DISSECTING INTERMOLECULAR GOLD CATALYSIS: APPLICATION TO THE TOTAL SYNTHESIS OF RUMPHELLAONE A.

Carla Obradors Llobet

Dipòsit Legal: T 75-2015

Carla Obradors Llobet

Dissecting Intermolecular Gold Catalysis: Application to the Total Synthesis of Rumphellaone A

DOCTORAL THESIS
Supervised by Prof. Antonio M. Echavarren

Institut Català d'Investigació Química (ICIQ)

UNIVERSITAT ROVIRA I VIRGILI

Tarragona 2014

UNIVERSITAT ROVIRA I VIRGILI

DEPARTAMENT DE QUIMICA ANALITICA I QUIMICA ORGANICA

C/ Marcel.lí Domingo s/n
Campus Sescelades
43007 Tarragona
Tel. 34 977 55 97 69
Fax 34 977 55 84 46
e-mail: secqaqo@urv.net

ICIQ
Institut Català d'Investigació Química

FAIG CONSTAR que aquest treball, titulat "Dissecting Intermolecular Gold Catalysis: Application to the Total Synthesis of Rumphellaone A", que presenta Carla Obradors Llobet per a l'obtenció del títol de Doctor, ha estat realitzat sota la meva direcció a l'Institut Català d'Investigació Química i que acompleix els requeriments per poder optar a Menció Internacional.

Tarragona, 13 d'Octubre 2014

El director de la tesi doctoral

Antonio M. Echavarren Pablos

Als meus pares.

A l'atzar agraeixo tres dons...
Maria Mercè Marçal i Serra

En primer lloc, agraeixo al Professor Antonio M. Echavarren l'oportunitat de formar-me en el seu grup a l'Institut Català d'Investigació Química (ICIQ). Li agraeixo les classes, els recursos, els seminaris, les conferències i l'accés a perspectives tan diferents. Per sobre de tot, li agraeixo la llibertat i absoluta confiança que he rebut des del primer dia.

A més, agraeixo a la Sònia Gavaldà i l'Imma Escofet la seva sublim eficiència. També que hagin decidit cuidar-nos a cada un de nosaltres simplement perquè tenen un bon cor. Agraeixo cada un dels seus ànims i somriures.

Agraeixo a tots els membres dels serveis tècnics de l'ICIQ la seva professionalitat i ajuda, en especial a David Pena i Ángel Mosquera d'Informàtica i als de Ressonància Magnètica Nuclear i de Difracció de Raigs X.

Agraeixo als Professors Vladimir Grushin, Rubén Martín, Feliu Maseras, Miquel Pericàs i la gent dels seus grups haver-me obert les portes i compartir el seu punt de vista cada cop que ho he demanat. Agraeixo també les col·laboracions amb Nicholas J. Green del grup del Professor Michael S. Sherburn a la Universitat Nacional d'Austràlia i amb el Doctor Iván Rivilla del grup del Professor Fernando P. Cossío a la Universitat del País Vasc.

Agraeixo a la Fundació ICIQ, Universitat Rovira i Virgili (URV), el projecte europeu ERC, AGAUR i el Ministeri espanyol amb una beca FPU haver-me finançat durant tot aquest temps.

També agraeixo l'oportunitat d'haver realitzat una estada a The Scripps Research Institute (USA). Agraeixo al Doctor Ryan Shenvi haver-me acceptat al seu grup i haver-me ensenyat tant durant aquells mesos. Agraeixo a Alberto Oppedisano, Doctor Sergey Pronin, Steven Crossley, Greg Trebor i Dennis Franco, entre tants d'altres personatges, tota la seva ajuda i amistat. Agraeixo a la Professora Donna Blackmond i als Doctors Erik Plata i Alex O'Brien la seva col·laboració en el meu projecte.

Agraeixo a tots els membres presents i passats del grup Echavarren qualsevol detall que m'hagin pogut ensenyar. Agraeixo al Doctor Paul McGonigal la seva immensa ajuda: la guia, les tècniques i la constant però no abatuda visió crítica del món. Agraeixo als Doctors Beatrice Ranieri, David Leboeuf, Juhannes Aydin, Javier Carreras, Michael Muratore i Laura López el seu granet de sorra. Per sobre de tot, agraeixo a aquells companys que han sigut amics: amb molt d'apreci a Yahui Wang, Anthony Pitaval i Pilar Calleja. També a Madeleine Livendahl, Núria Huguet, Morgane Gaydou, Masha Kirilova, Bart Herlé, Ana Escribano, Elena de Orbe, Ruth Dorel i tota la resta. *Last but not least*, agraeixo a l'Anna Homs cada dia que hem passat juntes i tots els que vindran.

Agraeixo a Tarragona haver-me acollit durant aquests anys. Per començar, al Doctor Xacobe Couso: agraeixo totes les cerveses, pitis i cafès. Fins i tot agraeixo totes les preguntes difícils que ens acompanyaven. A més, li agraeixo haver-me ensenyat a parlar amb un ordinador i ser capaç de portar a terme càlculs DFT. Amb moltíssim d'amor agraeixo a l'Asraa Ziadi cada moment que he passat amb ella i que mai m'hi hagi faltat un somriure o una abraçada. També agraeixo a totes aquelles persones que m'han fet sentir com a casa: per sobre de tot, Toni Moragas, David Bastida i cada una de les estones que hem passat tots junts al Delta. A la Berta Camafort, Jordi Ampurdanès, Álvaro Guitérrez, Arkaitz Correa, Piotr Jankowski, Andy Chapman, Alex Hamilton, Philipp Reeh, Andrea Henseler, Antonio Bazzo, Yolanda González, Claudio Martínez, Laura Fra, Jose Souto, Carles Rodríguez, Elena Arceo, Manuel Nappi, Paula Álvarez, Francisco Juliá, Anton

Lishchynski, Toni Bautista, Giulia Bergonzini, Charles Goery, Maria Basora, Miriam Sau, el Txepu i la Mariona i tants d'altres. I sobretot, a la senyora Azucena Obdulia del Carrer Sant Domènech.

Finalment, agraeixo a Manresa haver-me fet créixer fins a ser qui sóc avui i que encara ara senti que "ja he tornat" quan avanço Montserrat. Agraeixo a totes les persones que m'han acompanyat, ajudat i animat, cadascú en el seu moment i a la seva manera: a la Gemma Basiana, a la Miriam Raventós, al Josep M. Grané, al Jordi Guixé, a la Laura Fíguls, al Jordi Serra, a la Devi Tarragó, a l'Àstrid García, a la Sònia Cornejo, a l'Òscar Serra, al Victor Vallejo, al Marc Vila, a la Laura Vall, a la Tina Ribas, al Marc Khatib, a la Andrea Navarro, al Jordi Garcés, al Jordi Archs, a la Marta Vilar, al Joan Cantón, a la Txell Pons i a mil més que al recordar-los, em fan somriure. També agraeixo cada una de les converses que he tingut amb el senyor Pere, tot i que preferiria haver-lo conegut en unes altres circumstàncies.

I, per sobre de tot, agraeixo als meus pares, l'Emma i a tota la família l'amor, els consells i el suport incondicional que m'han regalat sempre. Aquesta tesis i la meva persona són obra seva, per haver construït un niu on sempre hi serem acceptats i estimats i per haver-me ensenyat a imitar-los: sempre creuré que són el millor exemple que hauria pogut tenir.

Per acabar, agraeixo haver conegut al Doctor Josep Cornellà: per mi, el Pep. Agraeixo cada una de les estones que hem passat junts: els riures, les discussions, l'ajuda i tot el que n'he pogut aprendre. Espero i desitjo que aquest hagi sigut només el començament del viatge.

En el moment de redactar aquesta memòria, els resultats aquí descrits han donat lloc a les següents publicacions:

Intermolecular Gold-Catalyzed Cycloaddition of Alkynes with Oxoalkenes
C. Obradors and A. M. Echavarren
Chem. –Eur. J. **2013**, *19*, 3547–3551

Dissecting Antion Effects in Gold(I)-Catalyzed Intermolecular Cycloadditions
C. Obradors, A. Homs, D. Leboeuf and A. M. Echavarren
Adv. Synth. Catal. **2014**, *356*, 221–228

Gold(I)-Catalyzed Macrocyclizations of 1,n-Enynes
C. Obradors, D. Leboeuf, J. Aydin and A. M. Echavarren
Org. Lett. **2013**, *15*, 1576–1579

Intriguing Mechanistic Labyrinths in Gold(I) Catalysis
C. Obradors and A. M. Echavarren
Chem. Commun. **2014**, *50*, 16–28

Gold-Catalyzed Rearrangements and Beyond
C. Obradors and A. M. Echavarren
Acc. Chem. Res. **2014**, *47*, 902–912

Gold-Catalyzed Intermolecular Cycloadditions of Alkynes and Allenes
M. Muratore, A. Homs, C. Obradors and A. M. Echavarren
Chem. Asian J. **2014**, DOI: 10.1002/asia.201402395

Chloro[1,3-dihydro-1,3-bis(2,4,6-trimethylphenyl)-2H-imidazol-2-ylidene]gold
C. Obradors and A. M. Echavarren
e–EROS Encyclopedia of Reagents in Organic Synthesis **2011**, DOI: 10.1002/047084289X.rn01338

Gold-Catalyzed Cyclizations of Alkynes with Alkenes and Arenes
M. Muratore, V. López-Carrillo, A. Escribano-Cuesta, N. Huguet, C. Obradors, A. M. Echavarren
Organic Reactions **2014**, *just accepted*

UNIVERSITAT ROVIRA I VIRGILI
DISSECTING INTERMOLECULAR GOLD CATALYSIS: APPLICATION TO THE TOTAL SYNTHESIS OF RUMPHELLAONE A.
Carla Obradors Llobet
Dipòsit Legal: T 75-2015

Table of Contents

This PhD manuscript is preceded by a **General Introduction** to gold chemistry and its applications. Part of this information was published in the form of reviews: *e–EROS Encyclopedia of Reagents in Organic Synthesis* (2011), *Chemical Communications* (2014), *Accounts of Chemical Research* (2014), *Chemistry Asian Journal* (2014) and *Organic Reactions* (2014).

At the same time, each chapter contains an outline with specific examples concerning our findings. Afterwards, the results are presented and discussed leading to the pertinent conclusions. Finally, a general overlook of the doctorate is exposed followed by all the experimental data: complete characterization of all the mentioned substrates, X-Ray crystallographic data and DFT calculations data. The references and numbering are organized by chapters as well.

The work performed during these four years has been divided in five chapters:

Chapter 1 gathers the development of the gold-catalyzed macrocyclization of large enynes via a [2+2] cycloaddition. This work was performed in collaboration with Dr. Juhanned Aydin at the beginning and with Dr. David Leboeuf at the end. I also thank Dr. Paul McGonigal for his guidance. The results were defended as my Master project in 2010 and published in *Organic Letters* in 2013.

Chapter 2 presents the development of the gold-catalyzed intermolecular cascade [2+2+2] cycloaddition of alkynes with oxoalkenes. I thank the lessons received by Dr. Xacobe Couso in order to perform DFT calculations. The results were published in *Chemistry European Journal* in 2013.

Chapter 3 contains a mechanistic study of the [2+2+2] cycloaddition, which led to the discovery of digold species. I thank Dr. Josep Cornellà for fruitful discussions. The results were published together with **Chapter 2**.

Chapter 4 included the design of new gold complexes for the intermolecular reactions accompanied with a mechanistic study of the [2+2] cycloaddition of alkynes with alkenes in order to explain the anion effects. This work was performed together with Anna Homs and in collaboration with Dr. David Leboeuf. The results were published in *Advanced Synthesis and Catalysis* in 2014.

Chapter 5 collects all the results obtained towards the total synthesis of the natural product Rumphellaone A as well as the attempts of an enantioselecective [2+2] version. This project is currently continued by Dr. Beatrice Ranieri. I thank Dr. Javier Carreras, Dr. Laura López and Dr. Josep Cornellà for crucial suggestions. These results are still unpublished.

In this manuscript, the abbreviations and acronyms most commonly used in organic and organometallic chemistry have been used following the recommendations of "Guidelines for authors" *J. Org. Chem.* **2006**, *71*, 1A-11A.

Additionally, we have also used the following ones:

DFT	Density Functional Theory
ESP	Electrostatic potential
Tol	Tolyl
DCE	1,2-Dichloroethane
THT	Tetrahydrothiophene
BIPHEP	(Biphenyl-2,2'-diyl)bis(diphenylphosphine)
TBHP	*Tert*-butylhydroperoxide
DTBB	4,4'-Di-*tert*-butylbiphenyl
CPME	Cyclopentyl methyl ether
iPr-DuPHOS	1,2-Bis[2,5-diisopropylphospholano]benzene
py	Pyridine
TsCl	Tosyl chloride
DIBAL	Diisobutyl aluminium hydride
TBS	*Tert*-butyldimethylsilyl
DIPT	Diisopropyltartrate
TMS	Trimethyl silyl
DME	Dimethoxyethane
TBAF	Tetrabutylammonium fluoride
BINAP	2,2´-Bis(diphenylphosphino)-1,1´-binaphthyl
TMBN	2,4,6-trimethoxybenzonitrile
NNf_2^-	Nonafluorobutanesulfimide

General Introduction

Gold as a Catalyst

For centuries, gold was considered a precious, purely decorative noble metal. It was not until 1998, in a groundbreaking report, that the hydration of alkynes catalyzed by Au(I) complexes under homogeneous conditions was reported.[1,2] Henceforth, numerous transformations were developed, nourishing the field of organic synthesis.[3] Gold salts and complexes emerged as powerful catalysts for the selective electrophilic activation of multiple bonds towards a variety of hetero- and carbonucleophiles under mild conditions. Cycloisomerizations and cycloadditions attracted particular attention for the construction of complex polycyclic structures present in diverse natural products.[4,5] Reactions catalyzed by gold usually proceed by multistep pathways that are rather complex. Although coherent mechanistic proposals advanced by means of DFT calculations, as well as labelling and kinetic experiments, isolation of key intermediates was proven to be challenging.[6]

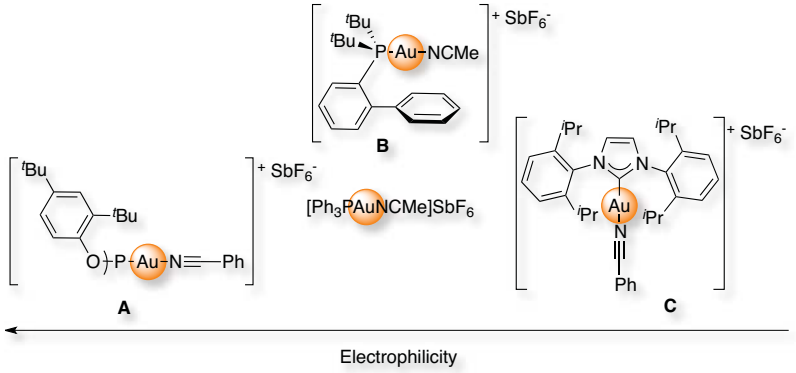

Figure 1. Gold complexes bearing different ligands.

Although simple gold salts such $NaAuCl_4$ or AuCl were active enough to catalyze many transformations, precatalysts LAuCl bearing phosphine or N-heterocyclic carbene as ligands found more widespread applications.[7] The active species were often generated *in situ* by chloride abstraction using a silver salt with distinct anions. However, the innocence

---

[1] For other precedents see: *(a)* R. O. C. Norman, W. J. E. Parr and C. B. Thomas, *J. Chem. Soc., Perkin Trans. 1* **1976**, 1983–1987; *(b)* Y. Fukuda and K. Utimoto, *J. Org. Chem.* **1991**, *56*, 3729–3731.
[2] J. H. Teles, S. Brode and M. Chabanas, *Angew. Chem. Int. Ed.* **1998**, *37*, 1415–1418.
[3] *(a)* A S. K. Hashmi, *Chem. Rev.* **2007**, *107*, 3180–3211; *(b)* A. Fürstner, P. W. Davies, *Angew. Chem. Int. Ed.* **2007**, *46*, 3410–3449; *(c)* E. Jiménez-Núñez and A. M. Echavarren, *Chem. Rev.* **2008**, *108*, 3326–3350; *(d)* D. J. Gorin, B. D. Sherry and F. D. Toste, *Chem. Rev.* **2008**, *108*, 3351–3378; *(e)* N. T. Patil and Y. Yamamoto, *Chem. Rev.* **2008**, *108*, 3395–3442; *(f)* A. Fürstner, *Chem. Soc. Rev.* **2009**, *38*, 3208–3221; *(g)* N. D. Shapiro and F. D. Toste, *Synlett* **2010**, 675–691; *(h)* C. Obradors and A. Echavarren, *Acc. Chem. Res.* **2014**, 47, 902–912.
[4] *(a)* N. Krause, V. Belting, C. Deutsch, J. Edrsack, H. T. Fan, B. Gockel, A. Hoffmann-Röder, N. Morita and F. Volz, *Pure Appl. Chem.* **2008**, *80*, 1063–1069; *(b)* M. Rudolph and A. S. K. Hashmi, *Chem. Soc. Rev.* **2012**, *41*, 2448–2462.
[5] For specific examples see: *(a)* E. Jiménez-Núñez, K. Molawi and A. M. Echavarren, *Chem. Commun.* **2009**, 7327–7329; *(b)* K. Molawi, N. Delpont and A. M. Echavarren, *Angew. Chem. Int. Ed.* **2010**, *49*, 3517–3519; *(c)* M. Gaydou, R. E. Miller, N. Delpont, J. Ceccon and A. M. Echavarren, *Angew. Chem. Int. Ed.* **2013**, *52*, 6396–6399.
[6] *(a)* A. S. K. Hashmi, *Angew. Chem. Int. Ed.* **2010**, *49*, 5232–5241; *(b)* L. P. Liu and G. B. Hammond, *Chem. Soc. Rev.* **2012**, *41*, 3129–3139.
[7] *(a)* P. Pérez-Galán, N. Delpont, E. Herrero-Gómez, F. Maseras and A. M. Echavarren, *Chem.–Eur. J.* **2010**, *16*, 5324–5332; *(b)* G. C. Fortman and S. P. Nolan, *Chem. Soc. Rev.* **2011**, *40*, 5151–5169.

of silver in the reaction mixture was recently questioned.[8] The most convenient catalysts are gold complexes [LAuL´]X or [LAuX] with weakly coordinating neutral (L´) or softer anionic ligands (X), which could enter the catalytic cycle by associative ligand exchange with the substrate (Figure 1).[9] The properties of the catalysts can be easily tuned sterically or electronically depending on the ligand. Thus, in general, complexes with phosphite (**A**) and related ligands are more electrophilic than those bearing more donating N-heterocyclic carbenes (**C**), whereas with phosphines show intermediate electrophilicity (**B** or $[Ph_3PAuNCMe]SbF_6$).[3d] The use of chiral ligands led to the development of efficient asymmetric processes.[10,11]

Activation of Unsaturated Substrates

Important structural features of gold are its aurophilicity, its linear geometry that limits the coordination potential and the fact that it does not undergo spontaneous oxidative addition nor β-hydride elimination. Gold has the highest electronegativity among the transition metals, which is attributed to relativistic effects.[12] Hence, the contraction of the 6s orbital in gold is much more significant than for the rest of the transition metals, which leads to an expansion of the 5d orbital, decreasing its electron-electron repulsion and becoming a remarkably soft Lewis acid. Furthermore, 5d electrons are too low in energy to experience a significant backbonding to anti-bonding orbitals but not to empty non-bonding orbitals. Thus, a 3 center – 4 electron σ-bond is proposed in gold(I)-carbenes $[L\text{-}Au{=}CR_2]^+$ accompanied with orthogonal weak π-backbonding from the metal to both the ligand and the substrate (Figure 2).

---

[8] *(a)* D. Wang, R. Cai, S. Sharma, J. Jirak, S. K. Thummanapelli, N. G. Akhmedov, H. Zhang, X. Liu, J. L. Petersen and X. Shi, *J. Am. Chem. Soc.* **2012**, *134*, 9012–9019; *(b)* Y. Zhu, C. S. Day, L. Zhang, K. J. Hauser and A. C. Jones, *Chem. –Eur. J.* **2013**, *19*, 12264–12271; *(c)* A. Homs, I. Escofet and A. M. Echavarren, *Org. Lett.* **2013**, *15*, 5782–5785.

[9] *(a)* N. Mézailles, L. Ricard and F. Gagosz, *Org. Lett.* **2005**, *7*, 4133–4136; *(b)* C Nieto-Oberhuber, M. P. Muñoz, S. López, E. Jiménez-Núñez, C. Nevado, E. Herrero-Gómez, M. Raducan and A. M. Echavarren, *Chem. –Eur. J.* **2006**, *12*, 1677–1693.

[10] *(a)* R. A. Widenhoefer, *Chem. –Eur. J.* **2008**, *14*, 5382–5391; *(b)* N. T. Patil, *Chem. Asian J.* **2012**, *7*, 2186–2194; (c) Y. M. Wang, A. D. Lackner and F. D. Toste, *Acc. Chem. Res.* **2014**, *47*, 889–901.

[11] For specific examples see: *(a)* M. P. Muñoz, J. Adrio, J. C. Carretero and A. M. Echavarren, *Organometallics* **2005**, *24*, 1293–1300; *(b)* G. L. Hamilton, E. J. Kang, M. Mba and F. D. Toste, *Science* **2007**, *317*, 496–499; *(c)* S. G. Sethofer, T. Mayer and F. D. Toste, *J. Am. Chem. Soc.* **2010**, *132*, 8276–8277; *(d)* K. Aikawa, M. Kojima and K. Mikami, *Adv. Synth. Catal.* **2010**, *352*, 3131–3135; *(e)* H. Teller, S. Flügge, R. Goddard and A. Fürstner, *Angew. Chem. Int. Ed.* **2010**, *49*, 1949–1953; *(f)* R. J. Felix, D. Weber, O. Gutierrez, D. J. Tantillo and M. R. Gagné, *Nat. Chem.* **2012**, *4*, 405–409; *(g)* J. Francos, F. Grande-Carmona, H. Faustino, J. Iglesias-Sigüenza, E. Díez, I. Alonso, R. Fernández, J. M. Lassaletta, F. López and J. L. Mascareñas, *J. Am. Chem. Soc.* **2012**, *134*, 14322–14325; *(h)* S. Handa and L. M. Slaughter, *Angew. Chem. Int. Ed.* **2012**, *51*, 2912–2915.

[12] D. J. Gorin and F. D. Toste, *Nature* **2007**, *446*, 395–403 and references citere therein.

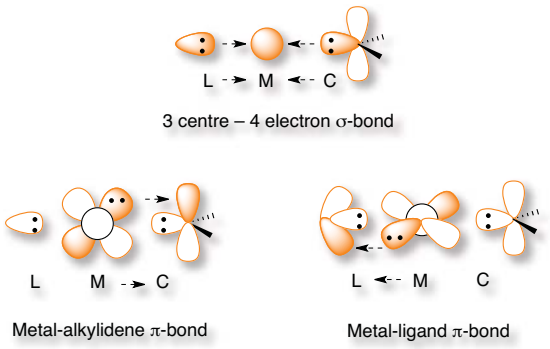

Figure 2. Ligand-metal-substrate orbital interactions in gold carbenes.

Gold(I) forms stable monomeric two coordinate π-complexes with alkenes,[13] 1,3-dienes,[14] substituted alkynes[15] and allenes.[16] Variations of the bond lengths as well as the ligand-metal-substrate angle suggest that the alkene orientation is controlled largely by steric factors. Thus, terminal alkenes bind unsymmetrically with gold(I) resulting in longer bonds with the substituted carbon atom. The X-ray structure of isobutylene IPr-gold(I) complex **1** revealed a 0.086 Å difference between the metal-carbon bonds, whereas for norbornene (**2**) and 2,3-dimethyl-2-butene (**3**), this difference is 0.024 Å and 0.009 Å, respectively (Figure 3).[13b] The angle between the metal and the centroid of the alkene also increased with the bulkiness of the alkene: 171.8º (isobutylene), 174.8º (norbornene), and 176.8º (2,3-dimethyl-2-butene).

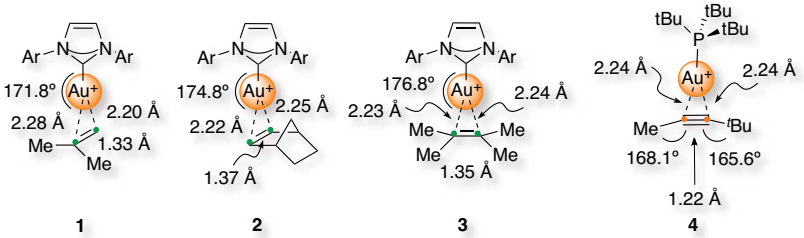

Figure 3. Analysis of alkene and alkyne gold complexes.

Internal alkyne gold(I) complex **4** showed almost symmetrical η^2-coordination. The triple bond length is identical to that of a free alkyne, although there is significant bending back of the alkyl substituents.[15c]

In the case of allenes, structural and solution analysis demonstrated that gold(I) preferentially binds to the less substituted C=C bond (Scheme 1). Although a theoretical study proposed that π-coordinated gold(I) complexes **5** with model NHC or phosphite

[13] *(a)* T. J. Brown, M. G. Dickens and R. A. Widenhoefer, *Chem. Commun.* **2009**, 6451–6453; *(b)* T. J. Brown, M. G. Dickens and R. A. Widenhoefer, *J. Am. Chem. Soc.* **2009**, *131*, 6350–6351; *(c)* R. E. M. Broomer and R. A. Widenhoefer, *Organometallics* **2012**, *31*, 768–771; *(d)* R. E. M. Brooner, T. J. Brown and R. A. Widenhoefer, *Chem.–Eur. J.* **2013**, *19*, 8276–8284.
[14] I. Krossing, *Angew. Chem. Int. Ed.* **2011**, *50*, 11576–11578 and references cited therein.
[15] For selected examples see: *(a)* S. Flügge, A. Anoop, R. Goddard, W. Thiel and A. Fürstner, *Chem.–Eur. J.* **2009**, *15*, 8558–8565; *(b)* T. N. Hooper, M. Green and C. A. Russell, *Chem. Commun.* **2010**, *46*, 2313–2315; *(c)* T. J. Brown and R. A. Widenhoefer, *J. Organomet. Chem.* **2011**, *696*, 1216–1220.
[16] T. J. Brown, A. Sugie, M. G. D. Leed and R. A. Widenhoefer, *Chem.–Eur. J.* **2012**, *18*, 6959–6971.

ligands could be in rapid equilibrium with η^1-allenyl species **5'**,[17] other experimental results with gold(I) complexes bearing bulky phosphine ligands ruled out the involvement of **5'** in the low energy π-face exchange processes (≤ 10 kcal mol^{-1}).[16]

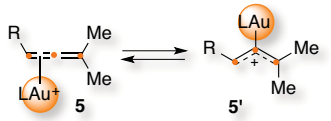

Scheme 1. Proposed equilibrium between η^2-allene (5) and η^1-allenyl (5′) gold species.

Nucleophilic Attack

In general, attack of nucleophiles to (η^2-alkyne)gold(I) complexes **6** gives *trans*-alkenyl species **7** (Scheme 2).[3,18] Although an outer-sphere mechanism is widely accepted and it has been verified many times in the stereoselectivity of gold(I)-catalyzed reactions, there are few exceptions. Although it is difficult to distinguish an outer-sphere attack from an insertion process, this type of mechanism was suggested in the gold(I)-catalysed hydroamination of alkynes and allenes with ammonia, since coordination to nitrogen was found to be preferred under catalytic condition in the presence of an excess of alkyne when using catalysts as **D**. 3-Hexyne was transformed to imine **8** with an excess of ammonia in toluene at 200 ºC for 20 h.[19] The *syn*-insertion of methyl propiolate in the Au-Si bond of a gold silyl complex was recently demonstrated.[20]

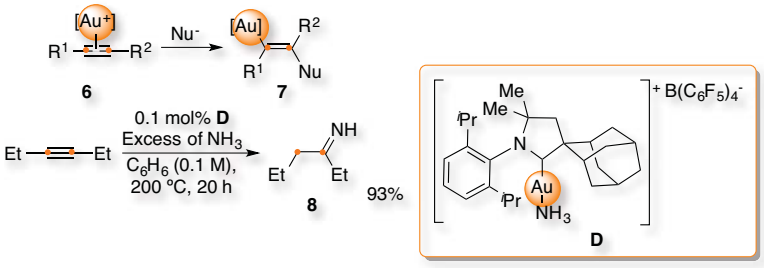

Scheme 2. Anti vs. syn nucleophilic attack to π-activated alkynes.

A wide range of carbon and heteronucleophiles such as arenes,[21] heteroarenes,[22] alcohols,[23] amines,[24] imines,[25] sulfoxides,[26] *N*-oxides[27] and thiols[28] have been used as nucleophiles in

[17] *(a)* B. Trillo, F. López, S. Montserrat, G. Ujaque, L. Castedo, A. Lledós and J. L. Mascareñas, *Chem.–Eur. J.* **2009**, *15*, 3336–3339; *(b)* I. Alonso, B. Trillo, F. López, S. Montserrat, G. Ujaque, L. Castedo, A. Lledós and J. L. Mascareñas, *J. Am. Chem. Soc.* **2009**, *131*, 13020–13030.
[18] J. A. Akana, K. X. Bhattacharyya, P. Müller and J. P. Sadighi, *J. Am. Chem. Soc.* **2007**, *129*, 7736–7737.
[19] V. Lavallo, G. D. Frey, B. Donnadieu, M. Soleilhavoup and G. Bertrand, *Angew. Chem. Int. Ed.* **2008**, *47*, 5224–5228 and references citere therein.
[20] M. Joost, P. Gualco, S. Mallet-Ladeira, A. Amgoune and D. Bourissou, *Angew. Chem. Int. Ed.* **2013**, *52*, 7160–7163.
[21] *(a)* M. T. Reetz and K. Sommer, *Eur. J. Org. Chem.* **2003**, 3485–3496; *(b)* C. Nevado and A. M. Echavarren, *Synthesis* **2005**, *2*, 167–182.
[22] *(a)* A. S. K. Hashmi, P. Haufe, C. Schmid, A. Rivas Nass and W. Frey, *Chem.–Eur. J.* **2006**, *12*, 5376–5382; *(b)* C. Ferrer and A. M. Echavarren, *Angew. Chem. Int. Ed.* **2006**, *45*, 1105–1109.
[23] *(a)* E. Mizushima, K. Sato, T. Hayashi and M. Tanaka, *Angew. Chem. Int. Ed.* **2002**, *41*, 4563–4565; *(b)* C. M. Krauter, A. S. K. Hashmi and M. Pernpointner, *ChemCatChem* **2010**, *2*, 1226–1230.

inter- or intramolecular processes. An early example was the intramolecular gold(III)-catalyzed cyclization of α-hydroxyallenes, such as **9**, that allowed the straightforward synthesis of 2,5-dihydrofurans like **10** in 78% isolated yield under mild conditions (Scheme 3).[29]

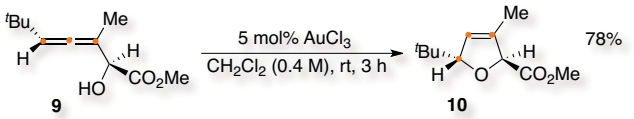

Scheme 3. Early gold-catalyzed cyclization of α-hydroxyallenes (9).

Noteworthy, the regioselectivity in the cyclization of halogenated allenones as **11** could be controlled depending on the oxidation state of the catalyst (Scheme 4).[30] Thus, gold(III) favoured a mechanism in which the ketone is preferentially activated leading to cyclisation with concomitant 1,2-halogen migration through bromonium intermediate **12** to finally build **13** whereas gold(I) coordinated to the allene leading to cyclization without halogen migration *via* **14** to form **15**.

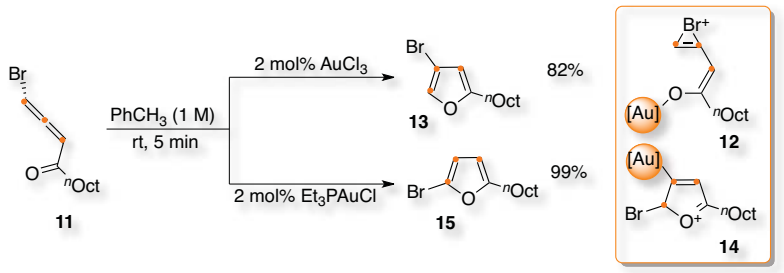

Scheme 4. Regioselective cyclization of halogenated allenone 11 depending on the metal oxidation state.

The intramolecular nucleophilic addition deserves a special mention when the nucleophile is located at the propargylic position.[31] Thus, propargylic carboxylates as **16** could undergo 1,2- or 1,3-acyloxy migrations leading to the formation of vinyl gold(I) carbenoid species **17** or allene gold(I) complexes **18**, which could be in rapid equilibrium (Scheme 5).[32] A double 1,2-shift, which also led to **18**, was found to be energetically more favoured than the direct 1,3-shift, although different substitution at the substrate could significantly influence this preference.

---

[24] *(a)* F. M. Istrate and F. Gagosz, *Org. Lett.* **2007**, *9*, 3181–3184; *(b)* J. Qian, Y. Liu, J. Cui and Z. Xu, *J. Org. Chem.* **2012**, *77*, 4484–4490.
[25] *(a)* H. Kusama, Y. Miyashita, J. Takay and, N. Iwasawa, *Org. Lett.* **2006**, *8*, 289–292; *(b)* E. Benedetti, G. Lemière, L. L. Chapellet, A. Penoni, G. Palmisano, M. Malacria, J. P. Goddard and L. Fensterbank, *Org. Lett.* **2010**, *12*, 4396–4399.
[26] *(a)* N. D. Shapiro and F. D. Toste, *J. Am. Chem. Soc.* **2007**, *129*, 4160–4161; *(b)* P. W. Davies and S. J. C. Albrecht, *Angew. Chem. Int. Ed.* **2009**, *48*, 8372–8375; (c) S. Shi, T. Wang, W. Yang, M. Rudolph and A. S. K. Hashmi, *Chem.–Eur. J.* **2013**, *19*, 6576–6580.
[27] L. Ye, L. Cui, G. Zhang and L. Zhang, *J. Am. Chem. Soc.* **2010**, *132*, 3258–3259.
[28] *(a)* I. Nakamura, T. Sato and Y. Yamamoto, *Angew. Chem. Int. Ed.* **2006**, *45*, 4473–4475; *(b)* I. Nakamura, T. Sato, M. Terada and Y. Yamamoto, *Org. Lett.* **2007**, *9*, 4081–4083.
[29] A. Hoffmann-Röder and N. Krause, *Org. Lett.* **2001**, *3*, 2537–2538.
[30] A. W. Sromek, M. Rubina and V. Gevorgyan, *J. Am. Chem. Soc.* **2005**, *127*, 10500–10501.
[31] *(a)* N. Marion and S. P. Nolan, *Angew. Chem. Int. Ed.* **2007**, *46*, 2750–2752; *(b)* S. Wang, G. Zhang and L. Zhang, *Synlett* **2010**, 692-706; *(c)* R. K. Shiroodi and V. Gevorgyan, *Chem. Soc. Rev.* **2013**, *42*, 4991–5001.
[32] A. Correa, N. Marion, L. Fensterbank, M. Malacria, S. P. Nolan and L. Cavallo, *Angew. Chem. Int. Ed.* **2008**, *47*, 718–721.

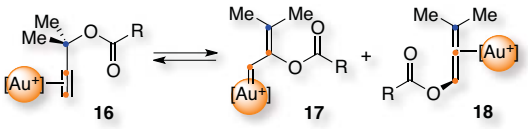

Scheme 5. Key intermediates in the propargylic migration of 16.

Cycloisomerization of 1,*n*-enynes are a class of emblematic transformations in which an alkene acts as the nucleophile towards an alkyne activated by gold (see **Chapters 1** and **2**).[3h] A diverse array of reactions are possible with a significant increase in molecular complexity and in a fully atom economic manner. A representative example was the single-cleavage rearrangement of 1,6-enyne **19** to form the conjugated diene **20** with 2 mol% of $Ph_3PAuCl/AgSbF_6$, which was proposed to proceed through a cyclopropyl gold(I) carbene (**21**) that could also be viewed as the homoallyl carbocation **21´** (Scheme 6).[9b,33] Gold(I) carbene intermediates could also be generated *via* a gold-catalyzed retro-Buchner reaction of 7-substituted cycloheptatrienes.[34]

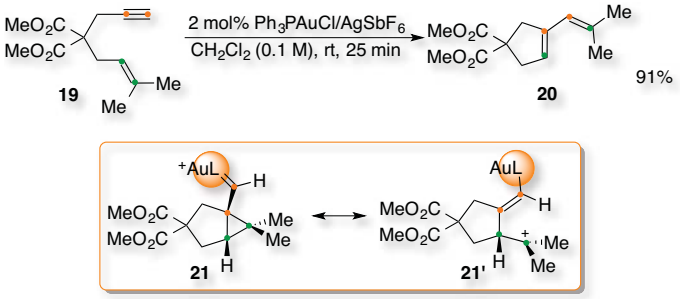

Scheme 6. Cyclopropyl gold carbene intermediate 21/21´ proposed in the cycloisomerization of enynes.

Gold Intermediates

Although many gold intermediates are too highly reactive to be readily isolated, some progress has been achieved in the observation of few key species.[6] In general, alkynes are selectively activated by gold(I) in the presence of other functional groups due to a higher reactivity of the η^2-alkyne gold(I) complexes towards nucleophilic attack.[35] In the case of the reaction between alkynes and alkenes, gold(I) carbenes and gold(I) stabilized carbocations could be conceived as the intermediates (Scheme 6).[33] An interesting debate, discussed in **Chapter 3**, was centred on the nature of the gold-carbon bond in complexes type $[LAuCHR]^+$.[36] However, spectroscopic or structural data for carbene-like structures of

[33] *(a)* C. Nieto-Oberhuber, M. P. Muñoz, E. Buñuel, C. Nevado, D. J. Cárdenas and A. M. Echavarren, *Angew. Chem. Int. Ed.* **2004**, *43*, 2402–2406; *(b)* C. Nieto-Oberhuber, S. López, E. Jiménez-Núñez and A. M. Echavarren, *Chem.–Eur. J.* **2006**, *12*, 5916–5923.
[34] C. R. Solorio, Y. Wang and A. M. Echavarren, *J. Am. Chem. Soc.* **2011**, *133*, 11952–11955.
[35] M. García-Mota, N. Cabello, F. Maseras, A. M. Echavarren, J. Pérez-Ramírez and N. Lopez, *ChemPhysChem* **2008**, *9*, 1624–1629.
[36] D. Benitez, N. D. Shapiro, E. Tkatchouk, Y. Wang, W. A. Goddard III and F. D. Toste, *Nat. Chem.* **2009**, *1*, 482–486.

relevance in homogeneous catalysis is lacking.[17,37] The interesting earlier structure of gold(I) carbene **22** showed C-Au length within the range of a single bond between a sp^2 carbon atom and the metal while the C-N bond was shorter than a typical imine as **22´** (Figure 4).[38,39] Neverthless, this scaffold is far from the intermediates generated in a catalytic cycle.

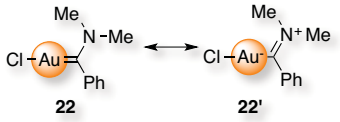

Figure 4. Isolated gold carbene 22/22´.

Evolution of the Gold Intermediates

Subsequently to the gold activation of the unsaturated scaffold and its nucleophilic attack, the intermediates could evolve through many different pathways leading to a huge variety of complex products.[3] The simplest evolution of the alkenyl gold(I) intermediates is their reaction with an electrophile, most usually by protodeauration regenerating the active catalyst. For example, intermediate **23** reacted with *p*-toluenesulfonic acid at 80 ºC to form **24** (Scheme 7).[40] Similarly, reaction with iodine and related electrophiles led to the corresponding halo-derivatives as **25**.[41]

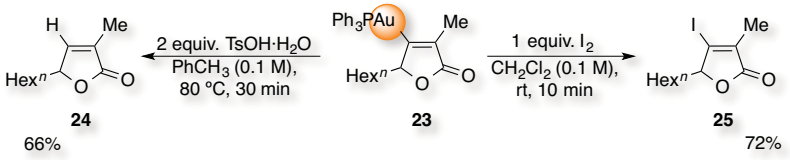

Scheme 7. Electrophilic attack to alkenyl gold complex 23.

The alkenyl gold(I) intermediate could further react in numerous multistep processes.[42] In the case of 1,*n*-enynes, they reacted with gold(I) by a series of fascinating rearrangements and related processes in the absence of external or internal nucleophiles (see **Chapter 1**).[9b,33a] On the other hand, they reacted both regio- and stereospecifically with a variety of them.[21-28] As an illustrative example, 1,6-enyne **26** reacted with Ph_3PAuMe/HBF_4 to form **27** in 80% isolated yield as a result of the intermolecular *anti* attack of methanol on the

---

[37] *(a)* R. E. M. Brooner and R. A. Widenhoefer, *Chem. Commun.* **2014**, *50*, 2420–2423; *(b)* M. Joost, L. Estévez, S. Mallet-Ladeira, K. Miqueu, A. Amgoune and D. Bourissou, *Angew. Chem. Int. Ed.* **2014**, DOI: 10.1002/anie.201407684.
[38] U. Schubert, K. Ackermann and R. Aumann, *Cryst. Struct. Comm.* **1982**, *11*, 591–594.
[39] For an analogous gold allenylidene see: M. M. Hansmann, F. Rominger and A. S. K. Hashmi, *Chem. Sci.* **2013**, *4*, 1552–1559.
[40] *(a)* L. P. Liu, B. Xu, M. S. Mashuta and G. B. Hammond, *J. Am. Chem. Soc.* **2008**, *130*, 17642–17643; *(b)* W. Wang, G. B Hammond and B. Xu, *J. Am. Chem. Soc.* **2012**, *134*, 5697–5705.
[41] L. Ye and L. Zhang, *Org. Lett.* **2009**, *11*, 3646–3649.
[42] For alternative reactivities not discussed in this manuscript see: *(a)* X. Shi, D. J. Gorin and F. D. Toste, *J. Am. Chem. Soc.* **2005**, *127*, 5802–5803; *(b)* G. Lemière, V. Gandon, K. Cariou, A. Hours, T. Fukuyama, A. L. Dhimane, L. Fensterbank and M. Malacria, *J. Am. Chem. Soc.* **2009**, *131*, 2993–3006; *(c)* L. Cui, Y. Peng and L. Zhang, *J. Am. Chem. Soc.* **2009**, *131*, 8394–8395; *(d)* L. Cui, L. Ye and L. Zhang, *Chem. Commun.* **2010**, *46*, 3351–3353; *(e)* B. Lu, Y. Li, Y. Wang, D. H. Aue, Y. Luo, and L. Zhang, *J. Am. Chem. Soc.* **2013**, *135*, 8512–8524; *(f)* W. He, L. Xie, Y. Xu, J. Xiang and L. Zhang, *Org. Biomol. Chem.* **2012**, *10*, 3168–3171; *(g)* K. Ji, Y. Zhao and L. Zhang, *Angew. Chem. Int. Ed.* **2013**, *52*, 6508–6512.

cyclopropyl ring intermediate analogous to **21** (Scheme 8).[33a]

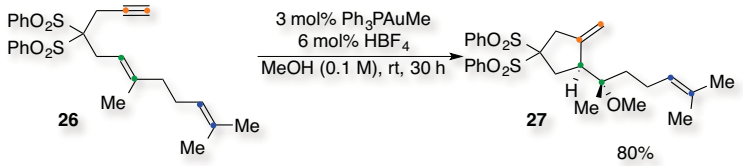

Scheme 8. Nucleophilic attack of methanol to 1,6-enyne 26.

Carbon nucleophiles reacted by similar mechanistic pathways.[43] A particular case was illustrated by the cycloaddition of aryl substituted enynes, such as **28**, which reacted readily with cationic gold(I) catalyst **B** to form smoothly tricyclic derivative **29** as well through a cyclopropyl gold carbene intermediate (Scheme 9).[44] This formal [4+2] cycloaddition was stereospecific and, according to DFT calculations, proceeded in a stepwise fashion in which the nucleophilic attack of the π-activated alkyne was the rate-determining step.

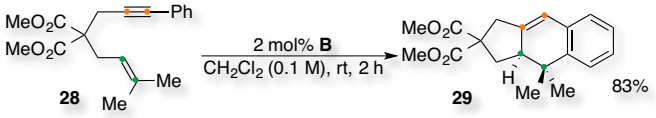

Scheme 9. [4+2] Cyclization of aryl-substituted 1,6-enyne 28.

Cyclopropyl gold(I) carbene intermediates could also be trapped by carbonyl groups inter- or intramolecularly as well as with alkenes via cyclopropanation (see **Chapters 2** and **3**).[33a,45,46] Dienynes such as ***Z*-30** bearing an alkoxy group at the propargylic position reacted differently leading to tricyclic products (**31**) as a result of a cyclization cascade process that involved a formal 1,5-migration of the RO- group (Scheme 10).[47] Thus, the reaction proceeded through intermediate **32**, which evolved by intramolecular attack of the RO- at the electrophilic site of the cyclopropane to form **33**. α,β-Unsaturated gold(I) carbene **34**, generated by cleavage of the oxonium bridge, then underwent cyclopropanation with the pending alkene. Intermediate **32** could also be trapped intermolecularly with an external nucleophile to generate the epimeric derivative **35**.

---

[43] *(a)* C. H. M. Amijs, C. Ferrer and A. M. Echavarren, *Chem. Commun.* **2007**, 698–700. *(b)* C. H. M. Amijs, V. López-Carrillo, M. Raducan, P. Pérez-Galán, C. Ferrer and A. M. Echavarren, *J. Org. Chem.* **2008**, *73*, 7721–7730.

[44] *(a)* C. Nieto-Oberhuber, S. López and A. M. Echavarren, *J. Am. Chem. Soc.* **2005**, *127*, 6178–6179; *(b)* C. Nieto-Oberhuber, P. Pérez-Galán, E. Herrero-Gómez, T. Lauterbach, C. Rodríguez, S. López, C. Bour, A. Rosellón, D. J. Cárdenas and A. M. Echavarren, *J. Am. Chem. Soc.* **2008**, *130*, 269–279.

[45] *(a)* E. Jiménez-Núñez, C. K. Claverie, C. Nieto-Oberhuber and A. M. Echavarren, *Angew. Chem. Int. Ed.* **2006**, *45*, 5452–5455; *(b)* M. Schelwies, A. L. Dempwolff, F. Rominger and G. Helmchen, *Angew. Chem. Int. Ed.* **2007**, *46*, 5598–5601; *(c)* A. Escribano-Cuesta, V. López-Carrillo, D. Janssen and A. M. Echavarren, *Chem.–Eur. J.* **2009**, *11*, 5646–5650.

[46] *(a)* P. Pérez-Galán, H. Herrero-Gómez, D. T. Hog, N. J. A. Martin, F. Maseras and A. M. Echavarren, *Chem. Sci.* **2011**, *2*, 141–149; *(b)* V. López-Carrillo, N. Huguet, A. Mosquera and A. M. Echavarren, *Chem.–Eur. J.* **2011**, *17*, 10972–10978.

[47] E. Jiménez-Núñez, M. Raducan, T. Lauterbach, K. Molawi, C. R. Solorio and A. M. Echavarren, *Angew. Chem. Int. Ed.* **2009**, *48*, 6152–6155.

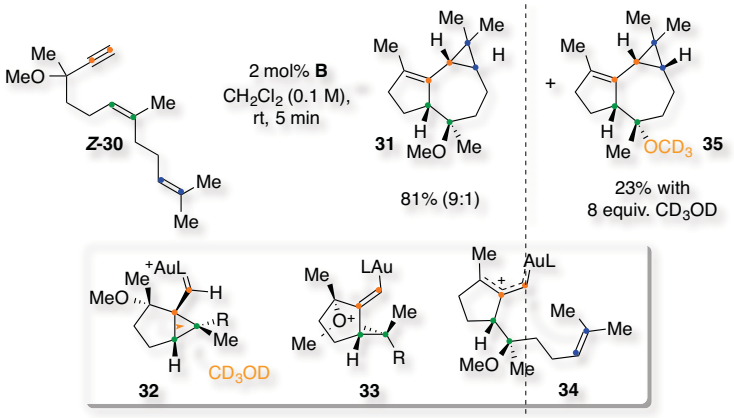

Scheme 10. 1,5-Propargylic ether migration of 1,6-enyne Z-30 followed by intramolecular cyclopropanation.

Intermolecular Processes

Although many transformations were developed using gold catalysis to build complex polycyclic structures, those methodologies generally relied on intramolecular processes.[3] In contrast, the corresponding intermolecular reactions were found to be more challenging (see the major advances in **Chapter 2**).[48] The first gold-catalyzed cycloaddition was developed between alkynes and alkenes to afford a cyclobutene moiety (Scheme 11).[49] As an example, reaction of ethynylbenzene with α-methylstyrene formed cyclobutene **36** when treated with [^{t}BuXPhosAuNCMe]SbF_6 (**E**) under mild conditions.

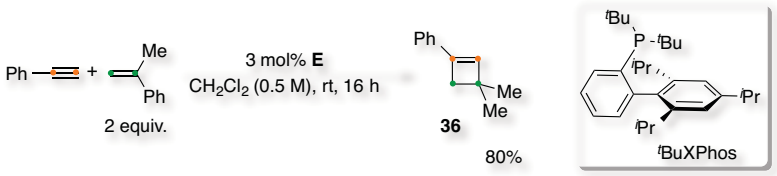

Scheme 11. Intermolecular [2+2] cycloaddition of alkynes and alkenes.

Afterwards, the presence of digold(I) complexes with bridging 3 center – 2 electron bond were observed in this reaction as well as in many different contexts, which triggered detailed analysis on their involvement in catalysis (see **Chapter 3**).[50,51] Moreover, several studies showed that the basicity and coordinating ability of the couteranion also played a

[48] M. Muratore, A. Homs, C. Obradors and A. M. Echavarren, *Chem. Asian J.* **2014**, *9*, 3066–3082 and references cited therein.
[49] V. López-Carrillo and A. M. Echavarren, *J. Am. Chem. Soc.* **2010**, *132*, 9292–9294.
[50] C. Obradors and A. M. Echavarren, *Chem. Commun.* **2014**, *50*, 16–28.
[51] For selected examples see: *(a)* P. H. Y. Cheong, P. Morganelli, M. R. Luzung, K. N. Houk and F. D. Toste, *J. Am. Chem. Soc.* **2008**, *130*, 4517–4526; *(b)* D. Weber, M. A. Tarselli and M. R. Gagné, *Angew. Chem. Int. Ed.* **2009**, *48*, 5733–5736; *(c)* G. Seidel, C. W. Lehmann and A. Fürstner, *Angew. Chem. Int. Ed.* **2010**, *49*, 8466–8470; *(d)* T. J. Brown and R. A. Widenhoefer, *Organometallics* **2011**, *30*, 6003–6009; *(e)* D. Weber, T. D. Jones, L. L. Adduci and M. R. Gagné, *Angew. Chem. Int. Ed.* **2012**, *51*, 2452–2456.

significant role in the reactivity as well as the selectivity of a specific transformation (see **Chapter 4**).[52]

Applications of Gold Chemistry

Therefore, gold-catalyzed reactions show many properties that prove them synthetically very useful. To start, gold chemistry allows a huge increment of the molecular complexity in really diverse types of transformations.[3] Thus, gold chemistry comprises a set of fully atom economy methodologies that also show excellent regio-, chemo- and stereoselectivities. Furthermore, most reactions proceed under mild conditions, with no additives and with rather robust catalysts. Finally, its reactivity is usually orthogonal to other transition metal catalyzed processes.

For these reasons, gold has been involved in many total syntheses of natural products with pharmaceutical interest (see **Chapter 5**).[53] Enantioselective processes are crucial in this area and, although asymmetric control has been shown possible in gold catalysis, there is still room for improvement regarding this specific feature.[10,11] As an example, a gold-catalyzed cascade [2+2+2] cyclization was used for the stereospecific synthesis of (–)-englerin A, which showed activity towards renal cancer cells (Figure 5).[54]

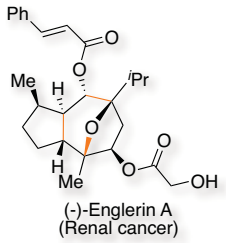

Figure 5. Englerin A synthesized using gold chemistry.

More recently, gold catalysis has also been combined with strong oxidants,[55] organocatalysts,[56] palladium, nickel or rhodium[57] and photoredox reactions[58] leading to a completely new set of interesting transformations. Finally, heterogeneous gold catalysis as well as the design of nanoparticles have shown great utilities in other contexts, for example, in the activation of small molecules, in supramolecular chemistry or in material science.[59]

---

[52] *(a)* A. S. K. Hashmi, T. Lauterbach, P. Nösel, M. H. Vilhemsen, M. Rudolph and F. Rominger, *Chem. –Eur. J.* **2013**, *19*, 1058–1065; *(b)* D. Zuccaccia, L. Belpassi, F. Tarantelli and A. Macchioni, *J. Am. Chem. Soc.* **2009**, *131*, 3170–3171.
[53] *(a)* A. S. K. Hashmi and M. Rudolph, *Chem. Soc. Rev.* **2008**, *37*, 1766–1775; *(b)* A. Fürstner, *Acc. Chem. Res.* **2014**, *47*, 925–938.
[54] *(a)* Q. Zhou, X. Chen and D. Ma, *Angew. Chem. Int. Ed.* **2010**, *49*, 3513–3516; *(b)* K. Molawi, N. Delpont and A. M. Echavarren, *Angew. Chem. Int. Ed.* **2010**, *49*, 3517–3519.
[55] M. N. Hopkinson, A. D. Gee and V. Gouverneur, *Chem. –Eur. J.* **2011**, *17*, 8248–8262 and references cited therein.
[56] For some illustrative examples see: *(a)* J. T. Binder, B. Crone, T. T. Haug, H. Menz and S. F. Kirsch, *Org. Lett.* **2008**, *10*, 1025–1028; *(b)* M. Bandini and A. Eichholzer, *Angew. Chem. Int. Ed.* **2009**, *48*, 9533–9537; *(c)* M. Bandini, A. Bottoni, M. Chiarucci, G. Cera and G. P. Miscione, *J. Am. Chem. Soc.* **2012**, *134*, 20690–20700; *(d)* C. Praveen, B. Montaignac, M. R. Vitale, V. Ratovelomanana-Vida and V. Michelet, *ChemCatChem* **2013**, DOI: DOI: 10.1002/cctc.201300313.
[57] J. J. Hirner, Y. Shi and S. A. Blum, *Acc. Chem. Res.* **2011**, *44*, 603–613 and references cited therein.
[58] B. Sahoo, M. N. Hopkinson and F. Glorius, *J. Am. Chem. Soc.* **2013**, *135*, 5505–5508.
[59] M. C. Daniel and D. Astruc, *Chem. Rev.* **2004**, *104*, 293–346 and references cited therein.

Chapter 1:

Gold-Catalyzed Macrocyclization of 1,n-Enynes via [2+2] Cycloaddition

1. Introduction

As explained in the **General Introduction**, gold-catalyzed cycloisomerizations of enynes emerged as a powerfull tool for the formation of C–C bonds due to the remarkable carbophilic properties of this metal.[1] These transformations allowed the construction of complex architectures under mild conditions from readily assembled starting materials and later led to the discovery of complex cascade reactions. In the absence of nucleophiles, 1,*n*-enynes could form products of skeletal rearrangement in fully intramolecular reactions through discrete cationic intermediates stabilized by gold.[2]

Broadly, gold selectively activates alkynes in the presence of other functional groups forming (π-alkyne)gold complexes, which can undergo nucleophilic attack from an alkene. In the case of 1,6-enyne **1**, this step formed cyclopropyl gold carbene intermediates **2** or **3** by an *anti-5-exo-dig* or a *6-endo-dig* cyclization, respectively (Scheme 1).[3] These intermediates were highly distorted according to DFT calculations and could later proceed *via* different pathways depending on the substitution pattern of the alkyne and the alkene.

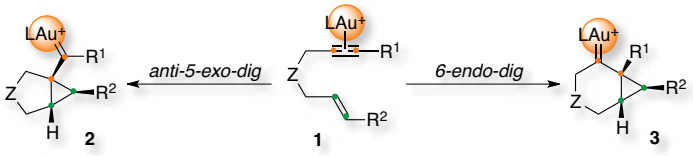

Scheme 1. Cyclopropyl gold carbene intermediates from 1,6-enyne 1.

As an example, intermediate **2** could evolve *via* one step single cleavage rearrangement followed by demetallation in which only the alkene was cleaved. Thus, 1,6-enyne **4** reacted with 2 mol% of $Ph_3PAuCl/AgBF_4$ in CH_2Cl_2 at 25 ºC to build 1,3-diene **5** in 96% isolated yield after 15 min (Scheme 2).[4]

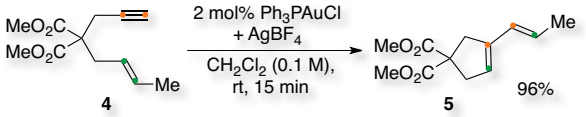

Scheme 2. Single cleavage rearrangement of 1,6-enyne 4.

On the other hand, 1,6-enyne **6** formed 1,3-diene **7** instead *via* a double cleavage rearrangement under similar conditions (Scheme 3).[4] Hence, intermediate **2** generated a

---

[1] *(a)* A S. K. Hashmi, *Chem. Rev.* **2007**, *107*, 3180–3211; *(b)* A. Fürstner, P. W. Davies, *Angew. Chem. Int. Ed.* **2007**, *46*, 3410–3449; *(c)* E. Jiménez-Núñez and A. M. Echavarren, *Chem. Rev.* **2008**, *108*, 3326–3350; *(d)* D. J. Gorin, B. D. Sherry and F. D. Toste, *Chem. Rev.* **2008**, *108*, 3351–3378; *(e)* N. T. Patil and Y. Yamamoto, *Chem. Rev.* **2008**, *108*, 3395–3442; *(f)* A. Fürstner, *Chem. Soc. Rev.* **2009**, *38*, 3208–3221; *(g)* N. D. Shapiro and F. D. Toste, *Synlett* **2010**, 675–691; *(h)* C. Obradors and A. Echavarren, *Acc. Chem. Res.* **2014**, 47, 902–912.

[2] For representative studies see: *(a)* L. Zhang, J. Sun and S. A. Kozmin, *Adv. Synth. Catal.* **2006**, *348*, 2271–2296; *(b)* M. García-Mota, N. Cabello, F. Maseras, A. M. Echavarren, J. Pérez-Ramírez and N. Lopez, *ChemPhysChem* **2008**, *9*, 1624–1629.

[3] *(a)* C. Nieto-Oberhuber, M. P. Muñoz, E. Buñuel, C. Nevado, D. J. Cárdenas and A. M. Echavarren, *Angew. Chem. Int. Ed.* **2004**, *43*, 2402–2406; *(b)* C. Nieto-Oberhuber, S. López, E. Jiménez-Núñez and A. M. Echavarren, *Chem. –Eur. J.* **2006**, *12*, 5916–5923.

[4] C. Nieto-Oberhuber, S. López, M. P. Muñoz, D. J. Cárdenas, E. Buñuel, C. Nevado and A. M. Echavarren, *Angew. Chem. Int. Ed.* **2005**, *44*, 6146–6148.

new rearranged gold carbene (**8**) by a formal insertion of the terminal alkene carbon into the alkyne carbons. Subsequent α-proton elimination formed the final product.

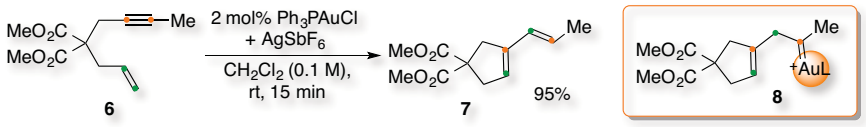

Scheme 3. Double cleavage rearrangement of 1,6-enyne 6.

In the case of intermediate **3**, α-proton elimination competed with single cleavage rearrangement through intermediate **9** (Scheme 4).[5] Thus, 1,6-enyne **10** cyclized in the presence of 2 mol% of $Ph_3PAuCl/AgSbF_6$ in CH_2Cl_2 at 0 ºC building 1,3-diene **11** in 67% isolated yield after 20 min.

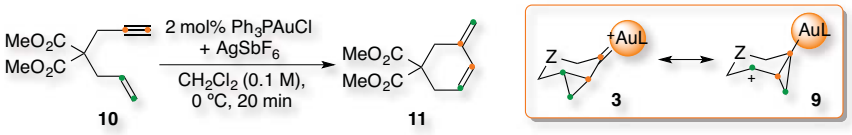

Scheme 4. Cyclization of 1,6-enyne 10 via 6-endo-dig pathway.

Analogous methodologies using 1,5-enynes were developed as well.[6] Moreover, similar cycloisomerizations of allenes are also possible.[7]

Alternatively, isomerization of **3** by ring expansion of the cyclopropane afforded 97% of cyclobutene **12** in the cyclization of 1,6-enyne **13** with JohnPhosAuCl/$AgSbF_6$ in CD_2Cl_2 at – 80 ºC (Scheme 5).[8] Cyclobutene **12** could be detected spectroscopically by ^{1}H NMR but isomerized to cyclobutene **14** at 25 ºC in 96% yield after 15 min.[9]

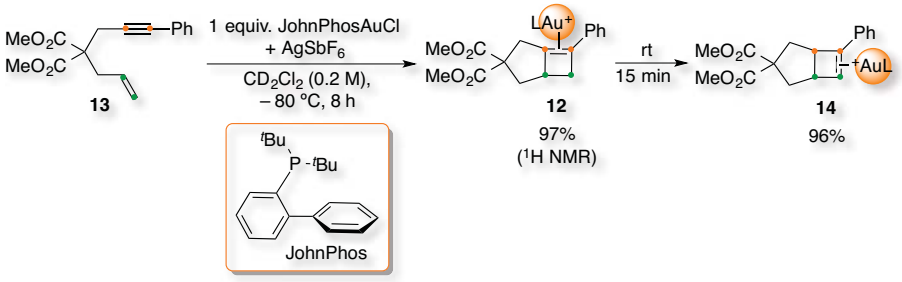

Scheme 5. Detection of cyclobutenes 12 and 14.

---

[5] C. Nieto-Oberhuber, M. P. Muñoz, S. López, E. Jiménez-Núñez, C. Nevado, E. Herrero-Gómez, M. Raducan and A. M. Echavarren, *Chem. –Eur. J.* **2006**, *12*, 1677–1693.
[6] For representative examples see: *(a)* L. Zhang and S. Kozmin, *J. Am. Chem. Soc.* **2004**, *126*, 11806–11807; *(b)* V. Mamane, T. Gress, H. Krause and A. Fürstner, *J. Am. Chem. Soc.* **2004**, *126*, 8654–8655.
[7] For representative examples see: (a) B. Trillo, F. López, S. Montserrat, G. Ujaque, L. Castedo, A. Lledós and J. L. Mascareñas, *Chem. –Eur. J.* **2009**, *15*, 3336–3339; (b) I. Alonso, B. Trillo, F. López, S. Montserrat, G. Ujaque, L. Castedo, A. Lledós and J. L. Mascareñas, *J. Am. Chem. Soc.* **2009**, *131*, 13020–13030.
[8] R. E. M. Brooner, T. J. Brown and R. A. Widenhoefer, *Angew. Chem. Int. Ed.* **2013**, *52*, 6259–6261.
[9] A. Escribano-Cuesta, P. Pérez-Galán, E. Herrero-Gómez, M. Sekine, A. A. C. Braga, F. Maseras and A. M. Echavarren, *Org. Biomol. Chem.* **2012**, *10*, 6105–6111.

Nevertheless, cyclobutenes emerged as the major products with 1,7- or 1,8-enynes. Hence, tricyclic structure **16** was obtained in 80% isolated yield from the cyclization of 1,7-enyne **15** with 2 mol% of [JohnPhosAuNCMe]SbF_6 (**B**) in CH_2Cl_2 at 25 ºC (Scheme 6).[4]

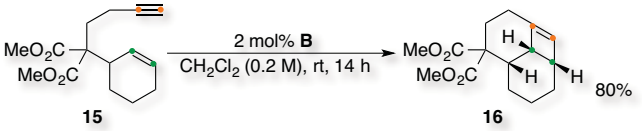

Scheme 6. Formation of a cyclobutene from 1,7-enyne 15.

Later on, cycloisomerization of 1,8-enynes catalysed by $XPhosAuNTf_2$ (**F**) was developed (Scheme 7).[10] Thus, 1,8-enyne **17** forged cyclobutene **18** in 90% isolated yield after 15 min in CD_2Cl_2 at 25 ºC using 4 mol% of the mentioned catalyst.

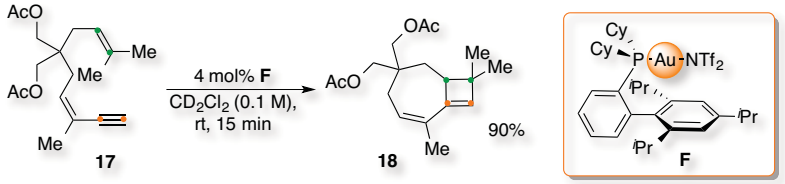

Scheme 7. Formation of a cyclobutene from 1,8-enyne 17.

So far, the largest 1,*n*-enyne involved in a gold-catalyzed cycloisomerization was 1,9-enyne **19**, which led to 10-membered ring **20** (Scheme 8).[11] However, this cyclization required 50 mol% of the gold catalyst to afford the final product in a moderate yield after 14 h in toluene at 50 ºC.

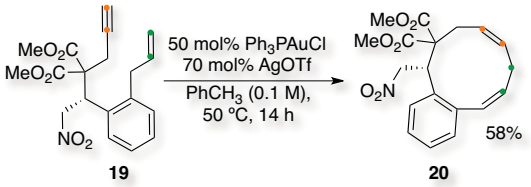

Scheme 8. Cyclization of 1,9-enyne 19.

On the other hand, the intermolecular [2+2] cycloaddition of terminal alkynes with an excess of an electron-rich alkene occurred using 3 mol% of [^{t}BuXPhosAuNCMe]SbF_6 (**E**) with a really sterically hindered ligand (Scheme 9).[12] The reaction proceeded in CH_2Cl_2 at 25 ºC to afford cyclobutene **21** regioselectively from ethynylbenzene and α-methylstyrene in 80% isolated yield.

[10] Y. Odabachian and F. Gagosz, *Adv. Synth. Catal.* **2009**, *351*, 379–386.
[11] E. Comer, E. Rohan, L. Deng and J. A. Porco, *Org. Lett.* **2007**, *9*, 2123–2126.
[12] V. López-Carrillo and A. M. Echavarren, *J. Am. Chem. Soc.* **2010**, *132*, 9292–9294.

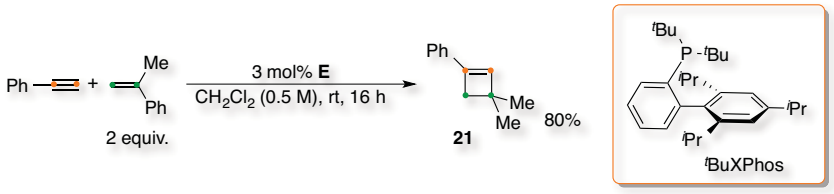

Scheme 9. Intermolecular [2+2] cycloaddition of alkynes and alkenes.

On the other hand, macrocycles are present in a multitude of important natural products that display a wide variety of biological activities.[13] Macrocycles are also commonly exploited in the fields of material science[14] and in supramolecular chemistry.[15] The most common methods for gaining access to macrocycles involve macrolactonizations,[16] ring-closing metathesis[17] or cross-coupling reactions (Figure 1).[18] For example, in the total synthesis of (–)-disorazole C_1, a late stage Yamaguchi lactonizaton was used to afford 30-membered ring **22** in 79% isolated yield under mild conditions.[19] Furthermore, during the synthesis of Taxol, an intramolecular Heck reaction with stoichiometric $Pd(PPh_3)_4$ at 90 ºC afforded 7-membered ring **23** in 49% yield.[20]

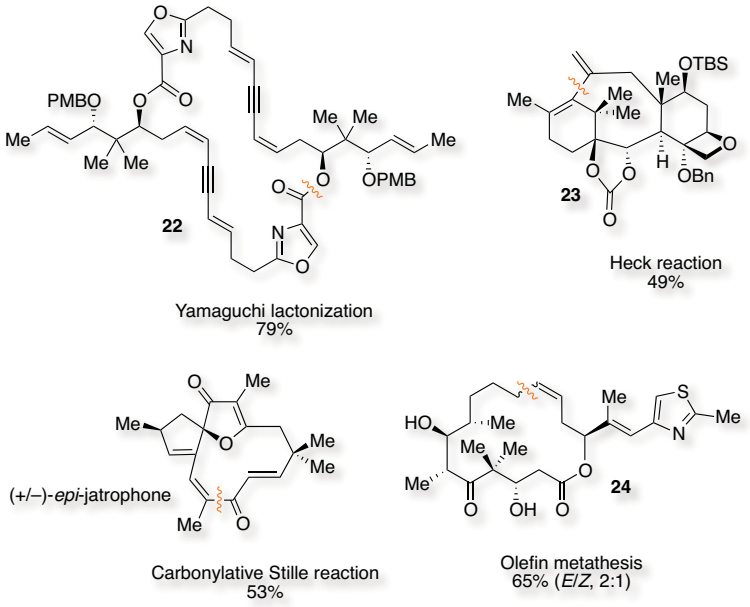

Figure 1. Examples of macrocyclizations in total synthesis.

---

[13] E. M. Driggers, S. P.Hale, J. Lee and N. K. Terrett, *Nat. Rev. Drug Discovery* **2008**, *7*, 608–624.
[14] S. H. Seo, T. V. Jones, H. Seyler, J. O. Peters, T. H. Kim, J. Y. Chang and G. N. Tew, *J. Am. Chem. Soc.* **2006**, *128*, 9264–9265.
[15] L. F. Indoy, K. M. Park and S. S. Lee, *Chem. Soc. Rev.* **2013**, *42*, 1713–1727.
[16] A. Parenty, X. Moreau and J. M. Campagne, *Chem. Rev.* **2006**, *106*, 911–939.
[17] *(a)* K. C. Nicolaou, P. G. Bulger and D. Sarlah, *Angew. Chem. Int. Ed.* **2005**, *44*, 4490–4527; *(b)* A. Gradillas and J. Pérez-Castells, *Angew. Chem. Int. Ed.* **2006**, *45*, 6086–6101.
[18] K. C. Nicolaou, P. G. Bulger and D. Sarlah, *Angew. Chem. Int. Ed.* **2005**, *44*, 4442–4489.
[19] P. Wipf and T. H. Graham, *J. Am. Chem. Soc.* **2004**, *126*, 15346–15347.
[20] J. J. Masters, J. T. Link, L. B. Snyder, W. B. Young and S. J. Danishefsky, *Angew. Chem. Int. Ed.* **1995**, *34*, 1723–1726.

(+/–)-2-*Epi*-jatrophone, which containes a 11-membered ring, was also obtained via an intramolecular carbonylative Stille coupling transformation in 53% isolated yield.[21] Finally, in the total synthesis of epothilones A and B, a ruthenium-catalyzed ring-closing olefin metathesis was applied to build 16-membered ring **24** in 65% (*E*/*Z*, 2:1) with 50 mol% of catalyst loading.[22]

Therefore, the construction of large carbon-based cyclic structures is not synthetically straightforward. Thus, the basic principles underlying the cyclization of bifunctional chain molecules to many-membered rings were expressed in terms of quantitative and systematic relationships applying physical-organic concepts.[23] The effective molarity, defined as k_{Intra}/k_{Inter}, determined the concentration limit in which a cyclization became favoured in front of polymerization. This factor relied on the type of transformation performed, the substrate involved, the most stable conformation as well as the size of the ring formed. Specifically, 3- to 7-membered rings, reaching the maximum in 5-, were the more straightforward rings formed due to entropic factors whereas it turned rather unfavoured from 8-membered rings and beyond (Figure 2).

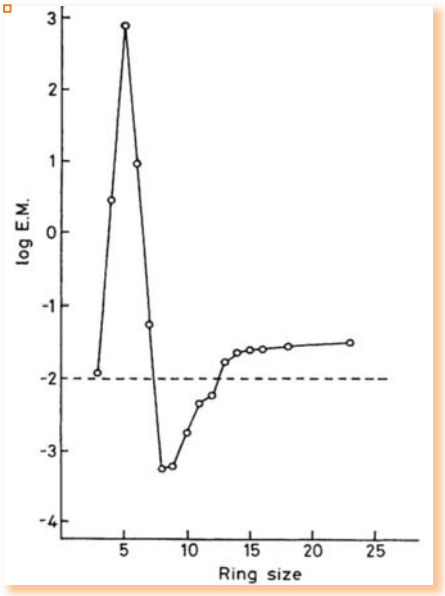

Figure 2. Relationship between the effective molarity in a cyclization and the size of the ring formed.

[21] A. C. Gyorkos, J. K. Stille and L. S. Hegedus, *J. Am. Chem. Soc.* **1990**, *112*, 8465–8472.
[22] D. Meng, P. Bertinato, A. Balog, D. S. Su, T. Kamenecka, E. J. Sorensen and S. J. Danishefsky, *J. Am. Chem. Soc.* **1997**, *119*, 10073 – 11092.
[23] C. Galli and L. Mandolini, *J. Chem. Soc., Chem. Commun.* **1982**, 251.

2. Objectives

Intramolecular cyclizations of 1,5-, 1,6-, 1,7- and 1,8-enynes were the benchmark to exploit gold-catalyzed reactions.[1h] Later on, the intermolecular cycloaddition between alkynes and alkenes led to the regioselective formation of cyclobutenes as **21**.[12] Due to the synthetic interest of macrocyclic structures, we reasoned we could develop a new methodology using this transformation. Thus, we decided to attempt the synthesis and gold-catalyzed cyclization of 1,*n*-enynes ($n \geq 9$) **25** to obtain frameworks such as **26** (Scheme 10).

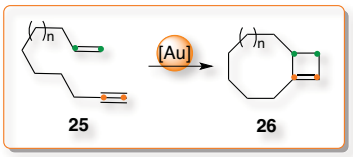

Scheme 10. Gold-catalyzed macrocyclization of 1,n-enynes (n≥9).

Therefore, we planned the development of a gold-catalyzed macrocyclization of large enynes as an extension of the intermolecular [2+2] cycloaddition.

3. Synthesis of Macrocycles

Optimization of the [2+2] Cyclization

In contrast to the transformations involving small 1,*n*-enynes (*n* = 5 – 8) that are entropically favoured, obtaining macrocycles from larger 1,*n*-enynes (*n* ≥ 9) is more challenging.[23] Preferably, the reacting partners must be in close proximity in a stable conformation to perform the reaction under mild conditions. For example, 1,10-enyne **27** did not lead to the formation of the corresponding macrocycle **28** with 3 mol% of catalyst **E** (Scheme 11). The reaction was attempted in CH_2Cl_2 at 25 ºC and only starting material was recovered after 24 h.

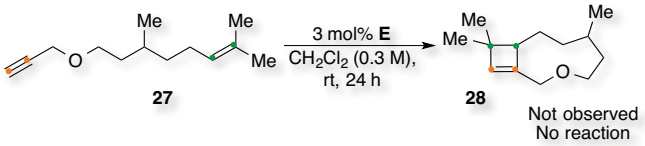

Scheme 21. Need of a spacer in order to react.

To circumvent this problem, we decided to add a spacer to favour the reactivity focusing on 1,14-enyne **29** towards 13-membered ring **30** (Table 1).

We first used catalyst **E** in CH_2Cl_2 but with distinct concentrations, temperatures and reaction times. To start, we could observe that the reaction outcome was highly dependant on the substrate concentration. Thus, when the reaction was performed under concentrated conditions (0.3 M) at 25 ºC, the yield of macrocycle **30** was not higher than 34% (entry 2). Interestingly, too long reaction times showed a decrease of the desired cyclobutene although complete conversion was reached in all cases. On the other hand, decreasing the concentration to 0.07 M and later to 0.007 M led to the formation of macrocycle **30** in good yields: 53 and 71%, respectively (entries 5 and 15). Nevertheless, the yield dropped to 57% (diastereoselectivity 2.3:1) after isolation. Heating the reaction allowed increasing the reaction rate but at the expense of the final yields. Presumably, oligomerization of the enyne or decomposition of the cyclobutene could occur more easily under these reaction conditions. Moreover, applying 10 mol% of catalyst **E** led to macrocycle **30** only in 64% yield (entry 22).

Afterwards, alternative gold complexes were examined in the macrocyclization of 1,14-enyne **29** to explore the impact of the ligand in the reactivity (Figure 3). The transformation was performed under the optimized conditions and analysed after 1 h (Table 2).

Table 1. Screening of the reaction conditions for the macrocyclization of large enynes.

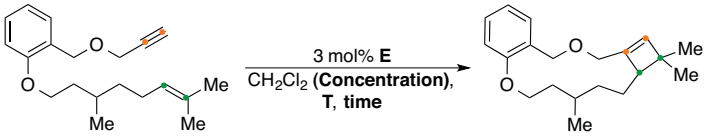

29 30

Enyne	Concentration (M)	Temperature (ºC)	Time (h)	Yield[a]
1			3	23
2	0.3	25	6	34
3			12	29
4			3	29
5		25	6	53
6			12	43
7			3	24
8	0.07	50	6	39
9			12	35
10			3	9
11		80	6	18
12			12	12
13			3	59
14		25	6	63
15			12	71
16			3	56
17	0.007	50	6	67
18			12	61
19			3	22
20		80	6	42
21			12	54
22[b]		25	12	64

[a]Crude analyzed by ^{1}H NMR spectroscopy using 1,4-diacetylbenzene as internal standard, yields referred to macrocycle **30**. [b]10 mol% **E**.

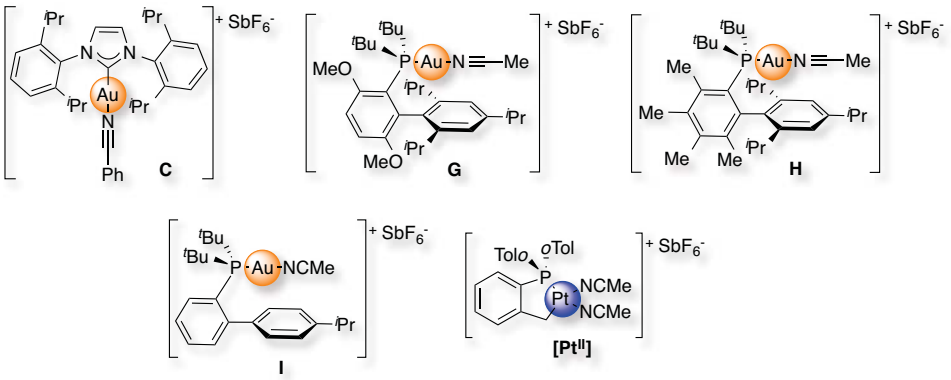

Figure 3. Other complexes screened.

In the case of catalyst **B**, a direct relationship between the bulkiness around the metal centre and the selectivity was observed. Thus, only 26% of macrocycle **30** was obtained with almost complete conversion (entry 1). Compared to complex **E**, new gold complexes **G** and **H** did not give macrocycle **30** in better yields (entries 3, 4 and 5). Study of the intermolecular [2+2] cycloaddition and the single cleavage of 1,6-enynes revealed the same behaviour for these new catalysts. Moderate results towards the macrocyclization were observed for catalysts **C** and **I**. On the other hand, when the active species were generated *in situ* from $Ph_3PAuCl/AgSbF_6$, the reaction proceeded very inefficiently (entry 7). Finally, no macrocycle **30** was observed using silver or platinum salts or complex **[Pt^{II}]** (entries 8 to 11).[2a]

Table 2. Screening of catalysts for the macrocyclization of large enynes.

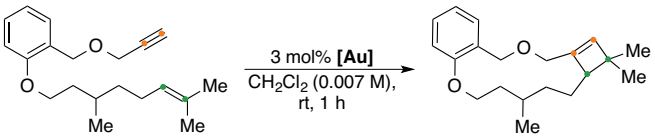

29 **30**

Entry	[Au]	Yield[a,b]
1	**A**	26% (91%)
2	**C**	22% (45%)
3	**E**	20% (35%)
4	**G**	8% (29%)
5	**H**	11% (23%)
6	**I**	29% (47%)
7	$Ph_3PAuCl/AgSbF_6$	10% (99%)
8	$AgSbF_6$	–
9	$PtCl_2$	–
10	$PtCl_4$	–
11	**[Pt^{II}]**	–

[a]Crude analyzed by ^{1}H NMR spectroscopy using 1,4-diacetylbenzene as internal standard, yields referred to macrocycle **30**. [b]Reaction conversion in brackets.

Scope of the [2+2] Cyclization

We started by examining the cyclization of 1,9-enyne **19** towards macrocycle **31** with catalyst **E** in CH_2Cl_2 (Scheme 12). The reaction was performed with 4 mol% at 25 ºC and led to no product, neither with 20 mol% at 50 ºC. On the contrary, catalyst **B** led to complete decomposition.

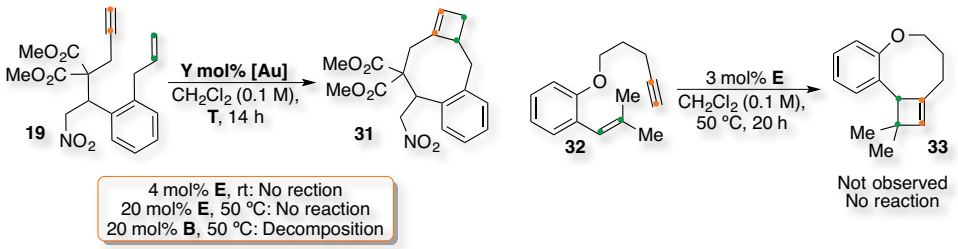

Scheme 12. Macrocyclization of 1,9-enynes.

Afterwards, 1,9-enyne **32** was treated with 3 mol% of catalyst **E** in CH_2Cl_2 at 50 ºC. Macrocycle **33** was not formed as no reaction was observed after 20 h. The analogous 1,10-enyne **34** did not lead to macrocycle **35** under the same conditions either (Scheme 13).

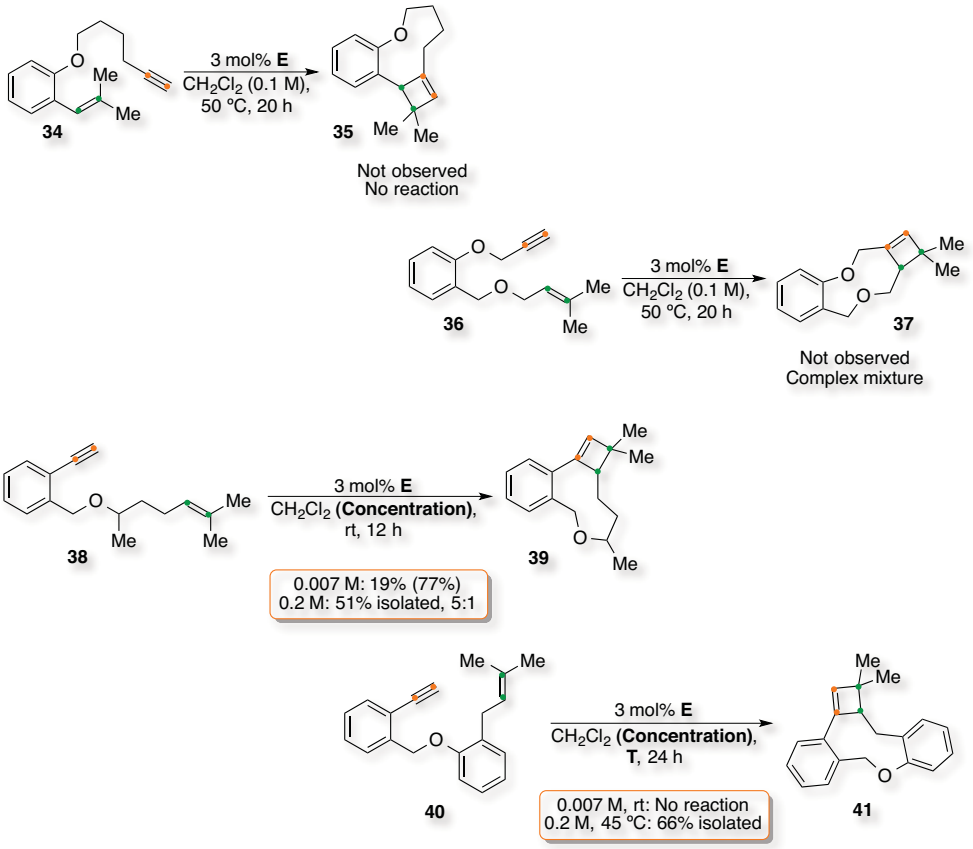

Scheme 13. Macrocyclization of 1,10-enynes.

A more flexible 1,10-enyne was synthesized (**36**) but reaction under the same conditions led to a very complex mixture and no cyclobutene **37** could be observed. In the case of 1,10-enyne **38** only 19% of macrocycle **39** was obtained with 77% of conversion under the optimized conditions. However, the yield increased to 51% (diastereoselectivity 5:1) when the concentration was increased to 0.2 M. Cyclization of 1,10-enyne **40** led to no reaction

under the optimized condition whereas formed macrocycle **41** in 66% isolated yield when the concentration was increased to 0.2 M and the temperature to 45 ºC. Furthermore, 9-membered ring **41** could be crystallized and the structure confirmed by X-ray diffraction (Figure 4). We could observe that the tetracyclic structure was rather rigid, which led to a distance between the aromatic rings of 2.82 Å.

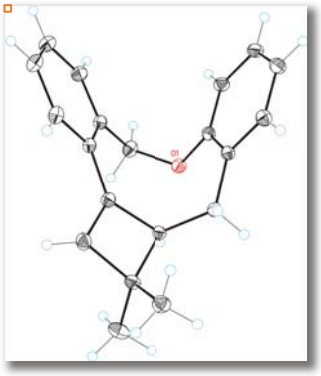

Figure 4. X-Ray crystal structure of macrocycle 41.

On the other hand, 1,11-enyne **42** led to 16% of macrocycle **43** and complete conversion under the optimized conditions (Scheme 14). When the reaction was performed in DCE (0.3 M) at 70 ºC the cyclobutene was obtained in 30% yield after 2 h, 20% (diastereoselectivity 4:1) after isolation.

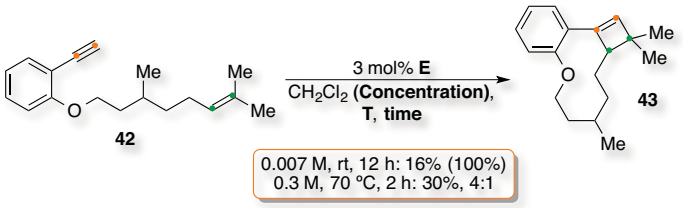

Scheme 14. Macrocyclization of 1,11-enyne 42.

In the case of 1,12-enynes, substrate **44** led to a very complex mixture and no macrocycle **45** was observed (Scheme 15). The reaction was attempted with 3 mol% of catalyst **E** in CH_2Cl_2 (0.1 M) at 25 and 50 ºC as well as at 0.05 M for 20 h.

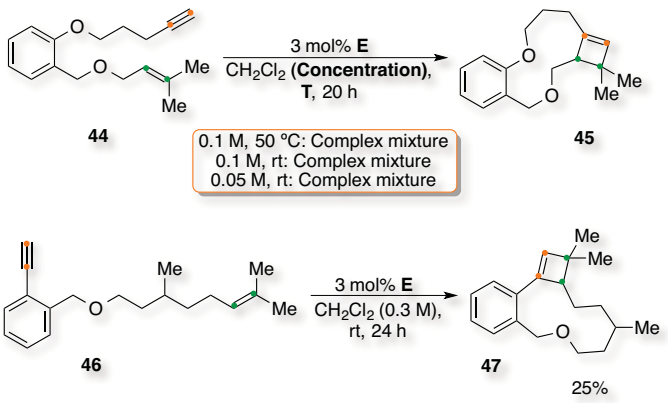

Scheme 15. Macrocyclization of 1,12-enynes.

Cyclization of 1,12-enyne **46** afforded macrocycle **47** in 25% yield when treated with 3 mol% of catalyst **E** in CH_2Cl_2 at 25 ºC. Due to co-elution with substrate **46**, the yield of **47** was determined by ^{1}H NMR spectroscopy using 1,4-diacetylbenzene as internal standard. We attempted a subsequent reaction with the crude mixture based on click chemistry,

specifically, a copper-catalyzed Huisgen cycloaddition between the remaining alkyne with a solid supported azide using 10 mol% of complex **[Cu^{I}]** (Figure 5).[24] The reaction was performed in DMF at 80 ºC, which led to the triazole but macrocycle **47** underwent decomposition under these conditions.

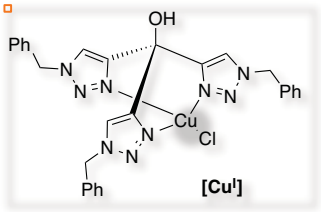

Figure 5. Copper catalyst for a Huisgen cycloaddition.

In the case of 1,13-enyne **48**, a very complex mixture with no cyclobutene **49** was also observed in the reaction with 3 mol% of catalyst **E** in CH_2Cl_2 at 25 or 50 ºC (Scheme 16). Otherwise, 1,13-enyne **50** afforded macrocycle **51** in 11% yield with complete conversion under the optimized conditions. However, it increased to 29% isolated yield when the reaction was performed at 0.3 M.

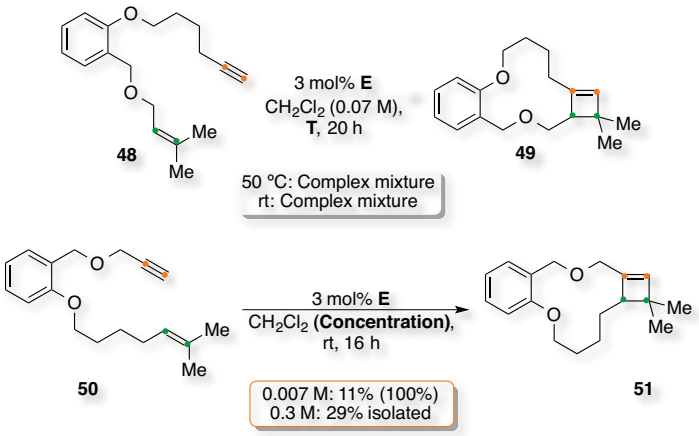

Scheme 16. Macrocyclization of 1,13-enynes.

On the other hand, cyclization of 1,14-enyne **52** led to macrocycle **53** in 57% isolated yield when treated with 3 mol% of catalyst **E** in CH_2Cl_2 (0.2 M) at 25 ºC (Scheme 17).

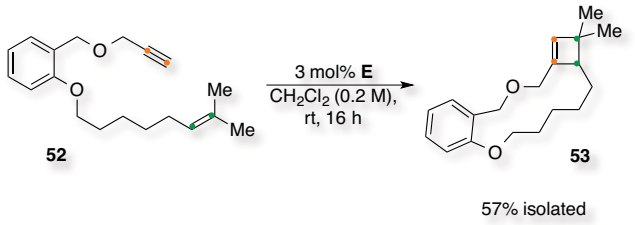

Scheme 17. Macrocyclization of 1,14-enyne 52.

[24] *(a)* V. V. Rostovtsev, L. G. Green, V. V. Fokin and K. B. Sharpless, *Angew. Chem. Int. Ed.* **2002**, *41*, 2596–2599; (b) S. Özçubukçu, E. Ozkal, C. Jimeno and M. A. Pericàs, *Org. Lett.* **2009**, *11*, 4680–4683.

Afterwards, 1,15-Enyne **54** afforded macrocycle **55** in 70% isolated yield under similar conditions (Scheme 18). Therefore, increasing the length of the enyne could lead to better yields as a consequence of a relief in transannular strain.

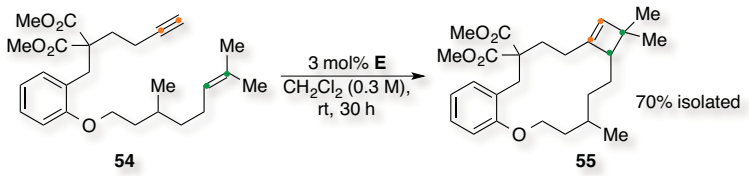

Scheme 18. Macrocyclization of 1,15-enyne 54.

Nevertheless, 1,16-enyne **56** led to a very complex mixture with no cyclobutene **57** (Scheme 19).

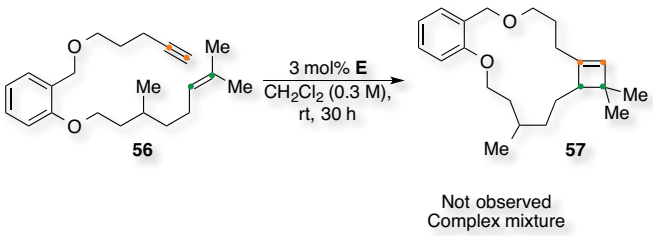

Scheme 19. Macrocyclization of 1,16-enyne 56.

Similarly, 1,17-enyne **58** formed only traces of macrocycle **59** when reacted in CH_2Cl_2 at 25 or 50 ºC for 20 h (Scheme 20).

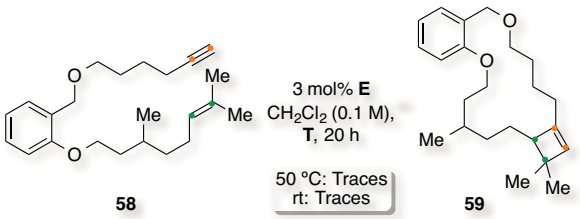

Scheme 20. Macrocyclization of 1,17-enyne 58.

Therefore, in order to explore the scope of the reaction, macrocyclizations were performed with 1,9- to 1,17- enynes bearing different spacers. In general, the reactions were carried out under mild conditions (**30**) although a few substrates required heating to furnish the macrocyclic products, for example, **41** and **43**. In addition, highly diluted conditions were counter-productive in some cases: **39**, **47**, **51**, **53** or **55**. Under these conditions, the macrocyclization reaction proceeded in moderate to good yields drastically depending on each substrate: the chain length, the spacer and the substituents.

This methodology also provided access to *m*-cyclophanes. This class of compounds exhibits interesting chemical and physical properties that result from their unusual

architecture.[25,26] Thus, 1,12-enyne **60** cyclized to form macrocycle **61** in 70% isolated yield with 3 mol% of catalyst **E** in CH_2Cl_2 (0.45 M) at 25 ºC for 1 day (Scheme 21).

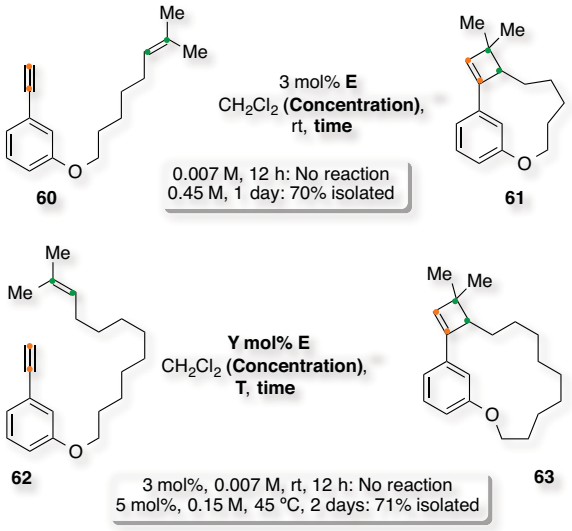

Scheme 21. Macrocyclization of meta-substituted arylenynes.

Finally, cyclization of 1,16-enyne **62** required 5 mol% of catalyst **E** to obtain macrocycle **63** in 71% isolated yield, which proceeded in CH_2Cl_2 (0.15 M) at 45 ºC for 2 days. Under more diluted conditions, no reaction was observed. Interestingly, macrocycle **61** was obtained as a mixture of atropoisomers 5:1 and macrocycle **63**, 4:1. NMR studies at high temperature (60 ºC) did not provide further information due to decomposition of the macrocycles.[27]

Derivatization of the Macrocycles

Finally, we decided to further modify these scaffolds with known transformations in order to prove the synthetic value of the methodology. Attempts of performing a ruthenium-catalyzed ring opening cross-metathesis with ethylene led to no reaction whereas oxidation of the cyclobutene moiety afforded very complex mixtures.[28,29]

Afterwards, we performed the hydrogenation of **30**. The cyclobutene could be reduced with 10 mol% of Pd/C in methanol at 25 ºC for 8 h under 1 atm of H_2 (Scheme 22). Under these conditions debenzylation of **30** was also observed and compound **64** was obtained in 79% isolated yield (diastereoselectivity 2.4:1). Attempts to derivatize the free alcohol with *p*-nitrobenzoyl chloride to crystallize the resulting product failed.

---

[25] R. Gleiter and H. Hopf, *Modern Cyclophane Chemistry*; Wiley VCH: Weinheim, **2004**.
[26] T. Gulder and P. Baran, *Nat. Prod. Rep.* **2012**, *29*, 899–934 and references cited therein.
[27] *(a)* T. Sato, M. Wakabayashi, K. Hata and M. Kainosho, *Tetrahedron* **1971**, *27*, 2737–2755; *(b)* K. Tomooka, C. Iso, K. Uehara, M. Suzuki, R. Nishikawa-Shimono and K. Igawa, *Angew. Chem. Int. Ed.* **2012**, *51*, 10355–10358.
[28] S. B. Garber, J. S. Kingsbury, B. L. Gray and A. H. Hoveyda, *J. Am. Chem. Soc.* **2000**, *122*, 8168–8179.
[29] B. R. Travis, R. S. Narayan and B. Borhan, *J. Am. Chem. Soc.* **2002**, *124*, 3824–3825.

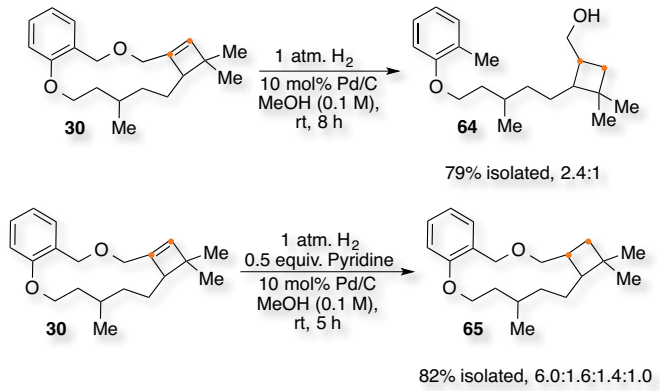

Scheme 22. Hydrogenation of macrocycle 30.

This problem could be circumvented by the addition of 0.5 equiv. of pyridine under similar conditions to furnish macrocycle **65** in 82% isolated yield.[30] However, this scaffold was obtained as a mixture of diastereoisomers (6.0:1.6:1.4:1.0). The configuration in the cyclobutane ring of the major diastereoisomer was assigned as trans by ^{1}H-^{13}C HSQC phase edited, ^{1}H-^{1}H COSY and ^{1}H-^{1}H NOESY NMR spectroscopy.

Furthermore, we compared the stability of the different diastereoisomers of substrates **64** and **65** by means of DFT calculations. In the case of compound **64**, the *trans*-cyclobutane was the more stable configuration and the effect of the methyl substituent was rather minor, $E_{CisTrans}$ = 0.7 kcal/mol (Figure 6). However, the *cis*-cyclobutane was significantly less stable, $E_{TransCis}$ = 2.6 kcal/mol and E_{CisCis} = 3.3 kcal/mol than the *trans-trans* diastereoisomer.

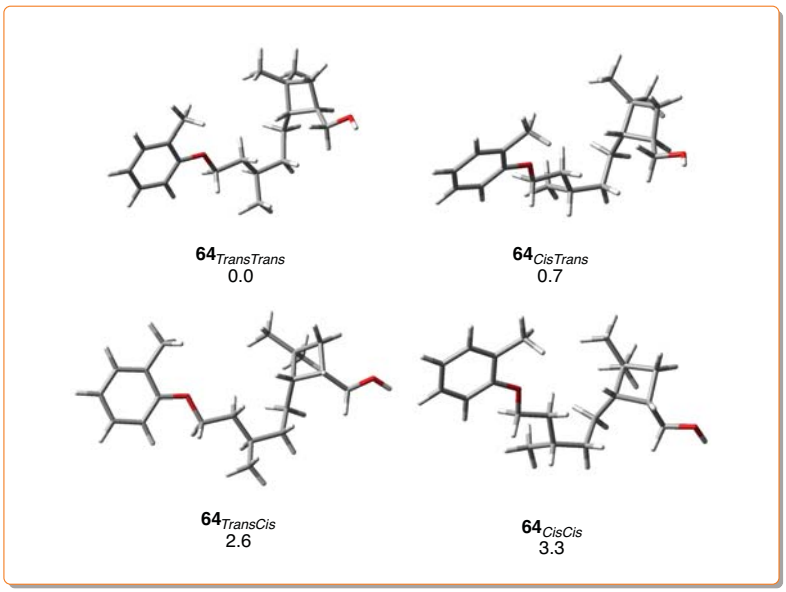

Figure 6. Diastereoisomers of compound 64 (relative energies in kcal/mol).

[30] H. Sajiki, *Tetrahedron Lett.* **1995**, *36*, 3465–3468.

On the other hand, macrocycle **65** was also more stable with a *trans* cyclobutane (Figure 7). Nevertheless, the effect of the methyl substituent was much more influential: $E_{CisTrans}$ = 2.4, E_{CisCis} = 2.8 and $E_{TransCis}$ = 3.7 kcal/mol.

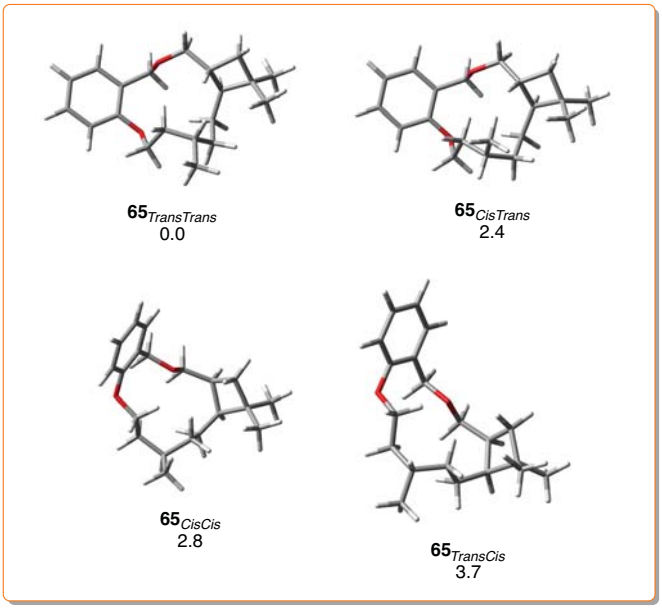

Figure 7. Diastereoisomers of compound 65 (relative energies in kcal/mol).

4. Conclusions

Although a wide variety of gold-catalyzed cycloisomerizations of 1,*n*-enynes were developed during the last decade, this class of emblematic transformations were limited from 1,5- to 1,8-substrates. Construction of larger rings was proven to be challenging due to entropic factors. In here, we have developed a gold-catalyzed macrocyclization of 1,*n*-enynes ($n \geq 9$) *via* a [2+2] cycloaddition towards a cyclobutene moiety.[31] As an example, 1,14-enyne **29** led to macrocycle **30** in 57% isolated yield under highly diluted conditions, at 25 ºC using 3 mol% of catalyst **E** (Scheme 23).

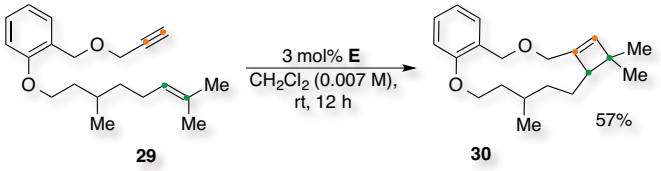

29 **30**

Scheme 23. Macrocyclization under highly diluted conditions.

Nevertheless, these optimized conditions were not general and other substrates required increasing the temperature and/or the concentration in order to react. Thus, 1,10-enyne **40** gave macrocycle **41** in 66% isolated yield at 0.2 M and 45 ºC (Scheme 24).

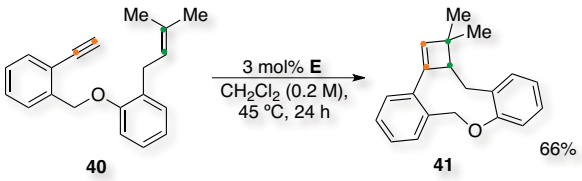

40 **41**

Scheme 24. Macrocyclization under harsher conditions.

The gold-catalyzed macrocyclization reaction proceeded smoothly with moderate to good yields forging 8- to 16-membered rings, including *m*-cyclophanes. However, the reactivity showed a strong dependence on the structure of each substrate.

[31] C. Obradors, D. Leboeuf, J. Aydin and A. M. Echavarren, *Org. Lett.* **2013**, *15*, 1576–1579.

Chapter 2:

Gold(I)-Catalyzed Intermolecular [2+2+2] Cycloaddition of Alkynes and Oxoalkenes

1. Introduction

As explained in the **General Introduction**, gold(I)-catalyzed intramolecular cycloisomerization reactions have been widely studied during the last decade.[1] Gold(I) complexes have been found to be powerful homogeneous catalysts for carbon-carbon, carbon-oxygen or carbon-nitrogen bond formation proceeding by nucleophilic additions to alkynes, allenes and alkenes giving access to new carbo- and heterocyclic compounds. Despite these major advances, the development of intermolecular cycloadditions using alkynes as the substrates has been shown to be challenging.[2] In these processes, different unsaturated substrates are involved and their possible competitive binding with the gold complex should be considered. Moreover, gold complexes are inherently acidic and therefore can promote the polymerization of alkenes *via* cationic mechanisms.[3]

The first intermolecular cycloaddition catalyzed by gold(I) involved terminal alkynes and electronrich alkenes that reacted to form cyclobutenes regioselectively, which are useful building blocks in synthesis (Scheme 1).[4]

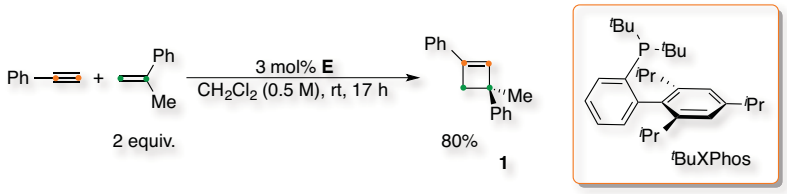

Scheme 1. Gold-catalyzed [2+2] cycloaddition of alkynes with alkenes.

This reaction required the use of the sterically hindered gold(I) complex [^{t}BuXPhosAu(NCMe)]SbF_6 (**E**) as catalyst, which circumvented the addition of any silver salt. Thus, reaction of ethynylbenzene and α-methylstyrene led to the cyclobutene adduct **1** in 80% isolated yield.

Further studies allowed the development of the [4+2] annulation of arylynamides with alkenes using IPrAuCl/$AgNTf_2$.[5] Attack of *p*-methoxystyrene to the activated alkyne **2** followed by a Friedel-Crafts reaction afforded structure **3** in 88% isolated yield (Scheme 2). In contrast, when terminal ynamide **4** and an enol ether were treated with a gold

---

[1] *(a)* L. Zhang, J. Sun and S. A. Kozmin, *Adv. Synth. Catal.* **2006**, *348*, 2271–2296; *(b)* A. Fürstner and P. W. Davies, *Angew. Chem. Int. Ed.* **2007**, *46*, 3410–3449; *(c)* A. S. K. Hashmi, *Chem. Rev.* **2007**, *107*, 3180–3211; *(d)* Z. Li, C. Brouwer and C. He, *Chem. Rev.* **2008**, *108*, 3239–3265; *(e)* A. Arcadi, *Chem. Rev.* **2008**, *108*, 3266–3325; *(f)* E. Jiménez-Núñez and A. M. Echavarren, *Chem. Rev.* **2008**, *108*, 3326–3350; *(g)* D. J. Gorin, B. D. Sherry and F. D. Toste, *Chem. Rev.* **2008**, *108*, 3351–3378; *(h)* V. Michelet, P. Y. Toullec and J.-P. Genêt, *Angew. Chem. Int. Ed.* **2008**, *47*, 4268–4315; *(i)* A. Fürstner, *Chem. Soc. Rev.* **2009**, *38*, 3208–3221; *(j)* C. Aubert, L. Fensterbank, P. Garcia, M. Malacria and A. Simonneau, *Chem. Rev.* **2011**, *111*, 1954–1993 ; *(j)* N. Krause and C. Winter, *Chem. Rev.* **2011**, *111*, 1994–2009; (k) C. Obradors and A. M. Echavarren, *Acc. Chem. Res.* **2014**, *47*, 902–912.

[2] M. E. Muratore, A. Homs, C. Obradors and A. M. Echavarren, *Chem. Asian J.* **2014**, DOI: 10.1002/asia.201402305. For related examples, see: *(a)* C. Ferrer, C. H. M. Amijs and A. M. Echavarren, *Chem. Eur. J.* **2007**, *13*, 1358– 1373; *(b)* S. Kramer and T. Skrydstrup, *Angew. Chem. Int. Ed.* **2012**, *51*, 4681–4684; *(c)* Y. Luo, K. Ji, Y. Li and L. Zhang, *J. Am. Chem. Soc.* **2012**, *134*, 17412–17415.

[3] J. Urbano, A. J. Hormigo, P. De Frémont, S. P. Nolan, M. M. Díaz-Requejo and P. J. Pérez, *Chem. Commun.* **2008**, 759–761.

[4] V. López-Carrillo and A. M. Echavarren, *J. Am. Chem. Soc.* **2010**, *132*, 9292–9294.

[5] R. B. Dateer, B. S. Shaibu and R. S. Liu, *Angew. Chem. Int. Ed.* **2012**, *51*, 113–117.

complex bearing a phosphine ligand, an intermolecular [2+2+2] reaction took place forming enamine **5** in 73% isolated yield diastereoselectively.

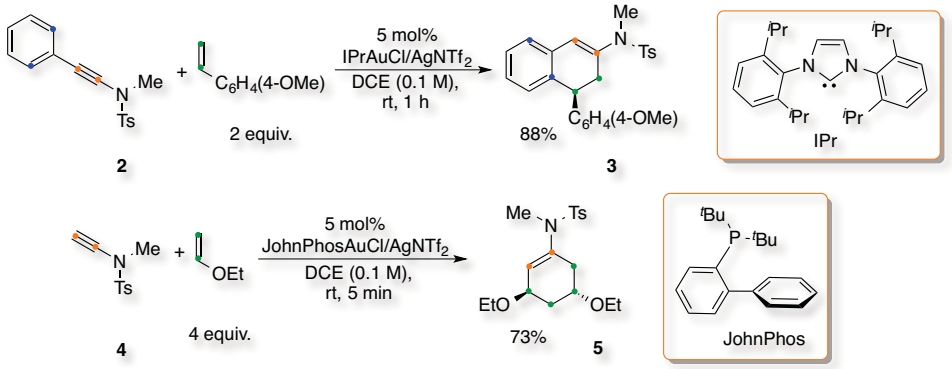

Scheme 2. Gold-catalyzed [4+2] and [2+2+2] annulation of ynamides with alkenes.

A [4+2] cycloaddition between propargylic esters or carboxylic acids with alkenes was also developed to build α,β-unsaturated lactones (Scheme 3).[6] Therefore, *tert*-butyl propiolate reacted with α-methylstyrene and [JohnPhosAuNCMe]SbF_6 (**B**) to build lactone **6** in 67% isolated yield. This transformation was also performed enantioselectively (up to 65% *ee*), being the first asymmetric example of an intermolecular gold-catalyzed cycloaddition. However, when 1,2-disubstituted alkenes were used, 1,3-dienes were formed stereospecifically by a metathesis-like process.

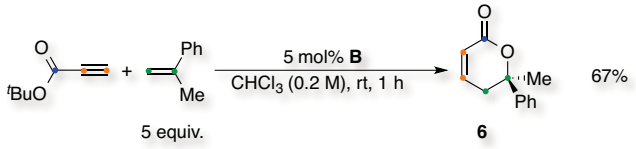

Scheme 3. Gold-catalyzed [4+2] cycloaddition of propargylic esters with alkenes.

The first intermolecular phenol synthesis was reported using the Schmidbauer–Bayer binuclear gold(I) complex $[(Mes_3PAu)_2Cl]BF_4$ as a catalyst with ethynylbenzene and 2,5-dimethylfuran (Scheme 4).[7]

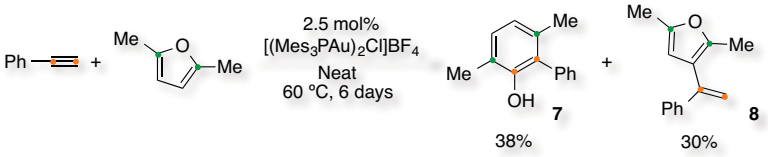

Scheme 4. Gold-catalyzed cycloaddition of alkynes with furans.

Phenol **7** was obtained in 38% isolated yield, along with large amounts of the hydroarylation product **8**. The process was later improved using IPr as ligand (see **Chapter 4** for more details).[8]

---

[6] H.-S. Yeom, J. Koo, H.-S. Park, Y. Liang, Z.-X. Yu and S. Shin, *J. Am. Chem. Soc.* **2012**, *134*, 208–211.
[7] A. S. K. Hashmi, M. C. Blanco, E. Kurpejovic, W. Frey and J. W. Bats, *Adv. Synth. Catal.* **2006**, *348*, 709–713.
[8] N. Huguet, D. Leboeuf and A. M. Echavarren, *Chem. –Eur. J.* **2013**, *19*, 6581–6585.

Finally, alkynes have been also used intermolecularly as nucleophiles (Scheme 5).[9] As an example, treatment of a terminal alkyne with gold complex **J** underwent deprotonation followed by addition to an imine.[10] Thus, ethynylbenzene reacted with imine **9** to build the propargylic amine **10**.

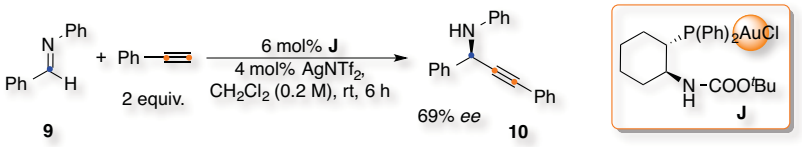

Scheme 5. Gold-catalyzed nucleophilic addition of alkynes to imines.

Besides, a noteworthy intramolecular cascade [2+2+2] reaction between an alkyne, an alkene and a carbonyl group was designed based on the nucleophilic attack towards enynes.[11] Thus, the cyclization of 1,6-enyne bearing a carbonyl moiety **11** using AuCl allowed the formation of tricyclic scaffold **12** *via* two C–C and one C–O bond (Scheme 6),[12] which has been used to build the core of several natural products as (+)-orientalol F or (-)-englerins A and B.[13, 14] Product **12** was obtained in 84% isolated yield (diastereoselectivity 50:1), together with diene **13** as a minor by-product.

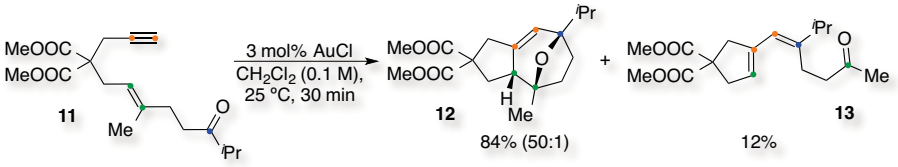

Scheme 6. Gold-catalyzed [2+2+2] tandem cyclization of an alkyne and an alkene bearing a carbonyl group.

Thus, the gold catalyst presumably activated preferentially the alkyne of 1,6-enyne **11**, which suffered a nucleophilic attack from the alkene (Scheme 7). This step led to the formation of the cyclopropyl gold carbene **14**. As discussed before, this intermediate is a highly distorted structure bearing a significant partial positive charge in the cyclopropyl ring. Therefore, it could undergo a subsequent intramolecular nucleophilic attack of the ketone forming a five-membered oxonium cation **15** stereospecifically. In the presence of

---

[9] For selected examples see: *(a)* L. Ye, Y. Wang, D. H. Aue and L. Zhang, *J. Am. Chem. Soc.* **2012**, *134*, 31–34; *(b)* A. S. K. Hashmi, I. Braun, P. Nösel, J. Schäldich, M. Wieteck, M. Rudolph and F. Rominger, *Angew. Chem. Int. Ed.* **2012**, *51*, 4456–4460; *(c)* A. S. K. Hashmi, M. Wieteck, I. Braun, M. Rudolph and F. Rominger, *Angew. Chem. Int. Ed.* **2012**, *51*, 10633–10637; *(d)* Y. Wang, A. Yepremyan, S. Ghorai, R. Todd, D. H. Aue and L. Zhang, *Angew. Chem. Int. Ed.* **2013**, *52*, 7795–7799; *(e)* D. D. Vachhani, M. Galli, J. Jacobs, L. Van Meervelt and E. V. Van der Eycken, *Chem. Commun.* **2013**, *49*, 7171–7173.

[10] M. J. Campbell and F. D. Toste, *Chem. Sci.* **2011**, *2*, 1369–1378.

[11] *(a)* C. Nieto-Oberhuber, M. P. Muñoz, E. Buñuel, C. Nevado, J. Cárdenas and A. M. Echavarren, *Angew. Chem. Int. Ed.* **2004**, *45*, 2402–2406; *(b)* M. P. Muñoz, J. Adrio, J. C. Carretero and A. M. Echavarren, *Organometallics* **2005**, *24*, 1293–1300; *(c)* C. Nieto-Oberhuber, M. P. Muñoz, S. López, E. Jiménez-Núñez, C. Nevado, E. Herrero-Gómez, M. Raducan and A. M. Echavarren, *Chem. –Eur. J.* **2006**, *12*, 1677–1693.

[12] E. Jiménez-Núñez, . K. Claverie, C. Nieto-Oberhuber and A. M. Echavarren, *Angew. Chem. Int. Ed.* **2006**, *45*, 5452–5455.

[13] *(a)* E. Jiménez-Núñez, K. Molawi and A. M. Echavarren, *Chem. Commun.* **2009**, 7327–7329; *(b)* Q. Zhou, X. Chen and D. Ma, *Angew. Chem. Int. Ed.* **2010**, *49*, 3513–3516; *(c)* K. Molawi, N. Delpont and A. M. Echavarren, *Angew. Chem. Int. Ed.* **2010**, *49*, 3517–3519.

[14] For alternative methodologies see: *(a)* B. Li, Y. J. Zhao, Y. C. Lai and T. P. Loh, *Angew. Chem. Int. Ed.* **2012**, *51*, 8041–8045; *(b)* Y. Bai, W. Tao, J. Ren and Z. Wang, *Angew. Chem. Int. Ed.* **2012**, *51*, 4112 –4116.

this alkenyl gold species, the intermediate proceeded through a Prins-type cyclization forming a tertiary carbocation first (**16**) and the final product **12** after demetallation (orange route). Simultaneous ring opening could explain the formation of the diastereoisomeric tricyclic scaffold **12´** (green route) and the diene product **13** (blue route).

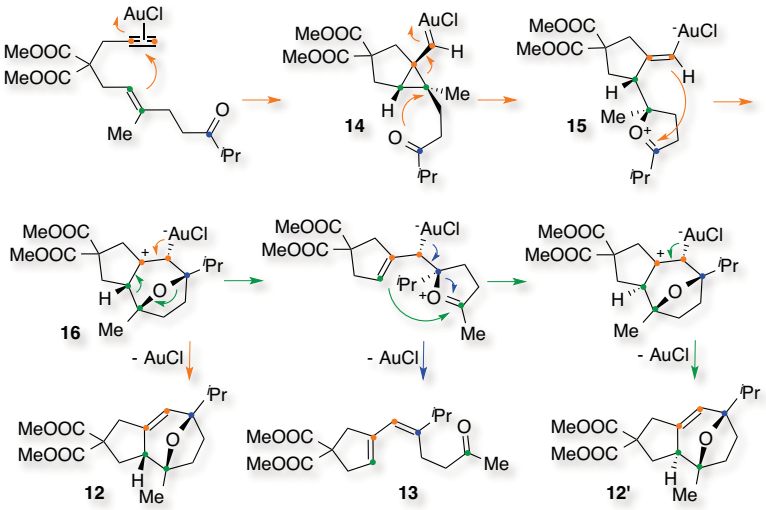

Scheme 7. Proposed mechanism of the [2+2+2] cyclization.

Trapping of cyclopropyl carbenes with carbonyl groups was also performed using 2 equiv. of an external aldehyde or ketone in the presence of a 1,6-enyne.[15,16] As an example, 1,6-enyne **17** reacted with 1,3,5-trimethylbenzaldehyde and [IPrAuNCPh]SbF_6 (**C**) to form oxacycle **18** as the main product (Scheme 8).

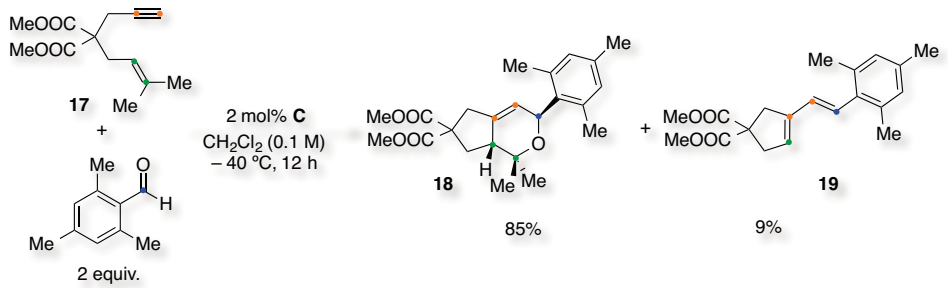

Scheme 8. Addition of a carbonyl to 1,6-enyne 17.

The transformation progressed at –40 ºC in CH_2Cl_2 with retention of the configuration and it was reasoned that this transformation proceeded analogously to the [2+2+2] cyclization. Traces of diene **19** were formed by the competitive ring opening.

---

[15] A. Escribano-Cuesta, V. López-Carrillo, D. Janseen and A. M. Echavarren, *Chem. –Eur. J.* **2009**, *15*, 5644–5650.

[16] For other examples see: *(a)* M. Schelwies, A. L. Dempwolff, F. Rominger and G. Helmchen, *Angew. Chem. Ibnt. Ed.* **2007**, *46*, 5598–5601; *(b)* D. B. Huple and R. S. Liu, *Chem. Commun.* **2012**, *48*, 10975–10977; (c) N. Huguet and A. M. Echavarren, *Synlett* **2012**, *23*, 49–53.

2. Objectives

Considering the challenge when applying a gold-catalyzed intermolecular cycloaddition of an alkyne with an alkene or another functional substrate, we decided to focus on expanding the scope of these methodologies. Furthermore, intermolecular cascade cycloadditions are even scarcer. Although several additions of carbonyls to 1,*n*-enynes have emerged successfully, the outcome was rather substrate-dependent leading to mixtures of products and always required the preparation of an elaborate unsaturated scaffold.

Therefore, we decided to attempt the development of an analogous [2+2+2] reaction between an alkyne (**20**) and an alkene linked to a carbonyl group (**21**) in an intermolecular fashion to build an oxabicycle scaffold such as **22** (Scheme 9).

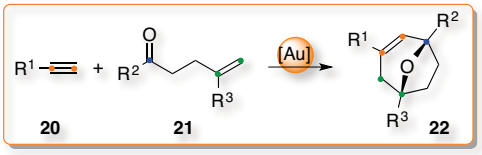

Scheme 9. Intermolecular gold-catalyzed [2+2+2] cycloaddition of an alkyne, an alkene and a carbonyl group.

3. Synthesis of Oxabicycles

Optimization of the [2+2+2] Cycloaddition

First, we examined the cycloaddition between ethynylbenzene and 5-methylhex-5-en-2-one in 0.5 M of CH_2Cl_2 and at 25 ºC for 24 h to form **23**. We screened several gold complexes as catalysts as well as the effect of the stoichiometry between the alkyne and the oxoalkene (Table 1). A slight excess of alkene was required in the formation of the cyclobutenes as dimerization of α-methylstyrene was observed as a competitive side-reaction.[4] Under these conditions, although the desired oxabicycle was detected using catalyst **A**, **B**, **C** and **E**, the yields were very low (entries 1 to 4).

Table 1. Screening of catalysts for the [2+2+2] cycloaddition.

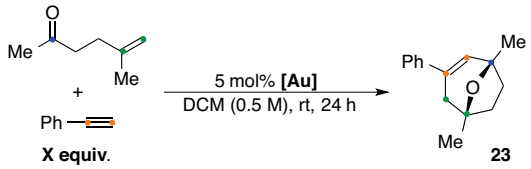

Entry	[Au]	X equiv.	Yield[a]
1	**A**	0.5	6%
2	**B**	0.5	19%
3	**C**	0.5	14%
4	**E**	0.5	13%
5	**B**	2	15%
6	**C**	2	15%
7	**E**	2	39%[b]
8	**K**	2	25%
9	**L**	2	Complex mixture
10	AuCl	2	Complex mixture

[a]Crude analyzed by ^{1}H NMR spectroscopy using 1,4-diacetylbenzene as internal standard, yields referred to oxabicycle **23**. [b]Isolated yield.

However, the amount of product was increased significantly to 39% isolated yield of **23** with catalyst **E** by switching the stoichiometry (entry 7). Catalyst **K** also delivered the desired product in 25% yield (Figure 1). A complex mixture was observed with **L** or AuCl (entries 8, 9 and 10).

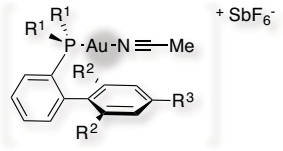

K: R^1=Cy; R^2=R^3=^{i}Pr
L: R^1=Cy; R^2= ^{i}Pr; R^3=H

Figure 1. Gold complexes tested.

Thus, we observed that, when increasing the steric bulkiness of the ligand in the gold complex, we obtained the maximum selectivity towards the intermolecular [2+2+2] cycloaddition. We centered our attention in catalyst **E** and attempted the reaction with 5 equiv. of ethynylbenzene for 15 h modifying both the temperature and the concentration (Table 2). The oxabicycle product **23** was obtained in 68% isolated yield in 0.5 M of DCE at 50 ºC (entry 3). Longer reaction times did not affect the results.

Table 2. Effect of the temperature and the concentration.[a]

Entry	Temperature (ºC)	Concentration (M)	Yield[b]
1	25	0.1	34%
2	25	0.5	41%
3	50	0.5	68%[c]
4	80	0.5	43%
5	50	1.0	53%

[a] Reaction of 5-methylhex-5-en-2-one with 5 equiv. of ethynylbenzene and 5 mol% of **E** in DCE for 15 h. [b]Crude analyzed by ^{1}H NMR spectroscopy using 1,4-diacetylbenzene as internal standard, yields referred to oxabicycle **23**. [c]Isolated yield.

New complexes (**G** and **H**) were also tested (Figure 2).[17] We reasoned that either the methoxy or the methyl groups could further increase the bulkiness around the metal as well as the rigidity of the catalyst. However, 63% and 57% yields, respectively, were observed under the optimized conditions.

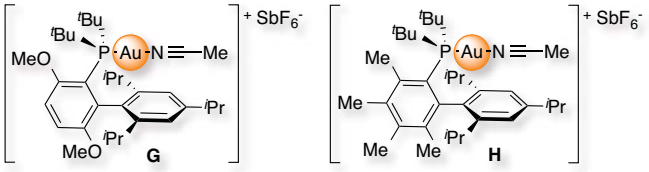

Figure 2. New gold complexes.

Interestingly, when the reaction was performed at 50 ºC or higher, an unprecedented trimerization of the alkyne was observed forming the 1,3,5-substituted benzene **24** (Figure 3).

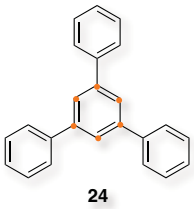

Figure 3. Formation of 1,3,5-substituted benzene 24.

Scope of the [2+2+2] Cycloaddition

The cycloaddition reaction proceeds in a general manner with aryl acetylenes **20** substituted at *ortho*, *meta*, or *para* positions with 6-methylhex-5-en-2-one to form cycloadducts **25** in moderate to excellent yields under the optimized conditions (Table 3). Aryl acetylenes **20** with electron-donating and electron-withdrawing substituents, alkyl groups, ethers and halides, react similarly.

[17] C. Obradors, D. Leboeuf, J. Aydin and A. M. Echavarren, *Org. Lett.* **2013**, *15*, 1576–1579.

Table 3. Alkyne scope of the [2+2+2] cycloaddition.

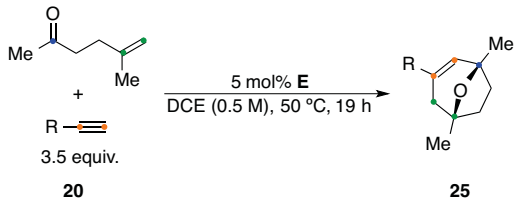

20 **25**

Entry	R-	Product	Yield[a,b]
1	Ph-	**23**	68%
2	2-Naphthyl-	**26**	62%
3	*p*-FC_6H_4-	**27**	68%
4	*p*-ClC_6H_4-	**28**	55%
5	*p*-BrC_6H_4-	**29**	49%
6	*m*-Tol-	**30**	70%
7	*m*-FC_6H_4-	**31**	49%
8	*m*-ClC_6H_4-	**32**	55%
9	*m*-HOC_6H_4-	**33**	65%
10	*m*-$MeOC_6H_4$-	**34**	91%
11	*o*-MeC_6H_4-	**35**	41%
12	3-Thienyl-	**36**	40% (79%)

[a]Isolated yields. [b]Reaction conversion in brackets, 100% if not stated.

2-Naphthylethynylbenzene, a polyaromatic acetylene, afforded oxabicycle **26** smoothly (entry 2). Moreover, a free phenol was also accommodated forming oxabicycle **33** (entry 9), the structure of which was confirmed by X-ray diffraction (Figure 4). Importantly, the reaction could be carried out on a 2 mmol scale without observing a decrease of the yield (74%). (3-Thienyl)acetylene reacted to furnish product **36** but never reached complete conversion (entry 12).

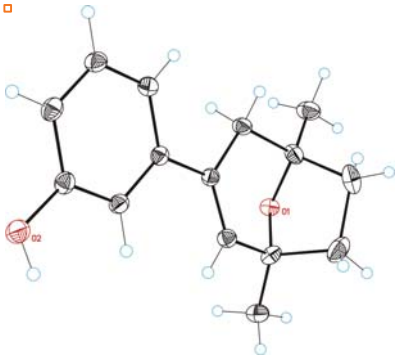

Figure 4. X-Ray crystal structure of oxabicycle 33.

Interestingly, we could also detect the formation of a tetrahydrofuran byproduct in low to moderate isolated yields for some of the substrates attempted (Figure 5).

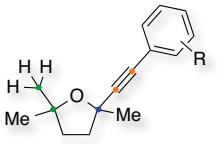

R=H (**37**); 14%
R=*p*-C (**38**); 28%
R=*p*-Br (**39**); 18%
R=*m*-F (**40**); 25%
R=*m*-Cl (**41**); 27%

Figure 5. Tetrahydrofurans formed as by-products.

However, the transformation did not tolerate amines or nitro substituents (entries 1 and 2, Table 4). Similar reactivities were also observed with alkyl acetylenes (entries 3, 4 and 5).

4-Acetylphenyl acetylene formed the corresponding oxabicycle **42** and 3,5-bis(trifluoromethyl) ethynylbenzene oxabicycle **43** in 17% and 6% yield, respectively (entries 6 and 7).

Table 4. Other alkynes tested.[a]

Entry	R-	Product	Outcome[b]
1	*p*-$NH_2C_6H_4$-	-	Complex mixture
2	*p*-$NO_2C_6H_4$-	-	Complex mixture
3	Cyclohexyl-	-	Complex mixture
4	Cyclopropyl-	-	Complex mixture
5	Benzyl-	-	Complex mixture
6	*p*-$CH_3C(O)C_6H_4$-	**42**	17%
7	3,5-$(CF_3)_2C_6H_3$-	**43**	6%

[a]Continuation of Table 3. [b]Crude analyzed by ^{1}H NMR spectroscopy using 1,4-diacetylbenzene as internal standard, yields referred to oxabicycles **25**.

Substrates bearing an electron-donating group in *para*-position led to the desired product in low yields (entries 1 and 2, Table 5): 13% (**44**) for the methoxy substituent and 38% (**45**) for the methyl derivative.

Table 5. Optimization of para-electron-donating groups.

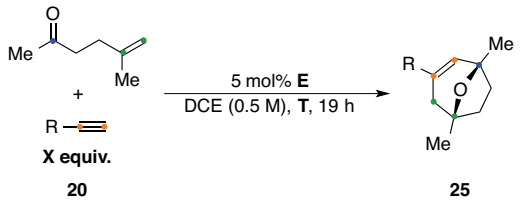

Entry	R-	X equiv.	Temperature (ºC)	Product	Yield[a]
1	*p*-$MeOC_6H_4$-	5	50	**44**	13%[b]
2	*p*-MeC_6H_4-	5	50	**45**	38%[b]
3	*p*-$MeOC_6H_4$-	5	80	**44**	13%
4[c]	*p*-$MeOC_6H_4$-	5	25	**44**	6%
5	*p*-$MeOC_6H_4$-	0.2	50	**44**	43%[b]
6	*p*-$MeOC_6H_4$-	0.2	80	**44**	24%
7	*p*-$MeOC_6H_4$-	0.2	0	**44**	8%
8[d]	*p*-$MeOC_6H_4$-	0.2	50	**44**	4%
9[e]	*p*-$MeOC_6H_4$-	0.2	25	**44**	9%
10[e]	*p*-$MeOC_6H_4$-	0.2	50	**44**	15%
11	*p*-MeC_6H_4-	0.2	50	**45**	52%[b]

[a]Crude analyzed by ^{1}H NMR using 1,4-diacetylbenzene as internal standard, yields referred to oxabicycle **25**. [b]Isolated yield. [c]Concentration = 1 M. [d]Complex **B** used as catalyst. [e]Complex **C** used as catalyst.

We reasoned that such an electon-rich alkyne could form a very stable gold complex that would not undergo nucleophilic attack from the oxoalkene. Thus, we decided to tune the reaction conditions for these specific substrates. First, we observed no improvement when modifying the temperature or increasing the concentration (entries 3 and 4). However, 43% isolated yield of **44** was obtained when switching the stoichiometry of the reaction (entry 5). Further variations of the ligand of the gold complex did not improve the result (entries

6 to 10). The same trend was observed for *p*-methylethynylbenzene and the oxabicycle **45** was isolated in 52% yield (entry11).

Later, we attempted the cycloaddition using 5-phenylhex-5-en-2-one and alkynes **20**. The corresponding oxabicycles **46** were built with similar yields (Table 6). In some cases, we observed an increase of the yield up to 20% due to the absence of the tetrahydrofuran byproduct (entry 4).

Table 6. Scope with 5-phenylhex-5-en-2-one.

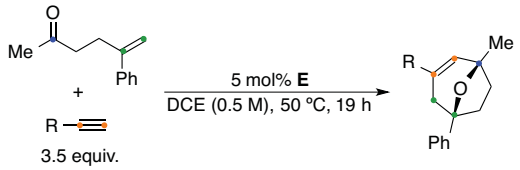

20 **46**

Entry	R-	Product	Yield[a]
1	Ph-	**47**	68%
2	*p*-FC_6H_4-	**48**	65%
3	*p*-ClC_6H_4-	**49**	61%
4	*p*-BrC_6H_4-	**50**	70%
5	*m*-FC_6H_4-	**51**	59%
6	*m*-ClC_6H_4-	**52**	60%

[a]Isolated yields.

Then, we decided to further explore the effect of the substitution pattern in the alkene as well as in the α-position of the carbonyl group and the reaction was performed using substrates **53**-**64** (Figure 6).[14b] Under the optimized conditions, monosubstituted alkene **53** led to only traces of the oxabicycle **65** (entry 1, Table 7).

Table 7. Oxoalkene scope in the [2+2+2] cycloaddition.[a]

Entry	Oxoalkene	Product	Yield[b]
1	**53**	**65**	4%[c]
2	**54**	**66**	87%
3	**55**	**67**	16%
4	**56**	**68**	54%

[a]Reaction with 3.5 equiv. of ethynylbenzene and 5 mol% of **E** at 50 ºC in DCE for 20 h. [b]Isolated yields. [c]Crude analyzed by ^{1}H NMR spectroscopy using 1,4-diacetylbenzene as internal standard, yields referred to oxabicycle **65**.

However, when the nucleophilicity of the α-substituent was increased (**54**), the yield improved to 87% isolated yield for **66** (entry 2) whereas decreased to 16% (**67**) by using aldehyde **55** (entry 3). T*ert*-butyl group (**56**) afforded the oxabicycle **68** in 54% isolated yield (entry 4). Substrates **57**-**64** led to very complex mixtures and no major product was detected.

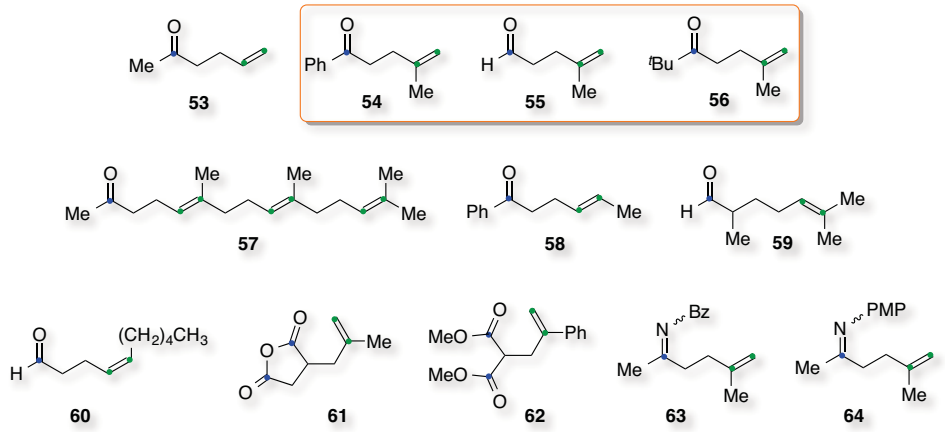

Figure 6. Other oxoalkenes tested.

On the other hand, reaction of ethynylbenzene with 6-methylhept-5-en-2-one led to the formation of cyclobutene **69** as the major product (56% isolated yield), along with oxabicycle **70** (Scheme 10). By changing the substitution pattern of the alkene, the cyclization *via* an oxonium cation would form preferentially a six-membered ring (**71**). However, ring expansion of the cyclopropyl intermediate **72** was faster and delivered cyclobutene **69** *via* **73**.

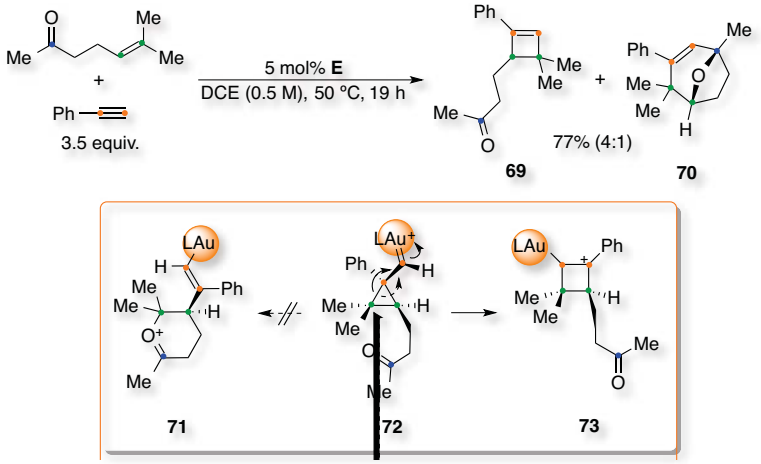

Scheme 10. Effect of the alkene substitution pattern.

Analogously, cycloaddition of ethynlbenzene and ethyl 4-methylpent-4-enoate afforded the cyclobutene scaffold **74** in 47% isolated yield (Scheme 11). Therefore, when using an ester the nucleophilic attack is also unfavorable.

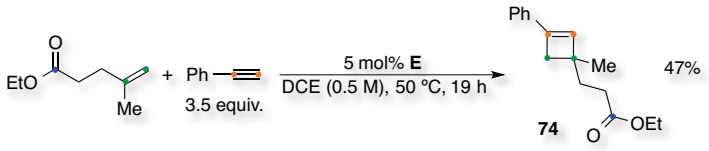

Scheme 11. Cycloaddition using an ester.

Finally, we designed the construction of a tricyclic structure in one step using this new gold catalyzed transformation. Hence, we synthesized several cyclic oxoalkenes (**75-79**) to further cyclize them with ethynylbenzene (Figure 7).

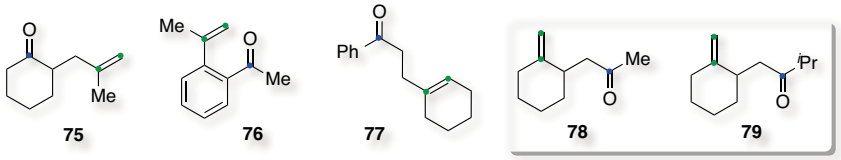

Figure 7. Challenging cyclic oxoalkenes.

Under the optimized conditions with 10 mol% of catalyst **E**, only traces of the corresponding cyclobutenes were detected for **75** and **76** by ^{1}H NMR spectroscopy (entries 1 and 2, Table 8). A very complex mixture with no major product was observed for **77** (entry 3).

Table 8. Formation of a tricyclic scaffold.[a]

Entry	Oxoalkene	Modification	Product	Yield[b,c]
1	**78**	–	**80**	5% (78%)
2	**76**	–	**81**	5%
3	**77**	–	-	Complex mixture
4	**78**	–	**82**	12%[d] (89%)
5	**78**	5 equiv.	**82**	31%[d]
6	**78**	*m*-MeOC$_6$H$_4$CCH	**83**	19% (87%)
7	**79**	*m*-MeOC$_6$H$_4$CCH	**84**	17% (94%)
8	**79**	5 equiv. *m*-MeOC$_6$H$_4$CCH	**84**	19%[d] (94%)

[a]Reaction with 3.5 equiv. of ethynylbenzene and 10 mol% of catalyst **E** at 50 ºC in DCE for 20 h. [b]Crude analyzed by ^{1}H NMR spectroscopy using 1,4-diacetylbenzene as internal standar, yields referred to tricyclic oxabicycles. [c]Reaction conversion in brackets, 100% if not stated. [d]Isolated yields.

On the other hand, tricyclic structure **82** could be obtained in 31% isolated yield *via* a gold catalyzed [2+2+2] cycloaddition of 5 equiv. of ethynylbenzene with oxoalkene **78** (entry 5). Use of *m*-methoxyenthynylbenzene to oxabicycle **83** or oxoalkene **79** did not improve the result (entries 6, 7 and 8). We reasoned that the most stable cyclopropyl intermediate might have a configuration that disfavors the nucleophilic attack of the carbonyl group. The configuration of the final product was confirmed by NOESY experiments (Scheme 12).

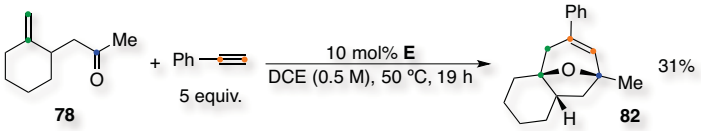

Scheme 12. Gold-catalyzed formation of a tricyclic scaffold.

Mechanistic Proposal for the [2+2+2] Cycloaddition

Initially a plausible mechanism for the [2+2+2] cycloaddition was based on the alkyne binding preferentially to the gold catalyst **E** forming complex **85**. This would further undergo nucleophilic attack from the alkene building the cyclopropyl gold carbene intermediate **86** (Scheme 13).[11,18] An intramolecular nucleophilic attack from the carbonyl occured forming oxonium cation **87**, which could undergo a Prins-type cyclization.[12] The carbocation **88** could proceed to **89** *via* demetalation and complex **85** would be recovered after ligand exchange with ethynylbenzene releasing **23**.

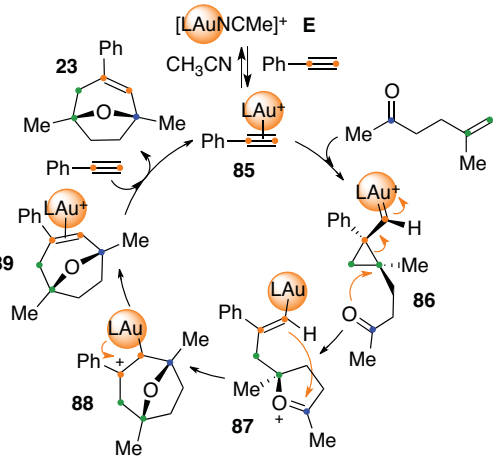

Scheme 13. Mechanistic proposal (L=^{t}BuXPhos).

Furthermore, we reasoned that the formation of tetrahydrofurans **37** could be explained due to the ability of gold complexes to deprotonate terminal alkynes (Scheme 14).[19] Simultaneously, the presence of an acid in the reaction conditions could promote the cationic cyclization of the oxoalkene.

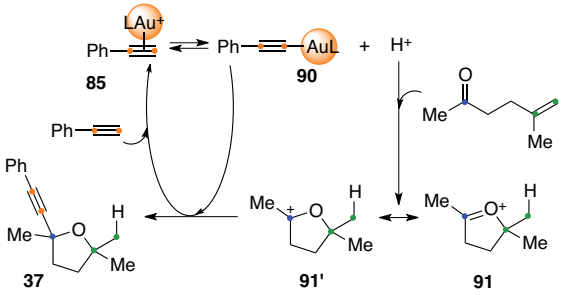

Scheme 14. Formation of tetrahydrofuran 37 (L=^{t}BuXPhos).

Thus, complex **85** evolved to **90** generating acid, which reacted with 5-methylhex-5-en-2-one to form oxonium cation **91**/**91´**. This could be easily trapped with complex **90** forming the tetrahydrofuran product **37** along with the regeneration of **85**.[9,10]

---

[18] C. Nieto-Oberhuber, S. López, E. Jiménez-Núñez and A. M. Echavarren, *Chem. –Eur. J.* **2006**, *12*, 5916–5923.
[19] *(a)* P. H. Y. Cheong, P. Morganelli, M. R. Luzung, K. N. Houk and F. D. Toste, *J. Am. Chem. Soc.* **2008**, *130*, 4517–4526; *(b)* T. J. Brown and R. A. Widenhoefer, *Organometallics*, **2011**, *30*, 6003–6009; *(c)* M. Raducan, M Moreno, C. Bour and A. M. Echavarren, *Chem. Commun.* **2012**, *48*, 52–54.

Derivatization of the Oxabicycles

Eventually, we also attempted the derivatization of the oxabicycle scaffold **33** by distinct organic transformations. To start, neither the epoxidation[13b], oxidation [20] nor the bromination of the double bond[21] led to the desired products and very complex mixtures were observed. Then, attempts of a Diels-Alder cycloaddition of with maleic anhydride led to no reaction.[22] Moreover, opening of the oxygen bridge also failed in all cases.[23]

Finally, we attempted the hydrogenation of the double bond of **33** using 1 atm of H_2 with Ni/Raney in ethanol at 80 ºC (Scheme 15).[13b] However, complete reduction of the oxabicycle product **33** was observed and **92** was isolated in 59% yield. The same product was obtained quantitavely when applying 60 atm of H_2 with Pd/C in CH_2Cl_2 at 25 ºC.

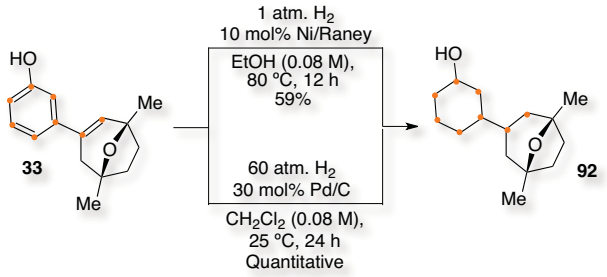

Scheme 15. Complete hydrogenation of the oxabicycle product 33.

Nevertheless, when the reaction was performed with 1 atm of H_2 with Pd/C in methanol at 25 ºC, the selective hydrogenation of the alkene in **33** occurred in 95% isolated yield (diastereomeric ratio 2:1) forming scaffold **93** (Scheme 16).[14b]

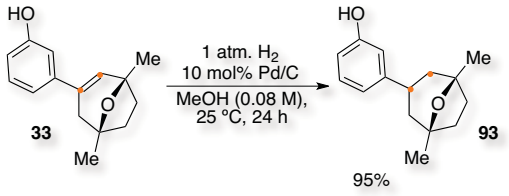

Scheme 16. Selective hydrogenation of the oxabicycle product 33.

[20] H. Hart and L. R. Lerner, *J. Org. Chem.* **1967**, *32*, 2669–2673.
[21] R. Knorr, E. Lattke and E. Räpple, *Chem. Ber.* **1981**, *14*, 1581–151.
[22] L. Minuti, A. Taticchi, D. Lanari, A. Marrocchi and E. Gacs-Baitz, *Tetrahedron: Asymmetry* **2003**, *14*, 775–2779.
[23] *(a)* A. M. Montaña and K. M. Nicholas, *J. Org. Chem.* **1990**, *55*, 1569–1578; *(b)* J. H. Rigby and J. A. Z. Wilson, *J. Org. Chem.* **1987**, *52*, 34–44; *(c)* S. Xing, Y. Li, Z. Li, C. Liu, J. Ren and Z. Wang, *Angew. Chem. Int. Ed.* **2011**, *50*, 12605–12609.

Enantioselective [2+2+2] Cycloaddition

Initially, we screened several chiral ligands using $[Au(tmbn)_2]SbF_6$ (**M**) as a cationic pre-catalyst for the optimized [2+2+2] cycloaddition of 3-ethynylphenol with 5-methylhex-5-en-2-one.[24] We attempted the reaction with ligands **94**-**102** (Figure 8)

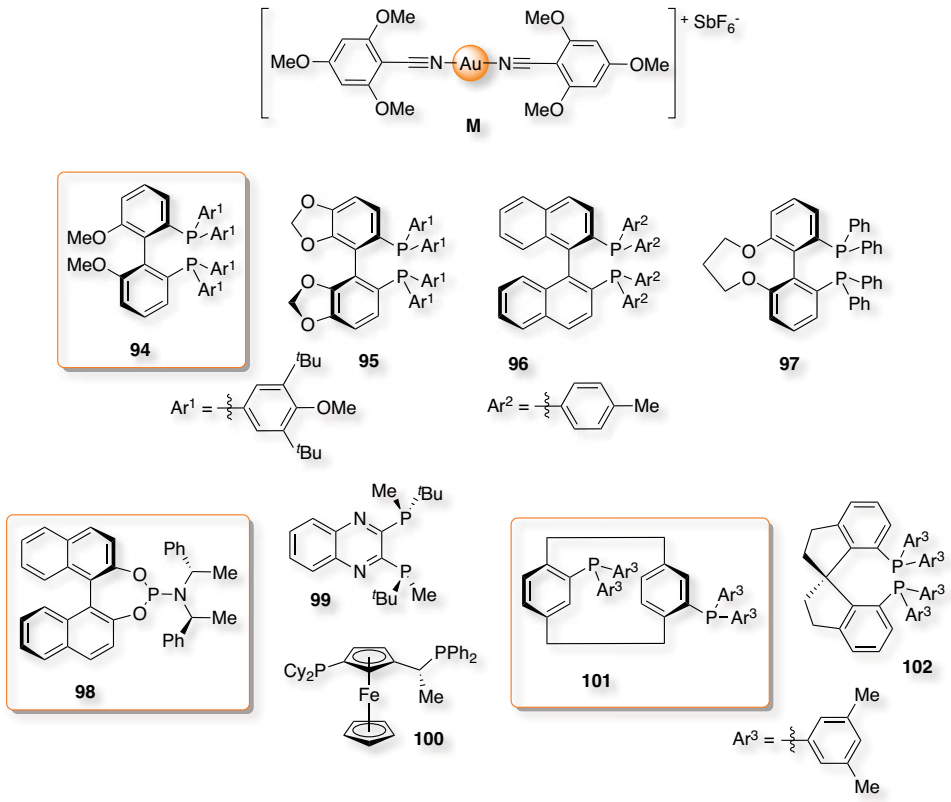

Figure 8. Gold pre-catalyst M and chiral ligands screened.

However, attempts to apply this strategy at 50 ºC failed due to the sensitivity of the gold complex and no reaction was obtained. Therefore, we synthesized the corresponding gold complexes with ligands **94**, **98** and **101** and (THT)AuCl.[25] We used these complexes under the optimized conditions along with $AgSbF_6$ (Table 9). The reaction proceeded in moderate yields when ligands **94** and **98** were used, 58% and 64% respectively. Only 18%

[24] M. Raducan, C. Rodrígez-Escrich, X. C. Cambeiro, E. C. Escudero-Adán, M. A. Pericàs and A. M. Echavarren, *Chem. Commun.* **2011**, *47*, 4893–4895.
[25] *(a)* G. L. Hamilton, E. J. Kang, M Mba and F. D. Toste, *Science* **2007**, *317*, 496–499; *(b)* R. A. Widenhoefer, *Chem. –Eur. J.* **2008**, *14*, 5382–5391; *(c)* K. Aikawa, M. Kojima and K. Mikami, *Angew. Chem. Int. Ed.* **2009**, *48*, 6073–6077; *(d)* H. Teller, S. Flügge, R. Goddard and A. Fürstner, *Angew. Chem. Int. Ed.* **2010**, *49*, 1949–1953; *(e)* K. Aikawa, M. Kojima and K. Mikami, *Adv. Synth. Catal.* **2010**, *352*, 3131–3135; *(f)* A. Z. González, D. Benitez, E. Tkatchouk, W. A. Goddard and F. D Toste, *J. Am. Chem. Soc.* **2011**, *133*, 5500–5507; *(g)* R. J. Felix, D. Weber, O. Gutierrez, D. J. Tantillo and M. R. Gagné, *Nat. Chem.* **2012**, *4*, 405–409; *(h)* H. S. Yeom, J. Koo, H. S. Park, Y. Wang, Y. Liang, Z. X. Yu and S. Shin, *J. Am. Chem. Soc.* **2012**, *134*, 208–211; *(i)* S. Handa and L. M. Slaughter, *Angew. Chem. Int. Ed.* **2012**, *51*, 2912–2915; *(j)* Y. M. Wang, A. D. Lackner and F. D. Toste, *Acc. Chem. Res.* **2014**, *47*, 889–901.

of isolated oxabicycle **33** was obtained with **101**. However, chiral HPLC analysis showed no enantioselectivity in the formation of **33** neither with **94** nor **98**.[26,27]

Table 9. Screening of chiral gold complexes for the [2+2+2] cycloaddition.

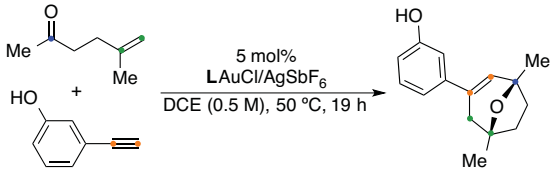

3.5 equiv. **33**

Entry	Ligand	Yield[a]	*ee*[b]
1	**94**	58%	0%
2	**98**	18%	Not determined
3	**101**	64%	0%

[a]Isolated yields. [b]ChiralPak IB, hexane : ethanol : diethylamine (97:3:0.1), 1 mL/min, 254 nm.

[26] At the same time, the analogous asymmetric cycloaddition with allenes was reported: E. Faustino, I. Alsonso, L. M. Mascareñas and F. López, *Angew. Chem. Int. Ed.* **2013**, *52*, 6526–6530.
[27] Collaboration started with Dr. Iván Rivilla from Prof. Fernando P. Cossio's research group in order to continue this work (Universidad del País Vasco).

4. Synthesis of Tetrahydrofurans

Optimization Towards a New Reaction Pathway

We decided to screen several solvents in order to check if the selectivity towards the formation of the tetrahydrofurans could be improved by modifying the polarity of the environment.[28] We performed the reaction under the optimized conditions using *p*-bromoethynylbenzene (Table 10). Chlorinated solvents as CH_2Cl_2, DCE or $CHCl_3$, showed an excellent reactivity but very low selectivity (entries 1, 2 and 3). Hydrocarbons followed the same trend with even lower yields (entries 4 to 7).

Table 10. Screening of solvents for the formation of tetrahydrofurans.

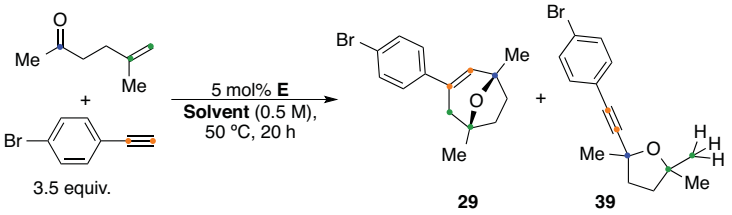

Entry	Solvent	Yield of 29[a]	Yield of 39[a]	Conversion[a]
1	DCM	43%	34%	98%
2	DCE	41%	35%	99%
3	$CHCl_3$	29%	21%	89%
4	Heptane	2%	15%	97%
5	Cyclohexane	17%	15%	99%
6	Benzene	35%	37%	96%
7	Toluene	33%	34%	98%
8	DMF	0%	0%	99%
9	MeOH	0%	0%	100%
10	MeCN	2%	3%	66%
11	Dioxane	2%	55%	99%
12	THF	0%	54%	100%
13	Acetone	8%	16%	75%
14	EtOAc	10%	42%	95%
15	Et_2O	10%	39%	95%
16	–	36%	18%	100%

[a]Crude analyzed by ^{1}H NMR spectroscopy using 1,4-diacetylbenzene as internal standard.

On the other hand, very polar solvents such as methanol, DMF or acetonitrile led to very complex mixtures with no major product observed (entries 8, 9 and 10). Then, the use of weak coordinative solvents, for example dioxane or THF, allowed an excellent selectivity, although the yields were still moderate (entries 11 to 15).

[28] V. M. Lau, C. F. Gorin and M. W. Kanan, *Chem. Sci.* **2014**, DOI: 0.1039/C4SC02058H.

Therefore, we decided to perform the reaction with distinct modifications to the optimized conditions (Table 11).

Table 11. Further modifications for the formation of tetrahydrofurans.[a]

Entry	Modification	Yield of 29[b]	Yield of 39[b]	Conversion[b]
1	Catalyst **C**	18%	0%	100%
2	Catalyst **N**	0%	26%	95%
3	Catalyst **O**	11%	0%	65%
4	10 mol% **E**	57%	43%	100%
5	3Å MS	40%	18%	92%
6	4Å MS	0%	0%	88%
7	5Å MS	8%	0%	90%
8	10 mol % TsOH	13%	51%[c]	91%
9	10 mol% $NaHCO_3$	22%	14%	80%
10	10 mol% AcOH	45%	35%	100%
11	10 mol% AcOH/AcONa (1:1)	0%	0%	94%
12	10 mol% $CsCO_3$	0%	0%	0%

[a]Continuation of Table 10 in DCE. [b]Crude analyzed by ^1H NMR spectroscopy using 1,4-diacetylbenzene as internal standard. [c]Isolated yield.

First, we performed the reaction with catalysts **C**, **N** or **O** (Figure 9). Those attempts led to low yields with disparate selectivities (entries 1, 2 and 3).

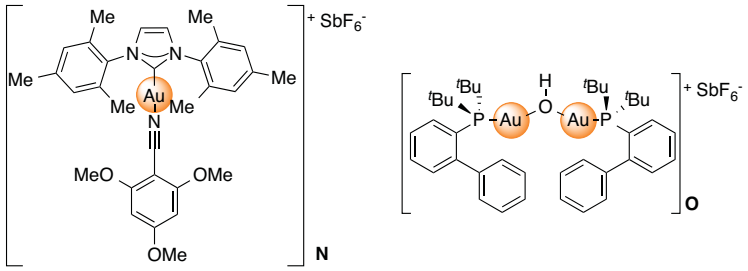

Figure 9. Gold complexes N and O.

Treatment with 10 mol% of catalyst **E** led to a higher yields but with a similar selectivity (entry 4). Then, the transformation was performed in the presence of molecular sieves: 3Å MS did not improve the results and 4Å MS or 5Å MS quenched the reactivity towards both cycloadditions (entries 5, 6 and 7). Finally, we screened several additives to promote the deprotonation of the terminal alkyne and the cyclization of the oxoalkene. The best outcome was obtained with catalytic amounts of *p*-toluensulfonic acid, which led to the tetrahydrofuran product **39** in 51% yield (entry 8). Addition of $NaHCO_3$ or acetic acid did not improve the selectivity (entries 9 and 10). A buffer solution of acetic acid and sodium acetate led to a complex mixture with no major product (entry 11). $CsCO_3$ led to no reaction, probably due to the inactivation of the catalyst (entry 12).

Therefore, when the reaction was performed under the optimized conditions adding 10 mol% of *p*-toluenesulfonic acid the yield towards the tetrahydrofuran product **39** was improved by 33% (Scheme 17).

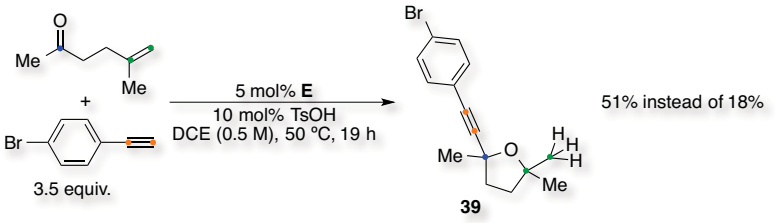

Scheme 17. Optimized conditions for the formation of tetrahydrofurans.

Expansion of the Scope

Successfully, when this modification was applied to the formation of tetrahydrofurans shown in Figure 5, the same trend was observed (Table 12).

Table 12. Scope of the tetrahydrofuran formation.[a]

Entry	20	Product	Yield[b]
1	PhCCH	**37**	50%
2	*p*-ClC_6H_4CCH	**38**	48%
3	*m*-FC_6H_4CCH	**40**	47%
4	*m*-ClC_6H_4CCH	**41**	57%

[a]Reaction with 5-methylhex-5-en-2-one, 5 mol% of catalyst **E** and 10 mol% of TsOH at 50 ºC in DCE.
[b]Isolated yields.

Thus, ethynylbenzene improved by 36% yield from 14% of **37** (entry 1), *p*-ClC_6H_4CCH in 20% from 28% of **38** (entry 2), *m*-FC_6H_4CCH in 16% from 31% of **40** (entry 3) and *m*-ClC_6H_4CCH in 15% from 42% of **41** (entry 4).

5. Gold-Catalyzed Trimerization of Terminal Alkynes

As we mentioned before, the formation of 1,3,5-substituted benzene products such as **24** was constantly observed during the construction of oxabicyclic structures **22**.

Although there are several reports of trimerization of alkynes promoted by gold in heterogenous catalysis,[29] very few examples using homogeneous complexes have been described. Thus, decomposition of tris(alkyne)gold complex **103** led to the corresponding arene **104** after heating under refluxing conditions in hexane: CH_2Cl_2 (Scheme 18). Tris(hexamethylene)benzene (**104**) was isolated from a mixture of compounds in 48% yield.

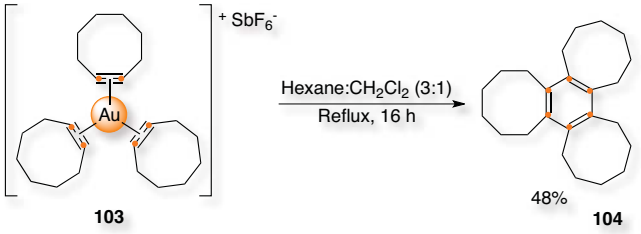

Scheme 18. Gold-catalyzed trimerization of cyclooctyne.

On the other hand, the homodimerization of terminal alkynes as dodec-1-yne was reported with ^{t}BuXPhosAuNTf$_2$ in the presence of sodium acetate in toluene under reflux for 24 h (Scheme 19).[30]

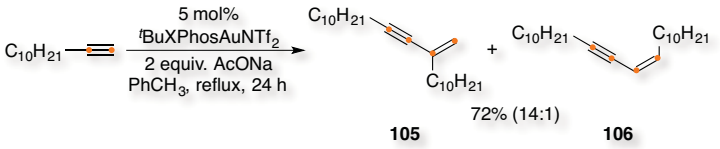

Scheme 19. Gold-catalyzed dimerization of alkynes.

Although harsh conditions were employed, good yields and selectivities were obtained. For example, 1,1´-disubstituted alkene **105** and *cis*-1,2-**106** were obtained as a mixture in 72% isolated yield and 14:1 regioselectivity. However, the scope was rather limited: in the case of ethynylbenzene, the product was obtained only in 8% yield.

Interestingly, the gold-catalyzed trimerization of alkynes was not a competitive pathway in the [2+2] cycloaddition of alkynes and alkenes leading to cyclobutenes, which was performed at 25 ºC (Scheme 1).[4]

---

[29] *(a)* R. M. Ormerod, C. J. Baddeley and R. M. Lambert, *Surface Science* **1991**, *259*, L709–L713; *(b)* C. J. Baddeley, R. M. Ormerod and R. M. Lambert, *Studies in Surface Science and Catalysis* **1993**, *75*, 371–382.
[30] S. Sun, J. Kroll, Y. Luo and L. Zhang, *Synlett* **2012**, *23*, 54–56.

Scope of the Trimerization

Therefore, we continued optimizing the trimerization of alkynes to structures like **107** by screening the concentration as well as the catalyst loading (Table 13). [^{t}BuXPhosAuNCMe]SbF_6 (**E**) was used in DCE at 50 ºC. The reaction of ethynylbenzene with 1 mol% of the gold catalyst afforded the terphenyl product **24** in 27% isolated yield (entry 1). The starting alkyne was completely consumed leading as well to distinct oligomerization products. Under the same conditions, the trimerization of *p*-bromo- and *p*-methoxy- substituted aryl akynes proceeded in 18% and 11% yields, respectively (entries 2 and 3).

Table 13. Expansion of the trimerization of terminal alkynes.

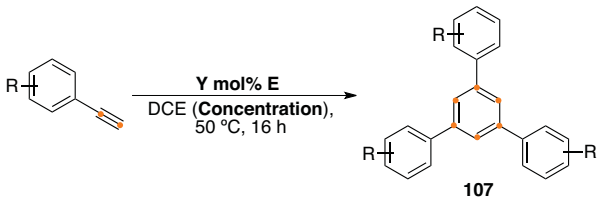

107

Entry	R-	Y mol%	Concentration (M)	Product	Yield[a]
1	H-	1	2.0	**24**	27%
2	*p*-Br	1	2.0	**108**	18%[b]
3	*p*-MeO	1	2.0	**109**	11%[b]
4	H-	3	2.0	**24**	40%
5	*m*-MeO	3	2.0	**110**	2%[b]
6	*m*-Cl	3	2.0	**111**	6%[b]
7	*p*-Me	3	2.0	**112**	33%
8	*p*-F	3	2.0	**113**	37%
9	*m*-Me	3	2.0	**114**	20%
10	H-	3	0.5	**24**	43%

[a]Isolated yields. [b]Crude analyzed by ^{1}H NMR spectroscopy using 1,4-diacetylbenzene as internal standard, yields referred to trimers **107**.

The reaction with ethynylbenzene could be improved to 40% yield of **24** with 3 mol% of catalyst (entry 4). Only traces of products **110** and **111** were observed with *m*-methoxy or *m*-chloro substitution (entries 5 and 6). Moderate yields were obtained for *p*-methyl, *p*-fluoro and *m*-methyl substitution (entries 7, 8 and 9). Thus, terphenyl **112** was obtained in 33% isolated yield, **113** in 37% and **114** only in 20%. Decrease of the concentration did not avoid the oligomerization and showed minimum improvement in the formation of **24** (entry 10).

6. Conclusions

Gold-catalyzed intramolecular cycloisomerizations have been the benchmark of the expansion of this type of chemistry whereas intermolecular transformations proved to the more challenging and related reports were rather limited. Therefore, we have developed a new intermolecular gold-catalyzed transformation based on a cascade [2+2+2] cycloaddition of an alkyne, an alkene and a carbonyl group.[31] As an example, we optimized the reaction between *m*-methoxyethynylbenzene and 5-methylhex-5-en-2-one to furnish oxabicycle **34** in 91% isolated yield (Scheme 20), which proceeded with 5 mol% of [^{t}BuXPhosAuNCMe]SbF_6 (**E**) in DCE at 50 ºC.

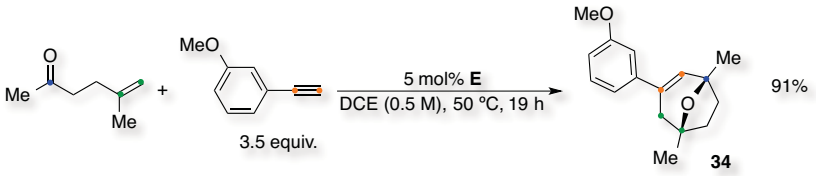

Scheme 20. Gold-catalyzed [2+2+2] cycloaddition to furnish 34.

The methodology showed a broad scope in the aryl substitution leading to the cycloadducts in moderate to excellent yields. Derivatization of the oxabicycle products showed the robustness of these scaffolds.

We also screened the effect of the alkene substitution pattern and the α-position of the carbonyl moiety. Interestingly, when the oxonium cation was not entropically favoured or the nucleophilicity of the carbonyl decreased, a cyclobutene scaffold was obtained instead. Thus, products **69** (54%) and **74** (47%) were formed from 6-methylhept-5-en-2-one and ethyl 4-methylpent-4-enoate, respectively (Figure 10).

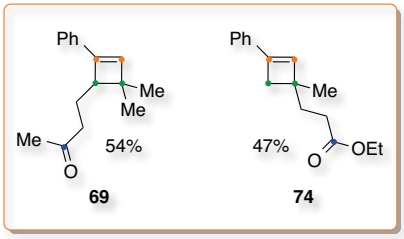

Figure 10. Cyclobutenes 69 and 74 formed as exceptions to the [2+2+2].

For similar reasons, cycloaddition with a cyclic oxoalkene such as **78** led to the tricyclic structure **82** only in 31% isolated yield (Scheme 12).

[31] C. Obradors and A. M. Echavarren, *Chem. –Eur. J.* **2013**, *19*, 3547–3551.

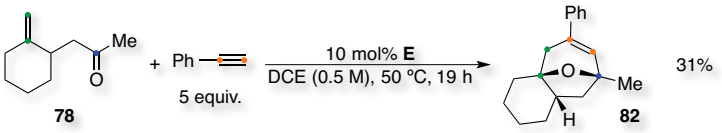

Scheme 12. Gold-catalyzed formation of a tricyclic scaffold.

Moreover, we could tune the reaction pathway towards the formation of a tetrahydrofuran scaffold by adding 10 mol% of *p*-toluenesulfonic acid. Thus, structure **39** was obtained in 51% isolated yield (Scheme 17).

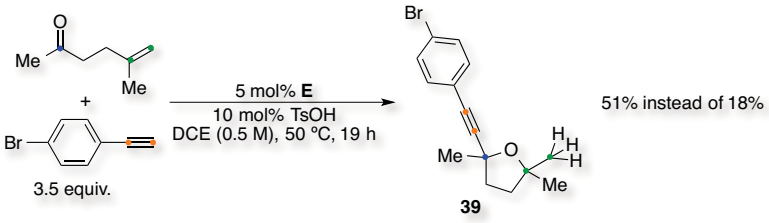

Scheme 17. Optimized conditions for the formation of tetrahydrofurans.

Analogously, trimerization of terminal alkynes was refined to give 43% yield of terphenyl **24** in the case of ethynylbenzene (Scheme 21).

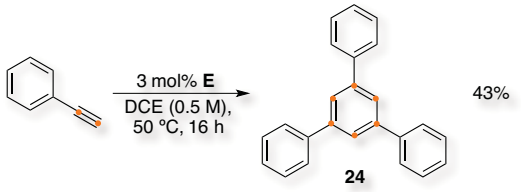

Scheme 21. Optimized trimerization of terminal alkynes.

Overall, we could selectively and effectively control the reaction pathways towards an oxabicycle, a cyclobutene, a tetrahydrofuran or a terphenyl starting from exactly the same commercially available building blocks by digging into a mechanistic reasoning and finely tuning the reaction conditions.

Chapter 3:

Mechanistic Study of a [2+2+2] Cycloaddition: Role of Digold Complexes

1. Introduction

As explained in the **General Introduction**, numerous transformations catalyzed by gold have been developed during the last decade nourishing the field of organic synthesis.[1] In most cases, these reactions proceed by multistep pathways that are rather complex. Therefore, a mechanistic understanding has been based often on analogy and speculation. Although coherent mechanistic schemes have been proposed by means of DFT calculations, as well as isotopic labelling and kinetic experiments, isolation of key intermediates has proven to be challenging.[2]

In **Chapter 2**, we presented the intramolecular cascade [2+2+2] reaction between an alkyne, an alkene and a carbonyl group. 1,6-Enyne bearing a ketone moiety **1** was synthesized and cyclized using AuCl (Scheme 1).[3] This reaction afforded the tricyclic scaffold **2** *via* two C–C and one C–O bond in 84% isolated yield (diastereoselectivity 50:1), together with diene **3** as a minor by-product.

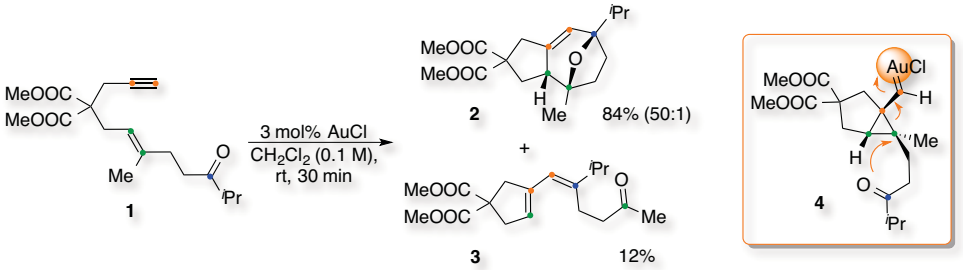

Scheme 1. Gold-catalyzed [2+2+2] cyclization of 1,6-enyne 1.

The gold catalyst presumably activated preferentially the alkyne of 1,6-enyne **1**, which could suffer a nucleophilic attack from the alkene forming cyclopropyl gold carbene **4**. The intermediate could be trapped *via* intramolecular nucleophilic attack of the ketone followed by a Prins-type cyclization. The stereochemistry of the final product **2** suggested that the intramolecular attack of the ketone proceeded through the lower face of the cyclopropyl ring (**4**). However, no further evidence to support this hypothesis was provided.

In general, alkynes are selectively activated by gold(I) in the presence of alkenes. This high site-selectivity of gold(I) is not directly related to a thermodynamic preference for the coordination to the alkynes, but to a higher reactivity of the (η^2-alkyne)gold(I) complexes towards nucleophilic attack.[4] Thus, NMR studies, supported by DFT calculations,

---

[1] *(a)* A. S. K. Hashmi, *Chem. Rev.* **2007**, *107*, 3180–3211; *(b)* A. Fürstner and P. W. Davies, *Angew. Chem. Int. Ed.* **2007**, *46*, 3410–3449; *(c)* E. Jiménez-Núñez and A. M. Echavarren, *Chem. Rev.* **2008**, *108*, 3326–3350; *(d)* D. J. Gorin, B. D. Sherry and F. D. Toste, *Chem. Rev.* **2008**, *108*, 3351–3378; *(e)* N. T. Patil and Y. Yamamoto, *Chem. Rev.* **2008**, *108*, 3395–3442; *(f)* A. Fürstner, *Chem. Soc. Rev.* **2009**, *38*, 3208–3221; *(g)* H. G. Raubenheimer and H. Schmidbaur, *S. Afr. J. Sci.* **2011**, *107*, 31–34; *(h)* C. Obradors and A. M. Echavarren, *Acc. Chem. Res.* **2014**, *47*, 902–912.

[2] *(a)* A. S. K. Hashmi, *Angew. Chem. Int. Ed.* **2010**, *49*, 5232–5241; *(b)* L. P. Liu and G. B. Hammond, *Chem. Soc. Rev.* **2012**, *41*, 3129–3139; *(c)* I. Braun, A. M. Asiri and A. S. K. Hashmi, *ACS Catal.* **2013**, *3*, 1902–1907; *(d)* C. Obradors and A. M. Echavarren, *Chem. Commun.* **2014**, *50*, 16–28.

[3] E. Jiménez-Núñez, C. K. Claverie, C. Nieto-Oberhuber and A. M. Echavarren, *Angew. Chem. Int. Ed.* **2006**, *45*, 5452–5455.

[4] *(a)* M. García-Mota, N. Cabello, F. Maseras, A. M. Echavarren, J. Pérez-Ramírez and N. López, *ChemPhysChem* **2008**, *9*, 1624-1629; *(b)* N. Cabello, C. Rodríguez and A. M. Echavarren, *Synlett* **2007**, 1753–1758.

confirmed that both **5** and **6** bearing $[JohnPhosAu]^+$ coexisted with free 1,7-enyne **7** and catalyst **B** (Scheme 2). However, this class of substrates exclusively reacted by intramolecular attack of the alkene to (η^2-alkyne)gold(I) species such as **5**.

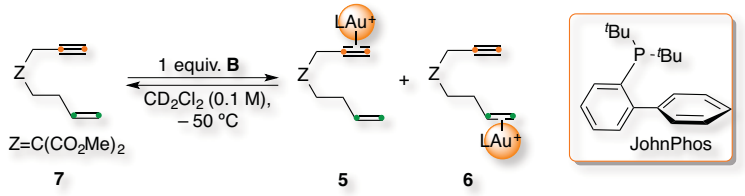

Scheme 2. Competitive coordination of gold to alkynes and alkenes.

Nucleophilic attack of (η^2-alkyne)gold complexes to give *trans*-alkenyl species *via* an outer-sphere mechanism is widely accepted.[5] The first stable organogold intermediate (**8**) was isolated in an intramolecular reaction between an allene and an ester in compound **9** (Scheme 3).[6] This result demonstrated the formation of a vinyl gold complex by nucleophilic attack onto an allene-gold complex.

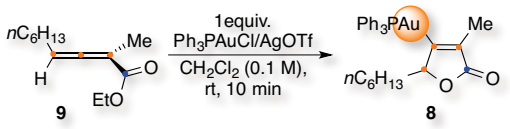

Scheme 3. Isolation of the first vinyl gold complex (8).

However, more complex carbenoid intermediates were suggested based on DFT calculations, for example, in the 1,2- or 1,3-acyloxy migrations of propargylic carboxylates or in the cycloisomerizations of 1,*n*-enynes.[1,3,7] Consequently, an interesting debate was

---

[5] Examples of nucleophilies. For arenes see: *(a)* M. T. Reetz and K. Sommer, Eur. *J. Org. Chem.* **2003**, 3485–3496; *(b)* C. Nevado and A. M. Echavarren, *Synthesis* **2005**, 167–182. For heteroarenes see: *(c)* A. S. K. Hashmi, P. Haufe, C. Schmid, A. Rivas Ness and W. Frey, *Chem. –Eur. J.* **2006**, *12*, 5376–5382; *(d)* C. Ferrer and A. M. Echavarren, *Angew. Chem. Int. Ed.* **2006**, *45*, 1105–1109. For alcohols see: *(e)* E. Mizushima, K. Sato, T. Hayashi and M. Tanaka, *Angew. Chem. Int. Ed.* **2002**, *41*, 4563–4565; *(f)* C. M. Krauter, A. S. K. Hashmi and M. Pernpointner, *ChemCatChem* **2010**, *2*, 1226–1230. For amines see: *(g)* F. M. Istrate and F. Gagosz, *Org. Lett.* **2007**, *9*, 3181–3184; *(h)* J. Qian, Y. Liu, J. Cui and Z. Xu, *J. Org. Chem.* **2012**, *77*, 4484–4490. For imines see: *(i)* H. Kusama, Y. Miyashita, J. Takay and N. Iwasawa, *Org. Lett.* **2006**, *8*, 289–292; *(j)* E. Benedetti, G. Lemière, L. L. Chapellet, A. Penoni, G. Palmisano, M. Malacria, J. P. Goddard and L. Fensterbank, *Org. Lett.* **2010**, *12*, 4396–4399. For sulfoxides see: *(k)* N. D. Shapiro and F. D. Toste, *J. Am. Chem. Soc.* **2007**, *129*, 4160–4161; *(l)* P. W. Davies and S. J. C. Albrecht, *Angew. Chem. Int. Ed.* **2009**, *48*, 8372–8375; *(m)* S. Shi, T. Wang, W. Wang, M. Rudolph and A. S. K. Hashmi, *Chem. –Eur. J.* **2013**, *19*, 6576–6580. For N-oxides see: *(n)* L. Ye, L. Cui, G. Zhang and L. Zhang, *J. Am. Chem. Soc.* **2010**, *132*, 3258–3259. And for thiols see: *(o)* I. Nakamura, T. Sato and Y. Yamamoto, *Angew. Chem. Int. Ed.* **2006**, *45*, 4473–4475; *(p)* I. Nakamura, T. Sato, M. Terada and Y. Yamamoto, *Org. Lett.* **2007**, *9*, 4081–4083.

[6] *(a)* L. P. Liu, B. Xu, M. S. Mashuta and G. B. Hammond, *J. Am. Chem. Soc.* **2008**, *130*, 17642–17643; *(b)* W. Wang, G. B. Hammond and B. Xu, *J. Am. Chem. Soc.* **2012**, *134*, 5697–5705.

[7] For propargylic carboxylates see: *(a)* N. Marion and S. P. Nolan, *Angew. Chem. Int. Ed.* **2007**, *46*, 2750–2752; *(b)* A. Correa, N. Marion, L. Fensterbank, M. Malacria, S. P. Nolan and L. Cavallo, *Angew. Chem. Int. Ed.* **2008**, *47*, 718–721; *(c)* S. Wang, G. Zhang and L. Zhang, *Synlett* **2010**, 692–706; *(d)* T. De Haro, E. Gómez-Bengoa, R. Cribiú, X. Huang and C. Nevado, *Chem. –Eur. J.* **2012**, *18*, 6811–6824; *(e)* R. K. Shiroodi and V. Gevorgyan, *Chem. Soc. Rev.* **2013**, *42*, 4991–5001. For 1,n-enynes see: *(f)* C. Nieto-Oberhuber, M. P. Muñoz, E. Buñuel, C. Nevado, D. J. Cárdenas and A. M. Echavarren, *Angew. Chem. Int. Ed.* **2004**, *43*, 2402–2406; *(g)* C. Nieto-Oberhuber, M. P Muñoz, S. López, E. Jiménez-Núñez, C. Nevado, E. Herrero-Gómez, M. Raducan and A. M. Echavarren, *Chem. –Eur. J.* **2006**, *12*, 1677–1693; *(h)* C. Nieto-Oberhuber, S. López, E. Jiménez-Núñez and A. M. Echavarren, *Chem. –Eur. J.* **2006**, *12*, 5916–5923.

centred on the nature of the gold–carbon bond in complexes of type $[LAuCHR]^+$.[8] The intermolecular cycloaddition between alkynes and alkenes led to cyclobutenes such as **10** using bulky phosphines as ligands, for example [^{t}BuXPhosAuNCMe]SbF_6 (**E**). Gold(I) carbene **11** or gold(I) stabilized carbocation **11´** could be conceived as intermediates, which explained the regioselectivity of the transformation (Scheme 4).[9] Although seldom reports with spectroscopic or structural data are presented in the literature, highly distorted cyclopropyl gold carbenes **11**/**11´** were also proposed in the reaction of propiolic acid with alkenes as well as in the cascade cyclizations of 1,*n*-enynes.[10]

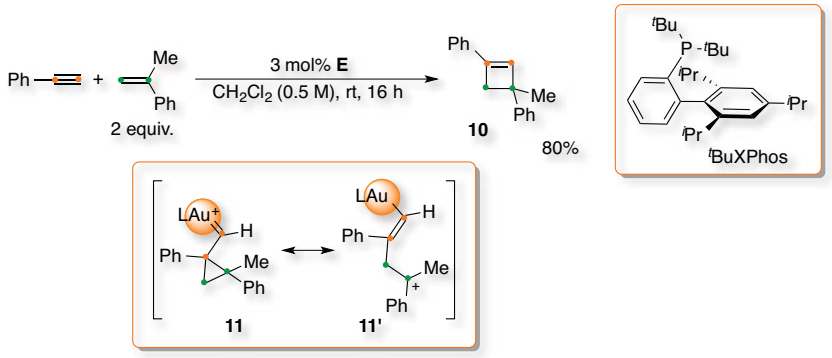

Scheme 4. [2+2] Cycloaddition of alkynes with alkenes.

On the other hand, the regioselective cyclization of enynes **12** with a pendant carboxylic acid formed selectively lactones **13** and/or **14** (Scheme 5).[11]

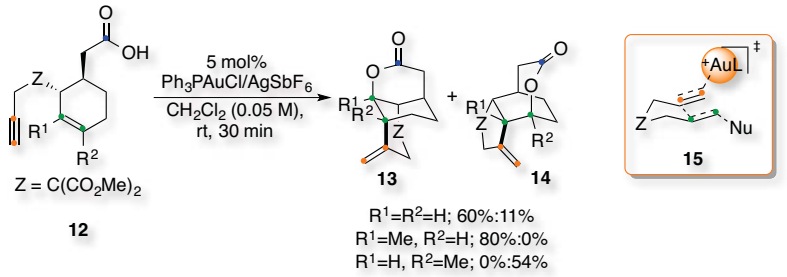

Scheme 5. Cascade cyclization of 1,6-enyne 12.

---

[8] *(a)* D. Benitez, N. D. Shapiro, E. Tkatchouk, Y. Wang, W. A. Goddard III and F. D. Toste, *Nat. Chem.* **2009**, *1*, 482–486; *(b)* A. M. Echavarren, *Nat. Chem.* **2009**, *1*, 431–433.

[9] *(a)* V. López-Carrilo and A. M. Echavarren, *J. Am. Chem. Soc.* **2010**, *132*, 9292–9294; *(b)* C. Obradors, D. Leboeuf, J. Aydin and A. M. Echavarren, *Org. Lett.* **2013**, *15*, 1576–1579.

[10] M. E. Muratore, A. Homs, C. Obradors and A. M. Echavarren, *Chem. Asian J.* **2014**, DOI: 10.1002/asia.201402305. For propiolic acid see: *(a)* H. S. Yeom, J. Koo, H. S. Park, Y. Wang, Y. Liang, Z. X. Yu and S. Shin, *J. Am. Chem. Soc.* **2012**, *134*, 208–211; *(b)* S. R. Park, C. Kim, D. Kim, D. Thrimurtulu, H. S. Yeom, J. Jun, S. Shin and Y. H. Rhee, *Org. Lett.* **2013**, *15*, 1166–1169. For nucleophilic additions to enynes see: *(c)* C. Nieto-Oberhuber, S. López, M. P. Muñoz, D. J. Cárenas, E. Buñuel, C. Nevado and A. M. Echavarren, *Angew. Chem. Int. Ed.* **2005**, *44*, 6146–6148; *(d)* P. Pérez-Galán, N. J. A. Martin, A. G. Campaña, D. J. Cárenas and A. M. Echavarren, *Chem. –Asian J.* **2011**, *6*, 482–486. For [4+2] cyclizations see: *(e)* C. Nieto-Oberhuber, S. López and A. M. Echavarren, *J. Am. Chem. Soc.* **2005**, *127*, 6178–6179; *(f)* C. Nieto-Oberhuber, P-Pérez-Galán, E. Herrero-Gómez, T. Lauterbach, C. Rodrígez, S. López, C. Bour, A. Rosellón, D. J. Cárdenas and A. M. Echavarren, *J. Am. Chem. Soc.* **2008**, *130*, 269–279. For a tandem 1,5-propargyl ether migration of a 1,6-enyne followed by intramolecular cyclopropanation see: *(g)* E. Jiménez-Núñez, M. Raducan, T. Lauterbach, K. Molawi, C. R. Solorio and A. M. Echavarren, *Angew. Chem. Int. Ed.* **2009**, *48*, 6152–6155.

[11] A. Fürstner and L. Morency, *Angew. Chem. Int. Ed.* **2008**, *47*, 5030–5033.

Following the Stork–Eschenmoser model for cyclizations of squalene and oxidosqualene,[12] these types of cascade cyclizations were rationalized as proceeding through concerted transition states such as **15**, not involving cyclopropyl gold(I) carbenes as discrete intermediates.[13]

However, other studies strongly suggested that gold-catalyzed 1,*n*-enyne cyclizations occurred in a step-wise fashion.[1,3,7,10] As an example, reaction of 1,6-enyne **16** with indole afforded adducts **17** and **18** by nucleophilic attack at the carbene *(a)* of intermediate **19** or the cyclopropyl ring *(b)* with retention of the configuration (Scheme 6).[14] The use of complex [IPrAu(NCPh)]SbF_6 (**C**) as catalyst, with a highly donating NHC ligand, enhanced the carbene-like nature of this intermediate, favouring nucleophilic attack at the carbene carbon leading to **18**.

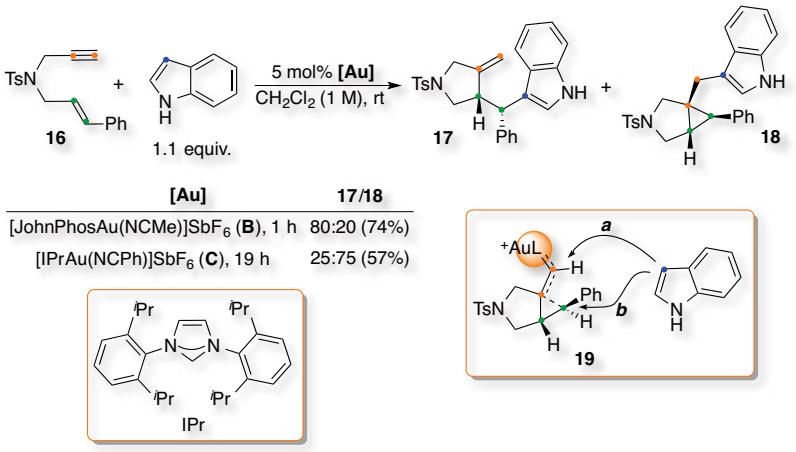

Scheme 6. Nucleophilic addition to the gold carbene position.

Furthermore, the carbene-like character of the intermediates generated by reaction of 1,*n*-enynes with gold was more clearly revealed by their trapping with alkenes.[7g] Thus, for example, reaction of dienyne **20** with [Ph_3PAuNCMe]SbF_6 led stereoselectively to tetracyclic compound **21** (Scheme 7).

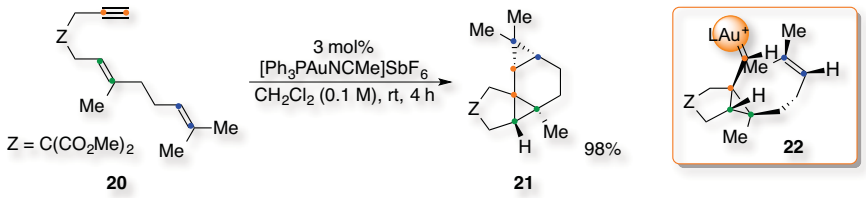

Scheme 7. Intramolecular cyclopropanation of 1,6-enyne 20.

---

[12] *(a)* A. Eschenmoser, L. Ruzicka, O. Jeger and D. Arigoni, *Helv. Chim. Acta* **1955**, *38*, 1890–1904; *(b)* G. Stork and A. W. Burgstahler, *J. Am. Chem. Soc.* **1955**, *77*, 5068–5077; *(c)* A. Eschenmoser and D. Arigoni, *Helv. Chem. Acta* **2005**, *88*, 3011–3050.

[13] *(a)* C. M. Chao, M. R. Vitale, P. Y. Toullec, J. P. Genêt and V. Michelet, *Chem. –Eur. J.* **2009**, *15*, 1319–1323; *(b)* S. G. Sethofer, T. Mayer and F. D. Toste, *J. Am. Chem. Soc.* **2010**, 132, 8276–8277.

[14] *(a)* C. H. M. Amijs, C. Ferrer and A. M. Echavarren, *Chem. Commun.* **2007**, 698–700; *(b)* C. H. M. Amijs, V. López-Carrillo, M. Raducan, P. Pérez-Galán, C. Ferrer and A. M. Echavarren, *J. Org. Chem.* **2008**, *73*, 7721–7730.

DFT calculations were consistent with a concerted, asynchronous cyclopropanation through intermediate **22**. A similar model was proposed for the intermolecular cyclopropanation of 1,6-enynes by alkenes.[15] The cyclopropanation was found to be concerted for symmetrical or less polarized alkenes whereas styrenes reacted in a stepwise manner. Nevertheless, the overall process was stereospecific since formation of the second carbon–carbon occurred through a very small energy barrier.

Oxygen transfer from diphenylsulfoxide to the carbene-like carbon of intermediate **23**, formed during the reaction of 1,6-enyne **24** with gold, led to the corresponding aldehyde **25** (Scheme 8).[16]

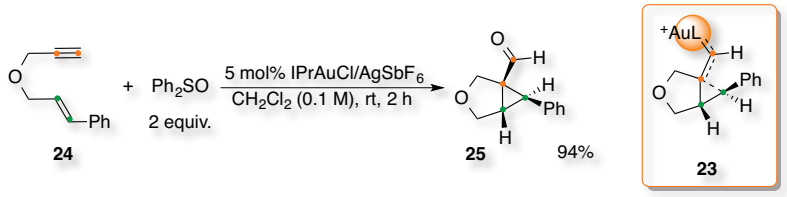

Scheme 8. Oxidation of the gold carbene intermediate.

Then, opening of cyclopropenone acetal **26** with $Ph_3PAuNTf_2$ led to ***Z*-27** that isomerised to ***E*-27** presumably through gold carbene **28** (Scheme 9).[17] The spectroscopic data of ***Z*-27** and ***E*-27** revealed an oxocarbenium cationic structure.

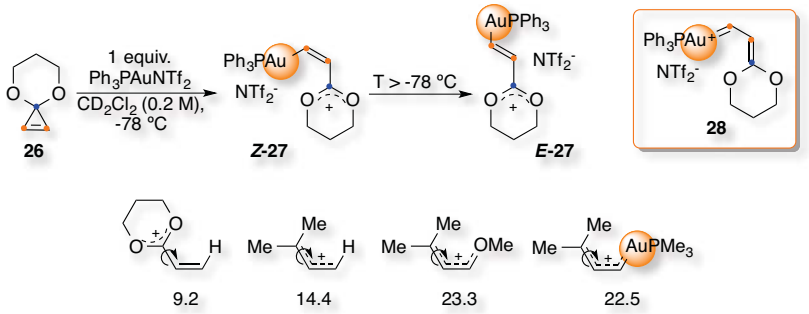

Scheme 9. Bond rotation analysis of organogold species (relative energies in kcal/mol).

An in-depth theoretical analysis of the bond rotation energy for different carbocations demonstrated that LAu- has a similar stabilizing effect as MeO- on an allyl carbocation (M06, 6-31G** (C, H, O, P, N, S, F) and LACVP** (Au) in CH_2Cl_2).[8] Moreover, the bond length between gold and the carbene carbon decreased with strong σ-donating ligands such as chloride or N-heterocyclic carbenes but it increased with less donating, π-acidic ligands such as phosphines or phosphites by reducing the back-donation to the substrate. This study concluded a continuum character of the organogold species ranging from metal stabilized singlet carbene to metal coordinated carbocation depending on the substitution pattern and the ligand on gold.

---

[15] *(a)* S. López, E. Herrero-Gómez, P. Pérez-Galán, C. Nieto-Oberhuber and A. M. Echavarren, *Angew. Chem. Int. Ed.* **2006**, *45*, 6029–6032; *(b)* P. Pérez, H. Herrero, D. T. Hog, N. J. A. Martin, F. Maseras and A. M. Echavarren, *Chem. Sci.* **2011**, *2*, 141–149.
[16] C. A. Witham, P. Mauleón, N. D. Shapiro, B. D. Sherry and F. D. Toste, *J. Am. Chem. Soc.* **2007**, *129*, 5838–5839.
[17] G. Seidel, R. Mynott and A. Fürstner, *Angew. Chem. Int. Ed.* **2009**, *48*, 2510–2513.

Finally, digold species were proposed to be involved as key intermediates in the cyclization of 1,5-allenynes such as **29** towards **30** using $[(Ph_3PAu)_3O]BF_4$.[18,19] The transformation proceeded by a stereospecific intramolecular hydrogen atom transfer from the allene to the alkyne based on deuterium labeling experiments (Scheme 10). According to DFT calculations, gold coordinated to the alkyne making the proton more acidic and leading to an alkynyl gold complex that reacted with a second equivalent of the catalyst to form **31**. Nucleophilic attack of the allene generated the allyl stabilized carbocation **32** in the rate-determining step, which was followed by an intramolecular 1,5-hydrogen shift leading to **30** through germinal diaurated species **33**.

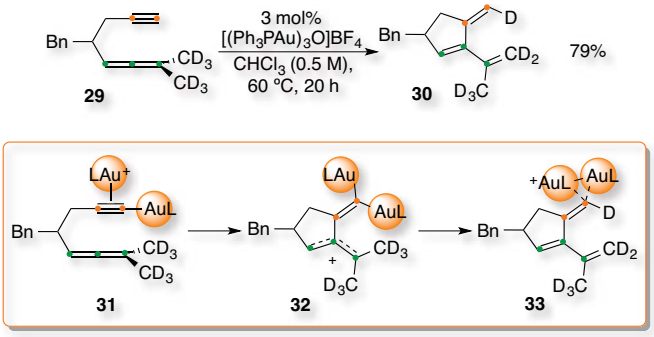

Scheme 10. Involvement of digold species as key intermediates.

Digold complexes related to **31**, **32** or **33** were later found to play relevant roles in catalysis. As an example, during the intramolecular hydroarylation of allenes, complex **34** was isolated as the catalyst resting state (Figure 1).[20] A species of type **35** was also generated by gold-boron transmetallation from a vinyl boronate.[21] The analysis of structure **35** revealed an important stabilization from the oxygen atom and two almost regular carbon-gold σ-bonds.

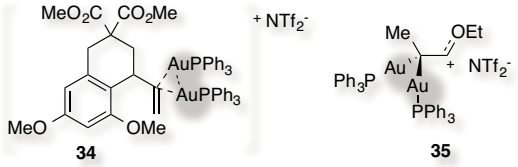

Figure 1. Isolated digold complexes.

[18] P. H. Y. Cheong, P. Morganelli, M. R. Luzung, K. N. Houk and F. D. Toste, *J. Am. Chem. Soc.* **2008**, *130*, 4517–4526.
[19] For related precedents see: *(a)* A. N. Nesmeyanov, E. G. Perevalova, K. I. Grandberg, D. A. Lemenovskii, T. V. Baukova and O. B. Afanassova, *J. Organomet. Chem.* **1974**, *65*, 131–144; *(b)* K. I. Grandberg, *Russ. Chem. Rev.* **1982**, *51*, 249–262; *(c)* K. I. Grandberg and V. P. Dyadchenko, *J. Organomet. Chem.* **1994**, *474*, 1–21; *(d)* K. A. Porter, A. Schier and H. Schmidbauer, *Organometallics* **2003**, *22*, 4922–4927; *(e)* V. Lavallo, G. D. Frey, S. Kousar, B. Donnadleu and G. Bertrand, *Proc. Natl. Acad. Sci. USA* **2007**, *104*, 13569–13573; *(f)* T. N. Hooper, M. Green and C. A. Russel, *Chem. Commun.* **2010**, *46*, 2313–2315.
[20] D. Weber, M. A. Tarselli and M. R. Gagné, *Angew. Chem. Int. Ed.* **2009**, *48*, 5733–5736.
[21] G. Seidel, C. W. Lehmann and A. Fürstner, *Angew. Chem. Int. Ed.* **2010**, *49*, 8466–8470.

2. Objectives

As reported in **Chapter 2**, the intermolecular gold-catalyzed [2+2+2] of an alkyne with an alkene bearing a carbonyl moiety was developed (Scheme 11).[22] [^{t}BuXPhosAuNCMe]SbF$_6$ (**E**) was used in DCE at 50 ºC. Thus, ethynlbenzene and 6-methylhept-5-en-2-one afforded oxabicycle **36** in 68% isolated yield.

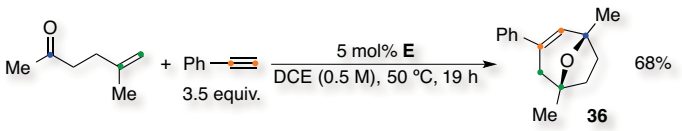

Scheme 11. Gold-catalyzed [2+2+2] cycloaddition of ethynylbenzene and 6-methylhept-5-en-2-one .

The preferential binding of the gold catalyst to the alkyne was suggested based on the precedents in other gold-catalyzed transformations (Scheme 12). Then, complex **37** would undergo nucleophilic attack of the alkene building the cyclopropyl gold carbene intermediate **38** regio- and stereoselectively. An intramolecular nucleophilic attack from the carbonyl could occur and the oxonium cation **39** would be formed, which could further experience a Prins-type cyclization. The carbocation **40** could proceed *via* demetalation to **41** and recover complex **37** after ligand exchange with ethynylbenzene releasing **36**. Therefore, a step-wise process was initially convieved.

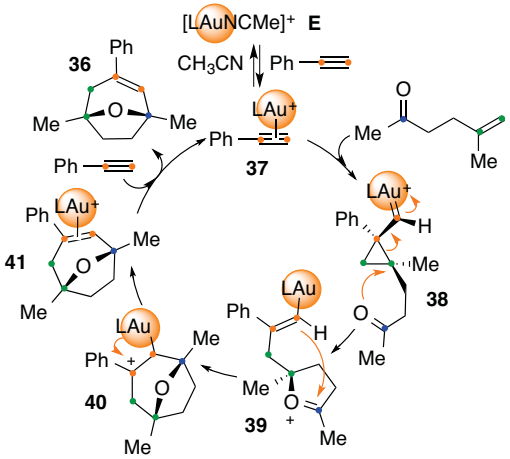

Scheme 12. Mechanistic proposal (L=^{t}BuXPhos).

Due to the lack of evidence in such transformations, we were challenged to study this cycloaddition more in depth to provide some insights that would allow the design of better catalysts to improve this type of reactions.

[22] C. Obradors and A. M. Echavarren, *Chem. –Eur. J.* **2013**, *19*, 3547–3551.

3. Theoretical Approach

First, we decided to check the feasibility of the proposal computationally. DFT calculations of the suggested pathway were performed (M06, 6-31G(d) (C, H, P, O) and SDD (Au) in CH_2Cl_2).[8]

Gold complex **37** was simplified to **42** bearing PMe_3 as ligand instead of ^{t}BuXPhos for time-consuming concerns. We analysed the competitive binding to the metal between the alkyne, the alkene and the carbonyl moiety by comparing the energies of the different complexes (Figure 2).[1,4,9]

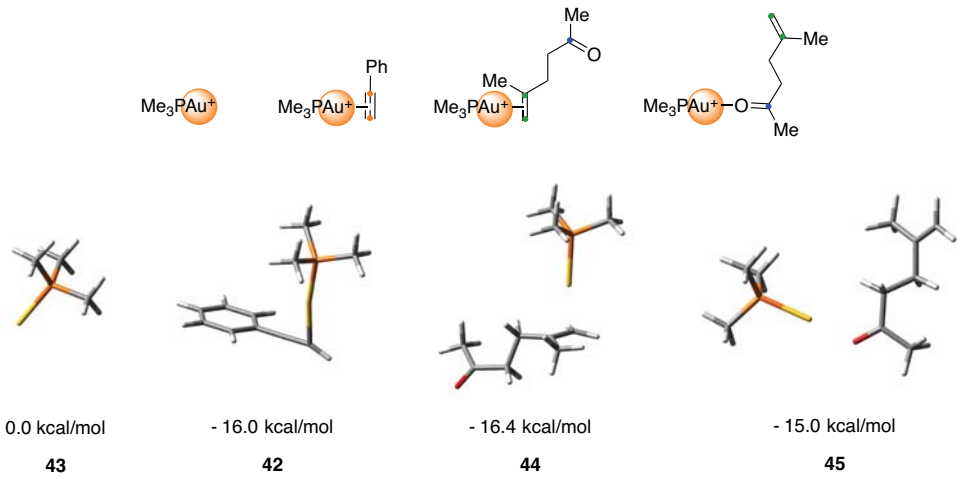

Figure 2. Me_3PAu^+ competitive coordination.

Thus, we could observe that Me_3PAu^+ (**43**) is at least 15.0 kcal/mol less stable than complexes as $[Me_3PAuL']^+$ in which L´ could be any substrate.[23] Coordination to the ketone (**45**) was 1 kcal/mol less stable for in the presence of unsaturated C–C bonds. Furthermore, we could determine that, when using PMe_3 as ligand, the coordination of the alkene was preferred by 0.4 kcal/mol (**44**). Nevertheless, when PMe_2(biphenyl) was used as ligand the difference in energy decreased (Figure 3).

[23] Although these are often invoked, there is yet no structural proof for their existance. For recent discussions see: *(a)* S. D. Weber, D. Zahner, F. Rominger and B. F. Straub, *Chem. Commun.* **2012**, *48*, 11325–11327; *(b)* A. Homs, I Escofet and A. M. Echavarren, *Org. Lett.* **2013**, *15*, 5782–5785.

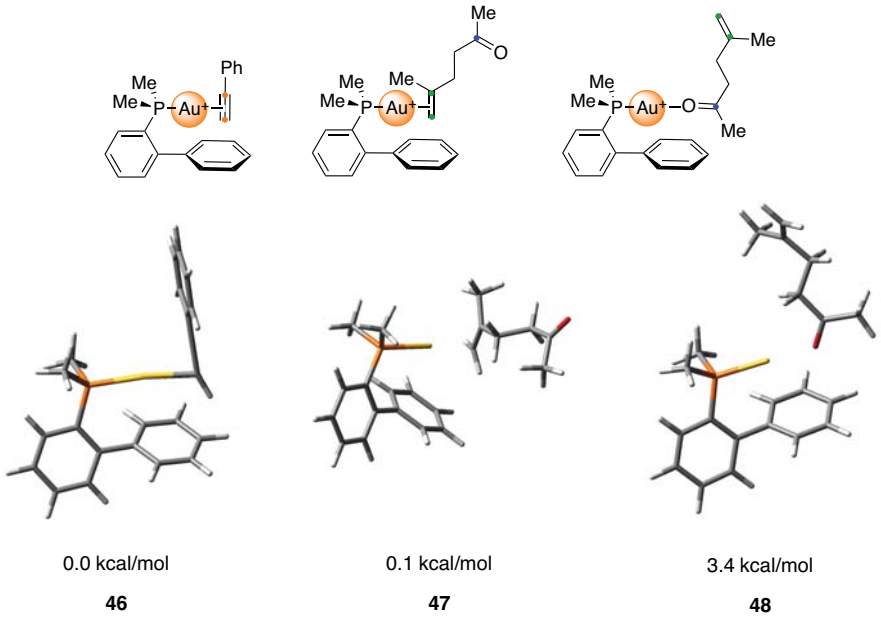

Figure 3. Me_2(biphenyl)PAu$^+$ competitive coordination.

Hence, the coordination of the alkyne (**46**) or the alkene (**47**) differed only by 0.1 kcal/mol. Therefore, the selectivity towards a triple bond observed experimentally when using bulky catalysts was unlikely due to its preferential binding.[9] In this case, coordination of the ketone (**48**) was 3.4 kcal/mol less stable.

Finally, we checked the coordination energies using ^{t}BuXPhosAu$^+$ (Figure 4). The alkene binding (**49**) was 0.5 kcal/mol more favoured comparing to the alkyne (**37**) and the corresponding ketone complex (**50**) was 5.0 kcal/mol less stable.

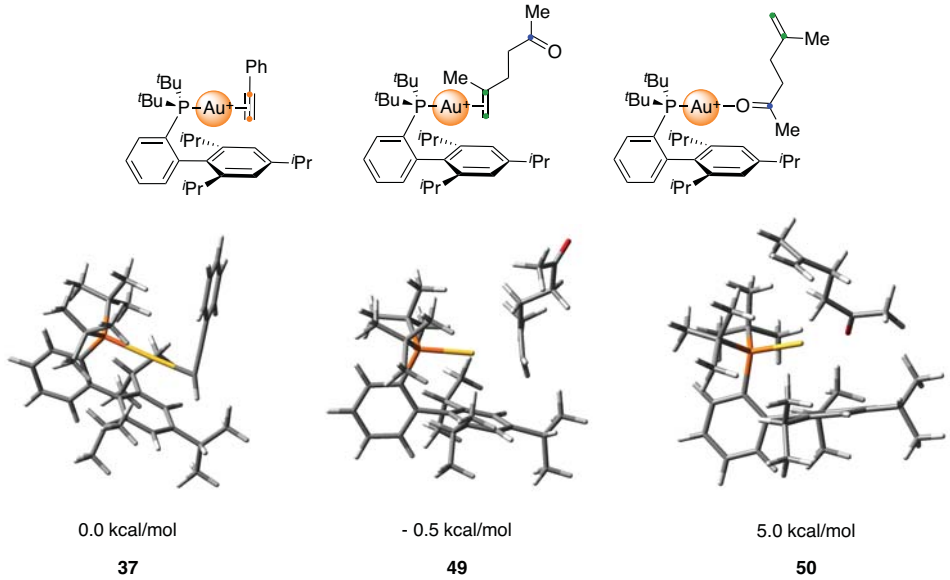

Figure 4. ^{t}BuXPhosAu$^+$ competitive coordination.

We analysed the nucleophilic attack of the alkene towards the activated alkyne **42**. We considered the initial regioselective formation of a cyclopropyl gold carbene in order to check if a step-wise process was possible (Figure 5).[1,3,9] The activation energy of this step was 15.9 kcal/mol towards $\mathbf{TS^{\neq}_{42\text{-}51}}$, which was both kinetically and thermodynamically feasible. Intermediate **51** was 1.2 kcal/mol less stable than its precursors so this step was endothermic.

Moreover, we contemplated that two stereogenic centres would be formed, which could lead to two diastereoisomers: **51** and **52** (Figure 6). In the case of intermediate **52**, 16.2 kcal/mol were necessary to build $\mathbf{TS^{\neq}_{42\text{-}52}}$ and it was 2.2 kcal/mol less stable than **51**.

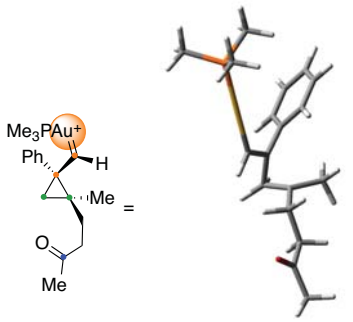

ΔG≠ = 15.9 kcal/mol
ΔG = 1.2 kcal/mol

51

Figure 5. Cyclopropylgold carbene 51.

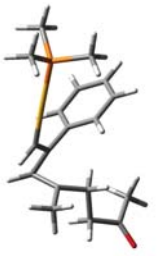

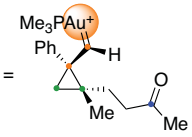

ΔG≠ = 16.2 kcal/mol
ΔG = 3.5 kcal/mol

52

Figure 6. Cyclopropyl gold carbene 52.

Alternatively, we also considered the opposite configuration of the gold carbene.[10c] Thus, cyclopropyl gold carbenes **53** and **54** were calculated (Figure 7). Intermediate **53** was 0.9 kcal/mol more stable than **51** and **54** 3.0 kcal/mol less stable. However, the activation energies were 19.4 and 22.3 kcal/mol, respectively.

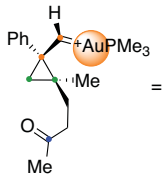

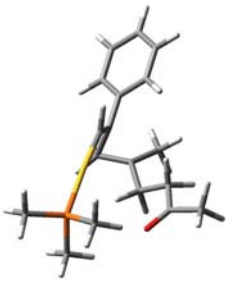

ΔG≠ = 19.4 kcal/mol
ΔG = 0.3 kcal/mol

53

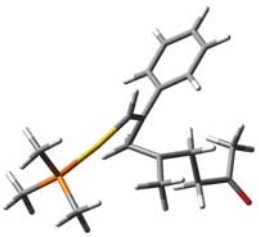

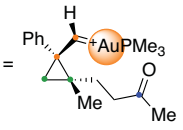

ΔG≠ = 22.3 kcal/mol
ΔG = 4.2 kcal/mol

54

Figure 7. Cyclopropyl gold carbenes 53 and 54.

Although the differences were rather low, we could assume that the transformation started with the stereoselective formation of the cyclopropyl gold carbene **51**. Furthermore, these results suggested a step-wise process towards the construction of the oxabicycle, as the C–C bond preceded the formation of the C–O bond.

Interestingly, we obtained the same type of scaffold for all the cyclopropyl gold carbene intermediates and we could confirm that those are highly unsymmetrical structures.[7f] Thereby, the new C–C bond lengths were 1.58 Å and 1.73 Å for **51**, 1.58 Å/1.72 Å for **52**, 1.59 Å/1.76 Å for **53** and 1.57 Å/1.75 Å for **54**. The largest bond length was in the substituted carbon atom in all the cases.

Subsequently, we studied the intramolecular regioselective nucleophilic attack of the ketone to the more substituted carbon of the cyclopropyl gold carbene **51**.[14] Beside the entropic factors, the bond lengths difference would imply an important positive charge in that position. Nevertheless, the nucleophilic attack could occur from both sides of the cyclopropyl ring. Consequently, we calculated both transition states, named **TS(up)**$^{\neq}_{\mathbf{51\text{-}55}}$ and **TS(down)**$^{\neq}_{\mathbf{51\text{-}55}}$, (Figure 8).

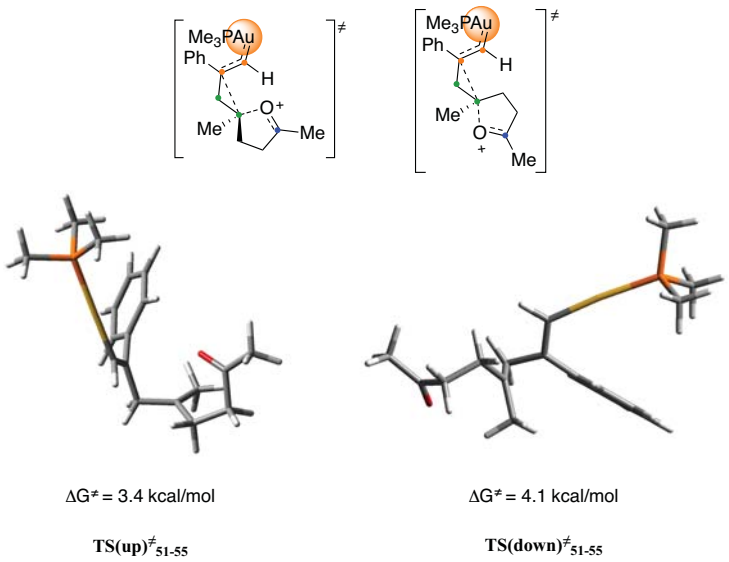

Figure 8. Intramolecular attack of the ketone to the cyclopropyl ring through the upper or the lower face.

According to the configuration of the final product (**2**), attack through the lower face of **4** was suggested in the case of the intramolecular gold-catalyzed [2+2+2] cyclization of **1** (Scheme 2). However, in the absence of the strains induced by the carbon tether,[3] the attack through the upper face of **51** was 3.4 kcal/mol, 0.7 kcal/mol below than though the lower face. Oxonium cation **55** was 10.1 kcal/mol more stable than the cyclopropyl gold carbene **51** (Figure 9).

Afterwards, the Prins-type cyclization of **55** required 9.1 kcal/mol to afford the carbocation **56**, which was 6.4 kcal/mol less stable but evolved to **57**, 40.5 kcal/mol more stable than **56** (Figure 10).[24]

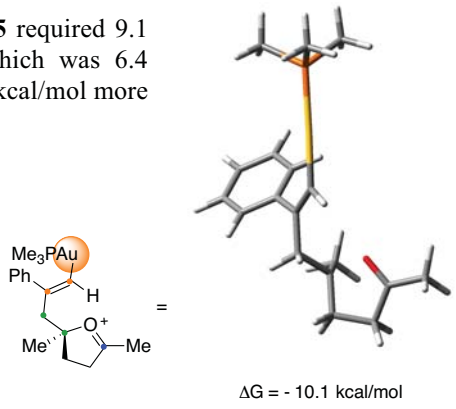

Figure 9. Oxonium cation 55.

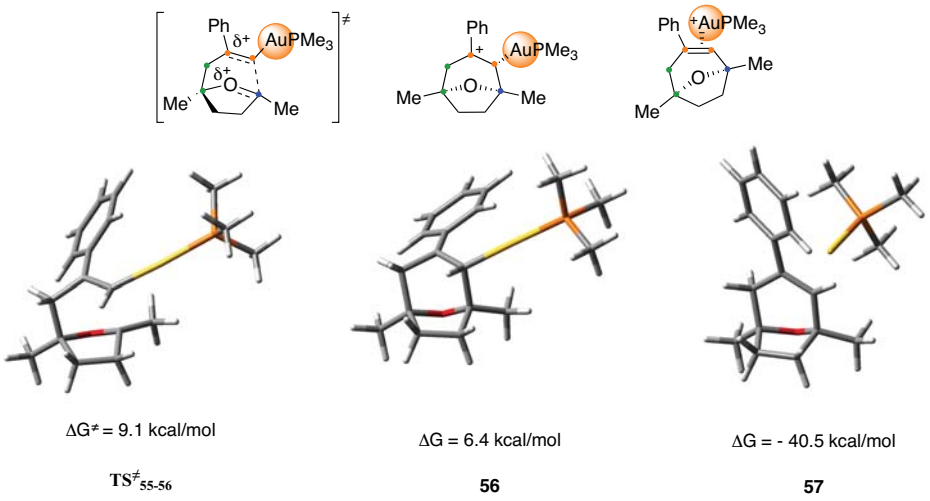

Figure 10. Prins cyclization of 55 to 57 through 56.

Accordingly, we suggested the most favoured pathway towards the formation of oxabicycle **36**. Using ethynylbenzene and 6-methylhept-5-en-2-one with gold catalysis, the metal would compete for the coordination of the alkyne and the alkene (Figure 2, 3 and 4). Then, complex **42** could undergo a regioselective nucleophilic attack from the alkene forming a cyclopropyl gold carbene **51** with *anti*-configuration in the rate-determining step of the process (Scheme 13). Regioselective intramolecular nucleophilic attack of the ketone to the more substituted carbon occurs preferentially at the upper face to form oxonium cation **55**. However, attack from the lower face is only 0.7 kcal/mol less favourable. Prins-type cylclization proceeds with 9.1 kcal/mol activation energy to form **56** and then the coordinated product **57**, 34.1 kcal/mol more stable than **55**. Ligand exchange with ethynylbenzene would restart the catalytic cycle.

[24] *(a)* X. Han, G. R. Peh and P. E. Floreancig, *Eur. J. Org. Chem.* **2013**, 1193–1208; *(b)* G. Drudis-Solé, G. Ujaque, F. Maseras and A. Lledós, *C. R. Chimie 7* **2004**, 885–893.

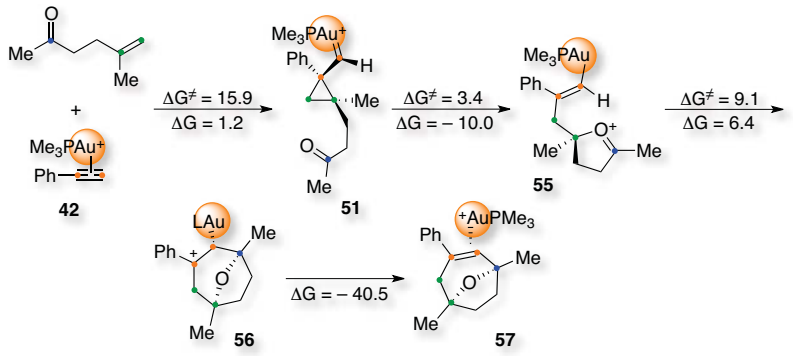

Scheme 13. Calculated mechanism of the [2+2+2] cycloaddition (relative energies in kcal/mol).

Finally, we also considered the formation of a cyclobutene **58** *via* a [2+2] cycloaddition between the alkyne and the alkene as a competitive pathway (Scheme 14).[9] However, ring expansion of the cyclopropyl gold carbene **51** would require 7.4 kcal/mol, compared to 3.4, and the coordinated product would be 22.6 kcal/mol more stable than **51**, compared to 44.1. Therefore, these results explained that the cyclobutene **58** was not usually observed during the [2+2+2] cycloaddition.

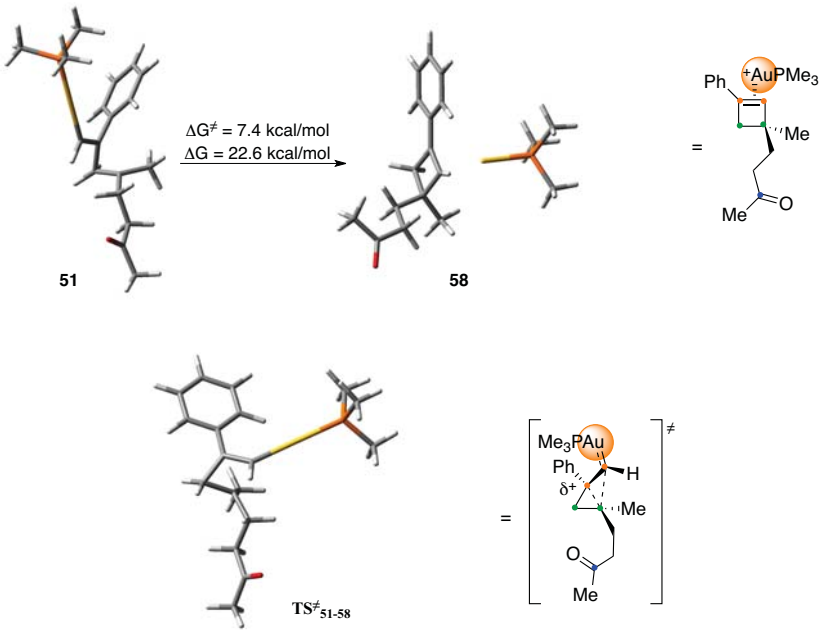

Scheme 14. Theoretical formation of cyclobutene 58.

4. Isotopic Labelling Experiments

We decided to study the deuterium incorporation in the final products when the gold-catalyzed [2+2+2] cycloaddition was performed between deuterated *p*-bromoethynylbenzene and 6-methylhept-5-en-2-one (Scheme 15). As explained in **Chapter 2**, the oxabicycle product **59** was formed in 56% isolated yield together with 17% of the tetrahydrofuran byproduct **60**.[22]

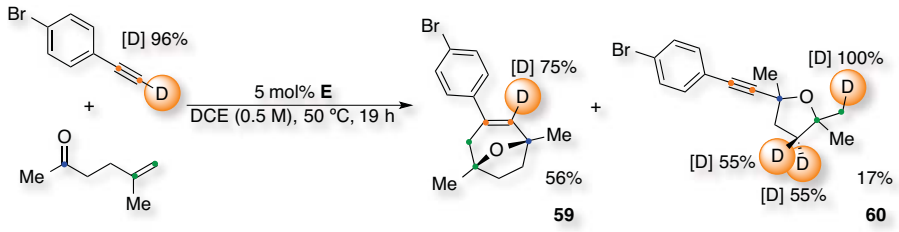

Scheme 15. Deuterium incorporation during the [2+2+2] cycloaddition.

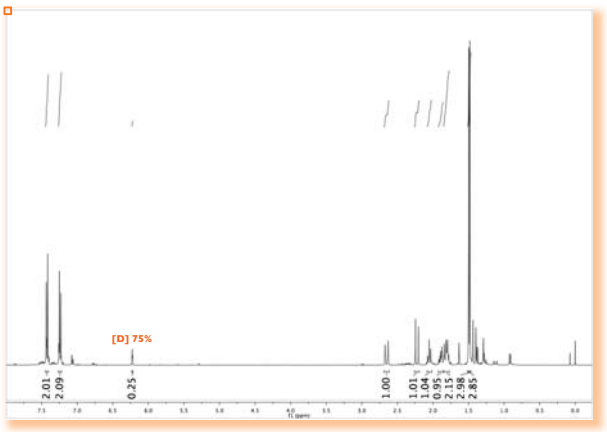

The isotopic transfer was totally selective during the formation of the oxabicycle **59**. Deuterium incorporation was observed only in the olefin moiety, which supported the theoretical results. However, the isotopic labelling was only 75% in contrast of 96% in the *p*-bromoethynylbenzene (Figure 11).

Figure 11. ^{1}H NMR spectra of deuterated oxabicycle 59.

On the other hand, the tetrahydrofuran **60** showed 100% of deuterium incorporation in the terminal position of the alkene and 55% for each of the diastereotopic CH_2 hydrogens in the five-membered ring (Figure 12).

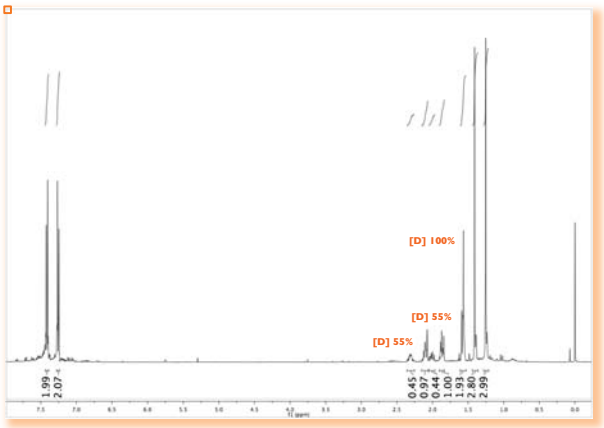

Figure 12. ^{1}H NMR spectra of deuterated tetrahydrofuran 60.

We reasoned that the formation of tetrahydrofurans such as **60** could be explained due to the ability of gold complexes to deprotonate terminal alkynes (Scheme 16).[19f, 25] Simultaneously, the presence of an acid in the reaction conditions can promote the cationic cyclization of the oxoalkene. Thus, complex **61** evolved to **62** generating acid, which reacted with 5-methylhex-5-en-2-one to form oxonium cation **63**/**63´**. This could be easily trapped with complex **62** forming the tetrahydrofuran product **60** along with the regeneration of **61**.

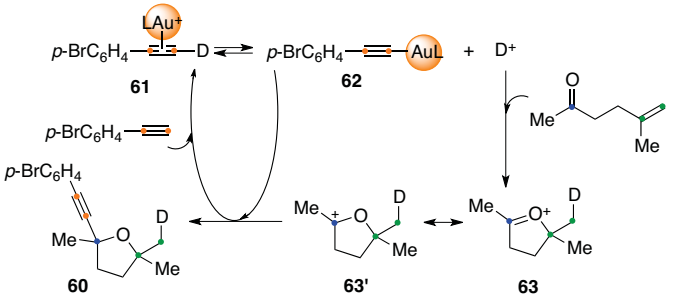

Scheme 16. Formation of tetrahydrofuran 60 (L=^{t}BuXPhos).

Nevertheless, this proposal only explained the deuterium incorporation to the terminal position of the alkene. If we assumed that the acid-promoted cyclization of the oxoalkene was a reversible reaction, the incorporation in the five-membered ring could be explained as well (Scheme 17). Hence, the equilibrium towards the more substituted alkene **64** would be more favored than 6-methylhept-5-en-2-one. The re-cyclization to **63**/**63´** would involve the incorporation of deuterium in the five-membered ring with no diastereoselectivity.

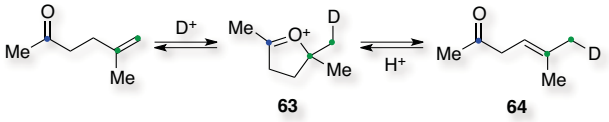

Scheme 17. Reversible cyclization of the oxoalkene.

Therefore, the formation of the tetrahydrofuran **60** presented a more complex scenario that was still consistent with the initial proposal.

[25] For selected examples see: *(a)* C. Wei and C. J. Li, *J. Am. Chem. Soc.* **2003**, *125*, 9584–9585; *(b)* M. J. Campbell and F. D. Toste, *Chem. Sci.* **2011**, *2*, 1369–1378; *(c)* M. Raducan, M. Moreno, C. Bour and A. M. Echavarren, *Chem. Commun.* **2012**, *48*, 52–54; *(d)* S. Sun, J. Kroll, Y. Luo and L. Zhang, *Synlett* **2012**, *23*, 54–56.

5. Formation of Digold Complexes

Monitoring of the [2+2+2] Cycloaddition

Attempts to detect any of the gold intermediates proposed were performed by monitoring the [2+2+2] cycloaddition between an excess of ethynylbenzene with 6-methylhept-5-en-2-one *via* ^{1}H NMR spectroscopy.[2] The reaction was performed in CD_2Cl_2 (0.5 M) at 30 ºC using 5 mol% of complex **E** (Scheme 18). The residual peak of the solvent was used as the internal standard.[10c]

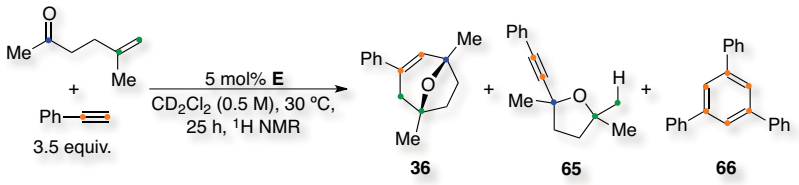

Scheme 18. [2+2+2] Cycloaddition followed by ^{1}H NMR spectroscopy.

Under these conditions, the oxabicycle product **36** was formed, along with tetrahydrofuran byproduct **65**, the trimerization product **66** and traces of the corresponding cyclobutene, dienes and alkyne di- or oligomerization.[9,22,25d] We could quantify the formation of oxabicycle **36** and trimer **66** as well as the consumption of the alkyne and the oxoalkene (Figure 13). However, the quantification of the tetrahydrofuran **65** was not reliable due to signal overlapping.

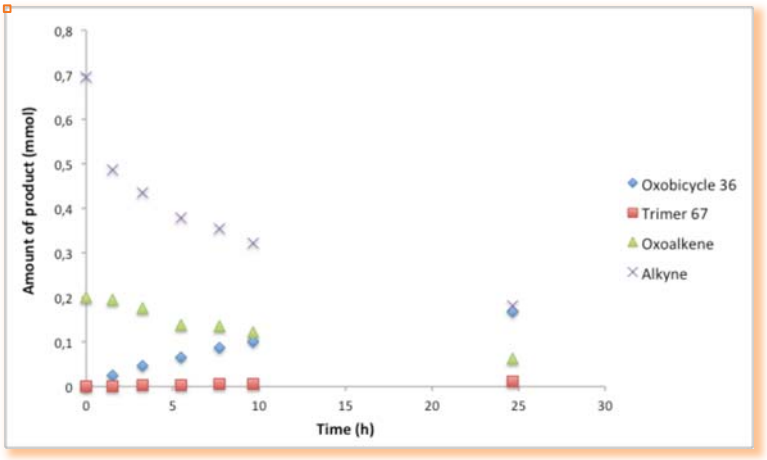

Figure 13. Variation of products with time.

In the variation of the amount of the different products with time, we could observe that the consumption of the alkyne was indeed much faster than the oxoalkene. Moreover, the oxabicycle **36** was the major product and no intermediates could be identified. This pattern was clearer when the percentage of formation or consumption were analysed (Figure 14).

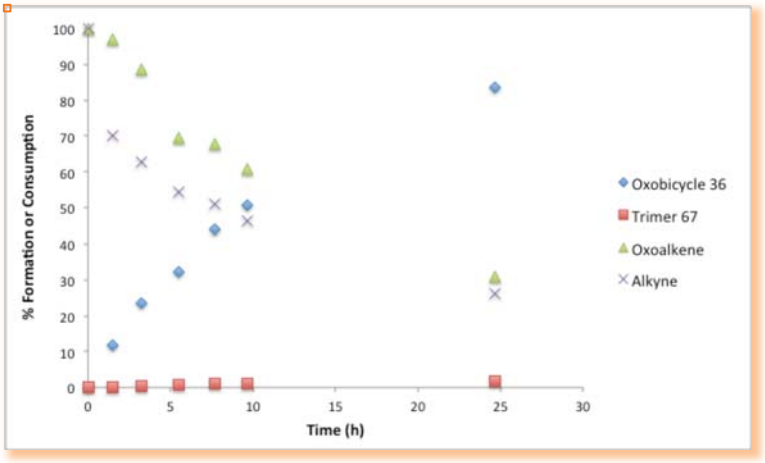

Figure 14. Percentages of products with time.

Attempts to determine the order of the reagents led to non-conclusive results due to the competitive pathways.[26] Furthermore, a single signal at δ = 65.22 ppm was observed by ^{31}P NMR spectroscopy over the whole process, which did not correspond to [^{t}BuXPhosAuNCMe]SbF_6 (**E**).

Crystallization of the Resting State

According to the DFT calculations, the nucleophilic attack of the alkene towards gold complex **37** was the rate-determining step due to the highest activation energy (Scheme 14). Therefore, complex **37** could be the resting state of the catalytic cycle. Nevertheless, the theoretical approach did not consider the formation of such species, which could involve a more complicated scenario. Addition of pentane to the reaction mixture allowed to isolate digold complex **67** (Figure 15).[18-21]

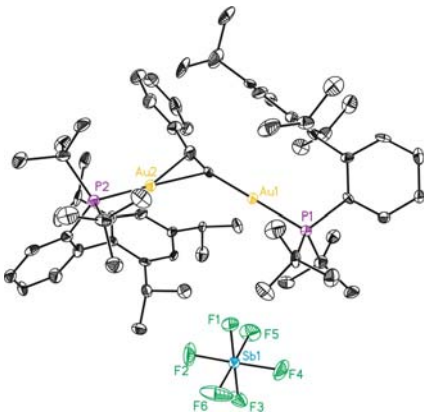

Figure 15. X-Ray crystal structure of digold complex 67.

In the solid state, ^{t}BuXPhosAu^{+} was bonded in the σ-position of the deprotonated ethynylbenzene whereas the second fragment was coordinated in the π-cloud of the triple bond. The distance C–Au for the first one was 2.05 Å and for the second one, 2.22 Å in the terminal position and 2.27 Å to the phenyl substituted one. However, both phosphorous atoms are chemically equivalent in solution after NMR scale, which corresponds to a fluxional dinuclear complex.

[26] For a review of kinetic experiments applied in mechanistic studies see: D. Blackmond, *Angew. Chem. Int. Ed.* **2005**, *44*, 4302–4320.

Analogously to the formation of the tetrahydrofuran byproduct (Scheme 16), we reasoned that, after ligand exchange, complex **37** could undergo deprotonation of ethynylbenzene building alkynyl gold complex **68** (Scheme 19).[19f,25] Apparently, reaction of **68** with another equivalent of [^{t}BuXPhosAuNCMe]SbF_6 (**E**) could form the more stable digold complex **67**.

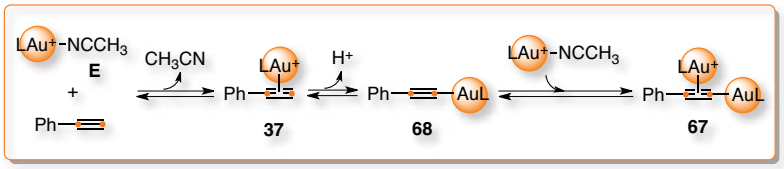

Scheme 19. Formation of digold complex 67 (L=^{t}BuXPhos).

We verified the involvement of digold complex **68** by synthesizing it though an alternative route (Scheme 20). Ethynylbenzene was deprotonated with LiHMDS at 0 ºC, which reacted with ^{t}BuXPhosAuCl at 25 ºC for 12 h forming the alkynyl gold complex **68**. The crude mixture was concentrated and added to a solution of one equivalent of ^{t}BuXPhosAuCl followed by $AgSbF_6$. Digold complex **67** was obtained after recrystallization in 99% isolated yield.

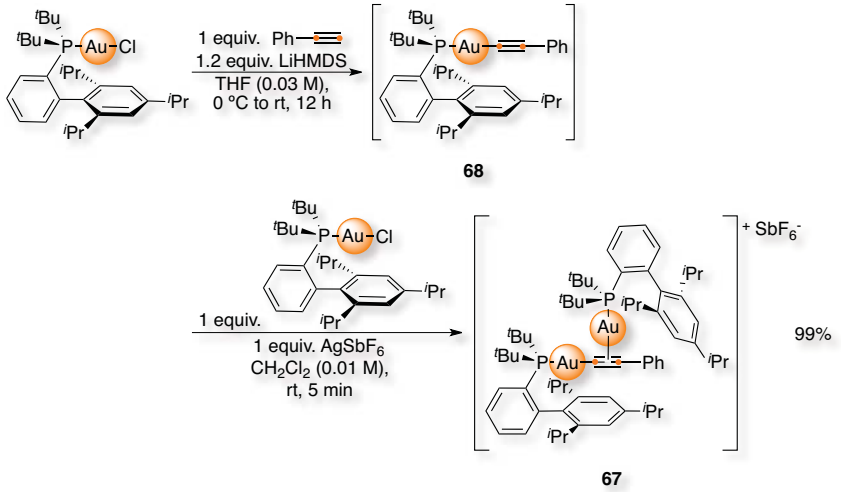

Scheme 20. Synthesis of digold complex 67.

Low Temperature NMR Experiments

Beside the role of digold complex **67**, we decided to prove the presence of complex **37** as it was theoretically the active species towards the nucleophilic attack of the alkene. Although gold forms stable monomeric dicoordinate π-complexes with alkenes,[27] 1,3-dienes,[28]

[27] For selected examples see: *(a)* T. J. Brown, M. G. Dickens and R. A. Widenhoefer, *Chem. Commun.* **2009**, 6451–6453; *(b)* T. J. Brown, M. G. Dickens and R. A. Widenhoefer, *J. Am. Chem. Soc.* **2009**, *131*, 6350–6351; *(c)* R. E. M. Brooner, T. J. Brown and R. A. Widenhoefer, *Chem. –Eur. J.* **2013**, 19, 8276–8284.

allenes[29] and substituted alkynes,[30] no examples with terminal alkynes were reported so far (see **General Introduction**). Therefore, 10 equiv. of ethynylbenzene were added over [^{t}BuXPhosAuNCMe]SbF_6 (**E**) in CD_2Cl_2 (0.04 M) at – 78 ºC and analysed by ^{1}H and ^{31}P NMR spectroscopy (Scheme 21).

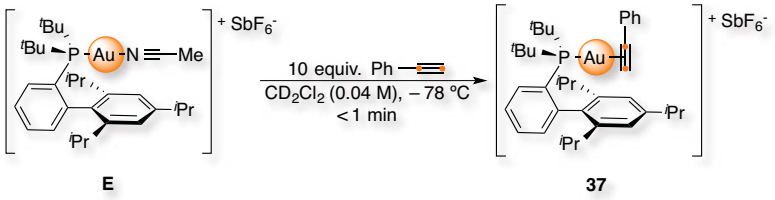

Scheme 21. Detection of gold complex 37.

At –60 ºC, [^{t}BuXPhosAuNCMe]SbF_6 (**E**) and complex **37** could be detected as well as digold complex **67**. The ^{31}P resonance of complex **37** appeared at δ = 65.43 ppm and it could be identified *via* the correlation proton-phosphorous performing a ^{1}H-^{31}P HMBC experiment (Figure 16). Thus, we could observe a cross peak between the phosphorous signal and the acetylene proton of the coordinated ethynylbenzene, which appeared at δ = 3.39 ppm splitted into a doublet (J (^{1}H-^{31}P) = 4.4 Hz). No cross peak could be observed when a ^{1}H COSY experiment was performed. The same result with lower resolution spectra was obtained when ^{t}BuXPhosAu$^+$ was generated *in situ* with one equivalent of ethynylbenzene.

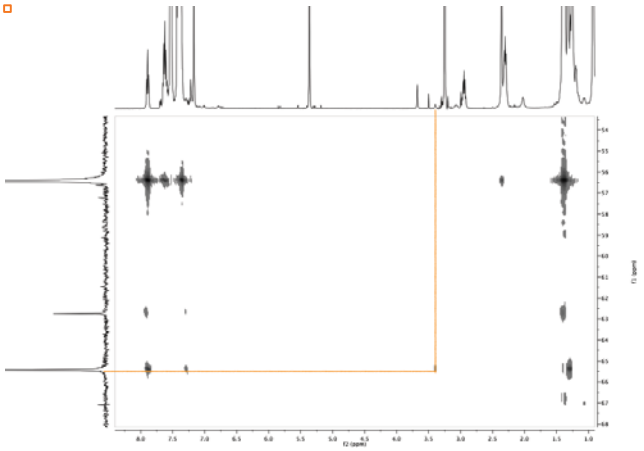

Figure 16. ^{1}H-^{31}P HMBC experiment of complex 37.

Furthermore, we analysed the evolution of those species when increasing the temperature by ^{31}P NMR spectroscopy recording the spectra every 20 ºC from – 60 ºC (213 K) to room temperature (Figure 17).

---

[28] For selected examples see: *(a)* R. A. Sanguramath, T. N. Hooper, C. P. Butts, M. Green, J. E. McGrady and C. A. Russel, *Angew. Chem. Int. Ed.* **2011**, *50*, 7592–7595; *(b)* R. E. M. Brooner and R. A. Widenhoefer, *Organometallics* **2011**, *30*, 3182–3193.
[29] T. J. Brown, A. Sugie, M. G. D. Leed and R. A. Widenhoefer, *Chem. –Eur. J.* **2012**, *18*, 6959–6971.
[30] For selected examples see: *(a)* N. D. Shapiro and F. D. Toste, *Proc. Natl. Acad. Sci. USA* **2008**, *105*, 2779–2782; *(b)* S. Flügge, A. Anoop, R. Goddard, W. Thhiel and A. Fürstner, *Chem. –Eur. J.* **2009**, *15*, 8558–8565; *(c)* T. J. Brown and R. A. Widenhoefer, *J. Organomet. Chem.* **2011**, *696*, 1216–1220.

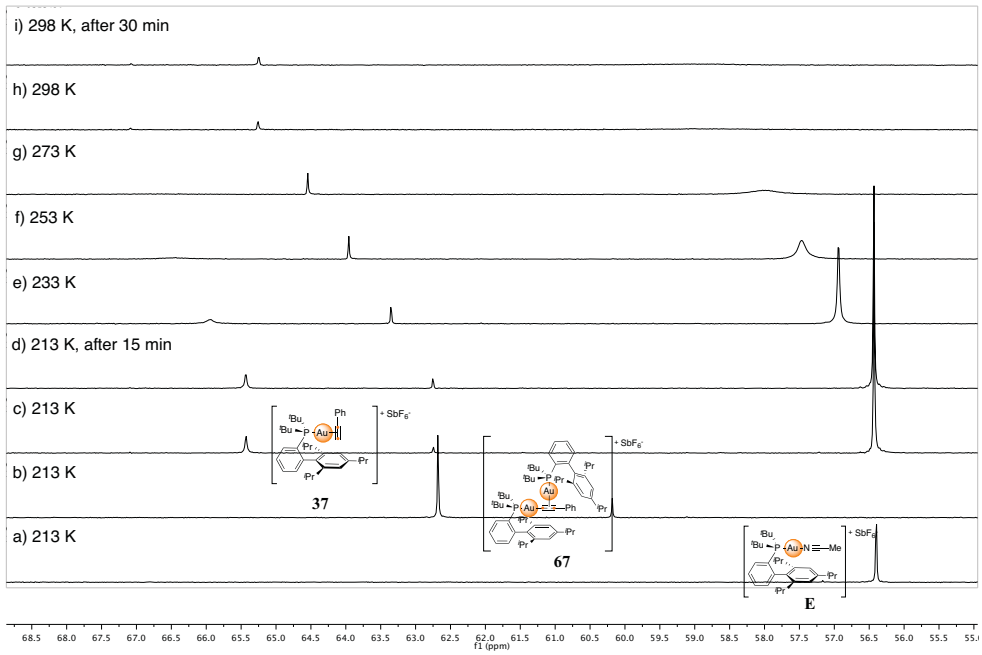

Figure 17.* ^{31}*P NMR spectroscopy from – 60 to 25 ºC: a) Pure E at 213 K; b) Pure 67 at 213 K; c) Reaction at 213 K; d) Reaction at 213 K after 15 min; e) Reaction at 233 K; f) Reaction at 253 K; g) Reaction at 273 K; h) Reaction at 298 K; i) Reaction at 298 K after 30 min.

In this manner, we could observe the consumption of [^{t}BuXPhosAuNCMe]SbF_6 (**E**) while digold complex **67** was formed. On the other hand, complex **37** was no longer observed at – 20 ºC (253 K).

Determination of the Equilibrium Constant

Later on, we checked that the formation of digold complex **67** was a reversible process by calculating the equilibrium constant with complex **E** (Scheme 22).[31] In this manner, we could prove that the resting state was coexisting with complex **37** (Scheme 19). Otherwise, we should consider an alternative active species and therefore a new catalytic cycle.

[31] For basic concepts see: *(a)* K. J. Laidler and M. C. King, *J. Phys. Chem.* **1983**, *87*, 2657–2664; *(b)* P. Ballester, *Acc. Chem. Res.* **2013**, *46*, 874–884.

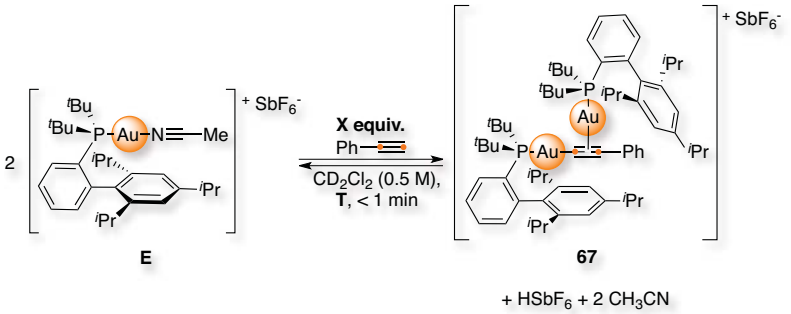

Scheme 22. Equilibrium between complex E and digold complex 67.

Thus, we decided to apply the Van't Hoff equation in order to calculate the equilibrium constant. Considering that Gibbs energy can be decomposed in enthalpy and entropy factors (Equation 1) as well as be related to the equilibrium constant of the same process (Equation 2), Van't Hoff equation represents the relationship between this equilibrium constant and its enthalpy/entropy factors (Equation 3). Therefore, the ratio between reagents and products would vary only depending on the temperature.

$$\Delta G^0 = \Delta H^0 - T\Delta S^0$$

Equation 1. Decomposition of Gibbs energy in ΔH^0 and ΔS^0.

$$\Delta G^0 = -RT \cdot lnK_{eq}$$

Equation 2. Relationship between Gibbs energy and K_{eq}.

$$lnK_{eq} = -\frac{\Delta H^0}{RT} + \frac{\Delta S^0}{R}$$

Equation 3. Van't Hoff equation.

Concurrently, the equilibrium constant between [^{t}BuXPhosAuNCMe]SbF$_6$ (**E**) and digold complex **67** could be represented as the quotient of their concentrations (Equation 4).

$$K_{eq} = \frac{[Digold\ Complex\ \mathbf{67}] \cdot [HSbF_6] \cdot [CH_3CN]^2}{[Complex\ \boldsymbol{E}]^2 \cdot [Ethynylbenzene]}$$

$$= \frac{4 \cdot [\mathbf{67}]^4}{[Complex\ \boldsymbol{E}]_0 - 2 \cdot [\mathbf{67}])^2 \cdot ([Ethynylbenzene]_0 - [\mathbf{67}])}$$

Equation 4. Equilibrium constant as a function of [67].

Therefore, reaction between [^{t}BuXPhosAuNCMe]SbF$_6$ (**E**) with 0.5, 1, 2, 3.5 and 5 equiv. of ethynylbenzene in CD_2Cl_2 (0.5 M) was analysed by ^{1}H and ^{31}P NMR spectroscopy at –10, 5, 20 and 35 ºC. Considering that we could measure the ratio between complex **E** and digold complex **67** under the different conditions, we could also determine their concentrations in the equilibrium (Equation 5).

$$Integrals\ Ratio = \frac{[Complex\ \boldsymbol{E}]_0 - 2 \cdot [\mathbf{67}]}{[\mathbf{67}]}$$

Equation 5. Relationship between catalyst E and digold complex 67.

Accordingly, we could calculate the equilibrium constant at each temperature (Table 1).

Table 1. Equilibrium constants depending on the temperature with increasing equiv. of ethynylbenzene. [a,b]

– 10 ºC	$1.79 \cdot 10^{-8}$	$6.67 \cdot 10^{-9}$	$6.38 \cdot 10^{-9}$	$6.99 \cdot 10^{-9}$	$1.82 \cdot 10^{-8}$
5 ºC	$3.53 \cdot 10^{-8}$	$1.10 \cdot 10^{-8}$	$1.07 \cdot 10^{-8}$	$7.64 \cdot 10^{-9}$	$5.51 \cdot 10^{-8}$
20 ºC	$4.84 \cdot 10^{-8}$	$3.77 \cdot 10^{-8}$	$2.97 \cdot 10^{-8}$	$1.77 \cdot 10^{-8}$	$1.03 \cdot 10^{-7}$
35 ºC	$6.37 \cdot 10^{-8}$	$9.16 \cdot 10^{-8}$	$3.76 \cdot 10^{-8}$	$2.81 \cdot 10^{-8}$	$1.59 \cdot 10^{-7}$

[a]Scheme 22, equations 4 and 5. [b]Equilibium constants (M).

Afterwards, we used these data for the Van't Hoff equation and we checked that fit in a linear regression with $R^2 = 0.991$ (Figure 18). Thus, we concluded that the formation of digold complex **67** was indeed reversible and determined that the equilibrium constant at 50 ºC was $1.08 \cdot 10^{-7}$ M. Moreover, we could calculate that the enthalpy of the process was 6.8 kcal/mol and the entropy – 11 cal/mol·K.

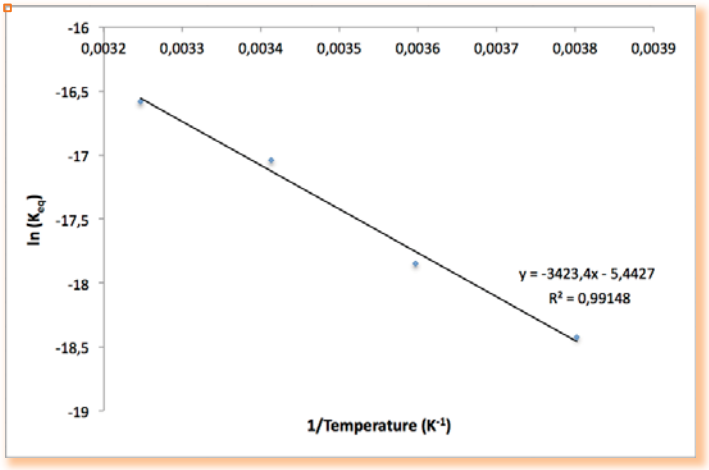

Figure 18. Relationship between the equilibrium constant towards 67 and the temperature.

6. Reactivity of Digold Complexes

Tests of the catalytic activity

Thereupon, we decided to prove whether digold complex **67** was catalytically involved in the formation of oxabicycle **36** (Table 2). The reaction was performed under the optimized conditions varying the stoichiometry and using half of the catalyst loading. No reaction was observed between **67** and 6-methylhept-5-en-2-one under stoichiometric conditions (entry 1). Furthermore, under catalytic conditions using 2.5 mol% of **67**, only 9% of **36** was observed after 19 h at 50 ºC (entry 2). Similarly, when switching the stoichiometry, only 8% was obtained after 4 days (entry 3).

Table 2. [2+2+2] Cycloaddition catalyzed by digold complex 67.

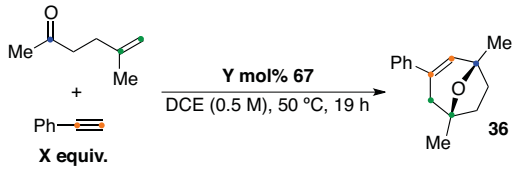

Entry	Y mol%	X equiv.	Additive	Yield[a]
1	100	0	–	–
2[b]	2.5	3.5	–	9%
3[c]	2.5	0.5	–	8%
4	2.5	5[d]	$HSbF_6 \cdot 6H_2O$ (2.5 mol%)	45%[e]
5	–	5[d]	$HSbF_6 \cdot 6H_2O$ (2.5 mol%)	–

[a]Crude analysed by ^{1}H NMR spectroscopy using 1,4-diacetylbenzene as internal standard, yield referred to oxabicycle **36**. [b]Dimerization of the alkyne was detected. [c]Reaction time of 4 days. [d]Proportion of the alkyne was increased to account for the competitive hydration. [e]Isolated yield.

Nevertheless, when $HSbF_6$ was added substoichiometrically, the equilibrium between the gold species was re-established allowing the formation of the active complex **37** and then, the reaction proceeded to give product **36** with slightly lower yield (Scheme 23).

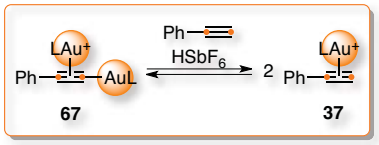

Scheme 23. Regeneration of gold complex 37 (L=^{t}BuXPhos).

Moreover, the same behaviour was observed in the reaction between 6-methylhept-5-en-2-one and ethynylbenzene to form cyclobutene **69** and oxabicycle **70**, which were described in **Chapter 2** (Table 3).[22] Traces of product **69** were observed performing the reaction with **67**, stoichiometrically or catalytically, and the equilibrium was re-established in the presence of substoichiometric amounts of $HSbF_6$ (entry 3).

Table 3. [2+2] Cycloaddition catalyzed by digold complex 67.

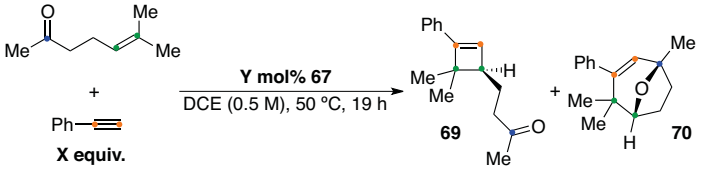

Entry	Y mol%	X equiv.	Additive	Yields (69:70)[a]
1[b]	2.5	3.5	–	6% (6:1)
2[c]	2.5	0.5	–	9% (3.5:1)
3	2.5	5[d]	$HSbF_6 \cdot 6H_2O$ (2.5 mol%)	44%[e] (2.1:1)
4	–	5[d]	$HSbF_6 \cdot 6H_2O$ (2.5 mol%)	–

[a]Crude analysed by ^{1}H NMR spectroscopy using 1,4-diacetylbenzene as internal standard, yields referred to cyclobutene **69** and oxabicycle **70**. [b]Dimerization of the alkyne was detected. [c]Reaction time of 4 days. [d]Proportion of the alkyne was increased to account for the competitive hydration. [e]Isolated yield.

Finally, we attempted the gold-catalyzed reaction between 6-methylhept-5-en-2-one and other nucleophilies in order to exclude the activation of the oxoalkene as the key step of the process (Scheme 24).[14] Thus, we used allyltrimethylsilane, indole, 1,3,5-trimethoxybenzene and 1,3-diphenylpropane-1,3-dione but no reaction was observed in any case.

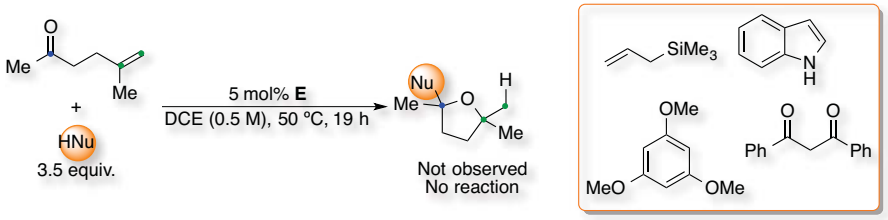

Scheme 24. Oxoalkene activation towards nucleophilic attack.

Therefore, we suggest the existence of a pre-equilibrium between [^{t}BuXPhosAuNCMe]SbF_6 (**E**) and ethynylbenzene with complex **37** and digold complex **67** (Scheme 25). Complex **37** was the active species towards the nucleophilic attack of the oxoalkene to enter the catalytic cycle that led to oxabicycle **36**. Thus, our results indicated that digold complex **67** acted as an unreactive resting state outside the catalytic cycle, sequestering most of the active gold(I) and lengthening the reaction times. This proposal could also explain the formation of the tetrahydrofuran byproduct **65**.

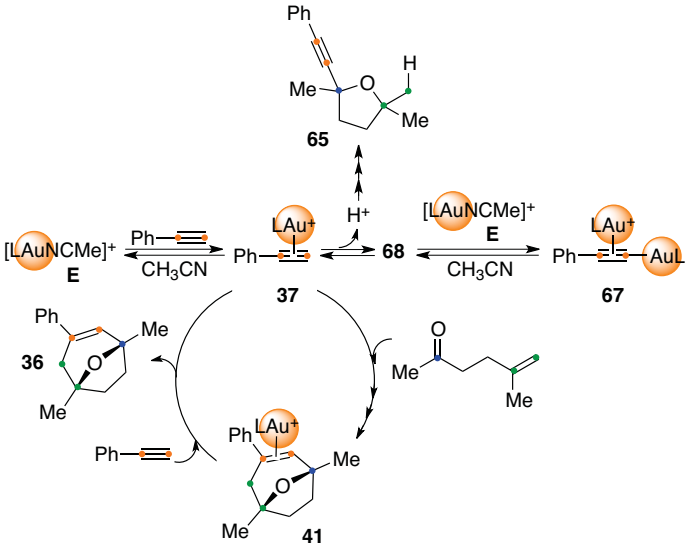

Scheme 25. Digold complex 67 as an off-cycle resting state.

DFT calculations

Computationally, we determined the activation energy for the key nucleophilic attack of the oxoalkene to the ethynylbenzene moiety of the model digold complex **71** with PMe_3 as ligand (Scheme 26). In this case, the activation energy was 25 kcal/mol, 10 kcal/mol higher than the attack to complex **42**.

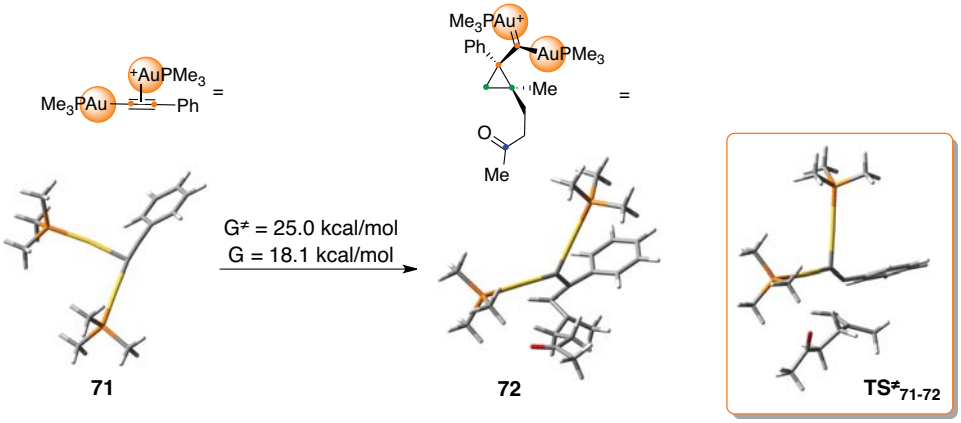

Scheme 26. Attack of the oxoalkene towards digold complex 71.

Moreover, the corresponding cyclopropyl gold carbene **72** would be 18.1 kcal/mol less stable than **71**, in contrast to 1.2 kcal/mol for **51**. Therefore, these results also suggested that digold complex **67** acts as a dead end.

7. Simultaneous Findings

While we were performing this study, other digold scaffolds were reported in the literature. An early example was digold complex **74** bearing an IPr ligand (Scheme 27).[32,33] This was isolated when increasing the temperature of complex **73**, which was generated *in situ* with ethynylbenzene, IPrAuCl and $AgSbF_6$ and detected spectroscopically at – 78 ºC.

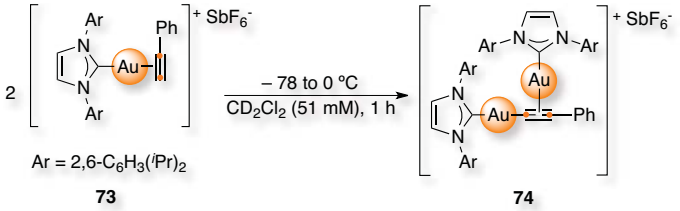

Scheme 27. Generation of digold complex 74.

Interestingly, digold complex **74** did not react with triflic acid but the corresponding alkynyl gold complex **75**, generated by the addition of pyridine to form **76**, led to the regeneration of ethynylbenzene building IPrAuOTf (Scheme 28). This result showed the robustness of this type of digold complexes.

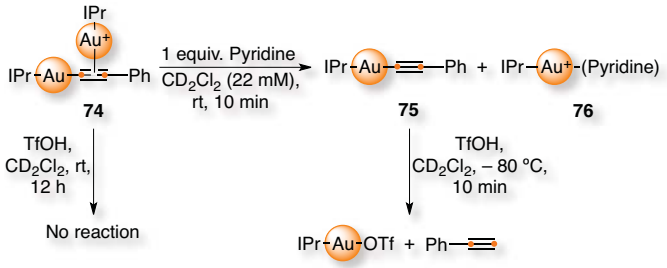

Scheme 28. Tests of the catalytic activity of 74.

Similar digold complexes with phosphine ligands were also detected in the intermolecular [2+2] cycloadditions of alkynes with alkenes.[34] However, their role in catalysis was still unclear. Their involvement in the cycloisomerization of 1,6-enynes was also examined. Experimental and computational work suggested that these types of σ,π-digold complexes were unreactive in these type of processes.[35]

The nature of the 3-centre 2-electron interaction between C–Au was also investigated by studying the equilibrium between aryl gold **77** and digold complexes **78** as a function of the electronic effects of the R- substituents in the aromatic ring and the counterions $\mathbf{A}^-$ of the gold complex (Scheme 29).[36,37] For this case, it was found that formation of **78** was

[32] T. J. Brown and R. A. Widenhoefer, *Organometallics* **2011**, *30*, 6003–6009.
[33] A. Himmelspach, M. Finze and S. Raub, *Angew. Chem. Int. Ed.* **2011**, *50*, 2628–2631.
[34] A. Grirrane, H. Garcia, A. Corma and E. Álvarez, *ACS Catal.* **2011**, *1*, 1647–1653.
[35] A. Simonneau, F. Jaroschik, D. Lesage, M. Karanik, R. Guillot, M. Malacria, J. C. Tabet, J. P. Goddard, L. Fensterbank, V. Gandon and Y. Gimbert, *Chem. Sci.* **2011**, *2*, 2417–2422.
[36] D. Weber, T. D. Jones, L. L. Adduci and M. R. Gagné, *Angew. Chem. Int. Ed.* **2012**, *51*, 2452–2456.
[37] D. Weber and M. R. Gagné, *Chem. Sci.* **2012**, *4*, 335–338.

favoured with less coordinating counterions as well as with more electron-rich substrates supporting the proposal of an electrondeficient Au_2C bond.

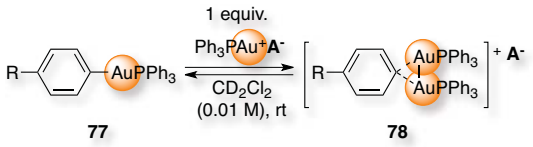

Scheme 29. Electronic effects in the formation of digold complexes 78.

Afterwards, a mechanistic investigation of the gold-catalyzed intramolecular allene hydroalkoxylation revealed a reversible C–O bond formation followed by a rate-determining protodeauration (Scheme 30).[38] Thus, in the transformation of **79** to **81**, vinyl gold complex **82** and vinyl digold complex **83** were detected. After testing their reactivity, it was reasoned that digold complex **83** was an off-cycle catalyst reservoir.

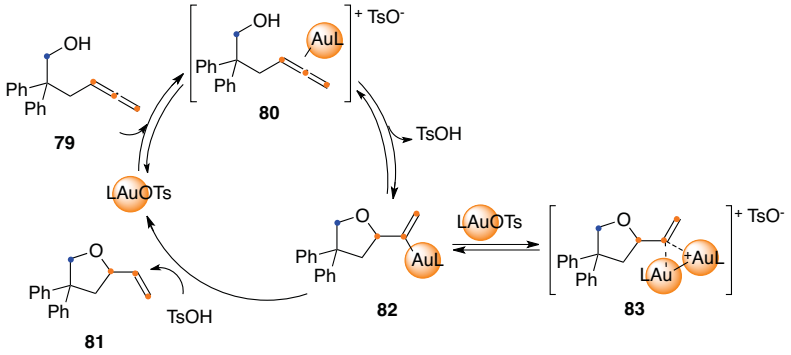

Scheme 30. Mechanistic study of allene 80 hydroxylation.

Later on, reactions of σ-alkynyl gold complexes with alkynes in intramolecular transformations leading to a new variety of interesting cyclic systems were also developed.[39] As an example, dyine **84** was cyclized with BrettPhosAuNTf$_2$ (**P**) to form 1,2-dihydrocyclopenta[*a*]indene **85** (Scheme 31).[40] The reaction was proposed to proceed by formation of alkynyl species **86**, which evolved by attack of the σ-alkynyl gold to the π-activated non-terminal alkyne in a *5-endo-dig* cyclization. The resulting gold vinylidene **87** could undergo a C–H insertion followed by protodemetallation to form tricyclic structure **85**.

[38] T. J. Brown, D. Weber, M. R. Gagné and R. A. Widenhoefer, *J. Am. Chem. Soc.* **2012**, *134*, 9134–9137.
[39] For selected examples see: *(a)* A. S. K. Hashmi, I. Braun, P. Nösel, J. Schädlich, M. Wieteck, M. Rudolph and F. Rominger, *Angew. Chem. Int. Ed.* **2012**, *51*, 4456–4460; *(b)* A. S. K. Hashmi, M. Wieteck, I. Braun, M. Rudolph and F. Rominger, *Angew. Chem. Int. Ed.* **2012**, *51*, 10633–10637; *(c)* A. S. K. Hashmi, I. Braun, M. Rudolph and F. Rominger, *Organometallics* **2012**, *31*, 644–661; *(d)* A. S. K. Hashmi, M. Wieteck, I. Braun, P. Nösel, L. Jongbloed, M. Rudolph and F. Rominger, *Adv. Synth. Catal.* **2012**, *354*, 555–562; *(e)* Y. Wang, A. Yepremyan, S. Ghorai, R. Todd, D. H. Aue and L. Zhang, *Angew. Chem. Int. Ed.* **2013**, *52*, 7795–7799.
[40] L. Ye, Y. Wang D. H. Aue and L. Zhang, *J. Am. Chem. Soc.* **2012**, *134*, 31–34.

It is interesting that, in contrast to the reactions between alkynes and alkenes, these type of diyne cyclizations were smoothly catalyzed with digold complexes *via* this novel alkyne dual activation.

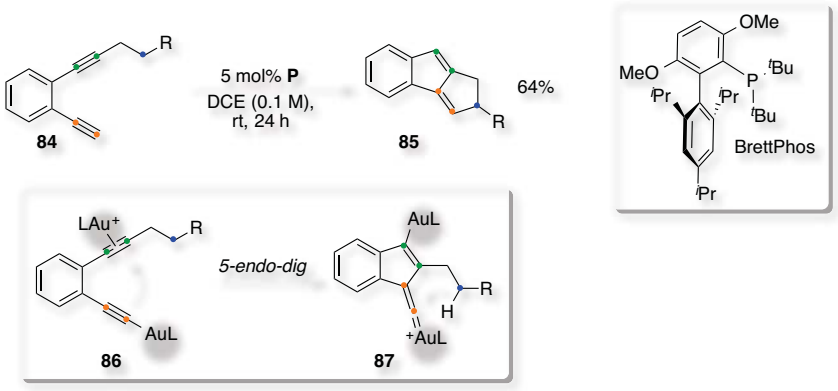

Scheme 31. Dual activation of dyine 84.

8. Conclusions

In spite of the advances of gold catalysis, very little evidence had been provided regarding the mechanistic aspects of these transformations. This lacking was due to the challenge in the identification of the key intermediates involved in the complex pathways proposed. Therefore, we performed a detailed mechanistic study of the gold-catalyzed intermolecular [2+2+2] cycloaddition of alkynes and oxoalkenes described in **Chapter 2**.

Monitoring of the reaction between ethynylbenzene and 6-methylhept-5-en-2-one by ^{1}H and ^{31}P NMR spectroscopy showed the formation of digold complex **67** as the resting state of the process (Figure 15).[22] Nevertheless, the tests performed to study the catalytic activity of **67** demonstrated that the structure was an unreactive structure outside the main catalytic cycle.

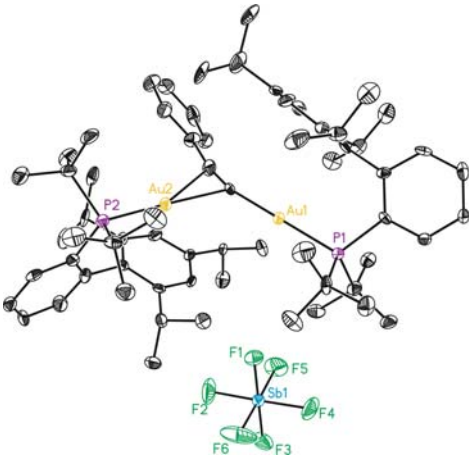

Figure 15. X-Ray crystal structure of digold complex 67.

Therefore, we checked that the formation of this digold complex was a reversible process by determining the equilibrium constant with catalyst **E** (K_{eq}(50 ºC) = $1.08 \cdot 10^{-7}$ M). Furthermore, we could detect the formation of complex **37** *via* low temperature NMR experiments. In this manner, we suggested a pre-equilibrium between those gold species before complex **37** entered the catalytic cycle (Scheme 19).

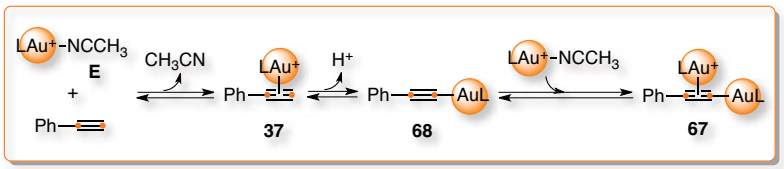

Scheme 19. Formation of digold complex 67 (L=^{t}BuXPhos).

Finally, complex **37** was simplified with PMe_3 as ligand (**42**) in order to use DFT calculations to analyse the main catalytic cycle (Scheme 32). Thus, complex **42** suffered nucleophilic attack from the oxoalkene in the rate-determining step of the process (15.9 kcal/mol). The *anti* cyclopropyl gold carbene **51** was formed regio- and stereoselectively and underwent intramolecular nucleophilic attack of the ketone from the upper face of the ring building the oxonium cation **55**.

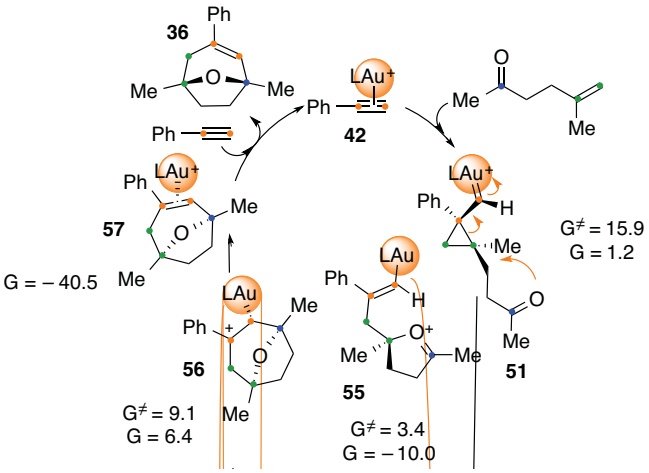

Scheme 32. DFT calculations of the main catalytic cycle with PMe_3 (relative energies in kcal/mol).

The transformation was followed by a Prins-type cyclization towards the carbocation **56**, which evolved to the coordinated product **57** (– 40.5 kcal/mol). Ligand exchange with ethynylbenzene would regenerate complex **42** whereas releasing oxabicycle **36**.

Isotopic labelling experiments also confirmed these results. Furthermore, they supported the formation of tetrahydrofuran **65** *via* an acid promoted cyclization of 6-methylhept-5-en-2-one to **63**/**63´** and **64** followed by trapping with alkynyl gold complex **68** (Scheme 33).

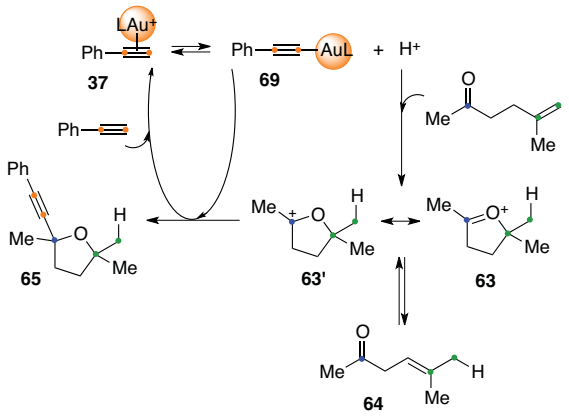

Scheme 33. Formation of tetrahydrofuran 65.

In summary, we suggest a stepwise process preceded by an equilibrium between different gold species towards the formation of **37**.

Chapter 4:

Anion Effects in Gold-Catalyzed Intermolecular Cycloadditions

1. Introduction

As mentioned in the **General Introduction**, the development of gold-catalyzed transformations relied on intramolecular reactions of functionalized 1,*n*-enynes and their allene analogues.[1] In contrast, the corresponding intermolecular processes were showed to be more challenging.[2] Thus, involvement of different unsaturated substrates would imply competitive binding with the gold complex. Moreover, gold catalysts are inherently acidic and could promote polymerization of alkenes by cationic mechanisms.[3]

Therefore, the first intermolecular gold-catalyzed cycloaddition, developed in 2010, was based on the reaction of electron-rich alkynes and alkenes to build regioselective cyclobutenes (Scheme 1).[4] Thus, ethynylbenzene and α-methylstyrene formed cyclobutene **1** in 80% isolated yield when treated with a sterically hindered gold catalyst such as [^{t}BuXPhosAuNCMe]SbF_6 (**E**).

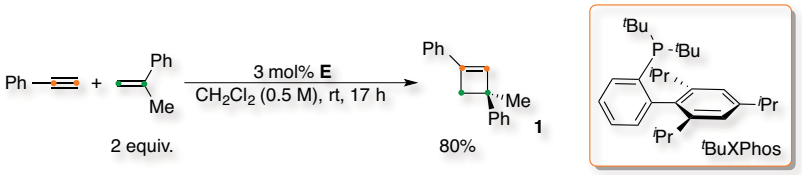

Scheme 1. Gold-catalyzed [2+2] cycloaddition of alkynes with alkenes.

In **Chapter 2**, we presented the development of the intermolecular cascade [2+2+2] reaction between an alkyne, an alkene and a carbonyl group catalyzed by the same gold complex.[5] As an example, the cycloaddition of *m*-methoxyethynylbenzene with 5-methylhex-5-en-2-one led to the oxabicycle scaffold **2** in 91% isolated yield (Scheme 2).

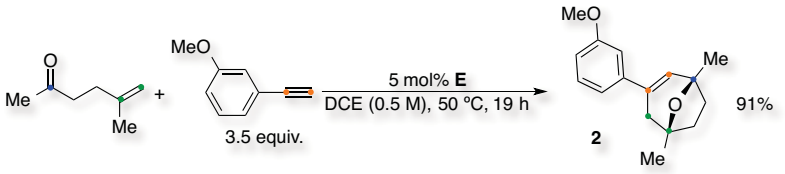

Scheme 2. Gold-catalyzed [2+2+2] cycloaddition towards oxabicycle 2.

---

[1] *(a)* A. S. K. Hashmi, *Chem. Rev.* **2007**, *107*, 3180–3211; *(b)* A. Fürstner and P. W. Davies, *Angew. Chem. Int. Ed.* **2007**, *46*, 3410–3449; *(c)* E. Jiménez-Núñez and A. M. Echavarren, *Chem. Rev.* **2008**, *108*, 3326–3350; *(d)* D. J. Gorin, B. D. Sherry and F. D. Toste, *Chem. Rev.* **2008**, *108*, 3351–3378; *(e)* N. T. Patil and Y. Yamamoto, *Chem. Rev.* **2008**, *108*, 3395–3442; *(f)* A. Fürstner, *Chem. Soc. Rev.* **2009**, *38*, 3208–3221; *(g)* H. G. Raubenheimer and H. Schmidbaur, *S. Afr. J. Sci.* **2011**, *107*, 31–34; *(h)* C. Obradors and A. M. Echavarren, *Acc. Chem. Res.* **2014**, *47*, 902–912.

[2] M. E. Muratore, A. Homs, C. Obradors and A. M. Echavarren, *Chem. Asian J.* **2014**, DOI: 10.1002/asia.201402305. For related examples, see: *(a)* C. Ferrer, C. H. M. Amijs and A. M. Echavarren, *Chem. Eur. J.* **2007**, *13*, 1358– 1373; *(b)* S. Kramer and T. Skrydstrup, *Angew. Chem. Int. Ed.* **2012**, *51*, 4681–4684; *(c)* Y. Luo, K. Ji, Y. Li and L. Zhang, *J. Am. Chem. Soc.* **2012**, *134*, 17412–17415.

[3] J. Urbano, A. J. Hormigo, P. de Frémont, S. P. Nolan, M. M. Díaz-Requejo and P. J. Pérez, *Chem. Commun.* **2008**, 759–761.

[4] V. López-Carrillo and A. M. Echavarren, *J. Am. Chem. Soc.* **2010**, *132*, 9292–9294.

[5] C. Obradors and A. M. Echavarren, *Chem. –Eur. J.* **2013**, *19*, 3547–3551.

It is interesting to note the differences between both optimized conditions: increased catalyst loading and temperature were required but also switching of the reaction stoichiometry. Thus, in the first case, an excess of the alkene was necessary partially due to its dimerization to **3** as a side-process and, in the second one, an excess of the alkyne due to the formation of trimer **4** as a side-product (Figure 1).

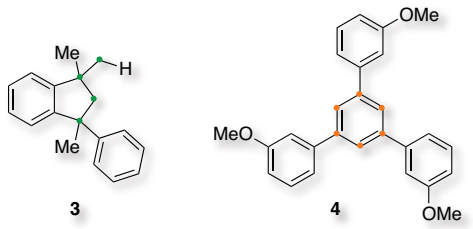

Figure 1. Side-products of the gold-catalyzed cycloadditions.

Based on analogy, the [2+2] cycloaddition between alkynes and alkenes was proposed to proceed *via* highly distorted cyclopropyl gold carbenes such as **5**/**5´** (Figure 2).[6] The contribution of resonance form **5´** (a gold(I) stabilized carbocation) explained the regioselectivity of the transformation.

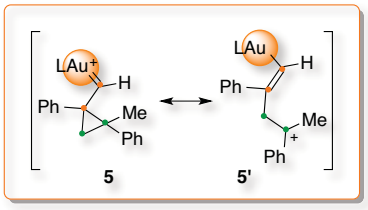

Figure 2. Highly distorted cyclopropyl gold carbene intermediate 5/5´ (L=^{t}BuXPhos).

In **Chapter 3**, we presented a detailed mechanistic study of the intermolecular gold-catalyzed [2+2+2] cycloaddition between ethynylbenzene and 5-methylhex-5-en-2-one.[5] A step-wise catalytic cycle starting from gold complex **6** was suggested *via* DFT calculations and supported by monitoring of the reaction, low-temperature NMR studies, determination of equilibrium constants and isotopic labelling experiments (Scheme 3).

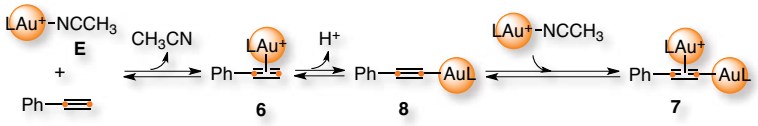

Scheme 3. Pre-equilibrium between gold species (L=^{t}BuXPhos).

Unreactive digold complex **7** was identified as the resting state of the transformation and we suggested a pre-equilibrium between the different gold species. Thus, we reasoned that

---

[6] *(a)* C. Nieto-Oberhuber, S. López, M. P. Muñoz, D. J. Cárenas, E. Buñuel, C. Nevado and A. M. Echavarren, *Angew. Chem. Int. Ed.* **2005**, *44*, 6146–6148; *(b)* P. Pérez-Galán, N. J. A. Martin, A. G. Campaña, D. J. Cárenas and A. M. Echavarren, *Chem. –Asian J.* **2011**, *6*, 482–486; *(c)* C. Nieto-Oberhuber, S. López and A. M. Echavarren, *J. Am. Chem. Soc.* **2005**, *127*, 6178–6179; *(d)* C. Nieto-Oberhuber, P-Pérez-Galán, E. Herrero-Gómez, T. Lauterbach, C. Rodrígez, S. López, C. Bour, A. Rosellón, D. J. Cárenas and A. M. Echavarren, *J. Am. Chem. Soc.* **2008**, *130*, 269–279; *(e)* E. Jiménez-Núñez, M. Raducan, T. Lauterbach, K. Molawi, C. R. Solorio and A. M. Echavarren, *Angew. Chem. Int. Ed.* **2009**, *48*, 6152–6155.

coordination of ethynylbenzene with gold formed complex **6**, which made the terminal proton very acidic. Deprotonation of terminal alkynes with gold catalysts towards complexes such as **8** was already known.[7] Coordination with a second molecule of the gold(I) complex formed the digold structure **7**.[8] This equilibrium could be modified by the ligand, the substrate and the counterion.

Tuning of the gold intermediates by the counterion has been used many times. In some examples, their influence could even modify the outcome of a transformation. This is the case of the gold-catalyzed synthesis of pyrroles from alkynyl aziridines (Scheme 4).[9] Substrate **9** cyclized towards 2,5-substituted pyrrol **10** or 2,4-**11** depending on the counterion of the gold catalyst.

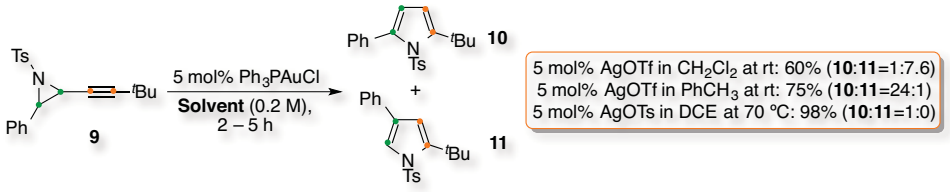

Scheme 4. Anion controlled regioselective synthesis of pyrroles.

The gold complex presumably coordinated to the alkyne (**12**), which would undergo intramolecular attack from the aziridine generating carbocation **13** (Scheme 5). Pyrrol **10** could be formed *via* direct proton elimination whereas pyrrole **11** *via* 1,2-aryl shift.

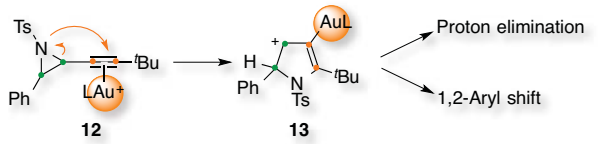

Scheme 5. Common carbocationic intermediate 13 (L=Ph$_3$P).

The lower activity of tosylate was assigned to the tighter ion pair. Thus, in the presence of a basic counterion, proton elimination of **13** was facilitated and pyrrol **10** was favoured. In the absence of it, the proton transfer pathway was suggested to proceed mediating an aromatic or a weakly Lewis basic solvent. Consequently, triflate in toluene also formed **10** preferentially. On the other hand, triflate in CH_2Cl_2 would be insufficiently basic and the

[7] C. Obradors and A. M. Echavarren, *Chem. Commun.* **2014**, *50*, 16–28. For specific examples see: *(a)* P. H. Y. Cheong, P. Morganelli, M. R. Luzung, K. N. Houk and F. D. Toste, *J. Am. Chem. Soc.* **2008**, *130*, 4517–4526; *(b)* T. J. Brown and R. A. Widenhoefer, *Organometallics*, **2011**, *30*, 6003–6009; *(c)* M. Raducan, M Moreno, C. Bour and A. M. Echavarren, *Chem. Commun.* **2012**, *48*, 52–54.

[8] *(a)* P. H. Y. Cheong, P. Morganelli, M. R. Luzung, K. N. Houk and F. D. Toste, *J. Am. Chem. Soc.* **2008**, *130*, 4517–4526; *(b)* D. Weber, M. A. Tarselli and M. R. Gagné, *Angew. Chem. Int. Ed.* **2009**, *48*, 5733–5736; *(c)* G. Seidel, C. W. Lehmann and A. Fürstner, *Angew. Chem. Int. Ed.* **2010**, *49*, 8466–8470; *(d)* T. J. Brown and R. A. Widenhoefer, *Organometallics* **2011**, *30*, 6003–6009; *(e)* A. Himmelspach, M. Finze and S. Raub, *Angew. Chem. Int. Ed.* **2011**, *50*, 2628–2631; *(f)* A. Simonneau, F. Jaroschik, D. Lesage, M. Karanik, R. Guillot, M. Malacria, J. C. Tabet, J. P. Goddard, L. Fensterbank, V. Gandon and Y. Gimbert, *Chem. Sci.* **2011**, *2*, 2417–2422; *(g)* D. Weber, T. D. Jones, L. L. Adduci and M. R. Gagné, *Angew. Chem. Int. Ed.* **2012**, *51*, 2452–2456; T. J. Brown, D. Weber, M. R. Gagné and R. A. Widenhoefer, *J. Am. Chem. Soc.* **2012**, *134*, 9134–9137.

[9] P. W. Davies and N. Martin, *Org. Lett.* **2009**, *11*, 2293–2296.

1,2-aryl shift took place towards **11**. However, this behavior could also be related to the different dielectric constants.[10]

In other cases, the counterion could also influence in the efficiency of a transformation by increasing the yield towards the desired product or by changing the reaction rate. As an example, the gold-catalyzed hydroarylating aromatization of diyne **14** led to phenylnaphthalenes **15** and **16** when treated with catalysts **17** in benzene at 80 ºC (Scheme 6).[11]

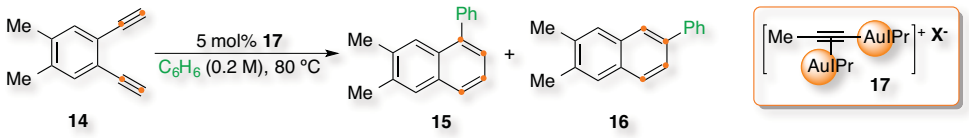

Scheme 6. Gold-catalyzed hydroarylating aromatization.

Very different reaction rates towards 2-phenylnaphthalene **16** were observed when changing the counterion of catalyst **17**. Monitoring the transformation with the different complexes showed great effiency for PF_6^- (Figure 3).

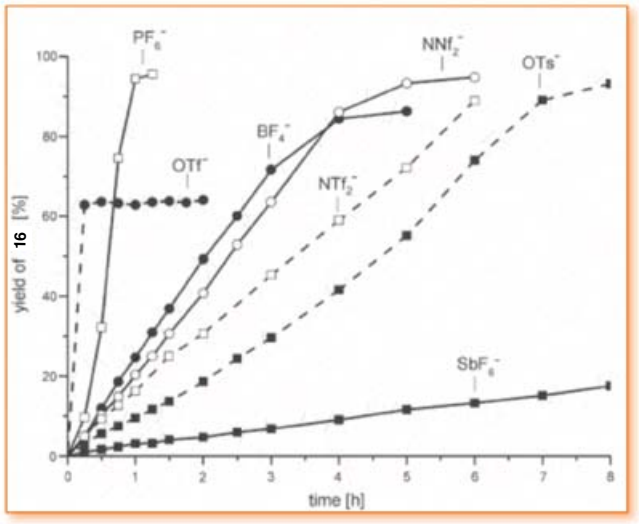

Figure 3. Reaction rates depending on the counterion of the catalyst 17.

Slightly lower reaction rates were detected for BF_4^- or NNf_2^-. NTf_2^- and TsO^- still led to acceptable results, and very a slow conversion was detected for SbF_6^-. Very fast transformation was observed for TfO^- but the reactivity drastically stopped around 60% yield.

[10] V. M. Lau, C. F. Gorin and M. W. Kanan, *Chem. Sci.* **2014**, DOI: 0.1039/C4SC02058H.
[11] A. S. K. Hashmi, T. Lauterbach, P. Nösel, M. H. Vilhelmsen, M. Rudolph and F. Rominger, *Chem. –Eur. J.* **2013**, *19*, 1058–1065.

Furthermore, important anion effects were observed in the enantioselectivity of several gold-catalyzed reactions.[12] As an example, the hydroamination of allenes, **18** to **19**, proceeded in very good yields when the cyclization was performed with *(R)*-xylylBINAP as the gold ligand in nitromethane at 50 ºC (Scheme 7).[13]

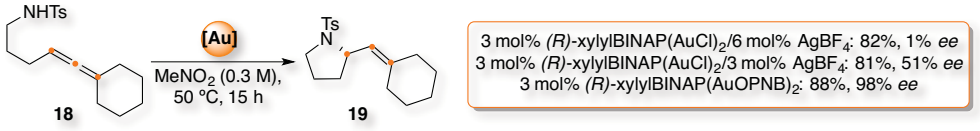

Scheme 7. Counterion-mediated enantioselective gold-catalyzed hydroamination of allenes.

However, the enatioselectivity of the reaction towards **19** was increased from 1 to 51% *ee* when 3 mol% of $AgBF_4$ instead of 6 was added. Noteworthy, when *p*-nitrobenzoate ($PNBO^-$) was used as the counterion of the gold complex, the enantioselectivity of **19** increased to 98% *ee*. A detailed mechanistic study, based on DFT calculations, showed an important interaction between the substrate and the anion *via* hydrogen bonding, which explained the large effect in the enantioselectivity of the process.

Later on, the development and study of new weakly coordinating anions was expanded.[14] These structures allowed the formation of highly soluble complexes due to the ion size prone to stabilize low charge species. These properties, along with the weak basicity and the stability in front of oxidation, formed robust Lewis acid-base adducts $[(L)_nM]^+X^-$.

The interionic structure of several (π-alkyne)gold(I) ion pairs (**20**) was studied by ^1H-^{19}F HOESY NMR spectroscopy combined with DFT calculations.[15] In all cases, the counterion was located close to the substrate but the specific distance strongly depended on the ligand on the metal. A new methodology, derived from diffusion NMR experiments and conductometry, was developed to determine the hydrodynamic volume of single ions as well as ion pairs.[16] This showed that complexes bearing poorly electron donating ligands as **21** formed stronger ion pairs whereas lower interactions were observed for strongly electron donating ligands as **23** (Figure 4).

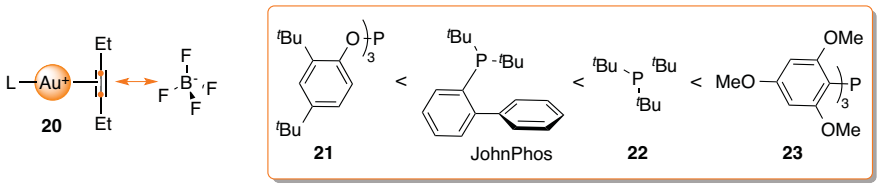

Figure 4. Distances between the anion and the substrate depending on the ligand.

[12] For selected examples see: *(a)* G. L. Hamilton, E. J. Kang, M. Mba and F. D. Toste, *Science* **2007**, *317*, 496–499; *(b)* K. Aikawa, M. Kojima and K. Mikami, *Angew. Chem. Int. Ed.* **2009**, *121*, 6189–6193; *(c)* K. Aikawa, M. Kojima and Koichi Mikami, *Adv. Synth. Catal.* **2010**, *352*, 3131–3135; *(d)* K. L. Butler, M. Tragni and R. A. Widenhoefer, *Angew. Chem. Int. Ed.* **2012**, *51*, 5175–5178.
[13] J. H. Kim, S. W. Park, S. R. Park, S. Lee and E. J. Kang, *Chem. –Asian J.* **2011**, *6*, 1982–1986.
[14] I. Krossing and I. Raabe, *Angew. Chem. Int. Ed.* **2004**, *43*, 2066–2090 and references cited therein.
[15] G. Ciancaleoni, L. Belpassi, F. Tarantelli, D. Zuccaccia and A. Macchioni, *Dalton Trans.* **2013**, *42*, 4122–4131.
[16] G. Ciancaleoni, C. Zuccaccia, D. Zuccaccia and A. Macchioni, *Organometallics* **2007**, *26*, 3624–3626.

These results were rationalized claiming that the electronic properties of the ligand finely tuned the charge accumulation on the alkyne and, consequently, its ability of attracting the anion.

Finally, when the same study was performed for NHC carbene ligands, it was observed that the position of that anion could be radically different.[17] Thus, BF_4^- was placed next to the substrate in complex $[Ph_3PAu(\eta^2\text{-alkene})]^+$ **24** but on the other side of the ligand in complex $[IPrAu(\eta^2\text{-alkene})]^+$ **25** (Figure 5).

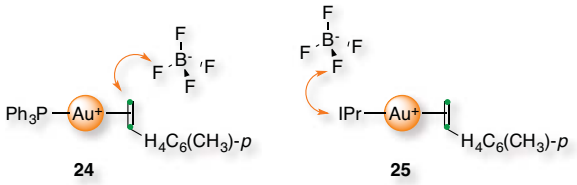

Figure 5. Distinct positions of the anion depending on the ligand.

[17] D. Zuccaccia, L. Belpassi, F. Tarantelli and A. Macchioni, *J. Am. Chem. Soc.* **2009**, *131*, 3170–3171.

2. Objectives

In this context, we focused on tuning the catalyst structure to minimize the generation of digold(I) complexes such as **7** during an intermolecular transformation, which are dead-ends of the catalytic cycle. In the cycloadditions involving alkynes, we reasoned that the use of more bulky, non-coordinating and less basic couterions could slow down the deprotonation and hamper the formation of the σ-acetylide gold(I) intermediates. Hence, we designed the synthesis of new gold complexes using $BAr^{F}_{4}^{-}$ as the anion, for example, **Q** or **R** bearing ^{t}BuXPhos and IPr ligands, respectively (Figure 6).

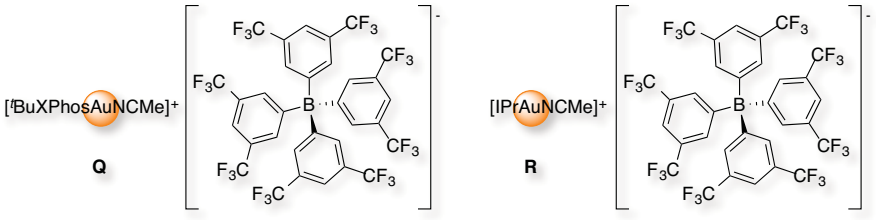

Figure 6. New gold(I) complexes using $BAr^{F}_{4}^{-}$.

We also performed a mechanistic study of the intermolecular [2+2] cycloaddition of alkynes with alkenes in order to further understand the influence of the counterion on the reactivity of these processes.

3. Synthesis and Reactivity of New Catalysts

Anion Effect in the [2+2] Cycloaddition

The [2+2] cycloaddition of alkynes with alkenes towards cyclobutene **1** was originally developed using catalyst **E** (Scheme 1).[4] As expected, the ligand had a strong influence on the selectivity but we decided to examine also the effect of changing the counterion (Table 1). The reaction was performed between ethynylbenzene and 2 equiv. of α-methylstyrene under the optimized conditions. We synthesized successfully gold complex **Q** from the corresponding chloride and $NaBAr^F_4$ in 97% isolated yield as well as complexes bearing BF_4^- (**S**) and PF_6^- (**T**). Thus, we could observe notable differences between them in the synthesis of cyclobutene **1**. Replacement of SbF_6^- by $BAr^F_4^-$ led to an increase of the isolated yield from 80 to 95% (entries 1 and 2).

Table 1. Screening of anions in the [2+2] cycloaddition.

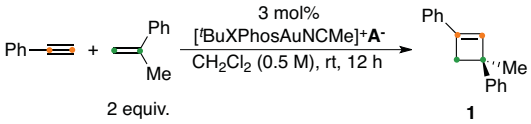

Entry	A^-	Yield[a]
1	SbF_6^-	80%
2	$BAr^F_4^-$	95%
3	BF_4^-	62%
4	PF_6^-	19%
5[b]	NTf_2^-	26%
6[b]	TfO^-	18%

[a]Crude analyzed by ^{1}H NMR spectroscopy using 1,4-diacetylbenzene as internal standard, yields referred to cyclobutene **1**. [b]Catalysts generated *in situ* with ^{t}BuXPhosAuCl and the corresponding silver salts.

The use of BF_4^- gave **1** in lower but still acceptable yield (entry 3). However, more coordinating couterions as NTf_2^- or TfO^- afforded the [2+2] cycloaddition product very inefficiently (entries 5 and 6). Surprisingly, the use of PF_6^- formed cyclobutene **1** only in 19% yield (entry 4).

These results suggested that the anion has a significant effect in this reaction. Therefore, we examined the scope of the improvement achieved with gold complex **Q**. The [2+2] cycloaddition between different terminal alkynes with α-methylstyrene towards cyclobutenes such as **26** was performed changing SbF_6^- by $BAr^F_4^-$ (Table 2). In most cases, yields using $BAr^F_4^-$ were 10 – 30% higher (Table 2), with the exception of MeO-substituted alkynes (entries 6, 14 and 24) and with 3-thienyl alkyne (entry 26). Moreover, in the case of the cyclopropyl ring, a lower yield was obtained (entry 28).

Table 2. Alkyne scope in the [2+2] cycloadditon.[a]

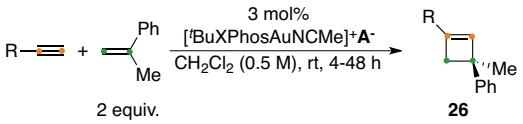

Entry	R-	A^-	Product	Yield[b]
1	Ph-	SbF_6^-	**1**	80%
2		$BAr^F{}_4^-$	**1**	95%
3	*p*-Tol-	SbF_6^-	**27**	74%
4		$BAr^F{}_4^-$	**27**	86%
5	*p*-$MeOC_6H_4$-	SbF_6^-	**28**	68%
6		$BAr^F{}_4^-$	**28**	64%
7	*p*-FC_6H_4-	SbF_6^-	**29**	75%
8		$BAr^F{}_4^-$	**29**	84%
9	*p*-ClC_6H_4-	SbF_6^-	**30**	61%
10		$BAr^F{}_4^-$	**30**	91%
11	*p*-BrC_6H_4-	SbF_6^-	**31**	74%
12		$BAr^F{}_4^-$	**31**	97%
13	*m*-$MeOC_6H_4$-	SbF_6^-	**32**	80%
14		$BAr^F{}_4^-$	**32**	78%
15	*m*-Tol-	SbF_6^-	**33**	78%
16		$BAr^F{}_4^-$	**33**	91%
17	*m*-HOC_6H_4-	SbF_6^-	**34**	74%
18		$BAr^F{}_4^-$	**34**	98%
19	*m*-FC_6H_4-	SbF_6^-	**35**	67%
20		$BAr^F{}_4^-$	**35**	77%
21	*m*-ClC_6H_4-	SbF_6^-	**36**	60%
22		$BAr^F{}_4^-$	**36**	83%
23	*o*-$MeOC_6H_4$-	SbF_6^-	**37**	30%
24		$BAr^F{}_4^-$	**37**	24%
25	3-Thienyl-	SbF_6^-	**38**	84%
26		$BAr^F{}_4^-$	**38**	86%
27	Cyclopropyl-	SbF_6^-	**39**	46%
28		$BAr^F{}_4^-$	**39**	35%

[a]These experiments were performed by Anna Homs. [b]Isolated yields.

Cyclobutene **1** could also be obtained in 95% yield by performing the reaction with complex **Q** on a larger scale (2.00 mmol). Furthermore, generating the catalyst *in situ* by mixing ^{t}BuXPhosAuCl and $NaBAr^F{}_4$ did not affect the yield.

We attempted the [2+2] cycloaddition between novel alkynes and α-methylstyrene using catalyst **Q**. However, very complex mixtures were obtained for *o*-methylethynylbenzene, (bromoethynyl)benzene and ethynyltrimethylsilane (Figure 7). Only 11% of the cyclobutene product was detected for the 1,3-enyne 2-methylut-1-n-3-yne. And, in the case

of non-terminal alkynes, no reaction was observed for hex-3-yne, 1,2-diphenylethyne or prop-1-yn-1-ylbenzene.[18]

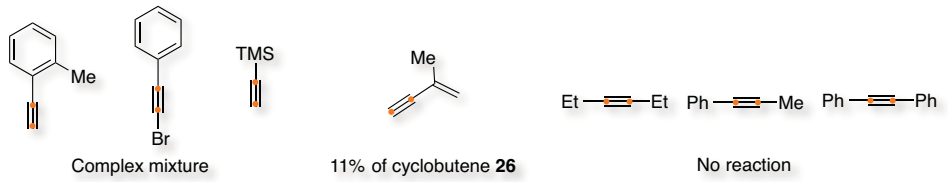

Figure 7. Expansion of the alkyne scope.

Improved yields were also obtained in general when ethynylbenzene was used with different alkenes to cyclobutenes **40** (Table 3). In these cases, the improvement ranged from 5 to 20% isolated yields. The reaction was also extended to allylsilanes (entries 5 and 6), allyl ethers (entries 7 and 8) and allylsilyl ethers (entries 9 and 10).

Table 3. Alkene scope of the [2+2] cycloaddition.[a]

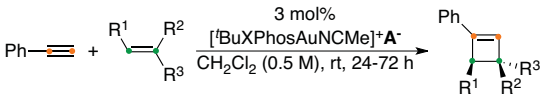

Entry	Alkene	A^-	Product	Yields
1		SbF_6^-	**41**	74%[b]
2		$BAr^F{}_4^-$	**41**	79%[b]
3		SbF_6^-	**42**	53%[b]
4		$BAr^F{}_4^-$	**42**	69%[b]
5	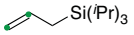	SbF_6^-	**43**	48%[c]
6		$BAr^F{}_4^-$	**43**	71%[c]
7		SbF_6^-	**44**	26%[c]
8		$BAr^F{}_4^-$	**44**	31%[c]
9		SbF_6^-	**45**	21%[c]
10		$BAr^F{}_4^-$	**45**	31%[c]

[a]These experiments were performed by Anna Homs. [b]Isolated yields. [c]Crude analyzed by ^{1}H NMR spectroscopy using 1,4-diacetylbenzene as internal standard, yields referred to cyclobutenes **40**.

Finally, the yield of the gold-catalyzed macrocyclization of 1,14-enyne **46** to form the 13-membered derivative **47** was also improved from 57% isolated yield when using SbF_6^- to 82% with $BAr^F{}_4^-$ maintaining the optimized conditions (Scheme 8).[19]

[18] For examples of gold complexes with substituted alkynes see: *(a)* N. D. Shapiro and F. D. Toste, *Proc. Natl. Acad. Sci. USA* **2008**, *105*, 2779–2782; *(b)* S. Flügge, A. Anoop, R. Goddard, W. Thiel and A. Fürstner, *Chem. – Eur. J.* **2009**, *15*, 8558–8565; *(c)* T. J. Brown and R. A. Widenhoefer, *J. Organomet. Chem.* **2011**, *696*, 1216–1220.
[19] C. Obradors and A. M. Echavarren, *Org. Lett.* **2013**, *15*, 1576–1579.

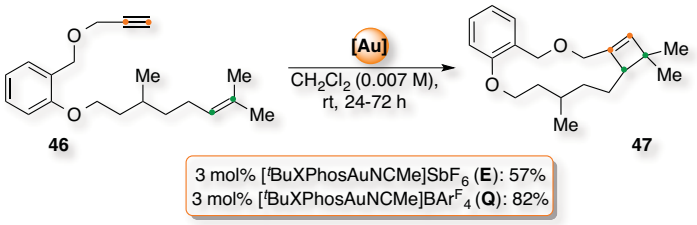

Scheme 8. Improved macrocyclization of 1,14-enyne 46.

Expansion to Other Transformations

At the same time, the intermolecular gold-catalyzed synthesis of phenols **48** from terminal alkynes and an excess of furans, using IPr as ligand, was developed in CH_2Cl_2 at 25 ºC (Table 4).[20] Thus, the cycloaddition proceeded under very mild conditions and with moderate to good yields when using [IPrAuNCMe]SbF_6 (**C**). Then, the yields increased up to 36% for catalyst **R** bearing $BAr^F{}_4^-$ (entry 4).

Table 4. Gold-catalyzed synthesis of phenols 48.[a]

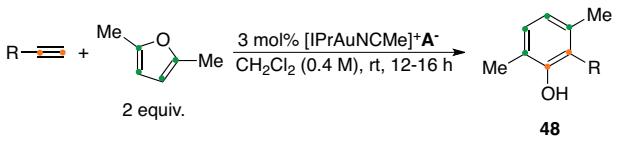

Entry	R-	A^-	Product	Yield[b]
1	Ph-	SbF_6^-	**49**	70%
2		$BAr^F{}_4^-$	**49**	85%
3	*p*-ClC_6H_4-	SbF_6^-	**50**	50%
4		$BAr^F{}_4^-$	**50**	86%
5	*m*-$MeOC_6H_4$-	SbF_6^-	**51**	77%
6		$BAr^F{}_4^-$	**51**	85%
7[c]	*p*-$NO_2C_6H_4$-	SbF_6^-	**52**	37%
8		$BAr^F{}_4^-$	**52**	66%
9	*o*-BrC_6H_4-	SbF_6^-	**53**	45%
10		$BAr^F{}_4^-$	**53**	76%

[a]These experiments were performed by Núria Huguet and Dr. David Leboeuf. [b]Isolated yields. [c]2,5-Dimethyl-3-(1-(4-nitrophenyl)vinyl)furan formed as a side-product.

Therefore, both the [2+2] cycloaddition and the synthesis of phenols followed the same trend when using $BAr^F{}_4^-$. We also examined its influence in the [2+2+2] cycloaddition of alkynes with oxoalkenes.[5] We performed the reaction between ethynylbenzene and 5-methylhex-5-en-2-one towards the oxabicycle **54** under the optimized conditions screening different counterions (Table 5). In this case, very similar results were obtained with SbF_6^- and $BAr^F{}_4^-$ (Table 5). Moderate yields were observed for BF_4^- and NTf_2^- and only traces of oxabicycle **54** were detected with TfO^-.

[20] N. Huguet, D. Leboeuf and A. M. Echavarren, *Chem. –Eur. J.* **2013**, *19*, 6581–6585.

Table 5. Screening of anions in the [2+2+2] cycloaddition.

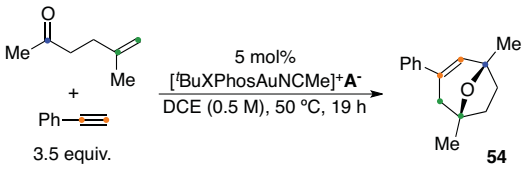

Entry	A^-	Yield[a]
1	SbF_6^-	68%
2	$BAr^F{}_4^-$	72%
3	BF_4^-	43%
5[b]	NTf_2^-	40%
6[b]	TfO^-	3%

[a]Crude analyzed by ^{1}H NMR spectroscopy using 1,4-diacetylbenzene as internal standard, yields referred to oxabicycle **54**. [b]Catalysts generated *in situ* with ^{t}BuXPhosAuCl and the corresponding silver salts.

Furthermore, we analysed the effect of other parameters of the reaction combined with $BAr^F{}_4^-$ (Table 6). Use of JohnPhos and IPr as ligands led to lower yields although they also improved with respect of SbF_6^- (entries 1 to 4). Use of 3 instead of 5mol% of catalyst **Q** dropped the yield to 52% (entry 5).

Table 6. Effect of other parameters.[a]

Entry	Modification	A^-	Yield[b]
1	JohnPhos	SbF_6^-	15%
2	JohnPhos	$BAr^F{}_4^-$	33%
3	IPr	SbF_6^-	15%
4	IPr	$BAr^F{}_4^-$	27%
5	3 mol%	$BAr^F{}_4^-$	52%
6	25 ºC	$BAr^F{}_4^-$	22%
7	1 equiv.	$BAr^F{}_4^-$	38%
8	0.25 equiv.	SbF_6^-	13%
9	0.25 equiv.	$BAr^F{}_4^-$	12%

[a]Continuation of Table 5. [b]Crude analyzed by ^{1}H NMR spectroscopy using 1,4-diacetylbenzene as internal standard, yields referred to oxabicycle **54**.

Decreasing the temperature to 25 ºC formed the oxabicycle **54** only in 22% yield (entry 6). Finally, performing the reaction with 1 equivalent of ethynylbenzene led to 38% yield and with an excess of oxoalkene only to 12%, which was already observed for SbF_6^- (entries 7, 8 and 9).

We examined the anion effect in the [2+2+2] cycloaddition between different alkynes with 5-methylhex-5-en-2-one towards **55** under the optimized conditions comparing SbF_6^- and $BAr^F{}_4^-$ with catalyst **E** and **Q** (Table 7). In most of the examples, the yields varied very little (Table 7). A significant improvement was observed for *p*-chloroethynylbenzene and

m-ethynylphenol (entries 4 and 12). However, a drop of the yield was observed for *o*-ethynyltoluene (entries 22).

Table 7. Alkyne scope of the [2+2+2] cycloaddition.

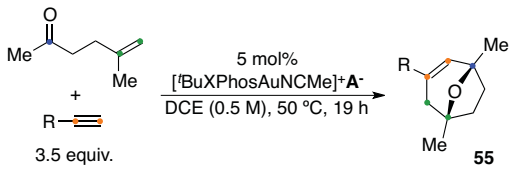

Entry	R-	A^-	Product	Yield[a,b]
1	Ph-	SbF_6^-	**54**	68%
2	Ph-	$BAr^F{}_4^-$	**54**	72%
3	*p*-ClC_6H_4-	SbF_6^-	**56**	51%
4	*p*-ClC_6H_4-	$BAr^F{}_4^-$	**56**	62%
5	*p*-BrC_6H_4-	SbF_6^-	**57**	49%
6	*p*-BrC_6H_4-	$BAr^F{}_4^-$	**57**	53%[c] (85%)
7	*p*-Tol-	SbF_6^-	**58**	55%
8	*p*-Tol-	$BAr^F{}_4^-$	**58**	40%[c] (80%)
9	*p*-FC_6H_4-	SbF_6^-	**59**	68%
10	*p*-FC_6H_4-	$BAr^F{}_4^-$	**59**	68%[c] (83%)
11	*m*-HOC_6H_4-	SbF_6^-	**60**	65%
12	*m*-HOC_6H_4-	$BAr^F{}_4^-$	**60**	81%
13	*m*-Tol-	SbF_6^-	**61**	70%
14	*m*-Tol-	$BAr^F{}_4^-$	**61**	72%
15	*m*-FC_6H_4-	SbF_6^-	**62**	49%
16	*m*-FC_6H_4-	$BAr^F{}_4^-$	**62**	49%[c]
17	*m*-ClC_6H_4-	SbF_6^-	**63**	55%
18	*m*-ClC_6H_4-	$BAr^F{}_4^-$	**63**	54%[c] (95%)
19	3-Thihenyl-	SbF_6^-	**64**	40% (79%)
20	3-Thihenyl-	$BAr^F{}_4^-$	**64**	41%[c] (56%)
21	*o*-Tol-	SbF_6^-	**65**	41% (100%)
22	*o*-Tol-	$BAr^F{}_4^-$	**65**	26%[c] (86%)
23	*p*-$MeOC_6H_4$-	SbF_6^-	**66**	13%[c] (100%)
24	*p*-$MeOC_6H_4$-	$BAr^F{}_4^-$	**66**	13%[c] (100%)
25[d]	*p*-$MeOC_6H_4$-	SbF_6^-	**66**	43% (100%)
26[d]	*p*-$MeOC_6H_4$-	$BAr^F{}_4^-$	**66**	8%[c] (100%)

[a]Isolated yields. [b]Conversion in brackets, 100% if not stated. [c]Crude analyzed by ^1H NMR spectroscopy using 1,4-diacetylbenzene as internal standard, yields referred to oxabicycle **55**. [d]Switched reaction stoichiometry.

In the case of *p*-methoxyethynylbenzene, the same result was obtained with the standard excess but no improvement was observed when switching the stoichiometry of the reaction (entries 23/24 and 25/26). Therefore, the improvement was moderate for this more challenging cascade transformation. In general, a lower reaction conversion was observed, presumably as a result of a faster catalyst decay with $BAr^F{}_4^-$ than with SbF_6^-.

Finally, we tested the catalytic activity of LAuCl/$NaBAr^F_4$ with several known intramolecular transformations. In the gold-catalyzed single cleavage rearrangement of 1,6-enyne **67** at 25 ºC in CH_2Cl_2, the cyclized product **68** and its isomer **69** were obtained in 67% yield (1:1.4) for SbF_6^- and 85% (11:1) for $BAr^F_4^-$ (Scheme 9).[21] Thus, both the yield and the selectivity were improved under these conditions.

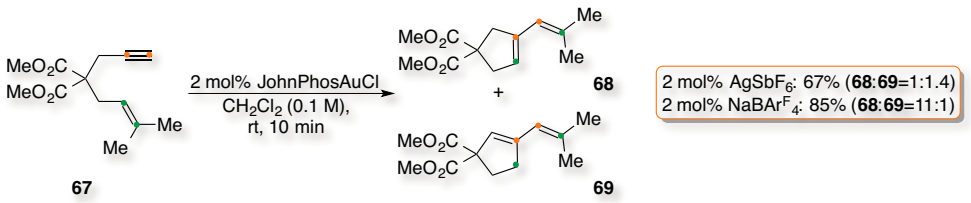

Scheme 9. Gold-catalyzed single cleavage rearrangement of 67.

Later, dienyne **70** cyclized using Ph_3PAuCl *via* the intramolecular cyclopropanation of the corresponding cyclopropyl gold carbene intermediate (Scheme 10).[22] The reaction was performed at – 30 ºC for 20 min and tetracycle **71** was obtained quantitavely with SbF_6^- and in 63% yield with $BAr^F_4^-$. This transformation using PPh_3 as the phosphine ligand was not more efficient by changing the counterion.

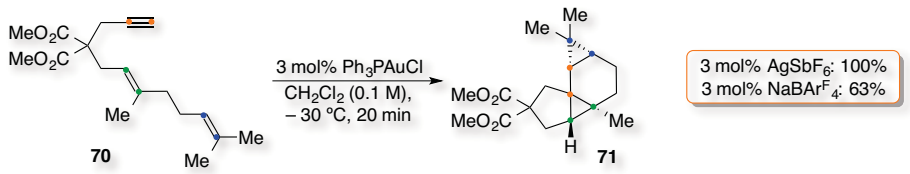

Scheme 10. Cascade cyclization of dienyne 70.

Furthermore, we attempted the [4+2] cyclization of enyne **72** using phosphite **21** gold chloride under mild conditions to afford the tricyclic structure **73** (Scheme 11).[6a] Interestingly, the reaction proceeded in very good yield with SbF_6^- but no reaction was observed when $BAr^F_4^-$ was used.

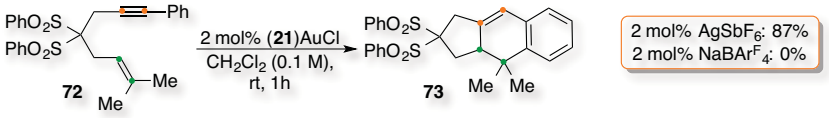

Scheme 11. [4+2] Cycloaddition of enyne 72.

[21] C. Nieto-Oberhuber, M. P. Muñoz, E. Buñuel, C. Nevado, D. J. Cárdenas and A. M. Echavarren, *Angew. Chem. Int. Ed.* **2004**, *34*, 2402–2406.
[22] C. Nieto-Oberhuber, S. López, M. P. Muñoz, E. Jiménez-Núñez, E. Buñuel, D. J. Cárdenas and A. M. Echavarren, *Chem. –Eur. J.* **2006**, *12*, 1694–1702.

We reasoned that the sodium salt could not abstract the chloride from this gold complex, which would impede the generation of the active species. However, catalyst (**21**)AuCl could cyclize cycloheptatriene **74** to indene **75** using SbF_6^- or $BAr^F{}_4^-$ with the same efficiency (Scheme 12).[23] The reaction proceeded quantitavely in toluene at 0 ºC *via* a complex mechanism through a gold-barbaralyl cation.

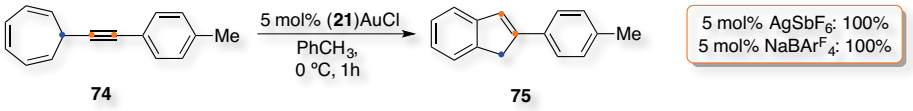

Scheme 12. Cyclization of cycloheptatriene 74.

[23] P. R. McGonigal, C. de León, Y. Wang, A. Homs, C. R. Rogelio and A. M. Echavarren, *Angew. Chem. Int. Ed.* **2012**, *51*, 13093–13096.

4. Kinetic Study of the [2+2] Cycloaddition

Monitoring of the Transformation

Subsequently, we decided to study the particular involvement of the counterion in the [2+2] cycloaddition of alkynes and alkenes. According to the previous theoretical work,[6] the catalytic cycle was expected to proceed by a rate-determining attack of the electron-rich alkene to the (π-alkyne)gold complex **6** forming the cyclopropyl gold carbene **5**/**5´** (Scheme 13). Then, the ring expansion would occur leading to benzylic carbocation **76**, which would form the coordinated cyclobutene **77** after demetallation. A presumably associative ligand exchange with ethynylbenzene would close the catalytic cycle to cyclobutene **1** and complex **6**.

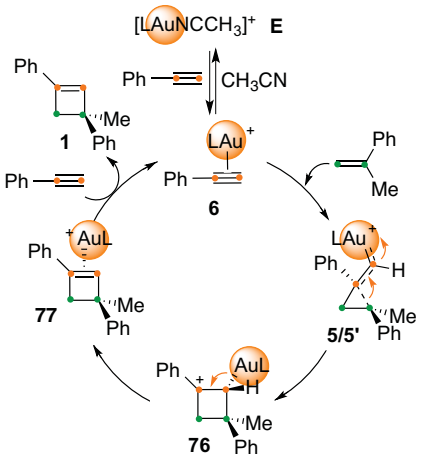

Scheme 13. Initial proposal for the [2+2] cycloaddition (L=^{t}BuXPhos).

However, this approach did not contemplate the formation of digold complexes **7** and did not explain the counterion effect observed.[5] Therefore, we monitored the [2+2] cycloaddition by ^{1}H NMR spectroscopy using ethynylbenzene and α-methylstyrene under the optimized conditions, along with diphenylmethane as internal standard (Scheme 14).

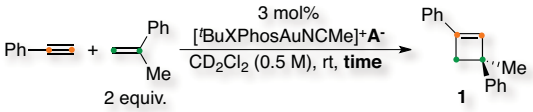

Scheme 14. Kinetic study of the [2+2] cycloaddition.

We performed these experiments using SbF_6^- (**E**), $BAr^F{}_4^-$ (**Q**) and BF_4^- (**S**). The results confirmed a great dependence on the anion (Figure 8). Beside the differences in the final yields, the reaction rate increased with the bulkiness and the softness of the counterion.

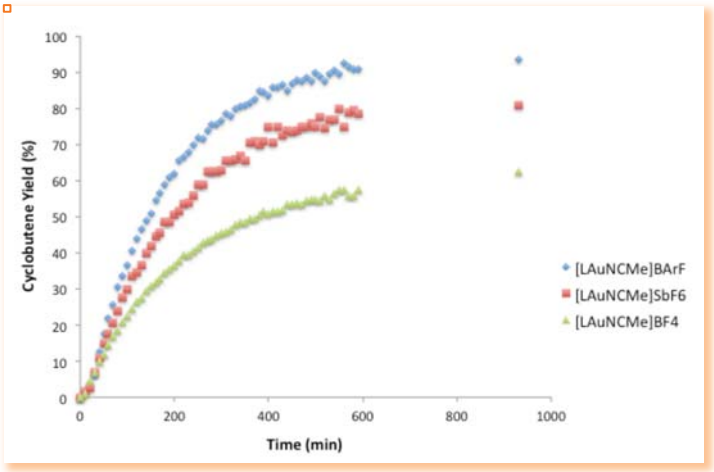

Thus, $BAr^{F}_{4}^{-}$ (**Q**) was faster than SbF_6^- (**E**), which was faster than BF_4^- (**S**). In this case, no intermediates could be detected either, only the starting substrates and the final products could be observed.

Figure 8. Kinetic study of the [2+2] cycloaddition (L=^{t}BuXPhos).

Order of the Reagents

We determined the order of the reagents of the rate equation to gain further insight into the mechanism applying the method of initial rates.[24] In chemical kinetics, the rate of a reaction is proportional to the concentration of each reagent with specific exponents (Equation 1). Therefore, when all the components remain constant except one, it is possible to determine these values right in the beginning of the transformation.

$$A + B \rightarrow C$$
$$v_0 = k \cdot [A]_0^{\,a} \cdot [B]_0^{\,b}$$

$$[B]_0 = Constant$$
$$v_0 = k' \cdot [A]_0^{\,a}$$

Equation 1. Rate equation of a reaction.

Then, when the initial rates (v_0) are determined, it is possible to calculate the order of the reagents by gradually modifying the initial concentration of the substrate ($[A]_0$) and plotting the logarithm of the results (Equation 2).

$$\ln(v_0) = \ln(k') + a \cdot \ln([A]_0)$$

Equation 2. Determination of the order of the reagents.

The initial rates can be measured as the variation of the product concentration in time when the conversion is smaller than 10-15% (Equation 3).

[24] K. A. Connors, *Chemical Kinetics, the Study of Reaction Rates in Solution* **1991**, VCH Publishers.

$$v_0 = \frac{d[C]}{dt} \; where \; [C] \sim 10 - 15\%$$

Equation 3. Determination of the initial rate.

Thus, we monitored the [2+2] cycloaddition between ethynylbenzene and α-methylstyrene using catalyst **Q** under the optimized conditions in CD_2Cl_2 by ^1H NMR spectroscopy with dipheylmethane as internal standard (Scheme 15). Methods using IR, GC or HPLC led to less reliable results.

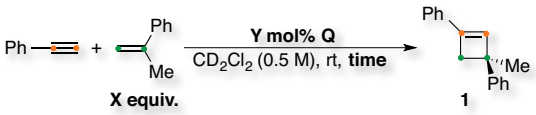

Scheme 15. Method of the initial rates.

To start, we used 0.50 mmol of alkene together with 7.2 μmol of catalyst in 0.56 mL of CD_2Cl_2 varying the quantities of ethynylbenzene and we determined the formation of cyclobutene **1** with time (Figure 9). We could observe that the reaction was faster by increasing the initial amount of ethynylbenzene.

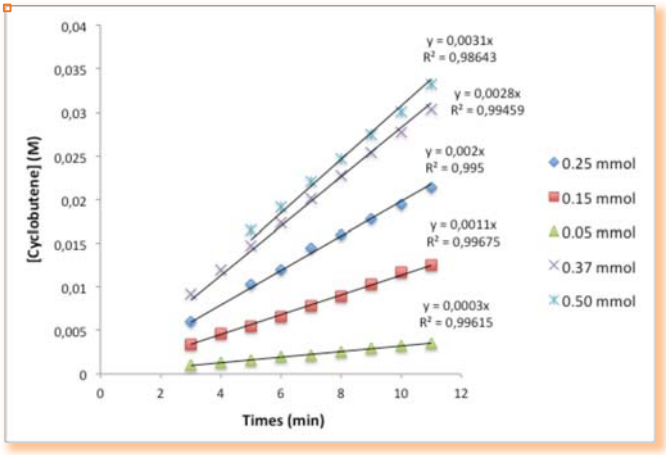

Figure 9. Variation of the alkyne.

Then, we performed the reaction with 0.25 mmol of alkyne and modifying the excess of α-methylstyrene (Figure 10). Although it was assumed that the nucleophilic attack of the alkene towards the activated alkyne was the rate-determining step of the process, the effect of α-methylstyrene was almost non-existent.

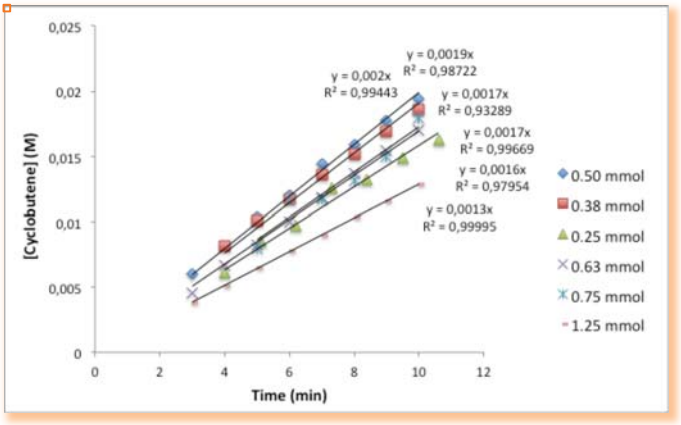

Figure 10. Variation of the alkene.

Finally, we kept 0.25 mmol of ethynylbenzene and 0.50 mmol of α-methylstyrene in order to determine the effect of the catalyst loading (Figure 11). In this case, the differences in the formation of cyclobutene **1** were significant.

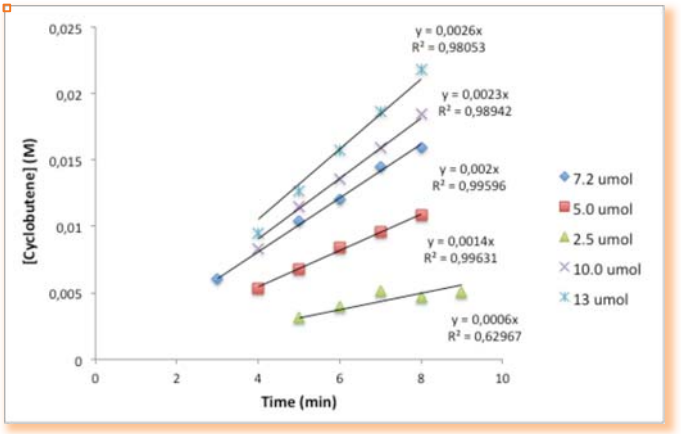

Figure 11. Variation of the catalyst.

With these results and according to the method described, we plotted the initial rates depending on the initial concentration of each substrate (Figure 12). We could observe first order for both ethynylbenzene and for catalyst **Q**, whereas the reaction showed zero order dependence for α-methylstyrene. This result contradicted the initial proposal, which involved the alkene in the rate-determining step of the catalytic cycle.

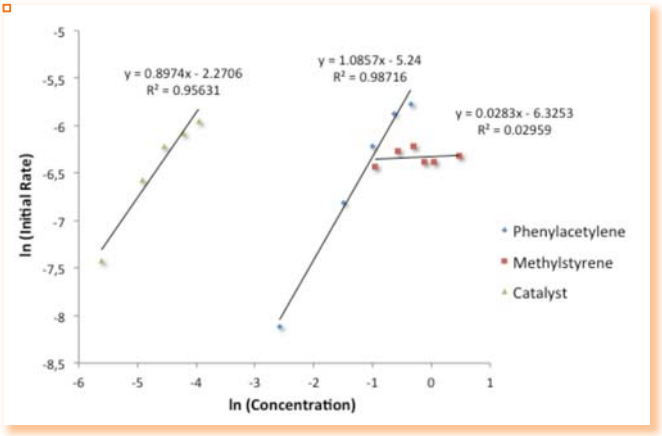

Figure 12. Order of the reagents in the [2+2] cycloaddition.

Furthermore, to confirm these results, we performed a kinetic experiment studying the effect of the ratio alkene:alkyne under the optimized conditions (Scheme 16).

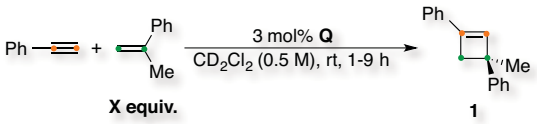

Scheme 16. Kinetic study depending on the stoichiometry.

Thus, the [2+2] cycloaddition between ethynylbenzene and α-methylstyrene was monitored by ^{1}H NMR spectroscopy using dipheylmethane as internal standard. The rate of cyclobutene **1** formation was compared with the ratio alkene:alkyne using 5:1, 2:1 and 5:2 as examples (Figure 13). We could observe that the rate between the two first experiments was almost the same but they showed a significant difference with the last one, therefore, the rate of the [2+2] cycloaddition did not depend on the concentration of α-methylstyrene.

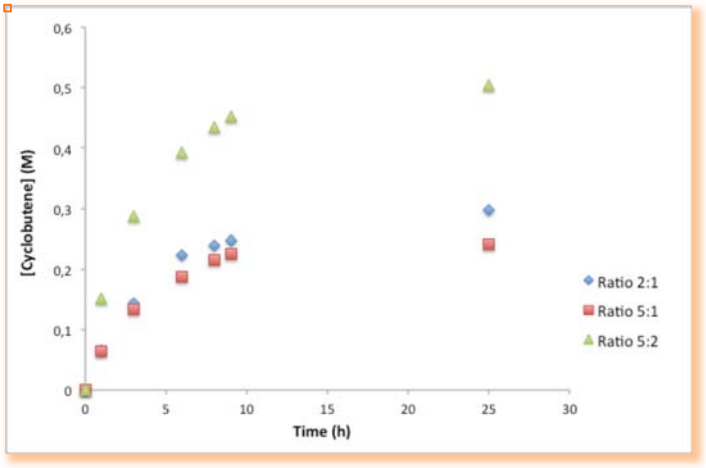

Figure 13. Kinetic study depending on the stoichiometry.

Accordingly, further studies were necessary to resolve the formation of cyclobutene **1** as the kinetic experiments showed a more complicated scenario than the DFT calculations had provided (Scheme 13).[4]

5. Involvement of Digold Complexes

Crystallization of Intermediates

Analysis of the reaction mixture by ^{31}P NMR spectroscopy showed a digold scaffold analogous to **7**, along with another new gold(I) complex. Crystallization of the reaction mixture with pentane led to [(^{t}BuXPhosAu)$_2$CCPh]BAr$^F{}_4$ (**78**) together with (π-alkene)gold(I) complex **79** (Figures 14 and 15, respectively).

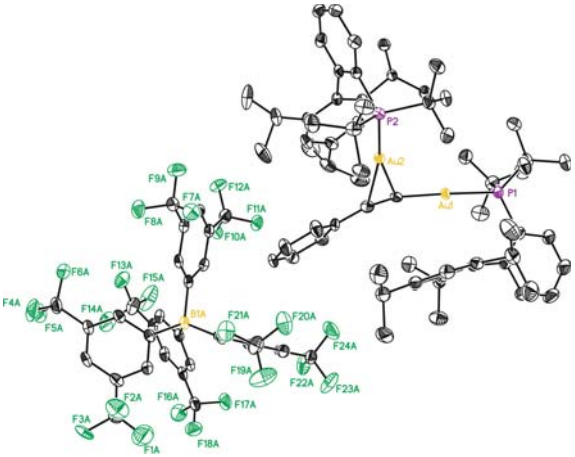

Figure 14. X-Ray crystal structure of digold complex 78.

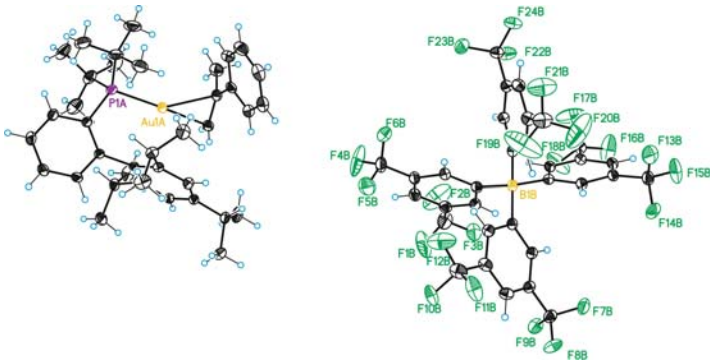

Figure 15. X-Ray crystal structure of (π-alkene)gold complex 79.

The main divergence between digold complex with SbF_6^- **7** (Figure 16, see **Chapter 3** for further information) and structure **78** in the solid state was the radically different position of the counterions. Whereas SbF_6^- was located between both gold atoms bending slightly the cation entity, BAr$^F{}_4^-$ was located alongside the ethynylbenzene moiety in the same plane. Thus, the angle of the π-coordinated gold(I) atom, the alkyne and the counterion was 130.3º for BAr$^F{}_4^-$ and 77.3º for SbF_6^- leading to rather significantly distinct distances with the metal: Au–B was 10.22Å while Au–Sb was 8.23Å. On the other hand, the angle with the σ-gold(I) atom was 210.0º for BAr$^F{}_4^-$ and 60.6º for SbF_6^- leading even more different distances: Au–B was 11.52Å and Au–Sb, 7.34Å.

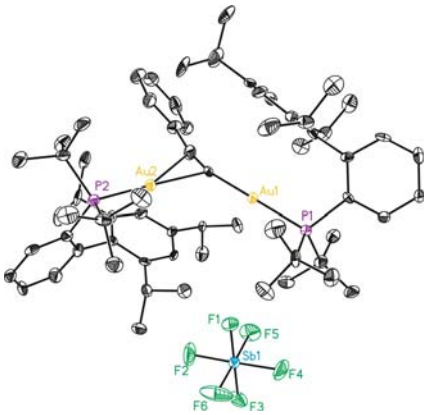

Figure 16. X-Ray crystal structure of digold complex 7

To recapitulate, the digold complex as well as the (π-alkene)gold coordination were observed during the monitoring of the [2+2] cycloaddition when using $BAr^F_4^-$ (**78** and **79**, respectively) but also with SbF_6^- (**7** and **80**, respectively) and BF_4^- (**81** and **82**, respectively).[25] Nevertheless, the ratios changed dramatically with the counterion: [**80**]/[**7**] (SbF_6^-) dropped to 30 from [**79**]/[**78**] = 115 ($BAr^F_4^-$) and finally to 4 for [**82**]/[**81**] (BF_4^-). Thus, the ratio between those species grew following a clear trend: $BAr^F_4^- > SbF_6^- > BF_4^-$, resulting in a larger reservoir of the cationic gold(I) species by increasing the bulkiness and the softness of the counterion (Figure 17).

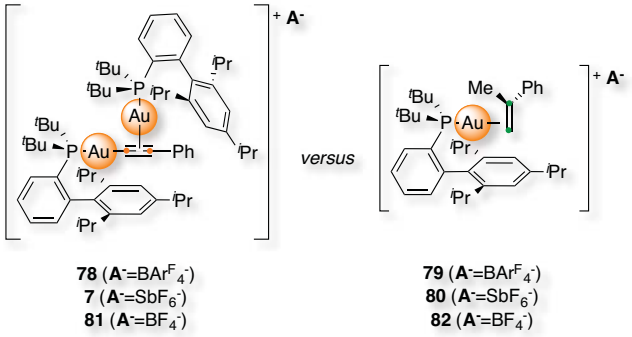

Figure 17. Ratio of the gold species dependant on the counterion.

Moreover, we prepared independently alkynyl gold complex **8** in 99% isolated yield by reaction of the gold chloride with pre-formed lithium phenylacetylide in THF (Scheme 17).

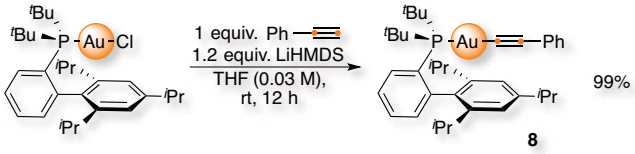

Scheme 17. Synthesis of alkynyl gold complex 8.

Crystallization in pentane showed a neutral structure with Au–C 2.04Å (Figure 18).

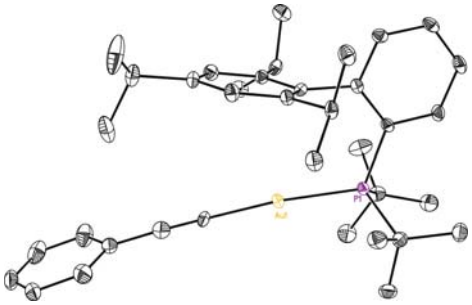

Figure 18. X-Ray crystal structure of alkynyl gold complex 8.

[25] For examples of gold complexes with alkenes see: *(a)* T. J. Brown, M. G. Dickens and R. A. Widenhoefer, *Chem. Commun.* **2009**, 6451–6453; *(b)* T. J. Brown, M. G. Dickens and R. A. Widenhoefer, *J. Am. Chem. Soc.* **2009**, *131*, 6350–6351; *(c)* R. E. M. Brooner, T. J. Brown and R. A. Widenhoefer, *Chem. –Eur. J.* **2013**, 19, 8276–8284.

Low Temperature NMR Experiments

These results suggested that the concentration of the catalytically active species **6** changed with the counterion, which should be higher with more bulky anions as $BAr^F_4^-$ (**83**). In order to study the evolution between the different gold complexes **Q**, **83**, **78** and **8**, we analysed the reaction between 10 equiv. of ethynylbenzene and catalyst **Q** in CD_2Cl_2 (0.04 M) at –78 ºC by ^{31}P NMR spectroscopy (Scheme 18).[8d]

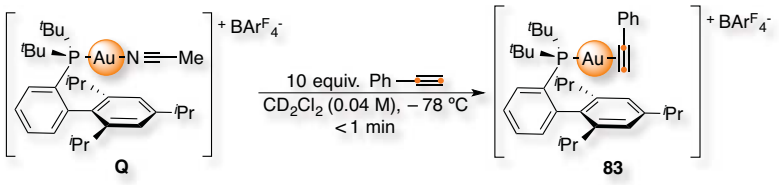

Scheme 18. Study of gold complex 83.

At – 60ºC, complexes **Q** and **83** could be detected but no digold complex **78** was observed (Figure 19). The temperature was increased slowly to 20 ºC while catalyst **Q** was consumed. Digold complex **78** was not observed until 0 ºC and the catalytically active species **83** was clearly observed up to the same temperature. On the other hand, when using SbF_6^-, we could observe complex **7** at – 60 ºC, becoming the only species at – 20 ºC (Figure 20, see **Chapter 3** for further information).[5]

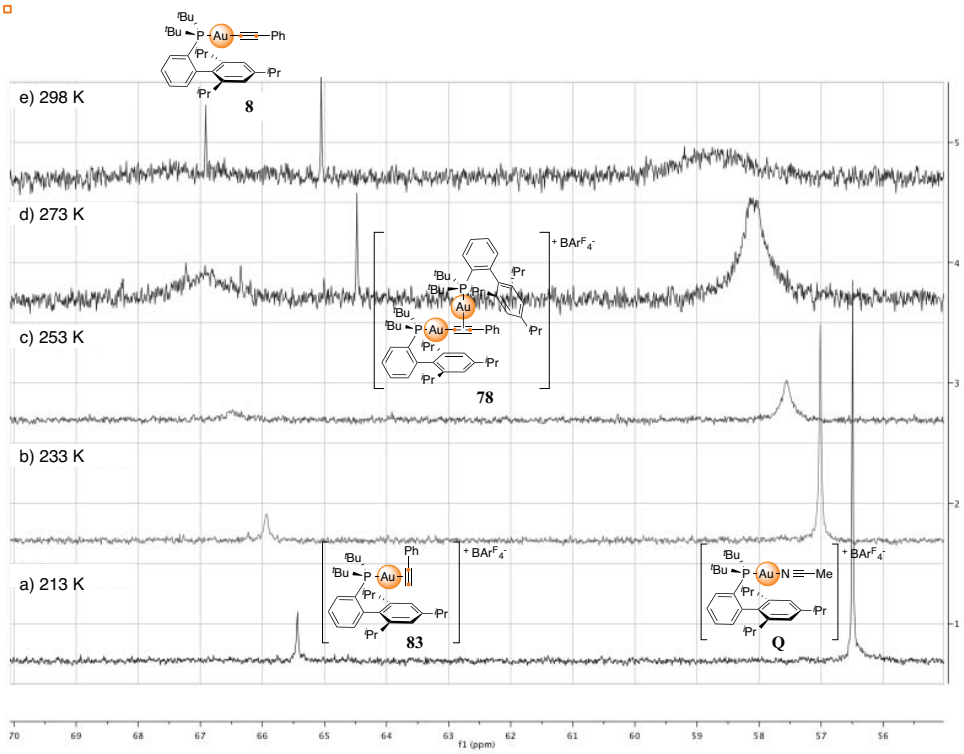

Figure 19. ^{31}P NMR spectroscopy from – 60 to 25 ºC ($BAr^F_4^-$): a) Reaction at 213 K; b) Reaction at 233 K; c) Reaction at 253 K; d) Reaction at 273 K; e) Reaction at 293 K.

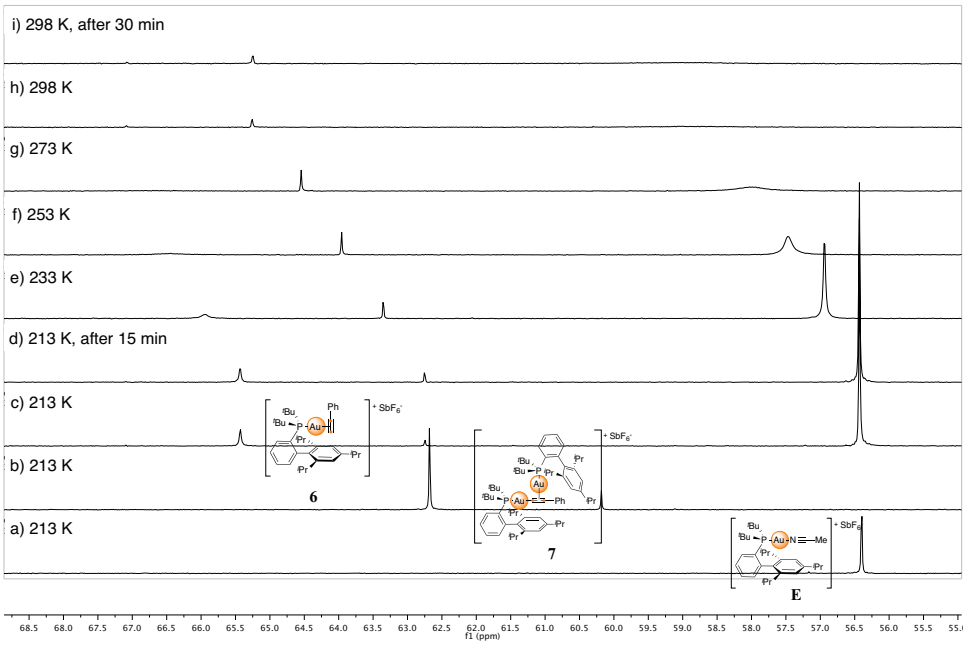

Figure 20. ^{31}P NMR spectroscopy from – 60 to 25 ºC (SbF_6^-): a) Pure E at 213 K; b) Pure 7 at 213 K; c) Reaction at 213 K; d) Reaction at 213 K after 15 min; e) Reaction at 233 K; f) Reaction at 253 K; g) Reaction at 273 K; h) Reaction at 298 K; i) Reaction at 298 K after 30 min.

Therefore, the deprotonation of terminal alkynes was more favoured when SbF_6^- was used as the counterion and digold structure **7** was the predominant species (Scheme 19). Otherwise, the life-time of the π-coordinated alkyne complex was longer with $BAr^F{}_4^-$ (**83**).

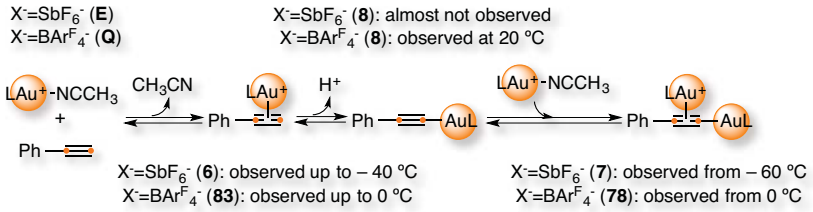

Scheme 19. Gold species formed with ethynylbenzene (L=^{t}BuXPhos).

DFT Calculations

Firstly, in order to gain further information of the nature of the (π-alkyne)gold complexes **6** and **83**, we performed DOSY and ^{1}H-^{19}F HOESY NMR spectroscopy experiments.[14,15,16] However, all the attempts led to non-conclusive results because of the low resolution spectra obtained.

Afterwards, by means of DFT calculations (M06, 6-31G(d) (C, H, P, B, F) and SDD (Au, Sb) in CH_2Cl_2), we studied these complexes to determine their steric and electronic features. We also calculated [^{t}BuXPhosAu(η^2-ethynylbenzene)]BF_4 (**84**) in order to determine a trend. First, we evidenced the steric congestion around the substrate hampering its deprotonation depending on the counterion. Later, we analysed the charge distribution by the electron density of the complexes mapped with ESP (ρ=0.03 eÅ^3) and the positive charge was widely distributed around the ligand instead of being concentrated in the metal centre for **83**, **6** and **84** (Figures 21, 22 and 23, respectively).

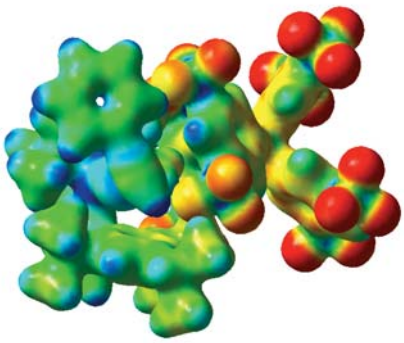

Figure 21. ESP of (η^2-ethynylbenezene)gold complex 83 (δ^+ in blue and δ^- in red).

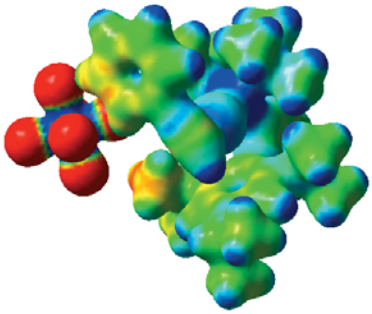

Figure 22. ESP of complex 6 (δ^+ in blue and δ^- in red).

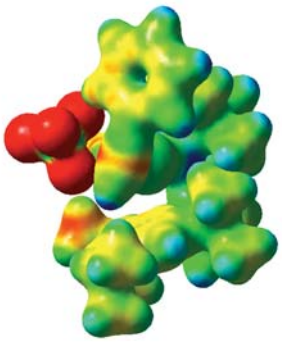

Figure 23. ESP of complex 84 (δ^+ in blue and δ^- in red).

We also checked the pattern between the bulkiness of the counterion and the acidity of ethynylbenzene by determining the Mulliken atomic charges. The electron density decreased with the anion size (BF_4^- < SbF_6^- < $BAr^F{}_4^-$), although the differences were modest: 0.250 (**84**), 0.243 (**6**) and 0.237 (**83**). Therefore, we reasoned that the large cation formed a more stable (π-alkyne)complex with a softer counterion, for example, $BAr^F{}_4^-$.

Determination of the Equilibrium Constants

Therefore, we decided to determine the equilibrium constant between catalyst **Q** and digold complex **78** using the Van't Hoff equation (Table 8).[26] In the case of SbF_6^-, K_{eq} (50ºC) = $1.08 \cdot 10^{-7}$ M and K_{eq} (25ºC) = $4.44 \cdot 10^{-8}$ M (see **Chapter 3**).[5] Thus, we performed the reaction between gold complex **Q** and 0.5, 1, 2, 3.5 or 5 equiv. of ethynylbenzene in CD_2Cl_2 (0.5 M) analysing the formation of **78** at – 10, 5, 20 and 35 ºC by ^1H and ^{31}P NMR spectroscopy. Then, we calculated the equilibrium constant at each temperature, and we used these data for the Van't Hoff equation by plotting the logarithm of K_{eq} with the inversed temperature and we checked that fit in a linear regression with $R^2 = 0.987$ (Figure 24).

Table 8. Equilibrium constants between catalyst Q and digold complex 78 depending on the temperature with increasing equivalents of ethynylbenzene.[a]

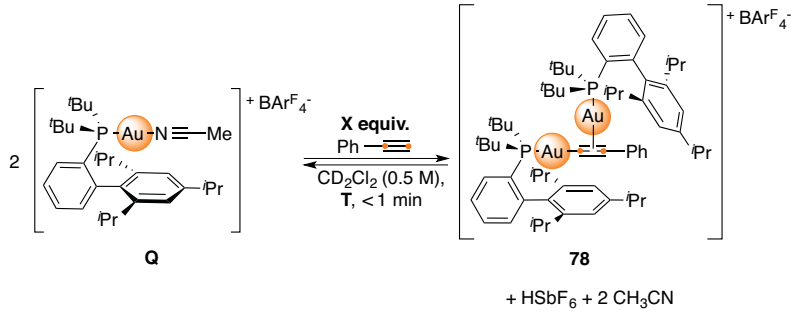

Equiv. =	0.5	1.0	2.0	3.5	5.0
– 10 ºC	$1.10 \cdot 10^{-9}$	$6.23 \cdot 10^{-10}$	$1.08 \cdot 10^{-9}$	$7.66 \cdot 10^{-10}$	$1.52 \cdot 10^{-9}$
5 ºC	$6.40 \cdot 10^{-9}$	$3.92 \cdot 10^{-9}$	$4.44 \cdot 10^{-9}$	$5.56 \cdot 10^{-9}$	$8.76 \cdot 10^{-9}$
20 ºC	$1.26 \cdot 10^{-8}$	$9.15 \cdot 10^{-9}$	$2.91 \cdot 10^{-8}$	$2.12 \cdot 10^{-8}$	$2.11 \cdot 10^{-8}$
35 ºC	$6.93 \cdot 10^{-8}$	$2.76 \cdot 10^{-8}$	$3.80 \cdot 10^{-8}$	$4.01 \cdot 10^{-8}$	$4.23 \cdot 10^{-8}$

[a]Equilibium constants (M).

In that case, the equilibrium constant at 25 ºC towards the digold complex **78** was $2.44 \cdot 10^{-8}$ M. Therefore, we could observe that, although the difference is rather small, the deprotonation of the alkyne was more favoured with SbF_6^- than with $BAr^F{}_4^-$, probably due to the lower stability of the bulkier conjugated acid. Moreover, we could calculate that the difference of enthalpy of the process was 13.4 kcal/mol and the entropy 10 cal/mol·K. Indeed, the enthalpy of this reaction was higher than with SbF_6^- (6.8 kcal/mol) although the entropy was slightly larger (– 11 cal/mol·K).

[26] For basic concepts see: *(a)* K. J. Laidler and M. C. King, *J. Phys. Chem.* **1983**, *87*, 2657–2664; *(b)* P. Ballester, *Acc. Chem. Res.* **2013**, *46*, 874–884.

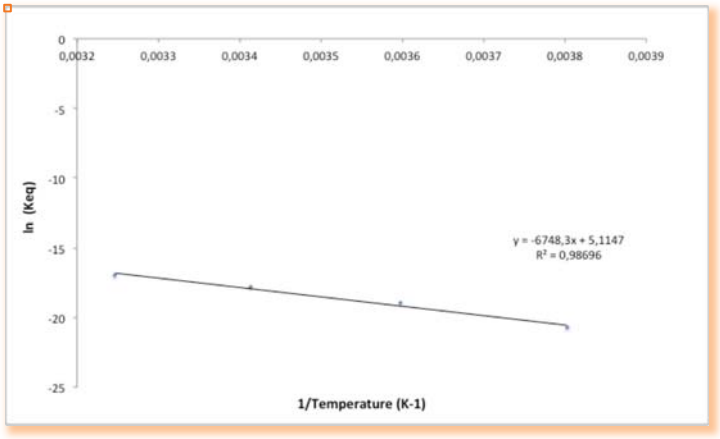

Figure 24. Relationship between the equilibrium constant towards 78 and the temperature.

Furthermore, using the same methodology, we compared the tendency of the cationic gold complex to coordinate to α-methylstyrene by determining the equilibrium constant towards **79** and **80**. Reaction between **E** or **Q** and 0.5, 1, 2, 3.5 or 5 equiv. of the alkene in CD_2Cl_2 (0.5 M) were also examined at – 10, 5, 20 and 35 ºC by ^{1}H and ^{31}P NMR spectroscopy (Scheme 20).

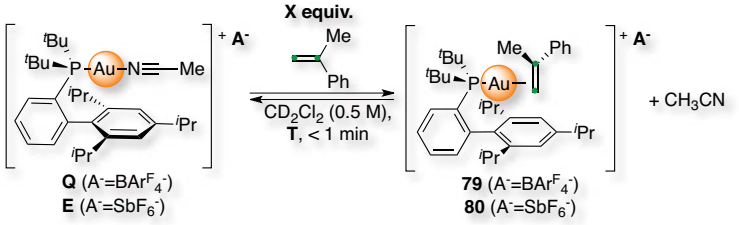

Scheme 20. Equilibrium between the cationic gold complex and the π-alkene coordination.

Accordingly, the equilibrium constant towards **79**, or **80**, was simpler (Equation 4). Considering that we could measure the ratio between complex **79** and catalyst **Q** under the different conditions, we could also determine their concentrations in the equilibrium (Equation 5). Analogously, we determined them for **80** as well.

$$K_{eq} = \frac{[\mathbf{79}] \cdot [CH_3CN]}{[\boldsymbol{Q}] \cdot [\alpha - methylstyrene]} = \frac{[\mathbf{79}]^2}{([\boldsymbol{Q}]_0 - [\mathbf{79}]) \cdot ([\alpha - methylstyrene]_0 - [\mathbf{79}])}$$

Equation 4. Equilibrium constant as a function of [79].

$$Integrals\ Ratio = \frac{[\mathbf{79}]}{[\boldsymbol{Q}]_0 - [\mathbf{79}]}$$

Equation 5. Relationship between catalyst Q and alkene complex 79.

Thus, we calculated the equilibrium constants at each temperature for $BAr^{F}_{4}^{-}$ and SbF_6^- (Tables 9 and 10, respectively). Then, we plotted the Van't Hoff equation and checked that it fit in a linear regression with $R^2 = 0.964$ for $BAr^{F}_{4}^{-}$ and $R^2 = 0.927$ for SbF_6^- (Figures 25 and 26, respectively).

Table 9. Equilibrium constants towards 79 depending on the temperature with increasing equivalents of α-methylstyrene.[a,b]

Equiv. =	0.5	1.0	2.0	3.5	5.0
– 10 ºC	0.108	0.110	0.115	0.106	0.115
5 ºC	0.105	0.109	0.102	0.101	0.101
20 ºC	0.101	0.091	0.096	0.090	0.093
35 ºC	0.098	0.080	0.085	0.080	0.071

[a]Scheme 20 with $A^- = BAr^{F}_{4}^{-}$. [b]Equilibium constants (no units).

Table 10. Equilibrium constants towards 80 depending on the temperature with increasing equivalents of α-methylstyrene.[a,b]

Equiv. =	0.5	1.0	2.0	3.5	5.0
– 10 ºC	0.068	0.062	0.055	0.064	0.059
5 ºC	0.068	---	0.055	0.055	0.054
20 ºC	0.058	0.044	0.055	0.053	0.047
35 ºC	0.049	0.029	0.033	0.054	0.045

[a]Scheme 20 with $A^- = SbF_6^-$. [b]Equilibium constants (no units).

With these results we could determine the equilibrium constants at 25 ºC: K_{eq} ($BAr^{F}_{4}^{-}$) = 0.090 and K_{eq} (SbF_6^-) = 0.047. In this case, we observed that the binding to α-methylstyrene was stronger with bulky counterions, although the differences were small again. However, their comparison with respect to the formation of the digold complexes was remarkably distinct: the constants increased from 10^{-8} to 10^{-2}.

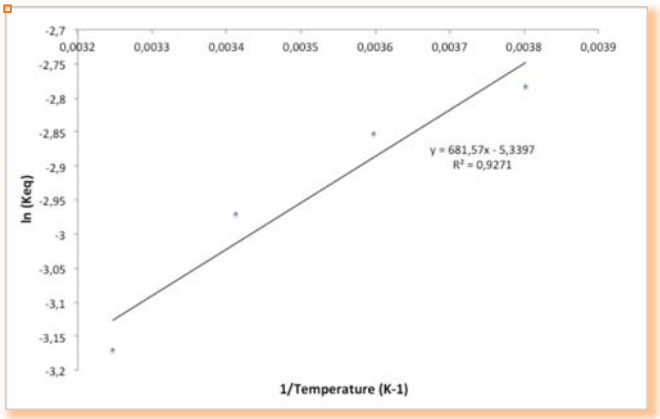

Figure 25. Relationship between the equilibrium constant towards 79 and the temperature.

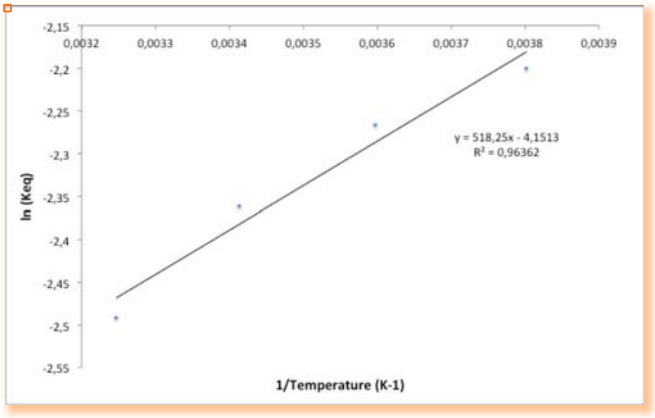

Figure 26. Relationship between the equilibrium constant towards 80 and the temperature.

In this case, the equilibrium was an exothermic process and the difference rather minor: ΔH = – 1.4 kcal/mol for $BAr^F_4^-$ and ΔH = – 1.0 kcal/mol for SbF_6^-. The entropy was – 11 and – 8 cal/mol·K, respectively .

Consequently, the initial proposal should be modified considering this pre-equilibrium described. According to the equilibrium constants, catalyst **Q** ought to bind preferentially to α-methylstyrene forming **79** in the presence of ethynylbenzene decreasing the concentration of **83** and **78** (Scheme 21). The extent of this effect would depend on the nucleophilicity of the alkene as well as the ratio of reagents of the reaction, as observed.

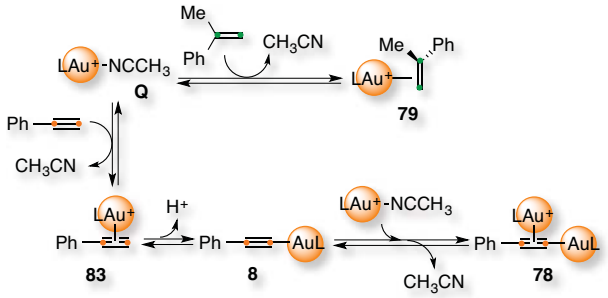

Scheme 21. Equilibrium between gold species including π-alkene coordination (L=^{t}BuXPhos).

The same scenario must be expected with SbF_6^- but the equilibrium between the corresponding gold species (**E**, **80**, **6**, **8** and **7**) would be more shifted towards the digold complex **7**, which would explain the results observed during the kinetic study and the low temperature NMR experiments.

At this point, we decided to determine if complex **79** and **83** were also in direct equilibrium, which would clarify if the coordination of the alkene was inhibiting the [2+2] cycloaddition or storing cationic gold(I) reservoirs.

Test of the Catalytic Activity

We performed some additional experiments to exclude other mechanistic pathways. We started by reacting the isolated intermediates under stoichiometric conditions with α-methlstyrene. Thus, gold complex **8** was submitted to the [2+2] cycloaddition with 2 equiv. of the alkene in CH_2Cl_2 at 25 ºC and no reaction was observed (Scheme 22). The same result was observed when the reaction was performed in the presence of 3 mol% of catalyst **Q**.

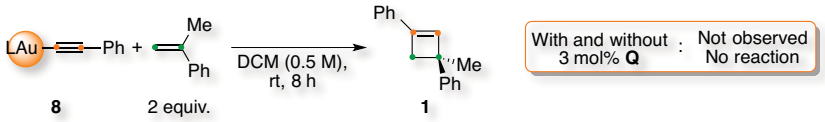

8 2 equiv. 1

Scheme 22. Stoichiometric experiments with gold complex 8.

The same tests were performed with digold complex **78** and no [2+2] cycloaddition was observed either (Scheme 23).

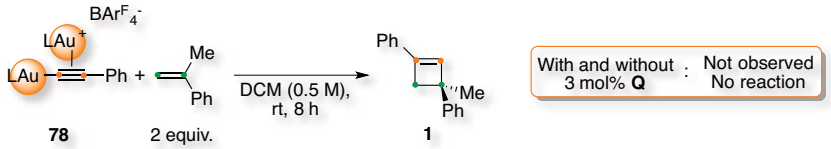

78 2 equiv. 1

Scheme 23. Stoichiometric experiments with digold complex 78.

On the other hand, (π-alkene)gold complex **79** reacted with ethynylbenzene under the optimized conditions in the absence of catalytic **Q** and afforded cyclobutene **1** in 72% isolated yield (Scheme 24).

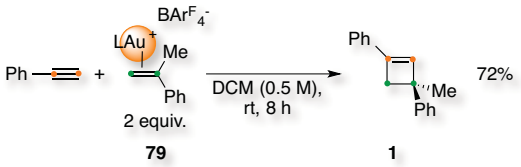

79 1

Scheme 24. Stoichiometric experiment with gold complex 79 (L=^{t}BuXPhos).

However, no cycloaddition was observed between **79** with alkynyl gold complex **8** (Scheme 25). These results demonstrated that (π-alkene)gold species **79** could exchange with ethynylbenzene to regenerate the reaction towards π-coordination of the alkyne (**83**).

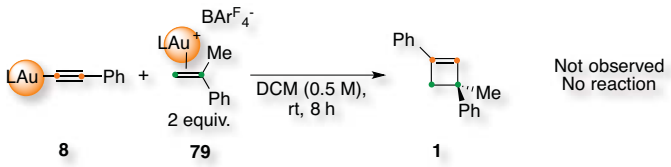

8 79 1

Scheme 25. Ending of the reactivity of gold complex 79 (L=^{t}BuXPhos).

Subsequently, we used complexes **8**, **78** and **7** as catalysts for the [2+2] cycloaddition between ethynylbenzene with 2 equiv. α-methylstyrene in CH_2Cl_2 (Table 11). These experiments proved that digold complex **7** was an unreactive resting state in the intermolecular gold-catalyzed [2+2+2] cycloaddition between alkynes and oxoalkenes (see **Chapter 3** for further information). In this case, complexes **8**, **78** and **7** were very inefficient in the absence of any additive. Complex **8** was completely inactive (entry 1) and digold complexes **78** and **7** were very poor catalysts (entries 2 and 3). Nevertheless, the catalytic activity was restored upon addition of $HSbF_6$, which cleaved the Au–C bond regenerating the equilibrium between the gold(I) species towards **6**. Thus, reaction between ethynylbenzene and α-methylstyrene with **8** or **7** and substoichiometric amounts of $HSbF_6$ proceeded smoothly under the optimized conditions towards cyclobutene **1** in 75 and 79% isolated yield, respectively (entries 4 and 5).

Table 11. [2+2] Cycloaddition catalyzed by the isolated gold intermediates.

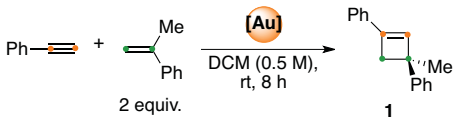

Entry	[Au]	X mol%	Additive	Yield[a]
1	**8**	3	–	–
2	**78**	1.5	–	13%
3	**7**	1.5	–	13%
4	**8**	3	$HSbF_6 \cdot 6H_2O$ (3 mol%)	75%[b]
5	**7**	1.5	$HSbF_6 \cdot 6H_2O$ (1.5 mol%)	79%[b]

[a]Crude analysed by ^1H NMR spectroscopy using 1,4-diacetylbenzene as internal standard, yield referred to cyclobutene **1**. [b]Isolated yield.

On the other hand, when ^{t}BuXPhosAuCl reacted with $NaBAr^F_4$ in the absence of a substrate, only one chloride abstraction occurred and digold complex **85** with a chloride bridge could be crystallized (Figure 27).[27]

[27] For other examples and their reactivity see: *(a)* S. G. Weber, D. Zahner, F. Rominger and B. F. Straub; *(b)* A. Homs, I. Escofet and A. M. Echavarren, *Org. Lett.* **2013**, *15*, 5782–5785 and references cited therein.

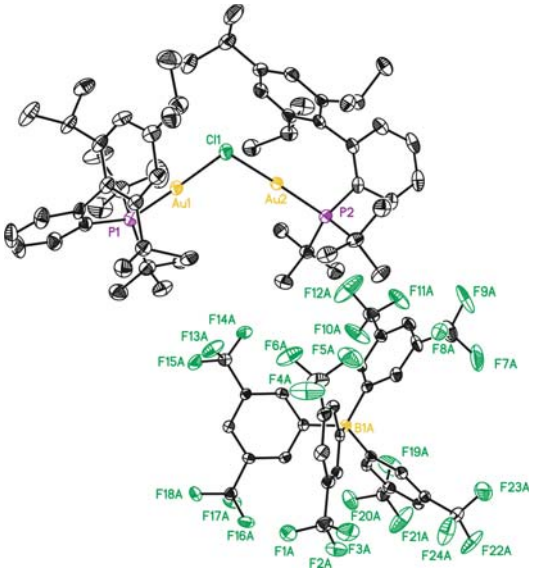

Figure 27. Formation of digold chloride bridge 85.

Finally, we attempted the gold-catalyzed reaction between α-methylstyrene and other nucleophilies in order to exclude the activation of the alkene as the key step of the process (Scheme 26). Thus, we used 0.5 equiv. allyltrimethylsilane, indole, 1,3,5-trimethoxybenzene or 1,3-diphenylpropane-1,3-dione in CH_2Cl_2 but no reaction was observed in any case.

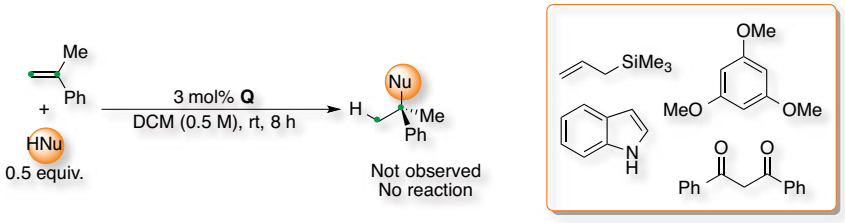

Scheme 26. Alkene activation towards nucleophilic attack.

These results suggested that the active gold species was [^{t}BuXPhosAu(η^2-ethynylbenzene)]BAr^F_4 (**83**), which entered the catalytic cycle *via* nucleophilic attack of α-methylstyrene to **86** followed by ring expansion (**87**) and demetallation (**88**). Thus, the coordinated product would enter into the equilibrium and **79** would be recovered after ligand exchange with α-methylstyrene releasing cyclobutene **1** (Scheme 27). Analogously, complexes **6** and **84** would be the active species when using SbF_6^- and BF_4^-, respectively.

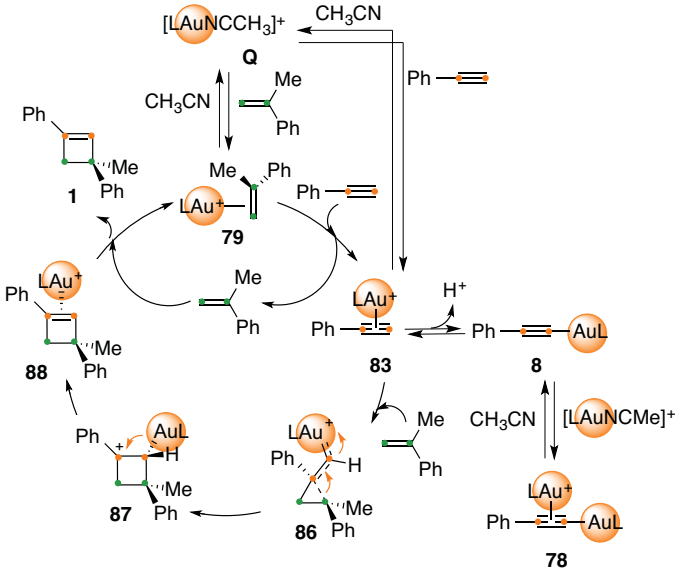

Scheme 27. Complete proposal for the [2+2] cycloaddition (L=^{t}BuXPhos).

Accordingly, the ligand exchange between complex **79** and ethynylbenzene to form the key intermediate **83** was the rate-determining step of the catalytic cycle. Therefore, the orders for the catalyst and the alkyne were close to 1 and we observed zero-dependence for α-methylstyrene. Thus, the coordination of the alkene would be more favoured (order 1) but exchange with the alkyne would be necessary to continue the catalytic cycle (order –1), which would formally be order 0. Simultaneously, digold complex **78** would be competitively formed as a minor inactive byproduct *via* a side-pathway based on the deprotonation of the alkyne. Hence, this was an off-cycle intermediate decreasing the concentration of the active species.

6. Conclusions

During the mechanistic study of the gold-catalyzed intermolecular [2+2+2] cycloaddition of alkynes with oxoalkenes described in **Chapter 3**, the formation of unreactive digold species outside the main catalytic cycle was revealed.[5] Thus, the activation of alkynes could competitively undergo deprotonation to form an alkynyl gold complex, which was detrimental for the efficiency of the transformation. Therefore, a new generation of gold(I) complexes bearing bulky, non-coordinating and less basic counterions, for example catalyst **Q**, were designed in order to refine the selectivity in the intermolecular cycloadditions (Figure 28).[28] Study of its efficiency showed improvements of the yields up to 36%. The reactivity was compared in the [2+2] cycloaddition between alkynes and alkenes, the macrocyclization of large enynes, the [2+2+2] cycloaddition of alkynes and oxoalkenes, the synthesis of phenols as well as in intramolecular reactions.

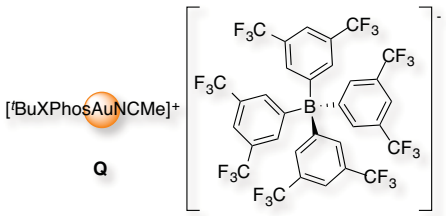

Figure 28. New gold complex Q using BAr^{F}_{4}.

A detailed mechanistic study of the [2+2] cycloaddition between ethynylbenzene and α-methylstyrene using catalyst **Q** revealed a complex pre-equilibrium between different gold species before the π -coordinated alkyne **83** entered the catalytic cycle (Scheme 28). Preferential coordination of the alkene (**79**) was observed under the reaction conditions. Determination of the equilibrium constants with **Q**, contrasting it with digold **78** formation, showed that this was indeed more favoured. Nevertheless, we could prove this was not inhibiting the formation of cyclobutene **1** by performing tests of the catalytic activity with the isolated gold intermediates. This scenario was confirmed by studying the evolution of these species with low-temperature NMR experiments, monitoring of the reaction and55 determination the order of the reagents. Thus, the formation of cyclobutene **1** was first order dependant with ethynylbenzene and catalyst **Q** but did not change with the concentration of α-methylstyrene concentration. These results suggested that the ligand exchange to form complex **83** was the rate-determining step of the transformation.

[28] C. Obradors, A. Homs, D. Leboeuf and A. M. Echavarren, *Adv. Synth. Catal.* **2014**, *356*, 221–228.

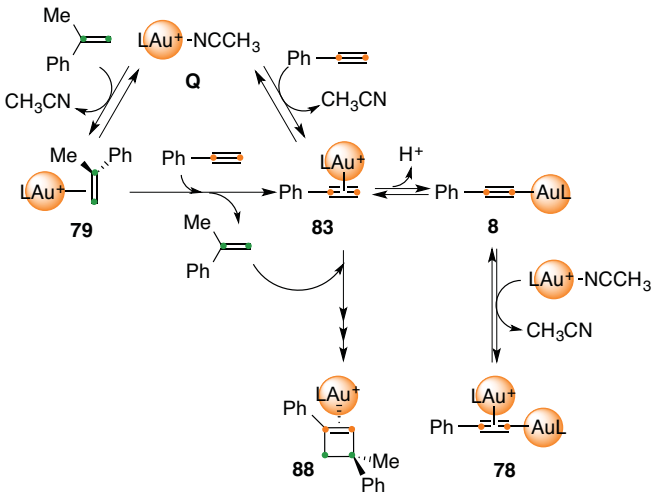

Scheme 28. Gold species involved during the [2+2] cycloaddition.

In this context, we could observe a significant effect of the counterion in the pre-equilibrium between these gold species and therefore in the efficiency of the cyclobutene **1** synthesis. Thus, kinetic studies showed that the reaction rate as well as the final yield increased with more bulky and less basic counterions, such as $BAr^{F}_{4}^{-}$. DFT calculations confirmed that large cations form more stable complexes with softer counterions.

Chapter 5:

Towards the Total Synthesis of Rumphellaone A

1. Introduction

As explained in the **General Introduction**, the application of gold catalysis in the total synthesis of natural products with interesting biological properties has grown during the last decade together with the development of new catalysts and methodologies.[1] Cycloisomerizations and cycloadditons attracted particular attention for the construction of polycyclic structures in an atom economy strategy and under mild conditions. As representative examples, (-)-englerin A, (-)-GSK1360707 and (+)-schisanwilsonene have been recently synthesized using gold catalysis in the key step of their total synthesis (Figure 1). In the first case, (-)-englerin A was isolated from *Phylanthus engleri* and showed selective inhibition of renal cancer cells growth. A gold-catalyzed [2+2+2] cyclization of an alkyne, an alkene and a ketone was used to build the main core of the natural product.[2] (-)-GSK1360707 represents a particularly promising "triple-uptake inhibitor" of neurotransmitters related to symptoms of depression, since the more advanced medication strategy nowadays is to interfere them simultaneously. The construction of the fused cyclopropyl piperidine was achieved enantioselectively from a 1,6-enyne using a chiral phosphoramidite gold catalyst.[3] Finally, (+)-schisanwilsonene was isolated from *Schisandra wilsoniana* used in the treatment of hepatitis. The scaffold was formed *via* a gold-catalyzed tandem cyclization of a 1,6-enyne followed by an acetate 1,5-migration and an intermolecular cyclopropanation.[4]

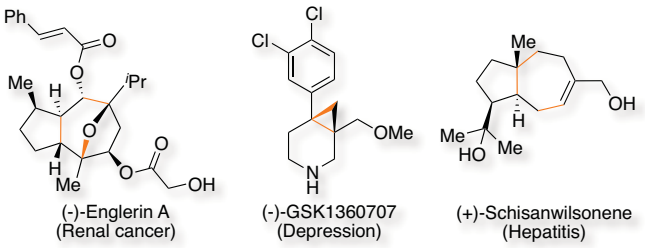

Figure 1. Natural products synthesized via gold catalysis.

This time we focused our attention to the presence of a cyclobutane moiety in natural products, some of them with significant biological activity. The four-membered ring carbocycle can be found from pretty simple to more complex structures, for example, in (-)-biyouyanagin A, nervonin A and (+)-kelsoene (Figure 2).[5]

---

[1] (*a*) A. S. K. Hashmi and M. Rudolph, *Chem. Soc. Rev.* **2008**, *37*, 1766–1775; (*b*) A. Fürstner, *Chem. Soc. Rev.* **2009**, *38*, 3208–3221; (*c*) Y. Zhang, T. Luo and Z. Yang, *Nat. Prod. Rep.* **2014**, *31*, 489–503; *(d)* A. Fürstner, *Acc. Chem. Res.* **2014**, *47*, 925–938; *(e)* C. Obradors and A. M. Echavarren, *Acc. Chem. Res.* **2014**, *47*, 902–912.
[2] (*a*) Q. Zhou, X. Chen and D. Ma, *Angew. Chem. Int. Ed.* **2010**, *49*, 3513–3516; (*b*) K. Molawi, N. Delpont and A. M. Echavarren, *Angew. Chem. Int. Ed.* **2010**, *49*, 3517–3519.
[3] H. Teller and A. Fürstner, *Chem. –Eur. J.* **2011**, *17*, 7764–7767.
[4] M. Gaydou, R. E. Miller, N. Delpont, J. Ceccon and A. M. Echavarren, *Angew. Chem. Int. Ed.* **2013**, *52*, 6396–6399.
[5] (*a)* Y. J. Hong and D. J. Tantillo, *Chem. Soc. Rev.* **2014**, *43*, 5042–5050; (*b*) B. Darses, A. E. Greene and J. F. Poisson, *J. Org. Chem.* **2012**, *77*, 1710–1721; (*c*) L. M. Li, G. Y. Li, L. S. Ding, L. B. Yang, Y. Zhao, J. X. Pu, W. L. Xiao, Q. B. Han and H. D. Sun, *J. Nat. Prod.* **2008**, *71*, 684–688.

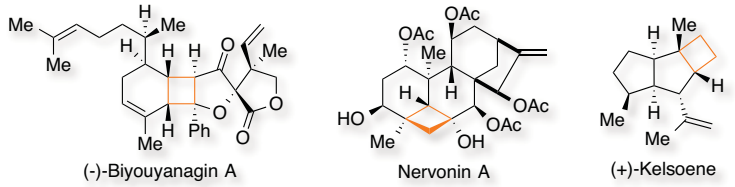

Figure 2. Natural products containing a cyclobutane moiety.

However, the assembly of cyclobutanes and the related cyclobutenes is not synthetically straightforward. Traditionally, four-member rings have been obtained *via* [2+2] photocycloadditions of α,β-unsaturated ketones or esters to alkenes, alkynes or allenes.[6] This transformation usually proceeds by photochemical reactions challenging the stereochemical control. A few examples have been reported in the synthesis of cyclobutenes using metal-catalysis, for example, with palladium or platinum.[7]

Our interest was centred in the caryophyllene-related sesquiterpenes, specifically rumphellaone A (Figure 3).[8] These natural products were isolated by the group of Sung in 2010 from the gorgonian coral *Rumphella antipathies*.[9] Rumphellaone A showed cytotoxicity towards CCRF-CEM (human T-cell acute lymphoblastic leukemia) tumor cells (IC_{50} = 12.6 μg/mL).

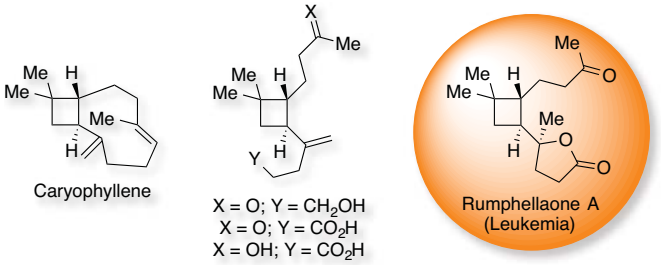

Figure 3. Caryophyllene and related natural products.

So far, one total synthesis of rumphellaone A has been reported by Kuwahara in 2012 (Scheme 1).[10] Their approach consisted in a stereospecific Stork epoxy nitrile cyclization. Hence, intermediate **7** was prepared from alcohol **1** by installing the nitrile group and performing a Horner-Wadsworth-Emmons reaction followed by an enantioselective Sharpless epoxidation. The Stork protocol employs a strong base to generate the delocalized anion that can undergo ring opening of the epoxide building simultaneously the three contiguous stereocenters of cyclobutane **9**. Subsequent carbon elongations led to

---

[6] (*a*) N. Hoffman, *Chem. Rev.* **2008**, *108*, 1052–1103. (b) J. Du and T. P. Yoon, *J. Am. Chem. Soc.* **2009**, *131*, 14604–14605.
[7] (*a*) A. Fürstner and C. Aïssa, *J. Am. Chem. Soc.* **2006**, *128*, 6306–6307; (*b*) M. Luparia, D. Audisio and N. Maulide, *Synlett* **2011**, *6*, 735–740.
[8] (*a*) L. Quijano, A. Vasquez and T. Rios, *Phytochemistry* **1995**, *38*, 1251–1255; (*b*) M. Wichlacz, W. A. Ayer, L. S. Trifonov, P. Chakravarty and D. Khasa, *Phytochemistry* **1999**, *52*, 1421–1425; (*c*) M. Wichlacz, W. A. Ayer, L. S. Trifonov, P. Chakravarty and D. Khasa, *J. Nat. Prod.* **1999**, *62*, 484–486; (d) H. M. Chung, W. H. Wang, T. L. Hwang, J. J. Li, L. S. Fang, Y. C. Wu and P. Y. Sung, *Molecules* **2014**, *19*, 12320–12327.
[9] H. M. Chung, Y. H. Chen, M. R. Lin, J. H. Su, W. H. Wang and P. J. Sung, *Tetrahedron Lett.* **2010**, *51*, 6025–6027.
[10] (*a*) T. Hirokawa and S. Kuwahara, *Tetrahedron* **2012**, *68*, 4581–4587; (*b*) T. Hirokawa, T. Nagasawa and S. Kuwahara, *Tetrahedron Lett.* **2012**, *53*, 705–706.

intermediate **15**, which was hydrogenated followed by an acid-catalyzed lactonization to obtain the final product.

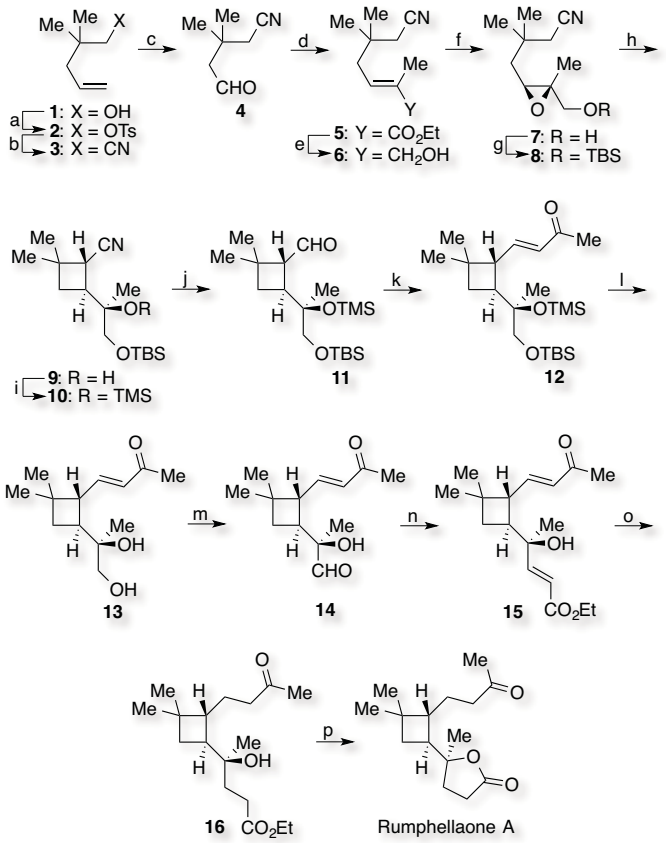

Reagents and conditions: a) TsCl, NEt_3, $Me_3N{\cdot}HCl$, CH_2Cl_2, 0 ºC to rt, 18 h; b) NaCN, DMSO, 50 ºC, 19 h; c) O_3, $NaHCO_3$, CH_2Cl_2/MeOH, – 78 ºC, 2 h, then Me_2S, – 78 ºC to rt, overnight; d) $Ph_3P{=}C(Me)CO_2Et$, THF, 40 ºC, 20 h (51% from **1**); e) DIBAL, CH_2Cl_2, – 78 to – 30 ºC, 4 h; f) TBHP, $Ti(O^iPr)_4$, L-(+)-DIPT, CH_2Cl_2, – 20 ºC, 17 h (64% from **5**); g) TBSCl, imidazole, DMF, 0 ºC to rt, 1.5 h (96%); h) NaHMDS, PhMe, reflux, 2.5 h (90%); i) TMSOTf, 2,6-lutidine, CH_2Cl_2, 45 min (80%); j) DIBAL, CH_2Cl_2, – 20 ºC to rt, 25 h (85%); k) $MeCOCH_2PO(OMe)_2$, NaH, DME, rt, 5 days (84%); l) TBAF, THF, rt, 1 h (84%); m) $SO_3{\cdot}Py$, $EtN(^iPr)_2$, DMSO, rt, 1 h (83%); n) $Ph_3P{=}CHCO_2Et$, THF, 50 ºC, 1 h (71%); o) H_2, 10% Pd/C, MeOH, rt, 2 h (87%); p) CSA, CH_2Cl_2, rt, 15 min (73%).

Scheme 1. Total synthesis of Rumphellaone A.

This approach requires of sixteen steps (5% overall yield) involving several protection-deprotection reactions. Therefore, we considered we could improve the synthetic route to rumphellaone A. Specifically, we reasoned that we could use an intermolecular gold-catalyzed [2+2] cycloaddition of an alkyne and an alkene to build a cyclobutene moiety, which could be derivatized towards the main core of this natural product. Thus, reaction of ethynylbenzene and α-methylstyrene with [^{t}BuXPhosAuNCMe]SbF_6 (**E**) afforded cyclobutene **17** regioselectively *via* a distorted cyclopropyl gold carbene **18**/**18´** (Scheme 2).[11]

[11] V. López-Carrillo and A. M. Echavarren, *J. Am. Chem. Soc.* **2010**, *132*, 9292–9294.

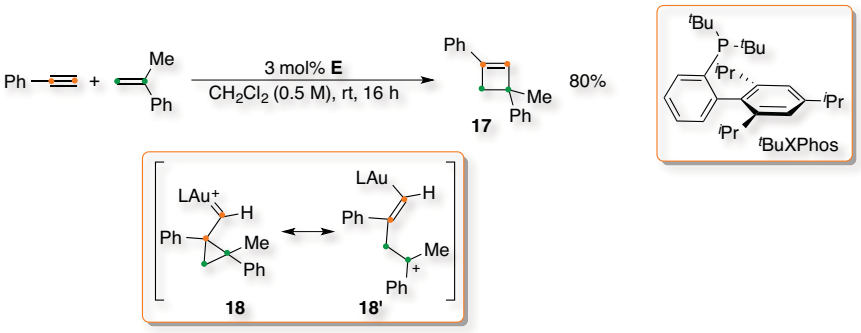

Scheme 2. Gold-catalyzed [2+2] cycloaddition of alkynes and alkenes.

Later, we also developed the gold-catalyzed [2+2+2] cycloaddition between alkynes and oxoalkenes where a carbonyl group opened an analogous cyclopropyl ring *via* an intramolecular nucleophilic attack (see **Chapter 2**).[12] Considering the result observed for 6-methylhept-5-en-2-one when studying the effect of the substitution pattern in the alkene, we envisioned we could use this particular example for the total synthesis of rumphellaone A (Scheme 3). Hence, when the terminal carbon is the more substituted one, oxonium cation **23** would be formed by the nucleophilic attack of the ketone. However, cyclobutene product **19** was more favoured by ring expansion of the cyclopropyl gold(I) carbene intermediate **22** towards **21**. Moreover, a detailed mechanistic study of this transformation was performed and allowed its improvement by tunning the counterion of the catalyst (see **Chapter 3** and **4**).

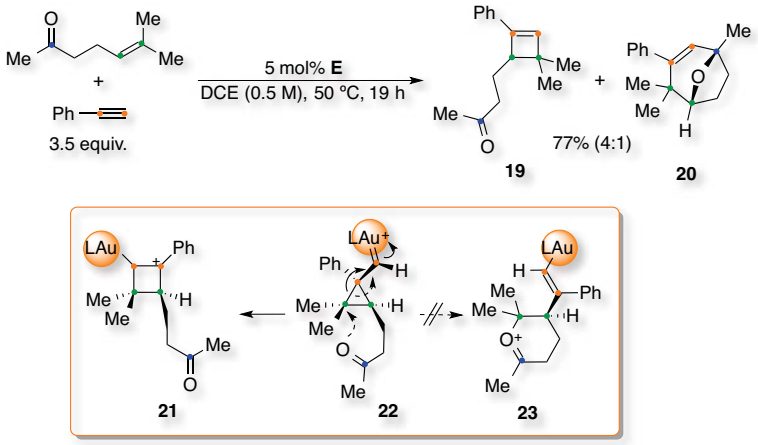

Scheme 3. Reaction of ethynylbenzene and 6-methylhept-5-en-2-one.

[12] C. Obradors and A. M. Echavarren, *Chem. –Eur. J.* **2013**, *19*, 3547–3551.

2. Objectives

Therefore, we designed a novel route to the natural product comprising a gold-catalyzed [2+2] cycloaddition of a suitable alkyne **24** and 6-methylhept-5-en-2-one to first form cyclobutene **25** followed by a diastereoselective hydrogenation to ***trans*-26** and, finally, derivatization of the R- group to the appropriate lactone (Scheme 4).

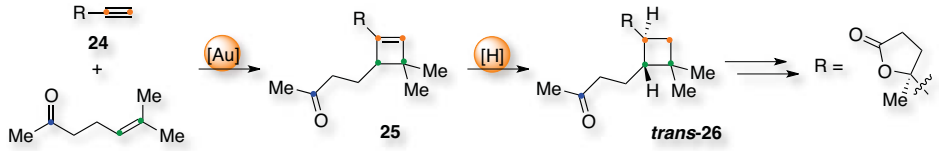

Scheme 4. Synthetic route to rumphellaone A.

3. Silyloxyalkynylfuran Approach

Retrosynthetic Analysis

First, we reasoned we could build a cyclobutene through a gold-catalyzed [2+2] cycloaddition between silyloxyalkynylfuran **27** and 6-methylhept-5-en-2-one (Scheme 5). The resulting intermediate **28** could undergo a vinylogous methylation and hydrogenation of **29** would lead to the natural product.

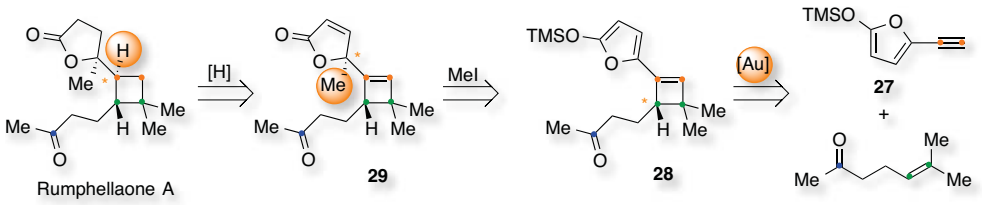

Scheme 5. Retrosynthetic analysis of rumphellaone A.

Beforehand, several challenges of the route could be already conceived. To start, the diastereoselective hydrogenation of cyclobutene **29** would require the attack through the sterically more hindered face of the four-membered ring. The same would occur in the methylation step of **28**. Nevertheless, similar transformations have been reported with additions to aldehydes, α,β-unsaturated ketones, allylacetates, hydroxylamines or acetals in the presence of an organocatalyst, a Lewis acid or a fluoride source.[13] Finally, the gold-catalyzed [2+2] cycloaddition between silyloxyalkynylfuran **27** and 6-methylhept-5-en-2-one would require an exquisite selectivity towards the cyclobutene.

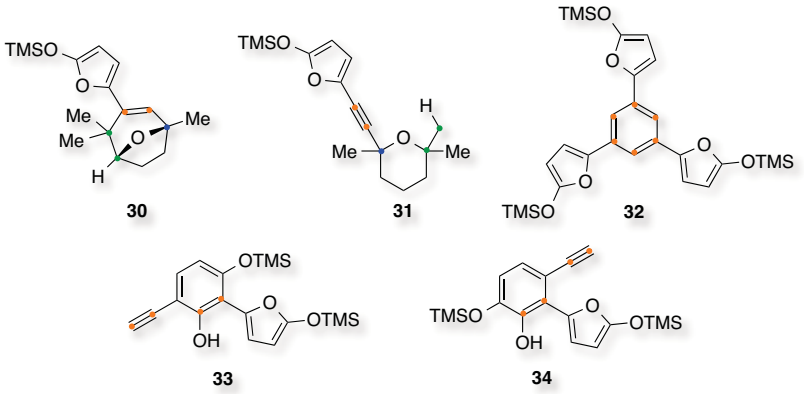

Figure 4. Possible by-products of the gold-catalyzed [2+2] cycloaddition.

[13] (*a*) M. Asaoka, N. Sugimura and H. Takei, *Bull. Chem. Soc. Jpn.* **1979**, *52*, 1953–1956; (*b*) M. Szlosek and B. Frigadère, *Angew. Chem. Int. Ed.* **2000**, *39*, 1799–1801; (*c*) C. W. Cho and M. J. Krische, *Angew. Chem. Int. Ed.* **2004**, *43*, 6689–6691; (*d*) S. Ma, L. Lu and P. Lu, *J. Org. Chem.* **2005**, *70*, 1063–1065; (*e*) R. K. Boeckman, J. E. Pero and D. J. Boehmler, *J. Am. Chem. Soc.* **2006**, *128*, 11032–11033; (*f*) B. Simmons, A. M. Walji and D. W. C. MacMillan, *Angew. Chem. Int. Ed.* **2009**, *48*, 4349–4353; (*g*) E. K. Kemppainen, G. Sahoo, A. Valkonen and P. M. Pihko, *Org. Lett.* **2012**, *14*, 1086–1089; (*h*) W. Chen and J. F. Hartwig, *J. Am. Chem. Soc.* **2012**, *134*, 15249–15252; (*i*) Y. H. Shi, Z. Wang and W. P. Deng, *Tetrahedron* **2012**, *68*, 3649–3653.

Thus, there is the possibility that oxabicycle **30**, tetrahydrofuran **31**, trimer **32** and phenols **33**/**34**, among others, are also formed (Figure 4).[12,14]

Synthesis of the Silyloxyalkynylfuran

We designed various pathways to synthesize the desired silyloxyalkynylfuran **27**. We started using trimethylsilyloxyfuran and attempting a deprotonation followed by the trapping with an electrophile to form either the iodo- or the aldehyde derivative **35** (Scheme 6).[15]

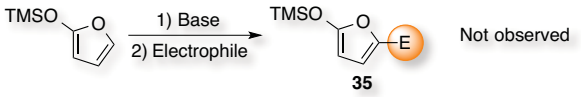

Scheme 6. Reaction of trimethylsilyloxyfuran with a base and an electrophile.

Attempts of deprotonation with ^{n}BuLi, LiHMDS or KHMDS and trapping with I_2, 1,2-diiodoethane or DMF from – 78 ºC to 25 ºC in diethyl ether led only to decomposition of the starting furan. Similar results were observed when a proton sponge, to avoid protonation, or 18-Crown ether, to stabilize the cation, were added. On the other hand, when Et_3N was used as a base, no reaction was observed. Decomposition was observed as well when I_2 or NIS were used in the absence of a base.[16] In the case of 1,2-diiodoethane, no reaction occurred.

Considering the instability of the silyloxy protecting group,[17] we reasoned that we could perform the cleavage of the TMS group followed by trapping with DMF forming the aldehyde **36** *in situ*.[18] The reaction was attempted in a mixture of CH_2Cl_2 and dried DMF in the presence of a fluoride source at room temperature. In particular, we screened KF, CsF, AgF, ZnF_2 and $KF/BF_3{\cdot}Et_2O$ but all the reactions led to the protonated lactone (Scheme 7).

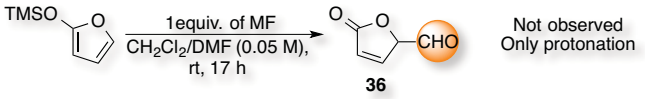

Scheme 7. Reaction of trimethylsilyloxyfuran with a fluorine source.

We continued with the synthesis of ethynylfuran, which could be further oxidized with LiHMDS/TBHP and enolized to build the desired silyloxyalkynylfuran.[19] Treatment of 2-acetylfuran with pyridine/PCl_3 at 110 ºC under microwave irradiation to dehydrate the ketone led to complete polymerization after 30 seconds.[20] Processing furan-2-carbaldehyde with the Bestman-Ohira reagent in the presence of K_2CO_3 in methanol to undergo an

[14] N. Huguet, D. Leboeuf and A. M. Echavarren, *Chem. –Eur. J.* **2013**, *19*, 6581–6585.
[15] P. Ribéreau and G. Quéguiner, *Tetrahedron Lett.* 1983, 39, 3593–3602.
[16] B. Zhong, L. Chen, J. Niu, D. Wu, H. Ma and M. Liao, *Acyclic nucleoside phosphonate derivative and its pharmaceutical use*, **2008**, CN 101293899.
[17] D. A. Dickman, Y. Y. Ku, H. E. Morton, S. R. Chemburkar, H. H. Patel, A. Thomas, D. J. Plata and D. P. Sawick, *Tetrahedron: Asymmetry,* **1997**, *8*, 1791–1795.
[18] F. Von der Ohe and R. Bruckner, *New J. Chem.* **2000**, *24*, 659–669.
[19] Y. E. Türkmen, T. J. Montavon, S. A. Kozmin and V. H. Rawal, *J. Am. Chem. Soc.* **2012**, *134*, 9062–9065.
[20] M. Ghaffarzadeh, M. Bolourtchian, Z. H. Fard, M. R. Halvagar and F. Mohsenzadeh, *Synth. Commun.* **2006**, *36*, 1973–1981.

homologation reaction resulted in the hydrolysis of the starting material.[21] Eventually, treatment of furan with ^{n}BuLi and I_2 afforded iodofuran in 65% isolated yield but the subsequent Negishi coupling reaction with ethynylmagnesium chloride, $ZnBr_2$ and $(Ph_3P)_4Pd$ led to decomposition.[22,23]

We later tried to oxidize 2-(diethoxymethyl)furan to further hydrolyze the acetal and build a terminal alkyne from the corresponding aldehyde.[24] Treatment with ^{n}BuLi and a mixture of BCl_3 and $B(OMe)_3$ would presumably generate the boronate intermediate **37** that could be oxidized in one pot to the corresponding lactone **38**. However, only traces of the desired product were observed (Scheme 8).

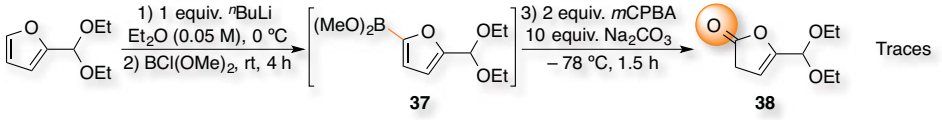

Scheme 8. Oxidation of 2-(diethoxymethyl)furan.

Moreover, we examined the possibility of oxidizing furan-2-carboxylic acid to 5-hydroxyfuran-2(5*H*)-one with air in the presence of rose Bengal with 450 nm light in $CHCl_3$ (Scheme 9).[25] We reasoned it could further undergo alkynylation and re–lactonization to intermediate **39**.[26] However, furan-2-carboxylic acid was recovered unchanged.

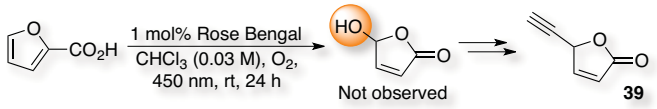

Scheme 9. Oxidation of furan-2-carboxylic acid.

Finally, we decided to attempt the synthesis of silyloxyalkynylfuran **27** avoiding the involvement of the furan scaffold in the early steps. We reasoned that we could selectively obtain the monoalkyne from either maleic anhydride or dimethyl maleate using 1 equivalent of ethynylmagnesium bromide and quenching with diluted HCl. Then, this could be selectively reduced with $NaBH_4$, cyclized and enolized to obtain the key furan. However, a very complex mixture was observed when the reactions were performed either at 0, – 50 or – 78 ºC.[27]

The same outcome was obtained when the reaction was attempted in the presence of LiCl, TMEDA, bis(methoxymethyl)ether or bis(2-dimethylaminoethyl)ether to stabilize the

---

[21] J. C. Gilbert and U. Weerasooriya, *J. Org. Chem.* **1982**, *47*, 1837–1845.
[22] R. W. Sinkelsam, A. J. Wheat, H. Boyaci and Y. Tor, *ChemPhysChem* **2011**, *12*, 567–570.
[23] E. Negishi, C. Xu, Z. Tan and M. Kotora, *Heterocycles* **1997**, *46*, 209–214.
[24] A. Pelter and M. Rowlands, *Tetrahedron Lett.* **1987**, *28*, 1203–1206.
[25] M. I. Burguete, R. Gavara, F. Galindo and S. V. Luis, *Tetrahedron Lett.* **2010**, *26*, 3360–3363.
[26] (*a*) R. A. Raphael, J. H. A. Stibbard and R. Tidbury, *Tetrahedron Lett.* **1982**, *23*, 2407–2410; (*b*) M. T. Reetz, K. Rölfing and N. Griebenow, *Tetrahedron Lett.* **1994**, *35*, 1969–1972.
[27] (*a*) D. Nightingale and F. T. Wadsworth, *J. Am. Chem. Soc.* **1947**, *69*, 1181–1183; (*b*) K. Y. Zhang, A. J. Borgerding and R. M. Carlson, *Tetrahedron Lett.* **1988**, *29*, 5703–5706; (*c*) W. Frosch, S. Back and H. Lang, *J. Organomet. Chem.* **2001**, *625*, 140–147; (*d*) R. Shintani and G. C. Fu, *Angew. Chem. Int. Ed.* **2002**, *41*, 1057–1059.

Grignard reagent as well as when it was performed by slow addition.[28] Still, if ethynyltrimethylsilane with ^{n}BuLi was used at – 60 ºC, the ring–opening product **40** was obtained in 40% isolated yield (Scheme 10).

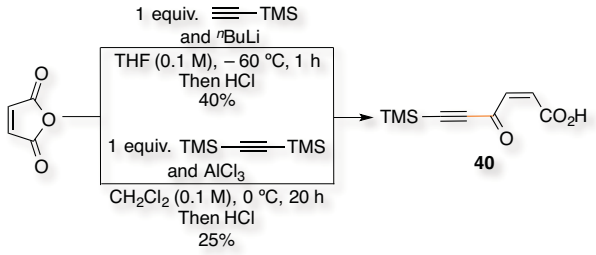

Scheme 10. Monoalkynylation of maleic anhydride.

Alternatively, the same carboxylic acid **40** could be synthesized using 1,2-bis(trimethylsilyl)ethyne and $AlCl_3$ in 25% isolated yield.[29,30]

2-Ethynyl-5-methylfuran as Model Substrate

In order to move forward, we synthesized 2-ethynyl-5-methylfuran as a model substrate and checked its reactivity towards the gold-catalyzed [2+2] cycloaddition with 6-methylhept-5-en-2-one. In this case, Negishi coupling from the iodo- derivative also failed to build the furan/alkyne C–C bond (Scheme 11).[22]

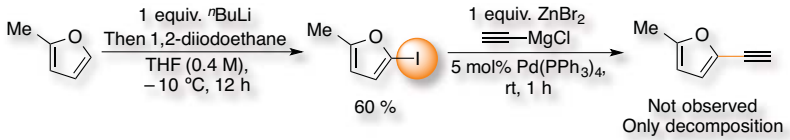

Scheme 11. Synthesis of 2-ethynyl-5-methylfuran via Negishi coupling.

Therefore, we build the protected alkyne **41** *via* Sonogashira reaction in 35% isolated yield over three steps (Scheme 12).[31] Although the deprotection led to decomposition when KOH was used, the desired alkynylfuran could be obtained with K_2CO_3 in methanol in 60% isolated yield. Unfortunately, the route was not productive when it was applied either to 2-methoxyfuran, 2-*tert*-butyldimethylsilyloxyfuran nor 2-triisopropylsilyloxyfuran.[13g]

---

[28] (*a*) X. J. Wang, L. Zhang, X. Sun, Y. Xu, D. Krishnamuthy and C. H. Senanayake, *Org. Lett.* **2005**, *7*, 5593–5595; (*b*) H. Zong, H. Huang, J. Liu, G. Bian and L. Song, *J. Org. Chem.* **2012**, *77*, 4645–4652.
[29] N. K. Nayyar, D. R. Hutchison and M. J. Martinelli, *J. Org. Chem.* **1997**, *62*, 982–991.
[30] Other possibilities considered: (*a*) E. J. Corey and P. L. Fuchs, *Tetrahedron Lett.* **1972**, *36*, 3769–3772; (*b*) A. Carpita, R. Rossi and C. A. Veracini, *Tetrahedron Lett.* **1985**, *41*, 1919–1929; (*c*) J. C. De Jong, F. Van Bolhuis and B. L. Feringa, *Tetrahedron: Asymmetry* **1991**, *2*, 1247–1262; (*d*) M. T. Crimmins, D. G. Washburn, J. D. Katz and F. J. Zawacki, *Tetrahedron Lett.* **1998**, *39*, 3439–3442; (*e*) P. Kumar and R. K. Pandey, *Green Chemistry* **2000**, 29–31; (*f*) L. Shen, Y. Zhang, A. Wang, E. Sieber-McMaster, X. Chen, P. Pelton, J. Z. Xu, M. Yang, P. Zhu, L. Zhou, M. Reuman, Z. Hu, R. Russel, A. C. Gibbs, H. Ross, K. Demarest, W. V. Murray and G. H. Kuo, *Bioorg. Med. Chem.* **2008**, *16*, 3321–3341.
[31] (*a*) H. Zhang and R. C. Larock, *J. Org. Chem.* **2002**, *67*, 7048–7056; (*b*) A. S. K. Hashmi, E. Enns, T. M. Frost, S. Schäfer, W. Frey and F. Rominger, *Synthesis* **2008**, *17*, 2707–2718.

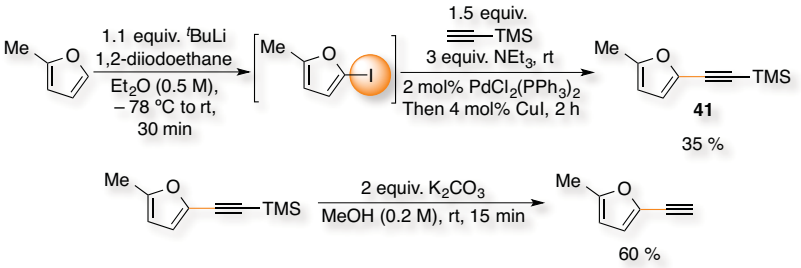

Scheme 12. Synthesis via Sonogashira coupling.

First, we performed the reaction between the alkynylfuran and α-methystyrene using ^{t}BuXPhosAuCl/NaBAr$^{F}_{4}$ in CH_2Cl_2 at 25 ºC for 24 h (Scheme 13). The desired cyclobutene **42** was obtained in 64% isolated yield.

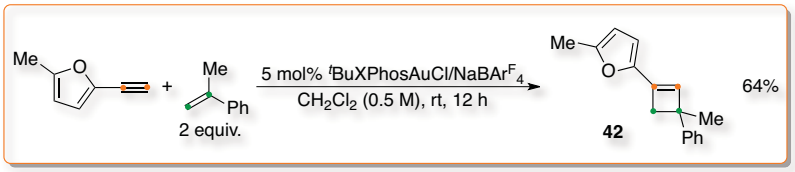

Scheme 13. [2+2] Cycloaddition using α-methylstyrene.

Then, we started the optimization of the gold cycloaddition with 6-methylhept-5-en-2-one by screening several ligands and counterions in the metal centre and maintaining the rest of conditions as in the original protocol (Table 1).[11]

Traces of the cyclobutene **43** were observed when JohnPhosAuCl, ^{t}BuXPhosAuCl or IPrAuCl (Figure 5) combined with NaBAr$^{F}_{4}$ were used as the catalytic system (entries 1, 2 and 3).[32] A complex mixture was obtained with Ph_3PAuCl (entry 4) but no reaction was observed with AuCl, (THT)AuCl or the gold complex with **44** (entries 5, 6 and 7). Interestingly, complete conversion with traces of the desired product was obtained when complex with **44** was activated with $AgSbF_6$ (entry 8). We also analyzed the reaction of ^{t}BuXPhosAuCl with $AgSbF_6$, $AgBF_4$ and $AgNTf_2$, which led to very complex mixtures (entries 9, 10 and 11) and $NaSbF_6$ did not show any reactivity (entry 12).

[32] C. Obradors, A. Homs, D. Leboeuf and A. M. Echavarren, *Adv. Synth. Catal.* **2013**, *356*, 221–228.

Table 1. Screening of catalysts for the [2+2] cycloaddition.

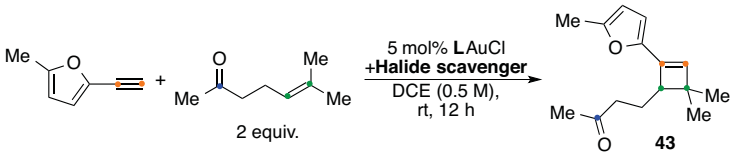

Entry	Ligand	Halide scavenger	Outcome[a]
1	JohnPhos	$NaBAr^F_4$	7%
2	^{t}BuXPhos	$NaBAr^F_4$	7%
3	IPr	$NaBAr^F_4$	12%
4	Ph_3P	$NaBAr^F_4$	Complex mixture
5	–	$NaBAr^F_4$	No reaction
6	THT	$NaBAr^F_4$	No reaction
7	**44**	$NaBAr^F_4$	No reaction
8	**44**	$AgSbF_6$	6%
9	^{t}BuXPhos	$AgSbF_6$	Complex mixture
10	^{t}BuXPhos	$AgBF_4$	Complex mixture
11	^{t}BuXPhos	$AgNTf_2$	4%
12	^{t}BuXPhos	$NaSbF_6$	No reaction

[a]Crude analysed by ^{1}H NMR using 1,4-diacetylbenzene as internal standard, yields referred to cyclobutene **43**.

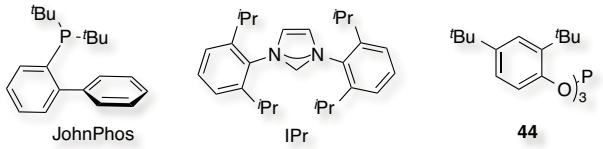

Figure 5. Ligands screened for the [2+2] cycloaddition.

We then tuned the stoichiometry, the concentration, the temperature and the reaction time (Table 2). Very low yields were observed at high concentrations (entries 1 to 4). No reaction was observed either at – 20 or 0 ºC (entries 5 and 6). However, a slight increment in the yield to **43** was observed by increasing the temperature and/or performing the reaction under more diluted conditions when using an excess of the oxoalkene (entries 7, 8 and 9). Further equivalents of the oxoalkene or decreasing the concentration did not improve the results (entries 10 to 13). The cycloaddition could be optimized to 31% isolated yield within 2 h reaction at 80 ºC (entry 16).

We also analysed the effect of the concentration, temperature and reaction time when using an NHC ligand on gold (Table 3). In this case, the optimum concentration was also 0.2 M (entry 1) but no further improvement was observed with the increment of the temperature (entries 4 and 5).

Table 2. Optimization for the [2+2] cycloaddition.

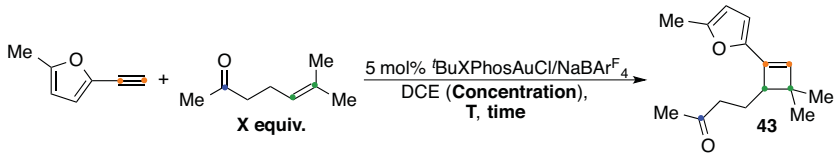

Entry	X equiv.	Concentration (M)	Temperature (ºC)	Reaction time (h)	Outcome[a,b]
1	2	1	25	12	Complex mixture
2	2	0.5	25	12	7%
3	1	0.5	25	12	5%
4	0.5	0.5	25	12	No reaction
5	2	0.5	0	12	No reaction
6	2	0.5	– 20	12	No reaction
7	2	0.5	50	12	13%
8	2	0.2	25	12	14%
9	2	0.2	50	12	21%
10	10	0.2	50	12	5% (80%)
11	2	0.04	50	12	10% (90%)
12	10	0.04	50	12	10% (65%)
13	2	0.02	50	12	9% (92%)
14	2	0.2	80	6	21%
15	2	0.02	80	6	21%
16	2	0.2	80	2	31%[c]
17	2	0.2	100	2	13%

[a]Crude analysed by ^{1}H NMR using 1,4-diacetylbenzene as internal standard, yields referred to cyclobutene **43**.
[b]Reaction conversion in brackets, 100% if not stated. [c]Isolated yield.

Table 3. Optimization using IPrAuCl for the [2+2] cycloaddition.

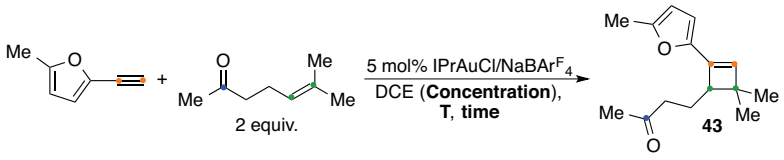

Entry	Concentration (M)	Temperature (ºC)	Reaction time (h)	Yield[a]
1	0.20	50	12	21%
2	0.04	50	12	16%
3	0.02	50	12	8%
4	0.20	80	2	14%
5	0.20	100	2	13%

[a]Crude analysed by ^{1}H NMR using 1,4-diacetylbenzene as internal standard, yields referred to cyclobutene **43**.

Thereby, the best result in the synthesis of cyclobutene **43** was obtained with ^{t}BuXPhosAuCl and NaBAr$^{F}_{4}$ (5 mol%) in DCE (0.2 M) at 80 ºC for 2 h between 2-ethynyl-5-methylfuran and 6-methylhept-5-en-2-one (Scheme 14).

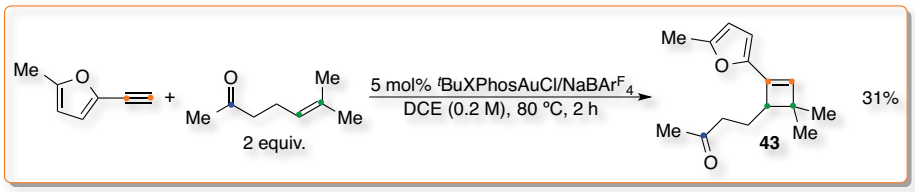

Scheme 14. Gold-catalyzed [2+2] cycloaddition of 2-ethynyl-5-methylfuran and 6-methylhept-5-en-2-one.

4. Oxidation Approach

Retrosynthetic Analysis

We considered an alternative approach based on the possibility of oxidizing an aromatic ring to a carboxylic acid.[33] We reasoned that we could perform the gold-catalyzed [2+2] cycloaddition between ethynylbenzene and 6-methylhept-5-en-2-one followed by a diastereoselective hydrogenation of the cyclobutene **19** to ***trans*-45** (Scheme 15). Then, the phenyl moiety could be oxidized with RuO_4. In this manner, the carboxylic acid ***trans*-46** could undergo a methylation reaction and a subsequent stereoselective allylation of the resulting ketone to **47**.

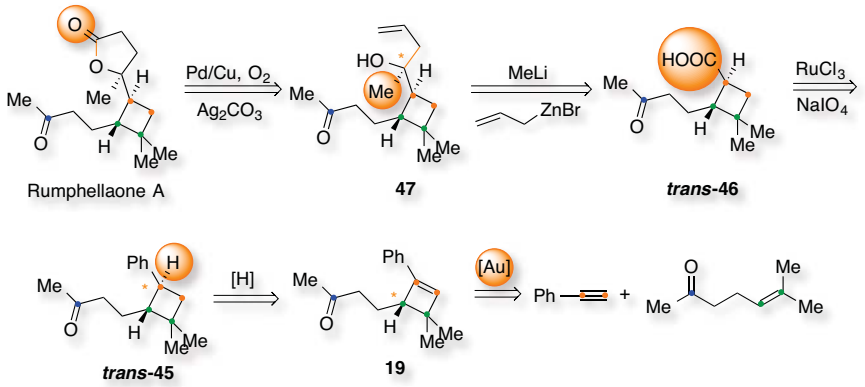

Scheme 15. Alternative retrosynthetic analysis of Rumphellaone A.

The feasibility of building a lactone from an homoallylic alcohol (**47**) was also a critical transformation in the design of our new synthetic route.[34] Hence, we planned a reverse Wacker oxidation to afford hemiacetal **48** followed by silver oxidation to form the lactone moiety present in rumphellaone A (Scheme 16).

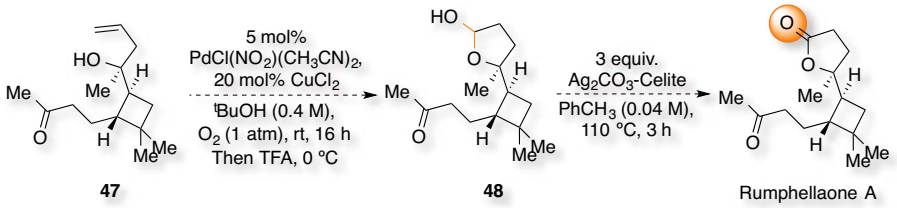

Scheme 16. Planned reverse Wacker oxidation.

Besides, we had to consider performing a gold-catalyzed [2+2] cycloaddition enantioselectively. Although several asymmetric gold catalysts have been developed recently using chiral ligands and/or counterions, these have been limited mainly to

[33] I thank Dr. Javier Carreras for suggesting this alternative pathway.
[34] (*a*) J. Muzart, *Tetrahedron* **2007**, *63*, 7505–7521; (*b*) S. Wan, H. Gunaydin, K. N. Houk and P. E. Floreancig, *J. Am. Chem. Soc.* **2007**, *129*, 7915–7923; *(c)* J. J. Dong, W. R. Browne and B. L. Feringa, *Angew. Chem. Int. Ed.* **2014**, *53*, 2–13.

intramolecular reactions. Otherwise, most of the gold-catalyzed transformations are stereospecific and enantioenriched products have been obtained *via* substrate-induced enantioselective reactions.[35]

Use of a Chiral Acetal

Since substrate–induced enantioselectivity has proved to be much more effective in gold catalysis, we reasoned we could attempt the [2+2] cycloaddition introducing a chiral element either in the oxoalkene or the alkyne. We considered that the more promising approach was to use an asymmetric protecting group in the ketone moiety like in **49** to build enantioenrich cyclobutene **50** (Scheme 17). Therefore, we seek for diols bulky enough to form an acetal that could influence the stereoselectivity occurring in the alkene group.

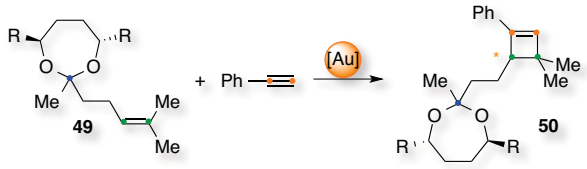

Scheme 17. Substrate–controlled enantioselective [2+2] gold cycloaddition.

First, we imagined an acetal derived from BINOL derivatives such as **51**, **52**, **53** and **54** (Figure 6).

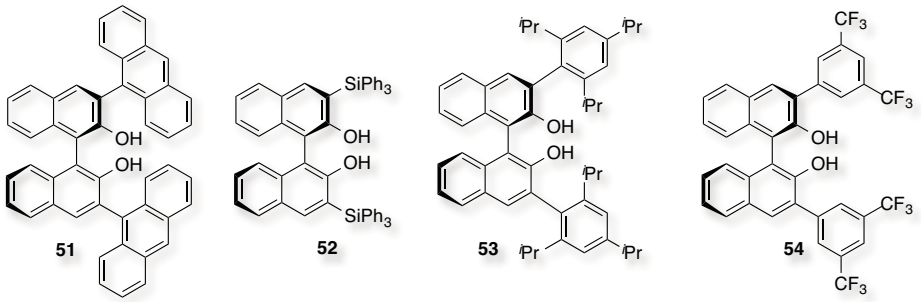

Figure 6. BINOL derivatives as protecting groups.

We calculated the optimized structures of the corresponding acetals with 6-methylhept-5-en-2-one using DFT analysis (M06, 6-31 G(d) (C, H, O), in CH_2Cl_2). In the case of the antracene-substituted BINOL **51**, we could observe a distance between the chiral unit and the alkene of 3.48 Å in the external position and 3.94 Å for the internal one after the acetal formation (Figure 7).

[35] (*a*) R. A. Widenhoefer, *Chem. –Eur. J.* **2008**, *14*, 5382–5391; (*b*) N. T. Patil, *Chem. Asian J.* **2012**, *7*, 2186–2194; (*c*) Y. M. Wang, A. D. Lackner and F. D. Toste, *Acc. Chem. Res.* **2014**, *47*, 889–901.

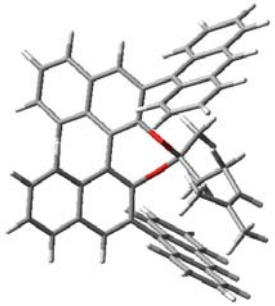

Figure 7. Chiral acetal with 51.

In the presence of triphenylsilyl groups (**52**) the distances were 3.37 Å and 3.81 Å, which are reasonably similar (Figure 8). Conversely, for the trifluoromethyl groups (**54**), 3.95 Å and 3.75 Å so in this case the internal position would be more crowded.

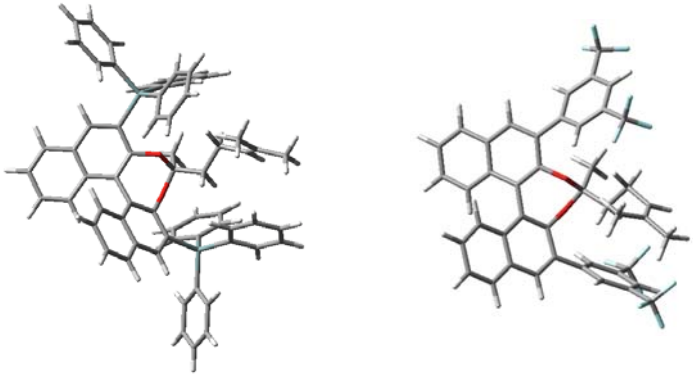

Figure 8. Chiral acetals with 52 and 54.

Finally, in the case of isopropyl groups (**53**), the distances were 2.70 Å and 2.75 Å. Both carbons are quite comparable and notably shorter than the rest of protecting groups (Figure 9).

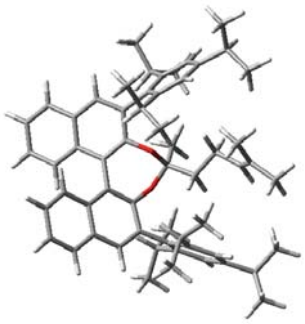

Figure 9. Chiral acetal with 53.

We first synthesized acetal **55** using butane-1,4-diol. Reaction with *p*-toluensulfonic acid in toluene under reflux led to decomposition of 6-methylhept-5-en-2-one.[36] Similar results were obtained with propane-1,3-diol or ethane-1,2-diol. However, acetal **55** was obtained in 65% isolated yield when treated with NH_4Cl and hydroquinone in a Dean-Stark apparatus. Purification difficulties forced us to attempt the reaction employing a Lewis acid and triethyl orthoformate (Table 4).[37] Then, acetal **55** was easily purified by distillation. $CeCl_3$ and $AuBr_3$ forged product **55** in modest yields (entries 1 and 2) whereas $ZrCl_4$ only afforded traces of it (entry 3). The best results were obtained using $FeCl_3$ (entry 4). No reaction was observed with $CuSO_4$ (entry 6).

Table 4. Screening of Lewis acids for an alternative synthesis of 55.

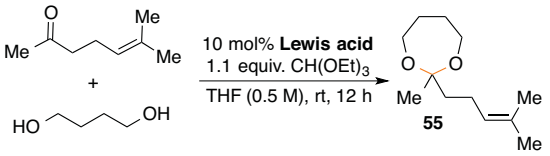

Entry	Lewis acid	Outcome[a]
1	$CeCl_3$	38%
2	$AuBr_3$	51%
3	$ZrCl_4$	8%
4	$FeCl_3$	83%[b]
5[c]	$FeCl_3$	No reaction
6	$CuSO_4$	No reaction

[a]Crude analysed by ^{1}H NMR using 1,4-diacetylbenzene as internal standard, yields referred to acetal **55**. [b]Isolated yield. [c]No triethyl orthoformate added.

We performed the gold-catalyzed [2+2] cycloaddition between ethynylbenzene and acetal **55** to construct cyclobutene **56** (Table 5). Keeping ^{t}BuXPhos as the ligand for gold and DCE as solvent, we screened the reaction conditions. Interestingly, the cationic catalyst was required in this case as the generation *in situ* of the active species with the corresponding gold chloride and $NaBAr^F_4$ was partially cleaving the acetal in **55** and **56**.

Very low yields to the desired product were observed when the reaction was performed at 50 ºC (entries 1 to 4). Gradual increment of the stoichiometry at 25 ºC showed higher yields with an excess of the alkyne and $BAr^F_4^-$ as the counterion (entries 5 to 8). Parallel experiments at 0 ºC led to lower yields and conversions (entries 9, 10 and 11). However, longer reaction times with larger amounts of ethynylbenzene slowly improved the result (entries 12, 13 and 14).

[36] K. Nagata, H. Ishikawa, A. Tanaka, M. Miyazaki, T. Kanemitsu and T. Itoh, *Heterocycles* **2010**, *81*, 1791–1798.
[37] (*a*) H. Firouzabadi, N. Iranpoor and B. Karimi, *Synlett* **1999**, *3*, 321–323; (*b*) I. Karamé, M. Alamé, A. Kanj, G. N. Baydoun, H. Hazimeh, M. el Masri and L. Christ, *C. R. Chimie* **2011**, *14*, 525–529.

Table 5. Optimization of the [2+2] cycloaddition using acetal 55.

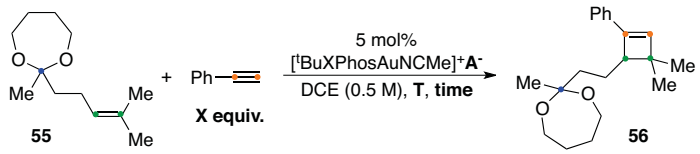

Entry	A^-	X equiv.	Temperature (ºC)	Reaction time (h)	Yield[a,b]
1	SbF_6^-	5.0	50	20	12%
2	BAr_F^-	5.0	50	20	16%
3	SbF_6^-	0.5	50	20	7%
4	BAr_F^-	0.5	50	20	12%
5	BAr_F^-	0.5	25	5	22%
6	BAr_F^-	1.0	25	5	21% (89%)
7	BAr_F^-	2.0	25	5	33% (73%)
8	SbF_6^-	2.0	25	5	16% (74%)
9	BAr_F^-	0.5	0	5	10% (55%)
10	BAr_F^-	1.0	0	5	10% (74%)
11	BAr_F^-	2.0	0	5	13% (38%)
12	SbF_6^-	2.0	0	48	30% (70%)
13	SbF_6^-	5.0	0	48	29% (78%)
14	SbF_6^-	10	0	48	31% (69%)
15	BAr_F^-	2.0	0	48	42% (74%)
16	BAr_F^-	5.0	0	48	45% (86%)
17	BAr_F^-	10	0	48	50%[c] (89%)
18	BAr_F^-	10	– 20	20	21% (41%)

[a]Crude analysed by ^{1}H NMR using 1,4-diacetylbenzene as internal standard, yields referred to cyclobutene **56**. [b]Reaction conversion in brackets, 100% if not stated. [c]Isolated yield. [d]10 mol% of catalyst used.

Therefore, the most efficient result was obtained when 10 equiv. of ethynylbenzene and [^{t}BuXPhosAuNCMe]BAr^F_4 (**Q**) were added at 0 ºC for 48 h in which cyclobutene **56** was obtained in 50% isolated yield (Scheme 18). Further decrease of the temperature to – 20 ºC did not improve the result (entry 18).

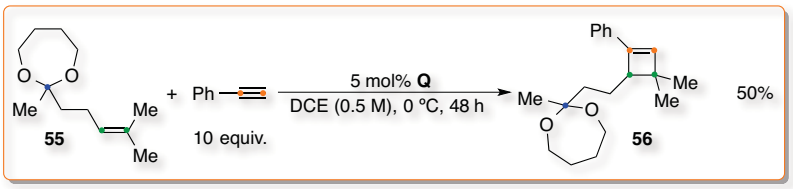

Scheme 18. Gold-catalyzed [2+2] cycloaddition of ethynylbenzene and acetal 55.

We attempted the formation of a chiral acetal such as **57** from 6-methylhept-5-en-2-one and BINOL to build the corresponding cyclobutene **58** with ethynylbenzene and [^{t}BuXPhosAuNCMe]BAr^F_4 (**Q**) under the optimized conditions (Scheme 19).

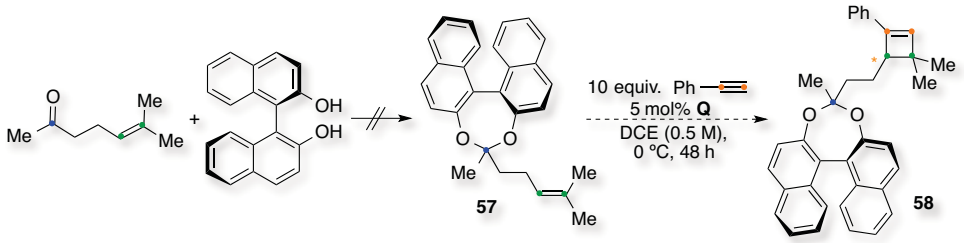

Scheme 19. Synthesis of acetal 57 and substrate – controlled enantioselective [2+2] cycloaddition.

Nevertheless, acetal **57** could not be prepared using the methodologies applied for the standard acetal **55**. Other Lewis acids such as $InCl_3$ or $BF_3{\cdot}Et_2O$ were also tested but unreacted BINOL was recovered.[38] Finally, the reaction was attempted with P_2O_5 in toluene at 75 ºC but complete decoposition of the oxoalkene was obtained.[39]

Due to the failure in forming a chiral acetal, a substrate – controlled gold-catalyzed asymmetric [2+2] cycloaddition to build an enantioenrich cyclobutene was dismissed.

Enantioselective Gold-Catalyzed [2+2] Cycloaddition

Consequently, we essayed several chiral gold complexes in the [2+2] cycloaddition of ethynylbenzene and 6-methylhept-5-en-2-one. We started by testing complex **V** and tuning the counterion, the stoichiometry and the temperature of the reaction (Scheme 20).[40]

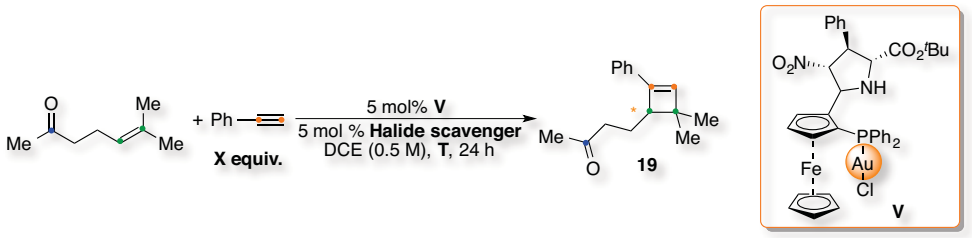

Scheme 20. [2+2] Cycloaddition using V.

A complex mixture was obtained at 50 ºC with 4 equiv. of ethynylbenzene either using SbF_6^- or $BAr^F{}_4^-$. The same outcome was observed at lower temperature (25 ºC) or when switching the stoichiometry. With the protected oxoalkene **55**, we obtained the same result altough at 0 ºC only cleavage of the acetal was observed.

We attempted the reaction with another ferrocene-based gold catalyst (**W**) with $BAr^F{}_4^-$ and at 25 ºC (Scheme 21).[41] Under these conditions we observed the formation of enantioenriched cyclobutene **19** in 13% yield (57% conversion) and 33% *ee*. This result is

[38] G. Tocco, M. Begala, G. Delogu, C. Piccaiau and G. Podda, *Tetrahedron Lett.* **2004**, *45*, 6909–6913.
[39] H. Q. Zhang, C. Bo. Zhang, Y. Zheng and Y. G. Ma, *Chem. Res. Chin. Univ.* **2008**, *24*, 798–804.
[40] Catalyst provided by Prof. Fernando P. Cossio's research group (Universidad del País Vasco). Complex **V** was prepared by Dr. Iván Rivilla, who collaborated in the enantioselective synthesis of oxabicycles (**Chapter 2**).
[41] Example performed by Dr. Laura López.

still rather poor but it is one of the few examples of inducing enantioselectivity in an intermolecular cycloaddition to an alkyne.

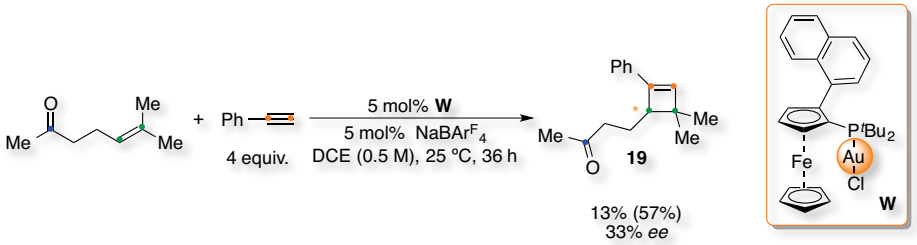

Scheme 21. [2+2] Cycloaddition using W.

Performing the reaction in the same conditions using complex **X** led to no reaction, even when heating at 50 ºC (Figure 10).[42] As observed before, NaBAr$^F_4$ is not always productive in the chloride abstraction of a phosphite gold complex.

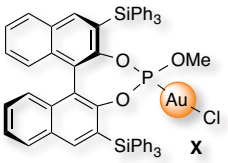

Figure 10. Complex X.

Simultaneously, it was determined by NMR experiments that triflimide could be a useful counterion for gold cycloadditions at low temperatures.[43] Thus, ligand exchange with ethynylbenzene was observed from – 78 ºC to 20 ºC when the corresponding digold scaffold started to abound significantly. Therefore, multiple attempts were essayed using $AgNTf_2$ as the halide scavenger (Scheme 22).

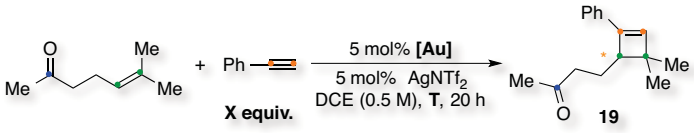

Scheme 22. Screening of ligands with NTf_2^-.

This time we focused in bidentate phosphines and a phosphoramidite as they have been more commonly and successfully used in enantioselective gold catalysis.[44] We started our screening using gold complexes **Y**, **Z**, **LL** and **SS** (Figure 11).

---

[42] N. Delpont, I. Escofet, P. Pérez-Galán, D. Spiegl, M. Raducan, C. Bour, R. Sinisi and A. M. Echavarren, *Catal. Sci. Tech.* **2013**, *3*, 3007–3012.
[43] Experiments performed by Imma Escofet.
[44] (*a*) G. L. Hamilton, E. J. Kang, M Mba and F. D. Toste, *Science* **2007**, *317*, 496–499; (*b*) R. L. LaLonde, B. D. Sherry, E. J. Kand and F. D. Toste, *J. Am. Chem. Soc.* **2007**, *129*, 2452–2453; (*c*) K. Aikawa, M. Kojima and K. Mikami, *Angew. Chem. Int. Ed.* **2009**, *48*, 6073–6077; (*d*) H. Teller, S. Flügge, R. Goddard and A. Fürstner, *Angew. Chem. Int. Ed.* **2010**, *49*, 1949–1953; (*e*) K. Aikawa, M. Kojima and K. Mikami, *Adv. Synth. Catal.* **2010**, *352*, 3131–3135; (*f*) A. Z. González, D. Benitez, E. Tkatchouk, W. A. Goddard and F. D Toste, *J. Am. Chem. Soc.* **2011**, *133*, 5500–5507; (*g*) M. Kojima and K. Mikami, *Chem. –Eur. J.* **2011**, *17*, 13950–13953; (*h*) R. J. Felix, D. Weber, O. Gutierrez, D. J. Tantillo and M. R. Gagné, *Nat. Chem.* **2012**, *4*, 405–409; (*i*) H. S. Yeom, J. Koo, H. S. Park, Y. Wang, Y. Liang, Z. X. Yu and S. Shin, *J. Am. Chem. Soc.* **2012**, *134*, 208–211; (*j*) S. Handa and L. M. Slaughter, *Angew. Chem. Int. Ed.* **2012**, *51*, 2912–2915; (*k*) K. L. Butler, M. Tragni and R. A. Widenhoefer, *Angew. Chem. Int. Ed.* **2012**, *51*, 5175–5178; (*l*) J. F. Briones and H. M. L. Davies, *J. Am. Chem. Soc.* **2012**, *134*, 11916–11919; (*m*) J. Francos, F. Grande-Carmona, H. Faustino, J. Iglesias-Sigüenza, E. Díez, I. Alonso, R. Fernández, J. M. Lassaletta, F. Lópe and J. L. Mascareñas, *J. Am. Chem. Soc.* **2012**, *134*, 14322–14325.

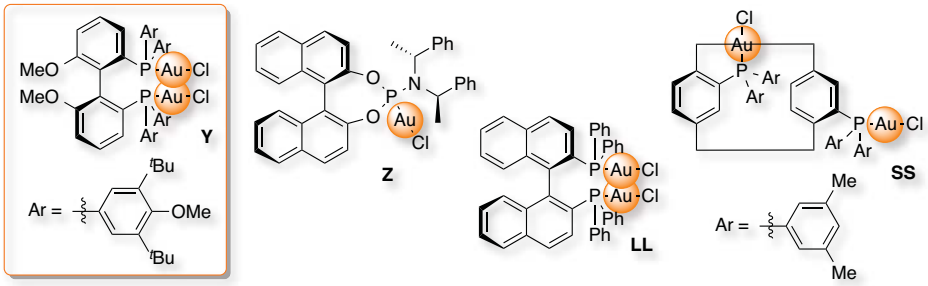

Figure 11. Other chiral gold complexes.

No cyclobutene **19** was observed when the reactions were performed at 0, 25 or 50 ºC using 1:4 or 4:1stoichiometries. Interestingly, we detected the formation of a new product that we identified as tetrahydropyran **59**, analogous to the tetrahydrofurans isolated during the formation of oxabicycles (see **Chapter 2**).[12] Thus, byproduct **59** was obtained in 38% isolated yield when the cycloaddition of ethynylbenzene and an excess of 6-methylhept-5-en-2-one was performed with complex **Z** and triflimide at 25 ºC (Scheme 23).

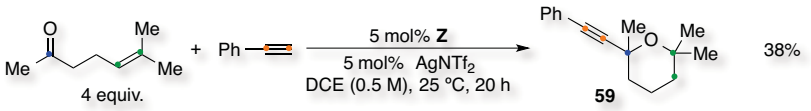

Scheme 23. Formation of by-product 59.

Therefore, we decided to continue the screening for the formation of the enantioenriched cyclobutene **19** using $BAr^{F}_{4}^{-}$ as the counterion (Table 6).[32]

Table 6. Screening of ligands with BAr_F^-.

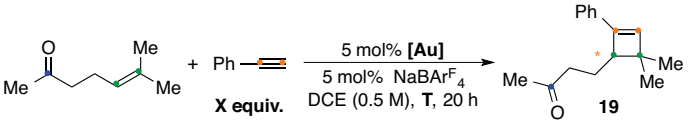

Entry	[Au]	X equiv.	Temperature (ºC)	Outcome[a,b]	*ee*[c]
1	**Y**	4	50	61%[d] (69%)	30%
2	**Z**	4	50	No reaction	Not determined
3	**LL**	4	50	6% (74%)	Not determined
4	**SS**	4	50	7% (68%)	Not determined
5	**LL**	4	25	Complex mixture	Not determined
6	**SS**	4	25	Complex mixture	Not determined
7	**SS**	4	0	No reaction	Not determined
8	**LL**	0.25	25	No reaction	Not determined
9	**LL**	0.25	0	No reaction	Not determined

[a]Crude analysed by ^{1}H NMR using 1,4-diacetylbenzene as internal standard, yields referred to cyclobutene **19**. [b]Reaction conversion in brackets. [c]ChiralPak IC, hexane : isopropanol : ethanol (97:2:1), 1 mL/min, 245 nm. [d]Isolated yield.

We could observe the clean formation of the desired product **19** when complex **Y** was used at 50 ºC (entry 1). No product was observed for **Z** (entry 2) and only traces for **LL** and **SS**. No improvements were observed for **Z**, **LL** or **SS** at lower temperatures or when switching the stoichiometry (entries 7 to 11).

Chiral HPLC determined that the cyclobutene **19** obtained with catalyst **Y** had 30% *ee* at 50 ºC (Scheme 24).

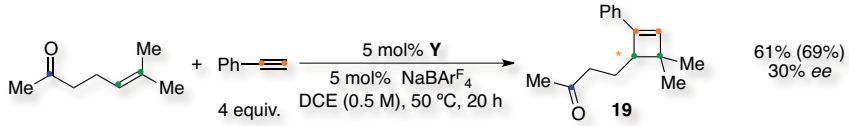

Scheme 24. Enantioselective [2+2] cycloaddition.

With these results result, we envisioned the study related BIPHEP bis-phosphine scaffolds tuning the backbond of the complex as well as the substituents of the phosphine: **Y2**, **Y3**, **Y4** and **Y5** (Figure 12).

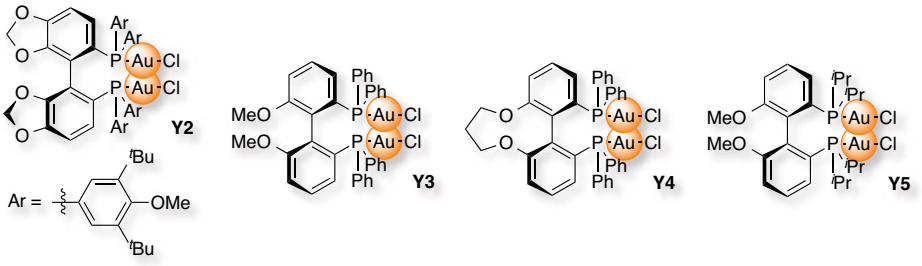

Figure 12. BIPHEP gold complexes related to Y.

Simultaneously, the effect of the reaction conditions is also on-going work.[45] Although the results are still modest, we proved that an intermolecular, enantioselective [2+2] cycloaddition between an alkyne and an alkene is certainly feasible.

Synthesis of the Racemic Rumphellaone A

Concurrently, we continued towards the total synthesis of rumphellaone A working on the racemic version.

- Gold-Catalyzed [2+2] Cycloaddition

As mentioned before, cyclobutene **19** could be obtained in 54% isolated yield using 6-methylhept-5-en-2-one and 3.5 equiv. of ethynylbenzene with 5 mol% of [^{t}BuXPhosAuNCMe]SbF$_6$ (**E**) in DCE (0.5 M) at 50 ºC for 19 h (Scheme 3).[12] The

[45] For the use of AgBAr$^F_4$ see: *(a)* M. Brookhart, B. Grant and A. F. Volpe Jr., *Organometallics* **1992**, *11*, 3920–3922; *(b)* S. Tanaka, M. Takashina, H. Tokimoto, Y. Fujimoto, K. Tanaka and K. Fukase, *Synlett* **2005**, *15*, 2325–2328; *(c)* H. Braunschweig, K. Radacki and A. Schneider, *Chem. Commun.* **2010**, *47*, 6473–6475; *(d)* K. Surendra and E. J. Corey, *J. Am. Chem. Soc.* **2014**, *136*, 10918–10920.

reaction yield could be improved to 78% when [^{t}BuXPhosAuNCMe]BAr$^{F}_{4}$ (**Q**) was used (Scheme 25).[32] In this case, just 18% of the corresponding oxabicycle (**20**) was observed.

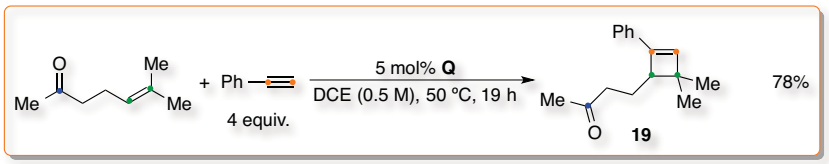

Scheme 25. Optimized synthesis of cyclobutene 19.

In order to explore the effect of the aromatic ring's substituents in the oxidation to carboxylic acid **46**, we also synthesized cyclobutenes **60**, **61** and **62** using 3-ethynylphenol, 1-ethynyl-3-methoxybenzene and 1-ethynyl-3-methylbenzene under the optimized conditions in 40, 65 and 44% isolated yields, respectively (Figure 13). Although the yields were lower than with ethynylbenzene, they could be useful substrates in the oxidation step.

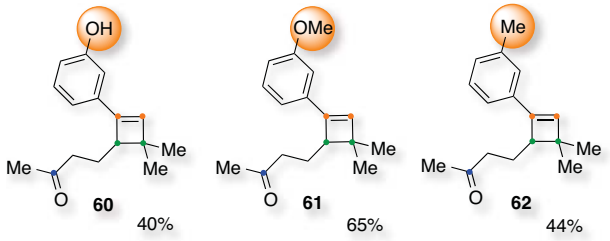

Figure 13. Alternative precursors of rumphellaone A.

- **Hydrogenation of the Cyclobutene.**

First, we reduced the alkene moiety of **19** using 10 mol% Pd/C in methanol at 25 ºC stirring for 5 h under 1 atm of H_2 to obtain the cyclobutane moiety (**45**) in 90% isolated yield (Scheme 26).[46] However, this conditions led to a 1.6:1 mixture of diastereoisomers.

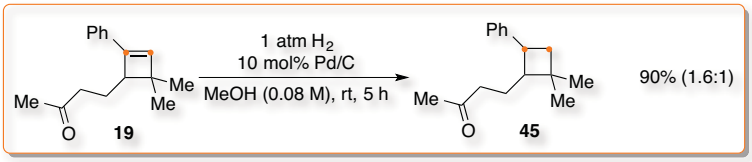

Scheme 26. Hydrogenation of 19 with Pd/C and H_2.

As suspected, the steric factors were not significant enough to undergo a diastereoselective hydrogenation. Hence, we reasoned we could use the carbonyl moiety as a directing group. We attempted the hydrogenation using Crabtree's catalyst, [Ir(cod)PCy$_3$(py)]PF$_6$, in CH_2Cl_2 (Scheme 27).[47,48] Although there are examples of free alcohols, ketones, ethers and

[46] M. Yamashita, Y. N. Dnyanoba, M. NagahamaT. Inaba, Y. Nishino, K. Miura, S. Kosaka, J. Fukao, I. Kawasaki and S. Ohta, *Heterocycles* **2005**, *65*, 2411–2430.
[47] R. H. Crabtree and M. W. Davis, *J. Org. Chem.* **1986**, *51*, 2655–2661.

esters behaving as directing groups up to four carbons distance by coordination to the metal, which slightly resembles our case, no reaction was observed.

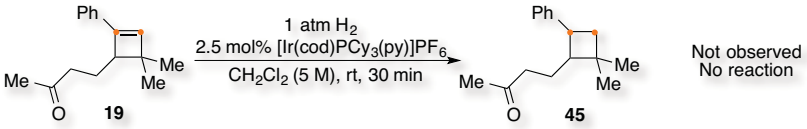

Scheme 27. Directing effect using Crabtree's catalyst.

The most promising alternatives relied on radical-based protocols as the thermodynamic product would be formed. However, these methodologies are rarely applied in styrenes. Very recently, a new procedure to reduce inactivated alkenes with thermodynamic stereocontrol was reported using a manganese complex with phenylsilane and TBHP in isopropanol.[49] Presumably, a metal–hydride is formed and undergoes a hydrogen atom transfer reaction to the alkene. Therefore, a carbon centred radical is formed and builds the more stable product when is finally reduced. We tested this reaction with cyclobutene **19** but only polymerization was observed (Scheme 28). Further attempts based on decreasing the concentration, increment of the equivalents of the silane or TBHP (decane) or use of THF as co-solvent led to the same result.

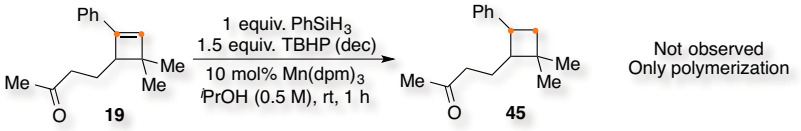

Scheme 28. Alkene reduction with thermodynamic stereocontrol.

Later, we applied the Birch reduction conditions as there are a few examples reported on the selective reduction of styrene's double bond.[50,51] After screening, the best results were obtained when cyclobutene **64**, synthesized analogously to **56** but with the six-membered ring acetal **63**, was treated with sodium metal in liquid ammonia at – 78 ºC for 30 min to obtain cyclobutane **65** in 40% yield with a 1:5 diastereoselectivity (Scheme 29). In spite of the improvement, the yield was still low.

---

[48] An enantioselective catalyst could be used as well: T. L. Church and P. G. Anderson, *Coord. Chem. Rev.* **2008**, *252*, 513–531.
[49] (*a*) R. P. Yu, J. M. Darmon, C. Milsmann, G. W. Margulieux, S. C. E. Stieber, S. DeBeer and P. J. Chirik, *J. Am. Chem. Soc.* **2013**, *135*, 13168–13184; (*b*) K. Iwasaki, K. K. Wan, A. Oppedisano, S. W. M. Crossley and R. Shenvi, *J. Am. Chem. Soc.* **2014**, *136*, 1300–1303.
[50] Screening performed by Dr. Laura López.
[51] (*a*) S. N. Ananchenko, V. Y. Limanov, V. N. Leonov, V. N. Rzheznikov and I. V. Torgov, *Tetrahedron* **1962**, *18*, 1355–1367; (*b*) Z. Lin, J. Chen and Z. Valenta, *Tetrahedron Lett.* **1997**, *38*, 3863–3866.

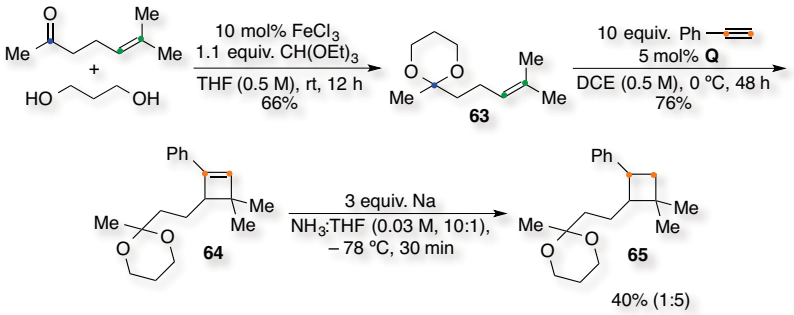

Scheme 29. Birch reduction of styrenes.

An alternative protocol consisted in adding magnesium turnings to cyclobutene **19** in methanol (Scheme 30).[52] However, no **45** was obtained as the double bond was recovered intact but partial reduction of the ketone to the secondary alcohol was observed.

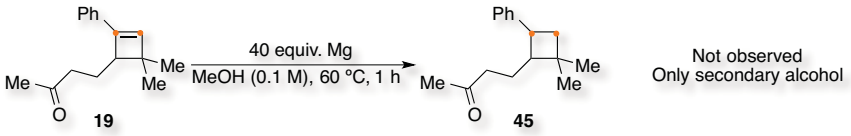

Scheme 30. Reduction with Mg/MeOH.

On the other hand, when potassium metal in dimethylamine was used, no reaction was occurred (Scheme 31).

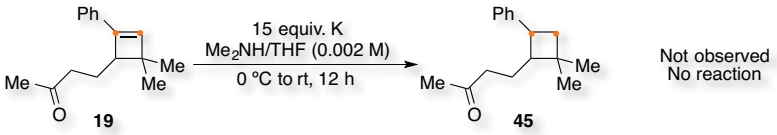

Scheme 31. Reduction with K/Me_2NH.

Finally, reaction with Li/naphthalene in the presence of $NiCl_2 \cdot 6H_2O$ in THF at 25 ºC did not lead to the desired product (Scheme 32).[53] Using DTBB as initiator led to no reaction as well as anhydrous $NiCl_2$ under H_2 atmosphere.

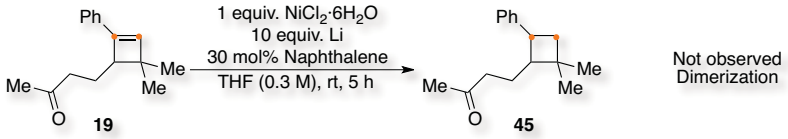

Scheme 32. Reduction with Li/naphthalene and $NiCl_2 \cdot 6H_2O$.

[52] G. H. Lee, I. K. Youn, E. B. Choi, H. K. Lee, G. H. Yon, H. C. Yang and C. S. Pak, *Curr. Org. Chem.* **2004**, *8*, 1263–1287.
[53] (*a*) F. Alsonso and M. Yus, *Tetrahedron* **1998**, *54*, 1921–1928; (*b*) F. Alonso, P. Candela, C. Gómez and M. Yus, *Adv. Synth. Catal.* **2003**, *345*, 275–279.

Regarding the challenge of the stereoselectivity, we reasoned that we could attempt the isomerization towards the *trans*-cyclobutane in a late stage of the total synthesis. After the oxidation of the phenyl ring and esterification, we could use a base to deprotonate the α-position of the ester **66**. The desired diastereoisomer would be obtained under thermodynamic conditions (Scheme 33).

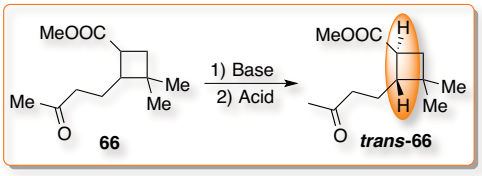

Scheme 33. Possible late stage isomerization.

Furthermore, we optimized both the *cis*- and the *trans*-cyclobutane by means of DFT calculations (M06, 6-31 G(d) (C, H, O), in CH_2Cl_2). Our calculations indicated that ***trans*-66** is 2.8 kcal/mol more stable than ***cis*-66** (Figure 14).

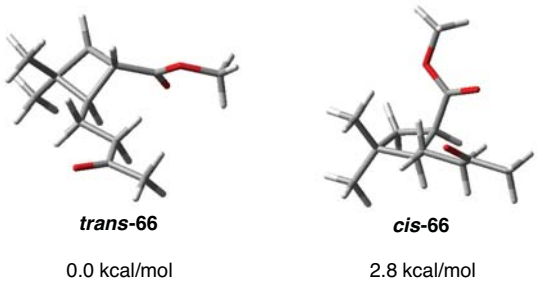

Figure 14. Diastereoisomers of ester 66.

We also submitted cyclobutenes **60**, **61** and **62** to the hydrogenation conditions with catalytic Pd/C in methanol (Figure 15). Cyclobutanes **67**, **68** and **69** were obtained in 86, 53 and 84% respectively.

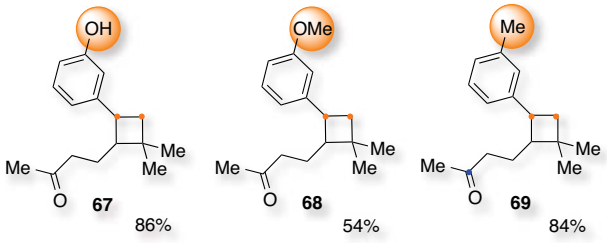

Figure 15. Synthesis of alternative cyclobutanes 67, 68 and 69.

- **Phenyl Oxidation Followed by Esterification**

According to the literature, the oxidation of aryl rings is commonly carried out using catalytic $RuCl_3$ with an excess of $NaIO_4$.[54,55] The transformation to carboxylic acids proceeds through the generation of RuO_4 *in situ*, which oxidizes any unsaturated C–C bond. We first performed the reaction with cyclobutane **45** using 3 mol% catalyst testing different solvent mixtures (Table 7). Only traces of the carboxylic acid **46** were observed when 15 equiv. of $NaIO_4$ were used in a mixture of CCl_4:CH_3CN:H_2O (2:2:3) for 4 h (entry 2). No reaction was observed with H_5IO_6 (entry 3) and very low reactivity was also obtained if $NaIO_4$ was combined with $NaHCO_3$ (entry 4).

Table 7. Screening for the phenyl oxidation using $RuCl_3$/$NaIO_4$.

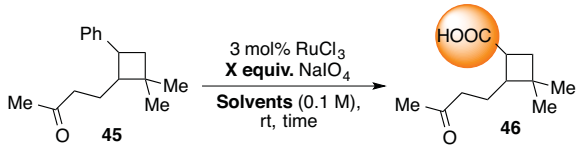

Entry	X equiv.	Solvents	Reaction time (h)	Outcome[a]
1	5	CCl_4:CH_3CN:H_2O (2:2:3)	4	No reaction
2	15	CCl_4:CH_3CN:H_2O (2:2:3)	4	Traces
3[b]	15	CCl_4:CH_3CN:H_2O (2:2:3)	4	No reaction
4[c]	5	EtOAc:CH_3CN:H_2O (1:1:8)	144	Traces

[a]Crude analysed by ^{1}H NMR using 1,4-diacetylbenzene as internal standard, yields referred to carboxylic acid **46**. [b]H_5IO_6 used as the oxidant. [c]1.2 equiv. of $NaHCO_3$ added.

On the other hand, we changed the protocol to 10 mol% RuO_2 with an excess of $NaIO_4$ in EtOAc:H_2O (1:3) under highly diluted conditions.[56] The transformation was performed from 4 to 25 ºC for 24 h to afford the carboxylic acid **46** in 80% isolated yield (Scheme 34).

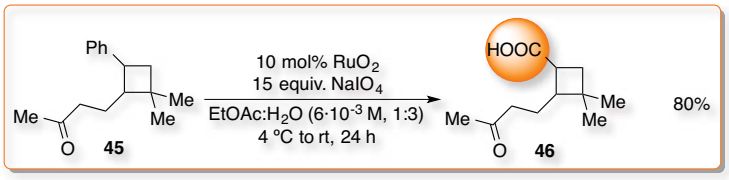

Scheme 34. Phenyl oxidation using RuO_2/$NaIO_4$.

Moreover, carboxylic acid **46** could be obtained from cyclobutane **67** in 83% isolated yield, **68** in 90% and **69** in 92%.

---

[54] (*a*) J. A. Caputo and R. Fuchs, *Tetrahedron Lett.* **1967**, *47*, 4729–4731; (*b*) P. H. J. Carlsen, T. Katsuki, V. S. Martin and K. B. Sharpless, *J. Org. Chem.* **1981**, *46*, 3936–3935; (*c*) M. Kasai and H. Ziffer, *J. Org. Chem.* **1983**, *48*, 2346–2349; (*d*) M. T. Núñez and V. S. Martin, *J. Org. Chem.* **1990**, *55*, 1928–1932.
[55] Alternatively: R. Liotta and W. S. Hoff, *J. Org. Chem.* **1980**, *45*, 2887–2890.
[56] W. R. Gutekunst and P. S. Baran, *J. Org. Chem.* **2014**, *79*, 2430–2452.

Afterwards, the esterification of **46** with TMS-diazomethane in a mixture of toluene and methanol at 0 ºC afforded the methyl ester **66** in 91% isolated yield (Scheme 35).[57]

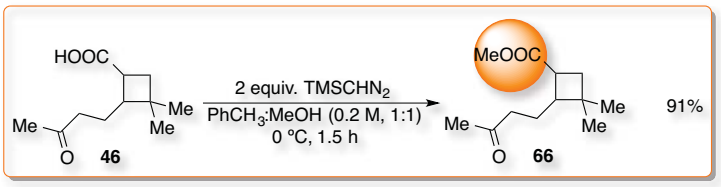

Scheme 35. Esterification of carboxylic acid 46.

- **Protection *via* Acetalization**

We first attempted the protection of the ketone functionality in **66** with propane-1,3-diol under the optimized conditions used to synthesize acetal **55**.[37b] We submitted the substrates to catalytic $FeCl_3$ and an excess of triethyl orthoformate in order to form a six-membered ring as in acetal **70** (Scheme 36).

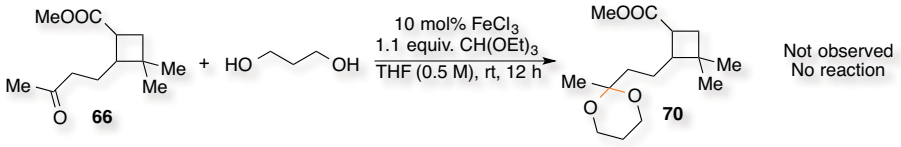

Scheme 36. Acetalization of ester 66.

Surprisingly, no reaction was observed under these circumstances. We performed the acetalization of ester **66** using 2 equiv. of TMS-protected ethylene glycol and catalytic TMSOTf in CH_2Cl_2 at 0 ºC (Scheme 37).[58] In this manner, acetal **71** was obtained quantitavely. Due to decomposition on silica gel, we optimized the purification by quenching the crude reaction mixture with pyridine and washing sequentially with saturated $NaHCO_3$, $CuSO_4$ 1% and water.[59] However, when the reaction was tested at larger scale, removal of the unreacted TMS-protected ethylene glycol was difficult. Consequently, cleavage of the silyl groups with TBAF was necessary, which was slightly detrimental for the final yield.

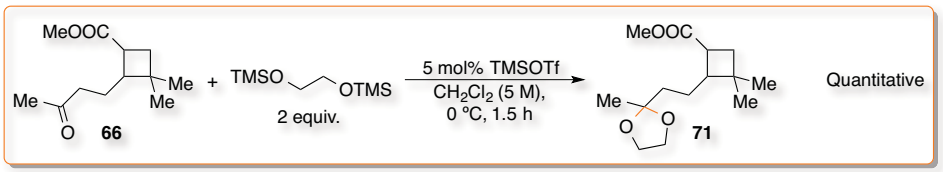

Scheme 37. Alternative acetalization of ester 66.

[57] H. Burghart-Stoll and R. Brueckner, *Eur. J. Org. Chem.* **2012**, 3978–4017.
[58] T. Tsunoda, M. Suzuki and R. Noyori, *Tetrahedron Lett.* **1980**, *21*, 1357–1358.
[59] J. R. Allan, D. H. Brown, R. H. Nuttail and D. W. A. Sharp, *J. Chem. Soc. A: Inorg. Phys. Theor.* **1966**, 1031–1034.

- **Isomerization to the Thermodynamic Cyclobutane**

We started testing the isomerization using ester **66** with 1 equivalent of sodium methoxide in a mixture of THF:methanol (1:1) at 45 ºC for 48 h, which led to a complex mixture (Scheme 38).[56]

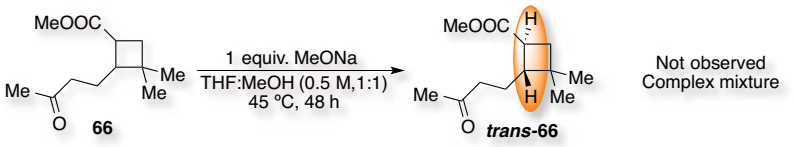

Scheme 38. Isomerization of ester 66.

On the other hand, applying the same conditions on protected ester **71** led to isomerization when modifying gradually the temperature and the reaction time (Table 8).

Table 8. Screening of the temperature and the reaction time for the isomerization of the protected ester 71.

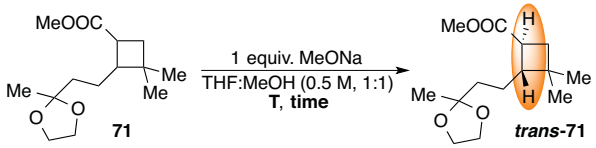

Entry	Experiment	Temperature (ºC)	Reaction time (h)	Ratio[a]
1	1	45	1	53:47
2	1	45	12	61:39
3	1	25	8	61:39
4	1	65	1	63:37
5	1	65	12	77:23
6	2	70	2	63:37
7	2	70	12	91:9
8	3	70	20	97:3

[a]Reaction monitored by GC-MS.

Almost no change was observed after 1 h at 45 ºC but it varied to 61:39 after 12 h (entries 1 and 2). Interestingly, if the reaction mixture was stirred for 8 h more at 25 ºC, this result was maintained (entry 3). When the temperature was further increased to 65 ºC, the ratio was 63:37 after 1 h and 77:23 after 12 h (entries 4 and 5). On the other hand, if the reaction was settled at 70 ºC, we could observe a mixture 63:37 after 2 h, 91:9 after 12 h and 97:3 after 20 h (entries 6, 7 and 8). Quenching with saturated NH_4Cl at 0 ºC followed with extraction with ethyl acetate afforded the pure product in 77% isolated yield. NOESY experiments confirmed that the isomer obtained is the protected ester ***trans*-71** (Figure 16: protons of the cyclobutane junction labeled with a circle and a star).

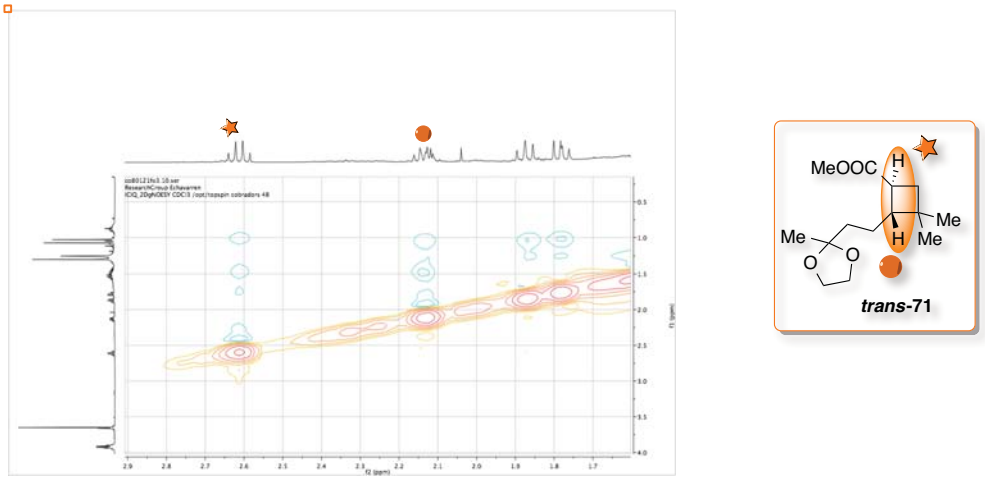

Figure 16. NOESY experiment of trans-71.

Thus, no interaction was observed between the hydrogens in the cyclobutane ring. Otherwise, when we analyzed the 1:1 *cis*:*trans* mixture of the protected ester **71**, we could identify ***cis*-71** with the cross-peak between the hydrogens in the cyclobutane ring (Figure 17: protons of the cyclobutane junction labeled with a triangle and a square).

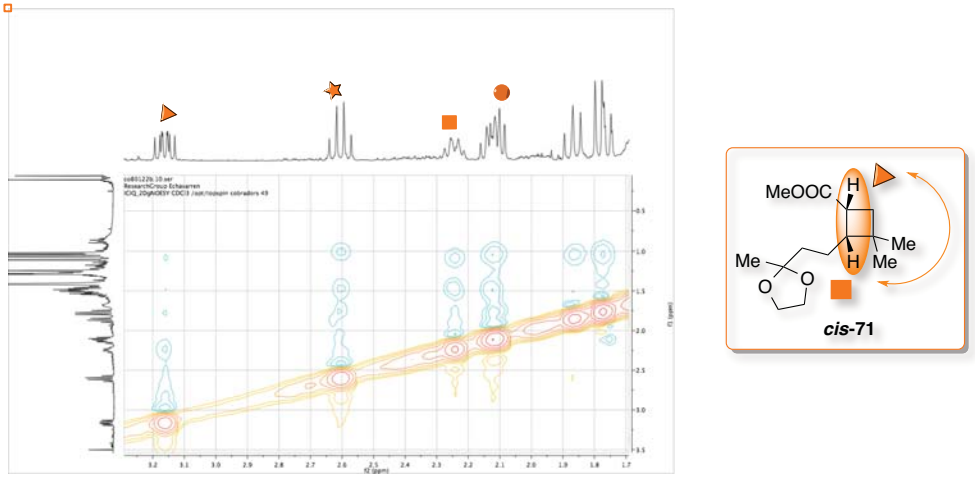

Figure 17. NOESY experiment of both diastereoisomers of 71.

- **Weinreb Amide and Methylation.**

In order to form the methyl ketone from ester ***trans*-71**, we decided to generate the corresponding Weinreb amide, which could later undergo nucleophilic attack with methyl magnesium bromide. Thus, we treated it with *N*,*O*-dimethylhydroxylamine hydrochloride and isopropyl magnesium chloride in THF at 0 ºC (Scheme 39).[60]

[60] B. M. Trost, J. L. Gunzner, O. Dirat and Y. H. Rhee, *J. Am. Chem. Soc.* **2002**, *124*, 10396–10415.

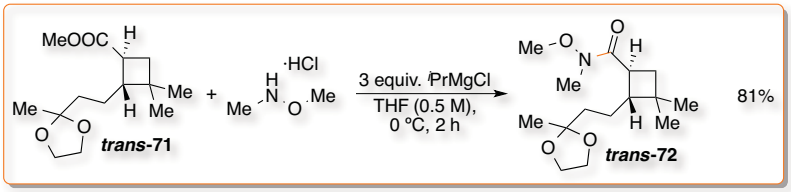

Scheme 39. Formation of the Weinreb amide trans-72.

The desired product ***trans*-72** was obtained in 81% yield as a single diastereoisomer. The methylation reaction was performed immediately with no further putification. Specifically, the Weinreb amide was dissolved in THF and treated with methyl magnesium bromide from 0 ºC to 25 ºC for 1.5 h to give methyl ketone ***trans*-73** as a single diastereoisomer in 65% isolated yield (Scheme 40).[61]

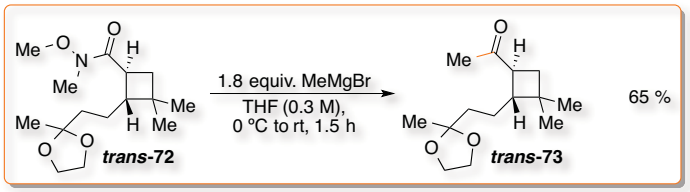

Scheme 40. Methylation of the Weinreb amide trans-73.

[61] C. Aciro, S. K. Bagal, J. W. Harvey, L. H. Jones, C. E. Mowbray, R. M. Owen, Y. A. Sabnis, R. I. Storer and S. K. Yeap, *Preparation of cyclobutenedione derivatives as modulators of CXCR-2 receptor for the treatment of asthma and COPD*, **2010**, WO 131145A1.

5. Outline

Final Steps Towards Rumphellaone A[62]

- **Stereoselective Allylation Reaction**

First, we considered the possibility to perform a diastereoselective allylation of ***trans*-73**.[63] As an example, an allyl boronate could undergo transmetallation to finally promote a nucleophilic attack to the ketone moiety *via* a Zimmerman-Traxler transition state (**74**) and build ***trans*-75** (Scheme 41).[64]

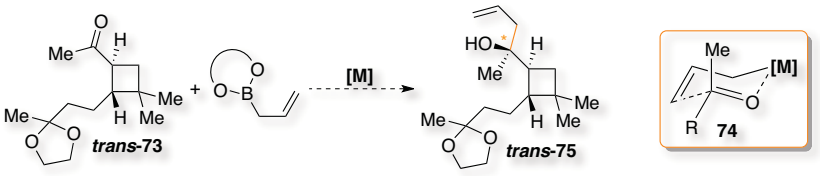

Scheme 41. Diastereoselective allylation of trans-73.

Due to the small steric difference between both faces of the cyclobutane, we also analyzed the feasibility of using a chiral reagent to perform the stereoselcetive allylation. However, we should take into consideration a match-mismatch situation with the asymmetric substrate during the process.

Although many efforts have been centered in developing enantioselective methodologies to add an allyl group to a wide variety of aldehydes, the examples on ketones are still rare. Several protocols using zinc, silver, iridium, nickel and titanium have been reported.[65,66,67]

---

[62] Project continued by Dr. Beatrice Ranieri.

[63] For representative examples see: *(a)* R. Hamasaki, Y. Chounan, H. Horino and Y. Yamamoto, *Tetrahedron Lett.* **2000**, *41*, 9883–9887; *(b)* S. Yamasaki, K. Fujii, R. Wada, M. Kanai and M. Shibasaki, *J. Am. Chem. Soc.* **2002**, *124*, 6536–6537; *(c)* M. Durandetti and J. Périchon, *Tetrahedron Lett.* **2006**, *47*, 6255–6258; *(d)* U. Schneider and S. Kobayashi, *Angew. Chem. Int. Ed.* **2007**, *46*, 5909–5912; *(e)* A. G. Campaña, B. Bazdi, N. Fuentes, R. Robles, J. M. Cuerva, J. E. Oltra, S. Porcel and A. M. Echavarren, *Angew. Chem. Int. Ed.* **2008**, *47*, 7515–7519; *(f)* T. J. Barker and E. R. Jarvo, *Org. Lett.* **2009**, *11*, 1047–1049; *(g)* T. Takeda, M. Yamamoto, S. Yoshida and A. Tsubouchi, *Angew. Chem. Int. Ed.* **2012**, *51*, 7263–7266; *(h)* F. J. Williams, R. E. Grote and E. R. Jarvo, *Chem. Commun.* **2012**, *48*, 1496–1498; *(i)* Y. Ciu, W. Li, T. Sato, Y. Yamashita and S. Kobayashi, *Adv. Synth. Catal.* **2013**, *355*, 1193–1205.

[64] K. R. Fandrick, D. R, Fandrick, J. J. Gao, J. T. Reeves, Z. Jan, W. Li, J. J. Song, B. Lu, N. K. Yee and C. H. Senanayake, *Org. Lett.* **2010**, *12*, 3748–3751.

[65] (*a*) S. Casolari, D. D'Addario and E. Tagliavini, *Org. Lett.* **1999**, *1*, 1061–1063; (*b*) K. M. Waltz, J. Gavenonis and P. J. Walsh, *Angew. Chem. Int. Ed.* **2002**, *41*, 3697–3699; (*c*) S. Yamasaki, K. Fujii, R. Wada, M. Kanai and M. Shibasaki, *J. Am. Chem. Soc.* **2002**, *124*, 6536–6537; (*d*) S. E. Denmark and J. Fu, *Chem Rev.* **2003**, *103*, 2763–2793; (*e*) J. G. Kim, K. M. Waltz, I. F. Garcia, D. Kwiatkowski and P. J. Walsh, *J. Am. Chem. Soc.* **2004**, *126*, 12580–12585; (*f*) M. Wadamoto and H. Yamamoto, *J. Am. Chem. Soc.* **2005**, *127*, 14556–14557; (*g*) J. Lu, M. L. Hong, S. J. Ji, Y. C. Teo and T. P Loh, *Chem. Commun.* **2005**, 4217–4218; (*h*) S. Lou, P. N. Mosquit and S. E. Schaus, *J. Am Chem. Soc.* **2006**, *128*, 12660–12661; (*i*) X. Zhang, D. Chen, X. Liu and X. Feng, *J. Org. Chem.* **2007**, *72*, 5227–5233; (*j*) J. J. Miller and M. S. Sigman, *J. Am. Chem. Soc.* **2007**, *129*, 2752–2753; (*k*) A. J. Wooten, J. G. Kim and P. J. Walsh, *Org. Lett.* **2007**, *9*, 381–384; (*l*) M. Kanai, R. Wada, T. Shibuguchi and M. Shibasaki, *Pure Appl. Chem.* **2008**, *80*, 1055–1062; (*m*) T. J. Baker and E. R. Jarvo, *Org. Lett.* **2009**, *11*, 1047–1049; (*n*) J. Itoh, S. B. Han and M. J. Krische, *Angew. Chem. Int. Ed.* **2009**, *48*, 6313–6316; (*o*) K. R. Fandrick, D. R. Fandrick, J. J. Gao, J. T. Reeves, Z. Tan, W. Li, J. J. Song, B. Lu, N. K. Yee and C. H. Senanayake, *Org. Lett.* **2010**, *12*, 3748–3751; (*p*) T. J. Baker and E. R. Jarvo, *Synthesis* **2010**, *19*, 3259–3262; (*q*) M. Yus, J. C. González-Gómez and F. Foubelo, *Chem. Rev.* **2011**, *111*, 7774–7854.

Therefore, for the completion of the total synthesis, we planned to perform an enantioselective allylation of ***trans*-73** to ***trans*-75** by treating the methyl ketone with an allyl boronate and a metal in the presence of a chiral ligand (Scheme 42).[68]

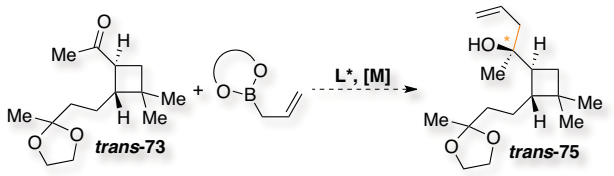

Scheme 42. Enantioselective allylation of trans-73.

Alternatively, a stereoselective reduction of the methyl ketone ***trans*-73** could be performed with a chiral aluminium or borohydride to obtain a secondary alcohol.[69] A ruthenium or rhodium catalyzed hydrogenation could be performed as well.[70] This could be transformed to the enantioenrich tertiary alcohol ***trans*-75** *via* a stereospecific lithiation/borylation reaction followed by hydrolysis .[71]

It is important to note that, until the first gold-catalyzed [2+2] cycloaddition is not enantioselective,[72] two different diastereoisomers will be obtained at this point. Thus, the enantiomer **(*S*,*R*)-73** would lead to **(*S*,*S*,*R*)-75** but the **(*R*,*S*)-73** to **(*S*,*R*,*S*,)-75** (Figure 18).

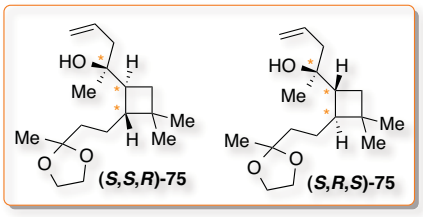

Figure 18. Diastereoisomers of alcohol 75.

---

[66] *(a)* L. F. Tietze, K. Schiemann and C. Wegner, *J. Am. Chem. Soc.* **1995**, *117*, 5851–5852; *(b)* L. F. Tietze, K. Schiemann, C. Wegner and C. Wulff, *Chem. –Eur. J.* **1998**, *4*, 1862–1869; (c) E. Canales, K. G. Prasad and J. A. Soderquist, *J. Am. Chem. Soc.* **2005**, *127*, 11572–11573.
[67] T. R. Wu, L. Shen and J. M. Chong, *Org. Lett.* **2004**, *6*, 2701–2704.
[68] R. Wada, K. Oisaki, M. Kanai and M. Shibasaki, *J. Am. Chem. Soc.* **2004**, *126*, 8910–8911.
[69] (*a*) P. V. Ramachandran, H. C. Brown and S. Swaminathan, *Tetrahedron: Asymmetry* **1990**, *1*, 433–436; (*b*) E. J. Corey and R. K. Balzski, *Tetrahedron Lett.* **1990**, *31*, 611–614;
[70] T. Ohkuma, H. Ooka, S. Hashiguchi, T. Ikariya and R. Noyori, *J. Am. Chem. Soc.* **1995**, *117*, 2675–2476.
[71] A. P. Pulis, D. J. Blair, E Torres and V. K. Aggarwal, *J. Am. Chem. Soc.* **2013**, *135*, 16054–16057.
[72] Current work performed in collaboration with Dr. Laura López and Imma Escofet using High Throughput Experimentation (CELLEX).

- **Reverse Wacker Oxidation**

Finally, as mentioned in Scheme 16, a reverse Wacker oxidation has been reported for homoallylic alcohols to generate an acetal that is further oxidized to a lactone. Thus, alcohol ***trans*-75** could cyclize to acetal **48** using catalytic $Pd(NO_2)Cl(CH_3CN)_2$ and $CuCl_2$ in *tert*-butanol and then treated with trifluoroacetic acid (Scheme 45).[73] It is expected that this could also cleave the five-membered ring acetal used to protect the ketone. Without further purification, acetal **48** could be oxidized to a lactone with Ag_2CO_3-Celite in toluene under reflux. These conditions would afford at last rumphellaone A.

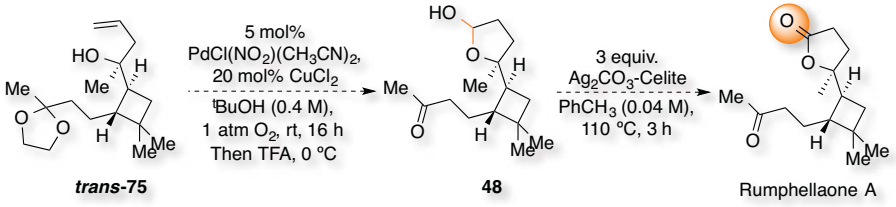

Scheme 45. Reverse Wacker oxidation to afford rumphellaone A.

[73] (*a*) T. M. Meulemans, N. H. Kiers, B. L. Feringa and P. W. N. M. van Leeuwen, *Tetrahedron Lett.* **1994**, *35*, 455–458; (*b*) J. A. Wright, M. J. Gaunt and J. B. Spencer, *Chem. –Eur. J.* **2006**, *12*, 949–955; (*c*) B. Weiner, A. Baeza, T. Jerphagnon and B. L. Feringa, *J. Am. Chem. Soc.* **2009**, *131*, 9473–9474; (*d*) S. K. Pandey and C. V. Ramana, *J. Org. Chem.* **2011**, *76*, 2315–2318.

6. Conclusions

Based on the results obtained in **Chapters 2**, **3** and **4** about the possible formation of a cyclobutene scaffold in a gold-catalyzed intermolecular [2+2] cycloaddition between an alkyne and an oxoalkene, we envisioned its application to the total synthesis of rumphellaone A. Our first approach consisted in using a silyloxyalkynylfuran, which led to the key cyclobutene **43** in only 31% isolated yield (Scheme 14).

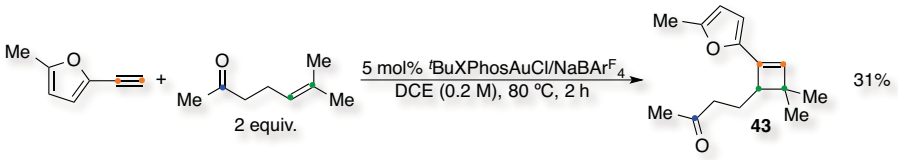

Scheme 14. Gold-catalyzed [2+2] cycloaddition of 2-ethynyl-5-methylfuran and 6-methylhept-5-en-2-one.

Therefore, we changed the strategy based on the oxidation of a phenyl ring to a carboxylic acid (Scheme 46).

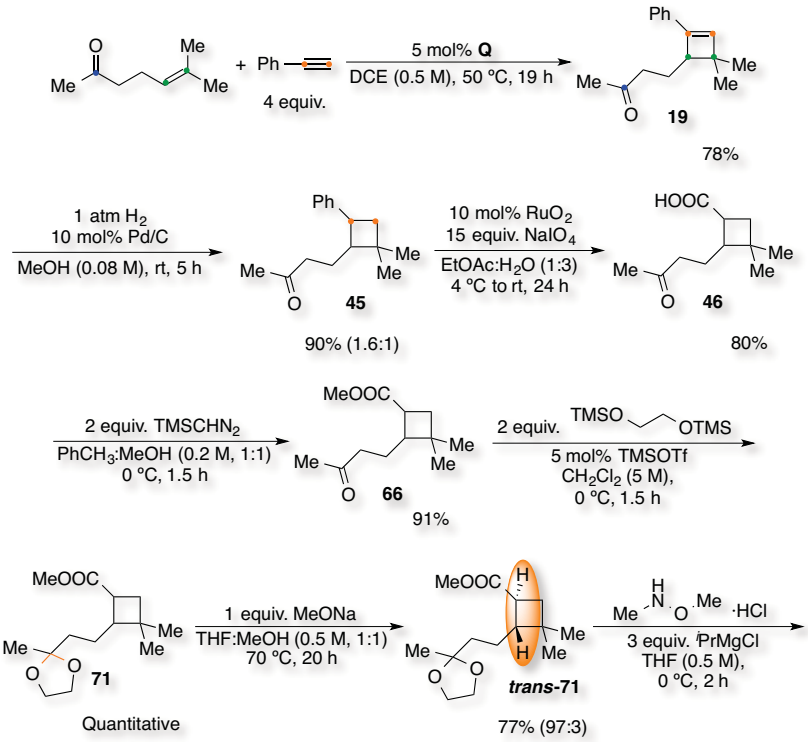

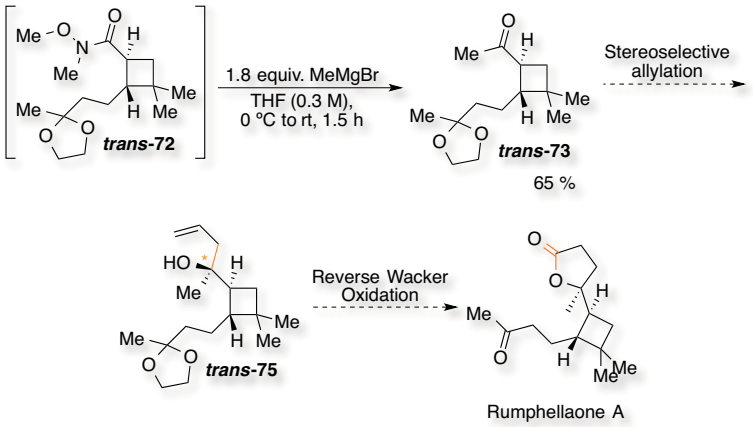

Scheme 56. Towards Rumphellaone A.

Thus, we performed the gold-catalyzed [2+2] cycloaddition of ethynylbenzene and 6-methylhept-5-en-2-one using complex **Q** (78% yield) followed by a non-diastereoselective hydrogenation of cyclobutene **19** with Pd/C in 90% yield. Oxidation afforded the carboxylic acid **46** in 80% isolated yield. Further esterification (**66**, 90%) and protection of the ketone (**71**, quantitative) allowed a late stage isomerization towards ***trans*-71** in 77% yield (97:3). Generation of the Weinreb amide (***trans*-72**) followed by methylation afforded our last intermediate ***trans*-73**. A consequent stereoselective allylation to ***trans*-75** followed by an oxidative cyclization are suggested to finally synthesize rumphellaone A.

A current challenge is still the enantioselective gold-catalyzed [2+2] cycloaddition of alkynes with alkenes. Although several asymmetric gold catalysts have been recently developed, their application has been mainly limited to intramolecular transformations. In our case, we first designed a substrate-induced enantioselective reaction *via* an asymmetric acetal since the transfer of chirality has proven to be much more effective in these reactions (Scheme 18).

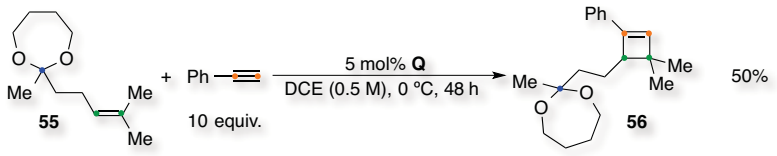

Scheme 18. Gold-catalyzed [2+2] cycloaddition of ethynylbenzene and acetal 55.

Acetal **55** could form the corresponding cyclobutene **56** in 50% isolated yield. However, the BINOL analogous could not be formed. Thus, preliminar screenings of chiral gold complexes have been performed.

For the moment, cyclobutene **19** has been obtained in 61% isolated yield (67% conversion) with 30% *ee* using catalyst **Y** and 1 equiv. of $NaBAr^{F}_{4}$ in the optimized conditions (Scheme 47). This result proves that the enantioselective [2+2] cycloaddition and its application to the total synthesis of rumphellaone A are possible and encourage us to continue this work.

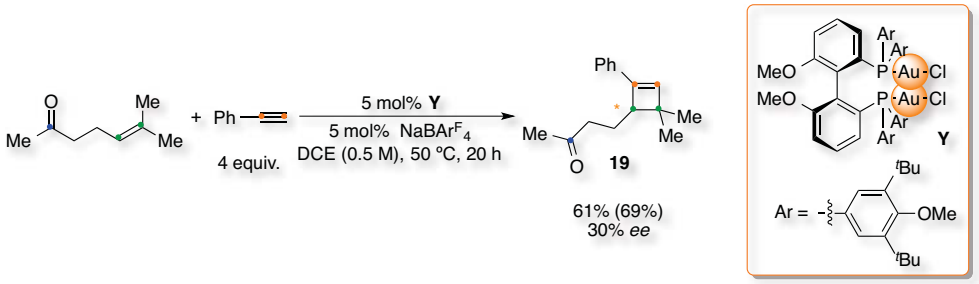

Scheme 47. Enantioselective [2+2] cycloaddition.

Although two steps are still remaining in order to accomplish the synthesis of this natural product, we have designed a straightforward synthetic route towards rumphellaone A and proved its feasibility by reaching a late-satge intermediate stereoselectively and in excellent yields.

General Conclusions

As explained in the **General Introduction**, gold-catalyzed transformations *via* the activation of unsaturated moieties towards nucleophilic attack emerged as a powerful tool for the construction of C–C, C–O and C–N bonds due to the remarkable carbophilic properties of this metal.[1,2] Thus, gold complexes allowed the construction of complex architectures under mild conditions from readily assembled starting materials. The understanding and combination of these new reactivities led to the discovery of complex cascade processes in a full atom economy, completely stereoselective fashion.

The cycloisomerizations of 1,*n*-enynes in the absence of nucleophiles underwent a wide variety of skeletal rearrangements affording very different carbo- and heterocyclic products.[3] However, these trasnsformations were limited from 1,5- to 1,8-enynes, which are entropically favoured. In the absence of a tether strain, very few intermolecular reactions were described.[4] As an example, the [2+2] cycloaddition between alkynes and alkenes using [^{t}BuXPhosAuNCMe]SbF_6 (**E**) in CH_2Cl_2 at 25 ºC led to the regioselective formation of cyclobutene scaffolds such as **1** in good yields (Scheme 1).[5]

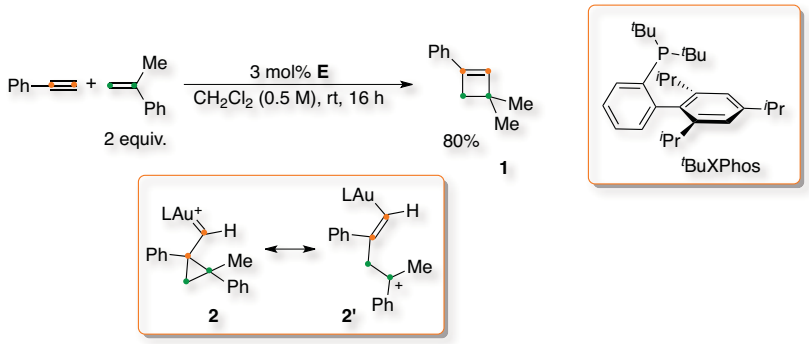

Scheme 1. [2+2] Cycloaddition of alkynes and alkenes.

These transformations were suggested to proceed through cyclopropyl gold carbenes like **2**. An interesting debate was centred on the nature of these intermediates as a gold-stabilized homoallyl carbocation (**2´**) could be also conceived. Further studies indicated the involvement of gradually distorted carbenes depending on the substitution pattern and the ligand on the metal.[6]

In **Chapter 1**, we developed the gold-catalyzed macrocyclization of large 1,*n*-enynes ($n \geq 9$) *via* a [2+2] cycloaddition.[7] In organic synthesis, forging 8- to 16- membered rings is not

---

[1] *(a)* A S. K. Hashmi, *Chem. Rev.* **2007**, *107*, 3180–3211; *(b)* A. Fürstner, P. W. Davies, *Angew. Chem. Int. Ed.* **2007**, *46*, 3410–3449; *(c)* E. Jiménez-Núñez and A. M. Echavarren, *Chem. Rev.* **2008**, *108*, 3326–3350; *(d)* D. J. Gorin, B. D. Sherry and F. D. Toste, *Chem. Rev.* **2008**, *108*, 3351–3378; *(e)* N. T. Patil and Y. Yamamoto, *Chem. Rev.* **2008**, *108*, 3395–3442; *(f)* A. Fürstner, *Chem. Soc. Rev.* **2009**, *38*, 3208–3221; *(g)* N. D. Shapiro and F. D. Toste, *Synlett* **2010**, 675–691; *(h)* C. Obradors and A. Echavarren, *Acc. Chem. Res.* **2014**, 47, 902–912.
[2] D. J. Gorin and F. D. Toste, *Nature* **2007**, *446*, 395–403 and references citere therein.
[3] For representative examples see: *(a)* C. Nieto-Oberhuber, M. P. Muñoz, E. Buñuel, C. Nevado, D. J. Cárdenas and A. M. Echavarren, *Angew. Chem. Int. Ed.* **2004**, *43*, 2402–2406; *(b)* C. Nieto-Oberhuber, S. López, E. Jiménez-Núñez and A. M. Echavarren, *Chem. –Eur. J.* **2006**, *12*, 5916–5923.
[4] M. E. Muratore, A. Homs, C. Obradors and A. M. Echavarren, *Chem. Asian J.* **2014**, DOI: 10.1002/asia.201402305.
[5] V. López-Carrillo and A. M. Echavarren, *J. Am. Chem. Soc.* **2010**, *132*, 9292–9294.
[6] D. Benitez, N. D. Shapiro, E. Tkatchouk, Y. Wang, W. A. Goddard III and F. D. Toste, *Nat. Chem.* **2009**, *1*, 482–486 and references cited therein.
[7] C. Obradors, D. Leboeuf, J. Aydin and A. M. Echavarren, *Org. Lett.* **2013**, *15*, 1576–1579.

a straightforward process and the methodology presented several challenges.[8] Optimization of the reaction conditions allowed the cyclization of 1,14-enyne **3**, bearing a spacer between both reacting partners, towards the macrocyclic structure **4** in good isolated yield (Scheme 2).

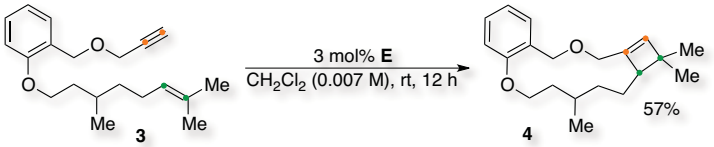

Scheme 2. Macrocyclization of large enynes.

In general, the reactions were carried out under mild conditions although some substrates required an increment of the temperature and/or the reaction concentration; for example, 1,10-enyne **5** demanded 45 ºC to form macrocycle **6** (Scheme 3). Nevertheless, expansion of the reaction scope showed that the macrocyclization proceeded in moderate to good yields drastically depending on each substrate: the chain length, the spacer and the substituents.

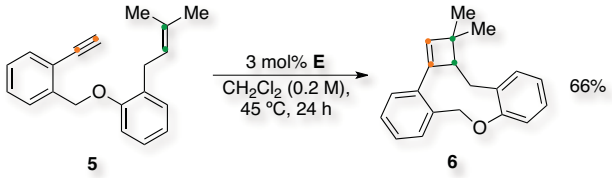

Scheme 3. Macrocyclization under harsher conditions.

This methodology also provided access to *m*-cyclophanes such as **7** or **8**, which exhibit interesting chemical and physical properties applied in supramolecular chemistry and material science (Figure 1).[9]

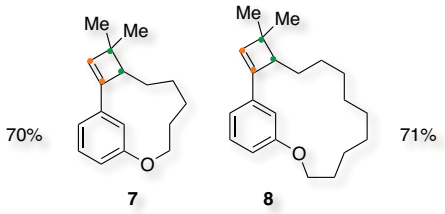

Figure 1. m-Cyclophanes synthesized via gold catalysis.

Subsequently to the gold activation and the nucleophilic attack, the intermediates formed could evolve though many different pathways affording a wide variety of products, for example, *via* trapping with nucleophiles or cyclopropanation. [1,3,10] Despite these major

[8] *(a)* K. C. Nicolaou, P. G. Bulger and D. Sarlah, *Angew. Chem. Int. Ed.* **2005**, *44*, 4490–4527; *(b)* K. C. Nicolaou, P. G. Bulger and D. Sarlah, *Angew. Chem. Int. Ed.* **2005**, *44*, 4442–4489; *(c)* A. Gradillas and J. Pérez-Castells, *Angew. Chem. Int. Ed.* **2006**, *45*, 6086–6101.
[9] *(a)* R. Gleiter and H. Hopf, *Modern Cyclophane Chemistry*; Wiley VCH: Weinheim, **2004**; *(b)* T. Gulder and P. Baran, *Nat. Prod. Rep.* **2012**, *29*, 899–934 and references cited therein.
[10] For selected examples see: *(a)* C. Nieto-Oberhuber, S. López and A. M. Echavarren, *J. Am. Chem. Soc.* **2005**, *127*, 6178–6179; *(b)* E. Jiménez-Núñez, . K. Claverie, C. Nieto-Oberhuber and A. M. Echavarren, *Angew. Chem. Int. Ed.* **2006**, *45*, 5452–5455.

advances, the presence of intermolecular cycloadditions in the literature was rather limited due to the competitive binding of the different unsaturated substrates with the gold complex. Striding forward, in **Chapter 2** we developed an intermolecular gold-catalyzed cascade [2+2+2] cycloaddition of an alkyne, an alkene and a carbonyl group.[11] Thus, *m*-methoxyethynylbenzene reacted with 5-methylhex-5-en-2-one and catalyst **E** at 50 ºC to form oxabicycle **9** in 91% isolated yield (Scheme 4).

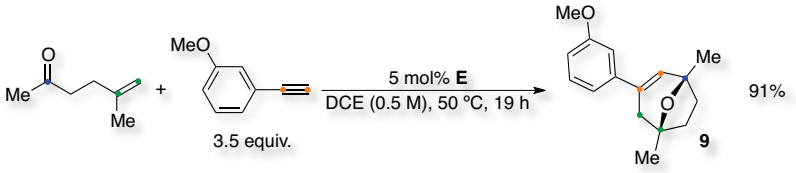

Scheme 4. [2+2+2] Cycloaddition of alkynes and oxoalkenes.

In most cases, the multistep mechanistic proposals of these reactions were rather complex and the isolation of key intermediates was proven to be challenging.[12] Therefore, its understanding was based often on analogy and speculation. Thus, in **Chapter 3** we performed a detailed mechanistic study of the intermolecular [2+2+2] cycloaddition of alkynes and oxoalkenes.[11] The initial framework was the selective π-coordination of the gold complex to the alkyne (**10**) allowing the nucleophilic attack of the oxoalkene to build the cyclopropyl gold carbene **11** (Scheme 5).

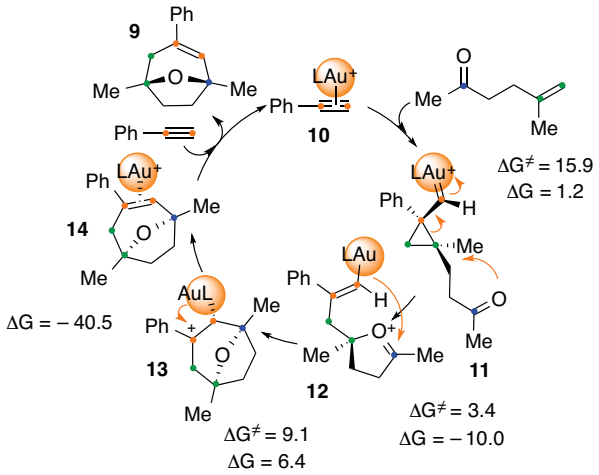

Scheme 5. Mechanistic proposal supported computationally (relative energies in kcal/mol).

This intermediate would undergo an intramolecular nucleophilic attack of the carbonyl group to form an oxonium cation (**12**) followed by a Prins-type cyclization with the alkenyl gold scaffold to **13**. Demetalation would afford the coordinated product **14** and complex **10** after ligand exchange. This proposal was supported by DFT calculations (M06, 6-31G(d) (C, H, P, O) and SDD (Au) in CH_2Cl_2), which suggested that the rate-

[11] C. Obradors and A. M. Echavarren, *Chem. –Eur. J.* **2013**, *19*, 3547–3551.
[12] *(a)* A. S. K. Hashmi, *Angew. Chem. Int. Ed.* **2010**, *49*, 5232–5241; *(b)* L. P. Liu and G. B. Hammond, *Chem. Soc. Rev.* **2012**, *41*, 3129–3139; *(c)* I. Braun, A. M. Asiri and A. S. K. Hashmi, *ACS Catal.* **2013**, *3*, 1902–1907; *(d)* C. Obradors and A. M. Echavarren, *Chem. Commun.* **2014**, *50*, 16–28.

detemining step of the process was the nucleophilic attack of the alkene towards the activated alkyne.

The scope of this methodology was expanded to 24 examples with good to excellent yields. The process showed a broad functional tolerance in the substitution of the aryl ring with both electron-deficient and electron-donating groups and including hetero- and polyaromatic moieties. Furthermore, varying the substituents in the alkene group and in the α-position of the ketone was also possible leading to a better efficiency by increasing their nucleophilicity. Interestingly, changing the substitution pattern of the olefin or utilization of an ester headed to the preferential formation of cyclobutenes such as **15** or **16** in 54% and 47% yield, respectively (Figure 2).

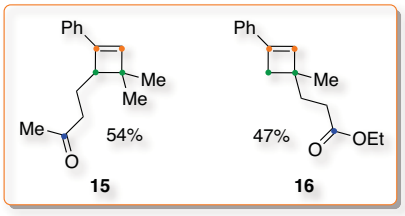

Figure 2. Preferential formation of cyclobutenes.

Therefore, the intramolecular nucleophilic attack of the carbonyl to a cyclopropyl gold carbene analogous to **11** was not favoured in those cases. Similarly, the reaction with the cyclic oxoalkene **17** afforded tricyclic structure **18** only in 31% isolated yield (Scheme 6).

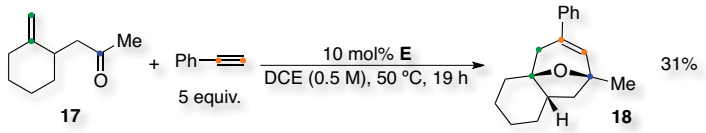

Scheme 6. Formation of a tricyclic scaffold.

Simultaneously, we could optimize the transformation towards a new reaction pathway that led to the formation of tetrahydrofurans such as **19** (Scheme 7).[11] Thus, reaction between *p*-bromoethynylbenzene and 5-methylhex-5-en-2-one with substoichiometric amounts of *p*-toluenesulfonic acid built **19** in 51% isolated yield.

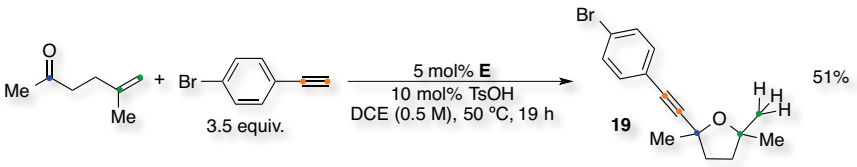

Scheme 7. Tuning of the reaction towards tetrahydrofurans.

We suggested that the π-coordinated gold complex with the alkyne (**20**) could undergo deprotonation forming **21** and releasing acid in the reaction media.[13] A proton-catalyzed cyclization of the oxoalkene would form cation **22**/**22′**, which would be in equilibrium with **23**. This intermediate could be easily trapped with **21** affording the tetrahydrofuran product **19** (Scheme 8). This proposal was supported with deuterium labelling experiments.

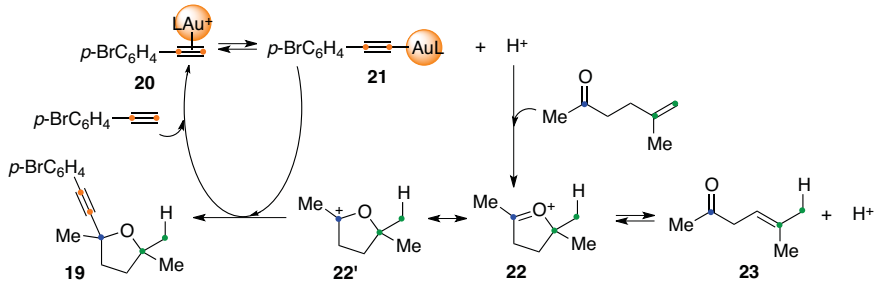

Scheme 8. Mechanistic proposal supported by deuterium labelling experiments.

Moreover, we developed an unprecedented gold-catalyzed trimerization of alkynes that led to 1,3,5-substituted benzenes such as **24** in moderate yields (Scheme 9).[11]

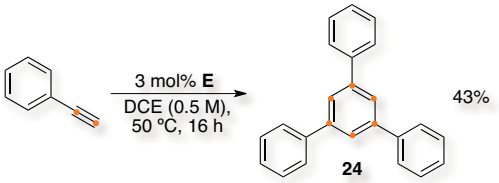

Scheme 9. Gold-catalyzed trimerization of alkynes.

Monitoring of the [2+2+2] cycloaddition by ^{1}H and ^{31}P NMR spectroscopy revealed a single gold species during the whole transformation. Crystallization of the resting state revealed digold complex **25** (Figure 3).[11,14]

---

[13] *(a)* P. H. Y. Cheong, P. Morganelli, M. R. Luzung, K. N. Houk and F. D. Toste, *J. Am. Chem. Soc.* **2008**, *130*, 4517–4526; *(b)* T. J. Brown and R. A. Widenhoefer, *Organometallics*, **2011**, *30*, 6003–6009; *(c)* M. Raducan, M Moreno, C. Bour and A. M. Echavarren, *Chem. Commun.* **2012**, *48*, 52–54.

[14] *(a)* D. Weber, M. A. Tarselli and M. R. Gagné, *Angew. Chem. Int. Ed.* **2009**, *48*, 5733–5736; *(b)* G. Seidel, C. W. Lehmann and A. Fürstner, *Angew. Chem. Int. Ed.* **2010**, *49*, 8466–8470; *(c)* A. Grirrane, H. Garcia, A. Corma and E. Álvarez, *ACS Catal.* **2011**, *1*, 1647–1653; *(d)* A. Simonneau, F. Jaroschik, D. Lesage, M. Karanik, R. Guillot, M. Malacria, J. C. Tabet, J. P. Goddard, L. Fensterbank, V. Gandon and Y. Gimbert, *Chem. Sci.* **2011**, *2*, 2417–2422; *(e)* D. Weber, T. D. Jones, L. L. Adduci and M. R. Gagné, *Angew. Chem. Int. Ed.* **2012**, *51*, 2452–2456; *(f)* D. Weber and M. R. Gagné, *Chem. Sci.* **2012**, *4*, 335–338; *(g)* T. J. Brown, D. Weber, M. R. Gagné and R. A. Widenhoefer, *J. Am. Chem. Soc.* **2012**, *134*, 9134–9137.

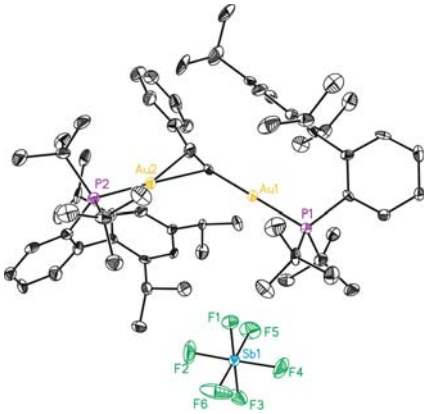

Figure 3. Digold complex 25 as the resting state.

This result suggested a more complex scenario. The formation was suggested to proceed *via* a competitive deprotonation of **10** to build **26** and reaction with another unit of catalyst **E** (Scheme 10). Determination of the equilibrium constant by the Van't Hoff equation proved this is a reversible process (K_{eq} (50 ºC) = $1.08 \cdot 10^{-7}$ M; ΔH = 6.79 kcal/mol; ΔS = – 11 cal/mol·K).

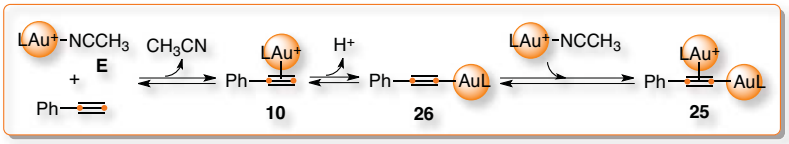

Scheme 10. Equilibrium between the involved gold species (L=^{t}BuXPhos).

Furthemore, we could detect complex **10** spectroscopically at – 78 ºC by observing the correlation between the proton of the alkyne and the phosphorous of the ligand.[15] Low temperature NMR studies revealed that this complex coexists with digold scaffold **25** to – 20 ºC, when it disappeared. Attempts to disclose the role of the digold complex in catalysis showed that this species were outside the catalytic cycle, which lowers the concentration of the active species **10** and explains the rather long reaction times. Digold complex **25** was unreactive until $HSbF_6$ was added to re-establish the equilibrium between the gold species, for example, in the synthesis of oxabicycle **27** (Scheme 11).

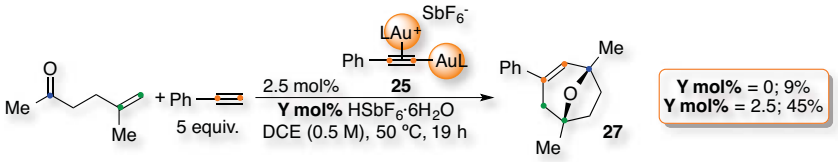

Scheme 11. Regeneration of the catalytic activity (L=^{t}BuXPhos).

These results shed light into the complex scenario composed in a gold-catalyzed intermolecular cycloaddition. In this context, we focused on tuning the catalyst structure to

[15] *(a)* T. J. Brown and R. A. Widenhoefer, *Organometallics* **2011**, *30*, 6003–6009; *(b)* A. Himmelspach, M. Finze and S. Raub, *Angew. Chem. Int. Ed.* **2011**, *50*, 2628–2631.

minimize the generation of digold complexes such as **25** and we reasoned that the use of more bulky, non-coordinating and less basic counterions could slow down the deprotonation of the alkynes and hamper the formation of the σ-alkynyl gold intermediates such as **26**.[16,17] Hence, we designed new gold complexes using $BAr^{F}_{4}^{-}$ as the anion, for example, catalyst **Q** (Figure 4).

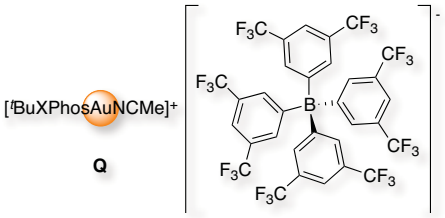

Figure 4. New gold complex Q bearing $BAr^{F}_{4}^{-}$.

This hypothesis was validated by performing a study of the anion effect in several gold-catalyzed intermolecular cycloadditions, which led to improvements up to 36% isolated yield. As an example, *p*-chloroethynylbenzene reacted with a slight excess of α-methylstyrene under the optimized conditions and led to cyclobutene **28** in 61% when using SbF_6^- and 91% with $BAr^{F}_{4}^{-}$ (Scheme 12).[5] Moreover, the same trend was observed in the macrocyclization of large enynes,[7] the gold-catalyzed synthesis of phenols[18] and the [2+2+2] cycloaddition of alkynes with oxoalkenes.[11] On the other hand, no pattern was observed in the intramolecular cyclizations.[3,10a,19]

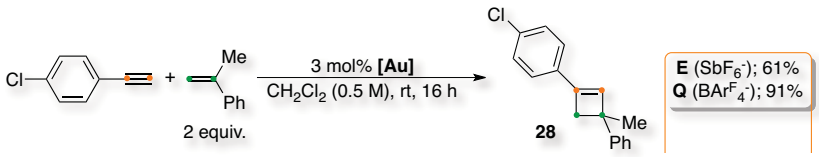

Scheme 12. Anion effect in the intermolecular cycloadditions.

In order to further understand this influence, we studied mechanistically the particular involvement of the couterion in the intermolecular [2+2] cycloaddition of alkynes with alkenes.[17] ^{1}H NMR monitoring of the transformation between ethynylbenzene and α-methylstyrene afforded the kinetic profile of the reaction and showed the great dependence with the anion. Thus, the final yield and the reaction rate increased along with its bulkiness: $BAr^{F}_{4}^{-}$ > SbF_6^- > BF_4^-. Additionally, ^{31}P NMR spectroscopy showed the presence of digold scaffolds analogous to **25** together with a major new gold species, which could be crystallized as the π-coordinated gold complex with α-methylstyrene **29** (Figure 5).[11]

[16] I. Krossing and I. Raabe, *Angew. Chem. Int. Ed.* **2004**, *43*, 2066–2090 and references cited therein.
[17] C. Obradors, A. Homs, D. Leboeuf and A. M. Echavarren, *Adv. Synth. Catal.* **2014**, *356*, 221–228.
[18] N. Huguet, D. Leboeuf and A. M. Echavarren, *Chem. –Eur. J.* **2013**, *19*, 6581–6585.
[19] P. R. McGonigal, C. de León, Y. Wang, A. Homs, C. R. Rogelio and A. M. Echavarren, *Angew. Chem. Int. Ed.* **2012**, *51*, 13093–13096.

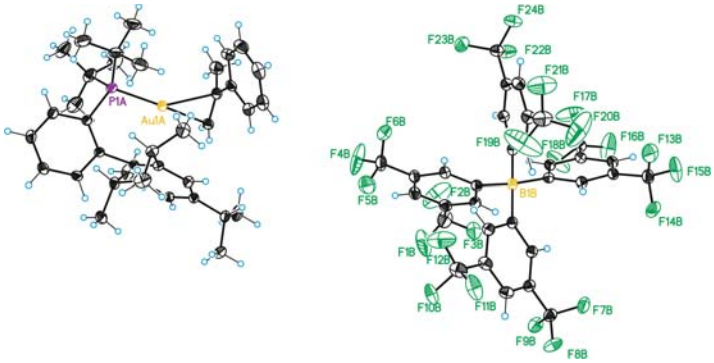

Figure 5. (α-Methylstyrene)gold(I) complex 29.

Interestingly, the ratios between the alkene *versus* the alkyne coordination changed dramatically with the counterion following the same trend: $BAr^F_4^-$ > SbF_6^- > BF_4^-. These results implied a larger reservoir of the cationic gold species in the reaction media. Determination of the equilibrium constant towards the digold complex showed it is slightly more favoured with smaller counterions: Keq (25 ºC) = $4.44 \cdot 10^{-8}$ M for SbF_6^- and Keq (25 ºC) = $2.44 \cdot 10^{-8}$ M for $BAr^F_4^-$. Notably, the enthalpy increased to 13.4 kcal/mol whereas the entropy turned 10 cal/mol·K. Performing the low temperature NMR studies with [^{t}BuXPhosAuNCMe]BAr^F_4 (**Q**) showed that the π-coordinated gold complex with the alkyne analogous to **10** was this time stable up to 0ºC, when the digold complex **25**-type was also formed (Scheme 13). These results were supported by DFT calculations as well.

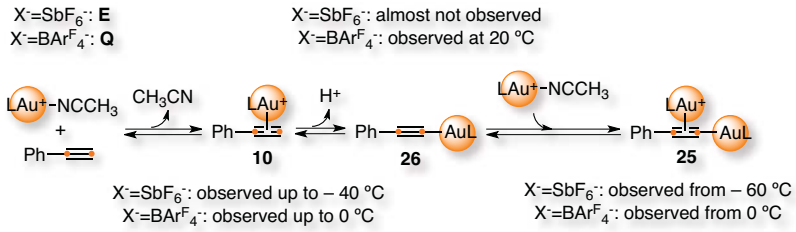

Scheme 13. Evolution of the different gold species by increasing the temperature (L=^{t}BuXPhos).

Furthermore, we measured the equilibrium constants towards the alkene complexes like **29** to observe that the binding to α-methylstyrene was stronger with bulky counterions, although the differences were small again: Keq (25 ºC) = 0.047 for SbF_6^- and Keq (25 ºC) = 0.090 for $BAr^F_4^-$. Nevertheless, their comparison with the formation of the digold complexes was remarkably distinct: the constants increased from 10^{-8} to 10^{-2}.

Concurrently, the method of the initial rates showed order one for both the alkyne and the gold catalyst but zero-dependance for α-methylstyrene. In the initial mechanistic proposal, the alkyne complex **10** was formed straightforward to undergo a rate-determining nucleophilic attack of the alkene and build a cyclopropyl gold carbene (**30**), analogous to **11** (Scheme 14). This intermediate was formed regioselectively and proceeded *via* ring expansion to form the stabilized carbocation **31** and the coordinated final product **32** after demetallation.

However, this proposal did not consider the pre-equilibrium described and did not explain the zero order observed for α-methylstyrene. Therefore, according to the equilibrium constants, the gold catalyst should bind preferentially to α-metylstyrene forming complex **29** in the presence of the ethynylbenzene, also decreasing **25** and **26**. The extent of this effect would depend on the nucleophilicity of the alkene as well as the stoichiometry of the reaction, as observed.

Therefore, it was mechanistically crucial to determine if complex **29** could lead directly to complex **10** as well, which would circumscribe if the coordination of the alkene was inhibiting the [2+2] cycloaddition or storing cationic gold(I) reservoirs.

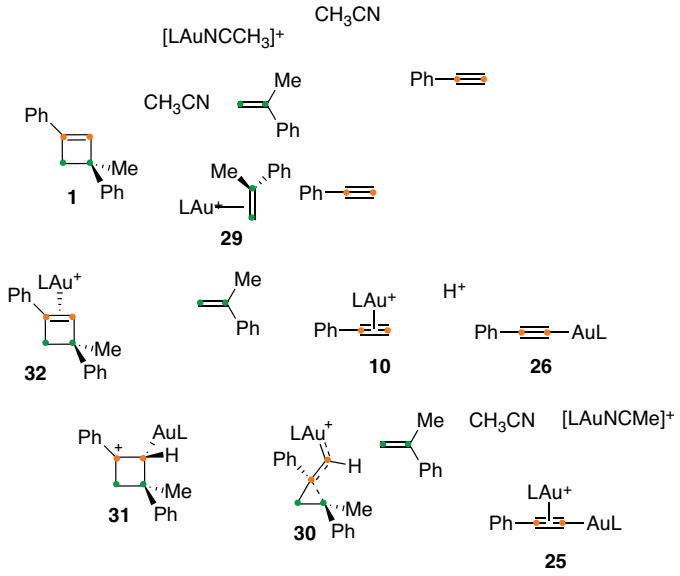

Scheme 14. Mechanistic proposal considering the counterion effect (L=^{t}BuXPhos).

Tests on the catalytic activity confirmed that digold complex **25** and **26** are off-cycle species, whose reactivity was restored upon an acid addition. Remarkably, complex **29** reacted stoichiometrically with ethynylbenzene in the absence of catalyst to forge cyclobutene **1** in 72% isolated yield (Scheme 15). Accordingly, the ligand exchange between complex **29** and ethynylbenzene to form the key intermediate **10** was the rate-detemining step of the catalytic cycle.

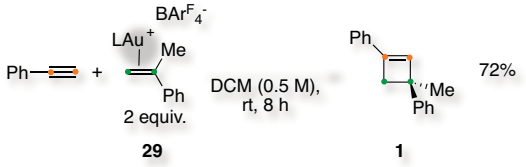

Scheme 15. Catalytic activity of (α-methylstyrene)gold complex 29.

Finally, we envisioned we could apply our findings in the total synthesis of rumphellaone A, a natural product that showed cytotoxicity towards leukemia tumor cells (Figure 6). [20,21] This scaffold contains a *trans* cyclobutane that could be built *via* an asymmetric gold-catalyzed [2+2] cycloaddition of an alkyne and an oxoalkene followed by a diastereoselective hydrogenation.

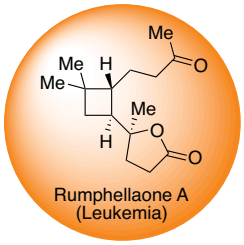

Figure 6. Application of gold chemistry to total synthesis.

Our first approach consisted on using a silyloxyalkynylfuran (**33**) to perform the key gold-catalyzed reaction to obtain **34**, **35** after a vinyligous methylation and the natural product after hydrogenation (Scheme 16). [22,23] However, the cycloaddition was not very efficient and intermediate **34** was obtained only in 31% isolated yield.

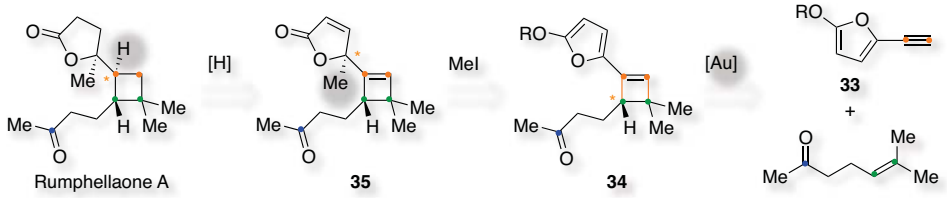

Scheme 16. Silyloxyalkynylfuran approach.

Therefore, we changed the strategy towards a gold-catalyzed [2+2] cycloaddition with ethynylbenzene followed by the oxidation of the aromatic ring to obtain a carboxylic acid, which could be transformed to the desired lactone *via* stereoselective allylation and an intramolecular reverse Wacker oxidation. [24,25]

---

[20] Application of gold chemistry to total synthesis: (*a*) A. S. K. Hashmi and M. Rudolph, *Chem. Soc. Rev.* **2008**, *37*, 1766–1775; (*b*) A. Fürstner, *Chem. Soc. Rev.* **2009**, *38*, 3208–3221; (*c*) Y. Zhang, T. Luo and Z. Yang, *Nat. Prod. Rep.* **2014**, *31*, 489–503; *(d)* A. Fürstner, *Acc. Chem. Res.* **2014**, *47*, 925–938.

[21] *a*) L. Quijano, A. Vasquez and T. Rios, *Phytochemistry* **1995**, *38*, 1251–1255; (*b*) M. Wichlacz, W. A. Ayer, L. S. Trifonov, P. Chakravarty and D. Khasa, *Phytochemistry* **1999**, *52*, 1421–1425; (*c*) M. Wichlacz, W. A. Ayer, L. S. Trifonov, P. Chakravarty and D. Khasa, *J. Nat. Prod.* **1999**, *62*, 484–486.

[22] (*a*) M. Szlosek and B. Frigadère, *Angew. Chem. Int. Ed.* **2000**, *39*, 1799–1801; (*b*) C. W. Cho and M. J. Krische, *Angew. Chem. Int. Ed.* **2004**, *43*, 6689–6691; (*c*) S. Ma, L. Lu and P. Lu, *J. Org. Chem.* **2005**, *70*, 1063–1065; (*d*) R. K. Boeckman, J. E. Pero and D. J. Boehmler, *J. Am. Chem. Soc.* **2006**, *128*, 11032–11033; (*e*) B. Simmons, A. M. Walji and D. W. C. MacMillan, *Angew. Chem. Int. Ed.* **2009**, *48*, 4349–4353.

[23] R. H. Crabtree and M. W. Davis, *J. Org. Chem.* **1986**, *51*, 2655–2661; K. Iwasaki, K. K. Wan, A. Oppedisano, S. W. M. Crossley and R. Shenvi, *J. Am. Chem. Soc.* **2014**, *136*, 1300–1303; S. N. Ananchenko, V. Y. Limanov, V. N. Leonov, V. N. Rzheznikov and I. V. Torgov, *Tetrahedron* **1962**, *18*, 1355–1367

[24] W. R. Gutekunst and P. S. Baran, *J. Org. Chem.* **2014**, *79*, 2430–2452.

[25] (*a*) J. Muzart, *Tetrahedron* **2007**, *63*, 7505–7521; (*b*) S. Wan, H. Gunaydin, K. N. Houk and P. E. Floreancig, *J. Am. Chem. Soc.* **2007**, *129*, 7915–7923.

Thus, reaction of ethynylbenzene with 5-methylhex-5-en-2-one and 5 mol% of catalyst **Q** afforded cyclobutene **15** in 78% isolated yield under the optimized conditions (Scheme 17). Attempts to perform a diastereoselective hydrogenation were unsuccessful and 90% cyclobutane **36** (1.6:1) was obtained with 10 mol% of Pd/C in methanol under 1 atm of H_2. Oxidation with RuO_2 afforded the carboxylic acid **37** in 80% isolated yield, which was followed by esterification (91% to **38**) and protection of the ketone moiety (quantitatively to **39**). A late stage isomerization afforded ***trans*-39** in 77% isolated yield (97:3) after treatment with sodium methoxide in THF:methanol (1:1) at 70 ºC for 20 h under strict anhydrous conditions. Formation *in situ* of the corresponding Weinreb amide ***trans*-40** followed by a methylation reaction afforded our last intermediate ***trans*-41** in 65% isolated yield. The already mentioned stereoselective allylation to **42** followed by a reverse Wacker oxidation to obtain rumphellaone A are on going work.

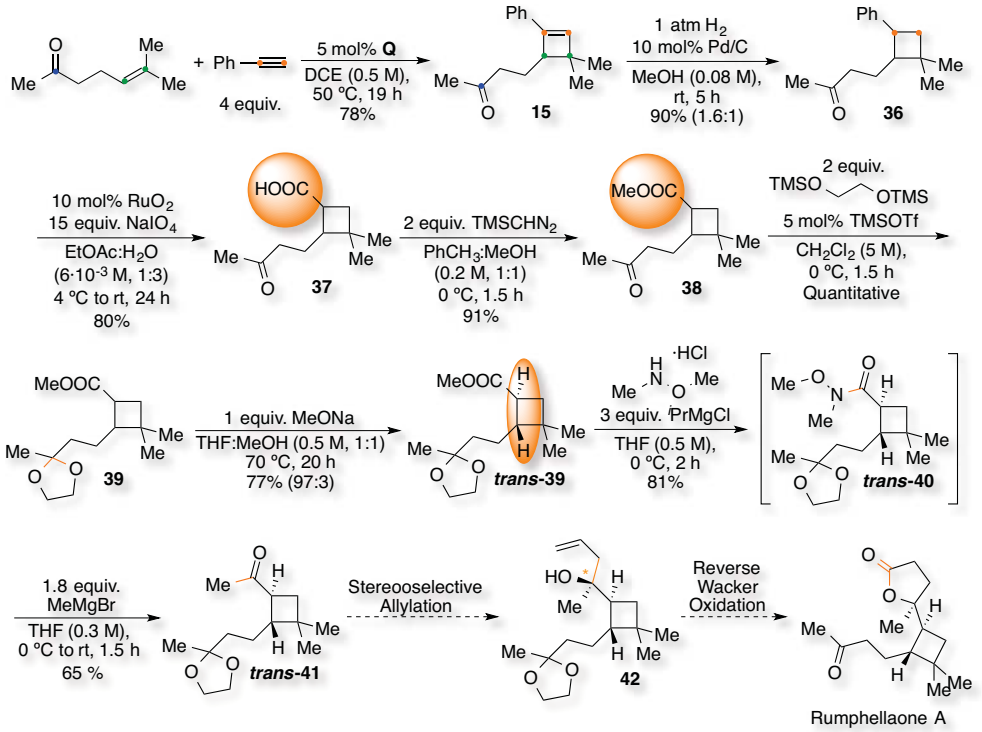

Scheme 17. Towards the total synthesis of Rumphellaone A.

Furthermore, attempts to perform an enantioselective intermolecular gold-catalyzed [2+2] cycloaddition between an alkyne and an oxoalkene were carried out. Initially, we designed a substrate-induced asymmetric reaction *via* a chiral acetal protecting the carbonyl group (Scheme 18). [26]

[26] (*a*) R. A. Widenhoefer, *Chem. –Eur. J.* **2008**, *14*, 5382–5391; (*b*) N. T. Patil, *Chem. Asian J.* **2012**, *7*, 2186–2194; (*c*) Y. M. Wang, A. D. Lackner and F. D. Toste, *Acc. Chem. Res.* **2014**, *47*, 889–901.

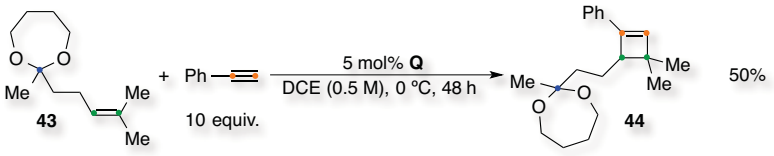

Scheme 18. Substrate-induced gold-catalyzed [2+2] cycloaddition.

Although acetal **43** afforded cyclobutene **44** in 50% isolated yield, the corresponding BINOL-derivative could not be formed.

Therefore, preliminar screenings of chiral gold complexes were performed. So far, cyclobutene **15** could be forged in 61% isolated yield (69% conversion) with 30% *ee* using catalyst **Y** under the optimized conditions (Scheme 19).[27] Although this result is still modest, it proved the feasibility of this approach and encouraged us to continue this project.

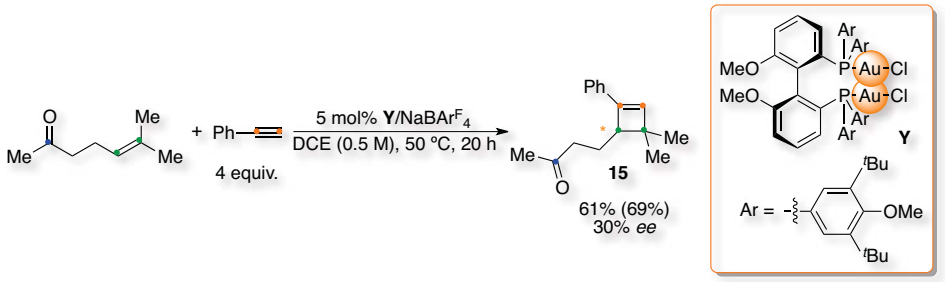

Scheme 19. Enantioselective gold-catalyzed [2+2] cycloaddition.

[27] (*a*) G. L. Hamilton, E. J. Kang, M Mba and F. D. Toste, *Science* **2007**, *317*, 496–499; ((*c*) K. Aikawa, M. Kojima and K. Mikami, *Angew. Chem. Int. Ed.* **2009**, *48*, 6073–6077; (*d*) H. Teller, S. Flügge, R. Goddard and A. Fürstner, *Angew. Chem. Int. Ed.* **2010**, *49*, 1949–1953;; (*f*) A. Z. González, D. Benitez, E. Tkatchouk, W. A. Goddard and F. D Toste, *J. Am. Chem. Soc.* **2011**, *133*, 5500–5507; (*h*) R. J. Felix, D. Weber, O. Gutierrez, D. J. Tantillo and M. R. Gagné, *Nat. Chem.* **2012**, *4*, 405–409; (*i*) H. S. Yeom, J. Koo, H. S. Park, Y. Wang, Y. Liang, Z. X. Yu and S. Shin, *J. Am. Chem. Soc.* **2012**, *134*, 208–211; (*k*) K. L. Butler, M. Tragni and R. A. Widenhoefer, *Angew. Chem. Int. Ed.* **2012**, *51*, 5175–5178; (*l*) J. F. Briones and H. M. L. Davies, *J. Am. Chem. Soc.* **2012**, *134*, 11916–11919;

Experimental Section

Unless otherwise stated, reactions were carried out under argon atmosphere in solvents dried by passing through an activated alumina column on a PureSolv^{TM} solvent purification system (Innovative Technologies, Inc., MA). Analytical thin layer chromatography was carried out using TLC-aluminium sheets with 0.2 mm of silica gel (Merck GF_{234}) using UV light as the visualizing agent and an acidic solution of vanillin in ethanol as the developing agent. Chromatograpy purifications were carried out using flash grade silica gel (SDS Chromatogel 60 ACC, 40-60 mm) or automated flash chromatographer CombiFlash Companion. Preparative TLC was performed on 20 cm × 20 cm silica gel plates (2.0 mm thick, catalogue number 02015, Analtech). Organic solutions were concentrated under reduced pressure on a Büchi rotary evaporator.

NMR spectra was recorded at 298 K on a Bruker Avance 400 Ultrashield and Bruker Avance 500 Ultrashield apparatus. Mass spectra was recorded on a Waters Micromass LCT Premier (ESI), Waters Micromass GCT (EI, CI) and Bruker Daltonics Autoflex (MALDI) spectrometers. Elemental analyses were performed on a LECO CHNS 932 micro-analyzer at the Universidad Complutense de Madrid. Melting points were determined using a Büchi melting point apparatus and are uncorrected.

Crystal structure determinations were carried out using a Bruker-Nonius diffractomer equipped with an APPEX 2 4K CCD area detector, a FR591 rotating anode with MoK_a radiation, Montel mirrors as monochromator and a Kryoflex low temperature device (T = -173 ºC). Full-sphere data collection was used with w and j scans. *Programs used*: Data collection APEX-2, data reduction Bruker Saint V/.60A and absorption correction SADABS. Structure Solution and Refinement: Crystal structure solution was achieved using direct methods as implement in SHELXTL and visualized using the program XP. Missing atoms were subsequently located from difference Fourier synthesis and added to the atom list. Least-squares refinement on F2 using all measured intensities was carried out using the program SHELXTL. All non hydrogen atoms were refined including anisotropic displacement parameters.

Calculations were carried out with DFT using the M06 functional[1] as implemented in Gaussian 09.[2] The 6-31G(d) basis set[3] was used for all atoms except gold, which was treated with SDD and the associated effective core potential.[4] Frequency calculations were performed to characterize the stationary points as minima. The solvent effect was taken into account by single-point calculations using the polarizable continuum model (PCM),[5,6,7,8] in particular IEF-PCM as implemented in Gaussian 09. Default options were

---

[1] *(a)* A. D. J. Becke, *Chem. Phys.* **1993**, *98*, 5648–5652; *(b)* C. T. Lee, W. T. Yang and R. G. Parr, *Phys. Rev. B* **1988**, *37*, 785–789; *(c)* P. J. Stephens, F. J. Devlin, C. F. Chabalowski and M. J. Frisch, *J. Phys. Chem.* **1994**, *98*, 11623–1627.

[2] M. J. Frisch, G. W. Trucks, H. B. Schlegel, G. E. Scuseria, M. A. Robb, J. R. Cheeseman, G. Scalmani, V. Barone, B. Mennucci, G. A. Petersson, H. Nakatsuji, M. Caricato, X. Li, H. P. Hratchian, A. F. Izmaylov, J. Bloino, G. Zheng, J. L. Sonnenberg, M. Hada, M. Ehara, K. Toyota, R. Fukuda, J. Hasegawa, M. Ishida, T. Nakajima, Y. Honda, O. Kitao, H. Nakai, T. Vreven, J. A. Montgomery, Jr., J. E. Peralta, F. Ogliaro, M. Bearpark, J. J. Heyd, E. Brothers, K. N. Kudin, K. N. Staroverov, R. Kobayashi, J. Normand, K. Raghavachari, A. Rendell, J. C. Burant, S. S. Iyengar, J. Tomasi, M. Cossi, N. Rega, N. J. Millam, M. Klene, J. E. Knox, J. B. Cross, V. Bakken, C. Adamo, J. Jaramillo, R. Gomperts, R. E. Stratmann, O. Yazyev, A. J. Austin, R. Cammi, C. Pomelli, J. W. Ochterski, R. L. Martin, K. Morokuma, V. G. Zakrzewski, G. A. Voth, P. Salvador, J. J. Dannenberg, S. Dapprich, A. D. Daniels, O. Farkas, J. B. Foresman, J. V. Ortiz, J. Cioslowski and D. J. Fox, Gaussian 09, revision 02; Gaussian, Inc.: Wallingford, CT, **2009**.

[3] *(a)* M. M. Francl, W. J. Pietro, W. J. Hehre, J. S. Binkley, M. S. Gordon, D. J. Defrees and J. A. Pople, *J. Chem. Phys.*, **1982**, *77*, 3654–3665; *(b)* W. J. Hehre, R. Ditchfield and J. A. Pople, *J. Chem. Phys.*, **1972**, *56*, 2257–2261.

[4] D. Andrae, U. Haussermann, M. Dolg, H. Stoll and H.Preuss, *Theor. Chim. Acta* **1990**, *77*, 123–141.

[5] E. Cances, B. Mennucci and J. J. Tomasi, *Chem. Phys.* **1997**, *107*, 3032–3041.

used, except that individual spheres were placed on all hydrogen atoms to get a more accurate cavity. The calculations were performed using CH_2Cl_2 ($\varepsilon = 8.93$) as solvent. The standard Gibbs energies in dichloromethane (ΔG_{DCM}) were obtained by adding the solvation energies to the gas-phase Gibbs energies computed at 298 K. The same procedure was employed to calculate zero-point corrected energies in CH_2Cl_2.

[6] M. Cossi, V. Barone, B. Mennucci and J. Tomasi, *Chem. Phys. Lett.* **1998**, *286*, 253-260.
[7] B. Mennucci and J. J. Tomasi, *Chem. Phys.* **1997**, *106,* 5151–5158.
[8] S. Miertus and J. Tomasi, *J. Chem. Phys.* **1982**, *65*, 239–245.

1. Gold-Catalyzed Macrocyclization *via* [2+2] Cycloaddition of 1,*n*-Enynes[1]

All the reactants, ligands and the following reagents were purchased from commercial sources and used without further purification: 3,7-dimethyloct-6-en-1-ol, 2-(hydroxymethyl)phenol, 3-bromoprop-1-yne, 2-hydroxybenzaldehyde, 2-(2-Methylprop-1-en-1-yl)phenol, (2-(prop-2-yn-1-yloxy)phenyl)methanol, 6-methylhept-5-en-2-ol, 1-(bromomethyl)-2-iodobenzene, 2-(3-methylbut-2-en-1-yl)phenol, 1-(bromomethyl)-2-ethynylbenzene, 2-iodophenol, 1-bromo-3-methylbut-2-ene, (2-(pent-4-yn-1-yloxy)phenyl)methanol, 1-(bromomethyl)-2-ethynylbenzene, (2-(hex-5-yn-1-yloxy)phenyl)methanol, 7-bromo-2-methylhept-2-ene, 8-bromo-2-methyloct-2-ene, 5-iodopent-1-yne, 6-iodohex-1-yne, dimethyl 2-(but-3-yn-1-yl)malonate, pent-4-yn-1-ol and 3-ethynylphenol. (THT)AuCl and (2-(hex-5-yn-1-yloxy)phenyl)methanol were synthesized as reported.[2,3] Enynes **19** and **27** were prepared according to the literature as well metal complexes **B**, **C**, **E**, **I**, **[Pt^{II}]** and **[Cu^{I}]**.[4,5,6,7]

Preparation of Gold Complexes

Chloro[(2′,4′,6′-triisopropyl-3,6-dimethoxy-1,1′-biphenyl-2-yl)di-tert-butylphosphine]gold(I)

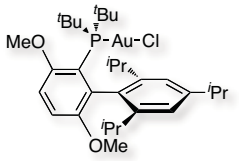

Chloro(tetrahydrothiophene) gold(I) (66.1 mg, 0.21 mmol) was dissolved in CH_2Cl_2 (0.3 ml) and a solution of 2-(di-*tert*-butylphosphino)-2',4',6'-triisopropyl-3,6-dimethoxy-1,1'-biphenyl (100.0 mg, 0.21 mmol) in CH_2Cl_2 (0.7 ml) was added. The reaction mixture was stirred at 25 ºC for 1 h and the solvent was removed under reduced pressure. The crude was purified with a chromatographic column using a mixture 2:1 of cyclohexane:ethyl acetate to obtain the product as a white powder in 92% isolated yield (136.0 mg, 0.19 mmol). ^{1}H NMR (500 MHz, CD_2Cl_2, ppm) δ 7.07 (d, *J* = 9.0 Hz, 1H), 7.03 (s, 2H), 6.99 (dd, *J* = 8.9 Hz, *J* (^{1}H-^{31}P) = 3.4 Hz, 1H), 3.83 (s, 3H), 3.55 (s, 3H), 2.97 (quintet, *J* = 7.0 Hz, 1H), 2.38 (quintet, *J* = 6.7 Hz, 2H), 1.41 (d, *J* (^{1}H-^{31}P) = 16.5 Hz, 18H), 1.37 (d, *J* = 7.0 Hz, 6H), 1.27 (d, *J* = 6.7 Hz, 6H), 0.86 (d, *J* = 6.7 Hz, 6H). DEPTQ-135 NMR (126 MHz, $CDCl_3$, ppm) δ 155.4 (s, C), 153.6 (d, *J* (^{13}C-^{31}P) = 12.0 Hz, C), 150.1 (s, C), 146.9 (s, C), 139.4 (d, *J* (^{13}C-^{31}P) = 15.2 Hz, C), 131.9 (d, *J* (^{13}C-^{31}P) = 7.5 Hz, C), 122.4 (s, CH), 119.7 (d, *J* (^{13}C-^{31}P) = 37.4 Hz, C), 114.7 (s, CH), 109.9 (d, *J* = 5.4 Hz, CH), 55.2 (CH_3), 54.7 (CH_3), 40.9 (d, *J* (^{13}C-^{31}P) = 25.5 Hz, C), 34.5 (CH), 32.8 (d, *J* (^{13}C-^{31}P) = 8.0 Hz, CH_3), 31.4 (s, CH), 25.5 (CH_3), 24.5 (CH_3), 24.4 (CH_3). ^{31}P {^{1}H} NMR (202 MHz, CD_2Cl_2, ppm) δ 73.10 (s). MALDI^{+} *m/z* calc for $C_{31}H_{49}AuClO_2P^{+}$ $[M]^{+}$ 716.2819, found 716.2728 (13 ppm).

---

[1] C. Obradors, D. Leboeuf, J. Aydin and A. M. Echavarren, *Org. Lett.* **2013**, *15*, 1576–1579.
[2] A. S. K. Hashmi, T. Hengst, C. Lothschütz and F. Rominguer, *Adv. Synth. Catal.* **2010**, *352*, 1315–1337.
[3] R. G. Iafe, D. G. Chan, J. L. Kuo, B. A. Boon, D. J. Faizi, T. Saga, J. W. Turner and C. A. Merlic, *Org. Lett.* **2012**, *14*, 4282–4285.
[4] E. Comer, E. Rohan, L. Deng and J. A. Porco, *Org. Lett.* **2007**, *9*, 2123–2126.
[5] R. R. Iyer and V. R. Mamdapur, *J. Agr. Food Chem.* **1989**, *37*, 1101–1103.
[6] *(a)* E. Herrero-Gómez, C. Nieto-Oberhuber, S. López, B. Benet-Buchholz and A. M. Echavarren, *Angew. Chem. Int. Ed.* **2006**, *45*, 5455–5459; *(b)* C. H. M. Amijs, V. López-Carrillo, M. Raducan, P. Pérez-Galán, C. Ferrer and A. M. Echavarren, *J. Org. Chem.* **2008**, *73*, 7721–7730.
[7] Complex **[Cu^{I}]** was provided by the group of Prof. Miquel Pericàs.

(Acetonitrile)[(2′,4′,6′-triisopropyl-3,6-dimethoxy-1,1′-biphenyl-2-yl)di-tert-butylphosphine]gold(I) hexafluoroantimonate (G)

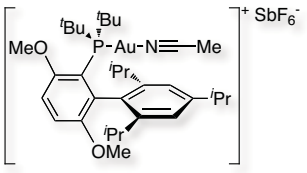

This synthesis was realized inside the glove box and in the dark (aluminium foil). Chloro[(2',4',6'-triisopropyl-3,6-dimethoxy-1,1'-biphenyl-2-yl)di-*tert*-butylphosphine] gold(I) (88.3 mg, 0.13 mmol) and acetonitrile (0.2 ml, 3.38 mmol) were added in CH_2Cl_2 (0.2 ml). Then, a suspension of $AgSbF_6$ (43.0 mg, 0.13 mmol) in CH_2Cl_2 (0.2 ml) was added and the reaction mixture was stirred at 25 ºC for 15 min. The crude was filtered twice through Teflon 0.22 and washed with CH_2Cl_2. The solvent was removed to afford complex **G** as a white powder in 94% isolated yield (111.0 mg, 0.17 mmol). ^{1}H NMR (500 MHz, CD_2Cl_2, ppm): δ 7.07 (s, 2 H), 7.06 (d, J = 8.2 Hz, 1 H), 6.99 (dd, J = 8.9 Hz, J (^{1}H-^{31}P) = 3.8 Hz, 1 H), 3.79 (s, 3 H), 3.46 (s, 3 H), 2.88 (quintet, J = 7.0 Hz, 1 H), 2.29 (quintet, J = 6.7 Hz, 2 H), 2.21 (br s, 3 H), 1.34 (d, J (^{1}H-^{31}P) = 17.3 Hz, 18 H), 1.26 (d, J = 7.0 Hz, 6 H), 1.18 (d, J = 6.7 Hz, 6 H), 0.81 (d, J = 6.6 Hz, 6 H). ^{13}C NMR (126 MHz, $CDCl_3$, ppm): δ 155.3 (s), 153.6 (d, J (^{13}C-^{31}P) = 11.9 Hz), 149.8 (s), 148.5 (s), 137.8 (d, J (^{13}C-^{31}P) = 13.6 Hz), 132.5 (d, J (^{13}C-^{31}P) = 7.6 Hz), 122.5 (s), 119.3 (s), 117.3 (d, J (^{13}C-^{31}P) = 37.4 Hz), 116.1 (s), 111.0 (d, J (^{13}C-^{31}P) = 5.9 Hz), 55.3 (s), 55.1 (s), 41.3 (d, J (^{13}C-^{31}P) = 27.3 Hz), 34.2 (s), 32.7 (d, J (^{13}C-^{31}P) = 7.1 Hz), 31.4 (s), 25.4 (s), 24.5 (s), 24.3 (s), 3.3 (s). ^{31}P {^{1}H} NMR (202 MHz, CD_2Cl_2, ppm): δ 70.5 (s). Structure confirmed by HMQC ^{13}C-^{1}H NMR and HMBC ^{31}P-^{1}H NMR. MALDI$^+$ *m/z* calcd for $C_{31}H_{49}AuO_2P^+$ [M-$C_2H_3F_6NSb$]$^+$ 681.3130, found 681.3485 (52 ppm). Anal. calcd. for $C_{33}H_{52}AuF_6NO_2PSb$: C, 41.35; H, 5.47; N, 1.46; found: C, 42.46; H, 5.44; N, 1.35. Structure confirmed also by X-Ray crystallography, CCDC 912986.

Chloro[(2′,4′,6′-triisopropyl-3,4,5,6-tetramethyl-1,1′-biphenyl-2-yl)di-tert-butylphosphine]gold(I)

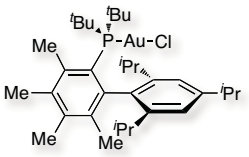

Chloro(tetrahydrothiophene) gold(I) (66.7 mg, 0.21 mmol) was dissolved in CH_2Cl_2 (0.3 ml) and a solution of 2-(di-*tert*-butylphosphino)-2',4',6'-triisopropyl-3,4,5,6-tetramethyl-1,1'-biphenyl (100.0 mg, 0.21 mmol) in CH_2Cl_2 (0.7 ml) was added. The reaction mixture was stirred at 25 ºC for 1 h and the solvent was removed under reduced pressure. The crude was purified with a chromatographic column using a mixture 2:1 of cyclohexane:ethyl acetate to obtain the product as a white powder in 95% isolated yield (140.6 mg, 0.20 mmol). ^{1}H NMR (500 MHz, CD_2Cl_2, ppm) δ 6.95 (s, 2H), 2.87 (quintet, J = 6.9 Hz, 1H), 2.53 (s, 3H), 2.31 (quintet, J = 6.7 Hz, 2H), 2.23 (s, 3H), 2.16 (s, 3H), 1.43 (d, J (^{1}H-^{31}P) = 16.2 Hz, 18H), 1.27 (d, J = 7.0 Hz, 6H), 1.19 (d, J = 6.9 Hz, 6H), 1.18 (s, 3H), 0.77 (d, J = 6.7 Hz, 6H). DEPTQ-135 NMR (126 MHz, CD_2Cl_2, ppm) δ 151.6 (s, C), 146.7 (s, C), 146.3 (s, C), 140.9 (d, J = 3.0 Hz, C), 138.9 (d, J = 4.0 Hz, C), 138.5 (d, J = 8.8 Hz, C), 137.9 (d, J = 8.0 Hz, C), 136.4 (d, J = 8.0 Hz, C), 128.7 (s, C), 122.9 (s, CH), 42.4 (d, J = 20.9 Hz, C), 34.9 (s, CH), 33.8 (d, J = 8.3 Hz, CH_3), 31.2 (s, CH), 28.5 (s, CH_3), 25.4 (s, CH_3), 25.2 (s, CH_3), 24.9 (s, CH_3), 22.5 (d, J = 2.7 Hz, CH_3), 18.1 (s, CH_3), 17.6 (s, CH_3). ^{31}P {^{1}H} NMR (202 MHz, CD_2Cl_2, ppm) δ 80.52 (s). MALDI$^+$ *m/z* calc for $C_{33}H_{53}AuClP^+$ [M]$^+$ 712.3233, found 712.3341 (15 ppm).

(Acetonitrile)[(2′,4′,6′-triisopropyl-3,4,5,6-tetramethyl-1,1′-biphenyl-2-yl)di-tert-butylphosphine]gold(I) hexafluoroantimonate (H)

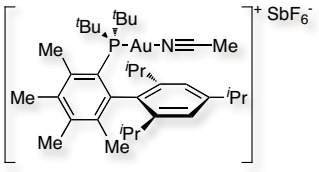

This synthesis was realized inside the glove box and in the dark (aluminum foil). Chloro[(2',4',6'-triisopropyl-3,4,5,6-tetramethyl-1,1'-biphenyl-2-yl)di-*tert*-butylphosphine] gold(I) (120.7 mg, 0.17 mmol) and acetonitrile (0.3 ml, 5.74 mmol) were added in CH_2Cl_2 (0.25 ml). Then, a suspension of $AgSbF_6$ (58.2 mg, 0.17 mmol) in CH_2Cl_2 (0.25 ml) was added and the reaction mixture was stirred at 25 ºC for 30 min. The crude was filtered twice through Teflon 0.22 and washed with CH_2Cl_2. The solvent was removed to afford complex **H** as a white powder in 98% isolated yield (159.1 mg, 0.167 mmol). ^{1}H NMR (500 MHz, CD_2Cl_2, ppm) δ 7.18 (s, 2 H), 2.99 (quintet, J = 6.9 Hz, 1 H), 2.63 (s, 3 H), 2.40 (quintet, J = 6.7 Hz, 2 H), 2.33 (s, 3 H), 2.30 (br s, 3 H), 2.26 (s, 3 H), 1.52 (d, J (^{1}H-^{31}P) = 17.0 Hz, 18 H), 1.47 (s, 3 H), 1.34 (d, J = 6.9 Hz, 6 H), 1.26 (d, J = 6.8 Hz, 6 H), 0.89 (d, J = 6.6 Hz, 6 H). ^{13}C NMR (126 MHz, CD_2Cl_2, ppm) δ 150.5 (s), 148.2 (s), 144.8 (d, J (^{13}C-^{31}P) = 19.3 Hz), 142.3 (d, J (^{13}C-^{31}P) = 2.3 Hz), 139.2 (d, J (^{13}C-^{31}P) = 5.4 Hz), 139.0 (d, J (^{13}C-^{31}P) = 8.6 Hz), 138.1 (d, J (^{13}C-^{31}P) = 8.6 Hz), 137.5 (d, J (^{13}C-^{31}P) = 8.6 Hz), 126.7 (s), 126.4 (s), 123.1 (s), 42.9 (d, J (^{13}C-^{31}P) = 22.6 Hz), 34.4 (s), 33.7 (d, J (^{13}C-^{31}P) = 7.5 Hz), 31.3 (s), 28.5 (s), 25.6 (s), 25.1 (s), 24.5 (s), 22.7 (d, J (^{13}C-^{31}P) = 2.8 Hz), 18.1 (s), 17.6 (s). ^{31}P {^{1}H} NMR (202 MHz, CD_2Cl_2, ppm): δ 78.2 (s). Structure confirmed by HMBC ^{31}P-^{1}H NMR. MALDI$^+$ *m/z* calcd for $C_{33}H_{53}AuP^+$ $[M\text{-}C_2H_3F_6NSb]^+$ 677.3545, found 677.3857 (46 ppm). Anal. calcd for $C_{35}H_{56}AuF_6NPSb$: C, 44.04; H, 5.91; N, 1.47; found: C, 48.13; H, 6.26; N, 1.65. Structure confirmed also by X-Ray crystallography, CCDC 912987.

Procedures for the Preparation of 1,*n*-Enynes

8-Bromo-2,6-dimethyloct-2-ene

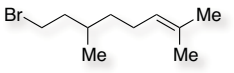

Triphenylphosphine (4.310 g, 16.43 mmol) was dissolved in CH_2Cl_2 (40.0 ml) to give a colourless solution that was cooled in an ice bath. A solution of dibromine (0.77 ml, 15.06 mmol) in tetrachloromethane (4.0 ml) was added and the reaction mixture was stirred at 25 ºC for 1 h. Then, a solution of pyridine (1.2 ml, 15.06 mmol) and 3,7-dimethyloct-6-en-1-ol (2.5 ml, 13.69 mmol) in CH_2Cl_2 (4.0 ml) was added and it was stirred 5.5 h more. The crude was concentrated under reduced pressure and it was filtered through a plug of silica gel with cyclohexane to obtain 8-bromo-2,6-dimethyloct-2-ene as a colourless oil in 94% isolated yield (2.8226 g, 12.88 mmol). ^{1}H NMR (500 MHz, $CDCl_3$, ppm) δ 5.11 – 5.07 (m, 1H), 3.49 – 3.44 (m, 1H), 3.42 – 3.37 (m, 1H), 2.05 – 1.93 (m, 2H), 1.93 – 1.85 (m, 1H), 1.71 – 1.63 (m, 2H), 1.69 (d, J = 1.0 Hz, 3H), 1.61 (s, 3H), 1.38 – 1.31 (m, 1H), 1.22 – 1.14 (m, 1H), 0.90 (d, J = 6.5, 3H). ^{13}C NMR (100 MHz, $CDCl_3$, ppm) δ 131.6 (s), 124.6 (s), 40.2 (s), 36.7 (s), 32.2 (s), 31.5 (s), 25.9 (s), 25.5 (s), 19.0 (s), 17.8 (s).

(2-((3,7-Dimethyloct-6-en-1-yl)oxy)phenyl)methanol

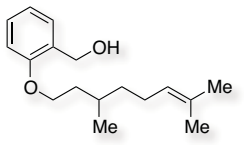

8-Bromo-2,6-dimethyloct-2-ene (2.506 g, 11.43 mmol), 2-(hydroxymethyl)phenol (1.561 g, 12.57 mmol), K_2CO_3 (7.90 g, 57.2 mmol), Cs_2CO_3 (1.118 g, 3.43 mmol) and tetrabutylammonium iodide (42.0 mg, 0.114 mmol) were dissolved in anhydrous acetone (18.0 ml) to give a white suspension that was stirred at 60ºC for 30 h. Then, the solvent was removed under reduced pressure and the crude was filtered in vacuum through celite washing with CH_2Cl_2. The solvent was removed again and the product was purified with a silica gel column and eluted with cyclohexane:ethyl acetate (0-100%) using a CombiFlash chromatographer to afford (2-((3,7-dimethyloct-6-en-1-yl)phenyl)methanol as a colourless oil in 90% isolated yield (2.703 g, 10.30 mmol). ^{1}H NMR (400 MHz, $CDCl_3$, ppm) δ 7.24 (dd, *J* = 7.4 Hz, *J* = 1.5 Hz, 1H), 7.17 (td, *J* = 8.0 Hz, *J* = 1.5 Hz, 1H), 6.86 (td, *J* = 7.4 Hz, *J* = 0.8 Hz, 1H), 6.78 (d, *J* = 8.1 Hz, 1H), 5.12 - 5.07 (m, 1H), 4.62 (s, 2H), 4.00 – 3.90 (m, 2H), 2.97 (s, 1H), 2.07 – 1.92 (m, 2H), 1.84 – 1.76 (m, 1H), 1.67 (d, *J* = 0.84 Hz, 3H), 1.65 – 1.51 (m, 2H), 1.59 (s, 3H), 1.42 – 1.33 (m, 1H), 1.25 – 1.16 (m, 1H), 0.93 (d, *J* = 6.6, 3H). ^{13}C NMR (100 MHz, $CDCl_3$, ppm) δ 156.5 (s), 131.1 (s), 129.3 (s), 128.3 (s), 128.1 (s), 124.5 (s), 120.3 (s), 110.7 (s), 66.0 (s), 61.2 (s), 36.9 (s), 36.0 (s), 29.4 (s), 25.5 (s), 25.3 (s), 19.4 (s), 17.5 (s). APCI$^+$ *m/z* calcd for $C_{17}H_{27}O_2^+$ $[M+H]^+$ 285.1831, found 285.1823.

1-((3,7-Dimethyloct-6-en-1-yl)oxy)-2-((prop-2-yn-1-yloxy)methyl)benzene (29)

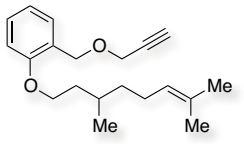

A solution of (2-((3,7-dimethyloct-6-en-1-yl)oxy)phenyl)methanol (4.25 g, 16.2 mmol) in THF (20.0 ml) was added to a suspension of NaH 60% wt (972 mg, 24.3 mmol) in THF (20.0 ml) at 0 ºC under argon. The reaction mixture was stirred at 70 ºC for 30 min. Then, a solution of 3-bromoprop-1-yne 80% wt (2.345 ml, 21.1 mmol) was added dropwise at 25 ºC. The solution was stirred under reflux for 12 h. The reaction mixture was quenched with saturated NH_4Cl and extracted with ethyl acetate. The combined organic layers were washed with brine, dried over $MgSO_4$ and filtered. The solvent was removed by rotary evaporation. The crude product was purified with a silica gel column and eluted with cyclohexane:ethyl acetate (0-100%) using a CombiFlash chromatographer to afford 1,14-enyne **29** as an orange oil in 93% isolated yield (4.5 g, 15 mmol). ^{1}H NMR (500 MHz, $CDCl_3$, ppm): δ 7.50 (d, *J* = 7.6 Hz, 1 H), 7.34 (t, *J* = 7.6 Hz, 1 H), 7.04 (t, *J* = 7.6 Hz, 1 H), 6.94 (d, *J* = 7.6 Hz, 1 H), 5.29 – 5.23 (m, 1 H), 4.77 (s, 2 H), 4.31 (d, *J* = 2.8 Hz, 2 H), 4.14 – 4.05 (m, 2 H), 2.54 (t, *J* = 2.7 Hz, 1 H), 2.19 – 2.13 (m, 2 H), 2.01 – 1.93 (m, 1 H), 1.88 – 1.83 (m, 1 H), 1.83 (s, 3 H), 1.81 – 1.75 (m, 4 H), 1.73 – 1.67 (m, 2 H), 1.09 (dd, *J* = 6.6 Hz, 3 H). ^{13}C NMR (126 MHz, $CDCl_3$, ppm) δ 156.8 (s), 131.1 (s), 129.3 (s), 128.9 (s), 126.2 (s), 124.9 (s), 120.4 (s), 111.2 (s), 80.2 (s), 74.5 (s), 66.7 (s), 66.3 (s), 57.5 (s), 37.3 (s), 36.3 (s), 29.7 (s), 25.8 (s), 25.7 (s), 19.7 (s), 17.8 (s). APCI$^+$ *m/z* calcd for $C_{20}H_{29}O_2^+$ $[M+H]^+$ 323.1987, found 323.1981.

2-(1-Hydroxy-2-methylpropyl)phenol

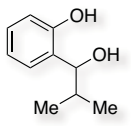

Dissolve 2-hydroxybenzaldehyde (10.99 g, 90.00 mmol) in diethyl ether (200.0 ml) and cool the solution to -78ºC. Isopropylmagnesium chloride (100 ml, 200 mmol) was added dropwise and the reaction mixture was stirred at 25 ºC for 2 h. It was quenched with HCl 10% wt and an extraction

with acidic water and a mixture of diethyl ether and ethyl acetate was carried out. The organic layers were collected and the solvent was removed. The product was purified with a silica gel column and eluted with cyclohexane:ethyl acetate (0-100%) using a CombiFlash chromatographer to afford 2-(1-hydroxy-2-methylpropyl)phenol as a colourless oil in 24% isolated yield (3.517 g, 21.16 mmol). ^{1}H NMR (400 MHz, $CDCl_3$, ppm) δ 8.33 (broad s, 1H), 7.10 (td, *J* = 7.5 Hz, *J* = 1.8 Hz, 1H), 6.86 (dd, *J* = 7.5 Hz, *J* = 1.6 Hz, 1H), 6.80 (d, *J* = 8.3, 1H), 6.78 (td, *J* = 7.3 Hz, *J* = 1.1 Hz, 1H), 4.42 (d, *J* = 7.0 Hz, 1H), 3.54 (broad s, 1H), 2.08-1.99 (m, 1H), 1.00 (d, *J* = 6.7 Hz, 3H), 0.81 (d, *J* = 6.8 Hz, 3H). ^{13}C NMR (126 MHz, $CDCl_3$, ppm) δ 155.6 (s), 128.7 (s), 128.4 (s), 126.3 (s), 119.5 (s), 117.0 (s), 81.8 (s), 34.4 (s), 19.3 (s), 18.2 (s).

2-(2-Methylprop-1-en-1-yl)phenol

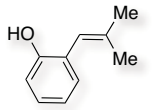

2-(1-Hydroxy-2-methylpropyl)phenol (3.417 g, 20.56 mmol) was dissolved in hexane (100.0 ml) and the solution was transferred into a high pressure reactor. Then, it was heated to 170ºC for 17 h. The solvent was removed and the product was purified with a silica gel column and eluted with cyclohexane:ethyl acetate (0-100%) using a CombiFlash chromatographer to afford 2-(2-methylprop-1-en-1-yl)phenol as an orange oil in 54% isolated yield (1.638 g, 11.05 mmol). ^{1}H NMR (500 MHz, $CDCl_3$, ppm) δ 7.10 (td, *J* = 8.0 Hz, *J* = 1.8 Hz, 1H), 7.04 (d, *J* = 7.7 Hz, 1H), 6.87 (d, *J* = 7.3, 1H), 6.85 (td, *J* = 7.4 Hz, *J* = 0.9 Hz, 1H), 6.12 (s, 1H), 5.34 (s, 1H), 1.89 (s, 3H), 1.67 (s, 3H). ^{13}C NMR (126 MHz, $CDCl_3$, ppm) δ 152.9 (s), 140.0 (s), 130.0 (s), 128.1 (s), 124.8 (s), 120.1 (s), 118.9 (s), 114.9 (s), 25.8 (s), 19.4 (s).

1-(2-Methylprop-1-en-yl)-2-(pent-4-yn-1-yloxy)benzene (32)

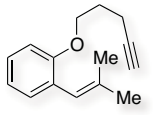

2-(2-Methylprop-1-en-1-yl)phenol (500.0 mg, 3.37 mmol), 5-chloropent-1-yne (0.39 ml, 3.71 mmol), K_2CO_3 (2.331 g, 16.87 mmol), Cs_2CO_3 (1.099 g, 3.37 mmol) and NaI (55.6 mg, 3.71 mmol) were dissolved in acetone (20.0 ml) to give a white suspension. The reaction mixture was stirred at 80ºC for four days. The solvent was removed and the crude was filtered in vacuum and washed with CH_2Cl_2. The product was purified with a silica gel column and eluted with cyclohexane:ethyl acetate (0-100%) using a CombiFlash chromatographer to afford 1,9-enyne **32** as an slightly pink oil in 56% isolated yield (404.3 mg, 1.887 mmol). ^{1}H NMR (400 MHz, $CDCl_3$, ppm) δ 7.17 (dd, *J* = 7.3 Hz, *J* = 1.6 Hz, 1H), 7.12 (td, *J* = 7.9 Hz, *J* = 1.5 Hz, 1H), 6.88 (dd, *J* = 7.4, *J* = 1.0 Hz, 1H), 6.82 (dd, *J* = 8.3 Hz, *J* = 0.9 Hz, 1H), 6.30 (s, 1H), 4.00 (t, *J* = 6.1 Hz, 2H), 2.37 (td, *J* = 7.1 Hz, *J* = 2.7 Hz, 2H), 2.00 – 1.94 (m, 2H), 1.93 (t, J = 2.7 Hz, 1H), 1.90 (d, *J* = 1.4 Hz, 3H), 1.79 (d, *J* = 1.2 Hz, 3H). ^{13}C NMR (100 MHz, $CDCl_3$, ppm) δ 156.2 (s), 135.0 (s), 130.4 (s), 127.8 (s), 127.3 (s), 120.6 (s), 120.1 (s), 111.7 (s), 83.5 (s), 68.8 (s), 66.5 (s), 28.3 (s), 26.6 (s), 19.5 (s), 15.2 (s). APCI$^+$ *m/z* calcd for $C_{15}H_{19}O^+$ $[M+H]^+$ 215.1436, found 215.1438.

1-(Hex-5-yn-1-yloxy)-2-(2-methylprop-1-en-1-yl)benzene (34)

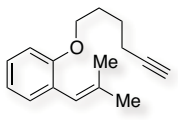

2-(2-Methylprop-1-en-1-yl)phenol (500.1 mg, 3.37 mmol), 6-chlorohex-1-yne (0.45 ml, 3.71 mmol), K_2CO_3 (2.331 g, 16.87 mmol), Cs_2CO_3 (1.099 g, 3.37 mmol) and NaI (55.6 mg, 3.71 mmol) were dissolved in acetone (20.0 ml) to give a white suspension. The reaction mixture was stirred at 80ºC for four days. The solvent was removed and the crude was filtered in vacuum and washed with CH_2Cl_2. The product was purified with a silica gel column and

eluted with cyclohexane:ethyl acetate (0-100%) using a CombiFlash chromatographer to afford 1,10-enyne **34** as a yellow oil in 46% isolated yield (354.8 mg, 1.554 mmol). ^{1}H NMR (500 MHz, $CDCl_3$, ppm) δ 7.17 (dd, *J* = 7.8 Hz, *J* = 1.5 Hz, 1H), 7.11 (td, *J* = 7.7 Hz, *J* = 1.7 Hz, 1H), 6.87 (t, *J* = 7.5, 1H), 6.78 (d, *J* = 8.3 Hz, 1H), 6.32 (s, 1H), 3.91 (t, *J* = 6.3 Hz, 2H), 2.23 (td, *J* = 7.1 Hz, *J* = 2.7 Hz, 2H), 1.93 (t, J = 2.7 Hz, 1H), 1.90 (d, *J* = 1.3 Hz, 3H), 1.88 – 1.84 (m, 2H), 1.79 (d, *J* = 1.2 Hz, 3H), 1.70 – 1.65 (m, 2H). ^{13}C NMR (126 MHz, $CDCl_3$, ppm) δ 156.3 (s), 134.8 (s), 130.3 (s), 127.7 (s), 127.2 (s), 120.7 (s), 119.9 (s), 111.5 (s), 84.0 (s), 68.6 (s), 67.5 (s), 28.2 (s), 26.6 (s), 25.2 (s), 19.5 (s), 18.1 (s). APCI$^+$ *m/z* calcd for $C_{16}H_{21}O^+$ $[M+H]^+$ 229.1592, found 229.1581.

1-(((3-Methylbut-2-en-1-yl)oxy)methyl)-2-(prop-2-yn-1-yloxy)benzene (36)

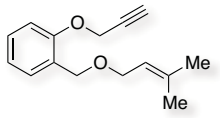

A suspension of NaH 60% wt (136.0 mg, 3.39 mmol) in THF (9.0 ml) was cooled in an ice bath and a solution of (2-(prop-2-yn-1-yloxy)phenyl)methanol (500.0 mg, 3.08 mmol) in THF (2.0 ml) was added dropwise. The solution was stirred at 25 ºC for 20 min. Then, 1-bromo-3-methylbut-2-ene (0.36 ml, 3.08 mmol) and tetrabutylammonium iodide (11.0 mg, 0.031 mmol) in THF (2.0 ml) was added carefully and it was stirred at 70ºC for 12 h. The reaction mixture was quenched with 1 ml of methanol and the crude was filtered in vacuum through celite washing with CH_2Cl_2. The product was purified with a silica gel column and eluted with cyclohexane:ethyl acetate (0-100%) using a CombiFlash chromatographer to afford 1,10-enyne **36** as a slightly yellowish oil in 72% isolated yield (510.6 mg, 2.217 mmol). ^{1}H NMR (400 MHz, $CDCl_3$, ppm) δ 7.40 (dd, *J* = 7.6 Hz, *J* = 1.6 Hz, 1H), 7.21 (td, *J* = 7.8 Hz, *J* = 1.8 Hz, 1H), 7.00 (td, *J* = 7.3 Hz, *J* = 1.0, 1H), 6.94 (dd, *J* = 8.3 Hz, *J* = 0.8, 1H), 5.44 – 5.39 (m, 1H), 4.65 (d, *J* = 2.4, 2H), 4.54 (s, 2H), 4.03 (d, *J* = 6.9, 2H), 2.47 (t, *J* = 2.3, 1H), 1.73 (d, *J* = 0.8, 3H), 1.65 (s, 3H). ^{13}C NMR (100 MHz, $CDCl_3$, ppm) δ 155.0 (s), 136.6 (s), 128.9 (s), 128.2 (s), 127.7 (s), 121.3 (s), 111.8 (s), 78.7 (s), 75.3 (s), 66.8 (s), 66.5 (s), 55.9 (s), 25.6 (s), 17.9 (s). APCI$^+$ *m/z* calcd for $C_{15}H_{19}O_2^+$ $[M+H]^+$ 253.1204, found 253.1192.

1-Ethynyl-2-(((6-methylhept-5-en-2-yl)oxy)methyl)benzene (38)

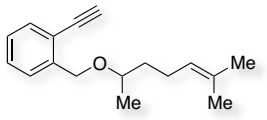

To a slurry of NaH 60 % wt (88.0 mg, 2.20 mmol) in THF (10.0 mL) at 0 ºC, a solution of 6-methylhept-5-en-2-ol (282.0 mg, 2.20 mmol) in THF (10.0 mL) was added dropwise and stirred for 15 min. Thereafter, 1-(bromomethyl)-2-iodobenzene (594.0 mg, 2.00 mmol) in THF (10.0 mL) was added over 10 minutes 0 ºC. The mixture was then stirred for 30 min at 0 ºC and subsequently the temperature was increased to 75 ºC and further stirred for 17 h. The reaction was quenched by addition of methanol followed by water and acidification with HCl 10 %. After complete evaporation of solvents and water, the residue was filtered through a plug of silica and washed with CH_2Cl_2. The solution was concentrated and the crude was dissolved in Et_3N (2.0 mL). Bis(triphenylphosphine)palladium(II)dichloride (46.7 mg, 0.07 mmol) and CuI (25.4 mg, 0.13 mmol) were added and the mixture was degassed with argon. Ethynyltrimethylsilane (0.30 mL, 2.00 mmol) was added via syringe and the solution was allowed to stir at 25 ºC for 20 h. After filtration through a plug of silica the solution was concentrated under reduced pressure. Finally, the residue was dissolved in THF (3.0 mL) and methanol (3.0 mL) at 0 ºC and K_2CO_3 (900.0 mg, 6.52 mmol) was added portionwise. Then, the solution was allowed to reach 25 ºC and stirred for 12 h. The crude was thereafter extracted using saturated NH_4Cl and diethylether and dried over $MgSO_4$. The crude product was purified with a silica gel column and eluted with cyclohexane:ethyl

acetate (0-100%) using a CombiFlash chromatographer to afford 1,10-enyne **38** as an orange oil in 44% isolated yield (216.3 mg, 0.89 mmol). ^{1}H NMR (400 MHz, $CDCl_3$, ppm) δ 7.54 (d, *J* = 7.6 Hz, 1 H), 7.50 (dd, *J* = 7.6, 1.4 Hz, 1 H), 7.37 (td, *J* = 7.6, 1.4 Hz, 1 H), 7.23 (td, *J* = 7.6, 1.4 Hz, 1 H), 5.16 – 5.11 (m, 1 H), 4.77 (d, *J* = 12.7 Hz, 1 H), 4.64 (d, *J* = 12.7 Hz, 1 H), 3.62 – 3.54 (m, 2 H), 3.30 (s, 1 H), 2.14 – 2.07 (m, 2 H), 1.73 – 1.67 (m, 4 H), 1.70 (s, 3 H), 1.54 – 1.45 (m, 1 H), 1.25 (d, *J* = 6.1 Hz, 3 H). ^{13}C NMR (101 MHz, $CDCl_3$, ppm) δ 141.7 (s), 132.6 (s), 131.5 (s), 129.0 (s), 127.6 (s), 127.0 (s), 124.4 (s), 120.4 (s), 81.6 (s), 81.5 (s), 75.0 (s), 68.2 (s), 36.8 (s), 25.7 (s), 24.2 (s), 19.7 (s), 17.7 (s). APCI$^+$ *m/z* calcd for $C_{17}H_{23}O^+$ $[M+H]^+$ 243.1743, found 243.1751.

1-Ethynyl-2-((2-(3-methylbut-2-en-1-yl)phenoxy)methyl)benzene (40)

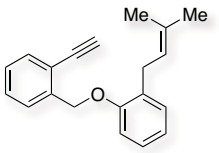

To a solution of 2-(3-methylbut-2-en-1-yl)phenol (2.039 g, 12.50 mmol) in acetone (18.0 mL) were added 1-(bromomethyl)-2-ethynylbenzene (2.230 g, 11.42 mmol), K_2CO_3 (7.90 g, 57.2 mmol), Cs_2CO_3 (1.118 g, 3.43 mmol) and NaI (17.0 mg, 0.11 mmol). The reaction mixture was stirred at 60ºC for 30 h and then filtered through a pad of celite washing with CH_2Cl_2. The solvent was removed and the product was purified with a silica gel column eluted with cyclohexane:ethyl acetate (0-100%) using a CombiFlash chromatographer to afford 1,10-enyne **40** as a pale yellow oil in 62% isolated yield (1.959 g, 7.09 mmol). ^{1}H NMR (400 MHz, $CDCl_3$, ppm) δ 7.77 (d, *J* = 7.8 Hz, 1 H), 7.71 (dd, 7.6, 1.4 Hz, 1 H), 7.52 (td, *J* = 7.6, 1.4 Hz, 1 H), 7.43 – 7.37 (m, 2 H), 7.33 (td, *J* 7.8, 1.8 Hz, 1 H), 7.12 – 7.08 (m, 2 H), 5.61 – 5.57 (m, 1 H), 5.46 (s, 2 H), 3.65 (d, *J* = 7.4 Hz, 2 H), 3.48 (s, 1H), 1.95 (s, 3 H), 1.89 (s, 3 H). ^{13}C NMR (126 MHz, $CDCl_3$, ppm) δ 156.5 (s), 140.1 (s), 132.9 (s), 132.4 (s), 130.6 (s), 129.7 (s), 129.3 (s), 127.5 (s), 127.2 (s), 127.1 (s), 123.0 (s), 121.1 (s), 120.4 (s), 111.8 (s), 82.7 (s), 81.2 (s), 68.1 (s), 29.1 (s), 26.0 (s), 18.0 (s). APCI$^+$ *m/z* calcd for $C_{20}H_{21}O^+$ $[M+H]^+$ 277.1587, found 277.1598.

1-((3,7-Dimethyloct-6-en-1-yl)oxy)-2-iodobenzene

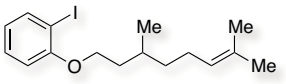

To a solution of 2-iodophenol (2.761 g, 12.55 mmol) in acetone (18.0 mL) were added 8-bromo-2,6-dimethyloct-2-ene (2.504 g, 11.43 mmol), K_2CO_3 (7.90 g, 57.2 mmol), Cs_2CO_3 (1.118 g, 3.43 mmol) and tetrabutylammonium iodide (42.0 mg, 0.114 mmol). The reaction mixture was stirred at 60ºC for 30 h and then filtered through a pad of celite washing with CH_2Cl_2. The solvent was removed and the product was purified with a silica gel column eluted with cyclohexane:ethyl acetate (0-100%) using a CombiFlash chromatographer to afford 1-((3,7-dimethyloct-6-en-1-yl)oxy)-2-iodobenzene as a pale yellow oil in 99% isolated yield (4.054 g, 11.32 mmol). ^{1}H NMR (400 MHz, $CDCl_3$, ppm) δ 7.78 (dd, *J* = 7.4, 1.5 Hz, 1 H), 7.29 (td, *J* = 8.0, 1.5 Hz, 1 H), 6.81 (d, *J* = 8.1, 1.4 Hz, 1 H), 6.70 (td, *J* = 7.4, 1.5 Hz, 1 H), 5.16 – 5.12 (m, 1 H), 4.10 – 4.00 (m, 2 H), 2.10 – 1.97 (m, 2 H), 1.94 – 1.89 (m, 1 H), 1.84 – 1.80 (m, 1 H), 1.70 (s, 3 H), 1.69 – 1.54 (m, 1 H), 1.63 (s, 3 H), 1.48 – 1.39 (m, 1 H), 1.30 – 1.20 (m, 1 H), 0.99 (d, *J* = 6.6 Hz, 3 H). ^{13}C NMR (101 MHz, $CDCl_3$, ppm) δ 157.7 (s), 139.4 (s), 131.3 (s), 129.4 (s), 124.7 (s), 122.3 (s), 112.1 (s), 86.8 (s), 67.5 (s), 37.1 (s), 36.0 (s), 29.5 (s), 25.8 (s), 25.5 (s), 19.6 (s), 17.7 (s).

((2-((3,7-Dimethyloct-6-en-1-yl)oxy)phenyl)ethynyl)trimethylsilane

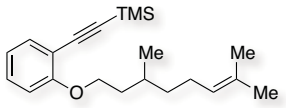

To a solution of 1-((3,7-dimethyloct-6-en-1-yl)oxy)-2-iodobenzene (0.71 g, 1.98 mmol) in Et_3N (3.0 mL) was added bis(triphenylphosphine)palladium dichloride (70 mg, 0.099 mmol) and CuI (38 mg, 0, 198 mmol) under argon. Then, ethynyltrimethylsilane (0.43 mL, 2.97 mmol) was added to the reaction mixture. The solution was stirred at 25 ºC for 12 h. After filtration over a pad of celite, the solvent was removed by rotary evaporation. The crude product was purified by flashed chromatography over silica gel (cyclohexane:ethyl acetate 98:2) to afford the product as an yellow oil in 99% isolated yield (648 mg, 1.97 mmol). ^{1}H NMR (400 MHz, $CDCl_3$, ppm) δ 7.47 (dd, *J* = 7.4, 1.5 Hz, 1 H), 7.28 (td, *J* = 7.5, 1.5 Hz, 1 H), 6.81 – 6.70 (m, 2 H), 5.22 – 5.18 (m, 1 H), 4.10 – 4.04 (m, 2 H), 2.16 – 2.04 (m, 2 H), 1.98 – 1.84 (m, 2 H), 1.76 (s, 3 H), 1.74 – 1.64 (m, 1 H), 1.64 (s, 3 H), 1.53 – 1.45 (m, 1 H), 1.35 – 1.26 (m, 1 H), 1.06 (d, *J* = 6.6 Hz, 3 H), 0.09 (s, 9H). ^{13}C NMR (101 MHz, $CDCl_3$, ppm) δ 160.3 (s), 133.7 (s), 131.0 (s), 129.9 (s), 124.9 (s), 120.2 (s), 112.9 (s), 111.9 (s), 101.7 (s), 98.1 (s), 66.8 (s), 37.33 (s), 36.2 (s), 29.7 (s), 25.8 (s), 25.7 (s), 19.7 (s), 17.7 (s), 0.1 (s).

1-((3,7-Dimethyloct-6-en-1-yl)oxy)-2-ethynylbenzene (42)

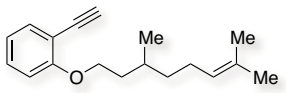

To a solution of (648 mg, 1.97 m((2-((3,7-dimethyloct-6-en-1-yl)oxy)phenyl)ethynyl)trimethylsilane mol) in methanol (5.0 mL) was added K_2CO_3 (1.37 g, 9.87 mmol). The reaction mixture was stirred at 25 ºC for 12 h and then quenched with quenched with saturated NH_4Cl and extracted with ethyl acetate. The combined organic layers were washed with brine, dried over $MgSO_4$ and filtered. The solvent was removed by rotary evaporation. The crude product was purified with a silica gel column and eluted with hexane:ethyl acetate (0-100%) using a CombiFlash chromatographer to afford 1,11-enyne **42** as a yellow oil in 75% isolated yield (380 mg, 1.48 mmol). ^{1}H NMR (500 MHz, $CDCl_3$, ppm) δ 7.48 (dd, *J* = 7.5, 1.8 Hz, 1 H), 7.29 (td, *J* = 8.1, 1.8 Hz, 1 H), 6.91 – 6.86 (m, 2 H), 5.18 – 5.14 (m, 1 H), 4.12 – 4.04 (m, 2 H), 3.28 (s, 1 H), 2.13 – 2.00 (m, 2 H), 1.95 – 1.89 (m, 1 H), 1.82 – 1.75 (m, 1 H), 1.73 (s, 3 H), 1.73 – 1.64 (m, 1 H), 1.64 (s, 3 H), 1.49 – 1.42 (m, 1 H), 1.31 – 1.24 (m, 1 H), 1.01 (dd, *J* = 6.6 Hz, 3 H). ^{13}C NMR (126 MHz, $CDCl_3$, ppm) δ 160.3 (s), 134.1 (s), 131.1 (s), 130.1 (s), 124.8 (s), 120.2 (s), 111.9 (s), 111.8 (s), 81.1 (s), 80.3 (s), 67.1 (s), 37.2 (s), 36.0 (s), 29.6 (s), 25.8 (s), 25.6 (s), 19.7 (s), 17.7 (s). APCI$^+$ *m/z* calcd for $C_{18}H_{25}O^+$ $[M+H]^+$ 257.1900, found 257.1907.

1-(((3-Methylbut-2-en-1-yl)oxy)methyl)-2-(pent-4-yn-1-yloxy)benzene (44)

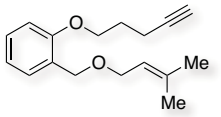

A suspension of NaH 60% wt (116.0 mg, 2.89 mmol) in THF (7.0 ml) was cooled in an ice bath and a solution of (2-(pent-4-yn-1-yloxy)phenyl)methanol (500.0 mg, 2.63 mmol) in THF (2.0 ml) was added dropwise. The solution was stirred at 25 ºC for 20 min. Then, 1-bromo-3-methylbut-2-ene (0.30 ml, 2.63 mmol) and tetrabutylammonium iodide (9.0 mg, 0.026 mmol) in THF (2.0 ml) was added carefully and it was stirred at 70ºC for 12 h. The reaction mixture was quenched with 1 ml of methanol and the crude was filtered in vacuum through celite with CH_2Cl_2. The product was purified with a silica gel column and eluted with cyclohexane:ethyl acetate (0-100%)

using a CombiFlash chromatographer to afford 1,12-enyne **44** as a slightly yellowish oil in 75% isolated yield (509.3 mg, 1.971 mmol). ^{1}H NMR (400 MHz, $CDCl_3$, ppm) δ 7.37 (dd, *J* = 7.7 Hz, *J* = 1.7 Hz, 1H), 7.19 (td, *J* = 7.8 Hz, *J* = 1.7 Hz, 1H), 6.92 (td, *J* = 7.5 Hz, *J* = 1.0, 1H), 6.81 (dd, *J* = 8.3 Hz, *J* = 0.7, 1H), 5.45 – 5.39 (m, 1H), 4.53 (s, 2H), 4.03 (d, *J* = 7.0, 2H), 4.02 (t, *J* = 5.9, 2H), 2.38 (td, *J* = 7.1, *J* = 2.6, 1H), 2.00 – 1.96 (m, 3H), 1.95 (t, *J* = 2.7, 1H), 1.74 (d, *J* = 0.9, 3H), 1.66 (s, 3H). ^{13}C NMR (100 MHz, $CDCl_3$, ppm) δ 156.2 (s), 136.4 (s), 128.8 (s), 128.3 (s), 127.1 (s), 121.3 (s), 120.4 (s), 111.0 (s), 83.3 (s), 68.8 (s), 66.8 (s), 66.6 (s), 66.0 (s), 28.2 (s), 25.6 (s), 17.9 (s), 15.1 (s). APCI$^+$ *m/z* calcd for $C_{17}H_{23}O_2^+$ $[M+H]^+$ 259.1698, found 259.1688.

1-(((3,7-Dimethyloct-6-en-1-yl)oxy)methyl)-2-ethynylbenzene (46)

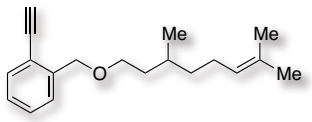

A solution of citronellol (1.69 mL, 9.23 mmol) in THF (5.0 ml) was added to a suspension of NaH 60% wt (369 mg, 9.23 mmol) in THF (5.0 ml) at 0 ºC under argon. The mixture was stirred at 25 ºC for 30 min and then, a solution of 1-(bromomethyl)-2-ethynylbenzene (1.5 g, 7.69 mmol) in THF (5.0 mL) was added dropwise. The solution was stirred under reflux for 12 h. The reaction mixture was quenched with saturated NH_4Cl and extracted with ethyl acetate. The combined organic layers were washed with brine, dried over $MgSO_4$ and filtered. The solvent was removed by rotary evaporation. The crude product was purified by flashed chromatography (eluent cyclohexane:ethyl acetate 97:3) to afford 1,12-enyne **46** as an orange oil in 72% isolated yield (1.5 g, 5.5 mmol). ^{1}H NMR (400 MHz, $CDCl_3$, ppm) δ 7.50 – 7.48 (m, 2 H), 7.36 (td, *J* = 7.6, 2.4 Hz, 1 H), 7.26 – 7.21 (m, 1 H), 5.13 – 5.09 (m, 1 H), 4.69 (s, 2 H), 3.61 – 3.53 (m, 2 H), 3.29 (s, 1 H), 2.04 – 1.95 (m, 2 H), 1.72 – 1.67 (m, 1 H), 1.69 (s, 3 H), 1.64 – 1.59 (m, 1 H), 1.61 (s, 3 H), 1.51 – 1.44 (m, 1 H), 1.42 – 1.32 (m, 1 H), 1.23 – 1.13 (m, 1 H), 0.92 (d, *J* = 6.6 Hz, 3 H). ^{13}C NMR (101 MHz, $CDCl_3$, ppm) δ 141.3 (s), 132.6 (s), 131.1 (s), 129.0 (s), 127.3 (s), 127.0 (s), 124.9 (s), 120.5 (s), 81.6 (s), 81.4 (s), 70.7 (s), 69.2 (s), 37.2 (s), 36.7 (s), 29.6 (s), 25.7 (s), 25.5 (s), 19.6 (s), 17.6 (s). APCI$^+$ *m/z* calcd for $C_{19}H_{27}O^+$ $[M+H]^+$ 271.2056, found 271.2057.

1-(Hex-5-yn-1-yloxy)-2-(((3-methylbut-2-en-1-yl)oxy)methyl)benzene (48)

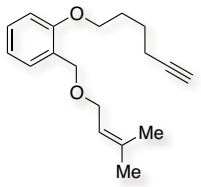

A suspension of NaH 60% wt (108.0 mg, 2.69 mmol) in THF (6.0 ml) was cooled in an ice bath and a solution of (2-(hex-5-yn-1-yloxy)phenyl)methanol (500.0 mg, 2.45 mmol) in THF (2.0 ml) was added dropwise. The solution was stirred at 25 ºC for 20 min. Then, 1-bromo-3-methylbut-2-ene (0.28 ml, 2.45 mmol) and tetrabutylammonium iodide (9.0 mg, 0.024 mmol) in THF (2.0 ml) was added carefully and it was stirred at 70ºC for 12 h. The reaction mixture was quenched with 1 ml of methanol and the crude was filtered in vacuum through celite washing with CH_2Cl_2. The product was purified with a silica gel column and eluted with cyclohexane:ethyl acetate (0-100%) using a CombiFlash chromatographer to afford 1,13-enyne **48** as a slightly yellowish oil in 73% isolated yield (487.7 mg, 1.791 mmol). ^{1}H NMR (400 MHz, $CDCl_3$, ppm) δ 7.37 (dd, *J* = 7.5 Hz, *J* = 1.9 Hz, 1H), 7.18 (td, *J* = 7.9 Hz, *J* = 1.7 Hz, 1H), 6.91 (td, *J* = 7.5 Hz, *J* = 1.0, 1H), 6.79 (dd, *J* = 8.2 Hz, *J* = 0.9, 1H), 5.44 – 5.40 (m, 1H), 4.53 (s, 2H), 4.04 (d, *J* = 6.8, 2H), 3.94 (t, *J* = 6.2, 2H), 2.24 (td, *J* = 7.0, *J* = 2.6, 2H), 1.95 (t, *J* = 2.7, 1H), 1.92 – 1.85 (m, 2H), 1.74 (d, *J* = 0.9, 3H), 1.72 – 1.68 (m, 2H), 1.66 (s, 3H). ^{13}C NMR (100 MHz, $CDCl_3$, ppm) δ 156.3 (s), 136.3 (s), 128.7 (s), 128.2 (s), 127.0 (s), 121.4 (s), 120.2 (s), 110.8 (s), 83.8 (s), 68.6 (s), 67.1 (s), 66.8 (s),

66.6 (s), 28.1 (s), 25.6 (s), 25.0 (s), 18.0 (s), 17.8 (s). APCI$^+$ *m/z* calcd for $C_{18}H_{25}O_2^+$ $[M+H]^+$ 295.1674, found 295.1670.

1-((6-Methylhept-5-en-1-yl)oxy)-2-((prop-2-yn-1-yloxy)methyl)benzene (50)

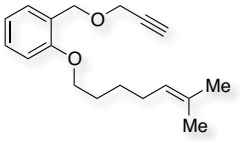

To a solution of 2-(hydroxymethyl)phenol (1.561 g, 12.57 mmol) in acetone (18.0 mL) were added 7-bromo-2-methylhept-2-ene (2.184 g, 11.43 mmol), K_2CO_3 (7.90 g, 57.2 mmol), Cs_2CO_3 (1.118 g, 3.43 mmol) and tetrabutylammonium iodide (42.0 mg, 0.114 mmol). The reaction mixture was stirred at 60ºC for 30 h and then filtered through a pad of celite with CH_2Cl_2. The solvent was removed and the crude was used directly in the next step (2.286 mg, 9.72 mmol). A solution of (2-((6-methylhept-5-en-1-yl)oxy)phenyl)methanol (3.796 g, 16.2 mmol) in THF (20.0 ml) was added to a suspension of NaH 60% wt (972 mg, 24.3 mmol) in THF (20.0 ml) at 0 ºC under argon. The reaction mixture was stirred at 70 ºC for 30 min. Then, a solution of 3-bromoprop-1-yne 80% wt (2.345 ml, 21.1 mmol) was added dropwise at 25 ºC. The solution was stirred under reflux for 12 h. The reaction mixture was quenched with saturated NH_4Cl and extracted with ethyl acetate. The combined organic layers were washed with brine, dried over $MgSO_4$ and filtered. The solvent was removed by rotary evaporation. The crude product was purified with a silica gel column and eluted with cyclohexane:ethyl acetate (0-100%) using a CombiFlash chromatographer to afford 1,13-enyne **50** as an yellow oil in 75% isolated yield (3.309 g, 12.15 mmol). ^{1}H NMR (400 MHz, $CDCl_3$, ppm) δ 7.44 (dd, *J* = 7.5, 1.8 Hz, 1 H), 7.28 (td, *J* = 8.1, 1.8 Hz, 1 H), 6.98 (td, *J* = 7.5, 1.1 Hz, 1 H), 6.89 (dd, *J* = 8.3, 1.1 Hz, 1 H), 5.24 – 5.19 (m, 1 H), 4.72 (s, 2 H), 4.27 (d, *J* = 2.8 Hz, 2 H), 4.02 (t, *J* = 6.4 Hz, 2 H), 2.49 (t, *J* = 2.7 Hz, 1 H), 2.15 – 2.09 (m, 2 H), 1.90 – 1.83 (m, 2 H), 1.77 (s, 3 H), 1.66 (s, 3 H), 1.63 – 1.55 (m, 2 H). ^{13}C NMR (101 MHz, $CDCl_3$, ppm) δ 156.9 (s), 131.7 (s), 129.4 (s), 128.9 (s), 126.1 (s), 124.5 (s), 120.3 (s), 111.3 (s), 80.2 (s), 74.4 (s), 68.0 (s), 66.7 (s), 57.5 (s), 29.0 (s), 27.8 (s), 26.4 (s), 25.8 (s), 17.8 (s). ESI$^+$ *m/z* calcd for $C_{18}H_{24}O_2Na^+$ $[M+Na]^+$ 295.1674, found 295.1674.

1-((7-Methyloct-6-en-1-yl)oxy)-2-((prop-2-yn-1-yloxy)methyl)benzene (52)

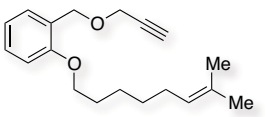

To a solution of 2-(hydroxymethyl)phenol (1.561 g, 12.57 mmol) in acetone (18.0 mL) were added 8-bromo-2-methyloct-2-ene (2.345 g, 11.43 mmol), K_2CO_3 (7.90 g, 57.2 mmol), Cs_2CO_3 (1.118 g, 3.43 mmol) and tetrabutylammonium iodide (42.0 mg, 0.114 mmol). The reaction mixture was stirred at 60ºC for 30 h and then filtered through a pad of celite with CH_2Cl_2. The solvent was removed and the crude was used directly in the next step (2.356 mg, 9.47 mmol). A solution of (2-((7-methyloct-6-en-1-yl)oxy)phenyl)methanol (4.023 g, 16.2 mmol) in THF (20.0 ml) was added to a suspension of NaH 60% wt (972 mg, 24.3 mmol) in THF (20.0 ml) at 0 ºC under argon. The reaction mixture was stirred at 70 ºC for 30 min. Then, a solution of 3-bromoprop-1-yne 80% wt (2.345 ml, 21.1 mmol) was added dropwise at 25 ºC. The solution was stirred under reflux for 12 h. The reaction mixture was quenched with saturated NH_4Cl and extracted with ethyl acetate. The combined organic layers were washed with brine, dried over $MgSO_4$ and filtered. The solvent was removed by rotary evaporation. The crude product was purified with a silica gel column and eluted with cyclohexane:ethyl acetate (0-100%) using a CombiFlash chromatographer to afford 1,14-enyne **52** as an yellow oil in 69% isolated yield (3.201 g, 11.18 mmol). ^{1}H NMR (400 MHz, $CDCl_3$, ppm) δ 7.45 (dd, *J* = 7.5, 1.8 Hz, 1 H), 7.34 (td, *J* = 8.1, 1.8 Hz, 1 H), 7.00 (dt, *J* = 7.5, 1.1 Hz, 1 H), 6.91 (dd, *J* = 8.3, 1.1 Hz, 1 H), 5.24 – 5.20 (m, 1 H), 4.74 (s, 2

H), 4.29 (d, *J* = 2.8 Hz, 2 H), 4.04 (t, *J* = 6.4 Hz, 2 H), 2.51 (t, *J* = 2.7 Hz, 1 H), 2.13 – 2.07 (m, 2 H), 1.91 – 1.84 (m, 2 H), 1.78 (s, 3 H), 1.70 (s, 3 H), 1.59 – 1.46 (m, 4 H). ^{13}C NMR (101 MHz, $CDCl_3$, ppm) δ 156.9 (s), 131.4 (s), 129.4 (s), 128.9 (s), 126.1 (s), 124.7 (s), 80.2 (s), 74.3 (s), 68.1 (s), 66.7 (s), 57.5 (s), 29.7 (s), 29.3 (s), 28.1 (s), 25.9 (s), 25.8 (s), 17.8 (s). APCI$^+$ *m/z* calcd for $C_{19}H_{27}O_2^+$ $[M+H]^+$ 287.2006, found 287.2005.

1-(Bromomethyl)-2-((3,7-dimethyloct-6-en-1-yl)oxy)benzene

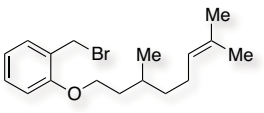

To a solution of (2-((3,7-dimethyloct-6-en-1-yl)oxy)phenyl)methanol (1.020 g, 3.89 mmol) in anhydrous CH_2Cl_2 (100.0 mL) was added triphenylphosphine (1.835 g, 7.00 mmol) under argon. The resulting solution was cooled in an ice bath and a solution of 1-bromopyrrolidine-2,5-dione (1.245 g, 7.00 mmol) in CH_2Cl_2 (100.0 ml) was added. The reaction mixture was stirred for 12 h at 25 ºC. Then, the solvent was removed and the product was purified with a silica gel column eluted with cyclohexane:ethyl acetate (0-100%) using a CombiFlash chromatographer to afford 1-(bromomethyl)-2-((3,7-dimethyloct-6-en-1-yl)oxy)benzene as a yellow oil quantitatively (1.265 g, 3.89 mmol). This compound was not very stable so it was kept in the freezer. ^{1}H NMR (500 MHz, $CDCl_3$, ppm) δ 7.31 (dd, *J* = 7.5, 1.6 Hz, 1 H), 7.26 (td, *J* = 7.8, 1.7 Hz, 1 H), 6.89 (td, *J* = 7.5, 0.7 Hz, 1 H), 6.86 (d, *J* = 8.1 Hz, 1 H), 5.14 – 5.10 (m, 1 H), 4.56 (s, 2 H), 4.10 – 4.02 (m, 2 H), 2.10 – 1.96 (m, 2 H), 1.92 – 1.86 (m, 1 H), 1.83 – 1.75 (m, 1 H), 1.68 (d, *J* = 0.40 Hz, 3 H), 1.67 – 1.62 (m, 1 H), 1.61 (s, 3 H), 1.46 – 1.39 (m, 1 H), 1.28 – 1.22 (m, 1 H), 0.97 (d, *J* = 6.7 Hz, 3 H). ^{13}C NMR (126 MHz, $CDCl_3$, ppm) δ 157.1 (s), 131.4 (s), 130.9 (s), 130.2 (s), 126.3 (s), 124.8 (s), 120.5 (s), 111.8 (s), 66.6 (s), 37.2 (s), 36.3 (s), 29.6 (s), 29.2 (s), 25.9 (s), 25.6 (s), 19.7 (s), 17.8 (s).

Dimethyl 2-(but-3-yn-1-yl)-2-(2-((3,7-dimethyloct-6-en-1-yl)oxy)benzyl)malonate (54)

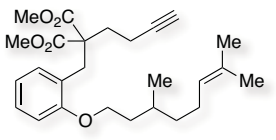

To a suspension of NaH 60% wt (49.0 mg, 1.23 mmol) in DMF (10.0 mL) at 0 ºC under argon was added a solution of dimethyl 2-(but-3-yn-1-yl)malonate (249.0 mg, 1.35 mmol) in DMF (2.5 mL). The mixture was stirred for 10 min and then, a solution of 1-(bromomethyl)-2-((3,7-dimethyloct-6-en-1-yl)oxy)benzene (400.0 mg, 1.23 mmol) in DMF (2.5 mL) was added dropwise. The reaction mixture was stirred at 25 ºC for 19 h. The solution was extracted with diethyl ether and brine and the combined organic layers were dried over $MgSO_4$ and filtered. The solvent was removed by rotary evaporation. The crude product was purified with a silica gel column and eluted with hexane:ethyl acetate (0-100%) using a CombiFlash chromatographer to afford 1,15-enyne **54** as a pale yellow oil in 55% isolated yield (288.7 mg, 0.67 mmol). ^{1}H NMR (400 MHz, $CDCl_3$, ppm) δ 7.18 (ddd, *J* = 8.2, 7.5, 1.7 Hz, 1 H), 6.95 (dd, *J* = 7.5, 1.7 Hz, 1 H), 6.88 – 6.79 (m, 2 H), 5.11 (ddt, *J* = 8.4, 5.7, 1.4 Hz, 1 H), 4.04 – 3.94 (m, 2 H), 3.71 (s, 3 H), 3.71 (s, 3 H), 3.30 (s, 2 H), 2.30 – 2.21 (m, 2 H), 2.12 – 1.96 (m, 4 H), 1.94 – 1.86 (m, 2 H), 1.70 – 1.63 (m, 5 H), 1.61 (s, 3 H), 1.43 – 1.36 (m, 1 H), 1.30 – 1.14 (m, 1 H), 0.96 (d, *J* = 6.4 Hz, 3 H). ^{13}C NMR (101 MHz, $CDCl_3$, ppm) δ 171.3 (s), 157.6 (s), 131.3 (s), 131.1 (s), 128.4 (s), 124.7 (s), 124.2 (s), 120.2 (s), 111.3 (s), 83.8 (s), 68.5 (s), 66.5 (s), 58.7 (s), 52.3 (s), 37.2 (s), 35.9 (s), 31.8 (s), 31.3 (s), 29.7 (s), 25.7 (s), 25.5 (s), 19.6 (s), 17.7 (s), 14.5 (s). ESI$^+$ *m/z* calcd for $C_{26}H_{36}O_5Na^+$ $[M+Na]^+$ 451.2455, found 451.2457.

1-((3,7-Dimethyloct-6-en-1-yl)oxy)-2-((pent-4-yn-1-yloxy)methyl)benzene (56)

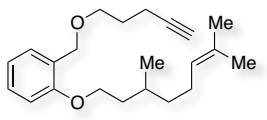

A solution of pent-4-yn-1-ol (160.6 mg, 1.909 mmol) in THF (5.0 ml) was added to a suspension of NaH 60% wt (74.8 mg, 1.870 mmol) in THF (10.0 ml) and the reaction mixture was stirred at 25 ºC for 30 min. Then, a solution of 1-(bromomethyl)-2-((3,7-dimethyloct-6-en-1-yl)oxy)benzene (599.4 mg, 1.843 mmol) and tetrabutylammonium iodide (10.0 mg, 0.027 mmol) in THF (5.0 ml) was added dropwise and it was stirred again at 25 ºC for four days. The reaction was quenched with 1 ml of methanol and the crude was filtered in vacuum through celite washing with CH_2Cl_2. Then, the product was purified with a silica gel column and eluted with cyclohexane:ethyl acetate (0-100%) using a CombiFlash chromatographer to afford 1,16-enyne **56** as a yellowish oil in 26% isolated yield (154.8 mg, 0.471 mmol). ^{1}H NMR (500 MHz, $CDCl_3$, ppm) δ 7.37 (dd, *J* = 7.5 Hz, *J* = 1.4 Hz, 1H), 7.23 (td, *J* = 7.8 Hz, *J* = 1.8 Hz, 1H), 6.93 (t, *J* = 7.4 Hz, 1H), 6.84 (d, *J* = 8.1 Hz, 1H), 5.12 – 5.09 (m, 1H), 4.55 (s, 2H), 4.04 – 3.96 (m, 2H), 3.61 (t, *J* = 6.1, 2H), 2.32 (td, *J* = 7.1, *J* = 2.6, 2H), 2.08 – 1.95 (m, 2H), 1.92 (t, *J* = 2.7, 1H), 1.88 – 1.81 (m, 3H), 1.74 – 1.67 (m, 1H), 1.69 (s, 3H), 1.65 – 1.57 (m, 1H), 1.61 (s, 3H), 1.44 – 1.37 (m, 1H), 1.25 – 1.19 (m, 1H), 0.96 (d, *J* = 6.6, 3H). ^{13}C NMR (126 MHz, $CDCl_3$, ppm) δ 156.6 (s), 131.4 (s), 128.7 (s), 128.5 (s), 127.1 (s), 124.8 (s), 120.3 (s), 111.1 (s), 84.2 (s), 69.0 (s), 68.4 (s), 67.7 (s), 66.3 (s), 37.2 (s), 36.3 (s), 29.7 (s), 28.9 (s), 25.8 (s), 25.6 (s), 19.7 (s), 17.8 (s), 15.4 (s).

1-((3,7-Dimethyloct-6-en-1-yl)oxy)-2-((hex-5-yn-1-yloxy)methyl)benzene (58)

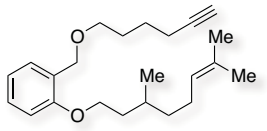

A solution of (2-((3,7-dimethyloct-6-en-1-yl)oxy)phenyl)methanol (500.0 mg, 1.906 mmol) in THF (2.0 ml) was added to a suspension of NaH 60% wt (99.0 mg, 2.477 mmol) in THF (4.0 ml) and the reaction mixture was stirred at 70ºC for 30 min. When the solution had cooled down to 25 ºC, a solution of 6-iodohex-1-yne (430.0 mg, 2.067 mmol) in THF (2.0 ml) was added dropwise and it was stirred again at 70ºC for 12 h. The reaction was quenched with 1 ml of methanol, the solvent was removed under reduced pressure and the crude was filtered through a plug of silica with CH_2Cl_2. Then, the product was purified with a silica gel column and eluted with cyclohexane:ethyl acetate (0-100%) using a CombiFlash chromatographer to afford 1,17-enyne **58** as a yellowish oil in 28% isolated yield (184.3 mg, 0.538 mmol). ^{1}H NMR (500 MHz, $CDCl_3$, ppm) δ 7.37 (dd, *J* = 7.5 Hz, *J* = 1.4 Hz, 1H), 7.20 (td, *J* = 7.9 Hz, *J* = 1.6 Hz, 1H), 6.92 (t, *J* = 7.3 Hz, 1H), 6.82 (d, *J* = 8.1 Hz, 1H), 5.12 – 5.09 (m, 1H), 4.53 (s, 2H), 4.02 – 3.94 (m, 2H), 3.53 (t, *J* = 6.3, 2H), 2.02 (td, *J* = 7.0, *J* = 2.6, 2H), 2.08 – 1.94 (m, 2H), 1.92 (t, *J* = 2.7, 1H), 1.87 – 1.80 (m, 1H), 1.76 – 1.70 (m, 3H), 1.68 (d, *J* = 0.5 Hz, 3H), 1.65 – 1.55 (m, 3H), 1.60 (s, 3H), 1.44 – 1.37 (m, 1H), 1.26 – 1.19 (m, 1H), 0.95 (d, *J* = 6.6, 3H). ^{13}C NMR (126 MHz, $CDCl_3$, ppm) δ 156.5 (s), 131.2 (s), 128.5 (s), 128.3 (s), 127.2 (s), 124.7 (s), 120.2 (s), 111.0 (s), 84.3 (s), 70.0 (s), 68.4 (s), 67.5 (s), 66.2 (s), 37.1 (s), 36.2 (s), 29.6 (s), 28.9 (s), 25.7 (s), 25.5 (s), 25.3 (s), 19.6 (s), 18.2 (s), 17.7 (s). APCI$^+$ *m/z* calcd for $C_{23}H_{35}O_2^+$ $[M+H]^+$ 343.2637, found 343.2633.

1-Ethynyl-3-((7-methyloct-6-en-1-yl)oxy)benzene (60)

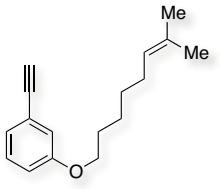

To a solution of 3-ethynylphenol (1.485 g, 12.57 mmol) in acetone (18.0 mL) were added 8-bromo-2-methyloct-2-ene (2.345 g, 11.43 mmol), K_2CO_3 (7.90 g, 57.2 mmol), Cs_2CO_3 (1.118 g, 3.43 mmol) and tetrabutylammonium iodide (42.0 mg, 0.114 mmol). The reaction mixture was stirred at 60ºC for 30 h and then filtered through a pad of celite with CH_2Cl_2. The solvent was removed and the product was purified with a silica gel column eluted with cyclohexane:ethyl acetate (0-100%) using a CombiFlash chromatographer to afford 1,12-enyne **60** as a colourless oil in 82% isolated yield (2.271 g, 9.37 mmol). ^{1}H NMR (400 MHz, $CDCl_3$, ppm) δ 7.22 (t, *J* = 7.5 Hz, 1 H), 7.08 (d, *J* = 7.6 Hz, 1 H), 7.04–7.02 (m, 1 H), 6.91 (dd, *J* = 7.6, 1.5 Hz, 1 H), 5.17–5.11 (m, 1 H), 3.95 (t, *J* = 6.6 Hz, 2 H), 3.06 (s, 1 H), 2.05–1.98 (m, 2 H), 1.83–1.74 (m, 2 H)1.71 (s, 3 H), 1.62 (s, 3 H), 1.50–1.37 (m, 4 H). ^{13}C NMR (101 MHz, $CDCl_3$, ppm) δ 158.9 (s), 131.5 (s), 129.4 (s), 124.6 (s), 124.5 (s), 123.0 (s), 117.6 (s), 116.0 (s), 83.7 (s), 76.9 (s), 68.1 (s), 29.6 (s), 29.2 (s), 28.0 (s), 25.8 (s), 25.7 (s), 17.7 (s). APCI$^+$ *m/z* calcd for $C_{17}H_{23}O^+$ $[M+H]^+$ 243.1743, found 243.1747.

1-Ethynyl-3-((11-methyldodec-10-en-1-yl)oxy)benzene (62)

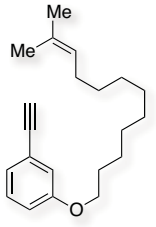

To a solution of 3-ethynylphenol (1.484 g, 12.57 mmol) in acetone (18.0 mL) were added 12-bromo-2-methyldodec-2-ene (2.985 g, 11.43 mmol), K_2CO_3 (7.90 g, 57.2 mmol), Cs_2CO_3 (1.118 g, 3.43 mmol) and tetrabutylammonium iodide (42.0 mg, 0.114 mmol). The reaction mixture was stirred at 60ºC for 30 h and then filtered through a pad of celite with CH_2Cl_2. The solvent was removed and the product was purified with a silica gel column eluted with cyclohexane:ethyl acetate (0-100%) using a CombiFlash chromatographer to afford 1,16-enyne **62** as a colourless oil in 57% isolated yield (1.946 g, 6.52 mmol). ^{1}H NMR (500 MHz, $CDCl_3$, ppm) δ 7.21 (t, *J* = 7.9 Hz, 1 H), 7.08 (d, *J* = 7.6 Hz, 1 H), 7.02 (s, 1 H), 6.90 (dd, *J* = 8.4, 2.6 Hz, 1 H), 5.13 (t, *J* = 7.2 Hz, 1 H), 3.94 (t, *J* = 6.5 Hz, 2 H), 3.05 (s, 1 H), 2.00–1.94 (m, 2 H), 1.82–1.73 (m, 2 H), 1.70 (s, 3 H), 1.61 (s, 3 H), 1.48–1.40 (m, 2 H), 1.39–1.29 (m, 10 H). ^{13}C NMR (126 MHz, $CDCl_3$, ppm) δ 158.9 (s), 131.1 (s), 129.3 (s), 124.9 (s), 124.4 (s), 123.0 (s), 117.6 (s), 116.0 (s), 83.7 (s), 76.8 (s), 68.1 (s), 29.9 (s), 29.6 (s), 29.5 (s), 29.5 (s), 29.4 (s), 29.3 (s), 29.2 (s), 28.1 (s), 26.0 (s), 25.7 (s). APCI$^+$ *m/z* calcd for $C_{21}H_{31}O^+$ $[M+H]^+$ 299.2369, found 299.2368.

General Procedure for the Preparation of Macrocycles

To a solution of the 1,*n*-enyne (1 equiv.) in CH_2Cl_2, gold(I) complex **C** (3 mol%) was added. The reaction mixture was stirred at 25 ºC or under reflux until complete consumption of the starting material. The reaction was quenched with 0.05 ml of Et_3N, the solvent was removed under reduced pressure and the crude was analysed by quantitative ^{1}H NMR using 1,4-diacetylbenzene as internal standard. The product was purified by preparative-TLC using different gradients of cyclohexane and ethyl acetate to obtain the pure macrocycle as a mixture of diastereoisomers.

8,11,11-Trimethyl-7,8,9,10,10a,11,13,15-octahydro-6H-benzo[b]cyclobuta[g][1,5]dioxacyclotridecine (30)

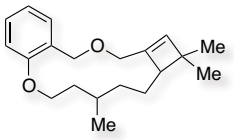

Macrocycle **30** was synthesized following the general procedure using 1,14-enyne **29** (78.1 mg, 0.26 mmol) and catalyst **C** (7.0 mg, 7.8 μmol) in CH_2Cl_2 (0.007 M) at 25 ºC. After 12 h, the product was obtained as a yellow oil in 57% isolated yield (44.5 mg, 0.15 mmol), diastereoselectivity 2.3:1. ^{1}H NMR for the mixture of diastereoisomers (400 MHz, $CDCl_3$, ppm) δ 7.30–7.22 (m, 2 H), 6.89–6.84 (m, 2 H), 6.10 (s, 0.3 H), 6.03 (s, 0.7 H), 4.59–4.56 (m, 1 H), 4.27 (d, *J* = 9.3 Hz, 0.7 H), 4.22–4.12 (m, 1.3 H), 4.05–3.90 (m, 3 H), 2.47–2.43 (m, 0.7 H), 2.26–2.22 (m, 0.3 H), 2.05–1.89 (m, 1 H), 1.75–1.47 (m, 6 H), 1.13 (s, 2.1 H), 1.12 (s, 0.9 H), 1.06 (s, 0.9 H), 1.05 (s, 2.1 H), 0.99 (d, *J* = 6.6 Hz, 0.9 H), 0.95 (d, *J* = 6.6 Hz, 2.1 H). ^{13}C NMR for the major diastereoisomer (101 MHz, $CDCl_3$, ppm) δ 158.2 (s), 146.8 (s), 141.2 (s), 131.8 (s), 129.9 (s), 126.3 (s), 120.0 (s), 111.3 (s), 69.8 (s), 68.5 (s), 67.7 (s), 52.1 (s), 42.9 (s), 35.9 (s), 33.3 (s), 30.2 (s), 27.0 (s), 24.7 (s), 22.4 (s), 20.7 (s). ^{13}C NMR for the minor diastereoisomer (101 MHz, $CDCl_3$, ppm) δ 158.1 (s), 146.6 (s), 142.8 (s), 130.1 (s), 130.0 (s), 126.0 (s), 119.9 (s), 110.9 (s), 69.8 (s), 68.9 (s), 67.0 (s), 55.8 (s), 42.7 (s), 35.2 (s), 34.9 (s), 34.1 (s), 30.5 (s), 29.1 (s), 22.2 (s), 21.0 (s). ESI$^+$ *m/z* calcd for $C_{20}H_{28}O_2Na^+$ $[M+Na]^+$ 323.1982; found 323.1989.

2,2,5-Trimethyl-2,2a,3,4,5,7-hexahydrobenzo[c]cyclobuta[e]oxonine (39)

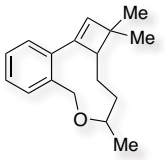

Macrocycle **39** was synthesized following the general procedure using 1,10-enyne **38** (63.0 mg, 0.26 mmol) and catalyst **C** (7.0 mg, 7.8 μmol) in CH_2Cl_2 (0.15 M) at 25 ºC. After 19 h, the product was obtained as a yellow oil in 51% isolated yield (32.1 mg, 0.13 mmol), diastereoselectivity 5:1. ^{1}H NMR for the major diastereoisomer (400 MHz, $CDCl_3$, ppm) δ 7.53–7.50 (m, 1 H), 7.32–7.25 (m, 3 H), 6.49 (s, 1 H), 4.99 (d, *J* = 12.4 Hz, 1 H), 4.47 (d, *J* = 12.4 Hz, 1 H), 3.39–3.32 (m, 1 H), 3.07–3.04 (m, 1 H), 1.93–1.79 (m, 2 H), 1.71–1.62 (m, 2 H), 1.24 (s, 3 H), 1.13 (d, *J* = 6.6 Hz, 3 H), 1.10 (s, 3 H). ^{13}C NMR for the major diastereoisomer (101 MHz ,$CDCl_3$, ppm) δ 148.0 (s), 140.0 (s), 136.1 (s), 133.7 (s), 131.2 (s), 127.8 (s), 127.7 (s), 127.6 (s), 71.6 (s), 66.5 (s), 57.2 (s), 42.6 (s), 37.1 (s), 28.7 (s), 27.1 (s), 22.6 (s), 22.4 (s). APCI$^+$ *m/z* calcd for $C_{17}H_{23}O^+$ $[M+H]^+$ 243.1743, found 243.1747.

1,1-Dimethyl-1,7,13,13a-tetrahydrodibenzo[b,g]cyclobuta[e]oxonine (41)

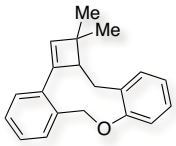

Macrocycle **41** was synthesized following the general procedure using 1,10-enyne **40** (71.9 mg, 0.26 mmol) and catalyst **C** (7.0 mg, 7.8 μmol) in CH_2Cl_2 (0.15 M) at 45 ºC. After 23 h, the product was obtained as a dark yellow solid in 66% isolated yield (47.4 mg, 0.17 mmol). ^{1}H NMR (400 MHz, $CDCl_3$, ppm) δ 7.42–7.40 (m, 1 H), 7.29–7.27 (m, 1 H), 7.25–7.18 (m, 2 H), 7.15–7.08 (m, 2 H), 7.01 (dd, *J* = 7.9, 1.4 Hz, 1 H), 6.96 (td, *J* = 7.3, 1.4 Hz, 1 H), 6.40 (s, 1 H), 5.12 (d, *J* = 10.8 Hz, 1 H), 5.07 (d, *J* = 10.8 Hz, 1 H), 3.15 (dd, *J* = 13.9, 9.7 Hz, 1 H), 2.92 (dd, *J* = 9.7, 2.9 Hz, 1 H), 2.74 (dd, *J* = 14.0, 3.0 Hz, 1 H), 1.29 (s, 3 H), 1.26 (s, 3 H). ^{13}C NMR (101 MHz, $CDCl_3$, ppm) δ 157.4 (s), 147.4 (s), 140.1 (s), 136.4 (s), 136.0 (s), 133.0 (s), 130.7 (s), 130.6 (s), 128.7 (s), 128.2 (s), 127.5 (s), 127.3 (s), 123.8 (s), 121.2 (s), 74.7 (s), 56.9 (s), 43.7 (s), 31.4 (s), 27.1 (s), 23.5 (s). APCI$^+$ *m/z* calcd for $C_{20}H_{21}O^+$ $[M+H]^+$ 277.1587, found

277.1591. Structure confirmed by X-Ray crystallography, CCDC 912988. Mp = 112.8 – 115.6 ºC.

8,11,11-Trimethyl-7,8,9,10,10a,11-hexahydro-6H-benzo[b]cyclobuta[d]oxecine (43)

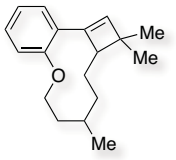

Macrocycle **43** was synthesized following the general procedure using 1,11-enyne **42** (66.7 mg, 0.26 mmol) and catalyst **C** (7.0 mg, 7.8 μmol) in CH_2Cl_2 (0.3 M) at 70 ºC. After 2 h, the product was obtained as a yellow oil in 20% isolated yield (13.3 mg, 0.05 mmol), diastereoselectivity 4:1. ^{1}H NMR for the major diastereoisomer (400 MHz, $CDCl_3$, ppm) δ 7.23–7.18 (m, 2 H), 6.91–6.87 (m, 1 H), 6.84–6.81 (m, 1 H), 6.21 (s, 1 H), 4.40–4.37 (m, 1 H), 3.83–3.78 (m, 1 H), 2.50 (dd, *J* = 11.8, 2.7 Hz, 1 H), 1.90–1.81 (m, 2 H), 1.73–1.66 (m, 2 H), 1.63–1.55 (m, 1 H), 3.44–1.39 (m, 2 H), 1.19 (s, 3 H), 1.14 (s, 3 H), 0.96 (d, *J* = 6.6 Hz, 3 H). ^{13}C NMR for the major diastereoisomer (101 MHz, $CDCl_3$, ppm) δ 156.8 (s), 147.8 (s), 139.6 (s), 129.5 (s), 128.6 (s), 128.2 (s), 120.8 (s), 113.0 (s), 69.4 (s), 56.1 (s), 42.8 (s), 33.1 (s), 32.3 (s), 32.1 (s), 27.0 (s), 23.0 (s), 22.9 (s), 20.8 (s). ESI$^+$ *m/z* calcd for $C_{18}H_{24}ONa^+$ $[M+Na]^+$ 279.1719; found 279.1724.

10,10-Dimethyl-6,7,8,9,9a,10,12,14-octahydrobenzo[b]cyclobuta[g][1,5]dioxacyclododecine (51)

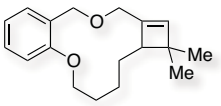

Macrocycle **51** was synthesized following the general procedure using 1,13-enyne **50** (70.8 mg, 0.26 mmol) and catalyst **C** (7.0 mg, 7.8 μmol) in CH_2Cl_2 (0.3 M) at 25 ºC. After 16 h, the product was obtained as a yellow oil in 29% isolated yield (20.5 mg, 0.08 mmol). ^{1}H NMR (500 MHz, $CDCl_3$, ppm) δ 7.30–7.22 (m, 2 H), 7.02–6.98 (m, 1 H), 6.92 (td, *J* = 7.4, 1.1 Hz, 1 H), 6.01 (s, 1 H), 4.59 (d, *J* = 8.9 Hz, 1 H), 4.30 (d, *J* = 8.9 Hz, 1 H), 4.28–4.24 (m, 1 H), 4.11 (dt, *J* = 11.3, 1.0 Hz, 1 H), 4.01–3.94 (m, 2 H), 2.42 (dd, *J* = 10.7, 3.6 Hz, 1 H), 2.07–2.00 (m, 1 H), 1.91–1.83 (m, 1 H), 1.59–1.45 (m, 4 H), 1.12 (s, 3 H), 1.02 (s, 3 H). ^{13}C NMR (126 MHz, $CDCl_3$, ppm) δ 158.9 (s), 146.5 (s), 140.7 (s), 131.5 (s), 129.8 (s), 128.6 (s), 121.4 (s), 116.2 (s), 69.9 (s), 69.8 (s), 68.4 (s), 53.4 (s), 42.6 (s), 28.4 (s), 28.0 (s), 27.0 (s), 24.0 (s), 21.9 (s). ESI$^+$ *m/z* calcd for $C_{18}H_{24}O_2Na^+$ $[M+Na]^+$ 295.1669; found 295.1665.

11,11-Dimethyl-7,8,9,10,10a,11,13,15-octahydro-6H-benzo[b]cyclobuta[g][1,5]dioxacyclotridecine (53)

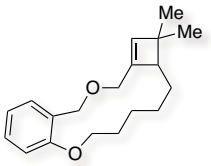

Macrocycle **53** was synthesized following the general procedure using 1,14-enyne **52** (74.4 mg, 0.26 mmol) and catalyst **C** (7.0 mg, 7.8 μmol) in CH_2Cl_2 (0.15 M) at 25 ºC. After 19 h, the product was obtained as a yellow oil in 57% isolated yield (42.4 mg, 0.15 mmol). ^{1}H NMR (400 MHz, $CDCl_3$, ppm) δ 7.27–7.23 (m, 2 H), 6.89–6.83 (m, 2 H), 6.06 (s, 1 H), 4.47 (d, *J* = 9.2 Hz, 1 H), 4.25 (d, *J* = 9.2 Hz, 1 H), 4.16–4.11 (m, 1 H), 4.05–4.01 (m, 1 H), 3.97 (s, 2 H), 2.39 (dd, *J* = 12.0, 2.9 Hz, 1 H), 2.04–1.97 (m, 1 H), 1.88–1.83 (m, 2 H), 1.81–1.75 (m, 1 H), 1.49–1.41 (m, 4 H), 1.12 (s, 3 H), 1.04 (s, 3 H). ^{13}C NMR (101 MHz, $CDCl_3$, ppm) δ 158.1 (s), 146.6 (s). 141.7 (s), 131.9 (s), 129.8 (s), 125.9 (s), 119.8 (s), 110.9 (s), 69.8 (s), 69.2 (s), 68.6 (s), 53.6 (s), 42.6 (s), 29.5 (s), 28.2 (s), 27.5 (s), 27.1 (s), 26.9 (s), 22.1 (s). APCI$^+$ *m/z* calcd for $C_{19}H_{27}O_2^+$ $[M+H]^+$ 287.2006, found 287.2009.

Dimethyl 8,11,11-trimethyl-7,8,9,10,10a,11,13,14-octahydro-6H-benzo[b]cyclobuta[h][1]oxacyclotetradecine-15,15(16H)-dicarboxylate (55)

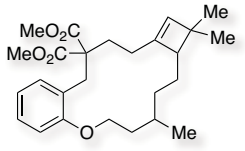

Macrocycle **55** was synthesized following the general procedure using 1,14-enyne **54** (111.5 mg, 0.26 mmol) and catalyst **C** (7.0 mg, 7.8 μmol) in CH_2Cl_2 (0.15 M) at 25 ºC. After 16 h, the product was obtained as a pale yellow oil in 70% isolated yield (79.0 mg, 0.18 mmol). ^{1}H NMR for the major diastereoisomer (500 MHz, $CDCl_3$, ppm) δ 7.16 (ddd, *J* = 8.5, 7.3, 1.8 Hz, 1 H), 6.88 (dd, *J* = 7.6, 1.6 Hz, 2 H), 6.80 (td, *J* = 7.4, 1.0 Hz, 1 H), 5.66 (s, 1 H), 4.17–4.08 (m, 1 H), 3.99 (td, *J* = 10.0, 2.7 Hz, 1 H), 3.76 (s, 3 H), 3.68 (s, 3 H), 3.56 (d, *J* = 14.0 Hz, 1 H), 3.22 (d, *J* = 13.9 Hz, 1 H), 2.34 (dd, *J* = 10.7, 3.7 Hz, 1 H), 2.13–2.04 (m, 3 H), 2.03–1.95 (m, 1 H), 1.92–1.82 (m, 2 H), 1.77–1.67 (m, 1 H), 1.65–1.48 (m, 2 H), 1.45–1.36 (m, 1 H), 1.18–1.09 (m, 1 H), 1.08 (s, 3 H), 0.96 (s, 3 H), 0.94 (d, *J* = 6.6 Hz, 3 H). ^{13}C NMR for the major diastereoisomer (126 MHz, $CDCl_3$, ppm) δ 172.5 (s), 172.2 (s), 157.8 (s), 149.8 (s), 136.7 (s), 130.8 (s), 128.3 (s), 124.8 (s), 120.4 (s), 111.6 (s), 65.8 (s), 59.3 (s), 52.4 (s), 52.3 (s), 50.3 (s), 42.2 (s), 37.4 (s), 32.0 (s), 31.9 (s), 30.0 (s), 27.4 (s), 27.4 (s), 25.3 (s), 25.0 (s), 22.6 (s), 19.9 (s). ESI$^+$ *m/z* calcd for $C_{26}H_{36}O_5Na^+$ $[M+Na]^+$ 451.2455; found 451.2453.

4,4-Dimethyl-11-oxatricyclo[10.3.1.0^{2,5}]hexadeca-1(16),2,12,14-tetraene (61)

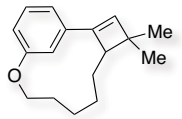

Macrocycle **61** was synthesized following the general procedure using 1,12-enyne **60** (63.0 mg, 0.26 mmol) and catalyst **C** (7.0 mg, 7.8 μmol) in CH_2Cl_2 (0.45 M) at 25 ºC. After 1 day, the product was obtained as a yellow oil in 70% isolated yield (44.1 mg, 0.18 mmol), mixture 5:1 of conformers. ^{1}H NMR (500 MHz, $CDCl_3$, ppm) δ 7.23–7.17 (m, 1 H), 6.91–6.84 (m, 2 H), 6.79–6.73 (m, 1 H), 6.28 (s, 1 H), 4.00–3.91 (m, 2 H), 2.75–2.69 (m, 1 H), 1.82–1.75 (m, 3 H), 1.52–1.44 (m, 5 H), 1.24 (s, 3 H), 1.16 (s, 3 H). ^{13}C NMR (126 MHz, $CDCl_3$, ppm) δ 159.2 (s), 145.8 (s), 136.6 (s), 136.2 (s), 129.3 (s), 124.6 (s), 117.5 (s), 113.4 (s), 67.9 (s), 51.9 (s), 42.9 (s), 29.3 (s), 28.7 (s), 27.9 (s), 26.5 (s), 25.7 (s), 21.9 (s). APCI$^+$ *m/z* calcd for $C_{17}H_{23}O^+$ $[M+H]^+$ 243.1743, found 243.1745.

4,4-Dimethyl-15-oxatricyclo[14.3.1.0^{2,5}]eicosa-1(20),2,16,18-tetraene (63)

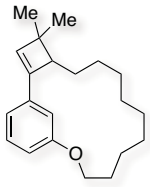

Macrocycle **63** was synthesized following the general procedure using 1,12-enyne **62** (77.6 mg, 0.26 mmol) but 5 mol% of catalyst **C** (11.7 mg, 13.0 μmol) in CH_2Cl_2 (0.15 M) at 45 ºC. After 2 days, the product was obtained as a yellow oil in 71% isolated yield (55.1 mg, 0.18 mmol), mixture 4:1 of conformers. ^{1}H NMR for the major diastereoisomer (400 MHz, $CDCl_3$, ppm) δ 7.21 (t, *J* = 7.9 Hz, 1 H), 6.96 – 6.86 (m, 2 H), 6.77 (d, *J* = 7.9 Hz, 1 H), 6.28 (s, 1 H), 3.95 (t, *J* = 6.7 Hz, 2 H), 2.72–2.67 (m, 1 H), 1.81–1.75 (m, 3 H), 1.46–1.30 (m, 13 H), 1.24 (s, 3 H), 1.16 (s, 3 H). ^{13}C NMR for the major diastereoisomer (101 MHz, $CDCl_3$, ppm) δ 159.2 (s), 145.9 (s), 136.5 (s), 136.3 (s), 129.2 (s), 124.9 (s), 117.5 (s), 113.5 (s), 67.9 (s), 52.0 (s), 42.9 (s), 30.1 (s), 29.9 (s), 29.6 (s), 29.5 (s), 29.4 (s), 29.3 (s), 28.9 (s), 27.9 (s), 26.1 (s), 21.8 (s). APCI$^+$ *m/z* calcd for $C_{21}H_{31}O^+$ $[M+H]^+$ 299.2369, found 299.2369.

Procedures for the Derivatization of Macrocycles

(3,3-Dimethyl-2-(3-methyl-5-(o-tolyloxy)pentyl)cyclobutyl)methanol (64)

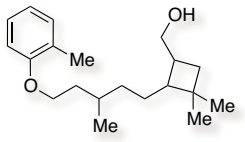

A solution of macrocycle 3**0** (50.0 mg, 0.17 mmol) in methanol (2.0 mL) was added over Pd/C 10 % (18.0 mg, 0.02 mmol). The resulting suspension was stirred at 25 ºC under H_2 atm for 8 h. Then, it was filtered through Teflon 0.22 and the solvent was removed under reduced pressure. The crude product was purified with Preparative-TLC and eluted with hexane:ethyl acetate (2:1) to afford compound **64** as a colourless oil in 79% isolated yield (39.9 mg, 0.13 mmol), diastereoselectivity retained to 2.4:1. ^{1}H NMR for the major diastereoisomer (500 MHz, $CDCl_3$, ppm) δ 7.15–7.11 (m, 2 H), 6.87–6.76 (m, 2 H), 4.01–3.95 (m, 2 H), 3.65–3.59 (m, 1 H), 3.56–3.47 (m, 1 H), 2.22 (s, 3 H), 2.06–1.96 (m, 1 H), 1.87–1.79 (m, 1 H), 1.72–1.64 (m, 2 H), 1.64–1.54 (m, 2 H), 1.41–1.33 (m, 2 H), 1.32–1.22 (m, 2 H), 1.18–1.13 (m, 1 H), 1.05–0.99 (m, 6 H), 0.97–0.92 (m, 3 H). ^{13}C NMR for the major diastereoisomer (126 MHz, $CDCl_3$, ppm) δ 157.3 (s), 130.7 (s), 126.9 (s), 126.8 (s), 120.2 (s), 111.0 (s), 67.6 (s), 66.2 (s), 47.6 (s), 38.6 (s), 36.4 (s), 36.3 (s), 35.6 (s), 34.4 (s), 31.3 (s), 30.3 (s), 28.0 (s), 22.9 (s), 19.8 (s), 16.4 (s). ESI$^+$ *m/z* calcd for $C_{20}H_{32}O_2Na^+$ $[M+Na]^+$ 327.2295; found 327.2297.

8,11,11-Trimethyl-7,8,9,10,10a,11,12,12a,13,15-decahydro-6H-benzo[b]cyclobuta[g][1,5]dioxacyclotridecine (65)

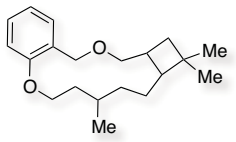

A solution of macrocycle **30** (50.0 mg, 0.17 mmol) and pyridine (6.7 μL, 0.08 mmol) in methanol (2.0 mL) was added over Pd/C 10 % (18.0 mg, 0.02 mmol). The resulting suspension was stirred at 25 ºC under H_2 atm for 5 h. Then, it was filtered through Teflon 0.22 and the solvent was removed under reduced pressure. The crude product was purified with Preparative-TLC and eluted with hexane:ethyl acetate (9:1) to afford compound **65** as a colourless oil in 82% isolated yield (41.1 mg, 0.14 mmol), diastereoselectivity 6.0:1.6:1.4:1.0. It was possible to assign *trans* configuration in the cyclobutane ring for the major diastereoisomer through ^{1}H–^{13}C HSQC phase edited, ^{1}H–^{1}H COSY and ^{1}H–^{1}H NOESY. ^{1}H NMR for the major diastereoisomer (500 MHz, $CDCl_3$, ppm) δ 7.28–7.23 (m, 1 H), 7.21 (dd, *J* = 7.4, 1.7 Hz, 1 H), 6.91–6.85 (m, 2 H), 4.56 (d, *J* = 9.1 Hz, 1 H), 4.24 (d, *J* = 9.2 Hz, 1 H), 4.19–4.15 (m, 1 H), 4.01–3.96 (m, 1 H), 3.55 (dd, *J* = 9.4, 2.7 Hz, 1 H), 3.31 (t, *J* = 9.2 Hz, 1 H), 2.13–2.06 (m, 1 H), 2.00–1.92 (m, 1 H), 1.90–1.81 (m, 1 H), 1.77–1.70 (m, 1 H), 1.70–1.65 (m, 1 H), 1.64–1.60 (m, 1 H), 1.51–1.44 (m, 1 H), 1.37–1.31 (m, 2 H), 1.30–1.25 (m, 1 H), 1.17–1.10 (m, 1 H), 0.99 (s, 3 H), 0.96 (s, 3 H), 0.86 (d, *J* = 6.7 Hz, 3 H). ^{13}C NMR for the major diastereoisomer (126 MHz, $CDCl_3$, ppm) δ 158.4 (s), 131.6 (s), 129.8 (s), 127.0 (s), 120.4 (s), 112.4 (s), 76.8 (s), 70.3 (s), 66.1 (s), 49.2 (s), 37.1 (s), 37.0 (s), 35.7 (s), 34.0 (s), 30.9 (s), 30.3 (s), 27.4 (s), 25.5 (s), 22.8 (s), 19.1 (s). ESI$^+$ *m/z* calcd for $C_{20}H_{30}O_2Na^+$ $[M+Na]^+$ 325.2138; found 325.2140.

X-Ray Crystallographic Data

(Acetonitrile)[(2′,4′,6′-triisopropyl-3,6-dimethoxy-1,1′-biphenyl-2-yl)di-tert-butylphosphine]gold(I) hexafluoroantimonate (G)

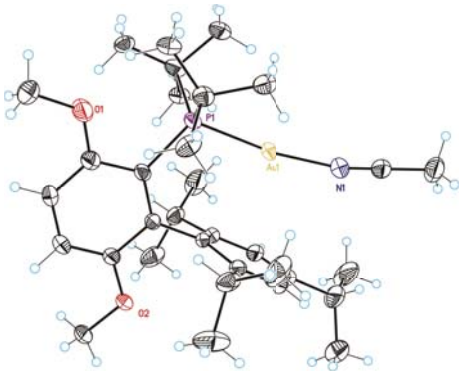

Table 1. Crystal data and structure refinement for complex G.

Empirical formula	C34.75 H56 Au Cl F6 N O2 P Sb
Formula weight	4075.83
Temperature	100(2) K
Wavelength	0.71073 Å
Crystal system	Monoclinic
Space group	P2(1)/n
Unit cell dimensions	a = 20.9905(9) Å α= 90.00 °. b = 8.7006(4) Å β = 114.731(2) °. c = 24.1270(11) Å γ = 90.00 °.
Volume	4002.2(3) $Å^3$
Z	4
Density (calculated)	1.691 Mg/m^3
Absorption coefficient	4.501 mm^{-1}
F(000)	2014
Crystal size	0.35x0.20x0.20mm^3
Theta range for data collection	1.08 to 30.01 °.
Index ranges	-29 <=h<=29 , -11 <=k<=11 , -33 <=l<=33
Reflections collected	43067
Independent reflections	10446 [R(int) = 0.0291]
Completeness to theta =30.01 °	0.895 %
Absorption correction	Empirical
Max. and min. transmission	0.8715 and 5421
Refinement method	Full-matrix least-squares on F^2
Data / restraints / parameters	10446 / 89 / 557
Goodness-of-fit on F^2	1.102
Final R indices [I>2sigma(I)]	R1 = 0.0262 , wR2 = 0.0681
R indices (all data)	R1 = 0.0314 , wR2 = 0.0747
Largest diff. peak and hole	1.328and-0.805e.$Å^{-3}$

Table 2. Bond lengths [Å] and angles [°] for complex G.

Bond lengths:		C5P-C1P#2	1.75(3)
Au1-N1	2.040(3)	Angles:	
Au1-P1	2.2534(8)		
P1-C1	1.854(3)	N1-Au1-P1	170.76(8)
P1-C24	1.895(3)	C1-P1-C24	110.89(14)
P1-C28	1.896(3)	C1-P1-C28	109.53(12)
N1-C32	1.129(4)	C24-P1-C28	113.30(13)
O1-C2	1.350(4)	C1-P1-Au1	110.59(9)
O1-C7	1.423(4)	C24-P1-Au1	105.49(9)
O2-C5	1.374(3)	C28-P1-Au1	106.90(10)
O2-C8	1.430(3)	C32-N1-Au1	166.9(3)
C1-C2	1.408(4)	C2-O1-C7	119.1(3)
C1-C6	1.415(4)	C5-O2-C8	116.5(2)
C2-C3	1.376(4)	C2-C1-C6	118.6(2)
C3-C4	1.387(4)	C2-C1-P1	117.6(2)
C4-C5	1.373(4)	C6-C1-P1	123.8(2)
C5-C6	1.412(4)	O1-C2-C3	122.5(3)
C6-C9	1.508(4)	O1-C2-C1	115.6(3)
C9-C14	1.406(5)	C3-C2-C1	121.9(3)
C9-C10	1.414(4)	C2-C3-C4	119.7(3)
C10-C11	1.390(5)	C5-C4-C3	119.9(3)
C10-C15	1.509(5)	C4-C5-O2	122.8(3)
C11-C12	1.374(6)	C4-C5-C6	122.0(3)
C12-C13	1.394(5)	O2-C5-C6	115.2(3)
C12-C18	1.503(5)	C5-C6-C1	118.0(3)
C13-C14	1.397(4)	C5-C6-C9	115.4(2)
C14-C21	1.521(4)	C1-C6-C9	126.6(2)
C15-C16	1.532(5)	C14-C9-C10	119.1(3)
C15-C17	1.535(5)	C14-C9-C6	120.3(2)
C18-C20	1.464(8)	C10-C9-C6	120.2(3)
C18-C20'	1.465(8)	C11-C10-C9	118.4(3)
C18-C19	1.493(6)	C11-C10-C15	119.0(3)
C21-C23	1.525(5)	C9-C10-C15	122.5(3)
C21-C22	1.534(5)	C12-C11-C10	123.6(3)
C24-C27'	1.502(6)	C11-C12-C13	117.4(3)
C24-C25	1.518(6)	C11-C12-C18	118.2(4)
C24-C26	1.532(6)	C13-C12-C18	124.4(4)
C24-C25'	1.540(7)	C12-C13-C14	121.7(4)
C24-C26'	1.564(6)	C13-C14-C9	119.6(3)
C24-C27	1.569(6)	C13-C14-C21	117.9(3)
C28-C31	1.475(6)	C9-C14-C21	122.4(3)
C28-C30'	1.516(6)	C10-C15-C16	110.1(3)
C28-C29'	1.536(6)	C10-C15-C17	112.1(4)
C28-C30	1.537(6)	C16-C15-C17	110.2(3)
C28-C29	1.565(5)	C20-C18-C20'	48.1(8)
C28-C31'	1.606(6)	C20-C18-C19	113.6(6)
C32-C33	1.457(5)	C20'-C18-C19	123.7(6)
Sb1-F3	1.856(2)	C20-C18-C12	113.6(4)
Sb1-F1	1.857(2)	C20'-C18-C12	121.5(6)
Sb1-F5	1.864(2)	C19-C18-C12	114.4(3)
Sb1-F2	1.867(2)	C14-C21-C23	114.1(3)
Sb1-F6	1.872(2)	C14-C21-C22	109.1(3)
Sb1-F4	1.874(2)	C23-C21-C22	109.2(3)
C1S-Cl2S	1.599(13)	C27'-C24-C25	129.4(5)
C1S-Cl1S	1.838(13)	C27'-C24-C26	78.8(5)
C1P-C2P	1.532(5)	C25-C24-C26	110.1(4)
C1P-C5P#1	1.75(3)	C27'-C24-C25'	108.8(6)
C2P-C3P	1.536(5)	C25-C24-C25'	25.1(3)
C3P-C4P	1.538(5)	C26-C24-C25'	125.2(4)
C4P-C5P	1.535(5)	C27'-C24-C26'	108.9(5)

C25-C24-C26'	84.6(5)	C31-C28-P1	117.4(3)
C26-C24-C26'	31.1(3)	C30'-C28-P1	110.8(3)
C25'-C24-C26'	106.4(5)	C29'-C28-P1	110.6(3)
C27'-C24-C27	29.8(4)	C30-C28-P1	104.5(3)
C25-C24-C27	108.1(5)	C29-C28-P1	103.0(3)
C26-C24-C27	106.6(5)	C31'-C28-P1	116.4(3)
C25'-C24-C27	83.9(5)	N1-C32-C33	179.1(4)
C26'-C24-C27	133.6(5)	F3-Sb1-F1	90.38(12)
C27'-C24-P1	107.0(3)	F3-Sb1-F5	179.16(12)
C25-C24-P1	115.9(3)	F1-Sb1-F5	90.01(13)
C26-C24-P1	108.2(3)	F3-Sb1-F2	89.90(13)
C25'-C24-P1	119.7(4)	F1-Sb1-F2	89.87(11)
C26'-C24-P1	105.7(3)	F5-Sb1-F2	90.84(14)
C27-C24-P1	107.6(3)	F3-Sb1-F6	89.32(12)
C31-C28-C30'	128.4(4)	F1-Sb1-F6	91.05(11)
C31-C28-C29'	68.5(4)	F5-Sb1-F6	89.93(13)
C30'-C28-C29'	110.7(4)	F2-Sb1-F6	178.80(12)
C31-C28-C30	114.6(4)	F3-Sb1-F4	89.42(12)
C30'-C28-C30	32.0(3)	F1-Sb1-F4	179.53(12)
C29'-C28-C30	137.8(4)	F5-Sb1-F4	90.19(13)
C31-C28-C29	109.7(4)	F2-Sb1-F4	89.70(12)
C30'-C28-C29	74.7(4)	F6-Sb1-F4	89.37(11)
C29'-C28-C29	43.5(4)	Cl2S-C1S-Cl1S	114.2(8)
C30-C28-C29	106.6(4)	C2P-C1P-C5P#1	103.2(18)
C31-C28-C31'	37.4(3)	C1P-C2P-C3P	119(2)
C30'-C28-C31'	104.3(4)	C2P-C3P-C4P	99.6(4)
C29'-C28-C31'	103.6(4)	C5P-C4P-C3P	99.6(4)
C30-C28-C31'	80.1(4)	C4P-C5P-C1P#2	78.4(15)
C29-C28-C31'	137.2(4)		

(Acetonitrile)[(2′,4′,6′-triisopropyl-3,4,5,6-tetramethyl-1,1′-biphenyl-2-yl)di-tert-butylphosphine]gold(I) hexafluoroantimonate (H)

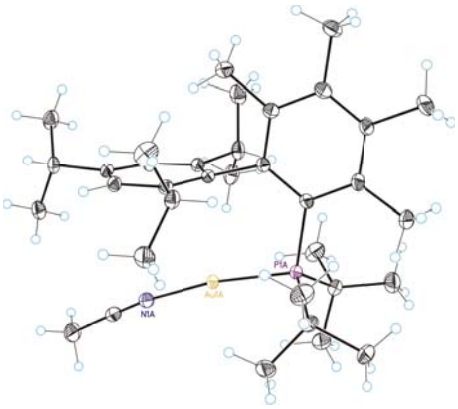

Table 3. Crystal data and structure refinement for complex H.

Empirical formula	C35.50 H57 Au Cl F6 N P Sb
Formula weight	996.96
Temperature	100(2) K
Wavelength	0.71073 Å
Crystal system	Triclinic
Space group	P-1
Unit cell dimensions	a = 8.7592(3) Å α= 88.1480(10) °. b = 19.0004(7) Å β = 84.8950(10) °. c = 23.7485(8) Å γ = 84.2550(10) °.
Volume	3915.9(2) $Å^3$

Z	4
Density (calculated)	1.691 Mg/m^3
Absorption coefficient	4.595 mm^{-1}
F(000)	1972
Crystal size	0.40x0.20x0.20mm^3
Theta range for data collection	0.86 to 30.07 °.
Index ranges	-11 <=h<=11 , -26 <=k<=26 , -31 <=l<=33
Reflections collected	87942
Independent reflections	20142 [R(int) = 0.0306]
Completeness to theta =30.07 °	0.876 %
Absorption correction	Empirical
Max. and min. transmission	0.4601 and 0.2608
Refinement method	Full-matrix least-squares on F^2
Data / restraints / parameters	20142 / 341 / 1009
Goodness-of-fit on F^2	1.093
Final R indices [I>2sigma(I)]	R1 = 0.0249 , wR2 = 0.0630
R indices (all data)	R1 = 0.0273 , wR2 = 0.0683
Largest diff. peak and hole	2.409and-1.370e.$Å^{-3}$

Table 4. Bond lengths [Å] and angles [°] for complex H.

Bond lengths:			
		C14A-C15A	1.390(4)
		C14A-C23A	1.522(3)
Au1A-N1A	2.049(2)	C15A-C16A	1.394(3)
Au1A-P1A	2.2656(6)	C16A-C20A	1.521(3)
Au1B-N1B	2.050(3)	C17A-C18A	1.528(4)
Au1B-P1B	2.2658(7)	C17A-C19A	1.536(4)
N1A-C34A	1.128(4)	C20A-C22A	1.532(4)
N1B-C34B	1.135(4)	C20A-C21A	1.533(4)
P1A-C1A	1.866(3)	C26A-C27A	1.526(4)
P1A-C26A	1.898(3)	C26A-C28A	1.536(4)
P1A-C30A	1.918(3)	C26A-C29A	1.540(4)
P1B-C1B	1.866(3)	C30A-C33A	1.527(4)
P1B-C26B	1.913(3)	C30A-C32A	1.537(4)
P1B-C30B	1.917(3)	C30A-C31A	1.546(4)
C1A-C2A	1.414(3)	C34A-C35A	1.462(4)
C1A-C6A	1.430(4)	C23A-C25A	1.527(4)
C2A-C3A	1.402(4)	C23A-C24A	1.534(4)
C2A-C7A	1.504(4)	C1B-C2B	1.415(3)
C3A-C4A	1.397(4)	C1B-C6B	1.421(3)
C3A-C8A	1.512(4)	C2B-C3B	1.402(3)
C4A-C5A	1.407(4)	C2B-C7B	1.503(4)
C4A-C9A	1.512(4)	C3B-C4B	1.395(3)
C5A-C6A	1.412(4)	C3B-C8B	1.513(4)
C5A-C10A	1.522(4)	C4B-C5B	1.401(3)
C6A-C11A	1.511(3)	C4B-C9B	1.511(4)
C11A-C12A	1.414(3)	C5B-C6B	1.409(3)
C11A-C16A	1.416(3)	C5B-C10B	1.515(4)
C12A-C13A	1.393(4)	C6B-C11B	1.518(3)
C12A-C17A	1.524(3)	C11B-C16B	1.414(3)
C13A-C14A	1.393(4)	C11B-C12B	1.414(3)

C12B-C13B	1.400(3)	C1B-P1B-C30B	111.57(14)
C12B-C17B	1.494(13)	C26B-P1B-C30B	112.25(16)
C12B-C17'	1.59(2)	C1B-P1B-Au1B	108.88(8)
C13B-C14B	1.390(3)	C26B-P1B-Au1B	106.09(11)
C14B-C15B	1.392(3)	C30B-P1B-Au1B	105.95(11)
C14B-C20B	1.518(3)	C2A-C1A-C6A	118.2(2)
C15B-C16B	1.398(3)	C2A-C1A-P1A	121.4(2)
C16B-C23B	1.514(4)	C6A-C1A-P1A	120.37(18)
C17B-C18B	1.526(14)	C3A-C2A-C1A	121.0(2)
C17B-C19B	1.553(11)	C3A-C2A-C7A	116.1(2)
C17'-C19'	1.486(19)	C1A-C2A-C7A	122.8(2)
C17'-C18'	1.51(2)	C4A-C3A-C2A	120.7(2)
C20B-C21B	1.528(4)	C4A-C3A-C8A	120.0(3)
C20B-C22B	1.528(4)	C2A-C3A-C8A	119.3(3)
C23B-C25B	1.528(4)	C3A-C4A-C5A	119.3(2)
C23B-C24B	1.536(4)	C3A-C4A-C9A	120.1(2)
C26B-C28'	1.418(14)	C5A-C4A-C9A	120.6(2)
C26B-C27'	1.515(16)	C4A-C5A-C6A	120.8(2)
C26B-C27B	1.534(6)	C4A-C5A-C10A	117.6(2)
C26B-C29B	1.541(6)	C6A-C5A-C10A	121.6(2)
C26B-C28B	1.571(6)	C5A-C6A-C1A	119.8(2)
C26B-C29'	1.577(14)	C5A-C6A-C11A	113.4(2)
C30B-C31'	1.403(14)	C1A-C6A-C11A	126.8(2)
C30B-C33B	1.490(7)	C12A-C11A-C16A	118.6(2)
C30B-C32B	1.495(6)	C12A-C11A-C6A	120.5(2)
C30B-C33'	1.552(19)	C16A-C11A-C6A	119.0(2)
C30B-C31B	1.598(6)	C13A-C12A-C11A	119.3(2)
C30B-C32'	1.790(16)	C13A-C12A-C17A	118.3(2)
C34B-C35B	1.458(4)	C11A-C12A-C17A	122.2(2)
Sb1A-F6A	1.8653(19)	C14A-C13A-C12A	122.5(2)
Sb1A-F3A	1.8694(18)	C15A-C14A-C13A	117.6(2)
Sb1A-F1A	1.8714(17)	C15A-C14A-C23A	121.5(2)
Sb1A-F4A	1.8740(18)	C13A-C14A-C23A	120.9(2)
Sb1A-F2A	1.8767(17)	C14A-C15A-C16A	122.0(2)
Sb1A-F5A	1.8775(18)	C15A-C16A-C11A	119.7(2)
Sb1B-F3B	1.867(2)	C15A-C16A-C20A	117.7(2)
Sb1B-F6B	1.868(2)	C11A-C16A-C20A	122.4(2)
Sb1B-F1B	1.871(2)	C12A-C17A-C18A	112.1(2)
Sb1B-F4B	1.873(2)	C12A-C17A-C19A	111.1(2)
Sb1B-F2B	1.874(2)	C18A-C17A-C19A	109.5(2)
Sb1B-F5B	1.877(2)	C16A-C20A-C22A	112.2(2)
Sb1'-F3'	1.863(4)	C16A-C20A-C21A	110.8(2)
Sb1'-F6'	1.866(4)	C22A-C20A-C21A	109.1(2)
Sb1'-F4'	1.871(4)	C27A-C26A-C28A	109.1(2)
Sb1'-F1'	1.873(4)	C27A-C26A-C29A	106.7(2)
Sb1'-F2'	1.878(4)	C28A-C26A-C29A	107.6(2)
Sb1'-F5'	1.880(4)	C27A-C26A-P1A	119.4(2)
C1S-Cl2'	1.732(5)	C28A-C26A-P1A	107.63(19)
C1S-Cl1S	1.749(4)	C29A-C26A-P1A	105.75(19)
C1S-Cl2S	1.800(6)	C33A-C30A-C32A	109.5(3)
		C33A-C30A-C31A	109.1(2)
Angles:		C32A-C30A-C31A	105.9(2)
		C33A-C30A-P1A	108.37(19)
N1A-Au1A-P1A	171.06(7)	C32A-C30A-P1A	106.89(19)
N1B-Au1B-P1B	170.96(8)	C31A-C30A-P1A	117.0(2)
C34A-N1A-Au1A	172.5(2)	N1A-C34A-C35A	178.6(3)
C34B-N1B-Au1B	168.7(3)	C14A-C23A-C25A	111.7(2)
C1A-P1A-C26A	111.50(12)	C14A-C23A-C24A	111.8(2)
C1A-P1A-C30A	112.13(12)	C25A-C23A-C24A	110.2(2)
C26A-P1A-C30A	112.02(13)	C2B-C1B-C6B	118.9(2)
C1A-P1A-Au1A	109.20(8)	C2B-C1B-P1B	120.78(18)
C26A-P1A-Au1A	103.67(9)	C6B-C1B-P1B	120.30(18)
C30A-P1A-Au1A	107.88(9)	C3B-C2B-C1B	120.7(2)
C1B-P1B-C26B	111.73(13)	C3B-C2B-C7B	116.3(2)

C1B-C2B-C7B	123.0(2)	C31'-C30B-C32B	62.3(7)
C4B-C3B-C2B	120.3(2)	C33B-C30B-C32B	112.2(4)
C4B-C3B-C8B	120.0(2)	C31'-C30B-C33'	116.1(10)
C2B-C3B-C8B	119.6(2)	C33B-C30B-C33'	22.1(7)
C3B-C4B-C5B	119.7(2)	C32B-C30B-C33'	130.9(8)
C3B-C4B-C9B	120.3(2)	C31'-C30B-C31B	44.8(7)
C5B-C4B-C9B	120.0(2)	C33B-C30B-C31B	105.4(4)
C4B-C5B-C6B	121.0(2)	C32B-C30B-C31B	107.1(3)
C4B-C5B-C10B	116.9(2)	C33'-C30B-C31B	87.0(8)
C6B-C5B-C10B	122.2(2)	C31'-C30B-C32'	101.7(8)
C5B-C6B-C1B	119.4(2)	C33B-C30B-C32'	73.3(5)
C5B-C6B-C11B	112.9(2)	C32B-C30B-C32'	45.1(5)
C1B-C6B-C11B	127.6(2)	C33'-C30B-C32'	95.3(9)
C16B-C11B-C12B	118.6(2)	C31B-C30B-C32'	141.1(5)
C16B-C11B-C6B	120.2(2)	C31'-C30B-P1B	128.3(6)
C12B-C11B-C6B	119.1(2)	C33B-C30B-P1B	108.5(3)
C13B-C12B-C11B	120.0(2)	C32B-C30B-P1B	109.0(2)
C13B-C12B-C17B	118.6(6)	C33'-C30B-P1B	106.6(8)
C11B-C12B-C17B	121.4(6)	C31B-C30B-P1B	114.6(3)
C13B-C12B-C17'	114.5(8)	C32'-C30B-P1B	101.9(4)
C11B-C12B-C17'	124.0(9)	N1B-C34B-C35B	179.2(4)
C17B-C12B-C17'	15.4(8)	F6A-Sb1A-F3A	90.10(10)
C14B-C13B-C12B	121.7(2)	F6A-Sb1A-F1A	90.40(10)
C13B-C14B-C15B	117.9(2)	F3A-Sb1A-F1A	179.39(9)
C13B-C14B-C20B	121.6(2)	F6A-Sb1A-F4A	90.57(10)
C15B-C14B-C20B	120.5(2)	F3A-Sb1A-F4A	90.27(9)
C14B-C15B-C16B	122.4(2)	F1A-Sb1A-F4A	90.07(9)
C15B-C16B-C11B	119.3(2)	F6A-Sb1A-F2A	90.43(10)
C15B-C16B-C23B	117.6(2)	F3A-Sb1A-F2A	89.97(9)
C11B-C16B-C23B	123.1(2)	F1A-Sb1A-F2A	89.68(8)
C12B-C17B-C18B	115.9(7)	F4A-Sb1A-F2A	178.96(10)
C12B-C17B-C19B	108.5(8)	F6A-Sb1A-F5A	179.09(10)
C18B-C17B-C19B	107.5(9)	F3A-Sb1A-F5A	89.89(9)
C19'-C17'-C18'	109.7(15)	F1A-Sb1A-F5A	89.60(9)
C19'-C17'-C12B	113.8(14)	F4A-Sb1A-F5A	90.34(10)
C18'-C17'-C12B	107.7(12)	F2A-Sb1A-F5A	88.65(9)
C14B-C20B-C21B	112.0(2)	F3B-Sb1B-F6B	89.69(14)
C14B-C20B-C22B	111.4(2)	F3B-Sb1B-F1B	179.77(16)
C21B-C20B-C22B	110.3(2)	F6B-Sb1B-F1B	90.13(14)
C16B-C23B-C25B	112.4(3)	F3B-Sb1B-F4B	90.54(14)
C16B-C23B-C24B	111.0(2)	F6B-Sb1B-F4B	90.47(15)
C25B-C23B-C24B	108.3(3)	F1B-Sb1B-F4B	89.61(13)
C28'-C26B-C27'	116.0(10)	F3B-Sb1B-F2B	90.08(14)
C28'-C26B-C27B	134.1(7)	F6B-Sb1B-F2B	89.78(14)
C27'-C26B-C27B	26.8(6)	F1B-Sb1B-F2B	89.77(14)
C28'-C26B-C29B	75.5(6)	F4B-Sb1B-F2B	179.33(15)
C27'-C26B-C29B	129.5(7)	F3B-Sb1B-F5B	90.52(13)
C27B-C26B-C29B	109.1(4)	F6B-Sb1B-F5B	179.72(18)
C28'-C26B-C28B	34.5(6)	F1B-Sb1B-F5B	89.65(14)
C27'-C26B-C28B	83.2(7)	F4B-Sb1B-F5B	89.72(14)
C27B-C26B-C28B	106.3(4)	F2B-Sb1B-F5B	90.03(14)
C29B-C26B-C28B	104.5(4)	F3'-Sb1'-F6'	90.5(3)
C28'-C26B-C29'	114.2(8)	F3'-Sb1'-F4'	90.9(3)
C27'-C26B-C29'	107.0(9)	F6'-Sb1'-F4'	90.7(3)
C27B-C26B-C29'	80.6(6)	F3'-Sb1'-F1'	179.0(4)
C29B-C26B-C29'	38.8(6)	F6'-Sb1'-F1'	90.0(3)
C28B-C26B-C29'	139.3(6)	F4'-Sb1'-F1'	89.9(3)
C28'-C26B-P1B	106.9(6)	F3'-Sb1'-F2'	89.6(3)
C27'-C26B-P1B	102.7(7)	F6'-Sb1'-F2'	89.7(3)
C27B-C26B-P1B	108.1(3)	F4'-Sb1'-F2'	179.3(4)
C29B-C26B-P1B	121.5(3)	F1'-Sb1'-F2'	89.6(3)
C28B-C26B-P1B	106.4(2)	F3'-Sb1'-F5'	90.5(3)
C29'-C26B-P1B	109.3(6)	F6'-Sb1'-F5'	178.7(4)
C31'-C30B-C33B	122.1(6)	F4'-Sb1'-F5'	90.2(3)

F1'-Sb1'-F5'	89.0(3)	Cl2'-C1S-Cl2S	15.7(2)
F2'-Sb1'-F5'	89.4(3)	Cl1S-C1S-Cl2S	112.8(3)
Cl2'-C1S-Cl1S	109.7(3)		

1,1-Dimethyl-1,7,13,13a-tetrahydrodibenzo[b,g]cyclobuta[e]oxonine (41)

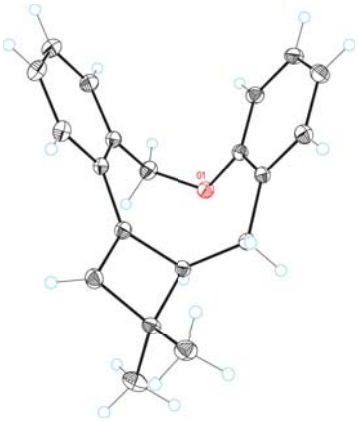

Table 5. Crystal data and structure refinement for macrocycle 41.

Empirical formula	C20 H20 O
Formula weight	276.36
Temperature	100(2) K
Wavelength	0.71073 Å
Crystal system	Monoclinic
Space group	P2(1)/c
Unit cell dimensions	a = 11.8987(3) Å α= 90.00 °. b = 6.0503(2) Å β = 104.9450(10) °. c = 21.0067(5) Å γ = 90.00 °.
Volume	1461.13(7) $Å^3$
Z	4
Density (calculated)	1.256 Mg/m^3
Absorption coefficient	0.075 mm^{-1}
F(000)	592
Crystal size	0.15x0.10x0.10mm^3
Theta range for data collection	1.77 to 33.26 °.
Index ranges	-17 <=h<=16 , -8 <=k<=8 , -31 <=l<=31
Reflections collected	12256
Independent reflections	5049 [R(int) = 0.0175]
Completeness to theta =33.26 °	0.896 %
Absorption correction	Empirical
Max. and min. transmission	0.9925 and 0.9888
Refinement method	Full-matrix least-squares on F^2
Data / restraints / parameters	5049 / 0 / 192
Goodness-of-fit on F^2	0.966
Final R indices [I>2sigma(I)]	R1 = 0.0440 , wR2 = 0.1165

R indices (all data)	R1 = 0.0521 , wR2 = 0.1235
Largest diff. peak and hole	0.535and-0.191e.Å^{-3}

Table 6. Bond lengths [Å] and angles [°] for macrocycle 41.

Bond lengths:			
		C2-C3-C4	119.75(8)
		C5-C4-C3	119.92(8)
C1-O1	1.3813(10)	C4-C5-C6	121.67(8)
C1-C2	1.3954(11)	C1-C6-C5	117.33(7)
C1-C6	1.3984(12)	C1-C6-C7	123.85(7)
C2-C3	1.3881(13)	C5-C6-C7	118.81(7)
C3-C4	1.3909(13)	C6-C7-C8	116.98(7)
C4-C5	1.3880(12)	C7-C8-C11	117.55(7)
C5-C6	1.3993(12)	C7-C8-C9	117.78(7)
C6-C7	1.5156(11)	C11-C8-C9	85.58(6)
C7-C8	1.5302(12)	C10-C9-C19	115.51(7)
C8-C11	1.5304(11)	C10-C9-C20	113.90(8)
C8-C9	1.5896(12)	C19-C9-C20	109.75(7)
C9-C10	1.5168(12)	C10-C9-C8	85.20(6)
C9-C19	1.5196(12)	C19-C9-C8	118.24(7)
C9-C20	1.5272(13)	C20-C9-C8	112.52(7)
C10-C11	1.3450(12)	C11-C10-C9	95.41(7)
C11-C12	1.4720(11)	C10-C11-C12	130.90(8)
C12-C13	1.4049(12)	C10-C11-C8	93.80(7)
C12-C17	1.4094(12)	C12-C11-C8	135.28(7)
C13-C14	1.3895(12)	C13-C12-C17	118.22(7)
C14-C15	1.3855(15)	C13-C12-C11	117.41(8)
C15-C16	1.3896(14)	C17-C12-C11	124.35(7)
C16-C17	1.3955(11)	C14-C13-C12	121.48(9)
C17-C18	1.5048(12)	C15-C14-C13	119.99(9)
C18-O1	1.4396(10)	C14-C15-C16	119.31(8)
		C15-C16-C17	121.53(9)
Angles:		C16-C17-C12	119.46(8)
		C16-C17-C18	117.38(8)
O1-C1-C2	120.64(8)	C12-C17-C18	123.12(7)
O1-C1-C6	117.75(7)	O1-C18-C17	114.66(7)
C2-C1-C6	121.58(8)	C1-O1-C18	116.22(6)
C3-C2-C1	119.75(8)		

Table 7. Torsion angles [°] for macrocycle 41.

O1-C1-C2-C3	-176.90(8)
C6-C1-C2-C3	0.73(13)
C1-C2-C3-C4	-0.56(13)
C2-C3-C4-C5	0.19(13)
C3-C4-C5-C6	0.02(13)
O1-C1-C6-C5	177.18(7)
C2-C1-C6-C5	-0.51(12)
O1-C1-C6-C7	-1.69(12)
C2-C1-C6-C7	-179.38(8)
C4-C5-C6-C1	0.13(12)
C4-C5-C6-C7	179.06(8)
C1-C6-C7-C8	-31.73(12)
C5-C6-C7-C8	149.41(8)
C6-C7-C8-C11	-55.00(10)
C6-C7-C8-C9	-155.17(7)
C7-C8-C9-C10	119.39(8)
C11-C8-C9-C10	0.47(6)
C7-C8-C9-C19	2.94(11)
C11-C8-C9-C19	-115.99(8)
C7-C8-C9-C20	-126.70(8)
C11-C8-C9-C20	114.38(8)
C19-C9-C10-C11	118.55(8)
C20-C9-C10-C11	-113.06(8)
C8-C9-C10-C11	-0.53(7)
C9-C10-C11-C12	-177.98(9)
C9-C10-C11-C8	0.55(7)
C7-C8-C11-C10	-119.67(8)
C9-C8-C11-C10	-0.52(7)
C7-C8-C11-C12	58.75(13)
C9-C8-C11-C12	177.90(10)
C10-C11-C12-C13	34.39(14)
C8-C11-C12-C13	-143.52(10)
C10-C11-C12-C17	-143.94(10)
C8-C11-C12-C17	38.15(15)
C17-C12-C13-C14	0.74(13)
C11-C12-C13-C14	-177.69(8)
C12-C13-C14-C15	0.21(15)
C13-C14-C15-C16	-0.79(15)
C14-C15-C16-C17	0.41(15)
C15-C16-C17-C12	0.55(14)
C15-C16-C17-C18	178.10(9)

C13-C12-C17-C16 -1.10(13)	C16-C17-C18-O1 127.77(8)
C11-C12-C17-C16 177.21(8)	C12-C17-C18-O1 -54.79(11)
C13-C12-C17-C18 -178.50(8)	C2-C1-O1-C18 -63.00(10)
C11-C12-C17-C18 -0.19(13)	C6-C1-O1-C18 119.29(8)
C17-C18-O1-C1 -38.94(10)	

DFT Calculations Data

Trans,trans-(3,3-Dimethyl-2-(3-methyl-5-(o-tolyloxy)pentyl)cyclobutyl)methanol (64$_{TransTrans}$)

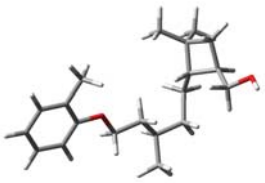

G = – 930.687472 Hartree/particle

Row	Symbol	X	Y	Z
1	C	5.9416150	0.6071870	-0.1547130
2	C	4.5727570	0.8758550	-0.1717520
3	C	3.6643130	-0.1471520	0.0955000
4	C	4.1128920	-1.4509810	0.3799600
5	C	5.4829410	-1.6861130	0.3877890
6	C	6.4036330	-0.6710850	0.1245870
7	H	6.6439640	1.4128400	-0.3632400
8	H	4.2274100	1.8822250	-0.3942360
9	H	5.8343330	-2.6951300	0.6076620
10	H	7.4710340	-0.8832900	0.1382310
11	C	3.1200620	-2.5348160	0.6656340
12	H	2.5092420	-2.2978200	1.5477110
13	H	2.4162310	-2.6687350	-0.1671970
14	H	3.6249890	-3.4909510	0.8458780
15	O	2.3158340	0.0158180	0.1032800
16	C	1.7866390	1.3018820	-0.1680750
17	H	2.0992010	1.6345360	-1.1745770
18	H	2.1860400	2.0273530	0.5596760
19	C	0.2806250	1.1972000	-0.0836410
20	H	-0.0193340	0.3160700	-0.6714120
21	H	-0.0093860	0.9941530	0.9624780
22	C	-0.4513260	2.4394120	-0.5876810
23	C	-1.9718350	2.3017400	-0.4742220
24	H	-2.4129040	3.2373470	-0.8505300
25	H	-2.2429720	2.2577870	0.5968180
26	C	-2.5870410	1.1099920	-1.2159640
27	H	-3.5635060	1.4023770	-1.6322650
28	H	-1.9575280	0.8606070	-2.0903140
29	C	-2.7792250	-0.1337390	-0.3681140
30	C	-3.9592470	-0.2455190	0.6190680
31	C	-3.2377850	-1.4660750	-1.0222720
32	H	-1.8566600	-0.3521140	0.1970190
33	C	-4.0369290	-1.7457320	0.2742990
34	H	-5.0308630	-2.2010320	0.1686480
35	H	-3.4506550	-2.3404700	0.9923430
36	C	-4.1671340	-1.2716010	-2.2112290
37	H	-3.6289040	-0.8764700	-3.0852740
38	H	-4.6104500	-2.2349270	-2.5030320
39	H	-4.9951530	-0.5844630	-1.9870070
40	C	-2.1163790	-2.4215230	-1.3781400
41	H	-1.4884850	-1.9996860	-2.1792850
42	H	-1.4667500	-2.6143810	-0.5118390
43	H	-2.5024270	-3.3878700	-1.7348190

44	H	-4.8436170	0.2943180	0.2434850
45	C	-3.7182950	0.1199900	2.0588650
46	H	-3.5602190	1.2101430	2.1605430
47	H	-2.7884330	-0.3748680	2.4027320
48	O	-4.8339310	-0.3059370	2.8133970
49	H	-4.6725380	-0.0850650	3.7402670
50	C	0.0070930	3.6957720	0.1445890
51	H	-0.5867950	4.5675670	-0.1609990
52	H	-0.1150900	3.5741880	1.2321630
53	H	1.0611550	3.9336200	-0.0486930
54	H	-0.2103950	2.5549340	-1.6612870

Cis,trans-(3,3-Dimethyl-2-(3-methyl-5-(o-tolyloxy)pentyl)cyclobutyl)methanol (64$_{CisTrans}$)

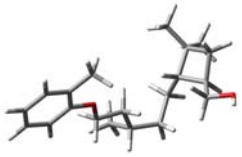

G = – 930.686361 Hartree/particle

Row	Symbol	X	Y	Z
1	C	-5.9634430	0.7172540	0.0127670
2	C	-4.5911410	0.9265960	-0.1271780
3	C	-3.7113850	-0.1470050	0.0041430
4	C	-4.1928270	-1.4417700	0.2755830
5	C	-5.5654300	-1.6167270	0.4096470
6	C	-6.4573010	-0.5514210	0.2808260
7	H	-6.6430570	1.5617010	-0.0912660
8	H	-4.2201410	1.9263700	-0.3384050
9	H	-5.9425220	-2.6181990	0.6211400
10	H	-7.5274550	-0.7166190	0.3908050
11	C	-3.2329560	-2.5827730	0.4111200
12	H	-2.6684670	-2.7480220	-0.5169670
13	H	-2.4873710	-2.3918240	1.1947490
14	H	-3.7619340	-3.5106130	0.6580370
15	O	-2.3621280	-0.0452140	-0.1156920
16	C	-1.7960590	1.2306440	-0.3580210
17	H	-2.1003900	1.9275600	0.4402310
18	H	-2.1711990	1.6358150	-1.3150520
19	C	-0.2940920	1.0604750	-0.4007520
20	H	0.0477650	0.7320230	0.5944000
21	H	-0.0638640	0.2413990	-1.1014110
22	C	0.4468640	2.3268170	-0.8261920
23	C	1.9381480	2.0836520	-1.0940340
24	H	2.3529900	3.0334680	-1.4660100
25	H	2.0406250	1.3701260	-1.9290820
26	C	2.7920240	1.5978880	0.0831360
27	H	3.8152340	1.9826490	-0.0487030
28	H	2.4313010	2.0447300	1.0266820
29	C	2.8685020	0.0908020	0.2459040
30	C	3.6533240	-0.7716960	-0.7664960
31	C	3.7288470	-0.5201270	1.3904800
32	H	1.8548400	-0.3356810	0.3361920
33	C	4.1097090	-1.6553190	0.4103820
34	H	5.1519790	-2.0014180	0.4213640
35	H	3.4482400	-2.5290540	0.5181920
36	C	4.9429560	0.3175780	1.7624010
37	H	4.6539030	1.2402110	2.2868670
38	H	5.5993740	-0.2550970	2.4338910
39	H	5.5410480	0.6020380	0.8852250
40	C	2.9558660	-0.9075390	2.6354100
41	H	2.5657860	-0.0121100	3.1448880

42	H	2.0996890	-1.5518550	2.3887600
43	H	3.5897870	-1.4478750	3.3539070
44	C	0.2314010	3.4701960	0.1627240
45	H	0.4864010	3.1717500	1.1900000
46	H	0.8542490	4.3369220	-0.0975460
47	H	-0.8122130	3.8105930	0.1732740
48	H	0.0158710	2.6446240	-1.7931260
49	H	4.4963030	-0.2096160	-1.2007180
50	C	2.8850240	-1.4586180	-1.8640580
51	H	2.4922370	-0.7222530	-2.5905980
52	H	2.0094800	-1.9703350	-1.4173860
53	O	3.7507080	-2.3819290	-2.4911790
54	H	3.2546840	-2.8377020	-3.1841190

Trans,cis-(3,3-Dimethyl-2-(3-methyl-5-(o-tolyloxy)pentyl)cyclobutyl)methanol (64$_{TransCis}$)

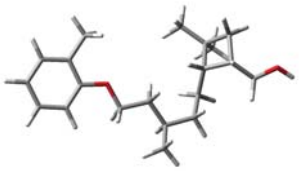

G = – 930.683260 Hartree/particle

Row	Symbol	X	Y	Z
1	C	-6.1019220	0.7342390	0.3196400
2	C	-4.7259290	0.9580910	0.2618320
3	C	-3.8717320	-0.0812700	-0.1027870
4	C	-4.3821220	-1.3562440	-0.4125460
5	C	-5.7575470	-1.5467310	-0.3448560
6	C	-6.6244910	-0.5152000	0.0177560
7	H	-6.7609520	1.5528380	0.6050240
8	H	-4.3328530	1.9425730	0.5026000
9	H	-6.1569000	-2.5333140	-0.5838320
10	H	-7.6974970	-0.6917790	0.0624510
11	C	-3.4468080	-2.4586640	-0.8016610
12	H	-2.8519620	-2.1877480	-1.6846200
13	H	-2.7255840	-2.6780540	-0.0022490
14	H	-3.9985680	-3.3785510	-1.0274670
15	O	-2.5212410	0.0365010	-0.1874360
16	C	-1.9294160	1.2896780	0.1072480
17	H	-2.1688660	1.5859020	1.1447000
18	H	-2.3439180	2.0607400	-0.5627760
19	C	-0.4354040	1.1375820	-0.0717800
20	H	-0.1370700	0.2154520	0.4501560
21	H	-0.2122480	0.9820790	-1.1411590
22	C	0.3683640	2.3248900	0.4546960
23	C	1.8742480	2.1141010	0.2803980
24	H	2.3824730	3.0146340	0.6580990
25	H	2.1003540	2.0780440	-0.8014350
26	C	2.4393280	0.8637740	0.9695310
27	H	3.3634430	1.1200700	1.5088900
28	H	1.7367020	0.5240300	1.7513400
29	C	2.6992030	-0.2877840	0.0139310
30	C	3.9321560	-0.2850830	-0.9262310
31	C	3.1122540	-1.6875740	0.5532860
32	H	1.8051310	-0.4282830	-0.6153570
33	C	4.1089590	-1.7917300	-0.6304800
34	H	3.7066390	-0.0442910	-1.9758890
35	H	5.1317090	-2.1099720	-0.3812290
36	H	3.7344910	-2.4325750	-1.4398950
37	C	-0.0550490	3.6290860	-0.2112540
38	H	0.5812420	4.4623220	0.1158470
39	H	0.0362050	3.5500050	-1.3056530
40	H	-1.0939320	3.8997690	0.0183540

41	H	0.1698500	2.4071690	1.5400170
42	C	3.8044890	-1.6850980	1.9086290
43	H	3.1023110	-1.4364020	2.7180020
44	H	4.2122530	-2.6847510	2.1194920
45	H	4.6414070	-0.9764880	1.9622690
46	C	1.9769300	-2.6952510	0.5661430
47	H	1.2082740	-2.4023180	1.2994290
48	H	1.4909650	-2.7630180	-0.4178980
49	H	2.3296040	-3.7009730	0.8388740
50	C	5.1022990	0.5745940	-0.5120840
51	H	4.8116810	1.6420170	-0.5297990
52	H	5.4121550	0.3434220	0.5235710
53	O	6.1552450	0.3165730	-1.4184570
54	H	6.9245630	0.8304220	-1.1391760

Cis,cis-(3,3-Dimethyl-2-(3-methyl-5-(o-tolyloxy)pentyl)cyclobutyl)methanol (64$_{CisCis}$)

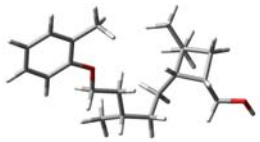

G = – 930.68221 Hartree/particle

Row	Symbol	X	Y	Z
1	C	-6.1341260	0.7899280	0.2173280
2	C	-4.7564070	0.9834280	0.1099270
3	C	-3.9291760	-0.0961650	-0.1958370
4	C	-4.4681890	-1.3803330	-0.3991600
5	C	-5.8446430	-1.5396640	-0.2849560
6	C	-6.6846900	-0.4684990	0.0212330
7	H	-6.7720210	1.6391650	0.4577450
8	H	-4.3391440	1.9757890	0.2629990
9	H	-6.2664540	-2.5338040	-0.4391170
10	H	-7.7589390	-0.6215370	0.1057730
11	C	-3.5628660	-2.5263070	-0.7287340
12	H	-3.0371070	-2.3642270	-1.6798380
13	H	-2.7839020	-2.6568410	0.0346060
14	H	-4.1288980	-3.4617460	-0.8072400
15	O	-2.5795490	-0.0087890	-0.3227230
16	C	-1.9556680	1.2406050	-0.0844200
17	H	-2.2228070	1.5989880	0.9232640
18	H	-2.3175900	1.9900610	-0.8113330
19	C	-0.4643480	1.0342970	-0.2228120
20	H	-0.1310400	0.3472640	0.5729260
21	H	-0.2806480	0.5198830	-1.1795480
22	C	0.3409130	2.3320370	-0.1781750
23	C	1.8352590	2.0821950	-0.4175040
24	H	2.3392420	3.0609950	-0.4168870
25	H	1.9674410	1.6770330	-1.4353870
26	C	2.5187140	1.1408610	0.5876310
27	H	3.4848120	1.5640240	0.9008500
28	H	1.9231490	1.0762940	1.5145770
29	C	2.7207630	-0.2645870	0.0494160
30	C	3.8289540	-0.5717970	-0.9917250
31	C	3.2759170	-1.3886670	0.9719690
32	H	1.7641360	-0.6201740	-0.3677180
33	C	4.1293040	-1.8798900	-0.2260180
34	H	3.4614810	-0.7146430	-2.0188530
35	H	5.1911780	-2.0783040	-0.0196350
36	H	3.7002910	-2.7665170	-0.7118820
37	C	4.1236290	-0.9048530	2.1390090
38	H	3.5084850	-0.4070740	2.9030120
39	H	4.6220380	-1.7595380	2.6196850

40	H	4.9079290	-0.2012900	1.8307390
41	C	2.2123450	-2.3469620	1.4752920
42	H	1.5157960	-1.8287550	2.1539350
43	H	1.6234810	-2.7610400	0.6442160
44	H	2.6536390	-3.1883500	2.0299960
45	C	4.9870100	0.3951050	-1.0638920
46	H	4.6331680	1.3851680	-1.4086780
47	H	5.4383480	0.5453600	-0.0660240
48	O	5.9333800	-0.1475340	-1.9627220
49	H	6.6996350	0.4409040	-1.9824390
50	C	0.1029060	3.1134980	1.1113570
51	H	0.2922390	2.4959730	2.0015730
52	H	0.7652440	3.9882390	1.1648700
53	H	-0.9290360	3.4810180	1.1830750
54	H	-0.0083970	2.9628760	-1.0152880

Trans,trans-8,11,11-Trimethyl-7,8,9,10,10a,11,12,12a,13,15-decahydro-6H-benzo[b]cyclobuta[g][1,5]dioxacyclotridecine (65$_{TransTrans}$)

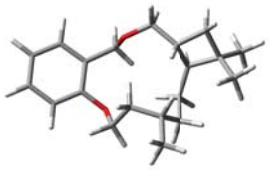

G = – 929.486054 Hartree/particle

Row	Symbol	X	Y	Z
1	C	-4.1041020	0.8094150	0.4724660
2	C	-2.8228470	0.2676100	0.5951100
3	C	-2.5955310	-1.0803900	0.2895180
4	C	-3.6720340	-1.8553560	-0.1473450
5	C	-4.9461860	-1.3193920	-0.2834560
6	C	-5.1592690	0.0212150	0.0307280
7	H	-4.2656750	1.8519190	0.7437460
8	H	-3.4897300	-2.9035260	-0.3886040
9	H	-5.7705960	-1.9424890	-0.6246330
10	H	-6.1543440	0.4543900	-0.0577530
11	C	-1.2318800	-1.6950400	0.3646880
12	H	-0.6005290	-1.1567730	1.0860140
13	H	-1.3092260	-2.7434190	0.7064990
14	C	0.6475760	-2.1976600	-0.9972350
15	H	0.7671270	-3.0101690	-0.2539510
16	H	0.7472660	-2.6570030	-1.9931510
17	C	1.7562370	-1.1825050	-0.8180310
18	C	2.1305780	-0.6743330	0.5975400
19	H	1.8906690	-1.5087250	1.2849540
20	C	3.6358620	-0.8563830	0.2396490
21	O	-0.6627160	-1.6700370	-0.9334300
22	C	3.1778910	-1.7721070	-0.9199440
23	H	3.7053000	-1.6694320	-1.8779580
24	H	3.1870510	-2.8342090	-0.6271190
25	C	4.4792300	-1.5008690	1.3233400
26	H	5.4916680	-1.7317940	0.9598940
27	H	4.5843810	-0.8276490	2.1882360
28	H	4.0266170	-2.4374980	1.6791630
29	C	4.3408310	0.3828410	-0.2908000
30	H	4.5653770	1.0964150	0.5151500
31	H	5.2981190	0.0934690	-0.7498290
32	H	3.7538250	0.9087830	-1.0570580
33	C	1.5767290	0.5785610	1.2709120
34	C	1.6747130	1.9660090	0.6291810
35	H	1.2472910	2.6720760	1.3628280
36	H	2.7272610	2.2699560	0.5356930
37	C	1.0030040	2.2283000	-0.7227070

38	H	1.5881310	1.7107840	-1.5026450
39	C	1.0735450	3.7212010	-1.0300940
40	H	0.6997770	3.9398130	-2.0395380
41	H	0.4665940	4.3016600	-0.3181660
42	H	2.1038100	4.0967860	-0.9609540
43	C	-0.4383020	1.7190190	-0.8574940
44	H	-0.8216570	2.0714240	-1.8276770
45	H	-0.4544500	0.6213160	-0.9155590
46	C	-1.4033970	2.1425130	0.2514000
47	O	-1.7979930	1.0384820	1.0754670
48	H	1.6132770	-0.3609700	-1.5343940
49	H	-2.3036140	2.6192690	-0.1628220
50	H	-0.9482590	2.8648980	0.9414920
51	H	2.0852100	0.6504080	2.2489400
52	H	0.5191230	0.3968450	1.5183520

Cis,trans-8,11,11-Trimethyl-7,8,9,10,10a,11,12,12a,13,15-decahydro-6H-benzo[b]cyclobuta[g][1,5]dioxacyclotridecine (65$_{CisTrans}$)

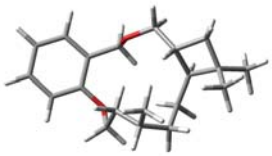

G = – 929.482220 Hartree/particle

Row	Symbol	X	Y	Z
1	C	4.1376540	0.8344240	-0.4352710
2	C	2.8970660	0.2511890	-0.6976260
3	C	2.6400630	-1.0707250	-0.3153550
4	C	3.6495080	-1.7844440	0.3334580
5	C	4.8848260	-1.2094310	0.6039130
6	C	5.1260890	0.1072260	0.2163730
7	H	4.3240480	1.8565330	-0.7619990
8	H	3.4452110	-2.8127180	0.6352120
9	H	5.6582240	-1.7834800	1.1105730
10	H	6.0932630	0.5678560	0.4114130
11	C	1.2991300	-1.7090400	-0.5157720
12	H	0.7356070	-1.2024290	-1.3153660
13	H	1.4259640	-2.7655640	-0.8142090
14	C	-0.6899590	-2.2245780	0.6900560
15	H	-0.7923910	-2.9004930	-0.1796540
16	H	-0.7849040	-2.8505980	1.5925500
17	C	-1.8067240	-1.2069640	0.6805760
18	C	-2.2003630	-0.4905810	-0.6324110
19	H	-2.0134230	-1.2370930	-1.4293810
20	C	-3.6994820	-0.6836390	-0.2537920
21	O	0.6030510	-1.6494320	0.7170680
22	C	-3.2305950	-1.7968120	0.7131200
23	H	-3.7358070	-1.8660340	1.6860150
24	H	-3.2562840	-2.7870130	0.2307890
25	C	-4.6083150	-1.1026460	-1.3928450
26	H	-5.6104950	-1.3709500	-1.0267680
27	H	-4.7313230	-0.2845820	-2.1192910
28	H	-4.2009890	-1.9714040	-1.9293860
29	C	-4.3344040	0.4618720	0.5204050
30	H	-4.5603000	1.3166640	-0.1329430
31	H	-5.2846460	0.1248950	0.9613180
32	H	-3.6968520	0.8174640	1.3418260
33	C	-1.6306730	0.8133930	-1.1888840
34	C	-1.6740500	2.1724790	-0.4644930
35	H	-1.4959270	2.9118700	-1.2612690
36	H	-2.6919050	2.3904980	-0.1141870
37	C	-0.6852140	2.4947310	0.6813130

38	C	0.6534630	1.7707230	0.5520470
39	H	1.2752790	2.0063860	1.4296630
40	H	0.4825020	0.6842830	0.5938160
41	C	1.4167040	2.1054380	-0.7289160
42	O	1.9360140	0.9454340	-1.3819720
43	H	-1.6545960	-0.5014000	1.5092830
44	H	2.2306410	2.8217490	-0.5353800
45	H	0.7606960	2.5649270	-1.4789280
46	H	-2.1710730	0.9723160	-2.1390610
47	H	-0.5911520	0.6161340	-1.4983250
48	C	-1.2679390	2.2783060	2.0723160
49	H	-1.4376720	1.2143540	2.2865450
50	H	-0.5834620	2.6554140	2.8448040
51	H	-2.2276110	2.8001090	2.1908810
52	H	-0.4838550	3.5787570	0.6014210

Cis,cis-8,11,11-Trimethyl-7,8,9,10,10a,11,12,12a,13,15-decahydro-6H-benzo[b]cyclobuta[g][1,5]dioxacyclotridecine (65_{CisCis})

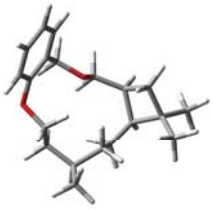

G = –929.481564 Hartree/particle

Row	Symbol	X	Y	Z
1	C	4.3009290	0.3550260	0.6164410
2	C	3.1869230	0.1512130	-0.1923680
3	C	2.6343220	-1.1256020	-0.3501180
4	C	3.2304690	-2.1913630	0.3247770
5	C	4.3410610	-1.9980140	1.1404920
6	C	4.8797270	-0.7215710	1.2812820
7	H	4.7028450	1.3631160	0.7092720
8	H	2.8133880	-3.1911510	0.1978620
9	H	4.7927170	-2.8431480	1.6565710
10	H	5.7532800	-0.5617610	1.9111030
11	C	1.4713410	-1.3504890	-1.2655840
12	H	1.5446270	-0.6879890	-2.1462270
13	H	1.5044880	-2.3922890	-1.6353150
14	C	-0.8193430	-1.5462270	-1.4625760
15	H	-0.8413810	-0.9113200	-2.3722210
16	H	-0.5930420	-2.5715260	-1.8130780
17	C	-2.1820480	-1.5551000	-0.8024970
18	H	-2.7544090	-2.3166430	-1.3529920
19	C	-3.1064330	-0.3068390	-0.6814980
20	H	-3.9119320	-0.3400120	-1.4340140
21	C	-3.5965900	-0.8945020	0.6894380
22	O	0.2317610	-1.1334230	-0.6138520
23	C	-2.3451070	-1.8052120	0.7037820
24	H	-1.5243020	-1.3482470	1.2727530
25	H	-2.4770250	-2.8430740	1.0423910
26	C	-4.8718550	-1.7025830	0.4687960
27	H	-5.1061570	-2.3102290	1.3551140
28	H	-5.7259790	-1.0337640	0.2849470
29	H	-4.7942520	-2.3832450	-0.3906140
30	C	-3.8020190	0.0122340	1.8911810
31	H	-4.4711990	0.8522240	1.6496810
32	H	-4.2686390	-0.5496590	2.7139620
33	H	-2.8618360	0.4242330	2.2737850
34	C	-2.4945050	1.0854900	-0.8127050
35	H	-1.9757790	1.1063390	-1.7887700

36	H	-3.3164020	1.8136280	-0.9194540
37	C	-1.5427780	1.6216270	0.2535160
38	H	-2.1218830	1.9374680	1.1320310
39	H	-0.8646120	0.8251610	0.5966070
40	C	-0.7319970	2.8269380	-0.2468280
41	C	0.5311090	2.3911550	-0.9970900
42	H	0.2839110	1.5991370	-1.7223470
43	H	0.9427270	3.2336010	-1.5739320
44	C	1.5965760	1.8467580	-0.0735860
45	H	1.1631810	1.1081810	0.6180410
46	H	2.0581120	2.6416860	0.5356510
47	O	2.6151520	1.2086180	-0.8463940
48	H	-1.3653850	3.3719540	-0.9688380
49	C	-0.4086660	3.7888190	0.8927570
50	H	0.2382460	4.6128770	0.5596850
51	H	-1.3279440	4.2264140	1.3041210
52	H	0.1026180	3.2759230	1.7205230

Trans,cis-8,11,11-Trimethyl-7,8,9,10,10a,11,12,12a,13,15-decahydro-6H-benzo[b]cyclobuta[g][1,5]dioxacyclotridecine (65$_{TransCis}$)

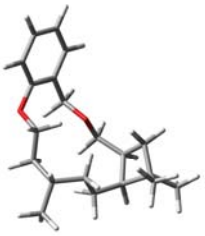

G = – 929.480212 Hartree/particle

Row	Symbol	X	Y	Z
1	C	4.3486180	0.4719870	0.7750360
2	C	3.2345020	0.3590050	-0.0505400
3	C	2.7684670	-0.8953950	-0.4644420
4	C	3.4509710	-2.0309720	-0.0273590
5	C	4.5637920	-1.9294840	0.8020280
6	C	5.0155960	-0.6736570	1.1987820
7	H	4.6794960	1.4661780	1.0718510
8	H	3.1013020	-3.0107020	-0.3551700
9	H	5.0836270	-2.8278510	1.1295090
10	H	5.8894760	-0.5845880	1.8420240
11	C	1.6021430	-1.0115350	-1.3962890
12	H	1.6125240	-0.1822370	-2.1263220
13	H	1.6934780	-1.9538430	-1.9678090
14	C	-0.6759970	-1.3362260	-1.5950450
15	H	-0.7602410	-0.5510420	-2.3746470
16	H	-0.3957290	-2.2643100	-2.1291360
17	C	-2.0187790	-1.5487810	-0.9265740
18	H	-2.5474450	-2.2609040	-1.5778960
19	C	-3.0296300	-0.4048560	-0.6116060
20	H	-3.8466020	-0.3922870	-1.3519790
21	C	-3.4449350	-1.2242910	0.6626100
22	O	0.3674160	-1.0145410	-0.6999580
23	C	-2.1302490	-2.0308390	0.5272300
24	H	-1.3307160	-1.6061970	1.1491100
25	H	-2.1813400	-3.1144650	0.7073950
26	C	-4.6608120	-2.0867330	0.3369260
27	H	-4.8233900	-2.8418790	1.1199370
28	H	-5.5683030	-1.4679060	0.2727340
29	H	-4.5530960	-2.6165480	-0.6197850
30	C	-3.6915510	-0.5279400	1.9901510
31	H	-4.4456810	0.2676480	1.8898220
32	H	-4.0746650	-1.2491650	2.7274200

33	H	-2.7822790	-0.0852560	2.4105840
34	C	-2.5287650	1.0389430	-0.5476700
35	H	-1.9913900	1.2182810	-1.4964790
36	H	-3.4090080	1.6996960	-0.5964100
37	C	-1.6595440	1.4980270	0.6228970
38	H	-2.3061980	1.6966380	1.4887330
39	H	-0.9764390	0.6912000	0.9277150
40	C	-0.8502050	2.7769310	0.3507600
41	H	-0.5081170	3.1466720	1.3347130
42	C	-1.7000220	3.8781190	-0.2712750
43	H	-1.1473700	4.8264990	-0.3021040
44	H	-1.9858460	3.6314440	-1.3035510
45	H	-2.6243810	4.0440360	0.2999560
46	C	0.4050070	2.5065210	-0.4799120
47	H	0.1670360	1.8708080	-1.3496050
48	H	0.8120170	3.4488380	-0.8789890
49	C	1.4606390	1.8153860	0.3473360
50	H	1.0547180	0.8890950	0.7797680
51	H	1.7947990	2.4590410	1.1803890
52	O	2.5843710	1.4880210	-0.4700480

2. Gold-Catalyzed Intermolecular [2+2+2] Cycloaddition of Alkynes and Oxoalkenes[1]

All the reactants, ligands and the following reagents were purchased from commercial sources and used without further purification: ethynylbenzene, 1-ethynyl-4-fluorobenzene, 1-ethynyl-4-chlorobenzene, 1-ethynyl-4-bromobenzene, 1-ethynyl-3-methylbenzene, 1-ethynyl-3-fluorobenzene, 1-ethynyl-3-chlorobenzene, 3-ethynylphenol, 1-ethynyl-3-methoxybenzene, 1-ethynyl-2-methylbenzene, 2-ethynylnaphthalene, 3-ethynylthiophene, 1-ethynyl-4-nitrobenzene, 4-ethynylaniline, ethynylcyclohexane, ethynylcyclopropane, prop-2-yn-1-ylbenzene, 1-(4-ethynylphenyl)ethanone, 1-ethynyl-3,5-bis(trifluoromethyl)benzene, 1-ethynyl-4-methoxybenzene, 1-ethynyl-4-methylbenzene, 5-methylhex-5-en-2-one, hex-5-en-2-one **53**, (5*E*,9*E*)-6,10,14-trimethylpentadeca-5,9,13-trien-2-one **57**, 2,6-dimethylhept-5-enal **59**, (*Z*)-dec-4-enal **60**, 3-(2-methylallyl)dihydrofuran-2,5-dione **61**, dimethyl 2-(2-phenylallyl)malonate **62**, 6-methylhept-5-en-2-one, ethyl 4-methylpent-4-enoate and 1-(2-(prop-1-en-2-yl)phenyl)ethanone **76**. Catalysts **G** and **H** were described in **Chapter 1**.[2] Gold complexes **A**, **B**, **E**, **K**, **L**, **M**, **N**, **O**, **94**$(AuCl)_2$, **98**(AuCl) and **101**$(AuCl)_2$ were synthesized according to the literature.[3,4]

Procedures for the Preparation of Starting Materials

5-Phenylhex-5-en-2-one

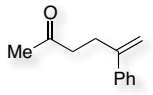

Dry 1-butyl-3-methylimidazolium tetrafluoroborate ($BmimBF_4$) by setting it under vacuum at 80 ºC for 24 h. Then, an oven-dried flask containing a stirring bar was charged with bromobenzene (1.57 g, 10.0 mmol) in $BmimBF_4$ (20 ml), diacetoxypalladium (56.0 mg, 0.25 mmol) and 1,3-bis(diphenylphosphino)propane (0.21 g, 0.50 mmol) at 25 ºC. After degassing the solution with N_2 three times, hex-5-en-2-one (1.28 ml, 11.0 mmol) and diisopropylamine (1.70 ml, 12.0 mmol) were injected sequentially. The reaction mixture was stirred at 115 ºC for 36 h. The flask was cooled down to 25 ºC and the crude was extracted with diethyl ether washing with water and brine. The organic layers were dried with $MgSO_4$, concentrated and the residue was purified with silica gel column chromatography using cyclohexane:ethyl acetate (30:1) as eluent. 5-Phenylhex-5-en-2-one was obtained in 23% isolated yield (0.41 g, 2.32 mmol). ^{1}H NMR (500 MHz, $CDCl_3$, ppm) δ 7.40 – 7.38 (m, 2H), 7.35 – 7.31 (m, 2H), 7.30 – 7.26 (m, 1H), 5.29 (s, 1H), 5.07 (q, *J* = 1.29 Hz, 1H), 2.81 – 2.78 (m, 2H), 2.60 – 2.57 (m, 2H), 2.12 (s, 3H). ^{13}C NMR (126 MHz, $CDCl_3$, ppm) δ 208.27 (s), 147.30 (s), 140.74 (s), 128.55 (s), 127.75 (s), 126.23 (s), 112.90 (s), 42.56 (s), 30.19 (s), 29.42 (s).

---

[1] C. Obradors and A. M. Echavarren, *Chem. –Eur. J.* **2013**, *19*, 3547–3551.
[2] C. Obradors, D. Leboeuf, J. Aydin and A. M. Echavarren, *Org. Lett.* **2013**, *15*, 1576–1579.
[3] *(a)* E. Herrero-Gómez, C. Nieto-Oberhuber, S. López, B. Benet-Buchholz and A. M. Echavarren, *Angew. Chem. Int. Ed.* **2006**, *45*, 5455–5459; *(b)* D. V. Partyka, T. J. Robilotto, M. Zelles, A. D. Hunter and T. G. Gray, *Organometallics* **2008**, *27*, 28–32; *(c)* C. H. M. Amijs, V. López-Carrillo, M. Raducan, P. Pérez-Galán, C Ferrer and A. M. Echavarren, *J. Org. Chem.* **2008**, *73*, 7721–7730; *(d)* Y. Wang, K. Ji, S. Lan and L. Zhang, *Angew. Chem. Int. Ed.* **2012**, *51*, 1915–1918; *(e)* A. S. K. Hashmi, M. Hamzic, F. Rominger and J. W. Bats, *Chem. –Eur. J.* **2009**, *15*, 13318–13322; *(f)* I. Alonso, B. Trillo, F. Lopez, S. Montserrat, G. Ujaque, L. Castedo, A. Lledós and J. L. Mascareñas, *J. Am. Chem. Soc.* **2009**, *131*, 13020–13030.
[4] R. J. Felix, D. Weber, O. Gutierrez, D. J. Tantillo and M. R. Gagné, *Nat. Chem.* **2012**, *4*, 405–409.

Ethyl 2-benzoyl-4-methylpent-4-enoate

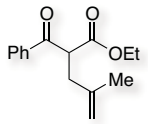

To a suspension of NaH 60% (125 mg, 3.12 mmol) in tetrehydrofuran (8 ml) at 0 ºC, ethyl 3-oxo-3-phenylpropanoate (0.45 ml, 2.60 mmol) was added slowly. The solution was stirred for 10 min and then, 3-bromo-2-methylprop-1-ene (0.26 ml, 2.60 mmol) was added. The reaction mixture was stirred at 25 ºC for 16 h and quenched with water (2 ml). After extraction with ethyl acetate, the organic layers were washed with brine and dried with $MgSO_4$. The residue was purified by silica gel column chromatography with cyclohexane:ethyl acetate (25:1) to obtain ethyl 2-benzoyl-4-methylpent-4-enoate in 49% isolated yield (0.31 g, 1.27 mmol). ^{1}H NMR (400 MHz, $CDCl_3$, ppm) δ 8.03 – 8.00 (m, 2H), 7.61 – 7.57 (m, 1H), 7.50 –7.46 (m, 2H), 4.78 (broad s, 1H), 4.72 (broad s, 1H), 4.55 (dd, *J* = 8.14, 6.66 Hz, 1H), 4.14 (qd, *J* = 7.15, 0.87 Hz, 2H), 2.79 – 2.67 (m, 2H), 1.77 (s, 3H), 1.17 (t, *J* = 7.23 Hz, 3H). ^{13}C NMR (101 MHz, $CDCl_3$, ppm) δ 194.42 (s), 169.50 (s), 142.21 (s), 136.56 (s), 133.47 (s), 128.92 (s), 128.72 (s), 112.30 (s), 61.34 (s), 52.93 (s), 36.65 (s), 21.69 (s), 14.01 (s).

4-Methyl-1-phenylpent-4-en-1-one (54)

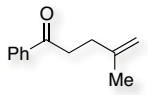

Ethyl 2-benzoyl-4-methylpent-4-enoate (100 mg, 0.41 mmol) was dissolved in a mixture 1:1 of water and THF (2 ml). LiOH (30 mg, 1.23 mmol) was added and the reaction mixture was stirred for 15 h at 50 ºC. After quenching with aqueous 0.1 M HCl (3 ml), the solution was extracted with diethyl ether. The organic layers were washed with brine, dried over $MgSO_4$ and concentrated. The residue was purified with silica gel column chromatography with hexane:ethyl acetate (30:1) to obtain 4-methyl-1-phenylpent-4-en-1-one **54** in 84% isolated yield (60 mg, 0.35 mmol). ^{1}H NMR (400 MHz, $CDCl_3$, ppm) δ 7.99 – 7.96 (m, 2H), 7.59 – 7.54 (m, 1H), 7.49 – 7.45 (m, 2H), 4.77 (broad s, 1H), 4.73 (broad s, 1H), 3.15 – 3.11 (m, 2H), 2.46 (t, *J* = 7.77 Hz, 2H), 1.79 (d, *J* = 0.49 Hz, 3H). ^{13}C NMR (101 MHz, $CDCl_3$, ppm) δ 199.71 (s), 144.70 (s), 136.97 (s), 132.98 (s), 128.59 (s), 128.03 (s), 110.19 (s), 36.85 (s), 31.90 (s), 22.76 (s).

4-Methylpent-4-enal (55)

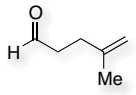

To an anhydrous solution of ethyl 4-methylpent-4-enoate (0.56 ml, 3.52 mmol) in CH_2Cl_2 at – 78 º C, diisobutylaluminium hydride 1 M in toluene (5.3 ml, 5.3 mmol) was added over 5 min. The reaction mixture was stirred for 40 min and then quenched with a solution 1:1 of water and methanol (20 ml). The solution was stirred for 3 h at 25 ºC and the resulting gel was filtered over a plug of Na_2SO_4/celite washing with CH_2Cl_2. The solvent was removed carefully (150 Torr, 25 ºC) and the residue was purified with a silica gel column chromatography eluting with pentane – pentane:diethyl ether (20:1) to obtain 4-methylpent-4-enal **55** in 97% isolated yield (0.33 g, 3.41 mmol). ^{1}H NMR (400 MHz, $CDCl_3$, ppm) δ 9.74 (t, *J* = 1.71 Hz, 1H), 4.76 (broad s, 1H), 4.68 (broad s, 1H), 2.57 – 2.53 (m, 2H), 2.33 (t, *J* = 7.41 Hz, 2H), 1.75 – 174 (m, 3H). ^{13}C NMR (101 MHz, $CDCl_3$, ppm) δ 202.57 (s), 158.84 (s), 110.76 (s), 42.34 (s), 30.37 (s), 22.86 (s).

Methyl 4-methyl-2-pivaloylpent-4-enoate

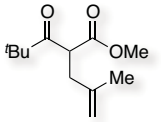

To a suspension of NaH 60% (152 mg, 3.79 mmol) in tetrehydrofuran (9.5 ml) at 0 ºC, methyl 3-oxo-3-phenylpropanoate (0.51 ml, 3.16 mmol) was added slowly. The solution was stirred for 10 min and then, 3-bromo-2-methylprop-1-ene (0.32 ml, 3.16 mmol) was added. The reaction mixture was stirred at 25 ºC for 15 h and quenched with water (2 ml). After extraction with ethyl acetate, the organic layers were washed with brine and dried with $MgSO_4$. The residue was purified by silica gel column chromatography with cyclohexane:ethyl acetate (50:1) to obtain methyl 4-methyl-2-pivaloylpent-4-enoate in 75% isolated yield (0.51 g, 2.39 mmol). ^{1}H NMR (500 MHz, $CDCl_3$, ppm) δ 4.77 (broad s, 1H), 4.71 (broad s, 1H), 4.13 (dd, *J* = 7.91, 6.17 Hz, 1H), 3.68 (s, 3H), 2.61 (dd, *J* = 15.12, 8.31 Hz, 1H), 2.42 (dd, *J* = 14.90, 6.36 Hz, 1H), 1.73 (s, 3H), 1.17 (s, 9H). ^{13}C NMR (126 MHz, $CDCl_3$, ppm) δ 209.26 (s), 169.93 (s), 142.17 (s), 112.74 (s), 52.48 (s), 51.26 (s), 45.57 (s), 37.61 (s), 26.31 (s), 22.65 (s).

2,2,6-Trimethylhept-6-en-3-one (56)

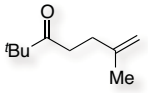

Methyl 4-methyl-2-pivaloylpent-4-enoate (204 mg, 0.96 mmol) was dissolved in a mixture 1:1 of water and THF (5 ml). LiOH (69 mg, 2.88 mmol) was added and the reaction mixture was stirred for 17 h at 50 ºC. After quenching with aqueous 0.1 M HCl (9 ml), the solution was extracted with diethyl ether. The organic layers were washed with brine, dried over $MgSO_4$ and concentrated. The residue was purified with silica gel column chromatography with hexane:ethyl acetate (30:1) to obtain 2,2,6-trimethylhept-6-en-3-one **56** in 16% isolated yield (23 mg, 0.15 mmol). ^{1}H NMR (400 MHz, $CDCl_3$, ppm) δ 4.72 (broad s, 1H), 4.66 (broad s, 1H), 2.65 – 2.61 (m, 2H), 2.25 (t, *J* = 7.73 Hz, 2H), 1.74 (s, 3H), 1.15 (s, 9H). ^{13}C NMR (126 MHz, $CDCl_3$, ppm) δ 215.40 (s), 145.22 (s), 110.01 (s), 44.32 (s), 34.96 (s), 31.76 (s), 26.62 (s), 22.89 (s).

(E)-Ethyl 2-benzoylhex-4-enoate

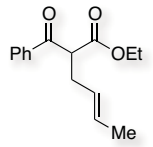

To a suspension of NaH 60% (125 mg, 3.12 mmol) in tetrehydrofuran (8 ml) at 0 ºC, ethyl 3-oxo-3-phenylpropanoate (0.45 ml, 2.60 mmol) was added slowly. The solution was stirred for 10 min and then, *(E)*-1-bromobut-2-ene (0.26 ml, 2.55 mmol) was added. The reaction mixture was stirred at 25 ºC for 19 h and quenched with water (2 ml). After extraction with ethyl acetate, the organic layers were washed with brine and dried with $MgSO_4$. The residue was purified by silica gel column chromatography with cyclohexane:ethyl acetate (30:1) to obtain *(E)*-ethyl 2-benzoylhex-4-enoate in 57% isolated yield (0.36 g, 1.47 mmol). ^{1}H NMR (400 MHz, $CDCl_3$, ppm) δ 8.00 – 7.97 (m, 2H), 7.60 – 7.56 (m, 1H), 7.50 – 7.45 (m, 2H), 5.59 – 5.50 (m, 1H), 5.46 – 5.38 (m, 1H), 4.35 – 4.31 (m, 1H), 4.17 – 4.11 (m, 2H), 2.74 – 2.61 (m, 2H), 1.62 (dd, *J* = 6.25, 1.40 Hz, 3H), 1.17 (t, *J* = 7.32 Hz, 3H). ^{13}C NMR (126 MHz, $CDCl_3$, ppm) δ 194.91 (s), 169.71 (s), 136.45 (s), 133.58 (s), 128.84 (s), 128.76 (s), 128.35 (s), 127.09 (s), 61.50 (s), 54.74 (s), 32.15 (s), 18.03 (s), 14.19 (s).

(E)-1-Phenylhex-4-en-1-one (58)

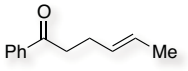

(E)-Ethyl 2-benzoylhex-4-enoate (0.37 g, 1.45 mmol) was dissolved in a mixture 1:1 of water and THF (6 ml). LiOH (0.10 g, 4.36 mmol)

was added and the reaction mixture was stirred for 15 h at 50 ºC. After quenching with aqueous 0.1 M HCl (9 ml), the solution was extracted with diethyl ether. The organic layers were washed with brine, dried over $MgSO_4$ and concentrated. The residue was purified with silica gel column chromatography with hexane:ethyl acetate (2:1) to obtain *(E)*-1-phenylhex-4-en-1-one **58** in 80% isolated yield (0.20 g, 0.16 mmol). ^{1}H NMR (500 MHz, $CDCl_3$, ppm) δ 7.97 – 7.95 (m, 2H), 7.57 – 7.54 (m, 1H), 7.47 – 7.44 (m, 2H), 5.54 – 5.48 (m, 2H), 3.03 (t, *J* = 7.51 Hz, 2H), 2.45 – 2.40 (m, 2H), 1.66 – 1.64 (m, 3H). ^{13}C NMR (126 MHz, $CDCl_3$, ppm) δ 199.95 (s), 137.19 (s), 133.07 (s), 129.90 (s), 128.71 (s), 128.19 (s), 126.09 (s), 38.71 (s), 27.33 (s), 18.05 (s).

N-(5-Methylhex-5-en-2-ylidene)benzamide (63)

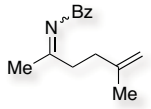

Benzylamine (0.32 ml, 2.94 mmol), 5-methyl-5-hexen-2-one (0.35 ml, 2.67 mmol) and 4-methylbenzenesulfonic acid (10 mg, 0.06 mmol) were dissolved in toluene (10 ml). Molecular sieves 4Å were added and the reaction mixture was stirred at 120 ºC for 24 h. Then, the solution was cooled down and concentrated. The residue was dissolved in cyclohexane, filtered though filter paper and washed with saturated $NaHCO_3$ and brine sequentially. The organic layers were dried over $MgSO_4$ and concentrated. *N*-(5-Methylhex-5-en-2-ylidene)benzamide **63** was obtained in 54% isolated yield (0.29 g, 1.44 mmol) and used immediately in the gold-catalyzed [2+2+2] cycloaddition. ^{1}H NMR (500 MHz, $CDCl_3$, ppm) δ 7.35 – 7.31 (m, 4H), 7.26 – 7.23 (m, 1H), 4.73 (s, 1H), 4.66 (s, 1H), 3.87 (s, 2H), 2.58 (t, *J* = 7.73 Hz, 2H), 2.28 (t, *J* = 7.73 Hz, 2H), 2.16 (s, 3H), 1.73 (s, 3H).

4-Methoxy-N-(5-methylhex-5-en-2-ylidene)aniline (64)

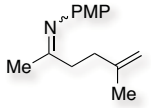

4-Methoxyaniline (0.36 g, 2.94 mmol), 5-methyl-5-hexen-2-one (0.35 ml, 2.67 mmol) and 4-methylbenzenesulfonic acid (10 mg, 0.06 mmol) were dissolved in toluene (10 ml). Molecular sieves 4Å were added and the reaction mixture was stirred at 120 ºC for 24 h. Then, the solution was cooled down and concentrated. The residue was dissolved in cyclohexane, filtered though filter paper and washed with saturated $NaHCO_3$ and brine sequentially. The organic layers were dried over $MgSO_4$ and concentrated. 4-Methoxy-*N*-(5-methylhex-5-en-2-ylidene)aniline **64** was obtained in 50% isolated yield (0.29 g, 1.34 mmol) and used immediately in the gold-catalyzed [2+2+2] cycloaddition. ^{1}H NMR (400 MHz, $CDCl_3$, ppm) δ 6.85 – 6.83 (m, 2H), 6.64 – 6.62 (m, 2H), 4.76 (broad s, 2H), 3.79 (s, 3H), 2.57 – 2.53 (m, 2H), 2.41 – 2.37 (m, 2H), 1.80 (s, 3H), 1.79 (s, 3H).

Methyl 1-(2-methylallyl)-2-oxocyclohexanecarboxylate

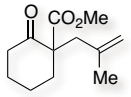

To a suspension of NaH 60% (338 mg, 8.45 mmol) in tetrehydrofuran (20 ml) at 0 ºC, methyl 2-oxocyclohexanecarboxylate (1.00 ml, 7.04 mmol) was added slowly. The solution was stirred for 10 min and then, 3-bromo-2-methylprop-1-ene (0.85 ml, 8.45 mmol) was added. The reaction mixture was stirred at 25 ºC for 19 h and quenched with water (2 ml). After extraction with ethyl acetate, the organic layers were washed with brine and dried with $MgSO_4$. The residue was purified by silica gel column chromatography with cyclohexane:ethyl acetate (20:1) to obtain methyl 1-(2-methylallyl)-2-oxocyclohexanecarboxylate in 37% isolated yield (0.54 g, 3.46 mmol). ^{1}H NMR (400 MHz, $CDCl_3$, ppm) δ 4.82 (dq, *J* = 2.32, 1.46 Hz, 1H), 4.65 (broad s, 1H), 3.71 (s, 3H), 2.74 (d, *J* = 13.88 Hz, 1H), 2.54 (dq, *J* = 13.81, 2.80 Hz, 1H), 2.49 – 2.43 (m, 1H), 2.43 – 2.36 (m, 1H), 2.33 (d, *J* = 13.81 Hz, 1H), 2.04 – 1.98 (m, 1H),

1.79 – 1,71 (m, 2H), 1.69 – 1.62 (m, 4H), 1.48 – 1.40 (m, 1H). ^{13}C NMR (101 MHz, $CDCl_3$, ppm) δ 207.32 (s), 172.16 (s), 141.37 (s), 115.41 (s), 61.03 (s), 52.34 (s), 42.44 (s), 41.27 (s), 36.17 (s), 27.77 (s), 23.81 (s), 22.66 (s).

2-(2-Methylallyl)cyclohexanone (75)

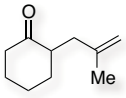

Methyl 1-(2-methylallyl)-2-oxocyclohexanecarboxylate (162 mg, 0.78 mmol) was dissolved in a mixture 1:1 of water and THF (4 ml). LiOH (37 mg, 1.54 mmol) was added and the reaction mixture was stirred for 23 h at 50 ºC. After quenching with aqueous 0.1 M HCl (6 ml), the solution was extracted with diethyl ether. The organic layers were washed with brine, dried over $MgSO_4$ and concentrated. 2-(2-Methylallyl)cyclohexanone **75** was obtained in 67% isolated yield (78 mg, 0.51 mmol). ^{1}H NMR (400 MHz, $CDCl_3$, ppm) δ 4.79 (broad s, 1H), 4.74 (broad s, 1H), 2.64 – 2.57 (m, 1H), 2.45 – 2.31 (m, 3H), 2.13 (dd, *J* = 14.95, 7.47 Hz, 1H), 1.75 – 1.68 (m, 4H), 1.68 – 1.65 (m, 3H), 1.41 – 1.31 (m, 2H). ^{13}C NMR (126 MHz, $CDCl_3$, ppm) δ 180.60 (s), 142.56 (s), 112.64 (s), 43.99 (s), 40.60 (s), 33.94 (s), 31.77 (s), 26.36 (s), 24.75 (s), 22.33 (s).

Cyclohex-1-en-1-ylmethanol

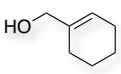

To a solution of $LiAlH_4$ (0.34 g, 9.00 mmol) in diethyl ether (17 ml), cyclohex-1-enecarboxylic acid (1.00 g, 7.93 mmol) was added at 0 ºC. The reaction mixture was stirred for 2 h and then quenched with a saturated solution of sodium potassium tartrate (20 ml). The solution was stirred at 25 ºC for 1.5 h and then extracted with diethyl ether. The organic layers were dried with $MgSO_4$ and concentrated. Cyclohex-1-en-ylmethanol was obtained in 87% isolated yield (0.78 g, 6.93 mmol). ^{1}H NMR (400 MHz, $CDCl_3$, ppm) δ 5.69 – 5.67 (m, 1H), 3.98 (s, 2H), 2.06 – 1.99 (m, 4H), 1.68 – 1.62 (m, 2H), 1.61 – 1.55 (m, 2H). ^{13}C NMR (101 MHz, $CDCl_3$, ppm) δ 137.70 (s), 123.19 (s), 67.88 (s), 25.77 (s), 25.07 (s), 22.69 (s), 22.59 (s).

1-(Bromomethyl)cyclohex-1-ene

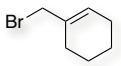

Cyclohex-1-en-1-ylmethanol (0.44 g, 3.88 mmol) was dissolved in CH_2Cl_2 (7 ml), cooled to 0 ºC and tribromophosphine (0.16 ml, 1.75 mmol) was added carefully. The reaction mixture was stirred for 3 h and diluted with CH_2Cl_2. The solution was washed with saturated $NaHCO_3$ and brine. The organic layers were dried with Na_2SO_4 and concentrated. The residue was purified by silica gel column chromatography using pure cyclohexane to obtain 1-(bromomethyl)cyclohex-1-ene in 63% isolated yield (0.43 g, 2.43 mmol). ^{1}H NMR (400 MHz, $CDCl_3$, ppm) δ 5.88 (broad s, 1H), 3.94 (s, 2H), 2.13 – 2.11 (m, 2H), 2.05 – 2.02 (m, 2H), 1.70 – 1.65 (m, 2H), 1.60 – 1.55 (m, 2H). ^{13}C NMR (101 MHz, $CDCl_3$, ppm) δ 134.81 (s), 128.32 (s), 40.04 (s), 26.53 (s), 25.65 (s), 22.56 (s), 22.08 (s).

3-(Cyclohex-1-en-1-yl)-1-phenylpropan-1-one (77)

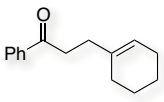

Acetophenone (67 μl, 0.57 mmol) was dissolved in benzene (2 ml) and potassium *tert*-butoxide (64 mg, 0.57 mmol) was added slowly. After stirring for 30 min at 25 ºC, 1-(bromomethyl)cyclohex-1-ene in benzene (1 ml) was added. The reaction mixture was then stirred at 25 ºC for 1.5 h. It was quenched with brine, extracted with cyclohexane and dried with Na_2SO_4. The residue was purified with silica gel preparative TLC with cyclohexane:ethyl

acetate (20:1) to obtain 3-(cyclohex-1-en-1-yl)-1-phenylpropan-1-one **77** in 23% isolated yield (14 mg, 0.07 mmol). ^{1}H NMR (500 MHz, $CDCl_3$, ppm) δ 7.95 (t, *J* = 7.13 Hz, 2H), 7.55 (t, *J* = 7.43 Hz, 1H), 7.46 (t, *J* = 7.89 Hz, 2H), 5.45 –5.44 (m, 1H), 3.08 – 3.05 (m, 2H), 2.36 (t, *J* = 7.53 Hz, 2H), 2.00 – 1.96 (m, 4H), 1.65 – 1.61 (m, 2H), 1.57 – 1.53 (m, 2H). ^{13}C NMR (101 MHz, $CDCl_3$, ppm) δ 200.80 (s), 137.70 (s), 137,18 (s), 133.53 (s), 129.18 (s), 128.69 (s), 122.05 (s), 37.73 (s), 32.99 (s), 29.18 (s), 25.86 (s), 23.58 (s), 23.09 (s).

Cyclohex-1-en-1-ylmethyl acetate

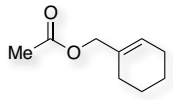

To an ice-cooled solution of cyclohex-1-en-1-ylmethanol (1.65 g, 14.68 mmol) in CH_2Cl_2 (40 ml) were added Et_3N (4.10 ml, 29.4 mmol) and a solution of *N*,*N*-dimethylpyridin-4-amine (18 mg, 0.15 mmol) in CH_2Cl_2 (7 ml). After 2 min, acetyl chloride (1.26 ml, 17.62 mmol) was added dropwise and the reaction mixture was stirred at 0 ºC for 1.5 h. The ice-bath was removed and the solution was stirred for an additional 30 min at 25 ºC. Then, it was quenched with cold 5% HCl (80 ml) and the phases were separated. The organic layers were washed with water, saturated $NaHCO_3$ and brine, dried with Na_2SO_4 and concentrated. Cyclohex-1-en-1-ylmethyl acetate was obtained in quantitative yield (2.26 g, 14.67 mmol). ^{1}H NMR (400 MHz, $CDCl_3$, ppm) δ 5.74 (broad s, 1H), 4.43 (s, 2H), 2.07 (s, 3H), 2.06 – 2.02 (m, 2H), 2.00 – 1.97 (m, 2H), 1.68 – 1.62 (m, 2H), 1.61 –1.56 (m, 2H). ^{13}C NMR (101 MHz, $CDCl_3$, ppm) δ 171.99 (s), 133.72 (s), 127.38 (s), 69.83 (s), 26.77 (s), 25.86 (s), 23.24 (s), 22.95 (s), 21.90 (s).

2-(2-Methylenecyclohexyl)acetic acid

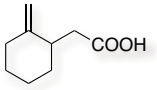

Lithium diisopropylamide (3.14 g, 29.3 mmol) was dissolved in THF (45 ml)and cooled down to – 78 ºC. Cyclohex-1-en-1-ylmethyl acetate (2.26 g, 14.67 mmol) in THF (4.5 ml) was added over 5 min. After 10 min, chlorotrimethylsilane (4.15 ml, 32.3 mmol) was added in one portion and, 2 min later, the solution was warmed up to 25 ºC. The reaction mixture was heated to reflux for 2.5 h and cooled down again to 25 ºC. Methanol (15 ml) was added and the solution was stirred for an additional 15 min. Then, it was quenched with aqueous 5% NaOH (250 ml) and washed with diethyl ether. The aqueous layer was cooled down to 0 ºC, acidified with concentrated HCl and extracted five times with CH_2Cl_2. The organic layers were collected, washed with brine, dried with Na_2SO_4 and concentrated. 2-(2-Methylenecyclohexyl)acetic acid was obtained in 53% isolated yield (1.21 g, 7.84 mmol). ^{1}H NMR (500 MHz, $CDCl_3$, ppm) δ 4.69 (broad s, 1H), 4.56 (broad s, 1H), 2.64 (dd, *J* = 15.10, 6.33 Hz, 1H), 2.58 – 2.52 (m, 1H), 2.34 (dd, *J* = 15.10, 8.03 Hz, 1H), 2.31 – 2.27 (m, 1H), 2.08 – 2.03 (m, 1H), 1.87 – 1.82 (m, 1H), 1.74 – 1.69 (m, 2H), 1.53 – 1.46 (m, 1H), 1.45 – 1.37 (m, 1H), 1.24 – 1.17 (m, 1H). ^{13}C NMR (101 MHz, $CDCl_3$, ppm) δ 179.82 (s), 151.61 (s), 105.89 (s), 39.97 (s), 38.21 (s), 35.96 (s), 34.45 (s), 28.83 (s), 25.43 (s).

1-(2-Methylenecyclohexyl)propan-2-one (78)

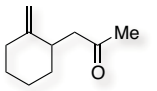

A stirred solution of 2-(2-methylenecyclohexyl)acetic acid (0.40 g, 2.59 mmol) in THF (26 ml) was cooled down to 0 ºC and treated rapidly with methyllithium 1.6 M in diethyl ether (13 ml, 20.75 mmol). The reaction mixture was stirred for 2 h and chlorotrimethylsilane (6.58 ml, 51.90 mmol) was added. The solution was warmed up to 25 ºC and quenched with 1 M HCl (70

ml). The phases were stirred at 25 ºC for 1 h and separated. The aqueous phase was extracted with diethyl ether and the combined organic layers were washed with water, dried with Na_2SO_4 and concentrated. The residue was purified with silica gel column chromatography using cyclohexane:ethyl acetate (20:1) to obtain 1-(2-methylenecyclohexyl)propan-2-one **78** in 55% isolated yield (0.22 g, 1.43 mmol). ^{1}H NMR (400 MHz, $CDCl_3$, ppm) δ 4.65 (broad s, 1H), 4.45 (broad s, 1H), 2.69 (dd, *J* = 15.97, 6.52 Hz, 1H), 2.62 – 2.55 (m, 1H), 2.39 (dd, *J* = 16.20, 7.20 Hz, 1H), 2.30 – 2.25 (m, 1H), 2.15 (s, 3H), 2.09 – 2.01 (m, 1H), 1.78 – 1.65 (m, 3H), 1.53 – 1.46 (m, 1H), 1.44 – 1.36 (m, 1H, 1.17 – 1.09 (m, 1H).

3-Methyl-1-(2-methylenecyclohexyl)butan-2-one (79)

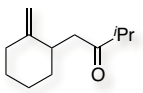

A stirred solution of 2-(2-methylenecyclohexyl)acetic acid (0.25 g, 1.62 mmol) in THF (16 ml) was cooled down to 0 ºC and treated rapidly with isopropyllithium 0.7 M in pentane (46 ml, 32.40 mmol). The reaction mixture was stirred for 2 h and chlorotrimethylsilane (8.23 ml, 64.81 mmol) was added. The solution was warmed up to 25 ºC and quenched with 1 M HCl (80 ml). The phases were stirred at 25 ºC for 1 h and separated. The aqueous phase was extracted with diethyl ether and the combined organic layers were washed with water, dried with Na_2SO_4 and concentrated. The residue was purified with silica gel column chromatography using cyclohexane:ethyl acetate (40:1) to obtain 3-methyl-1-(2-methylenecyclohexyl)butan-2-one **79** in 37% isolated yield (0.11 g, 0.60 mmol). ^{1}H NMR (500 MHz, $CDCl_3$, ppm) δ 4.66 (s, 1H), 4.48 (s, 1H), 2.71 (dd, *J* = 16.03, 5.84 Hz, 1H), 2.67 – 2.61 (m, 2H), 2.48 (dd, *J* = 16.03, 7.34 Hz, 1H), 2.32 – 2.28 (m, 1H), 2.11 – 2.06 (m, 1H), 1.76 – 1.69 (m, 3H), 1.51 – 1.47 (m, 1H), 1.43 – 1.39 (m, 1H), 1.17 –1.13 (m, 1H), 1.11(d, *J* = 6.90 Hz, 6H). ^{13}C NMR (101 MHz, $CDCl_3$, ppm) δ 214.09 (s), 152.20 (s), 105.15 (s), 43.77 (s), 41.33 (s), 38.65 (s), 35.84 (s), 34.36 (s), 28.72 (s), 25.28 (s), 18.41 (s), 18.26 (s). ESI$^+$ *m/z* calc for $C_{12}H_{20}NaO^+$ $[M+Na]^+$ 203.1406, found 203.1408 (0.2 ppm).

General Procedure for the Preparation of Oxabicycles

To a solution of the oxoalkene (1 equiv.) and the arylalkyne (3.5 equiv.) in DCE (0.5 M), the cationic gold (I) catalyst **A** (5 mol%) was added. Then, the reaction mixture was stirred at 50 ºC and followed by TLC. When it was finished, the catalyst was quenched by adding 0.05 ml of Et_3N, the solvent was removed and the crude was analysed by quantitative ^{1}H NMR using 1,4-diacetylbenzene as internal standard. Finally, the oxabicycle product was purified by preparative TLC and fully characterized.

1,5-Dimethyl-3-phenyl-8-oxabicyclo[3.2.1]oct-2-ene (23)

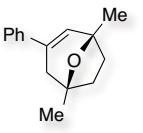

Compound **23** was synthesized following the general procedure starting from 5-methylhex-5-en-2-one (26.0 µl, 0.2 mmol) and ethynylbenzene (77.0 µl, 0.7 mmol) with catalyst **A** (9.0 mg, 0.01 mmol). The reaction time was 19 h and pure CH_2Cl_2 was used as eluent in the separation to obtain pure 1,5-dimethyl-3-phenyl-8-oxabicyclo[3.2.1]oct-3-ene as a yellow oil in 68% isolated yield (29.1 mg, 0.14 mmol). ^{1}H NMR (400 MHz, $CDCl_3$, ppm) δ 7.38 (d, *J* = 8.3 Hz, 2H), 7.31 (t, *J* = 7.5 Hz, 2H), 7.28 – 7.19 (m, 1H), 6.22 (t, *J* = 1.7 Hz, 1H), 2.70 (d, *J* = 16.7 Hz, 1H), 2.28 (dd, *J* = 16.7, 1.2 Hz, 1H), 2.11 – 2.04 (m, 1H), 1.96 – 1.85 (m, 1H), 1.84 – 1.78 (m, 2H), 1.50 (s, 3H), 1.49 (s, 3H). ^{13}C NMR (126 MHz, $CDCl_3$, ppm) δ

139.93 (s), 133.61 (s), 131.09 (s), 128.46 (s), 127.44 (s), 125.01 (s), 79.73 (s), 79.49 (s), 42.34 (s), 42.21 (s), 37.53 (s), 27.42 (s), 23.78 (s). Structure confirmed by ^{1}H COSY NMR and ^{1}H-^{13}C HMQC NMR. APCI^{+} m/z calc for $C_{15}H_{19}O^{+}$ [M+H]$^{+}$ 215.1436, found 215.1438 (0.9 ppm).

1,5-Dimethyl-3-(naphthalen-2-yl)-8-oxabicyclo[3.2.1]oct-2-ene (26)

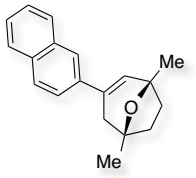

Compound **26** was synthesized following the general procedure starting from 5-methylhex-5-en-2-one (26.0 µl, 0.2 mmol) and 2-ethynylnaphthalene (107.0 mg, 0.7 mmol) with catalyst **A** (9.0 mg, 0.01 mmol). The reaction time was 20 h and a mixture of pentane and CH_2Cl_2 (1:99) was used as eluent in the separation to obtain pure 1,5-dimethyl-3-(naphthalen-2-yl)-8-oxabicyclo[3.2.1]oct-3-ene as a yellowish powder in 62% isolated yield (32.5 mg, 0.12 mmol). ^{1}H NMR (400 MHz, $CDCl_3$, ppm) δ 7.84 – 7.72 (m, 4H), 7.60 (dd, *J* = 8.6, 1.9 Hz, 1H), 7.50 – 7.37 (m, 2H), 6.39 (t, *J* = 1.6 Hz, 1H), 2.81 (d, *J* = 16.5 Hz, 1H), 2.43 (dd, *J* = 16.6, 1.2 Hz, 1H), 2.13 – 2.08 (m, 1H), 2.00 – 1.90 (m, 1H), 1.88 – 1.82 (m, 2H), 1.55 (s, 3H), 1.53 (s, 3H). ^{13}C NMR (101 MHz, $CDCl_3$, ppm) δ 137.06 (s), 133.59 (s), 133.38 (s), 132.91 (s), 131.70 (s), 128.23 (s), 127.93 (s), 127.65 (s), 126.29 (s) 125.88 (s), 123.55 (s), 123.43 (s), 79.83 (s), 79.55 (s), 42.33 (s), 42.19 (s), 37.56 (s), 27.48 (s), 23.85 (s). Structure confirmed by ^{1}H COSY NMR and ^{1}H-^{13}C HMQC NMR. APCI^{+} m/z calc for $C_{19}H_{21}O^{+}$ [M+H]$^{+}$ 265.1592, found 265.1588 (-1.5 ppm). Mp 128.5 – 129.3 ºC.

3-(4-Fluorophenyl)-1,5-dimethyl-8-oxabicyclo[3.2.1]oct-2-ene (27)

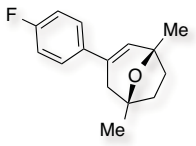

Compound **27** was synthesized following the general procedure starting from 5-methylhex-5-en-2-one (26.0 µl, 0.2 mmol) and 1-ethynyl-4-fluorobenzene (80.0 µl, 0.7 mmol) with catalyst **A** (9.0 mg, 0.01 mmol). The reaction time was 20 h and a mixture of pentane and CH_2Cl_2 (1:1) was used as eluent in the separation to obtain pure 3-(4-fluorophenyl)-1,5-dimethyl-8-oxabicyclo[3.2.1]oct-3-ene as a yellow oil in 68% isolated yield (31.6 mg, 0.14 mmol). ^{1}H NMR (500 MHz, $CDCl_3$, ppm) δ 7.37 – 7.31 (m, 2H), 7.04 – 6.95 (m, 2H), 6.16 (t, *J* = 1.6 Hz, 1H), 2.66 (d, *J* = 16.7 Hz, 1H), 2.24 (dd, *J* = 16.6, 1.2 Hz, 1H), 2.14 – 2.00 (m, 1H), 1.93 – 1.87 (m, 1H), 1.86 – 1.77 (m, 2H), 1.50 (s, 3H), 1.48 (s, 3H). ^{13}C NMR (126 MHz, $CDCl_3$, ppm) δ 162.32 (d, *J* (^{13}C-^{19}F) = 243.7 Hz), 136.02 (d, *J* (^{13}C-^{19}F) = 3.7 Hz), 132.72 (s), 130.96 (s), 126.56 (d, *J* (^{13}C-^{19}F) = 7.8 Hz), 115.25 (d, *J* (^{13}C-^{19}F) = 21.4 Hz), 79.69 (s), 79.42 (s), 42.36 (s), 42.29 (s), 37.51 (s), 27.38 (s), 23.76 (s). ^{19}F NMR (376 MHz, $CDCl_3$, ppm) δ -115.05 (s). Structure confirmed by ^{1}H COSY NMR and ^{1}H-^{13}C HMQC NMR. APCI^{+} m/z calc for $C_{15}H_{18}OF^{+}$ [M+H]$^{+}$ 233.1342, found 233.1342 (0.0 ppm).

3-(4-Chlorophenyl)-1,5-dimethyl-8-oxabicyclo[3.2.1]oct-2-ene (28)

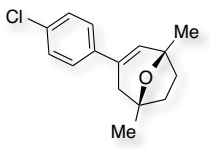

Compound **28** was synthesized following the general procedure starting from 5-methylhex-5-en-2-one (26.0 µl, 0.2 mmol) and 1-chloro-4-ethynylbenzene (96.0 mg, 0.7 mmol) with catalyst **A** (9.0 mg, 0.01 mmol). The reaction time was 18 h and a mixture of pentane and CH_2Cl_2 (1:10) was used as eluent in the separation to obtain pure 3-(4-chlorophenyl)-1,5-dimethyl-8-oxabicyclo[3.2.1]oct-3-ene as a yellow oil in 55% isolated yield (27.4 mg, 0.11 mmol). ^{1}H NMR (500 MHz, $CDCl_3$, ppm) δ 7.30 (d, *J* = 8.8 Hz, 2H), 7.27 (d, *J* = 8.9 Hz, 2H), 6.21 (t, *J* = 1.7 Hz, 1H),

2.65 (d, *J* = 16.6 Hz, 1H), 2.23 (d, *J* = 16.6 Hz, 1H), 2.14 – 2.00 (m, 1H), 1.94 – 1.84 (m, 1H), 1.84 – 1.78 (m, 2H), 1.50 (s, 3H), 1.48 (s, 3H). ^{13}C NMR (126 MHz, $CDCl_3$, ppm) δ 138.34 (s), 133.11 (s), 132.63 (s), 131.62 (s), 128.56 (s), 126.27 (s), 79.69 (s), 79.42 (s), 42.25 (s), 42.12 (s), 37.50 (s), 27.36 (s), 23.71 (s). Structure confirmed by ^{1}H COSY NMR and ^{1}H-^{13}C HMQC NMR. APCI^{+} m/z calc for $C_{15}H_{17}OCl^{+}$ $[M+H]^{+}$ 249.1046, found 249.1039 (-2.8 ppm).

3-(4-Bromophenyl)-1,5-dimethyl-8-oxabicyclo[3.2.1]oct-2-ene (29)

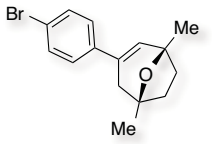

Compound **29** was synthesized following the general procedure starting from 5-methylhex-5-en-2-one (26.0 µl, 0.2 mmol) and 1-bromo-4-ethynylbenzene (127.0 mg, 0.7 mmol) with catalyst **A** (9.0 mg, 0.01 mmol). The reaction time was 20 h and a mixture of pentane and CH_2Cl_2 (1:2) was used as eluent in the separation to obtain pure 3-(4-bromophenyl)-1,5-dimethyl-8-oxabicyclo[3.2.1]oct-3-ene as a yellow oil in 49% isolated yield (28.7 mg, 0.10 mmol). ^{1}H NMR (500 MHz, $CDCl_3$, ppm) δ 7.43 (d, *J* = 8.6 Hz, 2H), 7.24 (d, J = 8.6 Hz, 2H), 6.23 (t, J = 1.7 Hz, 1H), 2.65 (d, *J* = 16.6 Hz, 1H), 2.23 (dd, *J* = 16.7, 1.1 Hz, 1H), 2.11 – 2.01 (m, 1H), 1.94 – 1.86 (m, 1H), 1.85 – 1.78 (m, 2H), 1.50 (s, 3H), 1.48 (s, 3H). ^{13}C NMR (101 MHz, $CDCl_3$, ppm) δ 138.81 (s), 132.69 (s), 131.71 (s), 131.51 (s), 126.63 (s), 121.25 (s), 79.70 (s), 79.43 (s), 42.23 (s), 42.06 (s), 37.50 (s), 27.36 (s), 23.70 (s). Structure confirmed by ^{1}H COSY NMR and ^{1}H-^{13}C HMQC NMR. APCI^{+} m/z calc for $C_{15}H_{18}OBr^{+}$ $[M+H]^{+}$ 293.0541, found 293.0527 (-4.8 ppm).

1,5-Dimethyl-3-(m-tolyl)-8-oxabicyclo[3.2.1]oct-2-ene (30)

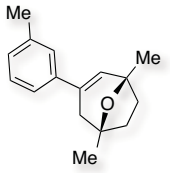

Compound **30** was synthesized following the general procedure starting from 5-methylhex-5-en-2-one (26.0 µl, 0.2 mmol) and 1-ethynyl-3-methylbenzene (90.0 µl, 0.7 mmol) with catalyst **A** (9.0 mg, 0.01 mmol). The reaction time was 19 h and a mixture of pentane and CH_2Cl_2 (1:10) was used as eluent in the separation to obtain pure 1,5-dimethyl-3-(m-tolyl)-8-oxabicyclo[3.2.1]oct-3-ene as a yellow oil in 70% isolated yield (31.9 mg, 0.14 mmol). ^{1}H NMR (400 MHz, $CDCl_3$, ppm) δ 7.22 – 7.17 (m, 3H), 7.07 – 7.05 (m, 1H), 6.20 (t, *J* = 1.7 Hz, 1H), 2.68 (d, *J* = 16.6 Hz, 1H), 2.35 (s, 3H), 2.27 (dd, *J* = 16.7, 1.2 Hz, 1H), 2.10 – 2.03 (m, 1H), 1.96 – 1.84 (m, 1H), 1.84 – 1.75 (m, 2H), 1.50 (s, 3H), 1.48 (s, 3H). ^{13}C NMR (126 MHz, $CDCl_3$, ppm) δ 139.93 (s), 137.95 (s), 133.65 (s), 130.91 (s), 128.35 (s), 128.18 (s), 125.76 (s), 122.14 (s), 79.71 (s), 79.47 (s), 42.35 (s), 42.26 (s), 37.51 (s), 27.41 (s), 23.78 (s), 21.64 (s). Structure confirmed by ^{1}H COSY NMR and ^{1}H-^{13}C HMQC NMR. APCI^{+} m/z calc for $C_{16}H_{21}O^{+}$ $[M+H]^{+}$ 229.1592, found 229.1588 (-1.7 ppm).

3-(3-Fluorophenyl)-1,5-dimethyl-8-oxabicyclo[3.2.1]oct-2-ene (31)

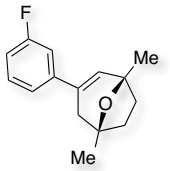

Compound **31** was synthesized following the general procedure starting from 5-methylhex-5-en-2-one (26.0 µl, 0.2 mmol) and 1-ethynyl-3-fluorobenzene (81.0 µl, 0.7 mmol) with catalyst **A** (9.0 mg, 0.01 mmol). The reaction time was 20 h and a mixture of pentane and CH_2Cl_2 (1:2) was used as eluent in the separation to obtain pure 3-(3-fluorophenyl)-1,5-dimethyl-8-oxabicyclo[3.2.1]oct-3-ene as a yellow oil in 49% isolated yield (22.6 mg, 0.10 mmol). ^{1}H NMR (500 MHz, $CDCl_3$, ppm) δ 7.31 – 7.27 (m, 1H), 7.22 – 7.16 (m, 1H), 7.13 – 7.05 (m, 1H), 6.96 (tdd, *J* = 8.3, 2.6, 0.8

Hz, 1H), 6.28 (t, *J* = 1.7 Hz, 1H), 2.69 (d, *J* = 16.6 Hz, 1H), 2.27 (dd, *J* = 16.6, 1.2 Hz, 1H), 2.17 – 2.03 (m, 1H), 1.97 – 1.90 (m, 1H), 1.89 – 1.80 (m, 2H), 1.53 (s, 3H), 1.51 (s, 3H). ^{13}C NMR (126 MHz, $CDCl_3$, ppm) δ 163.14 (s, *J* (^{13}C-^{19}F) = 245.4 Hz), 142.29 (d, *J* (^{13}C-^{19}F) = 9.6 Hz), 132.69 (s), 132.19 (s), 129.83 (d, *J* (^{13}C-^{19}F) = 9.7 Hz), 120.58 (d, *J* (^{13}C-^{19}F) = 3.7 Hz), 114.15 (d, *J* (^{13}C-^{19}F) = 21.7 Hz), 111.92 (d, *J* (^{13}C-^{19}F) = 22.8 Hz), 79.67 (s), 79.44 (s), 42.23 (s), 42.11 (s), 37.49 (s), 27.35 (s), 23.68 (s). ^{19}F NMR (376 MHz, $CDCl_3$, ppm) δ -113.66 (s). Structure confirmed by ^{1}H COSY NMR and ^{1}H-^{13}C HMQC NMR. APCI$^+$ m/z calc for $C_{15}H_{18}OF^+$ $[M+H]^+$ 233.1342, found 233.1339 (-1.3 ppm).

3-(3-Chlorophenyl)-1,5-dimethyl-8-oxabicyclo[3.2.1]oct-2-ene (32)

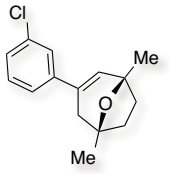

Compound **32** was synthesized following the general procedure starting from 5-methylhex-5-en-2-one (26.0 µl, 0.2 mmol) and 1-chloro-3-ethynylbenzene (86.0 µl, 0.7 mmol) with catalyst **A** (9.0 mg, 0.01 mmol). The reaction time was 20 h and a mixture of pentane and CH_2Cl_2 (1:2) was used as eluent in the separation to obtain pure 3-(3-chlorophenyl)-1,5-dimethyl-8-oxabicyclo[3.2.1]oct-3-ene as a yellow oil in 55% isolated yield (27.4 mg, 0.11 mmol). ^{1}H NMR (500 MHz, $CDCl_3$, ppm) δ 7.37 – 7.33 (m, 1H), 7.30 – 7.20 (m, 3H), 6.25 (t, *J* = 1.6 Hz, 1H), 2.66 (d, *J* = 16.7 Hz, 1H), 2.23 (dd, *J* = 16.7, 1.1 Hz, 1H), 2.16 – 2.00 (m, 1H), 1.94 – 1.87 (m, 1H), 1.86 – 1.75 (m, 2H), 1.50 (s, 3H), 1.49 (s, 3H). ^{13}C NMR (126 MHz, $CDCl_3$, ppm) δ 141.81 (s), 134.49 (s), 132.59 (s), 132.34 (s), 129.66 (s), 127.37 (s), 125.25 (s), 123.13 (s), 79.69 (s), 79.44 (s), 42.24 (s), 42.08 (s), 37.49 (s), 27.34 (s), 23.67 (s). Structure confirmed by ^{1}H COSY NMR and ^{1}H-^{13}C HMQC NMR. APCI$^+$ m/z calc for $C_{15}H_{18}OCl^+$ $[M+H]^+$ 249.1046, found 249.1041 (-2.0 ppm).

1,5-Dimethyl-8-oxabicyclo[3.2.1]oct-2-en-3-yl)phenol (33)

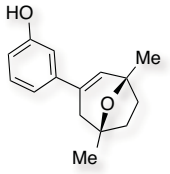

Compound **33** was synthesized following the general procedure starting from 5-methylhex-5-en-2-one (26.0 µl, 0.2 mmol) and 3-ethynylphenol (76.0 µl, 0.7 mmol) with catalyst **A** (9.0 mg, 0.01 mmol). The reaction time was 37 h and a mixture of cyclohexane and ethyl acetate (2:1) was used as eluent in the separation to obtain pure 3-(1,5-dimethyl-8-oxabicyclo[3.2.1]oct-3-en-3-yl)phenol as a yellowish powder in 65% isolated yield (22.8 mg, 0.10 mmol). Moreover, this compound was synthesized in larger scale. To a solution of 5-methylhex-5-en-2-one (0.26 ml, 2.00 mmol) and 3-ethynylphenol (1.0 g, 8.50 mmol) in DCE (5.6 ml) at 25 ºC, the cationic gold (I) catalyst (75.0 mg, 4 mol%) was added. Then, the reaction mixture was stirred at 50 ºC for 39 h and followed by TLC. When it was finished, it was quenched by adding 0.5 ml of Et_3N and the solvent was removed. Finally, the crude was purified by column chromatography using a mixture of cyclohexane and ethyl acetate (9:1) as eluent in the separation to obtain pure 3-(1,5-dimethyl-8-oxabicyclo[3.2.1]oct-3-en-3-yl)phenol as a yellowish powder in 74% isolated yield (339.2 mg, 1.47 mmol). ^{1}H NMR (500 MHz, CD_3OD, ppm) δ 7.12 (t, *J* = 7.9 Hz, 1H), 6.88 (ddd, *J* = 7.8, 1.8, 1.1 Hz, 1H), 6.83 (t, *J* = 2.1 Hz, 1H), 6.69 (ddd, *J* = 8.0, 2.5, 0.9 Hz, 1H), 6.21 (t, *J* = 1.7 Hz, 1H), 2.59 (d, *J* = 16.8 Hz, 1H), 2.31 (d, *J* = 16.8 Hz, 1H), 2.11 – 2.04 (m, 1H), 1.97 – 1.89 (m, 1H), 1.87 – 1.73 (m, 2H), 1.46 (s, 3H), 1.44 (s, 3H). ^{13}C NMR (126 MHz, CD_3OD, ppm) δ 158.44 (s), 142.44 (s), 134.95 (s), 131.23 (s), 130.35 (s), 117.34 (s), 115.38 (s), 112.75 (s), 81.22 (s), 81.04 (s), 43.10 (s), 42.95 (s), 38.08 (s), 27.41 (s), 23.78 (s). Structure confirmed by ^{1}H COSY NMR and ^{1}H-^{13}C HMQC NMR. ESI$^-$ m/z calc for $C_{15}H_{17}O_2^-$ $[M-H]^-$ 229.1229,

found 229.1223 (-2.6 ppm). Mp 129.8 – 130.5 ºC. Structure confirmed by X-Ray crystallography, CCDC 913001.

3-(3-Methoxyphenyl)-1,5-dimethyl-8-oxabicyclo[3.2.1]oct-2-ene (34)

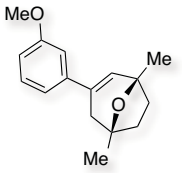

Compound **34** was synthesized following the general procedure starting from 5-methylhex-5-en-2-one (26.0 µl, 0.2 mmol) and 1-ethynyl-3-methoxybenzene (89.0 µl, 0.7 mmol) with catalyst **A** (9.0 mg, 0.01 mmol). The reaction time was 19 h and pure CH_2Cl_2 was used as eluent in the separation to obtain pure 3-(3-methoxyphenyl)-1,5-dimethyl-8-oxabicyclo[3.2.1]oct-3-ene as a yellow oil in 91% isolated yield (44.6 mg, 0.18 mmol). ^{1}H NMR (400 MHz, $CDCl_3$, ppm) δ 7.26 – 7.20 (m, 1H), 7.01 – 6.96 (m, 1H), 6.91 (t, *J* = 2.0 Hz, 1H), 6.84 – 6.77 (m, 1H), 6.22 (t, *J* = 1.7 Hz, 1H), 3.81 (s, 3H), 2.68 (d, *J* = 16.6 Hz, 1H), 2.26 (dd, *J* = 16.7, 1.2 Hz, 1H), 2.08 – 2.04 (m, 1H), 1.93 – 1.89 (m, 1H), 1.84 – 1.78 (m, 2H), 1.50 (s, 3H), 1.48 (s, 3H). DEPTQ-135 NMR (101 MHz, $CDCl_3$, ppm) δ 159.78 (s, C), 141.51 (s, C), 133.50 (s, C), 131.36 (s, CH), 129.37 (s, CH), 117.58 (s, CH), 112.67 (s, CH), 110.97 (s, CH), 79.68 (s, C), 79.46 (s, C), 55.35 (s, CH_3), 42.31 (s, CH_2), 42.27 (s, CH_2), 37.49 (s, CH_2), 27.38 (s, CH_3), 23.74 (s, CH_3). Structure confirmed by ^{1}H COSY NMR and ^{1}H-^{13}C HMQC NMR. APCI$^+$ m/z calc for $C_{16}H_{21}O_2^+$ $[M+H]^+$ 245.1542, found 245.1532 (-4.1 ppm).

1,5-Dimethyl-3-(o-tolyl)-8-oxabicyclo[3.2.1]oct-2-ene (35)

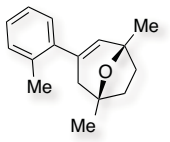

Compound **35** was synthesized following the general procedure starting from 5-methylhex-5-en-2-one (26.0 µl, 0.2 mmol) and 1-ethynyl-2-methylbenzene (88.0 µl, 0.7 mmol) with catalyst **A** (9.0 mg, 0.01 mmol). The reaction time was 20 h and a mixture of pentane and CH_2Cl_2 (1:1) was used as eluent in the separation to obtain pure 1,5-dimethyl-3-(o-tolyl)-8-oxabicyclo[3.2.1]oct-3-ene as a yellow oil in 41% isolated yield (18.5 mg, 0.08 mmol). ^{1}H NMR (400 MHz, $CDCl_3$, ppm) δ 7.18 –7.11 (m, 3H), 7.09 – 7.04 (m, 1H), 5.70 – 5.62 (m, 1H), 2.57 (d, *J* = 17.2 Hz, 1H), 2.30 (s, 3H), 2.14 – 1.99 (m, 3H), 1.89 – 1.78 (m, 2H), 1.45 (s, 3H), 1.45 (s, 3H). DEPTQ-135 NMR (101 MHz, $CDCl_3$, ppm) δ 141.64 (s, C), 135.70 (s, C), 135.16 (s, C), 133.39 (s, CH), 130.31 (s, CH), 128.24 (s, CH), 127.01 (s, CH), 125.74 (s, CH), 79.61 (s, C), 45.11 (s, CH_2), 42.62 (s, CH_2), 37.66 (s, CH_2), 27.21 (s, CH_3), 23.61 (s, CH_3), 19.88 (s, CH_3). Structure confirmed by ^{1}H COSY NMR and ^{1}H-^{13}C HMQC NMR. APCI$^+$ m/z calc for $C_{16}H_{19}^+$ $[MOH]^+$ 211.1487, found 211.1487 (0.0 ppm).

1,5-Dimethyl-3-(thiophen-3-yl)-8-oxabicyclo[3.2.1]oct-2-ene (36)

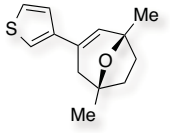

Compound **36** was synthesized following the general procedure starting from 5-methylhex-5-en-2-one (26.0 µl, 0.2 mmol) and 3-ethynylthiophene (69.0 µl, 0.7 mmol) with catalyst **A** (9.0 mg, 0.01 mmol). The reaction time was 19 h (no complete conversion was observed after after 67 h) and a mixture of pentane and CH_2Cl_2 (1:5) was used as eluent in the separation to obtain pure 1,5-dimethyl-3-(thiophen-3-yl)-8-oxabicyclo[3.2.1]oct-3-ene as a brownish oil in 40% isolated yield (17.5 mg, 0.08 mmol). ^{1}H NMR (500 MHz, $CDCl_3$, ppm) δ 7.28 – 7.24 (m, 1H), 7.22 (dd, *J* = 5.1, 1.3 Hz, 1H), 7.09 (dd, *J* = 2.9, 1.3 Hz, 1H), 6.18 (t, *J* = 1.6 Hz, 1H), 2.67 (d, *J* = 16.1 Hz, 1H), 2.24 (dd, *J* = 16.5, 1.2 Hz, 1H), 2.09 – 2.00 (m, 1H), 1.94 – 1.85 (m, 1H), 1.83 – 1.78 (m, 2H), 1.49 (s, 3H), 1.47 (s, 3H). ^{13}C NMR (126 MHz, $CDCl_3$, ppm) δ 142.04 (s), 130.22 (s), 129.15

(s), 125.69 (s), 124.68 (s), 119.25 (s), 79.57 (s), 79.39 (s), 42.43 (s), 42.26 (s), 37.51 (s), 27.38 (s), 23.83 (s). Structure confirmed by ^{1}H COSY NMR and ^{1}H-^{13}C HMQC NMR. APCI^{+} m/z calc for $C_{13}H_{17}OS^{+}$ [M+H]$^{+}$ 221.1000, found 221.1003 (1.4 ppm).

3-(4-Methoxyphenyl)-1,5-dimethyl-8-oxabicyclo[3.2.1]oct-2-ene (44)

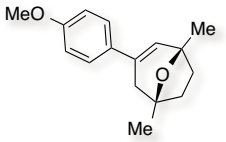

In this case, compound **44** was synthesized following the general procedure but switching the stoichiometry starting from 5-methylhex-5-en-2-one (112.0 µl, 0.99 mmol) and 1-ethynyl-4-methoxybenzene (28.4mg, 0.22 mmol) with catalyst **A** (9.0 mg, 0.01 mmol). The reaction time was 20 h and a mixture of pentane and CH_2Cl_2 (1:1) was used as eluent in the separation. If the starting material was not anhydrous, 1-(4-methoxyphenyl)ethanone was also formed and it had to be separated using an aluminium oxide preparative TLC plate and a mixture of pentane and CH_2Cl_2 (1:1) to obtain pure 3-(4-methoxyphenyl)-1,5-dimethyl-8-oxabicyclo[3.2.1]oct-3-ene as a yellowish doughy powder in 43% isolated yield (22.3 mg, 0.09 mmol). ^{1}H NMR (400 MHz, $CDCl_3$, ppm) δ 7.32 (d, *J* = 8.9 Hz, 2H), 6.85 (d, *J* = 8.9 Hz, 2H), 6.13 (t, *J* = 1.6 Hz, 1H), 3.80 (s, 3H), 2.66 (d, *J* = 16.6 Hz, 1H), 2.25 (dd, *J* = 16.6, 1.2 Hz, 1H), 2.18 – 2.01 (m, 1H), 1.92 – 1.86 (m, 1H), 1.83 – 1.77 (m, 2H), 1.50 (s, 3H), 1.48 (s, 3H). DEPTQ-135 NMR (101 MHz, $CDCl_3$, ppm) δ 159.12 (s, C), 132.93 (s, C), 132.53 (s, C), 129.38 (s, CH), 126.06 (s, CH), 113.82 (s, CH), 79.72 (s, C), 79.44 (s, C), 55.43 (s, CH_3), 42.38 (s, CH_2), 42.31 (s, CH_2), 37.53 (s, CH_2), 27.44 (s, CH_3), 23.87 (s, CH_3). Structure confirmed by ^{1}H COSY NMR and ^{1}H-^{13}C HMQC NMR. APCI^{+} m/z calc for $C_{16}H_{21}O_2^{+}$ [M+H]$^{+}$ 245.1542, found 245.1532 (-4.1 ppm).

1,5-Dimethyl-3-(p-tolyl)-8-oxabicyclo[3.2.1]oct-2-ene (45)

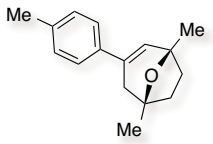

In this case, compound **45** was synthesized following the general procedure but switching the stoichiometry starting from 5-methylhex-5-en-2-one (104.0 µl, 0.80 mmol) and 1-ethynyl-4-methylbenzene (23.2mg, 0.20 mmol) with catalyst **A** (9.0 mg, 0.01 mmol). The reaction time was 20 h and a mixture of pentane and CH_2Cl_2 (1:3) was used as eluent in the separation to obtain pure 1,5-dimethyl-3-(p-tolyl)-8-oxabicyclo[3.2.1]oct-3-ene as a yellow oil in 52% isolated yield (23.7 mg, 0.10 mmol). ^{1}H NMR (500 MHz, $CDCl_3$, ppm) δ 7.28 (d, *J* = 8.2 Hz, 2H), 7.12 (d, *J* = 8.0 Hz, 2H), 6.18 (t, *J* = 1.6 Hz, 1H), 2.67 (d, *J* = 16.6 Hz, 1H), 2.33 (s, 3H), 2.26 (dd, *J* = 16.7, 1.1 Hz, 1H), 2.07 – 2.03 (m, 1H), 1.93 – 1.85 (m, 1H), 1.83 – 1.78 (m, 2H), 1.50 (s, 3H), 1.48 (s, 3H). DEPTQ-135 NMR (126 MHz, $CDCl_3$, ppm) δ 137.15 (s, C), 137.07 (s, C), 133.38 (s, C), 130.20 (s, CH), 129.13 (s, CH), 124.86 (s, CH), 79.70 (s, C), 79.45 (s, C), 42.36 (s, CH_2), 42.23 (s, CH_2), 37.52 (s, CH_2), 27.42 (s, CH_3), 23.81 (s, CH_3), 21.20 (s, CH_3). Structure confirmed by ^{1}H COSY NMR and ^{1}H-^{13}C HMQC NMR. APCI^{+} m/z calc for $C_{16}H_{21}O^{+}$ [M+H]$^{+}$ 229.1592, found 229.1587 (-4.1 ppm).

1-Methyl-3,5-diphenyl-8-oxabicyclo[3.2.1]oct-2-ene (47)

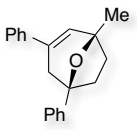

Compound **47** was synthesized following the general procedure starting from 5-phenyl-5-hexen-2-one (35.8 mg, 0.2 mmol) and ethynylbenzene (77.0 µl, 0.7 mmol) with catalyst **A** (9.0 mg, 0.01 mmol). The reaction time was 19 h and a mixture of pentane and CH_2Cl_2 (1:1) was used as eluent in the separation to obtain pure 1-methyl-3,5-diphenyl-8-oxabicyclo[3.2.1]oct-2-ene as a yellowish powder in 67% isolated yield (37.9 mg, 0.14 mmol).

^{1}H NMR (500 MHz, $CDCl_3$, ppm) δ 7.52 (d, *J* = 7.1 Hz, 2H), 7.41 (d, *J* = 7.1 Hz, 2H), 7.38 (t, *J* = 7.8 Hz, 2H), 7.32 (t, *J* = 7.5 Hz, 2H), 7.29 – 7.23 (m, 2H), 6.32 (t, *J* = 1.7 Hz, 1H), 2.90 (d, *J* = 16.5 Hz, 1H), 2.68 (d, *J* = 16.6 Hz, 1H), 2.42 – 2.27 (m, 1H), 2.22 – 2.16 (m, 2H), 1.89 – 1.83 (m, 1H), 1.60 (s, 3H). ^{13}C NMR (126 MHz, $CDCl_3$, ppm) δ 147.34 (s), 139.80 (s), 133.47 (s), 131.02 (s), 128.51 (s), 128.40 (s), 127.55 (s), 126.81 (s), 125.06 (s), 124.46 (s), 82.85 (s), 79.88 (s), 43.25 (s), 42.18 (s), 38.82 (s), 23.72 (s). Structure confirmed by ^{1}H COSY NMR and ^{1}H-^{13}C HMQC NMR. APCI$^+$ m/z calc for $C_{20}H_{21}O^+$ $[M+H]^+$ 277.1592, found 277.1586 (-2.2 ppm). Mp 113.8 – 114.9 ºC.

3-(4-Fluorophenyl)-1-methyl-5-phenyl-8-xabicyclo[3.2.1]oct-2-ene (48)

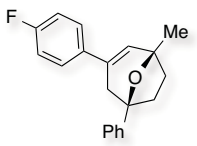

Compound **48** was synthesized following the general procedure starting from 5-phenyl-5-hexen-2-one (37.3 mg, 0.2 mmol) and 1-ethynyl-4-fluorobenzene (80.0 µl, 0.7 mmol) with catalyst **A** (9.0 mg, 0.01 mmol). The reaction time was 20 h and a mixture of pentane and CH_2Cl_2 (1:1) was used as eluent in the separation to obtain pure 3-(4-fluorophenyl)-1-methyl-5-phenyl-8-oxabicyclo[3.2.1]oct-2-ene as a yellow oil in 65% isolated yield (40.9 mg, 0.14 mmol). ^{1}H NMR (500 MHz, $CDCl_3$, ppm) δ 7.51 (dd, *J* = 8.3, 1.3 Hz, 2H), 7.40 – 7.30 (m, 4H), 7.26 (tt, *J* = 6.9, 1.3 Hz, 1H), 6.99 (t, *J* = 8.7 Hz, 2H), 6.25 (t, *J* = 1.6 Hz, 1H), 2.85 (d, *J* = 17.0 Hz, 1H), 2.63 (d, *J* = 16.6 Hz, 1H), 2.35 – 2.30 (m, 1H), 2.22 – 2.14 (m, 2H), 1.89 – 1.82 (m, 1H), 1.59 (s, 3H). DEPTQ-135 NMR (126 MHz, $CDCl_3$, ppm) δ 163.37 (d, *J* (^{13}C-^{19}F) = 246.5 Hz, C), 147.20 (s, C), 135.88 (d, *J* (^{13}C-^{19}F) = 3.4 Hz, C), 132.57 (s, C), 130.89 (s, CH), 128.40 (s, CH), 126.74 (d, *J* (^{13}C-^{19}F) = 25.7 Hz, CH), 126.57 (s, CH), 124.42 (s, CH), 115.31 (d, *J* (^{13}C-^{19}F) = 21.5 Hz, CH), 82.77 (s, C), 79.81 (s, C), 43.41 (s, CH_2), 42.10 (s, CH_2), 38.78 (s, CH_2), 23.70 (s, CH_3). ^{19}F NMR (376 MHz, CDCl3, ppm) δ -115.17 (s). Structure confirmed by ^{1}H COSY NMR and ^{1}H-^{13}C HMQC NMR. APCI$^+$ m/z calc for $C_{20}H_{20}OF^+$ $[M+H]^+$ 295.1498, found 295.1495 (-4.4 ppm).

3-(4-Chlorophenyl)-1-methyl-5-phenyl-8-xabicyclo[3.2.1]oct-2-ene (49)

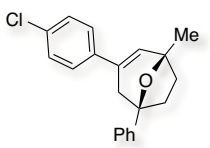

Compound **49** was synthesized following the general procedure starting from 5-phenyl-5-hexen-2-one (35.7 mg, 0.2 mmol) and 1-chloro-4-ethynylbenzene (96.0 mg, 0.7 mmol) with catalyst **A** (9.0 mg, 0.01 mmol). The reaction time was 18 h and a mixture of pentane and CH_2Cl_2 (1:10) was used as eluent in the separation to obtain pure 3-(4-chlorophenyl)-1-methyl-5-phenyl-8-oxabicyclo[3.2.1]oct-2-ene as a yellow oil in 62% isolated yield (38.9 mg, 0.13 mmol). ^{1}H NMR (500 MHz, $CDCl_3$, ppm) δ 7.51 (dd, *J* = 8.3, 1.2 Hz, 2H), 7.37 (t, *J* = 7.7 Hz, 2H), 7.34 – 7.29 (m, 2H), 7.29 – 7.24 (m, 3H), 6.31 (t, *J* = 8.3 Hz 1H), 2.84 (d, *J* = 16.6 Hz, 1H), 2.62 (d, *J* = 16.9 Hz, 1H), 2.35 – 2.29 (m, 1H), 2.26 – 2.13 (m, 2H), 1.89 – 1.83 (m, 1H), 1.59 (s, 3H). DEPTQ-135 NMR (126 MHz, $CDCl_3$, ppm) δ 147.13 (s, C), 138.20 (s, C), 133.23 (s, C), 132.49 (s, C), 131.55 (s, CH), 128.61 (s, CH), 128.42 (s, CH), 126.87 (s, CH), 126.31 (s, CH), 124.41 (s, CH), 82.77 (s, C), 79.82 (s, C), 43.20 (s, CH_2), 42.06 (s, CH_2), 38.76 (s, CH_2), 23.66 (s, CH_3). Structure confirmed by ^{1}H COSY NMR and ^{1}H-^{13}C HMQC NMR. APCI$^+$ m/z calc for $C_{20}H_{20}OCl^+$ $[M+H]^+$ 311.1203, found 311.1217 (4.5 ppm).

3-(4-Bromophenyl)-1-methyl-5-phenyl-8-xabicyclo[3.2.1]oct-2-ene (50)

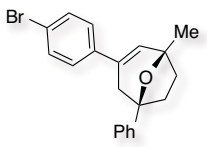

Compound **50** was synthesized following the general procedure starting from 5-phenyl-5-hexen-2-one (34.5 mg, 0.2 mmol) and 1-bromo-4-ethynylbenzene (125.0 mg, 0.7 mmol) with catalyst **A** (9.0 mg, 0.01 mmol). The reaction time was 15 h and a mixture of pentane and CH_2Cl_2 (1:1) was used as eluent in the separation to obtain pure 3-(4-bromophenyl)-1-methyl-5-phenyl-8-oxabicyclo[3.2.1]oct-2-ene as a yellow oil in 70% isolated yield (48.2 mg, 0.14 mmol). ^{1}H NMR (500 MHz, $CDCl_3$, ppm) δ 7.56 (dd, *J* = 8.3, 1.2 Hz, 2H), 7.47 (d, *J* = 8.6 Hz, 2H), 7.42 (t, *J* = 7.7 Hz, 2H), 7.36 – 7.28 (m, 3H), 6.37 (t, *J* = 1.6 Hz, 1H), 2.89 (d, *J* = 16.5 Hz, 1H), 2.67 (d, *J* = 17.0 Hz, 1H), 2.40 – 2.34 (m, 1H), 2.30 – 2.12 (m, 2H), 1.93 – 1.87 (m, 1H), 1.64 (s, 3H). ^{13}C NMR (101 MHz, $CDCl_3$, ppm) δ 147.09 (s), 138.65 (s), 132.54 (s), 131.62 (s), 131.55 (s), 128.42 (s), 126.88 (s), 126.64 (s), 124.40 (s), 121.37 (s), 82.77 (s), 79.83 (s), 43.12 (s), 42.04 (s), 38.75 (s), 23.64 (s). Structure confirmed by ^{1}H COSY NMR and ^{1}H-^{13}C HMQC NMR. APCI$^+$ m/z calc for $C_{20}H_{20}OBr^+$ $[M+H]^+$ 355.0698, found 355.0705 (2.0 ppm).

3-(3-fluorophenyl)-1-methyl-5-phenyl-8-xabicyclo[3.2.1]oct-2-ene (51)

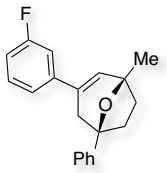

Compound **51** was synthesized following the general procedure starting from 5-phenyl-5-hexen-2-one (34.6 mg, 0.2 mmol) and 1-ethynyl-3-fluorobenzene (81.0 µl, 0.7 mmol) with catalyst **A** (9.0 mg, 0.01 mmol). The reaction time was 20 h and a mixture of pentane and CH_2Cl_2 (1:1) was used as eluent in the separation to obtain pure 3-(3-fluorophenyl)-1-methyl-5-phenyl-8-oxabicyclo[3.2.1]oct-2-ene as a yellow oil in 59% isolated yield (34.4 mg, 0.12 mmol). ^{1}H NMR (500 MHz, $CDCl_3$, ppm) δ 7.51 (dd, *J* = 8.3, 1.2 Hz, 2H), 7.37 (t, *J* = 7.7 Hz, 2H), 7.31 – 7.22 (m, 2H), 7.17 (dt, *J* = 7.8, 1.1 Hz, 1H), 7.09 (dt, *J* = 10.7, 2.1 Hz, 1H), 6.93 (td, *J* = 8.2, 3.3 Hz, 1H), 6.34 (t, *J* = 1.7 Hz, 1H), 2.86 (d, *J* = 16.4 Hz, 1H), 2.63 (d, *J* = 16.6 Hz, 1H), 2.35 – 2.29 (m, 1H), 2.25 – 2.08 (m, 2H), 1.89 – 1.83 (m, 1H), 1.60 (s, 3H). DEPTQ-135 NMR (126 MHz, $CDCl_3$, ppm) δ 163.15 (d, *J* (^{13}C-^{19}F) = 244.5 Hz, C), 147.09 (s, C), 142.14 (d, *J* (^{13}C-^{19}F) = 7.5 Hz, C), 132.56 (s, C), 132.12 (s, CH), 129.89 (d, J (^{13}C-^{19}F) = 9.5 Hz, CH), 128.43 (s, CH), 126.89 (s, C), 124.42 (s, C), 120.62 (d, *J* (^{13}C-^{19}F) = 2.6 Hz, CH), 114.28 (d, *J* (^{13}C-^{19}F) = 21.6 Hz, CH), 111.97 (d, *J* (^{13}C-^{19}F) = 22.5 Hz, CH), 82.77 (s, C), 79.81 (s, C), 43.16 (s, CH_2), 42.05 (s, CH_2), 38.77 (s, CH_2), 23.62 (s, CH_3). ^{19}F NMR (376 MHz, $CDCl_3$, ppm) δ -113.50 (s). Structure confirmed by ^{1}H COSY NMR and ^{1}H-^{13}C HMQC NMR. APCI$^+$ m/z calc for $C_{20}H_{20}OF^+$ $[M+H]^+$ 295.1498, found 295.1486 (-4.1 ppm).

3-(3-Chlorophenyl)-1-methyl-5-phenyl-8-oxabicyclo[3.2.1]oct-2-ene (52)

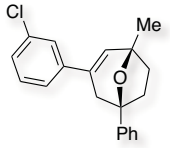

Compound **52** was synthesized following the general procedure starting from 5-phenyl-5-hexen-2-one (35.9 mg, 0.2 mmol) and 1-chloro-3-ethynylbenzene (86.0 ml, 0.7 mmol) with catalyst **A** (9.0 mg, 0.01 mmol). The reaction time was 20 h and a mixture of pentane and CH_2Cl_2 (1:1) was used as eluent in the separation to obtain pure 3-(3-chlorophenyl)-1-methyl-5-phenyl-8-oxabicyclo[3.2.1]oct-2-ene as a yellow oil in 60 % isolated yield (38.3 mg, 0.12 mmol). ^{1}H NMR (500 MHz, $CDCl_3$, ppm) δ 7.51 (dd, *J* = 8.3, 1.1 Hz, 2H), 7.37 (t, *J* = 7.4 Hz, 3H), 7.32 – 7.19 (m, 4H), 6.34 (t, *J* = 16.5 Hz, 1H), 2.85 (d, *J* = 16.5 Hz, 1H), 2.62 (d, *J* = 16.5 Hz, 1H), 2.35 – 2.29 (m, 1H), 2.25 – 2.06 (m, 2H), 1.89 – 1.83 (m, 1H), 1.59 (s, 3H). DEPTQ-135 NMR (126 MHz, $CDCl_3$, ppm) δ 147.05 (s,

C), 141.66 (s, C), 134.54 (s, C), 132.45 (s, C), 132.26 (s, CH), 129.71 (s, CH), 128.43 (s, CH), 127.48 (s, CH), 126.89 (s, CH), 125.28 (s, CH), 124.41 (s, CH), 123.15 (s, CH), 82.76 (s, C), 79.81 (s, C), 43.13 (s, CH_2), 42.05 (s, CH_2), 38.75 (s, CH_2), 23.62 (s, CH_3). Structure confirmed by ^{1}H COSY NMR and ^{1}H-^{13}C HMQC NMR. APCI$^+$ *m/z* calc for $C_{20}H_{19}OCl^+$ $[M+H]^+$ 311.1203, found 311.1218 (4.8 ppm).

5-Methyl-1,3-diphenyl-8-oxabicyclo[3.2.1]oct-2-ene (66)

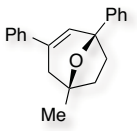

Compound **66** was synthesized following the general procedure starting from 4-methyl-1-phenyl-4-penten-1-one (34.8 mg, 0.2 mmol) and ethynylbenzene (77.0 µl, 0.7 mmol) with catalyst **A** (9.0 mg, 0.01 mmol). The reaction time was 19 h and a mixture of pentane and CH_2Cl_2 (1:1) was used as eluent in the separation to obtain pure 1-methyl-3,5-diphenyl-8-oxabicyclo[3.2.1]oct-3-ene as a yellowish powder in 87% isolated yield (48.0 mg, 0.17 mmol). ^{1}H NMR (400 MHz, $CDCl_3$, ppm) δ 7.54 (d, *J* = 7.0 Hz, 2H), 7.42 – 7.33 (m, 4H), 7.32 – 7.26 (m, 3H), 7.26 – 7.18 (m, 1H), 6.45 (t, *J* = 1.7 Hz, 1H), 2.80 (d, *J* = 16.6 Hz, 1H), 2.51 – 2.46 (m, 1H), 2.39 (d, *J* = 16.7 Hz, 1H), 2.19 – 2.12 (m, 1H), 2.07 – 2.00 (m, 1H), 1.96 – 1.86 (m, 1H), 1.59 (s, 3H). DEPTQ-135 NMR (126 MHz, $CDCl_3$, ppm) δ 143.49 (s, C), 139.76 (s, C), 133.50 (s, C), 131.16 (s, CH), 128.48 (s, CH), 128.45 (s, CH), 127.54 (s, CH), 127.22 (s, CH), 125.46 (s, CH), 125.08 (s, CH), 83.66 (s, C), 79.52 (s, C), 42.33 (s, CH_2), 42.14 (s, CH_2), 37.05 (s, CH_2), 27.45 (s, CH_3). Structure confirmed by ^{1}H COSY NMR and ^{1}H-^{13}C HMQC NMR. APCI$^+$ m/z calc for $C_{20}H_{21}O^+$ $[M+H]^+$ 277.1592, found 277.1587 (-1.8 ppm). Mp 78.9 – 79.5 ºC.

5-Methyl-3-phenyl-8-oxabicyclo[3.2.1]oct-2-ene (67)

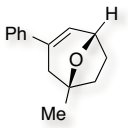

Compound **67** was synthesized following the general procedure starting from 4-methyl-4-pentenal (19.8 mg, 0.2 mmol) and ethynylbenzene (77.0 µl, 0.7 mmol) with catalyst **A** (9.0 mg, 0.01 mmol). The reaction time was 21 h and a mixture of pentane and CH_2Cl_2 (1:1) was used as eluent in the separation to obtain pure 1-methyl-3-phenyl-8-oxabicyclo[3.2.1]oct-3-ene as a yellow oil in 16% isolated yield (6.4 mg, 0.03 mmol). ^{1}H NMR (500 MHz, $CDCl_3$, ppm) δ 7.37 (d, *J* = 7.1 Hz, 2H), 7.31 (t, *J* = 7.6 Hz, 2H), 7.27 – 7.22 (m, 1H), 6.37 (dt, *J* = 4.6, 1.7 Hz, 1H), 4.67 (t, *J* = 5.4 Hz, 1H), 2.74 (d, *J* = 16.6 Hz, 1H), 2.32 (dd, *J* = 17.0, 1.0 Hz, 1H), 2.14 – 2.07 (m, 1H), 2.03 – 1.98 (m, 1H), 1.93 – 1.87 (m, 1H), 1.78 – 1.72 (m, 1H), 1.51 (s, 3H). ^{13}C NMR (126 MHz, $CDCl_3$, ppm) δ 139.88 (s), 133.58 (s), 128.48 (s), 127.68 (s), 127.47 (s), 124.96 (s), 78.95 (s), 74.76 (s), 42.78 (s), 36.04 (s), 35.75 (s), 27.20 (s). Structure confirmed by ^{1}H COSY NMR and ^{1}H-^{13}C HMQC NMR. APCI$^+$ m/z calc for $C_{14}H_{17}O^+$ $[M+H]^+$ 201.1279, found 201.1284 (2.5 ppm).

1-(Tert-butyl)-5-methyl-3-phenyl-8-oxabicyclo[3.2.1]oct-2-ene (68)

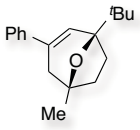

Compound **68** was synthesized following the general procedure starting from 2,2,6-trimethyl-6-hepten-3-one (23.3 mg, 0.15 mmol) and ethynylbenzene (58.1 µl, 0.53 mmol) with catalyst **A** (6.8 mg, 0.007 mmol). The reaction time was 19 h and a mixture of pentane and CH_2Cl_2 (2:1) was used as eluent in the separation to obtain pure 1-(tert-butyl)-5-methyl-3-phenyl-8-oxabicyclo[3.2.1]oct-2-ene as a yellow oil in 54% isolated yield (27.9 mg, 0.11 mmol). ^{1}H NMR (500 MHz, $CDCl_3$, ppm) δ 7.39 (d, *J* = 7.1 Hz, 2H), 7.32 (t, *J* = 7.6 Hz, 2H), 7.26 – 7.20 (m, 1H), 6.53 – 6.42 (m, 1H), 2.66 (d, *J* = 16.5 Hz, 1H), 2.26 (d, *J* = 16.5 Hz, 1H), 2.00 – 1.95 (m, 1H), 1.89 – 1.77 (m, 2H), 1.71 – 1.66 (m, 1H), 1.45 (s,

3H), 1.04 (s, 9H). ^{13}C NMR (126 MHz, $CDCl_3$, ppm) δ 140.68 (s), 133.51 (s), 129.22 (s), 128.45 (s), 127.21 (s), 124.98 (s), 87.11 (s), 78.96 (s), 42.37 (s), 37.08 (s), 35.56 (s), 34.74 (s), 27.47 (s), 25.62 (s). Structure confirmed by ^{1}H COSY NMR and ^{1}H-^{13}C HMQC NMR. APCI$^+$ m/z calc for $C_{18}H_{25}O^+$ $[M+H]^+$ 257.1905, found 257.1904 (-0.4 ppm).

4-(4,4-Dimethyl-2-phenylcyclobut-2-en-1-yl)butan-2-one (69)

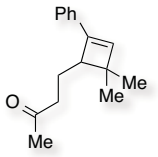

Compound **69** was synthesized following the general procedure starting from 6-mehtyl-5-hepten-2-one (30.0 µl, 0.2 mmol) and ethynylbenzene (77.0 µl, 0.7 mmol) with catalyst **A** (9.0 mg, 0.01 mmol). The reaction time was 19 h and a mixture of pentane and CH_2Cl_2 (1:3) was used as eluent in the separation to obtain a 1:3.6 mixture of 1,4,4-trimethyl-3-phenyl-8-oxabicyclo[3.2.1]oct-2-ene (**70**) and 4-(4,4-dimethyl-2-phenylcyclobut-2-en-1-yl)butan-2-one in 77% isolated yield. The isomers were separated by preparative TLC using a mixture of cyclohexane and ethyl acetate (9:1) as eluent to obtain 4-(4,4-dimethyl-2-phenylcyclobut-2-en-1-yl)butan-2-one as a yellow oil in 53% isolated yield (24.2 mg, 0.11 mmol). ^{1}H NMR (500 MHz, $CDCl_3$, ppm) δ 7.37 – 7.28 (m, 4H), 7.26 – 7.19 (m, 1H), 6.28 (s, 1H), 2.70 (dd, *J* = 10.6, 4.1 Hz, 1H), 2.56 – 2.45 (m, 2H), 2.15 (s, 3H), 2.13 – 2.08 (m, 1H), 1.68 (m, 1H), 1.25 (s, 3H), 1.17 (s, 3H). ^{13}C NMR (126 MHz, $CDCl_3$, ppm) δ 208.83 (s), 145.58 (s), 136.48 (s), 134.71 (s), 128.49 (s), 127.53 (s), 125.22 (s), 51.04 (s), 42.92 (s), 42.88 (s), 30.10 (s), 27.97 (s), 23.44 (s), 21.95 (s). Structure confirmed by ^{1}H COSY NMR and ^{1}H-^{13}C HMQC NMR. APCI$^+$ m/z calc for $C_{16}H_{21}O^+$ $[M+H]^+$ 229.1592, found 229.1594 (0.9 ppm).

1,4,4-Trimethyl-3-phenyl-8-oxabicyclo[3.2.1]oct-2-ene (70)

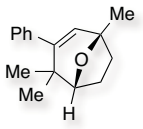

Compound **70** was synthesized following the general procedure starting from 6-mehtyl-5-hepten-2-one (30.0 µl, 0.2 mmol) and ethynylbenzene (77.0 µl, 0.7 mmol) with catalyst **A** (9.0 mg, 0.01 mmol). The reaction time was 19 h and a mixture of pentane and CH_2Cl_2 (1:3) was used as eluent in the separation to obtain a 1:3.6 mixture of 1,4,4-trimethyl-3-phenyl-8-oxabicyclo[3.2.1]oct-2-ene and 4-(4,4-dimethyl-2-phenylcyclobut-2-en-1-yl)butan-2-one (**69**) in 77% isolated yield. The isomers were separated by preparative TLC using a mixture of cyclohexane and ethyl acetate (9:1) as eluent to obtain 1,4,4-trimethyl-3-phenyl-8-oxabicyclo[3.2.1]oct-2-ene as a yellow oil in 16% isolated yield (7.5 mg, 0.03 mmol). ^{1}H NMR (500 MHz, $CDCl_3$, ppm) δ 7.29 – 7.23 (m, 3H), 7.17 – 7.12 (m, 2H), 5.46 (s, 1H), 4.02 (dd, *J* = 7.7, 2.1 Hz, 1H), 2.11 – 1.99 (m, 2H), 1.98 – 1.93 (m, 1H), 1.62 (td, *J* = 11.0, 7.5 Hz, 1H), 1.42 (s, 3H), 1.31 (s, 3H), 0.84 (s, 3H). ^{13}C NMR (126 MHz, $CDCl_3$, ppm) δ 143.92 (s), 140.88 (s), 131.67 (s), 129.01 (s), 127.72 (s), 126.75 (s), 85.00 (s), 78.97 (s), 40.37 (s), 39.84 (s), 28.50 (s), 25.80 (s), 23.09 (s), 22.21 (s). Structure confirmed by ^{1}H COSY NMR, ^{1}H-^{13}C HMQC NMR and ^{1}H-^{13}C HMBC NMR. APCI$^+$ m/z calc for $C_{16}H_{21}O^+$ $[M+H]^+$ 229.1592, found 229.1594 (0.9 ppm).

Ethyl 3-(1-methyl-3-phenylcyclobut-2-en-1-yl)propanoate (74)

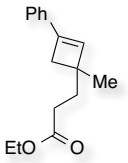

Compound **70** was synthesized following the general procedure starting from ethyl 4-methyl-4-pentenoate (32.0 ml, 0.2 mmol) and ethynylbenzene (77.0 ml, 0.7 mmol) with catalyst **A** (9.0 mg, 0.01 mmol). The reaction time was 20 h and a mixture of pentane and CH_2Cl_2 (3:1) was used as eluent in the separation to obtain pure ethyl 3-(1-methyl-3-phenylcyclobut-2-en-1-yl)propanoate as a yellow oil in 47% isolated yield (23.0 mg, 0.09 mmol).

^{1}H NMR (400 MHz, $CDCl_3$, ppm) δ 7.36 – 7.28 (m, 4H), 7.27 – 7.21 (m, 1H), 6.35 (s, 1H), 4.12 (q, *J* = 7.1 Hz, 2H), 2.56 (d, *J* = 12.7 Hz, 1H), 2.44 (d, *J* = 12.7 Hz, 1H), 2.35 (ddd, *J* = 8.7, 7.0, 1.5 Hz, 2H), 1.99 – 1.81 (m, 2H), 1.25 (s, 3H), 1.24 (t, *J* = 7.1 Hz, 3H). DEPTQ-135 (101 MHz, $CDCl_3$, ppm) δ 174.28 (s, C), 143.08 (s, C), 134.94 (s, C), 134.60 (s, CH), 128.41 (s, CH), 127.78 (s, CH), 124.56 (s, CH), 60.42 (s, CH_2), 42.31 (s, C), 40.38 (s, CH_2), 34.79 (s, CH_2), 31.20 (s, CH_2), 24.30 (s, CH_3), 14.36 (s, CH_3). Structure confirmed by ^{1}H COSY NMR, ^{1}H-^{13}C HMQC NMR and IR. APCI$^+$ *m/z* calc for $C_{16}H_{21}O_2^+$ $[M+H]^+$ 245.1542, found 245.1541 (-0.4 ppm).

8-Methyl-6-phenyl-1,2,3,4,5,8,9,9a-octahydro-4a,8-epoxybenzo[7]annulene (82)

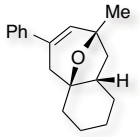

Compound **82** was synthesized following the general procedure starting from 1-(2-methylenecyclohexyl)propan-2-one **78** (30.0 mg, 0.2 mmol) and ethynylbenzene (110.0 µl, 1.0 mmol) with 10 mol% of catalyst **A** (18.0 mg, 0.02 mmol). The reaction time was 22 h and a silica gel column with pentane and diethyl ether (100:1) as eluent was used in the separation to obtain pure 8-methyl-6-phenyl-1,2,3,4,5,8,9,9a-octahydro-4a,8-epoxybenzo[7]annulene as a yellow oil in 31% isolated yield (15.7 mg, 0.06 mmol). ^{1}H NMR (400 MHz, $CDCl_3$, ppm) δ 7.33 – 7.29 (m, 2H), 7.26 – 7.21 (m, 2H), 7.19 – 7.14 (m, 1H), 6.23 (t, *J* = 1.7 Hz, 1H), 2.51 (dd, *J* = 17.0, 1.7 Hz, 1H), 2.28 – 2.18 (m, 2H), 1.99 – 1.93 (m, 1H), 1.91 – 1.85 (m, 1H), 1.68 – 1.55 (m, 4H), 1.48 – 1.43 (m, 1H), 1.42 (s, 3H), 1.39 – 1.33 (m, 1H), 1.24 – 1.15 (m, 2H). ^{13}C NMR (101 MHz, $CDCl_3$, ppm) δ 140.03 (s), 133.44 (s), 132.44 (s), 128.43 (s), 127.35 (s), 124.97 (s), 80.17 (s), 77.73 (s), 50.17 (s), 43.31 (s), 41.99 (s), 32.72 (s), 29.48 (s), 24.31 (s), 20.37 (s), 18.77 (s). Structure confirmed by ^{1}H COSY NMR, ^{1}H-^{13}C HMQC NMR, ^{1}H-^{13}C HMBC NMR and ^{1}H NOESY NMR (Figure 11). ESI$^+$ m/z calc for $C_{18}H_{22}NaO^+$ $[M+Na]^+$ 277.1563, found 277.1563 (0.0 ppm).

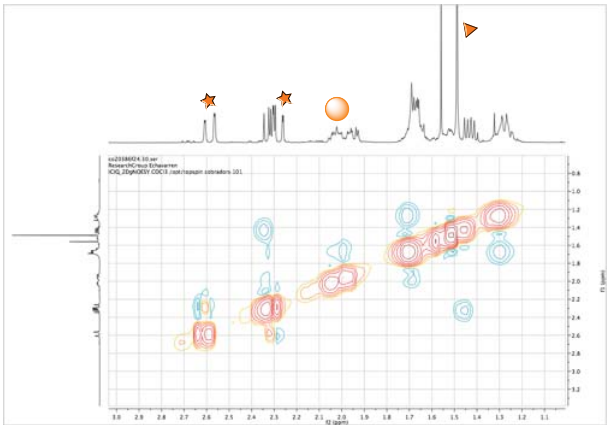

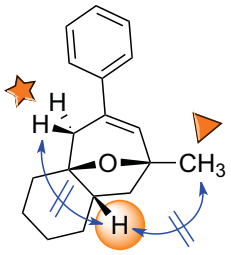

Figure 1. ^{1}H NOESY NMR spectra of 82, aliphatic region.

8-Isopropyl-6-(3-methoxyphenyl)-1,2,3,4,5,8,9,9a-octahydro-4a,8-epoxybenzo[7]annulene (84)

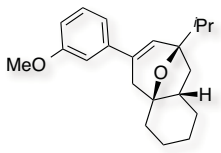

Compound **84** was synthesized following the general procedure starting from 3-methyl-1-(2-methylenecyclohexyl)butan-2-one **79** (36.0 mg, 0.2 mmol) and *m*-methoxyethynylbenzene (102.0 µl, 1.0 mmol) with 10 mol% of catalyst **A** (18.0 mg, 0.02 mmol). The reaction time was 21 h and a silica gel Prep-TLC with pentane and

diethyl ether (10:1) as eluent was used in the separation to obtain pure 8-isopropyl-6-(3-methoxyphenyl)-1,2,3,4,5,8,9,9a-octahydro-4a,8-epoxybenzo[7]annulene as a yellow oil in 19% isolated yield (10.5 mg, 0.03 mmol). ^{1}H NMR (400 MHz, $CDCl_3$, ppm) δ 7.23 (d, *J* = 7.88 Hz, 1H), 6.99 (ddd, *J* = 7.74, 1.72, 0.96 Hz, 1H), 6.92 – 6.91 (m, 1H), 6.79 (ddd, *J* = 8.20, 2.54, 0.82 Hz, 1H), 6.44 (t, *J* = 1.64 Hz, 1H), 3.82 (s, 3H), 2.58 (dd, *J* = 16.94 Hz, 1.48 Hz, 1H), 2.26 (dd, *J* = 17.04, 1.56 Hz, 1H), 2.16 (dd, *J* = 11.44, 8.09 Hz, 1H), 2.02 – 1.92 (m, 3H), 1.68 – 1.62 (m, 4H), 1.54 – 1.49 (m, 1H), 1.47 (dd, *J* = 11.79, 5.14 Hz, 1H), 1.30 – 1.19 (m, 2H), 1.05 (d, *J* = 7.00 Hz, 3H), 1.03 (d, *J* = 6.82 Hz, 3H). ^{13}C NMR (101 MHz, $CDCl_3$, ppm) δ 159.78 (s), 142.13 (s), 133.96 (s), 130.18 (s), 129.36 (s), 117.59 (s), 112.29 (s), 111.13 (s), 83.24 (s), 79.71 (s), 55.41 (s), 45.84 (s), 42.59 (s), 42.56 (s), 34.33 (s), 32.96 (s), 29.66 (s), 20.69 (s), 19.06 (s), 18.13 (s), 17.67 (s). Structure confirmed by ^{1}H COSY NMR, ^{1}H-^{13}C HMQC NMR, ^{1}H-^{13}C HMBC NMR and ^{1}H NOESY NMR. ESI$^+$ m/z calc for $C_{21}H_{28}NaO_2^+$ $[M+Na]^+$ 335.1982, found 335.1980 (0.3 ppm).

Procedures for the Derivatization of Oxabicycles

3-(1,5-Dimethyl-8-oxabicyclo[3.2.1]octan-3-yl)cyclohexanol (92)

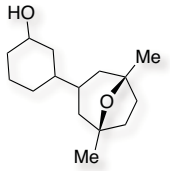

A high pressure steel autoclave was charged with 3-(1,5-dimethyl-8-oxabicyclo[3.2.1]oct-3-en-3-yl)phenol **33** (23 mg, 0.10 mmol) in ethanol (1.3 ml) and Ni-Raney (0.60 mg, 0.01 mmol). The autoclave was pressurized to 80 atm with H_2 and the reaction mixture was stirred at 80 ºC for 12 h. Then, the pressure was released slowly and the suspension was filtered though Celite washing with ethanol. The residue was concentrated and purified by silica gel column chromatography using cyclohexane:ethynl acetate (5:1) to obtain 3-(1,5-dimethyl-8-oxabicyclo[3.2.1]octan-3-yl)cyclohexanol **92** in 59% isolated yield as a mixture of diastereoisomers (14 mg, 0.06 mmol). ^{1}H NMR for the mixture of diastereoisomers (400 MHz, $CDCl_3$, ppm) δ 3.56 – 3.49 (m, 1H), 2.11 – 2.00 (m, 1.2H), 1.97 – 1.95 (m, 1.1H), 1.81 – 1.76 (m, 2H), 1.75 – 1.67 (m, 5H), 1.66 – 1.62 (m, 4.3H), 1.55 – 1.51 (m, 2.5H), 1.39 – 1.34 (m, 1.6H), 1.32 – 1.31 (m, 4.5H), 1.29 (m, 3H), 1.26 – 1.19 (m, 0.5H). ^{13}C NMR for the major diastereoisomer (126 MHz, $CDCl_3$, ppm) δ 79.08 (s), 71.20 (s), 40.98 (s), 40.08 (s), 39.46 (s), 39.15 (s), 38.66 (s), 38.63 (s), 36.67 (s), 35.93 (s), 35.31 (s), 30.49 (s), 27.95 (s), 27.07 (s), 24.22 (s). ^{13}C NMR for a minor diastereoisomer (126 MHz, $CDCl_3$, ppm) δ 80.45 (s), 66.82 (s), 42.08 (s), 41.31 (s), 41.20 (s), 39.87 (s), 38.66 (s), 36.70 (s), 35.96 (s), 35.77 (s), 29.15 (s), 27.99 (s), 27.07 (s), 24.15 (s), 20.18 (s). Structure confirmed by ^{1}H COSY NMR and ^{1}H-^{13}C HMQC NMR.

3-(1,5-Dimethyl-8-oxabicyclo[3.2.1]octan-3-yl)phenol (93)

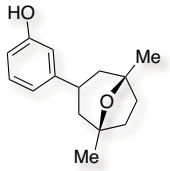

3-(1,5-Dimethyl-8-oxabicyclo[3.2.1]oct-3-en-3-yl)phenol **33** (23 mg, 0.10 mmol) and Pd/C 10% (11 mg, 0.01 mmol) were dissolved in methanol (1.2 ml). The solution was degassed three times with H_2 and stirred at 1 atm for 24 h at 25 ºC. The reaction mixture was filtered though Teflon 0.22 washing with CH_2Cl_2 and ethyl acetate. The combined filtrates were concentrated and the residue was purified with preparative TLC using cyclohexane:ethyl acetate (2:1) to obtain 3-(1,5-dimethyl-8-oxabicyclo[3.2.1]octan-3-yl)phenol **93** in 95% isolated yield as a 2:1 mixture of diastereoisomers (22 mg, 0.10 mmol). ^{1}H NMR for the mixture of diastereoisomers (400

MHz, $CDCl_3$, ppm) δ 7.18 – 7.14 (m, 1H), 6.86 – 6.76 (m, 2H), 6.72 – 6.67 (m, 1H), 3.10 – 2.96 (m, 1H), 2.07 – 2.01 (m, 1.5H), 1.99 – 1.85 (m, 0.6H), 1.85 – 1.65 (m, 6H), 1.40 – 1.38 (m, 6H). ^{13}C NMR for the major diastereoisomer (101 MHz, $CDCl_3$, ppm) δ 156.05 (s), 147.14 (s), 129.50 (s), 119.09 (s), 114.54 (s), 112.98 (s), 79.50 (s), 42.86 (s), 38.68 (s), 34.87 (s), 27.70 (s). ^{13}C NMR for the minor diastereoisomer (101 MHz, $CDCl_3$, ppm) δ 156.61 (s), 147.20 (s), 129.78 (s), 119.70 (s), 113.74 (s), 113.58 (s), 81.46 (s), 44.64 (s), 37.37 (s), 36.64 (s), 26.73 (s). Structure confirmed by ^1H COSY NMR and ^1H-^{13}C HMQC NMR.

General Procedure for the Preparation of Tetrahydrofurans

To a solution of the oxoalkene (1 equiv.) and the arylalkyne (3.5 equiv.) in DCE (0.5 M), *p*-toluensulphonic acid monohydrate (10 mol%) and the cationic gold (I) catalyst **C** (3 mol%) were added. Then, the reaction mixture was stirred at 50 ºC and followed by TLC. When it was finished, the catalyst was quenched by adding 0.05 ml of Et_3N, the solvent was removed and the crude was analysed by quantitative ^1H NMR using 1,4-diacetylbenzene as internal standard. Finally, the (arylehtynyl)tetrahydrofurane product was purified by Prep-TLC and fully characterized.

2,2,5-Trimethyl-5-(phenylethynyl)tetrahydrofuran (37)

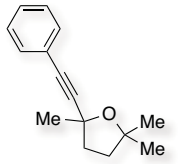

Compound **37** was synthesized following the general procedure starting from 5-methylhex-5-en-2-one (26.0 ml, 0.2 mmol) and ethynylbenzene (77.0 ml, 0.7 mmol) with *p*-toluensulphonic acid monohydrate (3.8 mg, 0.02 mmol) and catalyst **A** (5.4 mg, 0.006 mmol). The reaction time was 21 h and a mixture of pentane and CH_2Cl_2 (1:1) was used as eluent in the separation to obtain pure 2,2,5-trimethyl-5-(phenylethynyl)tetrahydrofuran as a yellow oil in 50% isolated yield (21.3 mg, 0.10 mmol). ^1H NMR (400 MHz, $CDCl_3$, ppm) δ 7.44 – 7.37 (m, 2H), 7.35 – 7.25 (m, 3H), 2.34 (ddd, *J* = 11.7, 6.9, 4.1 Hz, 1H), 2.13 (ddd, *J* = 11.6, 9.5, 7.2 Hz, 1H), 2.01 (ddd, *J* = 11.8, 9.6, 7.3 Hz, 1H), 1.87 (ddd, *J* = 11.4, 7.2, 4.0 Hz, 1H), 1.61 (s, 3H), 1.43 (s, 3H), 1.26 (s, 3H). ^{13}C NMR (101 MHz, $CDCl_3$, ppm) δ 131.68 (s), 128.29 (s), 128.05 (s), 123.43 (s), 93.93 (s), 82.53 (s), 82.45 (s), 76.55 (s), 40.91 (s), 39.00 (s), 29.71 (s), 29.47 (s), 29.27 (s). Structure confirmed by ^1H COSY NMR and ^1H-^{13}C HMQC NMR. APCI$^+$ *m/z* calc for $C_{15}H_{19}O^+$ $[M+H]^+$ 215.1436, found 215.1436 (0.0 ppm).

2-((4-Chlorophenyl)ethynyl)-2,5,5-trimethyltetrahydrofuran (38)

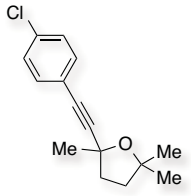

Compound **38** was synthesized following the general procedure starting from 5-methylhex-5-en-2-one (26.0 ml, 0.2 mmol) and 1-chloro-4-ethynylbenzene (96.0 mg, 0.7 mmol) with *p*-toluensulphonic acid monohydrate (3.8 mg, 0.02 mmol) and catalyst **A** (5.4 mg, 0.006 mmol). The reaction time was 21 h and a mixture of pentane and CH_2Cl_2 (1:10) was used as eluent in the separation to obtain pure 2-((4-chlorophenyl)ethynyl)-2,5,5-trimethyltetrahydrofuran as a yellow oil in 48% isolated yield (23.9 mg, 0.10 mmol). ^1H NMR (400 MHz, $CDCl_3$, ppm) δ 7.32 (d, *J* = 8.7 Hz, 2H), 7.25 (d, *J* = 8.7 Hz, 2H), 2.33 (ddd, *J* = 11.6, 6.7, 4.2 Hz, 1H), 2.11 (ddd, *J* = 11.3, 9.3, 6.8 Hz, 1H), 2.01 (ddd, *J* = 11.9, 9.3, 7.0 Hz, 1H), 1.87 (ddd, *J* = 11.1, 7.0, 4.2 Hz, 1H), 1.59 (s, 3H), 1.41 (s, 3H), 1.25 (s,

3H). ^{13}C NMR (126 MHz, $CDCl_3$, ppm) δ 134.06 (s), 132.92 (s), 128.62 (s), 121.93 (s), 94.98 (s), 82.59 (s), 81.35 (s), 76.47 (s), 40.83 (s), 38.98 (s), 29.69 (s), 29.45 (s), 29.26 (s). Structure confirmed by ^{1}H COSY NMR and ^{1}H-^{13}C HMQC NMR. APCI$^+$ *m/z* calc for $C_{15}H_{16}Cl^+$ $[M\text{-}OH]^+$ 231.0941, found 231.0940 (-0.4 ppm).

2-((4-Bromophenyl)ethynyl)-2,5,5-trimethyltetrahydrofuran (39)

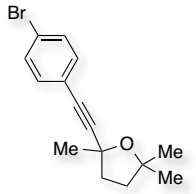

Compound **39** was synthesized following the general procedure starting from 5-methylhex-5-en-2-one (26.0 ml, 0.2 mmol) and 1-bromo-4-ethynylbenzene (127.0 mg, 0.7 mmol) with *p*-toluensulphonic acid monohydrate (3.8 mg, 0.02 mmol) and catalyst **A** (5.4 mg, 0.006 mmol). The reaction time was 21 h and a mixture of pentane and CH_2Cl_2 (1:1) was used as eluent in the separation to obtain pure 2-((4-bromophenyl)ethynyl)-2,5,5-trimethyltetrahydrofuran as yellow oil in 50% isolated yield (29.4 mg, 0.10 mmol). ^{1}H NMR (400 MHz, $CDCl_3$, ppm) δ 7.44 (d, *J* = 8.6 Hz, 2H), 7.28 (d, *J* = 8.6 Hz, 2H), 2.41 – 2.31 (m, 1H), 2.13 (ddd, *J* = 11.3, 9.3, 6.8 Hz, 1H), 2.04 (ddd, *J* = 11.8, 9.3, 7.0 Hz, 1H), 1.89 (ddd, *J* = 11.1, 7.0, 4.2 Hz, 1H), 1.61 (s, 3H), 1.43 (s, 3H), 1.28 (s, 3H). ^{13}C NMR (126 MHz, $CDCl_3$, ppm) δ 133.15 (s), 131.56 (s), 122.40 (s), 122.26 (s), 95.18 (s), 82.60 (s), 81.42 (s), 76.49 (s), 40.81 (s), 38.98 (s), 29.69 (s), 29.45 (s), 29.24 (s). Structure confirmed by ^{1}H COSY NMR and ^{1}H-^{13}C HMQC NMR. APCI$^+$ *m/z* calc for $C_{15}H_{18}OBr^+$ $[M+H]^+$ 293.0541, found 293.0555 (-0.4 ppm).

2-((3-Fluorophenyl)ethynyl)-2,5,5-trimethyltetrahydrofuran (40)

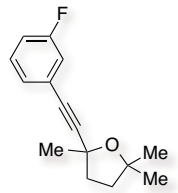

Compound **40** was synthesized following the general procedure starting from 5-methylhex-5-en-2-one (26.0 ml, 0.2 mmol) and 1-ethynyl-3-fluorobenzene (81.0 ml, 0.7 mmol) with *p*-toluensulphonic acid monohydrate (3.8 mg, 0.02 mmol) and catalyst **A** (5.4 mg, 0.006 mmol). The reaction time was 21 h and a mixture of pentane and CH_2Cl_2 (1:2) was used as eluent in the separation to obtain pure 2-((3-fluorophenyl)ethynyl)-2,5,5-trimethyltetrahydrofuran as a yellow oil in 47% isolated yield (21.8 mg, 0.09 mmol). ^{1}H NMR (400 MHz, $CDCl_3$, ppm) δ 7.24 (td, *J* = 7.9, 5.8 Hz, 1H), 7.18 (dt, *J* = 7.7, 1.2 Hz, 1H), 7.09 (ddd, *J* = 9.6, 2.5, 1.4 Hz, 1H), 6.99 (tdd, *J* = 8.5, 2.6, 1.1 Hz, 1H), 2.40 – 2.26 (m, 1H), 2.12 (ddd, *J* = 11.3, 9.4, 6.8 Hz, 1H), 2.02 (ddd, *J* = 11.8, 9.4, 7.1 Hz, 1H), 1.88 (ddd, *J* = 11.1, 7.0, 4.1 Hz, 1H), 1.60 (s, 3H), 1.42 (s, 3H), 1.26 (s, 3H). ^{13}C NMR (126 MHz, $CDCl_3$, ppm) δ 163.44 (d, *J* (^{13}C-^{19}F) = 246.9 Hz, 129.84 (d, *J* (^{13}C-^{19}F) = 7.9 Hz), 127.56 (d, *J* (^{13}C-^{19}F) = 3.1 Hz), 125.28 (d, *J* (^{13}C-^{19}F) = 9.4 Hz), 118.48 (d, *J* (^{13}C-^{19}F) = 22.1 Hz), 115.40 (d, *J* (^{13}C-^{19}F) = 20.4 Hz), 94.98 (s), 82.62 (s), 81.28 (d, *J* (^{13}C-^{19}F) = 3.6 Hz), 76.43 (s), 40.83 (s), 38.97 (s), 29.68 (s), 29.45 (s), 29.21 (s). ^{19}F NMR (376 MHz, $CDCl_3$, ppm) δ -113.42 (s). Structure confirmed by ^{1}H COSY NMR and ^{1}H-^{13}C HMQC NMR. APCI$^+$ *m/z* calc for $C_{15}H_{16}F^+$ $[M\text{-}OH]^+$ 215.1236, found 215.1237 (0.5 ppm).

2-((3-Chlorophenyl)ethynyl)-2,5,5-trimethyltetrahydrofuran (41)

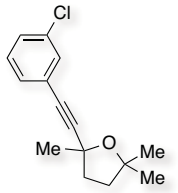

Compound **41** was synthesized following the general procedure starting from 5-methylhex-5-en-2-one (26.0 ml, 0.2 mmol) and 1-chloro-3-ethynylbenzene (86.0 ml, 0.7 mmol) with *p*-toluensulphonic acid monohydrate (3.8 mg, 0.02 mmol) and catalyst **A** (5.4 mg, 0.006 mmol). The reaction time was 21 h and a mixture of pentane and CH_2Cl_2 (1:2) was used as eluent in the separation to obtain pure 2-((3-chlorophenyl)ethynyl)-2,5,5-trimethyltetrahydrofuran as a yellowish doughy powder in 55% isolated yield (27.3 mg, 0.11 mmol). ^{1}H NMR (400 MHz, $CDCl_3$, ppm) δ 7.39 (t, *J* = 1.6 Hz, 1H), 7.30 – 7.24 (m, 2H), 7.24 – 7.16 (m, 1H), 2.33 (ddd, *J* = 11.7, 6.7, 4.2 Hz, 1H), 2.11 (ddd, *J* = 11.3, 9.4, 6.8 Hz, 1H), 2.02 (ddd, *J* = 11.9, 9.4, 7.0 Hz, 1H), 1.87 (ddd, *J* = 11.1, 7.0, 4.1 Hz, 1H), 1.60 (s, 3H), 1.42 (s, 3H), 1.26 (s, 3H). ^{13}C NMR (126 MHz, $CDCl_3$, ppm) δ 134.12 (s), 131.56 (s), 129.83 (s), 129.53 (s), 128.36 (s), 125.14 (s), 95.28 (s), 82.63 (s), 81.09 (s), 76.42 (s), 40.83 (s), 38.97 (s), 29.68 (s), 29.46 (s), 29.20 (s). Structure confirmed by ^{1}H COSY NMR and ^{1}H-^{13}C HMQC NMR. APCI$^+$ *m/z* calc for $C_{15}H_{16}Cl^+$ [M-OH]$^+$ 231.0941, found 231.0941 (0.0 ppm).

General Procedure for the Preparation of 1,3,5-Substituted Benzenes

To a solution of the arylalkyne (0.20 mmol) in DCE (2 M), the cationic gold (I) catalyst **C** (3 mol%) was added. Then, the reaction mixture was stirred at 50 ºC and followed by TLC. When it was finished, the catalyst was quenched by adding 0.02 ml of Et_3N, the solvent was removed and the crude was analysed by quantitative ^{1}H NMR using 1,4-diacetylbenzene as internal standard. Finally, the 1,3,5-triarylbenzene product was purified by preparative TLC and fully characterized.

5'-Phenyl-1,1':3',1''-terphenyl (24)

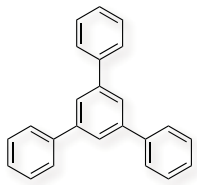

Compound **24** was synthesized following the general procedure starting from ethynylbenzene (22.0 ml, 0.2 mmol) with catalyst **A** (5.4 mg, 0.006 mmol). The reaction time was 16 h and a mixture of pentane and CH_2Cl_2 (3:1) was used as eluent in the separation to obtain pure 5'-phenyl-1,1':3',1''-terphenyl as a yellow oil in 40% isolated yield (8.0 mg, 0.03 mmol). ^{1}H NMR (400 MHz, $CDCl_3$, ppm) δ 7.79 (s, 3H), 7.70 (dd, *J* = 8.3, 1.2 Hz, 6H), 7.48 (t, *J* = 7.5 Hz, 6H), 7.43 – 7.36 (m, 3H). ^{13}C NMR (126 MHz, $CDCl_3$, ppm) δ 142.50 (s), 141.31 (s), 129.00 (s), 127.69 (s), 127.51 (s), 125.33 (s). Structure confirmed by ^{1}H COSY NMR and ^{1}H-^{13}C HMQC NMR.

4,4''-Dimethyl-5'-(p-tolyl)-1,1':3',1''-terphenyl (112)

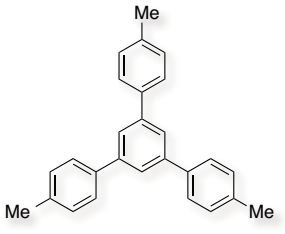

Compound **113** was synthesized following the general procedure starting from 1-ethynyl-4-methylbenzene (25.4 ml, 0.2 mmol) with catalyst **A** (5.4 mg, 0.006 mmol). The reaction time was 16 h and a mixture of pentane and CH_2Cl_2 (3:1) was used as eluent in the separation to obtain pure 4,4''-dimethyl-5'-(*p*-tolyl)-1,1':3',1''-terphenyl as a yellow oil in 33% isolated yield (7.6 mg, 0.02 mmol). ^{1}H NMR (400 MHz, $CDCl_3$, ppm) δ 7.73 (s, 3H), 7.59 (d, *J* = 8.1 Hz, 6H), 7.28 (d,

J = 7.9 Hz, 6H), 2.42 (s, 9H). ^{13}C NMR (126 MHz, $CDCl_3$, ppm) δ 142.31 (s), 138.55 (s), 137.41 (s), 129.68 (s), 127.33 (s), 124.72 (s), 21.29 (s). Structure confirmed by ^{1}H COSY NMR and ^{1}H-^{13}C HMQC NMR.

4,4''-Difluoro-5'-(4-fluorophenyl)-1,1':3',1''-terphenyl (113)

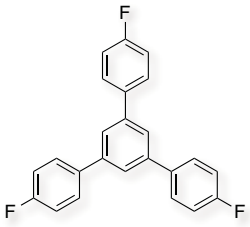

Compound **114** was synthesized following the general procedure starting from 1-ethynyl-4-fluorobenzene (22.9 ml, 0.2 mmol) with catalyst **A** (5.4 mg, 0.006 mmol). The reaction time was 16 h and a mixture of pentane and CH_2Cl_2 (3:1) was used as eluent in the separation to obtain pure 4,4''-difluoro-5'-(4-fluorophenyl)-1,1':3',1''-terphenyl as a yellow oil in 37% isolated yield (8.8 mg, 0.02 mmol). ^{1}H NMR (400 MHz, $CDCl_3$, ppm) δ 7.66 (s, 3H), 7.66 – 7.61 (m, 6H), 7.17 (t, *J* = 8.7 Hz, 6H). ^{13}C NMR (126 MHz, $CDCl_3$, ppm) δ 162.84 (d, *J* (^{13}C-^{19}F) = 246.83 Hz), 141.69 (s), 137.16 (d, *J* (^{13}C-^{19}F) = 3.41 Hz), 129.05 (d, *J* (^{13}C-^{19}F) = 7.97 Hz), 125.01 (s), 115.98 (d, *J* (^{13}C-^{19}F) = 21.37 Hz). ^{19}F NMR (376 MHz, $CDCl_3$, ppm) δ -115.15 (s). Structure confirmed by ^{1}H COSY NMR and ^{1}H-^{13}C HMQC NMR.

3,3''-Dimethyl-5'-(m-tolyl)-1,1':3',1''-terphenyl (114)

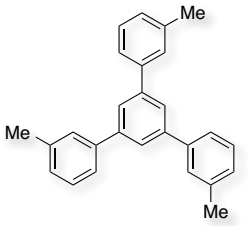

Compound **115** was synthesized following the general procedure starting from 1-ethynyl-3-methylbenzene (26.0 ml, 0.2 mmol) with catalyst **A** (5.4 mg, 0.006 mmol). The reaction time was 16 h and a mixture of pentane and CH_2Cl_2 (3:1) was used as eluent in the separation to obtain pure 3,3''-dimethyl-5'-(*m*-tolyl)-1,1':3',1''-terphenyl as a yellowish doughy powder in 20% isolated yield (4.5 mg, 0.01 mmol). ^{1}H NMR (400 MHz,$CDCl_3$, ppm) δ 7.75 (s, 3H), 7.54 – 7.47 (m, 6H), 7.37 (t, *J* = 8.0 Hz, 3H), 7.20 (d, *J* = 7.8 Hz, 3H), 2.45 (s, 9H). ^{13}C NMR (126 MHz, $CDCl_3$, ppm) δ 142.49 (s), 141.38 (s), 138.58 (s), 128.88 (s), 128.38 (s), 128.30 (s), 125.27 (s), 124.61 (s), 21.72 (s). Structure confirmed by ^{1}H COSY NMR and ^{1}H-^{13}C HMQC NMR.

X-Ray Crystallographic Data

1,5-Dimethyl-8-oxabicyclo[3.2.1]oct-2-en-3-yl)phenol (33)

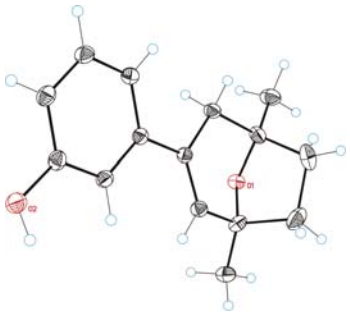

Table 1. Crystal data and structur refinement for 33.

Empirical formula	C15 H18 O2
Formula weight	230.29
Temperature	100(2) K
Wavelength	0.71073 Å

Crystal system	Monoclinic
Space group	P2(1)/c
Unit cell dimensions	a = 8.0849(16) Å α= 90.00 ° b = 7.3813(13) Å β = 99.419(7) ° c = 21.133(4) Å γ = 90.00 °
Volume	1244.1(4) $Å^3$
Z	4
Density (calculated)	1.229 Mg/m^3
Absorption coefficient	0.080 mm^{-1}
F(000)	496
Crystal size	0.40 x 0.20 x 0.20 mm^3
Theta range for data collection	1.95 to 36.37 °.
Index ranges	-10 <=h<=12, -12 <=k<=9, -31 <=l<=32
Reflections collected	17479
Independent reflections	4905 [R(int) = 0.0391]
Completeness to theta =36.37 °	0.808 %
Absorption correction	Empirical
Max. and min. transmission	0.9888 and 0.9701
Refinement method	Full-matrix least-squares on F^2
Data / restraints / parameters	4905 / 0 / 175
Goodness-of-fit on F^2	1.035
Final R indices [I>2sigma(I)]	R1 = 0.0484, wR2 = 0.1354
R indices (all data)	R1 = 0.0638, wR2 = 0.1459
Largest diff. peak and hole	0.550 and -0.295 e.$Å^{-3}$

Table 2. Bond lengths [Å] and angles [°] for 33.

Bond lengths:

C1-C2	1.4028(12)
C1-C6	1.4062(12)
C1-C7	1.4866(11)
C2-C3	1.3920(12)
C3-C4	1.3876(13)
C4-C5	1.3972(12)
C5-O2	1.3638(11)
C5-C6	1.3942(11)
C7-C8'	1.334(9)
C7-C13	1.346(4)
C7-C13'	1.505(7)
C7-C8	1.512(3)
C8-C9	1.542(4)
C8'-C9	1.496(10)
C9-O1	1.4518(11)
C9-C14	1.5128(14)
C9-C10	1.5451(15)
C10-C11	1.5292(16)
C11-C12	1.5409(14)
C12-O1	1.4491(11)
C12-C13	1.494(4)
C12-C15	1.5112(13)
C12-C13'	1.586(7)

Angles:

C2-C1-C6	118.47(7)
C2-C1-C7	120.32(7)
C6-C1-C7	121.20(7)
C3-C2-C1	120.31(8)
C4-C3-C2	121.00(8)
C3-C4-C5	119.33(8)
O2-C5-C6	122.77(8)
O2-C5-C4	117.14(7)
C6-C5-C4	120.09(8)
C5-C6-C1	120.80(8)

C8'-C7-C13	111.6(4)	C8'-C9-C10	100.8(2)
C8'-C7-C1	122.8(4)	C14-C9-C10	114.65(8)
C13-C7-C1	124.24(17)	C8-C9-C10	114.29(13)
C8'-C7-C13'	119.4(5)	C11-C10-C9	104.39(8)
C13-C7-C13'	14.3(2)	C10-C11-C12	103.71(8)
C1-C7-C13'	117.8(3)	O1-C12-C13	108.27(16)
C8'-C7-C8	13.7(3)	O1-C12-C15	108.30(7)
C13-C7-C8	118.3(2)	C13-C12-C15	115.70(13)
C1-C7-C8	117.49(16)	O1-C12-C11	101.88(8)
C13'-C7-C8	122.9(3)	C13-C12-C11	106.47(11)
C7-C8-C9	110.9(2)	C15-C12-C11	115.18(8)
C7-C8'-C9	125.3(7)	O1-C12-C13'	107.7(3)
O1-C9-C8'	107.2(4)	C13-C12-C13'	14.1(2)
O1-C9-C14	108.03(7)	C15-C12-C13'	103.5(2)
C8'-C9-C14	121.2(3)	C11-C12-C13'	119.7(2)
O1-C9-C8	107.12(16)	C7-C13-C12	123.6(3)
C8'-C9-C8	14.3(2)	C7-C13'-C12	108.2(4)
C14-C9-C8	108.82(13)	C12-O1-C9	104.02(6)
O1-C9-C10	103.36(8)		

Table 3. Torsion angles [°] for 33.

C6-C1-C2-C3	0.96(12)	C10-C11-C12-C15	149.97(8)
C7-C1-C2-C3	-179.92(8)	C10-C11-C12-C13'	-85.6(4)
C1-C2-C3-C4	-0.66(13)	C8'-C7-C13-C12	-16.1(4)
C2-C3-C4-C5	0.07(13)	C1-C7-C13-C12	177.23(13)
C3-C4-C5-O2	-179.15(8)	C13'-C7-C13-C12	110(2)
C3-C4-C5-C6	0.19(13)	C8-C7-C13-C12	-2.9(3)
O2-C5-C6-C1	179.43(8)	O1-C12-C13-C7	-25.0(2)
C4-C5-C6-C1	0.13(13)	C15-C12-C13-C7	-146.77(16)
C2-C1-C6-C5	-0.70(12)	C11-C12-C13-C7	83.8(2)
C7-C1-C6-C5	-179.82(7)	C13'-C12-C13-C7	-115.1(19)
C2-C1-C7-C8'	9.7(4)	C8'-C7-C13'-C12	8.7(6)
C6-C1-C7-C8'	-171.2(4)	C13-C7-C13'-C12	-51.0(16)
C2-C1-C7-C13	174.97(15)	C1-C7-C13'-C12	-171.5(2)
C6-C1-C7-C13	-5.93(18)	C8-C7-C13'-C12	24.2(5)
C2-C1-C7-C13'	-170.1(3)	O1-C12-C13'-C7	-49.3(4)
C6-C1-C7-C13'	9.0(3)	C13-C12-C13'-C7	45.3(15)
C2-C1-C7-C8	-4.89(18)	C15-C12-C13'-C7	-163.8(3)
C6-C1-C7-C8	174.21(16)	C11-C12-C13'-C7	66.3(5)
C8'-C7-C8-C9	55(2)	C13-C12-O1-C9	64.02(12)
C13-C7-C8-C9	-8.6(3)	C15-C12-O1-C9	-169.82(7)
C1-C7-C8-C9	171.29(14)	C11-C12-O1-C9	-47.98(8)
C13'-C7-C8-C9	-24.3(4)	C13'-C12-O1-C9	78.8(2)
C13-C7-C8'-C9	17.1(7)	C8'-C9-O1-C12	-62.6(2)
C1-C7-C8'-C9	-176.0(3)	C14-C9-O1-C12	165.27(7)
C13'-C7-C8'-C9	3.8(7)	C8-C9-O1-C12	-77.65(12)
C8-C7-C8'-C9	-105(3)	C10-C9-O1-C12	43.38(8)
C7-C8'-C9-O1	23.2(6)		
C7-C8'-C9-C14	147.7(4)		
C7-C8'-C9-C8	115(2)		
C7-C8'-C9-C10	-84.6(6)		
C7-C8-C9-O1	48.2(2)		
C7-C8-C9-C8'	-44(2)		
C7-C8-C9-C14	164.79(16)		
C7-C8-C9-C10	-65.6(3)		
O1-C9-C10-C11	-21.00(10)		
C8'-C9-C10-C11	89.8(4)		
C14-C9-C10-C11	-138.33(9)		
C8-C9-C10-C11	95.05(18)		
C9-C10-C11-C12	-7.22(10)		
C10-C11-C12-O1	33.00(9)		
C10-C11-C12-C13	-80.33(17)		

3. Mechanistic Study of A [2+2+2] Cycloaddition: Role of Digold Complexes[1]

Preparation of the Starting Materials

All the substrates and gold complexes used were already described in **Chapter 2** except for the following.

Deuterated para-bromoethynylbenzene

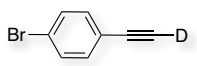

A flame-dried flask was charged with *p*-bromoethynylbenzene (0.47 g, 2.58 mmol) and K_2CO_3 (0.60 g, 3.87 mmol) in acetonitrile (5 ml). The reaction mixture was stirred at 25 ºC under N_2 atmosphere for 45 min. Then, deuterated water (2 ml) was added and the solution was stirred for 1 h. The crude was diluted with CH_2Cl_2 and the phases were separated. The organic layers were dried with MgSO4, filtered and concentrated under reduced pressure. Deuterated *p*-bromoethynylbenzene was obtained [D] 96% in 72% isolated yield (0.34 g, 1.85 mmol). ^{1}H NMR (500 MHz, $CDCl_3$, ppm) δ 7.46 (d, *J* = 8.58 Hz, 2H), 7.35 (d, *J* = 8.53 Hz, 2H), 3.13 (s, 0.04H). ^{13}C NMR (126 MHz, $CDCl_3$, ppm) δ 133.6 (s), 131.7 (s), 123.2 (s), 121.1 (s), 82.3 (t, *J* (^{2}H-^{13}C) = 7.60 Hz), 78.2 (t, *J* (^{2}H-^{13}C) = 38.58 Hz).

{Phenylethynyl[(2′,4′,6′-triisopropyl-1,1′-biphenyl-2-yl)di-tert-butylphosphine]gold(I) [(2′,4′,6′-triisopropyl-1,1′-biphenyl-2-yl)di-tert-butylphosphine]gold(I) hexafluoroantimonate (67)

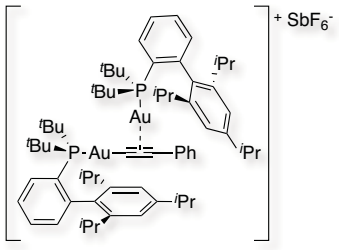

Ethynylbenzene (61.5 µl, 0.56 mmol) was dissolved in THF (10 ml) and the solution was cooled to 0 ºC. Then, LiHMDS (110 mg, 0.67 mmol) was added and the solution was stirred for 30 min. Afterwards, 1 ml of this stock solution was added to chloro[(2′,4′,6′-triisopropyl-1,1′-biphenyl-2-yl)di-tert-butylphosphine]gold(I) (50 mg, 0.06 mmol) dissolved in THF (1 ml). The reaction mixture was stirred at 25 ºC for 12 h. The solution was concentrated under vacuum and the residue was added to a solution of chloro[(2′,4′,6′-triisopropyl-1,1′-biphenyl-2-yl)di-tert-butylphosphine]gold(I) (40 mg, 0.06 mmol) in CH_2Cl_2 (5 ml). Then, $AgSbF_6$ (21 mg, 0.06 mmol) was added and the reaction mixture was stirred at 25 ºC for 5 min and afterwards filtered through celite. The solution was concentrated under reduced pressure to 1 ml approximately and the residue was diluted with pentane (6 ml) and cooled to 6 ºC for 12 h. The precipitate was washed with pentane and pure {phenylethynyl[(2′,4′,6′-triisopropyl-1,1′-biphenyl-2-yl)di-tert-butylphosphine]gold(I)} [(2′,4′,6′-triisopropyl-1,1′-biphenyl-2-yl)di-tert-butylphosphine]gold(I) hexafluoroantimonate (**67**) was obtained as a white powder in 99 % isolated yield (87.0 mg, 0.06 mmol). ^{1}H NMR (500 MHz, CD_2Cl_2, ppm) δ 7.95 – 7.86 (m, 2H), 7.56 – 7.53 (m, 4H), 7.43 – 7.36 (m, 2H), 7.32 – 7.30 (m, 2H), 7.25 – 7.22 (m, 2H), 6.84 (s, 4H), 2.37 – 2.30 (m, 6H), 1.44 (d, *J* = 15.6 Hz, 36H), 1.15 (d, *J* = 6.8 Hz, 12H), 1.08 (d, *J* = 6.9 Hz, 12H), 0.85 (d, *J* = 6.6 Hz, 12H). ^{13}C NMR (101 MHz, CD_2Cl_2, ppm) δ 149.9 (s), 148.0 (d, *J* (^{13}C-^{31}P) = 14.2 Hz), 147.1 (s), 136.2 (d, *J* (^{13}C-^{31}P) = 5.9 Hz), 135.5

[1] C. Obradors and A. M. Echavarren, *Chem. –Eur. J.* **2013**, *19*, 3547–3551.

(d, *J* (^{13}C-^{31}P) = 2.9 Hz), 135.4 (d, *J* (^{13}C-^{31}P) = 8.6 Hz), 133.1 (s), 131.3 (s), 130.5 (s), 128.9 (s), 127.9 (s), 127.6 (s), 127.5 (d, *J* (^{13}C-^{31}P) = 4.9 Hz), 122.2 (s), 122.1 (s), 121.3 (s), 39.3 (d, *J* (^{13}C-^{31}P) = 24.6 Hz), 33.9 (s), 31.8 (d, *J* (^{13}C-^{31}P) = 6.8 Hz), 31.3 (s), 26.3 (s), 24.2 (s), 23.6 (s). ^{31}P NMR (162 MHz, CD_2Cl_2, ppm) δ 65.17. ^{19}F NMR (376 MHz, CD_2Cl_2, ppm) δ not conclusive. Structure confirmed by ^{1}H COSY NMR and ^{1}H-^{13}C HMQC NMR. MALDI^{+} *m/z* calc for $C_{66}H_{95}Au_2P_2^{+}$ [M-SbF_6]$^{+}$ 1343.6235, found 1343.6238 (0.3 ppm). Structure confirmed by X-Ray crystallography, CCDC 913002.

X-Ray Crystallographic Data

{Phenylethynyl[(2′,4′,6′-triisopropyl-1,1′-biphenyl-2-yl)di-tert-butylphosphine]gold(I) [(2′,4′,6′-triisopropyl-1,1′-biphenyl-2-yl)di-tert-butylphosphine]gold(I) hexafluoroantimonate (67)

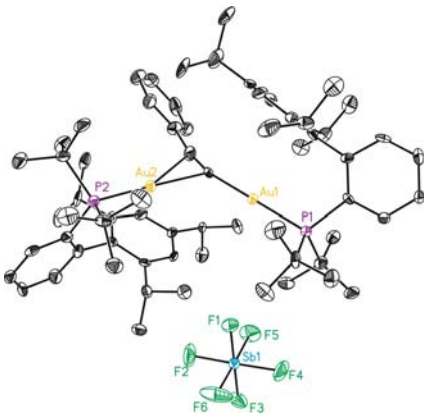

Table 1. Crystal data and structure refinement for 67.

Empirical formula	C72 H109 Au2 Cl2 F6 P2 Sb
Formula weight	1737.11
Temperature	100(2)K
Wavelength	0.71073 Å
Crystal system	Monoclinic
Space group	P2(1)
Unit cell dimensions	a = 13.6257(13) Å α = 90.00 °. b = 15.1869(13) Å β = 107.095(3) °. c = 18.6156(19) Å γ = 90.00 °.
Volume	3682.0(6) Å^3
Z	2
Density (calculated)	1.567 Mg/m^3
Absorption coefficient	4.509 mm^{-1}
F(000)	1736
Crystal size	0.25x0.12x0.12 mm^3
Theta range for data collection	1.14 to 29.97 °.
Index ranges	-18 <=h<=19, -19 <=k<=20, -25 <=l<=24
Reflections collected	37284

Independent reflections	17602 [R(int) = 0.0629]
Completeness to theta =29.97 °	0.879 %
Absorption correction	Empirical
Max. and min. transmission	0.6137 and 0.3986
Refinement method	Full-matrix least-squares on F^2
Data / restraints / parameters	17602 / 488 / 859
Goodness-of-fit on F^2	0.998
Final R indices [I>2sigma(I)]	R1 = 0.0515 , wR2 = 0.0968
R indices (all data)	R1 = 0.0736 , wR2 = 0.1082
Flack parameter	x =-0.017(5)
Largest diff. peak and hole	1.613 and -1.185e.$Å^3$

Table 2. Bond lengths [Å] and angles [°] for 67.

Bond lengths:			
		C30-C31	1.405(12)
		C30-C35	1.429(12)
Au1-C59	2.051(9)	C31-C32	1.370(12)
Au1-P1	2.292(2)	C32-C33	1.375(12)
Au2-C59	2.228(8)	C33-C34	1.375(12)
Au2-P2	2.274(2)	C34-C35	1.391(13)
Au2-C60	2.275(9)	C35-C36	1.501(11)
P1-C1	1.855(8)	C36-C41	1.395(12)
P1-C22	1.869(8)	C36-C37	1.431(11)
P1-C26	1.894(8)	C37-C38	1.395(11)
P2-C30	1.818(9)	C37-C42	1.474(12)
P2-C55	1.870(10)	C38-C39	1.388(12)
P2-C51	1.886(9)	C39-C40	1.382(11)
C1-C2	1.391(11)	C39-C45	1.526(11)
C1-C6	1.411(11)	C40-C41	1.384(11)
C2-C3	1.384(12)	C41-C48	1.521(11)
C3-C4	1.376(12)	C42-C43	1.529(12)
C4-C5	1.367(12)	C42-C44	1.533(12)
C5-C6	1.398(12)	C45-C46	1.498(12)
C6-C7	1.483(11)	C45-C47	1.524(12)
C7-C12	1.398(11)	C48-C49	1.508(13)
C7-C8	1.409(12)	C48-C50	1.512(13)
C8-C9	1.395(12)	C51-C52	1.497(13)
C8-C13	1.520(11)	C51-C54	1.529(13)
C9-C10	1.365(12)	C51-C53	1.535(12)
C10-C11	1.371(13)	C55-C57	1.535(12)
C10-C16	1.528(8)	C55-C58	1.544(12)
C11-C12	1.411(12)	C55-C56	1.549(13)
C12-C19	1.533(13)	C59-C60	1.180(12)
C13-C15	1.509(13)	C60-C61	1.460(13)
C13-C14	1.535(13)	C61-C66	1.389(12)
C16-C18	1.52(2)	C61-C62	1.391(12)
C16-C17	1.555(17)	C62-C63	1.319(13)
C19-C21	1.524(12)	C63-C64	1.416(14)
C19-C20	1.546(14)	C64-C65	1.369(14)
C22-C23	1.522(11)	C65-C66	1.369(13)
C22-C25	1.536(12)	Sb1-F6	1.832(6)
C22-C24	1.540(13)	Sb1-F2	1.864(6)
C26-C27	1.516(13)	Sb1-F4	1.867(6)
C26-C29	1.525(13)	Sb1-F1	1.867(5)
C26-C28	1.539(12)	Sb1-F5	1.870(6)

Sb1-F3	1.878(6)	C21-C19-C12	112.8(8)
C1S-Cl1S	1.740(9)	C21-C19-C20	110.6(8)
C1S-Cl2S	1.754(10)	C12-C19-C20	110.5(8)
C1T-C2T	1.555(10)	C23-C22-C25	106.4(8)
C2T-C3T	1.544(10)	C23-C22-C24	109.4(8)
C3T-C4T	1.552(10)	C25-C22-C24	107.1(7)
C4T-C5T	1.551(10)	C23-C22-P1	117.8(6)
C1T'-C2T'	1.545(10)	C25-C22-P1	106.2(6)
C2T'-C3T'	1.551(10)	C24-C22-P1	109.4(6)
C3T'-C4T'	1.555(10)	C27-C26-C29	108.5(9)
C4T'-C5T'	1.551(10)	C27-C26-C28	109.4(8)
C1T"-C2T"	1.558(10)	C29-C26-C28	107.0(8)
C2T"-C3T"	1.555(10)	C27-C26-P1	106.4(9)
C3T"-C4T"	1.548(10)	C29-C26-P1	107.4(10)
C4T"-C5T"	1.557(10)	C28-C26-P1	117.9(10)
		C31-C30-C35	117.6(8)
Angles:		C31-C30-P2	117.3(6)
		C35-C30-P2	125.1(6)
C59-Au1-P1	174.4(2)	C32-C31-C30	122.2(8)
C59-Au2-P2	169.1(2)	C31-C32-C33	120.3(8)
C59-Au2-C60	30.4(3)	C34-C33-C32	119.0(9)
P2-Au2-C60	157.4(2)	C33-C34-C35	122.9(9)
C1-P1-C22	106.9(4)	C34-C35-C30	118.1(8)
C1-P1-C26	105.9(4)	C34-C35-C36	115.6(8)
C22-P1-C26	112.6(4)	C30-C35-C36	126.4(8)
C1-P1-Au1	113.8(3)	C41-C36-C37	119.7(7)
C22-P1-Au1	110.4(3)	C41-C36-C35	121.6(7)
C26-P1-Au1	107.2(3)	C37-C36-C35	118.0(8)
C30-P2-C55	109.1(4)	C38-C37-C36	118.0(8)
C30-P2-C51	106.7(4)	C38-C37-C42	120.3(8)
C55-P2-C51	111.1(4)	C36-C37-C42	121.6(7)
C30-P2-Au2	114.3(3)	C39-C38-C37	122.5(8)
C55-P2-Au2	108.1(3)	C40-C39-C38	117.6(8)
C51-P2-Au2	107.7(3)	C40-C39-C45	120.8(8)
C2-C1-C6	120.0(8)	C38-C39-C45	121.6(7)
C2-C1-P1	115.5(6)	C39-C40-C41	122.9(9)
C6-C1-P1	124.4(6)	C40-C41-C36	119.2(8)
C3-C2-C1	121.3(8)	C40-C41-C48	119.1(8)
C4-C3-C2	119.2(8)	C36-C41-C48	121.5(7)
C5-C4-C3	119.8(9)	C37-C42-C43	113.1(8)
C4-C5-C6	123.1(8)	C37-C42-C44	112.5(8)
C5-C6-C1	116.5(8)	C43-C42-C44	109.3(7)
C5-C6-C7	117.1(8)	C46-C45-C47	109.3(7)
C1-C6-C7	126.3(8)	C46-C45-C39	113.6(7)
C12-C7-C8	119.2(8)	C47-C45-C39	110.8(7)
C12-C7-C6	119.5(8)	C49-C48-C50	110.0(8)
C8-C7-C6	120.8(7)	C49-C48-C41	112.0(8)
C9-C8-C7	118.2(8)	C50-C48-C41	111.6(8)
C9-C8-C13	119.8(8)	C52-C51-C54	110.2(8)
C7-C8-C13	121.5(8)	C52-C51-C53	109.5(8)
C10-C9-C8	123.5(9)	C54-C51-C53	106.0(8)
C9-C10-C11	118.1(8)	C52-C51-P2	109.4(7)
C9-C10-C16	121.7(9)	C54-C51-P2	105.1(6)
C11-C10-C16	120.2(9)	C53-C51-P2	116.4(6)
C10-C11-C12	121.6(8)	C57-C55-C58	108.6(8)
C7-C12-C11	119.4(9)	C57-C55-C56	108.1(8)
C7-C12-C19	122.8(8)	C58-C55-C56	106.4(8)
C11-C12-C19	117.5(8)	C57-C55-P2	115.6(7)
C15-C13-C8	112.4(8)	C58-C55-P2	109.2(6)
C15-C13-C14	110.3(8)	C56-C55-P2	108.6(6)
C8-C13-C14	112.3(8)	C60-C59-Au1	165.8(8)
C18-C16-C10	108.5(10)	C60-C59-Au2	77.0(6)
C18-C16-C17	105.4(13)	Au1-C59-Au2	116.9(4)
C10-C16-C17	108.9(9)	C59-C60-C61	168.3(9)

C59-C60-Au2	72.6(6)	F4-Sb1-F5	88.5(3)
C61-C60-Au2	119.0(6)	F1-Sb1-F5	89.3(3)
C66-C61-C62	118.0(9)	F6-Sb1-F3	89.6(3)
C66-C61-C60	122.2(8)	F2-Sb1-F3	89.4(3)
C62-C61-C60	119.7(8)	F4-Sb1-F3	89.6(3)
C63-C62-C61	121.6(10)	F1-Sb1-F3	179.3(3)
C62-C63-C64	120.2(10)	F5-Sb1-F3	90.0(3)
C65-C64-C63	119.7(9)	Cl1S-C1S-Cl2S	111.8(6)
C66-C65-C64	119.0(9)	C3T-C2T-C1T	120(2)
C65-C66-C61	121.6(10)	C2T-C3T-C4T	112.0(18)
F6-Sb1-F2	90.2(4)	C5T-C4T-C3T	119(2)
F6-Sb1-F4	92.9(4)	C1T'-C2T'-C3T'	107.6(9)
F2-Sb1-F4	176.7(4)	C2T'-C3T'-C4T'	122(3)
F6-Sb1-F1	91.1(3)	C5T'-C4T'-C3T'	112(3)
F2-Sb1-F1	90.6(3)	C3T"-C2T"-C1T"	107.1(9)
F4-Sb1-F1	90.4(3)	C4T"-C3T"-C2T"	94(3)
F6-Sb1-F5	178.5(4)	C3T"-C4T"-C5T"	163(4)
F2-Sb1-F5	88.4(3)		

Table 3. Torsion angles [°] for 67.

C59-Au1-P1-C1	94(3)	C8-C7-C12-C19	-171.1(8)
C59-Au1-P1-C22	-146(3)	C6-C7-C12-C19	1.4(13)
C59-Au1-P1-C26	-23(3)	C10-C11-C12-C7	-2.2(14)
C59-Au2-P2-C30	-135.5(12)	C10-C11-C12-C19	172.1(9)
C60-Au2-P2-C30	97.8(7)	C9-C8-C13-C15	75.3(11)
C59-Au2-P2-C55	-13.9(13)	C7-C8-C13-C15	-96.9(10)
C60-Au2-P2-C55	-140.5(7)	C9-C8-C13-C14	-49.6(12)
C59-Au2-P2-C51	106.2(12)	C7-C8-C13-C14	138.2(9)
C60-Au2-P2-C51	-20.5(8)	C9-C10-C16-C18	139.4(12)
C22-P1-C1-C2	65.4(7)	C11-C10-C16-C18	-37.9(15)
C26-P1-C1-C2	-54.9(7)	C9-C10-C16-C17	-106.4(12)
Au1-P1-C1-C2	-172.4(5)	C11-C10-C16-C17	76.3(13)
C22-P1-C1-C6	-118.2(7)	C7-C12-C19-C21	-142.7(9)
C26-P1-C1-C6	121.5(7)	C11-C12-C19-C21	43.2(12)
Au1-P1-C1-C6	4.1(8)	C7-C12-C19-C20	92.9(11)
C6-C1-C2-C3	-0.5(12)	C11-C12-C19-C20	-81.2(10)
P1-C1-C2-C3	176.1(6)	C1-P1-C22-C23	-44.7(8)
C1-C2-C3-C4	-0.9(12)	C26-P1-C22-C23	71.2(9)
C2-C3-C4-C5	1.8(13)	Au1-P1-C22-C23	-169.1(7)
C3-C4-C5-C6	-1.3(14)	C1-P1-C22-C25	74.3(7)
C4-C5-C6-C1	-0.2(13)	C26-P1-C22-C25	-169.7(6)
C4-C5-C6-C7	177.1(8)	Au1-P1-C22-C25	-50.0(7)
C2-C1-C6-C5	1.0(12)	C1-P1-C22-C24	-170.4(6)
P1-C1-C6-C5	-175.2(6)	C26-P1-C22-C24	-54.5(7)
C2-C1-C6-C7	-175.9(8)	Au1-P1-C22-C24	65.2(7)
P1-C1-C6-C7	7.8(12)	C1-P1-C26-C27	-54.3(9)
C5-C6-C7-C12	-84.8(10)	C22-P1-C26-C27	-170.9(8)
C1-C6-C7-C12	92.1(11)	Au1-P1-C26-C27	67.5(8)
C5-C6-C7-C8	87.6(10)	C1-P1-C26-C29	-170.3(8)
C1-C6-C7-C8	-95.5(11)	C22-P1-C26-C29	73.1(9)
C12-C7-C8-C9	-2.2(13)	Au1-P1-C26-C29	-48.5(9)
C6-C7-C8-C9	-174.6(8)	C1-P1-C26-C28	68.8(10)
C12-C7-C8-C13	170.2(8)	C22-P1-C26-C28	-47.7(10)
C6-C7-C8-C13	-2.2(13)	Au1-P1-C26-C28	-169.3(9)
C7-C8-C9-C10	1.0(14)	C55-P2-C30-C31	53.6(8)
C13-C8-C9-C10	-171.5(9)	C51-P2-C30-C31	-66.4(8)
C8-C9-C10-C11	-0.3(14)	Au2-P2-C30-C31	174.8(6)
C8-C9-C10-C16	-177.7(9)	C55-P2-C30-C35	-125.7(8)
C9-C10-C11-C12	0.9(14)	C51-P2-C30-C35	114.3(8)
C16-C10-C11-C12	178.3(9)	Au2-P2-C30-C35	-4.6(9)
C8-C7-C12-C11	2.8(13)	C35-C30-C31-C32	-0.5(13)
C6-C7-C12-C11	175.3(8)	P2-C30-C31-C32	-179.9(7)

C30-C31-C32-C33	0.0(14)
C31-C32-C33-C34	0.5(14)
C32-C33-C34-C35	-0.4(15)
C33-C34-C35-C30	-0.2(14)
C33-C34-C35-C36	178.5(9)
C31-C30-C35-C34	0.6(13)
P2-C30-C35-C34	179.9(7)
C31-C30-C35-C36	-177.9(8)
P2-C30-C35-C36	1.4(13)
C34-C35-C36-C41	79.1(11)
C30-C35-C36-C41	-102.4(11)
C34-C35-C36-C37	-90.9(10)
C30-C35-C36-C37	87.6(11)
C41-C36-C37-C38	2.8(13)
C35-C36-C37-C38	173.1(8)
C41-C36-C37-C42	-175.3(8)
C35-C36-C37-C42	-5.1(12)
C36-C37-C38-C39	-1.7(13)
C42-C37-C38-C39	176.4(8)
C37-C38-C39-C40	-0.4(13)
C37-C38-C39-C45	-179.0(8)
C38-C39-C40-C41	1.6(14)
C45-C39-C40-C41	-179.8(8)
C39-C40-C41-C36	-0.5(14)
C39-C40-C41-C48	-176.0(9)
C37-C36-C41-C40	-1.8(13)
C35-C36-C41-C40	-171.6(8)
C37-C36-C41-C48	173.6(8)
C35-C36-C41-C48	3.7(13)
C38-C37-C42-C43	43.2(11)
C36-C37-C42-C43	-138.7(9)
C38-C37-C42-C44	-81.3(10)
C36-C37-C42-C44	96.8(10)
C40-C39-C45-C46	140.2(9)
C38-C39-C45-C46	-41.3(11)
C40-C39-C45-C47	-96.4(10)
C38-C39-C45-C47	82.1(10)
C40-C41-C48-C49	-47.0(12)
C36-C41-C48-C49	137.7(9)
C40-C41-C48-C50	76.8(11)
C36-C41-C48-C50	-98.5(10)
C30-P2-C51-C52	174.7(6)
C55-P2-C51-C52	56.0(7)
Au2-P2-C51-C52	-62.3(7)
C30-P2-C51-C54	-67.0(7)
C55-P2-C51-C54	174.3(6)
Au2-P2-C51-C54	56.1(6)
C30-P2-C51-C53	49.9(8)
C55-P2-C51-C53	-68.8(8)
Au2-P2-C51-C53	173.0(6)
C30-P2-C55-C57	-81.7(8)
C51-P2-C55-C57	35.6(9)
Au2-P2-C55-C57	153.5(6)
C30-P2-C55-C58	41.1(7)
C51-P2-C55-C58	158.4(6)
Au2-P2-C55-C58	-83.7(6)
C30-P2-C55-C56	156.7(6)
C51-P2-C55-C56	-86.0(7)
Au2-P2-C55-C56	31.9(7)
P1-Au1-C59-C60	-58(5)
P1-Au1-C59-Au2	132(2)
P2-Au2-C59-C60	-142.3(10)
P2-Au2-C59-Au1	35.0(15)
C60-Au2-C59-Au1	177.4(9)
Au1-C59-C60-C61	8(8)
Au2-C59-C60-C61	178(5)
Au1-C59-C60-Au2	-170(3)
P2-Au2-C60-C59	162.6(5)
C59-Au2-C60-C61	-179.7(12)
P2-Au2-C60-C61	-17.1(12)
C59-C60-C61-C66	-127(5)
Au2-C60-C61-C66	51.2(12)
C59-C60-C61-C62	48(5)
Au2-C60-C61-C62	-133.4(8)
C66-C61-C62-C63	-0.2(15)
C60-C61-C62-C63	-175.8(9)
C61-C62-C63-C64	0.2(16)
C62-C63-C64-C65	0.6(17)
C63-C64-C65-C66	-1.2(18)
C64-C65-C66-C61	1.2(18)
C62-C61-C66-C65	-0.5(16)
C60-C61-C66-C65	175.0(10)
C1T-C2T-C3T-C4T	65(3)
C2T-C3T-C4T-C5T	170(2)
C1T'-C2T'-C3T'-C4T'	-64(6)
C2T'-C3T'-C4T'-C5T'	-164(4)
C1T"-C2T"-C3T"-C4T"	-42(5)
C2T"-C3T"-C4T"-C5T"	137(15)

DFT Calculations Data

Ethynylbenzene

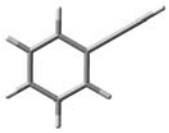

G = -308,060068 Hartree/particle.

Row	Symbol	X	Y	Z
1	C	0.1197040	-1.2102760	-0.0000050
2	C	-0.5888830	0.0000130	-0.0000110
3	C	0.1197110	1.2102790	-0.0000080
4	C	1.5083950	1.2061250	0.0000040
5	C	2.2057000	-0.0000030	0.0000090
6	C	1.5083750	-1.2061350	0.0000020

7	H	-0.4320960	-2.1487280	-0.0000070
8	H	-0.4320550	2.1487510	-0.0000110
9	H	2.0506370	2.1499080	0.0000100
10	H	3.2940630	-0.0000230	0.0000180
11	H	2.0506280	-2.1499120	0.0000060
12	C	-2.0174340	-0.0000040	-0.0000080
13	C	-3.2278000	-0.0000050	-0.0000040
14	H	-4.2977910	0.0000390	0.0001100

6-Methylhept-5-en-2-one

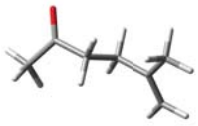

G = -348,775383 Hartree/particle.

Row	Symbol	X	Y	Z
1	C	2.6987830	1.0479830	0.3578270
2	H	2.8821240	1.1146360	1.4391660
3	H	2.1146180	1.9388000	0.0872750
4	H	3.6536920	1.0500010	-0.1755140
5	C	1.9187710	-0.1989370	0.0551430
6	C	0.4994190	-0.2486500	0.5711890
7	H	0.3558890	0.4426320	1.4139620
8	H	0.2952690	-1.2708780	0.9159010
9	O	2.3735380	-1.1123530	-0.6083670
10	C	-0.4614500	0.1212580	-0.5713740
11	H	-0.1771760	1.0996530	-0.9883200
12	H	-0.3254650	-0.6216160	-1.3746560
13	C	-1.9007120	0.1536490	-0.1408740
14	C	-2.6219810	1.2743440	-0.2114580
15	H	-2.1952010	2.2074020	-0.5794820
16	H	-3.6684270	1.2991280	0.0923600
17	C	-2.4760820	-1.1347460	0.3634800
18	H	-2.3151340	-1.9480610	-0.3599040
19	H	-1.9965300	-1.4534350	1.3004650
20	H	-3.5524440	-1.0488490	0.5520800

Naked gold complex, Me_3PAu^+ (43)

G = -596,507693 Hartree/particle.

Row	Symbol	X	Y	Z
1	P	-1.3272210	0.0012850	0.0000090
2	C	-2.0108940	1.6764000	-0.1379550
3	H	-3.1072900	1.6217800	-0.1518810
4	H	-1.6880810	2.2810430	0.7160080
5	H	-1.6581850	2.1460340	-1.0619710
6	C	-2.0152700	-0.9557440	-1.3795340
7	H	-1.6911920	-0.5245020	-2.3324540
8	H	-1.6696810	-1.9930920	-1.3209290
9	H	-3.1113760	-0.9337280	-1.3218360
10	C	-2.0200460	-0.7178910	1.5148210
11	H	-1.6868160	-1.7556430	1.6188650
12	H	-1.6883100	-0.1458350	2.3876960
13	H	-3.1159800	-0.6912950	1.4556620
14	Au	0.9569940	-0.0005140	0.0003380

Alkyne coordination, Me_3PAu^+(ethynylbenzene) (42)

G = -904,593267 Hartree/particle.

Row	Symbol	X	Y	Z
1	P	2.4228630	0.8568470	-0.0749760
2	C	3.9850850	0.0323230	-0.5113380
3	H	4.7958600	0.7709280	-0.5511450
4	H	4.2253700	-0.7300150	0.2373340
5	H	3.8878430	-0.4513000	-1.4894400
6	C	2.2127880	2.1694670	-1.3179190
7	H	2.0799760	1.7228030	-2.3091450
8	H	1.3284700	2.7699910	-1.0794920
9	H	3.0990620	2.8168350	-1.3270740
10	C	2.7555160	1.7236690	1.4901330
11	H	1.8819050	2.3196250	1.7756920
12	H	2.9593720	0.9945990	2.2816980
13	H	3.6236300	2.3847970	1.3727690
14	Au	0.6245840	-0.6207260	0.0341720
15	C	-2.9826680	0.3487790	1.1984670
16	C	-3.9534980	1.3362740	1.1330640
17	C	-4.6300570	1.5702950	-0.0638370
18	C	-4.3393120	0.8199830	-1.2022750
19	C	-3.3673940	-0.1679090	-1.1523320
20	C	-2.6864730	-0.4076850	0.0522280
21	H	-2.4458760	0.1498770	2.1245650
22	H	-4.1879470	1.9253700	2.0165860
23	H	-5.3917110	2.3458910	-0.1103170
24	H	-4.8717830	1.0084840	-2.1315480
25	H	-3.1264240	-0.7620280	-2.0314590
26	C	-1.6951550	-1.4258160	0.1130710
27	C	-0.8211560	-2.2981370	0.1600700
28	H	-0.4089170	-3.2886390	0.2500500

Alkene coordination, Me_3PAu^+(6-methylhept-5-en-2-one) (44)

G = -945,309177 Hartree/particle.

Row	Symbol	X	Y	Z
1	C	-0.9445200	-1.5945610	-1.1144560
2	H	-1.1446150	-1.0633760	-2.0471500
3	H	-0.5089920	-2.5916590	-1.1981240
4	C	-1.5415800	-1.1897210	0.0558600
5	C	-1.5125180	-2.0371720	1.2877670
6	H	-1.2702270	-1.4390440	2.1760400
7	H	-2.5080510	-2.4707820	1.4588090
8	H	-0.7966920	-2.8614070	1.2026610
9	C	-2.3893920	0.0521500	0.0970080
10	H	-2.1707560	0.6174100	1.0161740
11	H	-2.1389800	0.6977780	-0.7556880
12	C	-3.8809570	-0.3082470	0.0551550
13	H	-4.1590200	-0.9905010	0.8670250
14	Au	0.7778210	-0.3912050	-0.2510590
15	P	2.7694500	0.7261590	0.2510390
16	C	2.9550760	1.1262810	2.0169570

17	H	2.9397090	0.2059860	2.6107000
18	H	3.9077430	1.6465880	2.1795750
19	H	2.1301910	1.7698940	2.3408250
20	C	4.2581740	-0.2276650	-0.1795610
21	H	4.2681110	-0.4391930	-1.2542590
22	H	5.1538600	0.3487660	0.0856250
23	H	4.2641430	-1.1771140	0.3664900
24	C	2.9540730	2.3148070	-0.6180990
25	H	3.9177920	2.7696200	-0.3556110
26	H	2.9123610	2.1559920	-1.7008690
27	H	2.1436220	2.9930020	-0.3296440
28	H	-4.0938270	-0.8242300	-0.8961220
29	C	-4.8103680	0.8874670	0.1398870
30	C	-4.4797210	2.0840490	-0.7075260
31	H	-3.6284280	2.6264330	-0.2723360
32	H	-4.1871660	1.7893810	-1.7236360
33	H	-5.3383830	2.7600830	-0.7445470
34	O	-5.7914510	0.8556090	0.8555270

Ketone coordination, Me_3PAu^+(6-methylhept-5-en-2-one´) (45)

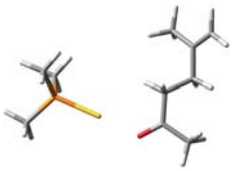

G = -945,306931 Hartree/particle.

Row	Symbol	X	Y	Z
1	C	5.2668890	1.8701210	0.7043780
2	H	5.9075050	1.0870590	1.1093250
3	H	5.5456830	2.8986760	0.9317100
4	C	4.1954130	1.5864230	-0.0380850
5	C	3.3116870	2.6537990	-0.6087930
6	H	3.7185090	3.6536830	-0.4198970
7	H	3.1953910	2.5295110	-1.6957680
8	H	2.2987720	2.6229190	-0.1807720
9	C	3.8256560	0.1613920	-0.3519550
10	H	3.7452550	0.0325460	-1.4441470
11	H	4.6245060	-0.5082500	-0.0055860
12	C	2.4945210	-0.2418900	0.2915310
13	H	1.6778510	0.4349280	-0.0019550
14	H	2.5870030	-0.1568810	1.3891480
15	C	2.0467170	-1.6437800	0.0305750
16	C	3.0539890	-2.7335760	-0.0504080
17	H	3.6347450	-2.6197720	-0.9766060
18	H	3.7693410	-2.6621250	0.7784320
19	H	2.5655720	-3.7107710	-0.0518310
20	O	0.8477040	-1.9320800	-0.0960910
21	Au	-0.8450870	-0.5673220	-0.0133270
22	P	-2.6669130	0.8126340	0.0483130
23	C	-4.2535550	-0.0720660	-0.0247350
24	H	-4.3362970	-0.7613330	0.8222460
25	H	-5.0789610	0.6504440	0.0119970
26	H	-4.3151390	-0.6457320	-0.9556110
27	C	-2.7136800	1.9952600	-1.3325180
28	H	-3.6039750	2.6308470	-1.2429440
29	H	-1.8167000	2.6236740	-1.3164370
30	H	-2.7489230	1.4535470	-2.2838880
31	C	-2.7452010	1.8283690	1.5542800
32	H	-3.6447980	2.4565270	1.5294420
33	H	-2.7775030	1.1832780	2.4387230
34	H	-1.8585190	2.4684610	1.6156580

Alkyne coordination, Me_2(biphenyl)PAu$^+$(ethynylbenzene) (46)

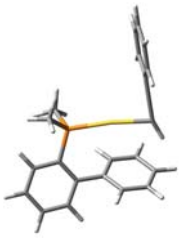

G = -1326,923356 Hartree/particle.

Row	Symbol	X	Y	Z
1	P	-0.9947230	-1.6379490	0.3458670
2	C	-0.5667800	-3.1028990	-0.6548340
3	H	-0.7366800	-2.8888300	-1.7153890
4	H	0.4975960	-3.3173410	-0.5060560
5	H	-1.1462970	-3.9856380	-0.3608230
6	C	-0.9630780	-2.2588210	2.0625240
7	H	0.0333650	-2.6604630	2.2799010
8	H	-1.1796960	-1.4513390	2.7693380
9	H	-1.7097540	-3.0535780	2.1850150
10	Au	0.4863700	0.1281660	-0.0468130
11	C	4.2278000	-0.0801360	0.9972460
12	C	5.3533140	-0.8835890	1.0942420
13	C	6.0649950	-1.2284850	-0.0544610
14	C	5.6540280	-0.7731720	-1.3060240
15	C	4.5272080	0.0280380	-1.4178650
16	C	3.8105350	0.3787110	-0.2630570
17	H	3.6605200	0.2002230	1.8835070
18	H	5.6810100	-1.2422810	2.0672910
19	H	6.9482860	-1.8585580	0.0265010
20	H	6.2149840	-1.0452360	-2.1971240
21	H	4.1928700	0.3919780	-2.3873200
22	C	2.6616220	1.2132000	-0.3680140
23	C	1.6700680	1.9440020	-0.4663250
24	H	1.0835840	2.8454200	-0.5657430
25	C	-2.7417020	-1.2595950	-0.0267760
26	C	-3.5939910	-2.3541660	-0.2277350
27	C	-3.2506370	0.0483680	-0.1690270
28	C	-4.9248690	-2.1782720	-0.5796500
29	H	-3.2148490	-3.3692730	-0.1157410
30	C	-4.5910870	0.2020140	-0.5455700
31	C	-5.4216870	-0.8906260	-0.7499010
32	H	-5.5662210	-3.0441000	-0.7277140
33	H	-4.9867960	1.2110430	-0.6540130
34	H	-6.4606790	-0.7349720	-1.0328830
35	C	-2.4807710	1.2927810	0.0753730
36	C	-2.3969880	2.2670770	-0.9265930
37	C	-1.9128430	1.5668440	1.3278770
38	C	-1.7574870	3.4799090	-0.6865400
39	H	-2.8420720	2.0685920	-1.9014690
40	C	-1.2795170	2.7836170	1.5704310
41	H	-2.0127550	0.8383840	2.1329810
42	C	-1.2008980	3.7432450	0.5638280
43	H	-1.7045110	4.2272430	-1.4761180
44	H	-0.8598900	2.9850210	2.5543200
45	H	-0.7178120	4.6995630	0.7568400

Alkene coordination, Me_2(biphenyl)PAu$^+$(6-methylhept-5-en-2-one) (47)

G = -1367,638453 Hartree/particle.

Row	Symbol	X	Y	Z
1	C	-1.9503500	1.3630900	-0.9308620
2	H	-1.8068200	1.9491560	-0.0200130
3	H	-1.7253010	1.8605030	-1.8764950
4	C	-2.7095230	0.2152910	-0.9089930
5	C	-3.1623360	-0.4492980	-2.1699410
6	H	-3.0841120	-1.5415810	-2.0947310
7	H	-4.2221090	-0.2155880	-2.3458940
8	H	-2.5952220	-0.1064580	-3.0417730
9	C	-3.2680420	-0.3137110	0.3839710
10	H	-3.1193140	-1.4034170	0.4314600
11	H	-2.7221870	0.1308680	1.2272970
12	C	-4.7648580	0.0028780	0.5037290
13	H	-5.3388400	-0.4259710	-0.3262960
14	Au	-0.2798230	-0.1481360	-0.7602870
15	P	1.6277520	-1.5103360	-0.6035910
16	C	2.4660130	-1.7710510	-2.2049020
17	H	2.7750890	-0.8163920	-2.6427750
18	H	3.3512120	-2.4041140	-2.0626350
19	H	1.7728410	-2.2671130	-2.8940480
20	C	1.1999220	-3.2035540	-0.0723250
21	H	2.0445290	-3.8940370	-0.1787290
22	H	0.8605090	-3.1961030	0.9687920
23	H	0.3797320	-3.5584760	-0.7068050
24	H	-4.9008620	1.0967920	0.4705700
25	C	-5.3975420	-0.4957340	1.7890570
26	C	-4.6635730	-0.2221700	3.0721510
27	H	-3.7876580	-0.8815330	3.1499800
28	H	-4.2912590	0.8100480	3.1088030
29	H	-5.3209220	-0.4155210	3.9242840
30	O	-6.4656670	-1.0741250	1.7683930
31	C	2.8998460	-0.9095610	0.5598060
32	C	2.9820010	0.4285860	1.0008930
33	C	3.7907490	-1.8601010	1.0754660
34	C	3.9317670	0.7470380	1.9796670
35	C	4.7394320	-1.5170890	2.0288460
36	H	3.7437350	-2.8943070	0.7371510
37	C	4.7994380	-0.2071930	2.4921900
38	H	3.9988190	1.7794720	2.3202560
39	H	5.4221690	-2.2721570	2.4120410
40	H	5.5309690	0.0761820	3.2460470
41	C	2.1494040	1.5388620	0.4799270
42	C	1.4361530	2.3543630	1.3675720
43	C	2.1236500	1.8528800	-0.8862170
44	C	0.7171280	3.4513280	0.9032300
45	H	1.4516260	2.1224330	2.4324060
46	C	1.4048470	2.9522910	-1.3507060
47	H	2.7155900	1.2611500	-1.5851470
48	C	0.7009990	3.7545600	-0.4563730
49	H	0.1731130	4.0770840	1.6084170
50	H	1.4111990	3.1898530	-2.4129950
51	H	0.1477980	4.6197400	-0.8169060

Ketone coordination,
Me_2(biphenyl)PAu$^+$(6-methylhept-5-en-2-one´) (48)

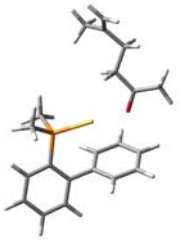

G = -1367,633211 Hartree/particle.

Row	Symbol	X	Y	Z
1	C	6.5529920	-1.7323670	-0.6154690
2	H	6.9519770	-1.1602010	-1.4527080
3	H	6.9557080	-2.7343830	-0.4700050
4	C	5.6211970	-1.2301600	0.1966120
5	C	5.0670970	-2.0049290	1.3539060
6	H	5.6018760	-2.9506910	1.4967370
7	H	5.1354700	-1.4253310	2.2866510
8	H	4.0027080	-2.2462020	1.2139030
9	C	5.0811890	0.1603140	-0.0069650
10	H	5.2438840	0.7534050	0.9083770
11	H	5.6410410	0.6522810	-0.8138790
12	C	3.5890590	0.1540330	-0.3335510
13	H	3.0015390	-0.3173820	0.4703980
14	H	3.4057210	-0.4654530	-1.2303330
15	C	2.9475060	1.4751710	-0.6252570
16	C	3.7783270	2.6504910	-0.9901530
17	H	4.4932790	2.8716120	-0.1868530
18	H	4.3774280	2.4135050	-1.8802490
19	H	3.1511290	3.5228440	-1.1864730
20	O	1.7139500	1.5999700	-0.6031510
21	Au	0.2792920	0.0214030	-0.1791960
22	P	-1.2451580	-1.6316860	0.2727370
23	C	-1.1755190	-2.2052340	2.0038630
24	H	-1.9452440	-2.9703200	2.1675640
25	H	-0.1867570	-2.6384420	2.1955640
26	H	-1.3372110	-1.3744800	2.6976640
27	C	-0.8790300	-3.1406190	-0.6825950
28	H	-1.4737920	-3.9948820	-0.3387610
29	H	-1.0618410	-2.9670640	-1.7482510
30	H	0.1818770	-3.3769410	-0.5418940
31	C	-2.9804260	-1.1927500	-0.0835020
32	C	-3.8524160	-2.2356460	-0.4224800
33	C	-3.4538610	0.1366080	-0.0895440
34	C	-5.1694330	-1.9823850	-0.7815320
35	H	-3.5043820	-3.2671950	-0.4182690
36	C	-4.7765750	0.3710330	-0.4803090
37	C	-5.6285470	-0.6705300	-0.8230950
38	H	-5.8286110	-2.8085580	-1.0384570
39	H	-5.1393070	1.3981910	-0.4906760
40	H	-6.6549690	-0.4567510	-1.1141790
41	C	-2.6352710	1.3084260	0.3065220
42	C	-2.1349790	1.4342260	1.6074460
43	C	-2.3992630	2.3402890	-0.6098220
44	C	-1.3939060	2.5537200	1.9770590
45	H	-2.3591490	0.6638500	2.3457080
46	C	-1.6561070	3.4574540	-0.2412590
47	H	-2.7980340	2.2555130	-1.6209020
48	C	-1.1489680	3.5652970	1.0517860
49	H	-1.0198480	2.6414170	2.9954890
50	H	-1.4775560	4.2490620	-0.9666670
51	H	-0.5736260	4.4426680	1.3412220

Alkyne coordination, ^{t}BuXPhosAu^{+}(ethynylbenzene) (37)

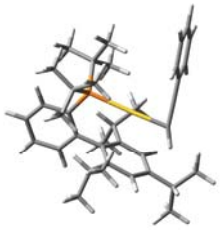

G = -1915,731964 Hartree/particle.

Row	Symbol	X	Y	Z
1	P	-0.8600140	1.7827480	0.0364240
2	C	-1.5771190	2.7452660	-1.4451540
3	C	-1.9903060	1.8896530	1.5607740
4	Au	-0.6473370	-0.4878300	-0.5552460
5	C	-3.2822320	-2.8180410	1.1213910
6	C	-4.5753410	-2.7376810	1.6171410
7	C	-5.6298200	-2.4117280	0.7650010
8	C	-5.3978350	-2.1662250	-0.5879900
9	C	-4.1095950	-2.2435270	-1.0966850
10	C	-3.0474470	-2.5733120	-0.2404290
11	H	-2.4434240	-3.0610760	1.7726070
12	H	-4.7638650	-2.9281240	2.6712400
13	H	-6.6418180	-2.3475620	1.1594150
14	H	-6.2255260	-1.9120370	-1.2461070
15	H	-3.9084670	-2.0477650	-2.1489420
16	C	-1.7148060	-2.6163730	-0.7478520
17	C	-0.5564990	-2.6332570	-1.1784940
18	H	0.3593220	-2.9963940	-1.6147510
19	C	0.7681620	2.5136430	0.4737120
20	C	0.8068280	3.8919010	0.7453380
21	C	1.9784830	1.7776830	0.5060930
22	C	1.9892840	4.5505920	1.0488580
23	H	-0.1094060	4.4776760	0.7144910
24	C	3.1594270	2.4694670	0.8122350
25	C	3.1768360	3.8306480	1.0823890
26	H	1.9787520	5.6187850	1.2531540
27	H	4.0925330	1.9059280	0.8286070
28	H	4.1178300	4.3260560	1.3127870
29	C	2.1669490	0.3118490	0.2373350
30	C	2.4718210	-0.1360060	-1.0682270
31	C	2.2374380	-0.5987140	1.3165650
32	C	2.7947180	-1.4810780	-1.2648470
33	C	2.5647550	-1.9313250	1.0644190
34	C	2.8403400	-2.3984920	-0.2186980
35	H	3.0349290	-1.8289880	-2.2725550
36	H	2.6220910	-2.6221090	1.9064780
37	C	-3.3965010	1.4382190	1.1648160
38	H	-3.3917310	0.4527450	0.6759090
39	H	-4.0032070	1.3498580	2.0777810
40	H	-3.9046980	2.1540810	0.5077730
41	C	-2.0429710	3.2710120	2.2108720
42	H	-2.7318360	3.2203650	3.0663140
43	H	-1.0638690	3.5750430	2.6004320
44	H	-2.4144070	4.0537950	1.5412520
45	C	-1.4391680	0.9050650	2.5896190
46	H	-1.4326640	-0.1265280	2.2106150
47	H	-0.4217620	1.1684030	2.9063230
48	H	-2.0795520	0.9296040	3.4834650
49	C	-0.4287560	3.0729590	-2.3980410
50	H	0.1221170	2.1734320	-2.6994320
51	H	-0.8504970	3.5194050	-3.3098820
52	H	0.2837970	3.7914020	-1.9735660
53	C	-2.5537470	1.8160270	-2.1771890
54	H	-2.9579570	2.3508550	-3.0489290
55	H	-2.0549910	0.9068460	-2.5422440
56	H	-3.4027420	1.5081930	-1.5547740
57	C	-2.3096800	4.0390280	-1.0891440
58	H	-2.6556470	4.5007030	-2.0252700
59	H	-3.1984270	3.8704390	-0.4696880
60	H	-1.6679070	4.7758760	-0.5922170
61	C	2.0391430	-0.1651780	2.7547600
62	H	1.5396060	0.8152990	2.7494500

63	C	1.1716150	-1.1378810	3.5525000
64	H	1.7200720	-2.0571950	3.7997960
65	H	0.8631290	-0.6814000	4.5024790
66	H	0.2670920	-1.4287440	2.9999370
67	C	3.3880980	0.0200950	3.4529170
68	H	3.2416580	0.3348600	4.4949850
69	H	3.9526190	-0.9232780	3.4619860
70	H	4.0056560	0.7773800	2.9532620
71	C	2.5305390	0.8071740	-2.2526210
72	H	2.0802500	1.7643630	-1.9502490
73	C	1.7533160	0.2883230	-3.4606820
74	H	1.7165470	1.0533800	-4.2482480
75	H	2.2243480	-0.6024780	-3.8985570
76	H	0.7181130	0.0198180	-3.1964810
77	C	3.9829770	1.0926420	-2.6368410
78	H	4.4941190	0.1721510	-2.9527910
79	H	4.0281080	1.8049880	-3.4714350
80	H	4.5466620	1.5173780	-1.7958860
81	C	3.2424930	-3.8329600	-0.4790880
82	H	3.0513410	-4.0354180	-1.5469990
83	C	2.4462450	-4.8426610	0.3405680
84	H	2.6768970	-4.7639040	1.4121370
85	H	1.3626980	-4.7055730	0.2211500
86	H	2.6962640	-5.8655180	0.0311850
87	C	4.7414810	-4.0071090	-0.2330770
88	H	5.0575880	-5.0356160	-0.4526970
89	H	5.3323650	-3.3245100	-0.8576480
90	H	4.9830060	-3.7957080	0.8189780

Alkene coordination,
^{t}BuXPhosAu^{+}(6-methylhept-5-en-2-one) (49)

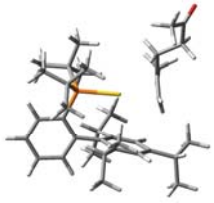

G = -1956,448140 Hartree/particle.

Row	Symbol	X	Y	Z
1	C	-2.0627850	1.7250990	0.4261710
2	H	-2.3123390	1.6299210	1.4860610
3	H	-1.3861350	2.5380580	0.1511130
4	C	-2.8244920	1.0898060	-0.5277220
5	C	-2.6822030	1.4114830	-1.9834070
6	H	-2.6711230	0.4970160	-2.5924360
7	H	-3.5453210	2.0056240	-2.3168730
8	H	-1.7724760	1.9892890	-2.1878750
9	C	-3.9670450	0.1951770	-0.1285690
10	H	-4.0095930	-0.6797730	-0.7961410
11	H	-3.8036300	-0.1775420	0.8922470
12	C	-5.2950720	0.9612640	-0.1953120
13	H	-5.4727770	1.3814410	-1.1924640
14	Au	-0.7718540	-0.1008550	0.0452250
15	P	0.5209650	-2.0757540	-0.1626870
16	C	0.2287910	-2.8031310	-1.8893940
17	C	0.0104060	-3.2835070	1.2237680
18	H	-5.2512420	1.8048790	0.5139110
19	C	-6.5101260	0.1300340	0.1658870
20	C	-6.4129900	-0.7409440	1.3874290
21	H	-5.7980900	-1.6252640	1.1661390
22	H	-5.9299180	-0.2148110	2.2212000
23	H	-7.4103080	-1.0780810	1.6831040
24	O	-7.5220950	0.1903790	-0.5037070
25	C	2.3189850	-1.7367640	0.0122640

26	C	2.8596210	-0.4395330	0.1869830
27	C	3.1884380	-2.8403870	0.0223290
28	C	4.2452680	-0.3248390	0.3706520
29	C	4.5565940	-2.6982460	0.2016170
30	H	2.7880640	-3.8437220	-0.1053620
31	C	5.0881820	-1.4271700	0.3796840
32	H	4.6650390	0.6714010	0.5128340
33	H	5.1975560	-3.5769590	0.2059250
34	H	6.1575740	-1.2909370	0.5272370
35	C	2.1149950	0.8643390	0.2066230
36	C	1.6721870	1.4068180	1.4354920
37	C	2.0393560	1.6500990	-0.9657060
38	C	1.1314690	2.6933630	1.4511590
39	C	1.4731000	2.9250960	-0.8964170
40	C	1.0113870	3.4676550	0.2999900
41	H	0.7910970	3.1184470	2.3985400
42	H	1.4217320	3.5231830	-1.8069890
43	C	-1.4872710	-3.0885740	1.4890800
44	H	-1.7963890	-3.7837420	2.2831820
45	H	-1.7083140	-2.0672670	1.8318640
46	H	-2.1105270	-3.2933510	0.6097060
47	C	0.7720430	-2.8967970	2.4915960
48	H	0.5979660	-1.8505700	2.7725230
49	H	0.4092360	-3.5226970	3.3195270
50	H	1.8536800	-3.0569880	2.3996930
51	C	0.2704470	-4.7607280	0.9270470
52	H	1.3298330	-4.9834510	0.7508990
53	H	-0.0320990	-5.3420110	1.8100780
54	H	-0.3160440	-5.1387800	0.0812760
55	C	1.1411420	-3.9721350	-2.2599860
56	H	1.0384240	-4.8362280	-1.5952480
57	H	0.8693110	-4.3066240	-3.2714570
58	H	2.1959870	-3.6734160	-2.2914740
59	C	-1.2363810	-3.2248790	-2.0013870
60	H	-1.4368500	-3.5164950	-3.0422760
61	H	-1.4819250	-4.0867590	-1.3697820
62	H	-1.9207830	-2.4002810	-1.7525320
63	C	0.4840630	-1.6767930	-2.8891540
64	H	-0.1824580	-0.8189920	-2.7221200
65	H	1.5234300	-1.3250840	-2.8574310
66	H	0.2950340	-2.0547440	-3.9045770
67	C	0.4618250	4.8741630	0.3973330
68	H	-0.2291630	4.8910490	1.2575290
69	C	-0.3123800	5.3252500	-0.8352460
70	H	0.3465270	5.4429910	-1.7067490
71	H	-1.1090590	4.6190820	-1.1093220
72	H	-0.7777730	6.3019860	-0.6515570
73	C	1.6005500	5.8513430	0.6944470
74	H	1.2182780	6.8735440	0.8165760
75	H	2.1402190	5.5739240	1.6093180
76	H	2.3225870	5.8553600	-0.1351280
77	C	1.8315120	0.6702220	2.7509360
78	H	2.1282140	-0.3661840	2.5300710
79	C	2.9526260	1.2966940	3.5814670
80	H	2.7148210	2.3386560	3.8384230
81	H	3.0940010	0.7435970	4.5195520
82	H	3.9064810	1.2960450	3.0382770
83	C	0.5365820	0.6242710	3.5598710
84	H	0.6703340	0.0087860	4.4600080
85	H	0.2286200	1.6250770	3.8927810
86	H	-0.2952110	0.1986330	2.9760340
87	C	2.6482650	1.1998750	-2.2791480
88	H	2.8217300	0.1152540	-2.2192630
89	C	1.7561680	1.4739950	-3.4878920

90	H	1.7159260	2.5454820	-3.7265750
91	H	2.1551570	0.9630230	-4.3743610
92	H	0.7263200	1.1265630	-3.3290870
93	C	4.0123340	1.8626290	-2.4845120
94	H	4.4644840	1.5256640	-3.4269790
95	H	3.9083340	2.9559960	-2.5320660
96	H	4.7088120	1.6261470	-1.6701820

Ketone coordination, ^{t}BuXPhosAu^{+}(6-methylhept-5-en-2-one´) (50)

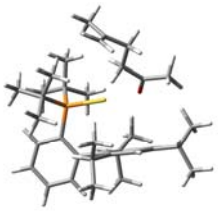

G = -1956,439283 Hartree/particle.

Row	Symbol	X	Y	Z
1	C	-6.6346890	-0.4944790	1.6051100
2	H	-6.7470340	0.4163570	2.1930150
3	H	-7.0767580	-1.4018670	2.0155850
4	C	-5.9935060	-0.4994100	0.4348330
5	C	-5.8463970	-1.7418650	-0.3904330
6	H	-6.3586130	-2.5931830	0.0720930
7	H	-6.2631370	-1.5957560	-1.3981100
8	H	-4.7920920	-2.0258600	-0.5292790
9	C	-5.3749630	0.7579840	-0.1179530
10	H	-5.7092640	0.9113100	-1.1570540
11	H	-5.7197500	1.6231570	0.4650550
12	C	-3.8500510	0.6815000	-0.0842970
13	H	-3.4769070	-0.1794420	-0.6628660
14	H	-3.5181840	0.5003210	0.9548080
15	C	-3.0755330	1.8771050	-0.5476530
16	C	-3.7378320	3.2008270	-0.6772890
17	H	-4.5605730	3.1423980	-1.4022510
18	H	-4.1910770	3.4836530	0.2827040
19	H	-3.0213390	3.9648160	-0.9898860
20	O	-1.8648940	1.7834820	-0.7940290
21	Au	-0.6663720	-0.0411740	-0.5091640
22	P	0.5257200	-2.0258390	-0.3076580
23	C	0.8526920	-2.6907780	-2.0520910
24	C	-0.4865530	-3.2485060	0.7539900
25	C	2.1541210	-1.7858450	0.5189540
26	C	2.8923390	-2.9446980	0.8134360
27	C	2.6741090	-0.5308250	0.9203250
28	C	4.1006290	-2.8977550	1.4932710
29	H	2.5156510	-3.9183020	0.5097680
30	C	3.8895110	-0.5125870	1.6186600
31	C	4.5992750	-1.6691460	1.9076540
32	H	4.6406310	-3.8184000	1.7028280
33	H	4.2797910	0.4523660	1.9420590
34	H	5.5385070	-1.6088340	2.4536830
35	C	2.0590710	0.8098160	0.6606650
36	C	2.4854080	1.5723210	-0.4494620
37	C	1.1491050	1.3668530	1.5846570
38	C	1.9254260	2.8337430	-0.6567960
39	C	0.6233910	2.6355600	1.3314310
40	C	0.9733290	3.3733190	0.2050820
41	H	2.2513600	3.4171150	-1.5191470
42	H	-0.0920930	3.0673850	2.0348540
43	C	-1.9738520	-3.0139850	0.4651550
44	H	-2.5615990	-3.7439440	1.0407460
45	H	-2.2919680	-2.0104810	0.7795730
46	H	-2.2339760	-3.1411190	-0.5931120

47	C	-0.2364100	-2.9184980	2.2251030
48	H	-0.4693610	-1.8698690	2.4520800
49	H	-0.9013920	-3.5429990	2.8387400
50	H	0.7954360	-3.1220120	2.5366230
51	C	-0.1788300	-4.7271140	0.5120400
52	H	0.8589620	-5.0009990	0.7347080
53	H	-0.8113370	-5.3175900	1.1903820
54	H	-0.4174300	-5.0507750	-0.5080040
55	C	1.8149100	-3.8768990	-2.1114890
56	H	1.4685270	-4.7485790	-1.5460900
57	H	1.9074630	-4.1860910	-3.1623380
58	H	2.8196660	-3.6077850	-1.7631020
59	C	-0.4825640	-3.0654390	-2.6963400
60	H	-0.3048150	-3.2959180	-3.7565710
61	H	-0.9407270	-3.9542930	-2.2445960
62	H	-1.2051590	-2.2377440	-2.6542750
63	C	1.4739640	-1.5412810	-2.8439600
64	H	0.8044340	-0.6717820	-2.9055550
65	H	2.4297230	-1.2167540	-2.4117740
66	H	1.6756240	-1.8838490	-3.8694220
67	C	0.3644070	4.7355460	-0.0315660
68	H	-0.5374950	4.7970520	0.6014460
69	C	0.7863370	0.6648400	2.8787120
70	H	1.1166600	-0.3825670	2.8030840
71	C	3.5896690	1.0995150	-1.3766270
72	H	3.6797160	0.0066900	-1.2734880
73	C	4.9291270	1.7080710	-0.9530110
74	H	5.7332750	1.3734050	-1.6221730
75	H	4.8830310	2.8054800	-1.0024110
76	H	5.2028240	1.4299870	0.0727010
77	C	3.3327100	1.4164720	-2.8486220
78	H	3.4594740	2.4872150	-3.0594090
79	H	4.0534140	0.8790560	-3.4792180
80	H	2.3211210	1.1320870	-3.1665170
81	C	1.3272500	5.8361820	0.4121410
82	H	2.2496270	5.8037890	-0.1860620
83	H	0.8762860	6.8291870	0.2815390
84	H	1.6076160	5.7215620	1.4674440
85	C	-0.0667780	4.9439380	-1.4796200
86	H	0.7999270	5.0103180	-2.1524820
87	H	-0.6996870	4.1160860	-1.8274090
88	H	-0.6289720	5.8817790	-1.5814950
89	C	-0.7133870	0.6625680	3.1641000
90	H	-1.2856060	0.2396140	2.3230080
91	H	-0.9319240	0.0634080	4.0587270
92	H	-1.0964180	1.6754750	3.3507030
93	C	1.5450600	1.2968900	4.0469080
94	H	1.2596410	2.3511460	4.1724450
95	H	1.3190300	0.7724290	4.9850410
96	H	2.6309960	1.2610280	3.8896380

Transition state to anti trans-cyclopropyl gold carbene 51 ($TS^{\neq}_{42\text{-}51}$)

G = -1253,343287 Hartree/particle.

Row	Symbol	X	Y	Z
1	C	0.8685360	0.7910770	-0.6879780
2	C	0.4216020	-0.4094400	-0.8113050
3	H	0.9657430	-1.2805420	-1.1674260
4	C	0.6593250	2.1209110	-0.1803390

5	C	0.6133670	2.3138310	1.2098330
6	C	0.4925200	3.2161270	-1.0410860
7	C	0.4005140	3.5847950	1.7273020
8	H	0.7458120	1.4556180	1.8684790
9	C	0.2839140	4.4828340	-0.5161360
10	H	0.5245620	3.0621300	-2.1187020
11	C	0.2417130	4.6681110	0.8659830
12	H	0.3638260	3.7317560	2.8044430
13	H	0.1521470	5.3306050	-1.1845940
14	H	0.0840210	5.6643770	1.2742070
15	Au	-1.6044720	-0.6343150	-0.2732610
16	P	-3.8542280	-0.9815340	0.3045080
17	C	-4.6099590	-2.4124010	-0.5352160
18	H	-5.6558820	-2.5222890	-0.2211400
19	H	-4.5707090	-2.2684620	-1.6204520
20	H	-4.0587850	-3.3247620	-0.2819900
21	C	-4.1334500	-1.2993300	2.0778030
22	H	-3.8032480	-0.4367670	2.6669650
23	H	-5.2006890	-1.4783390	2.2626570
24	H	-3.5599990	-2.1787900	2.3907080
25	C	-4.9598410	0.4133800	-0.0896940
26	H	-4.9281660	0.6190200	-1.1652820
27	H	-5.9897910	0.1703080	0.2019400
28	H	-4.6338660	1.3102410	0.4483990
29	C	3.4092440	0.7121350	-0.5328960
30	C	2.8128450	0.9345820	-1.7372330
31	H	2.6500610	0.1215270	-2.4419880
32	H	2.7075770	1.9447330	-2.1299600
33	C	3.8025340	1.8384620	0.3590270
34	H	3.3751920	2.7960570	0.0389250
35	H	3.5124690	1.6435850	1.4015050
36	H	4.8975170	1.9461840	0.3536000
37	C	3.7025490	-0.6754690	-0.0607530
38	H	3.2347470	-0.8393370	0.9230150
39	H	3.2691960	-1.4148930	-0.7469230
40	C	5.2000500	-0.9362270	0.0613380
41	H	5.6636340	-0.2752990	0.8110710
42	H	5.7213010	-0.7124750	-0.8833370
43	C	5.5086650	-2.3630410	0.4586400
44	C	6.9638450	-2.7370620	0.4703120
45	H	7.3485620	-2.7448330	-0.5587300
46	H	7.5571890	-1.9975830	1.0230000
47	H	7.0984560	-3.7293910	0.9098420
48	O	4.6284990	-3.1522710	0.7420190

Transition state to anti cis-cyclopropyl gold carbene 52 ($TS^{\neq}_{42\text{-}52}$)

G = -1253,342760 Hartree/particle.

Row	Symbol	X	Y	Z
1	C	0.7303400	-0.5377760	0.7135990
2	C	3.0147680	-1.6200620	0.2855130
3	C	2.4935800	-1.5606420	1.5433550
4	H	2.8159880	-0.7862410	2.2391820
5	H	1.9619940	-2.4071170	1.9730720
6	C	2.7082880	-2.7393560	-0.6478960
7	H	2.0870120	-3.5153510	-0.1892140

8	H	2.1996920	-2.3545910	-1.5445540
9	H	3.6368670	-3.2094970	-1.0015210
10	C	3.9301540	-0.5515720	-0.2180540
11	H	3.7024050	-0.3123790	-1.2678370
12	H	3.8080770	0.3765050	0.3583680
13	C	5.3875970	-0.9976110	-0.1201600
14	H	5.5634610	-1.9346440	-0.6725880
15	H	5.6588170	-1.2246020	0.9233280
16	C	6.3495410	0.0407010	-0.6568720
17	C	7.8091720	-0.2891900	-0.5168390
18	H	8.0838040	-0.3184660	0.5463010
19	H	8.0264920	-1.2838640	-0.9267870
20	H	8.4180740	0.4635070	-1.0251310
21	O	5.9586260	1.0737020	-1.1636510
22	C	1.1524440	0.8301590	0.5690570
23	C	1.2632040	1.3668160	-0.7236660
24	C	1.4525510	1.6266830	1.6836550
25	C	1.6645710	2.6849360	-0.8944740
26	H	1.0313490	0.7349060	-1.5812240
27	C	1.8547200	2.9424610	1.5040620
28	H	1.3644850	1.2043200	2.6836860
29	C	1.9645410	3.4692440	0.2171260
30	H	1.7514250	3.1005450	-1.8958730
31	H	2.0862320	3.5606420	2.3685530
32	H	2.2880760	4.4991400	0.0810840
33	C	-0.2154280	-1.4001980	0.5768550
34	H	-0.1396040	-2.4806700	0.6636140
35	Au	-2.0917610	-0.5438390	0.1355310
36	P	-4.2079780	0.3106560	-0.4204380
37	C	-5.3787550	0.4167750	0.9731170
38	H	-6.3431060	0.8065300	0.6219870
39	H	-5.5275520	-0.5770450	1.4094490
40	H	-4.9794020	1.0830430	1.7454460
41	C	-5.0832250	-0.6846940	-1.6726230
42	H	-6.0604570	-0.2359730	-1.8925830
43	H	-4.4897210	-0.7273730	-2.5925390
44	H	-5.2290050	-1.7048510	-1.3008410
45	C	-4.1808080	1.9940140	-1.1199940
46	H	-5.2019040	2.3123410	-1.3670710
47	H	-3.7495070	2.6922120	-0.3942170
48	H	-3.5677740	2.0086670	-2.0277960

Transition state to syn trans-cyclopropyl gold carbene 53 ($TS^{\neq}_{42\text{-}53}$)

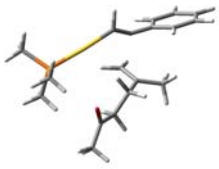

G = -1253,337747 Hartree/particle.

Row	Symbol	X	Y	Z
1	C	2.2258790	-0.8151450	-0.0166350
2	C	1.1422400	-1.4019890	-0.3890140
3	C	3.6452150	-0.6491260	-0.0373970
4	C	4.2578180	-0.1931960	-1.2174550
5	C	4.4357010	-0.9647750	1.0811890
6	C	5.6386930	-0.0588050	-1.2742810
7	H	3.6374170	0.0455330	-2.0804010
8	C	5.8115820	-0.8203270	1.0173020
9	H	3.9566750	-1.3218930	1.9916170
10	C	6.4124950	-0.3640080	-0.1576830
11	H	6.1114200	0.2903890	-2.1894560
12	H	6.4229150	-1.0666870	1.8824970

13	H	7.4935520	-0.2487870	-0.2013630
14	C	1.7261430	1.7482710	0.5054790
15	C	1.6209050	0.7943100	1.4709970
16	H	0.6599910	0.3447270	1.7169890
17	H	2.4293700	0.6250460	2.1803560
18	C	2.9992490	2.4736400	0.2574800
19	H	3.8158280	2.1474610	0.9120570
20	H	3.3153820	2.3616530	-0.7907130
21	H	2.8351660	3.5515050	0.4103110
22	C	0.5503630	2.1203210	-0.3417220
23	H	0.8780080	2.6615240	-1.2404520
24	H	0.0410880	1.2047040	-0.6875670
25	C	-0.4726770	2.9600630	0.4149020
26	H	-0.0886120	3.9630180	0.6536090
27	H	-0.7012260	2.4964540	1.3920950
28	C	-1.7992820	3.0676560	-0.3031020
29	C	-2.7004570	4.1807090	0.1430900
30	H	-2.7364650	4.2418340	1.2389640
31	H	-2.2962930	5.1389160	-0.2117120
32	H	-3.7075680	4.0458770	-0.2622860
33	O	-2.1298040	2.2666790	-1.1603210
34	H	1.3555760	-2.3343120	-0.9319220
35	Au	-0.9152560	-1.0797590	-0.1525890
36	P	-3.2325230	-0.8377620	0.1725800
37	C	-3.7017190	0.4261710	1.4010200
38	H	-4.7894690	0.4207340	1.5479780
39	H	-3.2059200	0.2277510	2.3575740
40	H	-3.3960230	1.4134570	1.0372730
41	C	-4.1885210	-0.3944700	-1.3131540
42	H	-4.0269090	-1.1409290	-2.0985140
43	H	-5.2578710	-0.3508910	-1.0684500
44	H	-3.8531950	0.5838460	-1.6723390
45	C	-4.0228240	-2.3645550	0.7828500
46	H	-3.5700550	-2.6658810	1.7339940
47	H	-5.0979740	-2.1988580	0.9298440
48	H	-3.8780980	-3.1706870	0.0552010

Tranisiotn state to syn cis-cyclopropyl gold carbene 54 ($TS^{\neq}_{42\text{-}54}$)

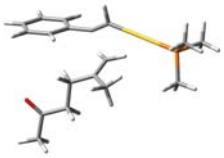

G = -1253,333136 Hartree/particle.

Row	Symbol	X	Y	Z
1	C	-0.8865860	-1.5271570	0.0996800
2	C	-1.5127910	1.0428660	0.3760950
3	C	-1.0295560	0.2944970	1.4071820
4	H	-1.7068860	-0.1494240	2.1354390
5	H	0.0235520	0.3254160	1.6800490
6	C	-0.6163540	1.8399650	-0.5080040
7	H	0.4266600	1.4950400	-0.4569940
8	H	-0.9535300	1.8108510	-1.5533140
9	H	-0.6246890	2.8957020	-0.1971820
10	C	-2.9750100	1.0923000	0.0834040
11	H	-3.1511360	0.7449670	-0.9484270
12	H	-3.5319470	0.4105350	0.7396830
13	C	-3.5590160	2.4943840	0.2125850
14	H	-3.0683210	3.2023880	-0.4743190
15	H	-3.3948610	2.9071010	1.2206100
16	C	-5.0428470	2.5182730	-0.0879390
17	C	-5.7289490	3.8379860	0.1241450
18	H	-5.7175120	4.0936690	1.1924370

19	H	-5.1969780	4.6435380	-0.3983270
20	H	-6.7647130	3.7895510	-0.2232910
21	O	-5.6324520	1.5273070	-0.4727870
22	C	-2.2486550	-1.9580250	0.0372970
23	C	-2.9319670	-1.8659120	-1.1877500
24	C	-2.9076940	-2.4738850	1.1666200
25	C	-4.2563300	-2.2729720	-1.2756880
26	H	-2.4096770	-1.4672630	-2.0568540
27	C	-4.2284430	-2.8790410	1.0690460
28	H	-2.3725910	-2.5470810	2.1122330
29	C	-4.9046820	-2.7694240	-0.1479190
30	H	-4.7856760	-2.1960510	-2.2225330
31	H	-4.7388600	-3.2796150	1.9419270
32	H	-5.9462040	-3.0768380	-0.2149750
33	C	0.3563090	-1.6777900	-0.2116520
34	H	0.5296590	-2.6738940	-0.6456700
35	Au	2.0962130	-0.5327050	-0.0830790
36	P	4.0512170	0.7712770	0.0239730
37	C	5.0301480	0.5811970	1.5498620
38	H	5.3616870	-0.4579920	1.6509520
39	H	5.9082980	1.2386760	1.5160910
40	H	4.4173550	0.8402990	2.4202810
41	C	5.2422330	0.4607930	-1.3207280
42	H	4.7613050	0.6319750	-2.2900040
43	H	6.1039840	1.1330000	-1.2202350
44	H	5.5869250	-0.5782130	-1.2796320
45	C	3.7069820	2.5597060	-0.0775080
46	H	4.6435770	3.1312080	-0.0442710
47	H	3.1800720	2.7817480	-1.0127120
48	H	3.0702960	2.8602080	0.7626170

Anti trans-cyclopropyl gold carbene (51)

G = -1253,366678 Hartree/particle.

Row	Symbol	X	Y	Z
1	C	2.5820290	1.1667120	-1.4838610
2	C	2.9177830	0.8717580	-0.1187160
3	C	1.2697450	0.9172010	-0.6451480
4	H	2.6439180	2.1999310	-1.8236540
5	H	2.7710230	0.4198070	-2.2537020
6	C	3.1922270	1.9861280	0.8472430
7	H	2.8536390	1.7320170	1.8595180
8	H	4.2792290	2.1390830	0.8897500
9	H	2.7400510	2.9353150	0.5466140
10	C	3.5135020	-0.4634730	0.2511630
11	H	3.2008340	-0.7552250	1.2635880
12	H	3.1831960	-1.2575960	-0.4263910
13	C	5.0354410	-0.4144200	0.1749780
14	H	5.4752990	0.2270080	0.9531810
15	H	5.3670930	0.0219150	-0.7826350
16	C	5.6612330	-1.7895190	0.2898970
17	C	7.1603830	-1.8140970	0.3782550
18	H	7.6134560	-1.1727550	-0.3883050
19	H	7.4747940	-1.4134240	1.3518290
20	H	7.5310970	-2.8379870	0.2782280
21	O	4.9878970	-2.8008940	0.3151000
22	C	0.6731840	-0.3284950	-0.7163980
23	H	1.3288260	-1.1352530	-1.0575590

24	C	0.4659690	2.0965440	-0.2027810
25	C	0.2115330	3.1670860	-1.0601370
26	C	-0.1008040	2.1025510	1.0773830
27	C	-0.6045780	4.2196630	-0.6516310
28	H	0.6341420	3.1740470	-2.0646450
29	C	-0.9133560	3.1535070	1.4863310
30	H	0.1066990	1.2735720	1.7562760
31	C	-1.1685280	4.2150240	0.6202860
32	H	-0.8021770	5.0436930	-1.3344640
33	H	-1.3425280	3.1474750	2.4866900
34	H	-1.8024000	5.0401360	0.9392710
35	Au	-1.2920570	-0.7409860	-0.2692000
36	P	-3.5662610	-1.1660350	0.2425760
37	C	-4.4087450	0.2834610	0.9612440
38	H	-5.4443400	0.0322810	1.2244320
39	H	-3.8739420	0.6141910	1.8591830
40	H	-4.4098150	1.1041170	0.2350690
41	C	-3.8388570	-2.4996320	1.4567060
42	H	-3.3244670	-2.2605360	2.3939530
43	H	-4.9124250	-2.6158470	1.6529050
44	H	-3.4387310	-3.4427440	1.0685610
45	C	-4.6053140	-1.6344950	-1.1812330
46	H	-4.2311600	-2.5642670	-1.6237530
47	H	-5.6436780	-1.7801070	-0.8565300
48	H	-4.5714510	-0.8462980	-1.9415640

Anti cis-cyclopropyl gold carbene (52)

G = -1253,363129 Hartree/particle.

Row	Symbol	X	Y	Z
1	C	2.3683560	-1.2202850	-1.7776850
2	C	2.6573510	-1.4326060	-0.3859500
3	C	1.2105160	-0.6442300	-0.8743980
4	H	2.8943560	-0.4211200	-2.3011370
5	H	2.0801180	-2.0637950	-2.4021200
6	C	2.5469090	-2.7951300	0.2377070
7	H	3.5485180	-3.2444330	0.2517790
8	H	2.1961280	-2.7365770	1.2749410
9	H	1.9077290	-3.4812570	-0.3241870
10	C	3.5768630	-0.4708410	0.3285030
11	H	3.2779330	-0.3848190	1.3839720
12	H	3.4895320	0.5269590	-0.1174350
13	C	5.0319240	-0.9428750	0.2320250
14	H	5.1847520	-1.9130520	0.7180580
15	H	5.3003730	-1.0580330	-0.8317390
16	C	6.0279310	0.0220910	0.8484130
17	C	5.9137520	1.4725090	0.4700490
18	H	5.7349900	1.5958390	-0.6061270
19	H	5.0606890	1.9303270	0.9906810
20	H	6.8230830	2.0043790	0.7630410
21	O	6.8926150	-0.3813830	1.6001570
22	C	1.1311550	0.8320450	-0.6529990
23	C	0.8164080	1.3207860	0.6207560
24	C	1.2916390	1.7340610	-1.7049280
25	C	0.6579560	2.6848080	0.8349750
26	H	0.7014180	0.6185100	1.4481290
27	C	1.1293790	3.1013410	-1.4912350
28	H	1.5237970	1.3691460	-2.7053680

29	C	0.8132730	3.5787250	-0.2232230
30	H	0.4209980	3.0521860	1.8318720
31	H	1.2488540	3.7946400	-2.3214780
32	H	0.6920660	4.6473890	-0.0570820
33	C	0.0745510	-1.4169150	-0.6963870
34	H	0.2098520	-2.4860730	-0.8874690
35	Au	-1.7637110	-0.6871300	-0.1341360
36	P	-3.8394390	0.2626560	0.5039840
37	C	-3.7766270	1.0529720	2.1468300
38	H	-2.9848360	1.8113360	2.1585260
39	H	-4.7386240	1.5295420	2.3749200
40	H	-3.5550150	0.3023140	2.9134790
41	C	-4.3820630	1.5997720	-0.6116650
42	H	-5.3225530	2.0355290	-0.2503580
43	H	-3.6124920	2.3791750	-0.6509370
44	H	-4.5314420	1.2038460	-1.6220940
45	C	-5.2697650	-0.8643660	0.5938580
46	H	-5.0799360	-1.6479160	1.3354060
47	H	-6.1691790	-0.3046320	0.8816050
48	H	-5.4343390	-1.3361000	-0.3810370

Syn trans-cyclopropyl gold carbene (53)

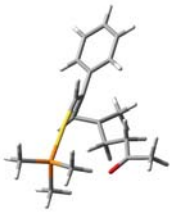

G = -1253,368096 Hartree/particle.

Row	Symbol	X	Y	Z
1	C	1.8101580	-0.2778740	1.9931680
2	C	1.7612980	1.0405660	1.4279200
3	C	2.0726400	-0.3914670	0.4505490
4	H	2.6884900	-0.5591710	2.5734730
5	H	0.8800470	-0.7470140	2.3102930
6	C	2.9760100	1.9195470	1.4410910
7	H	3.1230820	2.4359340	0.4839550
8	H	2.8102600	2.6918690	2.2060660
9	H	3.8929750	1.3803880	1.6934940
10	C	0.4520550	1.7600650	1.2713230
11	H	-0.3910330	1.0627730	1.3248270
12	H	0.3670640	2.3896570	2.1731730
13	C	0.3256980	2.6299710	0.0333060
14	H	0.7050190	2.0947230	-0.8567620
15	H	0.9353160	3.5433820	0.0975050
16	C	-1.1017510	3.0179880	-0.2906170
17	C	-1.2635090	4.0841170	-1.3328300
18	H	-0.9149130	5.0449760	-0.9300610
19	H	-0.6428630	3.8685050	-2.2122170
20	H	-2.3126390	4.1771010	-1.6271700
21	O	-2.0575260	2.4855420	0.2465630
22	C	3.4847400	-0.5219900	-0.0241020
23	C	4.4142740	-1.3176960	0.6489480
24	C	3.8756240	0.1271800	-1.1996960
25	C	5.7078060	-1.4606740	0.1557630
26	H	4.1246450	-1.8482500	1.5556340
27	C	5.1682330	-0.0121020	-1.6907010
28	H	3.1556150	0.7564550	-1.7267940
29	C	6.0890780	-0.8059940	-1.0114050
30	H	6.4190350	-2.0910480	0.6860210
31	H	5.4588380	0.5062030	-2.6025340
32	H	7.1022260	-0.9149620	-1.3934370

33	C	1.0354120	-0.7593930	-0.3919350
34	H	1.4210040	-1.1029890	-1.3623750
35	Au	-1.0169570	-0.8371860	-0.2018500
36	P	-3.3761150	-0.7767900	0.0078370
37	C	-4.1775550	0.2771560	-1.2452470
38	H	-3.9821040	-0.1141120	-2.2496860
39	H	-5.2610390	0.3122850	-1.0731200
40	H	-3.7626400	1.2886540	-1.1645920
41	C	-4.2678710	-2.3654290	-0.0800770
42	H	-3.8955170	-3.0478150	0.6917760
43	H	-5.3426260	-2.2016850	0.0708090
44	H	-4.1089890	-2.8260190	-1.0612900
45	C	-3.8798350	-0.0357730	1.5952040
46	H	-4.9721330	0.0601640	1.6452050
47	H	-3.5333370	-0.6595920	2.4268900
48	H	-3.4173100	0.9556360	1.6729910

Syn cis-cyclopropyl gold carbene (54)

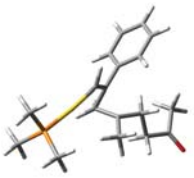

G = -1253,361936 Hartree/particle.

Row	Symbol	X	Y	Z
1	C	-1.2449160	-0.4138710	1.3227800
2	C	-1.6206200	-0.9604350	0.0474140
3	C	-1.1663120	0.7217630	0.2460170
4	H	-2.0340370	-0.2268840	2.0518950
5	H	-0.2781690	-0.6814470	1.7463890
6	C	-3.0786880	-1.0658610	-0.3132880
7	H	-3.2161460	-0.9202720	-1.3945300
8	H	-3.6695750	-0.2909640	0.1868860
9	C	-0.7101220	-1.8670920	-0.7225680
10	H	0.3434010	-1.7497350	-0.4541340
11	H	-0.9923930	-2.9018640	-0.4817520
12	C	-2.2857170	1.7099330	0.1602230
13	C	-2.8715990	2.2368810	1.3129420
14	C	-2.7165650	2.1661510	-1.0894190
15	C	-3.8707980	3.2012150	1.2175550
16	H	-2.5355800	1.9067610	2.2958460
17	C	-3.7170960	3.1257720	-1.1846980
18	H	-2.2673530	1.7514460	-1.9933550
19	C	-4.2978190	3.6449550	-0.0300240
20	H	-4.3131990	3.6090630	2.1244940
21	H	-4.0490080	3.4657900	-2.1638510
22	H	-5.0825450	4.3952450	-0.1045430
23	C	0.0652140	1.0470950	-0.2995110
24	H	0.0248230	2.0141600	-0.8199470
25	Au	1.9604660	0.2499740	-0.1404460
26	P	4.2017680	-0.4777220	0.1236430
27	C	4.8712990	-1.4235650	-1.2846490
28	H	4.8396800	-0.8102270	-2.1918830
29	H	5.9104390	-1.7124080	-1.0803040
30	H	4.2719670	-2.3254910	-1.4499830
31	C	5.3852930	0.8930530	0.3465550
32	H	5.1117180	1.4814620	1.2294650
33	H	6.4007930	0.4968570	0.4760110
34	H	5.3625600	1.5478470	-0.5314610
35	C	4.4825460	-1.5536430	1.5689970
36	H	5.5407030	-1.8396480	1.6253670
37	H	4.2035510	-1.0217490	2.4853430
38	H	3.8688830	-2.4575710	1.4878330
39	H	-0.8251440	-1.7338430	-1.8049130

40	C	-3.6348620	-2.4261850	0.0975770
41	H	-3.1947550	-3.2489900	-0.4858180
42	H	-3.3922910	-2.6524700	1.1492920
43	C	-5.1387760	-2.5059740	-0.0702220
44	C	-5.7682610	-3.8035930	0.3522530
45	H	-5.2953670	-4.6494510	-0.1635900
46	H	-5.6135160	-3.9632920	1.4278020
47	H	-6.8402950	-3.7922890	0.1376630
48	O	-5.7844580	-1.5789690	-0.5164090

Transition state to oxonium cation 55 thourgh the upper face (TS(up)$^{\neq}_{51\text{-}55}$)

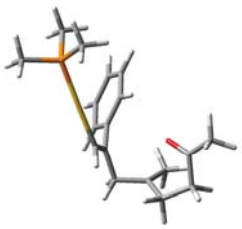

G = -1253,361233 Hartree/particle.

Row	Symbol	X	Y	Z
1	C	2.8198800	0.5325130	-1.8102120
2	C	3.7654120	-0.0384750	-0.8435520
3	C	1.4311480	0.5821620	-1.1148270
4	H	3.1323640	1.5473380	-2.0888560
5	H	2.7528000	-0.0873820	-2.7099450
6	C	4.4494620	0.8810810	0.0757770
7	H	5.0138800	0.3967850	0.8750050
8	H	5.1465540	1.4738890	-0.5407940
9	H	3.7363480	1.6053330	0.4948910
10	C	4.1977300	-1.4360550	-1.0278450
11	H	3.4449110	-1.9726130	-1.6206210
12	H	5.0893450	-1.3596850	-1.6793990
13	C	4.5335040	-2.2015020	0.2366830
14	H	5.4602220	-1.8493740	0.7155960
15	H	4.6966220	-3.2654980	0.0259610
16	C	3.4040170	-2.0077160	1.2189390
17	C	3.2613610	-2.9845020	2.3358310
18	H	2.9000130	-3.9382090	1.9269270
19	H	4.2357830	-3.1877970	2.7971610
20	H	2.5523630	-2.6211640	3.0839550
21	O	2.6538620	-1.0559440	1.0630620
22	C	0.5401750	-0.4006760	-1.3365400
23	H	0.8860510	-1.2181260	-1.9813590
24	C	1.2041610	1.7405050	-0.2181700
25	C	1.4738600	3.0501700	-0.6378890
26	C	0.6815550	1.5544800	1.0703780
27	C	1.1928930	4.1375800	0.1829950
28	H	1.8799220	3.2288610	-1.6341560
29	C	0.4001130	2.6408120	1.8918140
30	H	0.5151810	0.5388880	1.4260840
31	C	0.6508820	3.9374610	1.4499540
32	H	1.3937540	5.1467540	-0.1725130
33	H	-0.0070150	2.4721480	2.8878800
34	H	0.4328700	4.7883330	2.0928280
35	Au	-1.3824100	-0.4505210	-0.5791070
36	P	-3.5575060	-0.4382980	0.3590940
37	C	-3.8440990	1.0268650	1.4120680
38	H	-4.8459960	0.9913140	1.8593350
39	H	-3.0908610	1.0597710	2.2083010
40	H	-3.7479840	1.9376960	0.8098030
41	C	-3.9443270	-1.8445170	1.4593250
42	H	-3.2090160	-1.8934920	2.2703140
43	H	-4.9482290	-1.7277390	1.8881420

44	H	-3.9008400	-2.7818770	0.8933570
45	C	-4.9588930	-0.4120510	-0.8121730
46	H	-4.9389110	-1.3123430	-1.4362450
47	H	-5.9098390	-0.3728710	-0.2647570
48	H	-4.8812080	0.4653840	-1.4636390

Transition state to oxonium cation 55 thourgh the lower face (TS(down)$^{\neq}_{51\text{-}55}$)

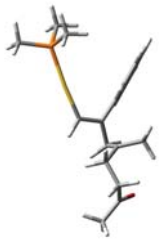

G = -1253,360076 Hartree/particle.

Row	Symbol	X	Y	Z
1	C	2.8298250	0.4543510	-1.1238350
2	C	2.9752090	0.2464010	0.2868930
3	C	1.4064960	0.4299330	-0.4453670
4	H	3.0634020	1.4405990	-1.5248980
5	H	3.0160480	-0.3720250	-1.8083110
6	C	3.2883980	1.4076650	1.1794710
7	H	2.9261100	1.2487270	2.2027990
8	H	4.3824320	1.4964840	1.2040160
9	H	2.8928050	2.3533430	0.7989930
10	C	3.3162030	-1.1187460	0.8443180
11	H	2.7093030	-1.3203570	1.7371050
12	H	3.0925420	-1.9050760	0.1118020
13	C	4.7987910	-1.2405580	1.2394380
14	H	4.9562540	-2.2487940	1.6424300
15	H	5.0438070	-0.5236020	2.0331150
16	C	5.7041420	-0.9814800	0.0515100
17	C	6.3416230	-2.1778570	-0.5866170
18	H	7.0192100	-2.6637270	0.1289160
19	H	5.5750410	-2.9240050	-0.8410420
20	H	6.8970880	-1.8913200	-1.4837750
21	O	5.8595320	0.1505500	-0.3706950
22	C	0.6696400	-0.7393330	-0.4844460
23	H	1.2451310	-1.6485850	-0.6847420
24	C	0.7038610	1.7282240	-0.2109580
25	C	0.6392190	2.6988050	-1.2104390
26	C	0.0242600	1.9464240	0.9934340
27	C	-0.1021190	3.8626710	-1.0170970
28	H	1.1526580	2.5384700	-2.1584680
29	C	-0.7121100	3.1090790	1.1888290
30	H	0.0853280	1.1967110	1.7842300
31	C	-0.7792400	4.0694480	0.1805420
32	H	-0.1524320	4.6074520	-1.8089890
33	H	-1.2275390	3.2701090	2.1341390
34	H	-1.3535280	4.9812430	0.3327330
35	Au	-1.3684380	-0.8103830	-0.2080970
36	P	-3.7069440	-0.7037750	0.1530080
37	C	-4.1254070	-0.3966030	1.9021600
38	H	-5.2110770	-0.2823030	2.0167150
39	H	-3.7822210	-1.2315230	2.5228110
40	H	-3.6268070	0.5199090	2.2403060
41	C	-4.7172230	-2.1478590	-0.3113130
42	H	-4.3877510	-3.0294050	0.2494320
43	H	-5.7735930	-1.9514070	-0.0872940
44	H	-4.6070570	-2.3511800	-1.3819130
45	C	-4.4690890	0.6990460	-0.7297780

46	H	-4.3554440	0.5659360	-1.8112150
47	H	-5.5359440	0.7714640	-0.4820950
48	H	-3.9641220	1.6276840	-0.4371880

Oxonium cation (55)

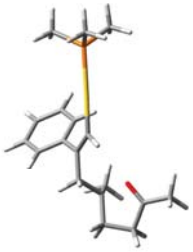

G = -1253,382691 Hartree/particle.

Row	Symbol	X	Y	Z
1	C	3.8355820	0.0614670	-0.1596400
2	O	3.4908590	-1.3232950	0.4118460
3	C	4.5178390	-2.0498140	0.5130370
4	C	5.7557350	-1.3980090	0.0375290
5	C	5.2358210	-0.1811610	-0.7255440
6	H	6.3477460	-1.1403350	0.9315800
7	H	6.3769800	-2.0887090	-0.5441230
8	H	5.8686510	0.7013380	-0.5921820
9	H	5.1806290	-0.4018130	-1.7984790
10	C	2.7902380	0.3430000	-1.2243930
11	H	3.1465350	1.2500180	-1.7386420
12	H	2.8465550	-0.4663010	-1.9664030
13	C	3.8096240	0.9800880	1.0364650
14	H	3.9231200	2.0153950	0.6924180
15	H	2.8571460	0.9032110	1.5717650
16	H	4.6283770	0.7556420	1.7316400
17	C	1.3672730	0.4974580	-0.7265880
18	C	0.5188120	-0.5523570	-0.7605350
19	H	0.9662720	-1.4770230	-1.1498800
20	C	0.9707930	1.8396140	-0.2246820
21	C	1.3022730	3.0063880	-0.9260660
22	C	0.2492970	1.9799490	0.9702690
23	C	0.9013290	4.2591660	-0.4714240
24	H	1.8563700	2.9366380	-1.8625750
25	C	-0.1473250	3.2307410	1.4310390
26	H	0.0172780	1.0864470	1.5508690
27	C	0.1740830	4.3778830	0.7094070
28	H	1.1586280	5.1477110	-1.0461110
29	H	-0.6980640	3.3107360	2.3674250
30	H	-0.1336390	5.3579660	1.0697230
31	Au	-1.4878510	-0.5937130	-0.2770230
32	P	-3.8148920	-0.6431710	0.1974770
33	C	-4.2627000	-0.9271620	1.9462000
34	H	-3.8204020	-0.1438680	2.5721100
35	H	-5.3537480	-0.9128090	2.0670720
36	H	-3.8757300	-1.8971720	2.2781330
37	C	-4.7655900	-1.9201760	-0.6990440
38	H	-5.8293590	-1.8623130	-0.4340180
39	H	-4.6538590	-1.7723410	-1.7791280
40	H	-4.3836980	-2.9150570	-0.4438230
41	C	-4.6922830	0.9063930	-0.2151080
42	H	-5.7577640	0.8235350	0.0368620
43	H	-4.2515160	1.7399890	0.3435670
44	H	-4.5892480	1.1148720	-1.2860230
45	C	4.4055760	-3.3987400	1.0690660
46	H	3.4136090	-3.5835000	1.4861780

47	H	4.6120730	-4.1196050	0.2648670
48	H	5.1855200	-3.5537970	1.8251240

Transition state to carbocation 56 ($TS^{\neq}_{55\text{-}56}$)

G = -1253,368244 Hartree/particle.

Row	Symbol	X	Y	Z
1	C	3.7404960	-1.1829840	-0.2367620
2	O	3.1335710	-0.6940930	0.9882660
3	C	1.8992650	-1.2132190	1.0294370
4	C	2.0255220	-2.6617680	0.6459840
5	C	3.2117070	-2.6334580	-0.3307770
6	H	2.2915500	-3.1915140	1.5752890
7	H	1.1036170	-3.1116780	0.2684000
8	H	3.9924740	-3.3385080	-0.0245490
9	C	3.1734680	-0.2325760	-1.3414290
10	C	0.8182060	-0.6947300	-0.7554330
11	C	1.8142500	0.2535320	-0.9284810
12	C	5.2372840	-1.0788950	-0.1179260
13	H	5.7000190	-1.3996380	-1.0593330
14	H	5.5504670	-0.0471020	0.0833320
15	H	5.6083110	-1.7245980	0.6865820
16	H	3.8711390	0.5950170	-1.5130200
17	H	3.1004220	-0.7954580	-2.2821140
18	C	1.0800400	-0.7213510	2.1638800
19	H	0.1111320	-1.2278460	2.2001490
20	H	1.6310720	-0.9366350	3.0916600
21	H	0.9286920	0.3631640	2.1048740
22	C	1.6735310	1.6388990	-0.4766840
23	C	0.4560620	2.3261690	-0.6365800
24	C	2.7417630	2.3154320	0.1381090
25	C	0.3051890	3.6258210	-0.1752800
26	H	-0.3641900	1.8410390	-1.1654520
27	C	2.5808860	3.6060620	0.6230220
28	H	3.6976610	1.8155720	0.2765780
29	C	1.3632730	4.2645530	0.4679350
30	H	-0.6386260	4.1463550	-0.3266220
31	H	3.4115270	4.1032040	1.1195180
32	H	1.2434690	5.2815760	0.8363070
33	H	2.9242400	-2.8931380	-1.3551510
34	H	1.0478480	-1.6197380	-1.2933760
35	Au	-1.2043110	-0.4651890	-0.2828010
36	P	-3.5001240	-0.1317290	0.1644660
37	C	-4.6679380	-1.0426550	-0.9011030
38	H	-5.7018400	-0.7726730	-0.6498770
39	H	-4.4763470	-0.7996440	-1.9522390
40	H	-4.5329370	-2.1210790	-0.7628280
41	C	-3.9630240	1.6205490	-0.0605630
42	H	-5.0262210	1.7769230	0.1633130
43	H	-3.3555410	2.2481130	0.6026750
44	H	-3.7644460	1.9195550	-1.0965960
45	C	-4.0443750	-0.5248400	1.8611150
46	H	-3.4591300	0.0591730	2.5802160
47	H	-5.1092040	-0.2893490	1.9854030
48	H	-3.8849400	-1.5897320	2.0642450

Carbocation (56)

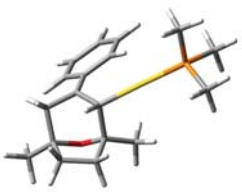

G = -1253,372438 Hartree/particle.

Row	Symbol	X	Y	Z
1	C	3.4432950	-1.5559020	-0.2617860
2	O	2.9077590	-1.0139260	0.9404750
3	C	1.5198380	-1.3415170	0.8979390
4	C	1.5781550	-2.8426050	0.6283960
5	C	2.7547190	-2.9421610	-0.3624300
6	H	1.8152160	-3.3521200	1.5728480
7	H	0.6331910	-3.2492420	0.2486270
8	H	3.4597040	-3.7260360	-0.0605420
9	C	3.0295640	-0.5492710	-1.4252440
10	C	0.8205790	-0.6977470	-0.4504990
11	C	1.8753440	0.1973930	-0.8675430
12	C	4.9450830	-1.6251500	-0.1502860
13	H	5.3757110	-2.0196720	-1.0790750
14	H	5.3752180	-0.6330820	0.0368340
15	H	5.2310540	-2.2881000	0.6753660
16	H	3.8739890	0.0776370	-1.7288150
17	H	2.7114050	-1.1215120	-2.3068970
18	C	0.9073070	-0.8863560	2.1927300
19	H	-0.1189830	-1.2623690	2.2860780
20	H	1.5039080	-1.2684150	3.0320620
21	H	0.8833370	0.2100100	2.2501450
22	C	2.0041550	1.5588160	-0.4402370
23	C	0.8644200	2.3442150	-0.1510260
24	C	3.2806790	2.1464550	-0.2633950
25	C	0.9928290	3.6444050	0.3029960
26	H	-0.1258470	1.9281430	-0.3322730
27	C	3.4040080	3.4374680	0.2127290
28	H	4.1813910	1.5687240	-0.4507120
29	C	2.2615980	4.1901680	0.4917670
30	H	0.1059010	4.2403150	0.5044030
31	H	4.3909600	3.8659100	0.3685020
32	H	2.3630250	5.2118430	0.8521770
33	H	2.4369560	-3.1767400	-1.3847830
34	H	0.8245050	-1.5285470	-1.1675820
35	Au	-1.2467840	-0.2614810	-0.1928710
36	P	-3.5769950	0.0490520	0.0106870
37	C	-4.4740500	-1.4180200	0.6202770
38	H	-4.0979980	-1.6988240	1.6104360
39	H	-5.5484980	-1.2041760	0.6883480
40	H	-4.3159700	-2.2584370	-0.0645970
41	C	-4.4240760	0.4698000	-1.5501770
42	H	-5.5014600	0.5869030	-1.3748220
43	H	-4.0198790	1.4065910	-1.9498960
44	H	-4.2626180	-0.3232270	-2.2887840
45	C	-4.0765210	1.3826700	1.1521320
46	H	-5.1711060	1.4554400	1.1930550
47	H	-3.6904120	1.1772390	2.1566890
48	H	-3.6654450	2.3383950	0.8078820

Coordinated product (57)

G = -1253,436946 Hartree/particle.

Row	Symbol	X	Y	Z
1	C	2.6696890	-1.3612080	1.0984260
2	O	1.7435720	-2.1445840	0.3309020
3	C	1.8738590	-1.6613680	-1.0018750
4	C	3.3974110	-1.6328230	-1.2090260
5	C	3.9167240	-1.2610850	0.1876860
6	H	3.7314320	-2.6346600	-1.5092660
7	H	3.7050290	-0.9296890	-1.9928460
8	H	4.6897770	-1.9625910	0.5232190
9	C	2.0406930	0.0157160	1.3253610
10	C	1.3572120	-0.2361480	-1.0536050
11	H	1.1510740	0.1812020	-2.0432650
12	C	1.4792390	0.5937940	0.0430040
13	C	2.9216290	-2.0697050	2.4058520
14	H	3.6270210	-1.4956960	3.0204590
15	H	1.9881430	-2.1866990	2.9714290
16	H	3.3483560	-3.0636480	2.2245070
17	H	1.2571510	-0.0518070	2.0976200
18	H	2.7975250	0.7096860	1.7211620
19	C	1.1335190	-2.5841570	-1.9392030
20	H	1.2415580	-2.2418670	-2.9763860
21	H	1.5419030	-3.5988340	-1.8616000
22	H	0.0623430	-2.6205460	-1.6967620
23	C	1.2216050	2.0516670	-0.0126970
24	C	1.3002200	2.7626370	-1.2179070
25	C	0.8880240	2.7457060	1.1588590
26	C	1.0416360	4.1264480	-1.2505810
27	H	1.5910230	2.2507700	-2.1341060
28	C	0.6228270	4.1090500	1.1224270
29	H	0.8226690	2.2119480	2.1063130
30	C	0.6977170	4.8031440	-0.0822160
31	H	1.1194240	4.6662870	-2.1921330
32	H	0.3597910	4.6320140	2.0396870
33	H	0.4975010	5.8722790	-0.1097000
34	H	4.3573130	-0.2566400	0.2196050
35	Au	-0.7910880	-0.2142720	-0.1745740
36	P	-3.0585620	-0.5780130	0.2303850
37	C	-3.6965660	0.3047840	1.6883820
38	H	-4.7590760	0.0680250	1.8288500
39	H	-3.1376040	0.0025090	2.5804860
40	H	-3.5808250	1.3848900	1.5475770
41	C	-3.4472920	-2.3315250	0.5225370
42	H	-4.5262670	-2.4503490	0.6851290
43	H	-3.1433740	-2.9290130	-0.3442190
44	H	-2.9048210	-2.6895230	1.4043480
45	C	-4.1399230	-0.0743640	-1.1436230
46	H	-3.8691510	-0.6253980	-2.0506550
47	H	-5.1854090	-0.2898190	-0.8877330
48	H	-4.0260450	0.9981240	-1.3341360

Transition state to cyclobutene 58 ($TS^{\neq}_{51\text{-}58}$)

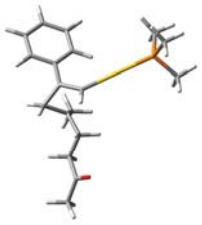

G = -1253,354943 Hartree/particle.

Row	Symbol	X	Y	Z
1	C	2.6350610	1.6836740	-0.8556020
2	C	2.2777110	0.6172540	0.1530190
3	C	1.1460140	1.5976260	-0.8175320
4	H	3.0687400	2.6072110	-0.4713440
5	H	3.1405010	1.2994480	-1.7439640
6	C	2.0968860	0.9884700	1.6011760
7	H	1.5234330	0.2140200	2.1275870
8	H	3.0842150	1.0558040	2.0757330
9	H	1.6044850	1.9537640	1.7484690
10	C	2.9073210	-0.7614000	-0.0406470
11	H	2.2697140	-1.5377010	0.4051180
12	H	3.0121800	-1.0066500	-1.1025460
13	C	4.2988070	-0.8102190	0.5785870
14	H	4.2677590	-0.8042140	1.6782470
15	H	4.8914990	0.0772160	0.2974410
16	C	5.0686260	-2.0429520	0.1478550
17	C	6.4529320	-2.1765560	0.7154170
18	H	7.0666300	-1.3121240	0.4291330
19	H	6.4169070	-2.1880900	1.8125840
20	H	6.9229060	-3.0952560	0.3538710
21	O	4.5897270	-2.8655470	-0.6078920
22	C	0.6721580	0.2946640	-0.9755070
23	H	1.2769590	-0.3069770	-1.6531990
24	C	0.3746920	2.7278210	-0.2574370
25	C	0.7504840	4.0187820	-0.6497430
26	C	-0.7465840	2.5741930	0.5692040
27	C	0.0075330	5.1247810	-0.2523890
28	H	1.6133850	4.1584680	-1.2992470
29	C	-1.4730010	3.6810910	0.9849040
30	H	-1.0407440	1.5801350	0.9089650
31	C	-1.1025240	4.9586940	0.5689820
32	H	0.3024960	6.1187020	-0.5817860
33	H	-2.3321540	3.5458450	1.6389750
34	H	-1.6788260	5.8244840	0.8889970
35	Au	-1.0894790	-0.6250760	-0.3730530
36	P	-3.0893250	-1.7002320	0.2846710
37	C	-4.1866640	-0.6268650	1.2714300
38	H	-5.1031330	-1.1657690	1.5444390
39	H	-3.6699300	-0.3086650	2.1841330
40	H	-4.4506320	0.2645270	0.6906970
41	C	-2.8723840	-3.1903930	1.3134100
42	H	-2.3231590	-2.9342470	2.2261230
43	H	-3.8503770	-3.6079470	1.5854060
44	H	-2.3002220	-3.9435760	0.7604000
45	C	-4.1363820	-2.2553570	-1.1014340
46	H	-3.5935800	-2.9884020	-1.7080990
47	H	-5.0585080	-2.7118760	-0.7193400
48	H	-4.3937300	-1.3990990	-1.7347080

Cyclobutene (58)

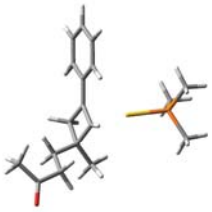

G = -1253,402721 Hartree/particle.

Row	Symbol	X	Y	Z
1	C	1.4022890	0.6624210	1.7063330
2	C	2.0338170	-0.4919690	0.8597090
3	C	1.2158400	0.0658270	-0.3108780
4	C	0.7395730	1.1380050	0.4314550
5	H	0.7327150	0.3529870	2.5197700
6	H	2.1307140	1.3824670	2.1054920
7	H	1.3286940	-0.0744670	-1.3893720
8	C	0.0588690	2.3898970	0.1397290
9	C	-0.2935040	3.2346400	1.1995550
10	C	-0.2467140	2.7681230	-1.1773880
11	C	-0.9459230	4.4357890	0.9493900
12	H	-0.0514060	2.9428590	2.2212600
13	C	-0.8958310	3.9682930	-1.4224630
14	H	0.0323780	2.1177340	-2.0068340
15	C	-1.2482510	4.8018440	-0.3594610
16	H	-1.2170590	5.0881330	1.7766140
17	H	-1.1275260	4.2603590	-2.4445420
18	H	-1.7573640	5.7434160	-0.5555570
19	Au	-0.9925720	-0.5353760	-0.0644980
20	P	-3.1201990	-1.4931840	-0.1687720
21	C	-3.0910030	-3.2939150	-0.4314250
22	H	-2.5590090	-3.7825510	0.3919890
23	H	-4.1189800	-3.6758210	-0.4767390
24	H	-2.5773900	-3.5254550	-1.3708100
25	C	-4.1447480	-0.8329680	-1.5205910
26	H	-5.1250760	-1.3266370	-1.5150470
27	H	-4.2816020	0.2458680	-1.3895400
28	H	-3.6543750	-1.0121640	-2.4835670
29	C	-4.1104070	-1.2472330	1.3381660
30	H	-4.2354080	-0.1761040	1.5297770
31	H	-5.0970170	-1.7109470	1.2099180
32	H	-3.6044090	-1.7037040	2.1956570
33	C	1.7213370	-1.9018030	1.3257880
34	H	0.6708260	-1.9896840	1.6397640
35	H	1.8872010	-2.6381520	0.5284790
36	H	2.3526760	-2.1790320	2.1817730
37	C	3.5338680	-0.2637880	0.6554590
38	H	3.6918640	0.7891540	0.3717980
39	H	4.0387500	-0.4055120	1.6251000
40	C	4.1588500	-1.1790180	-0.3931740
41	H	4.0088350	-2.2382880	-0.1502100
42	H	3.6765560	-0.9991830	-1.3701640
43	C	5.6457480	-0.9793580	-0.5954860
44	C	6.1424610	0.4347310	-0.7262370
45	H	5.4848450	1.0384750	-1.3650260
46	H	6.1567260	0.9155790	0.2621980
47	H	7.1605990	0.4353900	-1.1256320
48	O	6.4014750	-1.9299260	-0.6625680

Digold complex 71

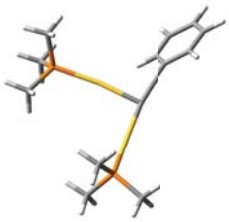

G = -1500,716605 Hartree/particle.

Row	Symbol	X	Y	Z
1	P	1.4473830	3.1111290	0.0819970
2	C	-0.0614060	4.1234600	-0.0532480
3	H	0.1990600	5.1896330	-0.0330710
4	H	-0.5773660	3.8953120	-0.9925600
5	H	-0.7346250	3.8990090	0.7816370
6	C	2.2590870	3.6919180	1.6051360
7	H	1.6395930	3.4481920	2.4750030
8	H	3.2315390	3.2002500	1.7175940
9	H	2.4063960	4.7785520	1.5556320
10	C	2.5209640	3.7071940	-1.2634460
11	H	3.4979600	3.2151980	-1.2054380
12	H	2.0666600	3.4770160	-2.2332470
13	H	2.6557200	4.7929640	-1.1743290
14	Au	1.0063630	0.8291550	0.0333310
15	C	3.7688390	-1.7136650	-0.9476400
16	C	5.0513960	-2.2440320	-0.9503860
17	C	5.3878050	-3.2644740	-0.0627900
18	C	4.4411120	-3.7517910	0.8357230
19	C	3.1586660	-3.2201010	0.8550640
20	C	2.8120900	-2.1980030	-0.0417500
21	H	3.4917940	-0.9197680	-1.6404890
22	H	5.7914500	-1.8628400	-1.6510160
23	H	6.3930970	-3.6809300	-0.0708840
24	H	4.7046190	-4.5486710	1.5279780
25	H	2.4139670	-3.5904820	1.5571160
26	C	1.4866540	-1.6661640	-0.0349000
27	C	0.3105650	-1.2643480	-0.0210520
28	Au	-1.7070200	-0.8764780	-0.0314170
29	P	-4.0236720	-0.4957610	-0.0359280
30	C	-4.6185510	0.5580180	-1.4000420
31	H	-5.7079220	0.6740740	-1.3321180
32	H	-4.1458870	1.5447490	-1.3422540
33	H	-4.3630650	0.1018280	-2.3626560
34	C	-5.0217930	-2.0146590	-0.1750230
35	H	-4.8096120	-2.6772500	0.6712910
36	H	-6.0899350	-1.7617910	-0.1792710
37	H	-4.7707130	-2.5407850	-1.1026050
38	C	-4.6544250	0.3232040	1.4660900
39	H	-4.1828290	1.3058850	1.5780260
40	H	-5.7423430	0.4500020	1.3947640
41	H	-4.4172940	-0.2814690	2.3482540

Transition state to the cyclopropyl digold carbene 72 ($TS^{\neq}_{71\text{-}72}$)

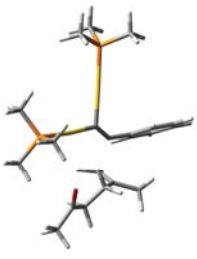

G = -1849,452114 Hartree/particle.

Row	Symbol	X	Y	Z
1	C	-0.5444700	1.9566510	-0.4939640
2	C	-0.3106020	0.7017230	-0.3217100
3	C	-1.5960970	2.9524380	-0.2787730
4	C	-2.1415510	3.0895120	1.0054590
5	C	-2.0926600	3.7555430	-1.3130020
6	C	-3.1546300	4.0100340	1.2486780
7	H	-1.7529340	2.4655390	1.8103880
8	C	-3.1086590	4.6714810	-1.0685770
9	H	-1.6870770	3.6504680	-2.3190440
10	C	-3.6386410	4.8053920	0.2131400
11	H	-3.5644350	4.1099390	2.2522450
12	H	-3.4891830	5.2845260	-1.8834260
13	H	-4.4281420	5.5299700	0.4034370
14	Au	-1.8915420	-0.6564520	-0.0524290
15	P	-3.5996770	-2.2430450	0.2617920
16	C	-2.9889030	-3.9416520	0.5341950
17	H	-3.8303170	-4.6342740	0.6667270
18	H	-2.3889910	-4.2612180	-0.3255600
19	H	-2.3567660	-3.9662600	1.4291160
20	C	-4.6796700	-1.9256260	1.6976460
21	H	-5.1639660	-0.9488570	1.5882840
22	H	-5.4485580	-2.7054430	1.7729530
23	H	-4.0816330	-1.9177710	2.6158440
24	C	-4.7589970	-2.4068980	-1.1376770
25	H	-4.2100110	-2.6919920	-2.0419930
26	H	-5.5136500	-3.1724960	-0.9156140
27	H	-5.2577190	-1.4484270	-1.3193850
28	C	1.4887380	3.3671000	0.0161130
29	C	0.9953260	2.9749260	-1.2093930
30	H	1.4939130	2.1809210	-1.7619950
31	H	0.4612570	3.6970230	-1.8252590
32	C	0.9903730	4.5773040	0.7178800
33	H	0.2648690	5.1495050	0.1298480
34	H	0.5312440	4.3063940	1.6817740
35	H	1.8408790	5.2318270	0.9630440
36	C	2.4895550	2.5208770	0.7199260
37	H	2.6181530	2.8493350	1.7605000
38	H	2.0958630	1.4839720	0.7548730
39	C	3.8441850	2.4707530	0.0240260
40	H	4.3542000	3.4454430	0.0492760
41	H	3.7232020	2.2380400	-1.0483950
42	C	4.7612360	1.4069550	0.5794640
43	C	6.2020230	1.5060700	0.1710110
44	H	6.7555310	0.6178640	0.4896590
45	H	6.2902810	1.6355550	-0.9158900
46	H	6.6528460	2.3965860	0.6297360
47	O	4.3478970	0.5066390	1.2900010
48	Au	1.2389830	-0.6733500	-0.2375270
49	P	2.8898690	-2.3564550	-0.0939400
50	C	2.3231350	-3.9852630	-0.6969040
51	H	3.1182730	-4.7333860	-0.5807720
52	H	1.4418330	-4.3042810	-0.1285260
53	H	2.0473420	-3.9138300	-1.7552030
54	C	4.4173770	-2.0486620	-1.0431180
55	H	4.9039570	-1.1480190	-0.6519300
56	H	5.1028630	-2.9003150	-0.9440340
57	H	4.1803770	-1.8964740	-2.1020180
58	C	3.4855680	-2.6888770	1.5975060
59	H	2.6426530	-2.9606090	2.2426390
60	H	4.2131990	-3.5109920	1.5853960
61	H	3.9609170	-1.7832280	1.9904950

Cyclopropyl digold carbene (72)

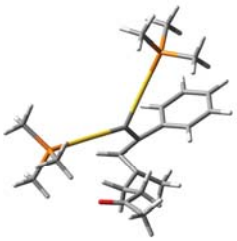

G = -1849,463118 Hartree/particle.

Row	Symbol	X	Y	Z
1	C	0.3899390	2.6756700	-1.8398790
2	C	0.5730830	3.1241680	-0.4780100
3	C	-0.4791670	1.9005570	-0.7744100
4	H	-0.2170470	3.2801300	-2.5139160
5	H	1.1595980	2.0737910	-2.3180040
6	C	-0.1022930	4.4005050	-0.0395400
7	H	-0.4274090	4.3598540	1.0077360
8	H	0.6274670	5.2175090	-0.1279690
9	H	-0.9687370	4.6577310	-0.6568430
10	C	1.8580230	2.8231060	0.2577980
11	H	2.3962260	1.9991880	-0.2252810
12	H	2.5009180	3.7106100	0.1429710
13	C	1.6808010	2.5119690	1.7340820
14	H	0.8315710	1.8158540	1.8738210
15	H	1.4217410	3.4035630	2.3241970
16	C	2.8706060	1.8257190	2.3697150
17	C	2.9192810	1.8677850	3.8688070
18	H	3.1789610	2.8857070	4.1911460
19	H	1.9354730	1.6441180	4.3012830
20	H	3.6685830	1.1699210	4.2530190
21	O	3.7233420	1.2560280	1.7102980
22	C	-1.9416490	2.2526370	-0.7021970
23	C	-2.7191450	2.3031820	-1.8589350
24	C	-2.5701210	2.3955380	0.5392660
25	C	-4.1009660	2.4655290	-1.7799240
26	H	-2.2435430	2.1850050	-2.8333760
27	C	-3.9479510	2.5650620	0.6218180
28	H	-1.9702620	2.3497660	1.4505030
29	C	-4.7195310	2.5925700	-0.5396030
30	H	-4.6952600	2.4890480	-2.6918990
31	H	-4.4221100	2.6754400	1.5959840
32	H	-5.7984910	2.7214230	-0.4759680
33	C	-0.1150450	0.5664880	-0.4899930
34	Au	1.7033670	-0.3915600	-0.5597320
35	P	3.8040930	-1.4998930	-0.5647200
36	C	4.3532290	-2.0636300	1.0808930
37	H	3.6380590	-2.7859520	1.4898400
38	H	5.3438200	-2.5317130	1.0095660
39	H	4.4050140	-1.1949190	1.7463860
40	C	3.9551110	-2.9791120	-1.6236670
41	H	3.7335790	-2.7176130	-2.6644720
42	H	4.9725300	-3.3868060	-1.5625160
43	H	3.2411080	-3.7434020	-1.2968470
44	C	5.1549230	-0.4073040	-1.1215810
45	H	6.1195060	-0.9286860	-1.0679140
46	H	4.9734920	-0.0880410	-2.1542630
47	H	5.1812970	0.4786740	-0.4768310
48	Au	-1.5693320	-0.7916630	0.0637490
49	P	-3.2803060	-2.3277460	0.6834870
50	C	-2.8262530	-4.0853190	0.8736910

51	H	-3.7073000	-4.6761390	1.1563860
52	H	-2.4243100	-4.4676720	-0.0712050
53	H	-2.0583500	-4.1908090	1.6479590
54	C	-4.6644940	-2.3531160	-0.5070010
55	H	-5.4591830	-3.0237800	-0.1552200
56	H	-5.0675250	-1.3396980	-0.6207120
57	H	-4.3077030	-2.6974650	-1.4843080
58	C	-4.0799980	-1.8975430	2.2675980
59	H	-4.4721110	-0.8751080	2.2102710
60	H	-4.9045400	-2.5903100	2.4803410
61	H	-3.3476460	-1.9450220	3.0813060

4. Anion Effects in Gold-Catalyzed Intermolecular Cycloadditions[1]

All the reactants, ligands and the following reagents were purchased from commercial sources and used without further purification: ethynylbenzene, 1-ethynyl-4-fluorobenzene, 1-ethynyl-4-chlorobenzene, 1-ethynyl-4-bromobenzene, 1-ethynyl-3-methylbenzene, 1-ethynyl-3-fluorobenzene, 1-ethynyl-3-chlorobenzene, 3-ethynylphenol, 1-ethynyl-3-methoxybenzene, 1-ethynyl-2-methylbenzene, 3-ethynylthiophene, 1-ethynyl-4-nitrobenzene, ethynylcyclopropane, 1-ethynyl-4-methoxybenzene, 1-ethynyl-4-methylbenzene, 1-ethynyl-2-methoxybenzene, 1-ethynyl-2-bromobenzene, ethynyltrimethylsilane, 2-methylbut-1-en-3-yne, hex-3-yne, prop-1-yn-1-ylbenzene, 1,2-diphenylethyne, , α-methylstyrene, 2,5-dimethylfuran, 5-methylhex-5-en-2-one, 2-methylpent-2-ene, methylenecyclohexane, (2-bromoethynyl)benzene, tris(1-methylethyl)-2-propen-1-yl-silane, [(2-methyl-2-propen-1-yl)oxy]benzene, allyltrimethylsilane, indole, 1,3,5-trimethoxybenzene and 1,3-diphenylpropane-1,3-dione. Cyclobutenes **26** and **40** agreed as reported in the literature[2] as well as phenols **48**,[3] enynes **67**, **70**, **72**, **74** and the cyclized polycycles **68**/**69**,[4] **71**,[5] **73**[6] and **75**.[7] Gold chlorides with JohnPhos, ^{t}BuXPhos, IPr, Ph_3P and phosphite **21** were prepared according to the literature.[8] Catalyst **R** was prepared as described.[3] Enyne **46** and the corresponding macrocycles **47** were characterized in **Chapter 1**,[9] oxabicycles **55** in **Chapter 2** and digold complex **7** in **Chapter 3**.[10]

Preparation of Gold Complexes

(Acetonitrile) [(2′,4′,6′-triisopropyl-1,1′-biphenyl-2-yl) di-tert-butylphosphine] gold(I) tetrakis[3,5-bis(trifluoromethyl)phenyl] borate (Q)

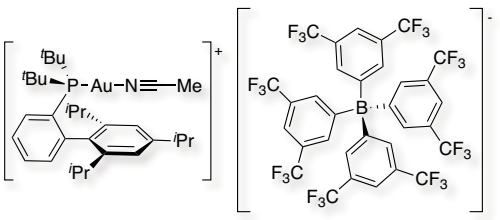

Chloro [(2',4',6'-triisopropyl-1,1'-biphenyl-2-yl)di-*tert*-butylphosphine] gold(I) (100.0 mg, 0.15 mmol) and acetonitrile (9.5 µl, 0.18 mmol) were dissolved in CH_2Cl_2 (6.6 ml). Then, $NaBAr^F_4$ (135.0 mg, 0.15 mmol) was added and the reaction mixture was

[1] C. Obradors, A. Homs, D. Leboeuf and A. M. Echavarren, *Adv. Synth. Catal.* **2014**, *356*, 221–228.
[2] V. López-Carrillo and A. M. Echavarren, *J. Am. Chem. Soc.* **2010**, *132*, 9292–9294.
[3] N. Huguet, D. Leboeuf and A. M. Echavarren, *Chem. –Eur. J.* **2013**, *19*, 6581–6585.
[4] C. Nieto-Oberhuber, M. P. Muñoz, E. Buñuel, C. Nevado, D. J. Cárdenas and A. M. Echavarren, *Angew. Chem. Int. Ed.* **2004**, *34*, 2402–2406.
[5] C. Nieto-Oberhuber, S. López, M. P. Muñoz, E. Jiménez-Núñez, E. Buñuel, D. J. Cárdenas and A. M. Echavarren, *Chem. –Eur. J.* **2006**, *12*, 1694–1702.
[6] C. Nieto-Oberhuber, S. López and A. M. Echavarren, *J. Am. Chem. Soc.* **2005**, *127*, 6178–6179.
[7] P. R. McGonigal, C. de León, Y. Wang, A. Homs, C. R. Rogelio and A. M. Echavarren, *Angew. Chem. Int. Ed.* **2012**, *51*, 13093–13096.
[8] *(a)* E. Herrero-Gómez, C. Nieto-Oberhuber, S. López, B. Benet-Buchholz and A. M. Echavarren, *Angew. Chem. Int. Ed.* **2006**, *45*, 5455–5459; *(b)* D. V. Partyka, T. J. Robilotto, M. Zelles, A. D. Hunter and T. G. Gray, *Organometallics* **2008**, *27*, 28–32; *(c)* C. H. M. Amijs, V. López-Carrillo, M. Raducan, P. Pérez-Galán, C Ferrer and A. M. Echavarren, *J. Org. Chem.* **2008**, *73*, 7721–7730.
[9] C. Obradors and A. M. Echavarren, *Org. Lett.* **2013**, *15*, 1576–1579.
[10] C. Obradors and A. M. Echavarren, *Chem. –Eur. J.* **2013**, *19*, 3547–3551.

stirred at 25 ºC for 30 min. The crude was filtered through Celite and concentrated. Finally, it was filtered through Teflon 0.22 and washed with CH_2Cl_2. The solvent was removed to afford [^{t}BuXPhosAuNCMe]BAr$^F{}_4$ **Q** as a white powder in 97% isolated yield (224.3 mg, 0.15 mmol). ^{1}H NMR (400 MHz, CD_2Cl_2, ppm) δ 7.92 – 7.85 (m, 1H), 7.75 – 7.70 (m, 8H), 7.66 – 7.58 (m, 2H), 7.56 (s, 4H), 7.32 (m, 1H), 7.16 (s, 2H), 2.94 (p, *J* = 6.9 Hz, 1H), 2.33 (dt, *J* = 13.4, 6.7 Hz, 2H), 2.25 (broad s, 3H), 1.41 (d, *J* = 16.3 Hz, 18H), 1.32 (d, *J* = 6.9 Hz, 6H), 1.25 (d, *J* = 6.8 Hz, 6H), 0.93 (d, *J* = 6.6 Hz, 6H). ^{13}C NMR (101 MHz, CD_2Cl_2, ppm) δ 162.3 (q, *J* (^{13}C-^{11}B) = 50.1 Hz), 150.4 (s), 148.0 (s), 147.6 (d, *J* (^{13}C-^{31}P) = 12.8 Hz), 136.7 (d, *J* (^{13}C-^{31}P) = 6.1 Hz), 135.5 (s), 135.4 (s), 134.7 (d, *J* (^{13}C-^{31}P) = 4.6 Hz), 132.1 (d, *J* (^{13}C-^{31}P) = 2.6 Hz), 129.5 (q, *J* (^{13}C-^{19}F) = 28.6 Hz), 128.1 (d, *J* (^{13}C-^{31}P) = 8.1 Hz), 126.0 (d, *J* (^{13}C-^{31}P) = 50.2 Hz), 125.2 (q, *J* (^{13}C-^{19}F) = 272.3 Hz), 122.5, 118.1 (p, *J* (^{13}C-^{19}F) = 4.0 Hz), 39.2 (d, *J* (^{13}C-^{31}P) = 29.3 Hz), 34.6 (s), 31.5 (d, *J* (^{13}C-^{31}P) = 4.3 Hz), 31.5 (s), 26.3 (s), 24.5 (s), 23.4 (s), 3.3 (s). ^{31}P {^{1}H} NMR (162 MHz, CD_2Cl_2, ppm) δ 58.68 (s). ^{19}F {^{1}H} NMR (376 MHz, CD_2Cl_2, ppm) δ -62.97 (s). ^{11}B {^{1}H} NMR (128 MHz, CD_2Cl_2, ppm) δ -6.68 (s). MALDI$^+$ *m/z* calcd for $C_{31}H_{48}AuNP^+$ [M-$C_{32}H_{12}BF_{24}$]$^+$: 662.3175, found 662.3184. Anal. calcd for $C_{63}H_{60}AuBF_{24}NP$: C, 49.59; H, 3.97; N, 0.92; found: C, 49.56; H, 3.94; N, 0.97.

(Acetonitrile) [(2′,4′,6′-triisopropyl-1,1′-biphenyl-2-yl) di-tert-butylphosphine] gold(I) tetrafluoroborate (S)

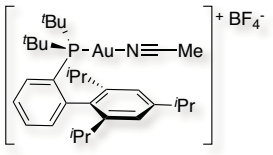

Chloro [(2',4',6'-triisopropyl-1,1'-biphenyl-2-yl)di-*tert*-butylphosphine] gold(I) (100.0 mg, 0.15 mmol) and acetonitrile (9.5 µl, 0.18 mmol) were dissolved in CH_2Cl_2 (6.6 ml). Then, $AgBF_4$ (29.6 mg, 0.15 mmol) was added and the reaction mixture was stirred at 25 ºC for 20 min. The crude was filtered through and concentrated. Finally, it was filtered through Teflon 0.22 and washed with CH_2Cl_2. The solvent was removed to afford [^{t}BuXPhosAuNCMe]BF_4 **S** as a white powder in quantitative isolated yield (113.9 mg, 0.152 mmol). ^{1}H NMR (400 MHz, CD_2Cl_2, ppm) δ 7.90 (td, *J* = 8.9, 8.1, 2.3 Hz, 1H), 7.69 – 7.54 (m, 2H), 7.32 (ddd, *J* = 6.9, 4.9, 2.5 Hz, 1H), 7.17 (s, 2H), 2.97 (hept, *J* = 6.8 Hz, 1H), 2.39 (s, 3H), 2.33 (hept, *J* = 6.7 Hz, 2H), 1.43 (d, *J* = 16.3 Hz, 18H), 1.33 (d, *J* = 6.9 Hz, 6H), 1.27 (d, *J* = 6.8 Hz, 6H), 0.93 (d, *J* = 6.6 Hz, 6H). ^{13}C NMR (101 MHz, CD_2Cl_2, ppm) δ 150.5 (s), 147.8 (s), 147.7 (d, *J* (^{13}C-^{31}P) = 12.7 Hz), 136.6 (d, *J* (^{13}C-^{31}P) = 6.0 Hz), 135.4 (d, *J* (^{13}C-^{31}P) = 8.1 Hz), 134.8 (d, *J* (^{13}C-^{31}P) = 4.3 Hz), 132.0 (s), 128.0 (d, *J* (^{13}C-^{31}P) = 7.8 Hz), 126.3 (d, *J* (^{13}C-^{31}P) = 47.8 Hz), 122.5 (s), 120.0 (d, *J* (^{13}C-^{31}P) = 4.4 Hz), 39.2 (d, *J* (^{13}C-^{31}P) = 28.2 Hz), 34.5 (s), 31.6 (d, *J* (^{13}C-^{31}P) = 5.8 Hz), 31.5 (s), 26.4 (s), 24.5 (s), 23.4 (s), 3.3 (s). ^{31}P {^{1}H} NMR (162 MHz, CD_2Cl_2, ppm): δ 58.58 (s). ^{19}F {^{1}H} NMR (376 MHz, CD_2Cl_2, ppm) δ -153.10 (s). ^{11}B {^{1}H} NMR (128 MHz, CD_2Cl_2, ppm) δ -1.23 (s). MALDI$^+$ *m/z* calcd for $C_{31}H_{48}AuNP^+$ [M-BF_4]$^+$ 662.3184, found 662.3180. Anal. calcd for $C_{63}H_{60}AuBF_{24}NP$: C, 49.68; H, 6.46; N, 1.87; found: C, 48.89; H, 6.20; N, 1.64.

(Acetonitrile) [(2′,4′,6′-triisopropyl-1,1′-biphenyl-2-yl) di-tert-butylphosphine] gold(I) hexafluorophosphate (T)

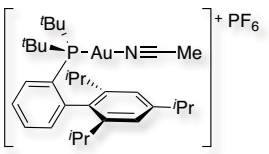

Chloro [(2',4',6'-triisopropyl-1,1'-biphenyl-2-yl)di-*tert*-butylphosphine] gold(I) (350.0 mg, 0.53 mmol) and acetonitrile (33.0 μl, 0.64 mmol) were dissolved in CH_2Cl_2 (23 ml). Then, $AgPF_6$ (135.0 mg, 0.53 mmol) was added and the reaction mixture was stirred at 25 ºC for 20 min. The crude was filtered through Celite and concentrated. Finally, it was filtered through Teflon 0.22 and washed with CH_2Cl_2. The solvent was removed to afford [^{t}BuXPhosAuNCMe]PF_6 **E** as a white powder in 51% isolated yield (221.0 mg, 0.27 mmol, 51%). ^{1}H NMR (400 MHz, CD_2Cl_2, ppm) δ 7.90 (ddd, *J* = 9.0, 7.1, 2.2 Hz, 1H), 7.60 (dq, *J* = 7.1, 2.0 Hz, 2H), 7.33 (td, *J* = 6.6, 5.7, 3.2 Hz, 1H), 7.17 (s, 1H), 2.95 (hept, *J* = 6.9 Hz, 1H), 2.38 – 2.27 (m, 4H), 1.43 (d, *J* = 16.3 Hz, 18H), 1.33 (d, *J* = 6.9 Hz, 6H), 1.27 (d, *J* = 6.7 Hz, 6H), 0.93 (d, *J* = 6.6 Hz, 6H). ^{13}C NMR (101 MHz, CD_2Cl_2, ppm) δ 149.9 (s), 147.8 (s), 136.6 (d, *J* (^{13}C-^{31}P) = 7.1 Hz), 135.3 (d, *J* (^{13}C-^{31}P) = 9.3 Hz), 134.8 (d, *J* (^{13}C-^{31}P) = 4.2 Hz), 132.0 (s), 128.0 (d, *J* (^{13}C-^{31}P) = 7.2 Hz), 122.4 (s), 117.9 (s), 39.2 (d, *J* (^{13}C-^{31}P) = 29.2 Hz), 34.55 (s), 31.56 (d, *J* = 5.6 Hz), 26.35 (s), 24.47 (s), 23.39 (s), 3.23 (s). ^{31}P {^{1}H} NMR (162 MHz, CD_2Cl_2, ppm) δ 58.53 (s), -139.23 (hept, *J* (^{31}P-^{19}F) = 715.0 Hz). ^{19}F {^{1}H} NMR (376 MHz, CD_2Cl_2, ppm) δ -73.46 (d, *J* (^{19}F-^{31}P)= 710.3 Hz). ESI$^+$ *m/z* calcd for $C_{31}H_{48}AuNP^+$ [M-PF_6]$^+$ 662.3184, found: 662.3176.

[(2′,4′,6′-Triisopropyl-1,1′-biphenyl-2-yl)di-tert-butylphosphine](2-phenylethynyl)gold(I) (8)

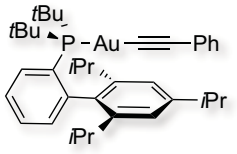

LiHMDS (53.5 mg, 0.32 mmol) was dissolved in THF (4.0 ml) and cooled to 0 ºC. Ethynylbenzene (35.1 μl, 0.32 mmol) was added and the solution was stirred for 30 min. Afterwards, chloro [(2',4',6'-triisopropyl-1,1'-biphenyl-2-yl)di-*tert*-butylphosphine] gold(I) (200.0 mg, 0.30 mmol) dissolved in THF (3.0 ml) was added and the solution was stirred overnight at 25 ºC. The crude was concentrated, dissolved in CH_2Cl_2 and filtered through Teflon 0.22. The solvent was removed to afford complex **8** as a white powder in 99% isolated yield (219.0 mg, 0.30 mmol). ^{1}H NMR (500 MHz, CD_2Cl_2, ppm) δ 7.92 (td, *J* = 7.4, 1.8 Hz, 1H), 7.53 – 7.46 (m, 2H), 7.30 – 7.28 (m, 3H), 7.21 – 7.18 (m, 2H), 7.15 – 7.12 (m, 3H), 2.93 (p, *J* = 6.9 Hz, 1H), 2.40 (p, *J* = 6.7 Hz, 2H), 1.43 (d, *J* = 14.8 Hz, 18H), 1.36 (d, *J* = 6.8 Hz, 6H), 1.27 (d, *J* = 6.9 Hz, 6H), 0.92 (d, *J* = 6.7 Hz, 6H). ^{13}C NMR (126 MHz, CD_2Cl_2, ppm) δ 150.0 (s), 148.7 (d, *J* (^{13}C-^{31}P) = 15.6 Hz), 146.4 (s), 137.3 (d, *J* (^{13}C-^{31}P) = 133.1 Hz), 136.6 (d, *J* (^{13}C-^{31}P) = 5.1 Hz), 136.1 (d, *J* (^{13}C-^{31}P) = 1.6 Hz), 135.2 (d, *J* (^{13}C-^{31}P) = 7.9 Hz), 132.2 (s), 130.4 (d, *J* (^{13}C-^{31}P) = 2.2 Hz), 129.9 (d, *J* (^{13}C-^{31}P) = 37.0 Hz), 128.3 (s), 127.4 (d, *J* (^{13}C-^{31}P) = 2.7 Hz), 126.9 (d, *J* (^{13}C-^{31}P) = 6.0 Hz), 126.0 (s), 122.3 (s), 101.5 (d, *J* (^{13}C-^{31}P) = 23.9 Hz), 38.5 (d, *J* (^{13}C-^{31}P) = 23.2 Hz), 34.5 (s), 31.7 (d, *J* (^{13}C-^{31}P) = 6.8 Hz), 31.4 (s), 26.5 (s), 24.4 (s), 23.2 (s). ^{31}P {^{1}H} NMR (202 MHz, CD_2Cl_2, ppm) δ 66.89 (s). MALDI$^+$ *m/z* calcd for $C_{37}H_{50}AuPNa^+$ [M+Na]$^+$ 745.3208, found 745.3216. Structure confirmed by X-ray crystallography: CCDC 953709.

{Phenylethynyl [(2′,4′,6′-triisopropyl-1,1′-biphenyl-2-yl) di-tert-butylphosphine] gold(I)} [(2′,4′,6′-triisopropyl-1,1′-biphenyl-2-yl) di-tert-butylphosphine] gold(I) tetrakis[3,5-bis(trifluoromethyl)phenyl] borate (78)

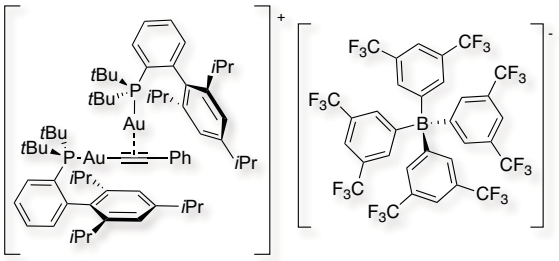

Chloro [(2',4',6'-triisopropyl-1,1'-biphenyl-2-yl)di-*tert*-butylphosphine] gold(I) (68.2 mg, 0.10 mmol) and [(2′,4′,6′-triisopropyl-1,1′-biphenyl-2-yl)di-*tert*-butylphosphine](2-phenylethynyl) gold(I) (75 mg, 0.10 mmol) were dissolved in CH_2Cl_2 (9.4 ml). Then, $NaBAr^F_4$ (92 mg, 0.10 mmol) was added and the reaction mixture was stirred at 25 ºC for 30 min. The crude was filtered through Celite and concentrated. Finally, it was filtered through Teflon 0.22 and washed with CH_2Cl_2. The solvent was removed to afford complex **78** as a white powder in 97% isolated yield (223.0 mg, 0.10 mmol). ^{1}H NMR (400 MHz, CD_2Cl_2, ppm) δ 7.95 – 7.87 (m, 2H), 7.73 (dd, *J* = 4.2, 2.0 Hz, 8H), 7.57 (broad s, 4H), 7.56 – 7.49 (m, 4H), 7.48 – 7.42 (m, 1H), 7.42 – 7.37 (m, 2H), 7.34 – 7.30 (m, 2H), 7.26 – 7.22 (m, 2H), 6.84 (s, 4H), 2.39 – 2.29 (m, 6H), 1.42 (d, *J* = 15.6 Hz, 36H), 1.14 (d, *J* = 6.8 Hz, 12H), 1.09 (d, *J* = 6.9 Hz, 12H), 0.85 (d, *J* = 6.6 Hz, 12H). ^{13}C NMR (101 MHz, CD_2Cl_2, ppm) δ 162.3 (q, *J* (^{13}C-^{11}B) = 50.0 Hz), 150.0 (s), 148.1 (d, *J* (^{13}C-^{31}P) = 14.3 Hz), 147.1 (s), 136.2 (d, *J* (^{13}C-^{31}P) = 5.6 Hz), 135.5 (s), 135.4 (s), 135.0 (d, *J* (^{13}C-^{31}P) = 1.2 Hz), 133.1 (s), 131.4 (s), 130.6 (s), 130.0 – 129.0 (m), 129.0 (s), 127.7 (d, *J* (^{13}C-^{31}P) = 42.5 Hz), 127.6 (s), 127.5 (s), 125.2 (q, *J* (^{13}C-^{19}F) = 272.6 Hz), 122.2 (s), 121.3 (s), 118.2 – 118.0 (m), 39.3 (d, *J* (^{13}C-^{31}P) = 24.6 Hz), 34.0 (s), 31.9 (d, *J* (^{13}C-^{31}P) = 6.8 Hz), 31.4 (s), 26.4 (s), 24.3 (s), 23.6 (s). ^{31}P {^{1}H} NMR (162 MHz, CD_2Cl_2, ppm) δ 65.09 (s). ^{19}F {^{1}H} NMR (376 MHz, CD_2Cl_2, ppm) δ -62.95 (s). ^{11}B {^{1}H} NMR (128 MHz, CD_2Cl_2, ppm) δ -6.67 (s). MALDI$^+$ *m/z* calcd for $C_{66}H_{95}Au_2P_2^+$ $[M\text{-}C_{32}H_{12}BF_{24}]^+$ 1343.6235, found: 1343.5751. Structure confirmed by X-ray crystallography: CCDC 953710.

(α-Methylstyrene) [(2′,4′,6′-triisopropyl-1,1′-biphenyl-2-yl)di-tert-butylphosphine] gold(I) tetrakis[3,5-bis(trifluoromethyl)phenyl] borate (79)

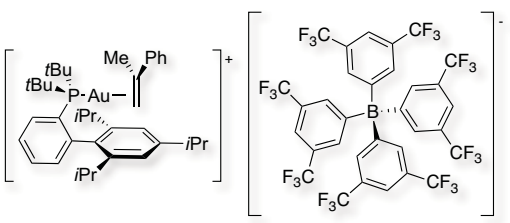

Chloro [(2',4',6'-triisopropyl-1,1'-biphenyl-2-yl)di-*tert*-butylphosphine] gold(I) (100.0 mg, 0.15 mmol) and α-methylstyrene (30.0 μl, 0.23 mmol) were dissolved in CH_2Cl_2 (10.0 ml). Then, $NaBAr^F_4$ (135.0 mg, 0.15 mmol) was added and the reaction mixture was stirred at 25 ºC for 30 min. The crude was filtered through Celite and concentrated. Finally, it was filtered through Teflon 0.22 and washed with CH_2Cl_2. The solvent was removed to afford complex **79** as a white powder in 86% isolated yield (210.4 mg, 0.131 mmol). ^{1}H NMR (400 MHz, CD_2Cl_2, 298 K, ppm) δ 7.82 (td, *J* = 7.8, 1.6 Hz, 1H), 7.76 – 7.70 (m, 8H), 7.63 – 7.53 (m, 6H), 7.50 – 7.39 (m, 5H), 7.29 (s, 2H), 7.21 (ddd, *J* = 7.3, 3.7, 1.7 Hz, 1H), 4.27 (dd, *J* = 4.5, 0.8 Hz, 1H), 3.95 (d, *J* = 4.5 Hz, 1H), 3.12 (p, *J* = 6.9 Hz, 1H), 2.50 (s, 3H), 2.42 – 2.19 (m, 2H), 1.43 (d, *J* = 6.9 Hz, 6H), 1.39 – 1.03 (m, 24H), 0.92 (d, *J* = 6.6 Hz, 6H). ^{13}C NMR (101

MHz, CD_2Cl_2, 213 K, ppm) δ 162.9, 162.5, 162.1, 161.7, 155.9, 151.7, 149.0, 147.0, 146.9, 135.9, 135.7, 135.4, 135.3, 135.0, 133.4, 132.9, 132.6, 132.2, 130.2, 129.7, 129.6, 129.3, 129.0, 128.4, 127.1, 126.6, 126.2, 124.1, 123.6, 123.1, 121.9, 118.5, 118.2, 117.8, 117.5, 89.0, 88.6, 38.6, 38.4, 34.7, 31.6, 31.4, 31.1, 26.2, 26.0, 25.9, 25.0, 24.8, 24.6, 24.4, 23.8. It was not possible to properly assign all the signals due to the broadening of some peaks because of the weak coordination of the metal to the alkene combined with the complexity of the heterocouplings with ^{31}P, ^{19}F and ^{11}B. ^{31}P $\{^1H\}$ NMR (162 MHz, CD_2Cl_2, 298 K, ppm) δ 69.34. ^{19}F $\{^1H\}$ NMR (376 MHz, CD_2Cl_2, 298 K, ppm) δ -62.83 (s). ^{11}B $\{^1H\}$ NMR (128 MHz, CD_2Cl_2, 298 K, ppm) δ -6.67 (s). ESI^+ *m/z* calcd for $C_{29}H_{45}AuP^+$ $[M\text{-}C_{31}H_{22}BF_{24}]^+$ 621.2919, found: 621.2916. Structure confirmed by X-ray crystallography: CCDC 953708.

General Procedure for the Preparation of Cyclobutenes[11]

To a solution of the alkyne (1 equiv.) and the alkene (2 equiv.) in CH_2Cl_2 (0.5 M), the cationic gold (I) catalyst [^{t}BuXPhosAuNCMe]X (3 mol%) was added. Then, the reaction mixture was stirred at 25 ºC and followed by TLC. When it was finished, the catalyst was quenched by adding 0.05 ml of Et_3N, the solvent was removed and the crude was analysed by quantitative ^1H NMR using 1,4-diacetylbenzene as internal standard. Finally, the cyclobutene product was purified by preparative TLC and fully characterized.

1-Methoxy-3-(3-methyl-3-phenylcyclobut-1-en-1-yl)benzene (32)

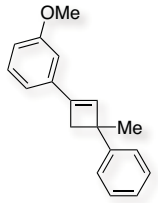

Cyclobutene **32** was synthetized following the general procedure starting from 1-ethynyl-3-methoxybenzene (21 μl, 0.17 mmol) and α-methylstyrene (44 μl, 0.34 mmol) with [^{t}BuXPhosAuNCMe]BAr^F_4 **B** (7.7 mg, 0.05 mmol). The reaction time was 8 h and a mixture of pentane and diethyl ether (9:1) was used as eluent in the separation to obtain cyclobutene **32** as a colorless oil in 78% isolated yield (33 mg, 0.13 mmol). ^1H NMR (500 MHz, $CDCl_3$, ppm) δ 7.47 – 7.43 (m, 2H), 7.40 – 7.35 (m, 2H), 7.33 – 7.28 (m, 1H), 7.25 (td, *J* = 7.2, 1.4 Hz, 1H), 7.05 (dt, *J* = 7.7, 1.2 Hz, 1H), 7.00 – 6.95 (m, 1H), 6.87 (dd, *J* = 7.8, 3.2 Hz, 1H), 6.78 (s, 1H), 3.87 (s, 3H), 3.02 (d, *J* = 12.7 Hz, 1H), 2.95 (d, *J* = 12.5 Hz, 1H), 1.68 (s, 3H). ^{13}C NMR (126 MHz, $CDCl_3$, ppm) δ 159.8 (s), 147.7 (s), 143.8 (s), 136.2 (s), 134.2 (s), 129.5 (s), 128.2 (s), 125.9 (s), 125.8 (s), 117.3 (s), 113.7 (s), 109.9 (s), 55.3 (s), 46.0 (s), 44.4 (s), 27.6 (s). HRMS-APCI m/z calculated for $C_{18}H_{18}O$ $[M+H]^+$ 251.1430, found 251.1434.

1-Fluoro-3-(3-methyl-3-phenylcyclobut-1-en-1-yl)benzene (35)

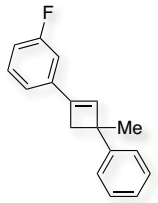

Cyclobutene **35** was synthetized following the general procedure starting from 1-ethynyl-3-fluorobenzene (21 μl, 0.17 mmol) and α-methylstyrene (44 μl, 0.34 mmol) with [^{t}BuXPhosAuNCMe]BAr^F_4 **B** (7.7 mg, 0.05 mmol). The reaction time was 24 h and a mixture of pentane and diethyl ether (90:1) was used as eluent in the separation to obtain cyclobutene **35** as a yellowish oil in 77% isolated yield (31 mg, 0.13 mmol). ^1H NMR (500 MHz, $CDCl_3$, ppm) δ 7.40 – 7.35 (m, 2H), 7.34 – 7.29 (m, 2H), 7.29 – 7.24 (m, 1H), 7.21 – 7.17 (m, 1H), 7.14 (dt, *J* = 7.7, 1.2 Hz,

[11] Synthesized by Anna Homs.

1H), 7.05 (ddd, *J* = 9.8, 2.6, 1.5 Hz, 1H), 6.94 (tdd, *J* = 8.3, 2.6, 1.0 Hz, 1H), 6.75 (s, 1H), 2.95 (d, *J* = 12.6 Hz, 1H), 2.88 (d, *J* = 12.5 Hz, 1H), 1.62 (s, 3H). ^{13}C NMR (126 MHz, $CDCl_3$, ppm) δ 163.1 (d, *J* = 245.8 Hz), 147.4 (s), 142.9 (d, *J* = 2.5 Hz), 137.0 (d, *J* = 7.6 Hz), 135.3 (s), 129.9 (d, *J* = 8.3 Hz), 128.3 (s), 125.9 (s), 125.9 (s), 120.4 (d, *J* = 2.8 Hz), 114.7 (d, *J* = 21.4 Hz), 111.5 (d, *J* = 21.4 Hz), 46.2 (s), 44.3 (s), 27.6 (s). HRMS-APCI m/z calculated for $C_{17}H_{15}F$ $[M+H]^+$ 239.1234, found 239.1231.

1-Chloro-3-(3-methyl-3-phenylcyclobut-1-en-1-yl)benzene (36)

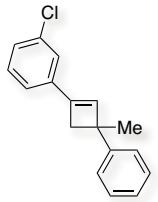

Cyclobutene **36** was synthetized following the general procedure starting from 1-ethynyl-3-chlorobenzene (21 μl, 0.17 mmol) and α-methylstyrene (44 μl, 0.34 mmol) with [^{t}BuXPhosAuNCMe]BAr^F_4 **B** (7.7 mg, 0.05 mmol). The reaction time was 24 h and a mixture of pentane and diethyl ether (90:1) was used as eluent in the separation to obtain cyclobutene **36** as a yellowish oil in 83% isolated yield (36 mg, 0.141 mmol). ^{1}H NMR (500 MHz, $CDCl_3$, ppm) δ 7.40 – 7.35 (m, 3H), 7.35 – 7.30 (m, 2H), 7.27 – 7.17 (m, 4H), 6.77 (s, 1H), 2.96 (d, *J* = 12.5 Hz, 1H), 2.89 (d, *J* = 12.5 Hz, 1H), 1.63 (s, 3H). ^{13}C NMR (126 MHz, $CDCl_3$, ppm) δ 147.3 (s), 142.7 (s), 136.6 (s), 135.5 (s), 134.5 (s), 129.7 (s), 128.3 (s), 127.8 (s), 125.9 (s), 124.9 (s), 122.8 (s), 46.3 (s), 44.3 (s), 27.6 (s). HRMS-APCI m/z calculated for $C_{17}H_{15}Cl$ $[M+H]^+$ 255.0935, found 255.0935.

1-Methoxy-3-(3-methyl-3-phenylcyclobut-1-en-1-yl)benzene (37)

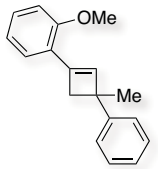

Cyclobutene **37** was synthetized following the general procedure starting from 1-ethynyl-2-methoxybenzene (22 μl, 0.17 mmol) and α-methylstyrene (44 μl, 0.34 mmol) with [^{t}BuXPhosAuNCMe]BAr^F_4 **B** (7.7 mg, 0.05 mmol). The reaction time was 48 h and a mixture of pentane and diethyl ether (9:1) was used as eluent in the separation to obtain cyclobutene **37** as a colorless oil in 24% isolated yield (11 mg, 0.044 mmol). ^{1}H NMR (300 MHz, $CDCl_3$, ppm) δ 7.47 – 7.39 (m, 2H), 7.36 – 7.28 (m, 2H), 7.25 – 7.14 (m, 3H), 6.98 – 6.86 (m, 2H), 6.80 (s, 1H), 3.92 (s, 3H), 3.03 (d, *J* = 12.4 Hz, 1H), 2.95 (d, *J* = 12.3 Hz, 1H), 1.65 (s, 3H). ^{13}C NMR (75 MHz, $CDCl_3$, ppm) δ 158.6 (s), 148.2 (s), 140.2 (s), 138.7 (s), 128.9 (s), 128.1 (s), 127.1 (s), 126.0 (s), 125.6 (s), 123.5 (s), 120.3 (s), 110.5 (s), 55.2 (s), 46.8 (s), 45.4 (s), 27.8 (s). HRMS-APCI m/z calculated for $C_{18}H_{18}O$ $[M+H]^+$ 251.1430, found 251.1433.

3-(3-Methyl-3-phenylcyclobut-1-en-1-yl)thiophene (38)

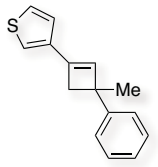

Cyclobutene **38** was synthetized following the general procedure starting from 3-ethynylthiophene (17 μl, 0.17 mmol) and α-methylstyrene (44 μl, 0.34 mmol) with [^{t}BuXPhosAuNCMe]BAr^F_4 **B** (7.7 mg, 0.05 mmol). The reaction time was 24 h and a mixture of pentane and diethyl ether (90:1) was used as eluent in the separation to obtain cyclobutene **38** as a brownish oil in 86% yield (33 mg, 0.146 mmol). ^{1}H NMR (500 MHz, $CDCl_3$, ppm) δ 7.43 – 7.39 (m, 2H), 7.36 – 7.31 (m, 2H), 7.30 (dd, *J* = 5.0, 2.9 Hz, 1H), 7.23 – 7.19 (m, 2H), 7.17 (dd, *J* = 3.0, 1.2 Hz, 1H), 6.51 (s, 1H), 2.97 (d, *J* = 12.5 Hz, 1H), 2.91 (d, *J* = 12.4 Hz, 1H), 1.65 (s, 3H). ^{13}C NMR (126 MHz, $CDCl_3$, ppm) δ 147.8 (s), 139.3 (s), 137.8 (s), 132.7 (s), 128.2 (s), 126.0 (s), 125.9 (s), 125.8 (s), 125.1 (s), 121.1 (s), 47.1 (s), 45.2 (s), 27.7 (s). HRMS-APCI m/z calculated for $C_{15}H_{14}S$ $[M+H]^+$ 239.0889, found 239.0896.

Triisopropyl((1-methyl-3-phenylcyclobut-2-en-1-yl)methyl)silane (43)

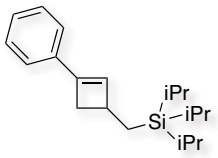

Cyclobutene **43** was synthetized following the general procedure starting from phenylacetylene (19 μl, 0.17 mmol) and allyltriisopropylsilane (81 μl, 0.34 mmol) with [^{t}BuXPhosAuNCMe]BAr$^F_4$ **B** (7.7 mg, 0.05 mmol). The reaction time was 72 h and a mixture of pentane 100% was used as eluent in the separation. Cyclobutene **43** was isolated as a colorless oil. ^{1}H NMR (400 MHz, $CDCl_3$, ppm) δ 7.38 – 7.28 (m, 4H), 7.25 – 7.20 (m, 1H), 6.39 (d, *J* = 1.1 Hz, 1H), 3.07 – 2.94 (m, 2H), 2.31 (dd, *J* = 12.4, 1.4 Hz, 1H), 1.08 (s, 23H). ^{13}C NMR (101 MHz, $CDCl_3$, ppm) δ 143.8 (s), 135.2 (s), 133.7 (s), 128.4 (s), 127.5 (s), 124.4 (s), 38.6 (s), 35.5 (s), 19.0 (s), 15.3 (s), 11.4 (s). HRMS-APCI m/z calculated for $C_{20}H_{32}Si$ $[M+H]^+$ 301.2346, found 301.2352.

(3-Methyl-3-(phenoxymethyl)cyclobut-1-en-1-yl)benzene (44)

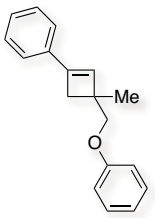

Cyclobutene **44** was synthetized following the general procedure starting from phenylacetylene (19 μl, 0.17 mmol) and ((2-methylallyl)oxy)benzene (52 μl, 0.34 mmol) with [^{t}BuXPhosAuNCMe]BAr$^F_4$ **B** (7.7 mg, 0.05 mmol). The reaction time was 72 h and a mixture of pentane and diethyl ether (20:1) was used as eluent in the separation in a preparative TLC in alumina oxide. Cyclobutene **44** was isolated as a colorless oil. ^{1}H NMR (500 MHz, $CDCl_3$, ppm) δ 7.39 – 7.36 (m, 2H), 7.36 – 7.31 (m, 2H), 7.30 – 7.26 (m, 3H), 6.96 – 6.91 (m, 3H), 6.47 (s, 1H), 3.98 (d, *J* = 8.7 Hz, 1H), 3.95 (d, *J* = 8.7 Hz, 1H), 2.74 (d, *J* = 12.8 Hz, 1H), 2.56 (d, *J* = 12.8 Hz, 1H), 1.42 (s, 3H). ^{13}C NMR (126 MHz, $CDCl_3$, ppm) δ 159.6 (s), 144.3 (s), 134.8 (s), 132.9 (s), 129.5 (s), 128.4 (s), 128.0 (s), 124.7 (s), 120.6 (s), 114.7 (s), 75.4 (s), 42.9 (s), 38.9 (s), 21.7 (s). HRMS-APCI m/z calculated for $C_{18}H_{18}O$ $[M+H]^+$ 251.1426, found 251.1430.

((1-methyl-3-phenylcyclobut-2-en-1-yl)methoxy)triphenylsilane (45)

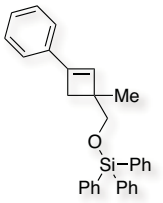

Cyclobutene **45** was synthetized following the general procedure starting from phenylacetylene (19 μl, 0.17 mmol) and ((2-methylallyl)oxy)triphenylsilane (112 mg, 0.34 mmol) with [^{t}BuXPhosAuNCMe]BAr$^F_4$ **B** (7.7 mg, 0.05 mmol). The reaction time was 72 h and a mixture of pentane and diethyl ether (20:1) was used as eluent in the separation in a preparative TLC in alumina oxide. Cyclobutene **45** was isolated as a colorless oil. ^{1}H NMR (300 MHz, $CDCl_3$, ppm) δ 7.68 – 7.57 (m, 6H), 7.46 – 7.28 (m, 14H), 6.29 (s, 1H), 3.80 (s, 2H), 2.61 (d, *J* = 12.7 Hz, 1H), 2.40 (d, *J* = 12.7 Hz, 1H), 1.30 (s, 3H). ^{13}C NMR (75 MHz, $CDCl_3$, ppm) δ 143.9 (s), 135.6 (s), 135.0 (s), 134.6 (s), 133.5 (s), 130.0 (s), 128.3 (s), 127.9 (s), 127.7 (s), 124.6 (s), 71.0 (s), 44.6 (s), 38.3 (s), 21.5 (s). HRMS-APCI m/z calculated for $C_{30}H_{28}OSi$ $[M+H]^+$ 433.1982, found 433.1984.

X-Ray Crystallographic Data

[(2′,4′,6′-Triisopropyl-1,1′-biphenyl-2-yl)di-tert-butylphosphine](2-phenylethynyl)gold(I) (8)

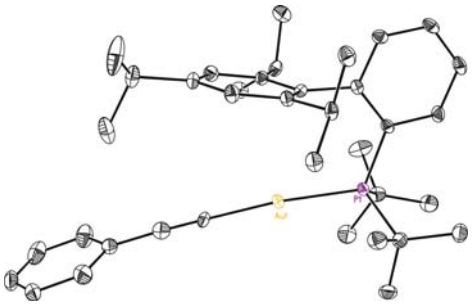

Table 1. Crystal data and structure refinement for complex 8.

Empirical formula	C37 H50 Au P
Formula weight	724.71
Temperature	100(2) K
Wavelength	0.71073 Å
Crystal system	Triclinic
Space group	P-1
Unit cell dimensions	a = 10.8245(8) Å α= 101.506(2) °. b = 12.6401(9) Å β = 95.285(2) °. c = 13.3697(10) Å γ = 112.126(2) °.
Volume	1632.1(2) $Å^3$
Z	2
Density (calculated)	1.475 Mg/m^3
Absorption coefficient	4.580 mm^{-1}
F(000)	734
Crystal size	0.25x0.12x0.10mm^3
Theta range for data collection	1.80 to 30.39 °.
Index ranges	-14 <=h<=13, -14 <=k<=17, -17 <=l<=17
Reflections collected	26200
Independent reflections	8605 [R(int) = 0.0279]
Completeness to theta =30.39 °	87.1%
Absorption correction	Empirical
Max. and min. transmission	0.6573 and 0.3939
Refinement method	Full-matrix least-squares on F^2
Data / restraints / parameters	8605 / 0 / 364
Goodness-of-fit on F^2	1.039
Final R indices [I>2sigma(I)]	R1 = 0.0196, wR2 = 0.0483
R indices (all data)	R1 = 0.0213, wR2 = 0.0490
Largest diff. peak and hole	1.618 and -1.437 e.$Å^{-3}$

Table 2. Bond lengths [Å] and angles [°] for complex 8.

Bond lengths:		C2-C1-C6	117.98(17)
		C2-C1-P1	118.07(14)
Au1-P1	2.2890(5)	C6-C1-P1	123.87(14)
Au1-C37	2.042(2)	C3-C2-C1	122.56(19)
P1-C1	1.8389(19)	C2-C3-C4	119.63(18)
P1-C26	1.888(2)	C5-C4-C3	118.96(18)
P1-C22	1.8954(19)	C4-C5-C6	122.76(18)
C1-C2	1.405(3)	C5-C6-C1	118.08(17)
C1-C6	1.419(3)	C5-C6-C7	113.96(17)
C2-C3	1.384(3)	C1-C6-C7	127.96(16)
C3-C4	1.385(3)	C8-C7-C12	119.20(17)
C4-C5	1.384(3)	C8-C7-C6	119.68(15)
C5-C6	1.407(3)	C12-C7-C6	120.16(15)
C6-C7	1.504(3)	C9-C8-C7	119.51(17)
C7-C8	1.408(2)	C9-C8-C13	118.61(16)
C7-C12	1.413(2)	C7-C8-C13	121.84(17)
C8-C9	1.394(3)	C10-C9-C8	122.00(17)
C8-C13	1.521(2)	C9-C10-C11	117.70(18)
C9-C10	1.388(3)	C9-C10-C16	122.61(17)
C10-C11	1.398(3)	C11-C10-C16	119.67(18)
C10-C16	1.520(3)	C12-C11-C10	122.31(17)
C11-C12	1.385(3)	C11-C12-C7	119.27(16)
C12-C19	1.523(2)	C11-C12-C19	119.91(16)
C13-C15	1.532(3)	C7-C12-C19	120.79(17)
C13-C14	1.536(3)	C8-C13-C15	111.50(16)
C16-C17	1.518(3)	C8-C13-C14	112.06(16)
C16-C18	1.521(4)	C15-C13-C14	109.84(15)
C19-C21	1.530(3)	C17-C16-C10	114.12(18)
C19-C20	1.530(3)	C17-C16-C18	111.6(2)
C22-C24	1.531(3)	C10-C16-C18	109.27(19)
C22-C25	1.533(3)	C12-C19-C21	112.51(16)
C22-C23	1.545(3)	C12-C19-C20	111.52(15)
C26-C27	1.530(3)	C21-C19-C20	110.20(16)
C26-C29	1.538(3)	C24-C22-C25	108.75(18)
C26-C28	1.538(3)	C24-C22-C23	107.65(17)
C30-C31	1.434(3)	C25-C22-C23	106.78(18)
C31-C32	1.396(3)	C24-C22-P1	117.21(14)
C31-C36	1.400(3)	C25-C22-P1	107.41(14)
C32-C33	1.375(4)	C23-C22-P1	108.58(14)
C33-C34	1.404(4)	C27-C26-C29	109.42(17)
C34-C35	1.345(4)	C27-C26-C28	107.92(16)
C35-C36	1.395(4)	C29-C26-C28	108.85(16)
C37-C30	1.170(3)	C27-C26-P1	116.13(14)
		C29-C26-P1	108.27(14)
Angles:		C28-C26-P1	106.02(14)
		C31-C30-C37	177.4(2)
P1-Au1-C37	173.31(6)	C32-C31-C36	117.2(2)
C1-P1-C26	106.92(8)	C32-C31-C30	121.2(2)
C1-P1-C22	106.31(8)	C36-C31-C30	121.6(2)
C26-P1-C22	111.07(9)	C33-C32-C31	121.9(2)
C1-P1-Au1	115.61(6)	C32-C33-C34	119.3(3)
C26-P1-Au1	108.82(6)	C35-C34-C33	120.0(2)
C22-P1-Au1	108.10(7)	C34-C35-C36	120.8(2)
C30-C37-Au1	178.3(2)	C35-C36-C31	120.7(2)

Table 3. Torsion angles [°] for complex 8.

P1-Au1-C37-C30 103(7)	C37-Au1-P1-C22 48.7(5)
C37-Au1-P1-C1 167.7(5)	C26-P1-C1-C2 67.63(16)
C37-Au1-P1-C26 -72.0(5)	C22-P1-C1-C2 -51.09(16)

Au1-P1-C1-C2	-171.05(12)
C26-P1-C1-C6	-115.65(15)
C22-P1-C1-C6	125.62(15)
Au1-P1-C1-C6	5.67(16)
C6-C1-C2-C3	-1.5(3)
P1-C1-C2-C3	175.37(14)
C1-C2-C3-C4	0.9(3)
C2-C3-C4-C5	0.2(3)
C3-C4-C5-C6	-0.6(3)
C4-C5-C6-C1	0.0(3)
C4-C5-C6-C7	179.74(16)
C2-C1-C6-C5	1.1(2)
P1-C1-C6-C5	-175.66(13)
C2-C1-C6-C7	-178.66(16)
P1-C1-C6-C7	4.6(2)
C5-C6-C7-C8	-81.0(2)
C1-C6-C7-C8	98.8(2)
C5-C6-C7-C12	87.7(2)
C1-C6-C7-C12	-92.6(2)
C12-C7-C8-C9	1.3(3)
C6-C7-C8-C9	170.14(17)
C12-C7-C8-C13	-176.54(17)
C6-C7-C8-C13	-7.8(3)
C7-C8-C9-C10	-1.0(3)
C13-C8-C9-C10	177.00(18)
C8-C9-C10-C11	0.3(3)
C8-C9-C10-C16	178.61(19)
C9-C10-C11-C12	-0.1(3)
C16-C10-C11-C12	-178.44(18)
C10-C11-C12-C7	0.5(3)
C10-C11-C12-C19	-177.69(18)
C8-C7-C12-C11	-1.1(3)
C6-C7-C12-C11	-169.87(17)
C8-C7-C12-C19	177.06(17)
C6-C7-C12-C19	8.3(3)
C9-C8-C13-C15	-76.2(2)
C7-C8-C13-C15	101.7(2)
C9-C8-C13-C14	47.4(2)
C7-C8-C13-C14	-134.72(18)
C9-C10-C16-C17	31.3(3)
C11-C10-C16-C17	-150.4(2)
C9-C10-C16-C18	-94.4(3)
C11-C10-C16-C18	83.9(3)
C11-C12-C19-C21	-41.6(2)
C7-C12-C19-C21	140.18(18)
C11-C12-C19-C20	82.8(2)
C7-C12-C19-C20	-95.4(2)
C1-P1-C22-C24	74.18(17)
C26-P1-C22-C24	-41.78(18)
Au1-P1-C22-C24	-161.10(14)
C1-P1-C22-C25	-48.51(17)
C26-P1-C22-C25	-164.47(15)
Au1-P1-C22-C25	76.21(16)
C1-P1-C22-C23	-163.64(14)
C26-P1-C22-C23	80.40(16)
Au1-P1-C22-C23	-38.92(15)
C1-P1-C26-C27	-45.30(17)
C22-P1-C26-C27	70.29(17)
Au1-P1-C26-C27	-170.82(13)
C1-P1-C26-C29	-168.80(13)
C22-P1-C26-C29	-53.22(16)
Au1-P1-C26-C29	65.67(14)
C1-P1-C26-C28	74.53(15)
C22-P1-C26-C28	-169.89(13)
Au1-P1-C26-C28	-51.00(14)
Au1-C37-C30-C31	-77(10)
C37-C30-C31-C32	74(6)
C37-C30-C31-C36	-104(6)
C36-C31-C32-C33	1.9(4)
C30-C31-C32-C33	-176.8(2)
C31-C32-C33-C34	-0.3(4)
C32-C33-C34-C35	-1.6(4)
C33-C34-C35-C36	1.9(4)
C34-C35-C36-C31	-0.3(4)
C32-C31-C36-C35	-1.6(3)
C30-C31-C36-C35	177.1(2)

{Phenylethynyl [(2′,4′,6′-triisopropyl-1,1′-biphenyl-2-yl) di-tert-butylphosphine] gold(I)} [(2′,4′,6′-triisopropyl-1,1′-biphenyl-2-yl) di-tert-butylphosphine] gold(I) tetrakis[3,5-bis(trifluoromethyl)phenyl] borate (78)

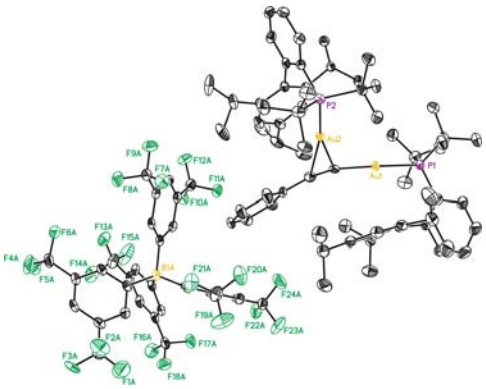

Table 4. Crystal data and structure refinement for complex 78.

Empirical formula	C98.25 H108.50 Au2 B Cl0.50 F24 P2
Formula weight	2229.76
Temperature	100(2) K
Wavelength	0.71073 Å
Crystal system	Triclinic
Space group	P-1

Unit cell dimensions	a = 12.7748(13) Å α= 107.801(3) °. b = 17.3827(17) Å β = 95.994(4) °. c = 22.973(2) Å γ = 93.979(3) °.
Volume	4802.8(8) $Å^3$
Z	2
Density (calculated)	1.542 Mg/m^3
Absorption coefficient	3.190 mm^{-1}
F(000)	2231
Crystal size	0.20x0.12x0.02mm^3
Theta range for data collection	0.94 to 26.48 °.
Index ranges	-15 <=h<=16, -21 <=k<=21, -28 <=l<=28
Reflections collected	138270
Independent reflections	19731 [R(int) = 0.0485]
Completeness to theta =26.48 °	99.4%
Absorption correction	Empirical
Max. and min. transmission	0.9390 and 0.5679
Refinement method	Full-matrix least-squares on F^2
Data / restraints / parameters	19731 / 108 / 1263
Goodness-of-fit on F^2	1.046
Final R indices [I>2sigma(I)]	R1 = 0.0275, wR2 = 0.0615
R indices (all data)	R1 = 0.0397, wR2 = 0.0670
Largest diff. peak and hole	1.871 and -0.734 e.$Å^{-3}$

Table 5. Bond lengths [Å] and angles [°] for complex 78.

Bond lengths:			
		C6-C7	1.513(5)
		C7-C12	1.409(5)
Au1-C59	2.021(3)	C7-C8	1.413(5)
Au1-P1	2.2892(9)	C8-C9	1.383(5)
Au2-C59	2.212(3)	C8-C13	1.525(5)
Au2-C60	2.265(3)	C9-C10	1.386(5)
Au2-P2	2.2690(9)	C10-C11	1.379(5)
P1-C1	1.837(4)	C10-C16	1.528(5)
P1-C26	1.887(4)	C11-C12	1.397(5)
P1-C22	1.892(4)	C12-C19	1.514(5)
P2-C30	1.833(3)	C13-C14	1.529(5)
P2-C55	1.891(3)	C13-C15	1.529(5)
P2-C51	1.892(4)	C16-C17	1.520(6)
C1-C2	1.410(5)	C16-C18	1.532(5)
C1-C6	1.412(5)	C19-C21	1.526(6)
C2-C3	1.375(5)	C19-C20	1.536(6)
C3-C4	1.376(6)	C22-C23	1.520(6)
C4-C5	1.385(6)	C22-C25	1.540(5)
C5-C6	1.402(5)	C22-C24	1.544(5)

C26-C27	1.530(5)	C11A-C15A	1.487(5)
C26-C28	1.536(5)	C12A-C13A	1.379(5)
C26-C29	1.540(6)	C13A-C14A	1.392(5)
C30-C31	1.405(5)	C13A-C16A	1.493(5)
C30-C35	1.415(5)	C15A-F9A	1.336(4)
C31-C32	1.384(5)	C15A-F7A	1.344(4)
C32-C33	1.383(5)	C15A-F8A	1.345(4)
C33-C34	1.370(5)	C16A-F10'	1.216(14)
C34-C35	1.399(5)	C16A-F12A	1.318(5)
C35-C36	1.506(5)	C16A-F11A	1.333(17)
C36-C37	1.408(5)	C16A-F11'	1.34(3)
C36-C41	1.409(5)	C16A-F10A	1.397(6)
C37-C38	1.385(5)	C16A-F12'	1.403(11)
C37-C42	1.528(5)	C17A-C22A	1.395(5)
C38-C39	1.387(5)	C17A-C18A	1.414(5)
C39-C40	1.385(5)	C18A-C19A	1.373(5)
C39-C45	1.511(5)	C19A-C20A	1.386(5)
C40-C41	1.398(5)	C19A-C23A	1.491(5)
C41-C48	1.511(5)	C20A-C21A	1.384(5)
C42-C44	1.530(6)	C21A-C22A	1.396(5)
C42-C43	1.533(6)	C21A-C24A	1.498(5)
C45-C47	1.529(6)	C23A-F15A	1.322(5)
C45-C46	1.532(6)	C23A-F13A	1.327(5)
C48-C49	1.532(5)	C23A-F14A	1.355(5)
C48-C50	1.534(5)	C24A-F18A	1.328(5)
C51-C54	1.528(5)	C24A-F17A	1.333(4)
C51-C53	1.530(5)	C24A-F16A	1.339(4)
C51-C52	1.533(5)	C25A-C30A	1.398(5)
C55-C58	1.532(5)	C25A-C26A	1.404(5)
C55-C57	1.536(5)	C26A-C27A	1.387(5)
C55-C56	1.537(5)	C27A-C28A	1.386(5)
C59-C60	1.218(5)	C27A-C31A	1.493(5)
C60-C61	1.443(5)	C28A-C29A	1.386(5)
C61-C62	1.386(5)	C29A-C30A	1.394(5)
C61-C66	1.392(5)	C29A-C32A	1.499(5)
C62-C63	1.379(5)	C31A-F20'	1.293(8)
C63-C64	1.372(6)	C31A-F19A	1.294(5)
C64-C65	1.372(6)	C31A-F21'	1.318(9)
C65-C66	1.377(5)	C31A-F21A	1.332(6)
B1A-C17A	1.633(5)	C31A-F20A	1.383(5)
B1A-C1A	1.644(5)	C31A-F19'	1.398(8)
B1A-C9A	1.647(5)	C32A-F23A	1.321(4)
B1A-C25A	1.650(5)	C32A-F22A	1.330(4)
C1A-C2A	1.394(5)	C32A-F24A	1.332(4)
C1A-C6A	1.399(5)	Cl1S-C1S	1.7545
C2A-C3A	1.389(5)	Cl2S-C1S	1.7892
C3A-C4A	1.383(5)		
C3A-C7A	1.489(5)	Angles:	
C4A-C5A	1.381(5)		
C5A-C6A	1.388(5)	C59-Au1-P1	174.73(10)
C5A-C8A	1.485(5)	C59-Au2-C60	31.54(13)
C7A-F1A	1.275(6)	C59-Au2-P2	163.24(9)
C7A-F2'	1.279(7)	C60-Au2-P2	163.13(10)
C7A-F3'	1.318(9)	C1-P1-C26	108.05(17)
C7A-F3A	1.319(7)	C1-P1-C22	106.12(17)
C7A-F2A	1.422(6)	C26-P1-C22	111.77(18)
C7A-F1'	1.461(7)	C1-P1-Au1	111.37(12)
C8A-F6A	1.334(5)	C26-P1-Au1	111.09(12)
C8A-F4A	1.337(5)	C22-P1-Au1	108.34(12)
C8A-F5A	1.352(5)	C30-P2-C55	106.35(15)
C9A-C10A	1.393(5)	C30-P2-C51	108.88(15)
C9A-C14A	1.404(5)	C55-P2-C51	111.44(16)
C10A-C11A	1.390(5)	C30-P2-Au2	113.92(11)
C11A-C12A	1.394(5)	C55-P2-Au2	110.39(12)

C51-P2-Au2	105.95(12)	C40-C39-C45	121.6(3)
C2-C1-C6	118.1(3)	C38-C39-C45	120.9(3)
C2-C1-P1	117.6(3)	C39-C40-C41	122.4(3)
C6-C1-P1	124.1(3)	C40-C41-C36	118.6(3)
C3-C2-C1	122.2(4)	C40-C41-C48	119.4(3)
C2-C3-C4	119.8(4)	C36-C41-C48	122.0(3)
C3-C4-C5	119.3(4)	C37-C42-C44	111.9(3)
C4-C5-C6	122.4(4)	C37-C42-C43	109.9(3)
C5-C6-C1	118.1(3)	C44-C42-C43	110.7(4)
C5-C6-C7	113.7(3)	C39-C45-C47	113.5(3)
C1-C6-C7	128.2(3)	C39-C45-C46	110.2(3)
C12-C7-C8	119.5(3)	C47-C45-C46	111.2(4)
C12-C7-C6	119.2(3)	C41-C48-C49	112.8(3)
C8-C7-C6	120.3(3)	C41-C48-C50	111.1(3)
C9-C8-C7	119.1(3)	C49-C48-C50	110.1(3)
C9-C8-C13	119.0(3)	C54-C51-C53	110.2(3)
C7-C8-C13	121.9(3)	C54-C51-C52	107.1(3)
C8-C9-C10	122.3(3)	C53-C51-C52	107.8(3)
C11-C10-C9	118.2(3)	C54-C51-P2	116.1(3)
C11-C10-C16	121.9(4)	C53-C51-P2	108.7(2)
C9-C10-C16	119.8(3)	C52-C51-P2	106.5(2)
C10-C11-C12	122.2(4)	C58-C55-C57	108.4(3)
C11-C12-C7	118.7(3)	C58-C55-C56	108.9(3)
C11-C12-C19	118.4(3)	C57-C55-C56	108.1(3)
C7-C12-C19	122.6(3)	C58-C55-P2	107.7(2)
C8-C13-C14	112.4(3)	C57-C55-P2	114.7(3)
C8-C13-C15	110.0(3)	C56-C55-P2	109.0(2)
C14-C13-C15	110.2(3)	C60-C59-Au1	165.9(3)
C17-C16-C10	113.1(3)	C60-C59-Au2	76.6(2)
C17-C16-C18	109.9(4)	Au1-C59-Au2	115.65(15)
C10-C16-C18	109.8(3)	C59-C60-C61	165.8(3)
C12-C19-C21	110.5(3)	C59-C60-Au2	71.8(2)
C12-C19-C20	113.3(4)	C61-C60-Au2	122.3(2)
C21-C19-C20	109.2(4)	C62-C61-C66	118.5(3)
C23-C22-C25	108.0(3)	C62-C61-C60	122.1(3)
C23-C22-C24	108.8(3)	C66-C61-C60	119.4(3)
C25-C22-C24	108.0(3)	C63-C62-C61	120.9(4)
C23-C22-P1	107.4(3)	C64-C63-C62	119.8(4)
C25-C22-P1	108.7(3)	C63-C64-C65	120.3(3)
C24-C22-P1	115.7(3)	C64-C65-C66	120.3(4)
C27-C26-C28	110.0(3)	C65-C66-C61	120.3(4)
C27-C26-C29	107.7(3)	C17A-B1A-C1A	105.3(3)
C28-C26-C29	107.6(3)	C17A-B1A-C9A	110.5(3)
C27-C26-P1	115.8(3)	C1A-B1A-C9A	111.3(3)
C28-C26-P1	109.6(3)	C17A-B1A-C25A	115.7(3)
C29-C26-P1	105.8(2)	C1A-B1A-C25A	110.5(3)
C31-C30-C35	118.0(3)	C9A-B1A-C25A	103.7(3)
C31-C30-P2	117.7(3)	C2A-C1A-C6A	115.1(3)
C35-C30-P2	124.1(3)	C2A-C1A-B1A	122.5(3)
C32-C31-C30	122.6(3)	C6A-C1A-B1A	122.3(3)
C33-C32-C31	118.9(3)	C3A-C2A-C1A	122.7(3)
C34-C33-C32	119.6(3)	C4A-C3A-C2A	120.6(3)
C33-C34-C35	123.0(3)	C4A-C3A-C7A	118.8(3)
C34-C35-C30	117.9(3)	C2A-C3A-C7A	120.5(3)
C34-C35-C36	114.6(3)	C5A-C4A-C3A	118.2(3)
C30-C35-C36	127.5(3)	C4A-C5A-C6A	120.6(3)
C37-C36-C41	119.9(3)	C4A-C5A-C8A	119.4(3)
C37-C36-C35	120.1(3)	C6A-C5A-C8A	120.0(3)
C41-C36-C35	119.3(3)	C5A-C6A-C1A	122.7(3)
C38-C37-C36	118.5(3)	F1A-C7A-F2'	58.5(6)
C38-C37-C42	119.3(3)	F1A-C7A-F3'	117.5(10)
C36-C37-C42	122.2(3)	F2'-C7A-F3'	117.6(10)
C37-C38-C39	123.0(3)	F1A-C7A-F3A	112.8(6)
C40-C39-C38	117.4(3)	F2'-C7A-F3A	127.9(7)

F3'-C7A-F3A	13.9(12)	C18A-C17A-B1A	119.2(3)
F1A-C7A-F2A	102.6(5)	C19A-C18A-C17A	122.8(3)
F2'-C7A-F2A	46.0(5)	C18A-C19A-C20A	120.9(3)
F3'-C7A-F2A	87.2(8)	C18A-C19A-C23A	121.0(3)
F3A-C7A-F2A	101.1(6)	C20A-C19A-C23A	118.1(3)
F1A-C7A-F1'	36.4(4)	C21A-C20A-C19A	117.9(3)
F2'-C7A-F1'	94.7(6)	C20A-C21A-C22A	121.1(3)
F3'-C7A-F1'	99.7(10)	C20A-C21A-C24A	118.9(3)
F3A-C7A-F1'	89.0(6)	C22A-C21A-C24A	120.0(3)
F2A-C7A-F1'	136.3(5)	C17A-C22A-C21A	122.0(3)
F1A-C7A-C3A	116.8(4)	F15A-C23A-F13A	107.0(4)
F2'-C7A-C3A	115.4(5)	F15A-C23A-F14A	106.1(4)
F3'-C7A-C3A	117.8(10)	F13A-C23A-F14A	105.0(3)
F3A-C7A-C3A	113.2(5)	F15A-C23A-C19A	112.6(3)
F2A-C7A-C3A	108.3(4)	F13A-C23A-C19A	114.0(3)
F1'-C7A-C3A	106.2(4)	F14A-C23A-C19A	111.5(4)
F6A-C8A-F4A	107.3(4)	F18A-C24A-F17A	105.6(3)
F6A-C8A-F5A	105.0(3)	F18A-C24A-F16A	106.4(3)
F4A-C8A-F5A	106.0(3)	F17A-C24A-F16A	106.4(3)
F6A-C8A-C5A	113.5(3)	F18A-C24A-C21A	112.7(3)
F4A-C8A-C5A	113.0(3)	F17A-C24A-C21A	112.8(3)
F5A-C8A-C5A	111.5(4)	F16A-C24A-C21A	112.3(3)
C10A-C9A-C14A	115.9(3)	C30A-C25A-C26A	115.5(3)
C10A-C9A-B1A	122.7(3)	C30A-C25A-B1A	124.3(3)
C14A-C9A-B1A	121.3(3)	C26A-C25A-B1A	119.6(3)
C11A-C10A-C9A	122.3(3)	C27A-C26A-C25A	122.7(3)
C10A-C11A-C12A	120.6(3)	C28A-C27A-C26A	120.5(3)
C10A-C11A-C15A	119.3(3)	C28A-C27A-C31A	118.9(3)
C12A-C11A-C15A	120.0(3)	C26A-C27A-C31A	120.6(3)
C13A-C12A-C11A	118.2(3)	C29A-C28A-C27A	118.4(3)
C12A-C13A-C14A	120.8(3)	C28A-C29A-C30A	120.7(3)
C12A-C13A-C16A	120.1(3)	C28A-C29A-C32A	117.8(3)
C14A-C13A-C16A	119.2(3)	C30A-C29A-C32A	121.5(3)
C13A-C14A-C9A	122.2(3)	C29A-C30A-C25A	122.3(3)
F9A-C15A-F7A	106.5(3)	F20'-C31A-F19A	68.1(7)
F9A-C15A-F8A	106.9(3)	F20'-C31A-F21'	115.4(11)
F7A-C15A-F8A	105.5(3)	F19A-C31A-F21'	121.4(9)
F9A-C15A-C11A	113.1(3)	F20'-C31A-F21A	124.9(7)
F7A-C15A-C11A	112.0(3)	F19A-C31A-F21A	109.2(6)
F8A-C15A-C11A	112.3(3)	F21'-C31A-F21A	17.3(10)
F10'-C16A-F12A	83.7(6)	F20'-C31A-F20A	37.5(6)
F10'-C16A-F11A	113.9(9)	F19A-C31A-F20A	103.8(4)
F12A-C16A-F11A	114.3(8)	F21'-C31A-F20A	87.7(8)
F10'-C16A-F11'	122.0(13)	F21A-C31A-F20A	103.1(5)
F12A-C16A-F11'	105.0(13)	F20'-C31A-F19'	99.9(8)
F11A-C16A-F11'	12.0(15)	F19A-C31A-F19'	32.9(4)
F10'-C16A-F10A	21.9(6)	F21'-C31A-F19'	100.9(9)
F12A-C16A-F10A	104.1(4)	F21A-C31A-F19'	84.7(6)
F11A-C16A-F10A	97.6(6)	F20A-C31A-F19'	132.3(6)
F11'-C16A-F10A	107.9(11)	F20'-C31A-C27A	116.3(6)
F10'-C16A-F12'	108.7(7)	F19A-C31A-C27A	114.3(4)
F12A-C16A-F12'	25.9(4)	F21'-C31A-C27A	113.9(9)
F11A-C16A-F12'	96.8(8)	F21A-C31A-C27A	114.1(5)
F11'-C16A-F12'	85.5(12)	F20A-C31A-C27A	111.2(3)
F10A-C16A-F12'	127.3(5)	F19'-C31A-C27A	107.7(5)
F10'-C16A-C13A	114.5(7)	F23A-C32A-F22A	106.2(3)
F12A-C16A-C13A	114.7(3)	F23A-C32A-F24A	106.5(3)
F11A-C16A-C13A	112.8(8)	F22A-C32A-F24A	105.2(3)
F11'-C16A-C13A	112.8(14)	F23A-C32A-C29A	112.7(3)
F10A-C16A-C13A	111.6(3)	F22A-C32A-C29A	113.5(3)
F12'-C16A-C13A	108.6(5)	F24A-C32A-C29A	112.1(3)
C22A-C17A-C18A	115.2(3)	Cl1S-C1S-Cl2S	109.3
C22A-C17A-B1A	125.3(3)		

Table 6. Torsion angles [°] for complex 78.

C59-Au1-P1-C1 -80.2(10)	C26-P1-C22-C25 -82.3(3)
C59-Au1-P1-C26 159.3(10)	Au1-P1-C22-C25 40.4(3)
C59-Au1-P1-C22 36.2(10)	C1-P1-C22-C24 -78.2(3)
C59-Au2-P2-C30 118.1(3)	C26-P1-C22-C24 39.3(3)
C60-Au2-P2-C30 -102.0(3)	Au1-P1-C22-C24 162.1(3)
C59-Au2-P2-C55 -122.3(3)	C1-P1-C26-C27 43.8(3)
C60-Au2-P2-C55 17.6(4)	C22-P1-C26-C27 -72.6(3)
C59-Au2-P2-C51 -1.6(3)	Au1-P1-C26-C27 166.3(3)
C60-Au2-P2-C51 138.3(3)	C1-P1-C26-C28 168.9(3)
C26-P1-C1-C2 -66.2(3)	C22-P1-C26-C28 52.5(3)
C22-P1-C1-C2 53.8(4)	Au1-P1-C26-C28 -68.6(3)
Au1-P1-C1-C2 171.6(3)	C1-P1-C26-C29 -75.4(3)
C26-P1-C1-C6 118.8(3)	C22-P1-C26-C29 168.2(2)
C22-P1-C1-C6 -121.1(3)	Au1-P1-C26-C29 47.1(3)
Au1-P1-C1-C6 -3.4(4)	C55-P2-C30-C31 58.7(3)
C6-C1-C2-C3 2.6(6)	C51-P2-C30-C31 -61.4(3)
P1-C1-C2-C3 -172.7(4)	Au2-P2-C30-C31 -179.4(2)
C1-C2-C3-C4 -1.6(7)	C55-P2-C30-C35 -116.5(3)
C2-C3-C4-C5 0.0(7)	C51-P2-C30-C35 123.3(3)
C3-C4-C5-C6 0.7(7)	Au2-P2-C30-C35 5.3(3)
C4-C5-C6-C1 0.3(6)	C35-C30-C31-C32 0.8(5)
C4-C5-C6-C7 -179.2(4)	P2-C30-C31-C32 -174.8(3)
C2-C1-C6-C5 -1.9(6)	C30-C31-C32-C33 -1.2(5)
P1-C1-C6-C5 173.1(3)	C31-C32-C33-C34 0.9(5)
C2-C1-C6-C7 177.5(4)	C32-C33-C34-C35 -0.2(5)
P1-C1-C6-C7 -7.5(6)	C33-C34-C35-C30 -0.2(5)
C5-C6-C7-C12 86.7(4)	C33-C34-C35-C36 179.4(3)
C1-C6-C7-C12 -92.7(5)	C31-C30-C35-C34 -0.1(5)
C5-C6-C7-C8 -81.6(4)	P2-C30-C35-C34 175.2(2)
C1-C6-C7-C8 99.0(5)	C31-C30-C35-C36 -179.6(3)
C12-C7-C8-C9 1.2(5)	P2-C30-C35-C36 -4.4(5)
C6-C7-C8-C9 169.4(3)	C34-C35-C36-C37 -79.6(4)
C12-C7-C8-C13 -174.7(3)	C30-C35-C36-C37 99.9(4)
C6-C7-C8-C13 -6.5(5)	C34-C35-C36-C41 90.6(4)
C7-C8-C9-C10 -0.2(5)	C30-C35-C36-C41 -89.8(4)
C13-C8-C9-C10 175.9(3)	C41-C36-C37-C38 4.8(5)
C8-C9-C10-C11 -0.5(5)	C35-C36-C37-C38 175.0(3)
C8-C9-C10-C16 -176.2(3)	C41-C36-C37-C42 -172.3(3)
C9-C10-C11-C12 0.2(5)	C35-C36-C37-C42 -2.1(5)
C16-C10-C11-C12 175.7(3)	C36-C37-C38-C39 -2.5(5)
C10-C11-C12-C7 0.9(5)	C42-C37-C38-C39 174.8(3)
C10-C11-C12-C19 -172.9(3)	C37-C38-C39-C40 -0.9(5)
C8-C7-C12-C11 -1.6(5)	C37-C38-C39-C45 -177.5(3)
C6-C7-C12-C11 -169.9(3)	C38-C39-C40-C41 1.9(5)
C8-C7-C12-C19 172.0(3)	C45-C39-C40-C41 178.5(3)
C6-C7-C12-C19 3.7(5)	C39-C40-C41-C36 0.5(5)
C9-C8-C13-C14 53.2(4)	C39-C40-C41-C48 -176.0(3)
C7-C8-C13-C14 -130.8(4)	C37-C36-C41-C40 -3.9(5)
C9-C8-C13-C15 -70.0(4)	C35-C36-C41-C40 -174.2(3)
C7-C8-C13-C15 106.0(4)	C37-C36-C41-C48 172.5(3)
C11-C10-C16-C17 33.3(5)	C35-C36-C41-C48 2.2(5)
C9-C10-C16-C17 -151.3(4)	C38-C37-C42-C44 50.0(5)
C11-C10-C16-C18 -89.9(5)	C36-C37-C42-C44 -132.9(4)
C9-C10-C16-C18 85.6(5)	C38-C37-C42-C43 -73.5(5)
C11-C12-C19-C21 76.3(5)	C36-C37-C42-C43 103.7(4)
C7-C12-C19-C21 -97.3(4)	C40-C39-C45-C47 36.8(5)
C11-C12-C19-C20 -46.6(5)	C38-C39-C45-C47 -146.7(4)
C7-C12-C19-C20 139.8(4)	C40-C39-C45-C46 -88.7(5)
C1-P1-C22-C23 43.5(3)	C38-C39-C45-C46 87.8(4)
C26-P1-C22-C23 161.0(3)	C40-C41-C48-C49 -41.8(4)
Au1-P1-C22-C23 -76.2(3)	C36-C41-C48-C49 141.8(3)
C1-P1-C22-C25 160.1(3)	C40-C41-C48-C50 82.4(4)

C36-C41-C48-C50 -94.0(4)
C30-P2-C51-C54 45.9(3)
C55-P2-C51-C54 -71.1(3)
Au2-P2-C51-C54 168.8(2)
C30-P2-C51-C53 170.8(2)
C55-P2-C51-C53 53.8(3)
Au2-P2-C51-C53 -66.3(3)
C30-P2-C51-C52 -73.3(3)
C55-P2-C51-C52 169.7(2)
Au2-P2-C51-C52 49.6(2)
C30-P2-C55-C58 40.7(3)
C51-P2-C55-C58 159.2(3)
Au2-P2-C55-C58 -83.3(3)
C30-P2-C55-C57 -80.1(3)
C51-P2-C55-C57 38.5(3)
Au2-P2-C55-C57 155.9(2)
C30-P2-C55-C56 158.7(2)
C51-P2-C55-C56 -82.8(3)
Au2-P2-C55-C56 34.7(3)
P1-Au1-C59-C60 57(2)
P1-Au1-C59-Au2 -153.3(9)
P2-Au2-C59-C60 159.1(2)
C60-Au2-C59-Au1 -172.7(3)
P2-Au2-C59-Au1 -13.6(4)
Au1-C59-C60-C61 -25(3)
Au2-C59-C60-C61 -176.7(16)
Au1-C59-C60-Au2 151.8(13)
P2-Au2-C60-C59 -159.2(3)
C59-Au2-C60-C61 179.1(4)
P2-Au2-C60-C61 19.8(5)
C59-C60-C61-C62 140.2(15)
Au2-C60-C61-C62 -36.1(5)
C59-C60-C61-C66 -38.0(17)
Au2-C60-C61-C66 145.6(3)
C66-C61-C62-C63 -0.2(6)
C60-C61-C62-C63 -178.5(4)
C61-C62-C63-C64 -0.9(6)
C62-C63-C64-C65 1.7(6)
C63-C64-C65-C66 -1.3(6)
C64-C65-C66-C61 0.2(6)
C62-C61-C66-C65 0.5(5)
C60-C61-C66-C65 178.8(3)
C17A-B1A-C1A-C2A 91.5(4)
C9A-B1A-C1A-C2A -148.8(3)
C25A-B1A-C1A-C2A -34.1(5)
C17A-B1A-C1A-C6A -85.2(4)
C9A-B1A-C1A-C6A 34.6(4)
C25A-B1A-C1A-C6A 149.2(3)
C6A-C1A-C2A-C3A -3.0(5)
B1A-C1A-C2A-C3A -179.9(3)
C1A-C2A-C3A-C4A 2.2(6)
C1A-C2A-C3A-C7A -174.8(4)
C2A-C3A-C4A-C5A -0.2(6)
C7A-C3A-C4A-C5A 176.9(4)
C3A-C4A-C5A-C6A -0.9(5)
C3A-C4A-C5A-C8A 178.4(4)
C4A-C5A-C6A-C1A -0.1(6)
C8A-C5A-C6A-C1A -179.3(4)
C2A-C1A-C6A-C5A 1.9(5)
B1A-C1A-C6A-C5A 178.8(3)
C4A-C3A-C7A-F1A 170.6(6)
C2A-C3A-C7A-F1A -12.3(7)
C4A-C3A-C7A-F2' -123.5(7)
C2A-C3A-C7A-F2' 53.6(8)
C4A-C3A-C7A-F3' 22.5(11)
C2A-C3A-C7A-F3' -160.4(10)
C4A-C3A-C7A-F3A 37.0(7)
C2A-C3A-C7A-F3A -145.9(6)
C4A-C3A-C7A-F2A -74.2(5)
C2A-C3A-C7A-F2A 102.9(5)
C4A-C3A-C7A-F1' 133.0(4)
C2A-C3A-C7A-F1' -49.9(5)
C4A-C5A-C8A-F6A 149.8(4)
C6A-C5A-C8A-F6A -31.0(6)
C4A-C5A-C8A-F4A 27.3(6)
C6A-C5A-C8A-F4A -153.5(4)
C4A-C5A-C8A-F5A -91.9(4)
C6A-C5A-C8A-F5A 87.3(4)
C17A-B1A-C9A-C10A 150.9(3)
C1A-B1A-C9A-C10A 34.3(4)
C25A-B1A-C9A-C10A -84.5(4)
C17A-B1A-C9A-C14A -34.0(4)
C1A-B1A-C9A-C14A -150.6(3)
C25A-B1A-C9A-C14A 90.6(4)
C14A-C9A-C10A-C11A 0.9(5)
B1A-C9A-C10A-C11A 176.3(3)
C9A-C10A-C11A-C12A 0.1(5)
C9A-C10A-C11A-C15A -179.7(3)
C10A-C11A-C12A-C13A -0.7(5)
C15A-C11A-C12A-C13A 179.0(3)
C11A-C12A-C13A-C14A 0.3(5)
C11A-C12A-C13A-C16A -178.6(3)
C12A-C13A-C14A-C9A 0.7(5)
C16A-C13A-C14A-C9A 179.6(3)
C10A-C9A-C14A-C13A -1.3(5)
B1A-C9A-C14A-C13A -176.7(3)
C10A-C11A-C15A-F9A -174.5(3)
C12A-C11A-C15A-F9A 5.7(5)
C10A-C11A-C15A-F7A 65.1(4)
C12A-C11A-C15A-F7A -114.7(4)
C10A-C11A-C15A-F8A -53.5(4)
C12A-C11A-C15A-F8A 126.8(3)
C12A-C13A-C16A-F10' -120.6(7)
C14A-C13A-C16A-F10' 60.4(7)
C12A-C13A-C16A-F12A -26.2(6)
C14A-C13A-C16A-F12A 154.9(4)
C12A-C13A-C16A-F11A 107.0(7)
C14A-C13A-C16A-F11A -71.9(7)
C12A-C13A-C16A-F11' 94.0(12)
C14A-C13A-C16A-F11' -84.9(12)
C12A-C13A-C16A-F10A -144.3(4)
C14A-C13A-C16A-F10A 36.7(5)
C12A-C13A-C16A-F12' 1.0(6)
C14A-C13A-C16A-F12' -177.9(5)
C1A-B1A-C17A-C22A -92.8(4)
C9A-B1A-C17A-C22A 147.0(3)
C25A-B1A-C17A-C22A 29.5(5)
C1A-B1A-C17A-C18A 81.2(4)
C9A-B1A-C17A-C18A -39.0(4)
C25A-B1A-C17A-C18A -156.4(3)
C22A-C17A-C18A-C19A -1.3(5)
B1A-C17A-C18A-C19A -175.9(3)
C17A-C18A-C19A-C20A -0.1(6)
C17A-C18A-C19A-C23A -179.8(3)
C18A-C19A-C20A-C21A 1.6(5)
C23A-C19A-C20A-C21A -178.7(3)
C19A-C20A-C21A-C22A -1.7(5)
C19A-C20A-C21A-C24A 179.3(3)

C18A-C17A-C22A-C21A 1.1(5)
B1A-C17A-C22A-C21A 175.3(3)
C20A-C21A-C22A-C17A 0.4(5)
C24A-C21A-C22A-C17A 179.3(3)
C18A-C19A-C23A-F15A 120.5(4)
C20A-C19A-C23A-F15A -59.2(5)
C18A-C19A-C23A-F13A -1.7(5)
C20A-C19A-C23A-F13A 178.6(3)
C18A-C19A-C23A-F14A -120.3(4)
C20A-C19A-C23A-F14A 60.0(5)
C20A-C21A-C24A-F18A -140.0(3)
C22A-C21A-C24A-F18A 41.1(5)
C20A-C21A-C24A-F17A 100.5(4)
C22A-C21A-C24A-F17A -78.5(4)
C20A-C21A-C24A-F16A -19.8(5)
C22A-C21A-C24A-F16A 161.2(3)
C17A-B1A-C25A-C30A 30.4(5)
C1A-B1A-C25A-C30A 150.0(3)
C9A-B1A-C25A-C30A -90.7(4)
C17A-B1A-C25A-C26A -159.0(3)
C1A-B1A-C25A-C26A -39.5(4)
C9A-B1A-C25A-C26A 79.8(4)
C30A-C25A-C26A-C27A 0.9(5)
B1A-C25A-C26A-C27A -170.4(3)
C25A-C26A-C27A-C28A 0.2(5)
C25A-C26A-C27A-C31A -179.7(3)
C26A-C27A-C28A-C29A -0.9(5)
C31A-C27A-C28A-C29A 179.0(3)
C27A-C28A-C29A-C30A 0.5(5)
C27A-C28A-C29A-C32A 179.3(3)
C28A-C29A-C30A-C25A 0.7(5)
C32A-C29A-C30A-C25A -178.0(3)
C26A-C25A-C30A-C29A -1.4(5)
B1A-C25A-C30A-C29A 169.5(3)
C28A-C27A-C31A-F20' 10.5(9)
C26A-C27A-C31A-F20' -169.6(8)
C28A-C27A-C31A-F19A -66.0(6)
C26A-C27A-C31A-F19A 114.0(5)
C28A-C27A-C31A-F21' 148.4(9)
C26A-C27A-C31A-F21' -31.7(9)
C28A-C27A-C31A-F21A 167.3(5)
C26A-C27A-C31A-F21A -12.7(7)
C28A-C27A-C31A-F20A 51.2(5)
C26A-C27A-C31A-F20A -128.9(4)
C28A-C27A-C31A-F19' -100.6(6)
C26A-C27A-C31A-F19' 79.4(6)
C28A-C29A-C32A-F23A 44.6(5)
C30A-C29A-C32A-F23A -136.7(3)
C28A-C29A-C32A-F22A 165.3(3)
C30A-C29A-C32A-F22A -15.9(5)
C28A-C29A-C32A-F24A -75.6(4)
C30A-C29A-C32A-F24A 103.2(4)

(α-Methylstyrene) [(2′,4′,6′-triisopropyl-1,1′-biphenyl-2-yl)di-tert-butylphosphine] gold(I) tetrakis[3,5-bis(trifluoromethyl)phenyl] borate (79)

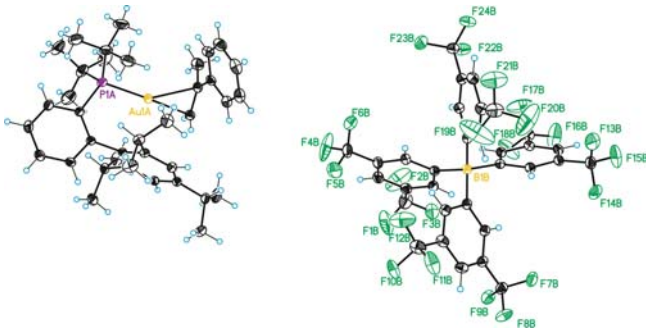

Table 7. Crystal data and structure refinement for complex 79.

Empirical formula	C70 H67 Au B F24 P
Formula weight	1602.98
Temperature	100(2) K
Wavelength	0.71073 Å
Crystal system	Monoclinic
Space group	P2(1)/n
Unit cell dimensions	a = 12.876(11) Å
	α = 90.00 °.
	b = 14.771(3) Å
	β = 90.39(2) °.
	c = 36.339(8) Å
	γ = 90.00 °.
Volume	6911(6) Å^3

Z	4
Density (calculated)	1.541 Mg/m^3
Absorption coefficient	2.257 mm^{-1}
F(000)	3208
Crystal size	0.20x0.20x0.20mm^3
Theta range for data collection	2.37 to 36.40 °.
Index ranges	-20 <=h<=21 , 0 <=k<=24 , 0 <=l<=59
Reflections collected	31125
Independent reflections	31125 [R(int) = 0.0000]
Completeness to theta =36.40 °	92.299995%
Absorption correction	Empirical
Max. and min. transmission	0.6610 and 0.6610
Refinement method	Full-matrix least-squares on F^2
Data / restraints / parameters	31125 / 790 / 1353
Goodness-of-fit on F^2	1.035
Final R indices [I>2sigma(I)]	R1 = 0.0347 , wR2 = 0.0866
R indices (all data)	R1 = 0.0506 , wR2 = 0.0902
Largest diff. peak and hole	2.035 and -0.829 $e.Å^{-3}$

Table 8. Bond lengths [Å] and angles [°] for complex 79.

Bond lengths:			
		C19A-C25A	1.531(3)
		C20A-C21A	1.405(3)
Au1A-C1A	2.247(2)	C21A-C28A	1.536(3)
Au1A-P1A	2.3125(14)	C22A-C23A	1.548(3)
Au1A-C2A	2.405(3)	C22A-C24A	1.556(3)
C1A-C2A	1.389(3)	C25A-C27A	1.542(3)
C2A-C4A	1.498(3)	C25A-C26A	1.552(3)
C2A-C3A	1.524(3)	C28A-C30A	1.552(3)
C4A-C9A	1.398(3)	C28A-C29A	1.553(3)
C4A-C5A	1.409(3)	C31A-C32A	1.535(4)
C5A-C6A	1.392(3)	C31A-C33A	1.544(3)
C6A-C7A	1.390(4)	C31A-C34A	1.568(4)
C7A-C8A	1.406(4)	C31A-P1A	1.906(2)
C8A-C9A	1.391(3)	C35A-C37A	1.540(4)
C10A-C15A	1.421(2)	C35A-C36A	1.559(3)
C10A-C11A	1.422(3)	C35A-C38A	1.560(3)
C10A-P1A	1.852(2)	C35A-P1A	1.892(2)
C11A-C12A	1.410(3)	Au1'-C1'	2.255(3)
C12A-C13A	1.392(3)	Au1'-P1'	2.318(3)
C13A-C14A	1.401(3)	Au1'-C2'	2.404(4)
C14A-C15A	1.429(3)	C1'-C2'	1.389(4)
C15A-C16A	1.523(2)	C2'-C4'	1.501(4)
C16A-C21A	1.416(2)	C2'-C3'	1.523(4)
C16A-C17A	1.426(2)	C4'-C9'	1.401(4)
C17A-C18A	1.407(2)	C4'-C5'	1.412(4)
C17A-C22A	1.530(3)	C5'-C6'	1.392(4)
C18A-C19A	1.398(3)	C6'-C7'	1.391(5)
C19A-C20A	1.404(3)	C7'-C8'	1.407(5)

C8'-C9'	1.391(5)	C15B-F11"	1.393(10)
C10'-C15'	1.421(4)	C15B-F12"	1.412(7)
C10'-C11'	1.424(4)	C15B-F12'	1.473(7)
C10'-P1'	1.851(3)	C16B-F8B	1.353(2)
C11'-C12'	1.411(4)	C16B-F7B	1.358(3)
C12'-C13'	1.393(4)	C16B-F9B	1.358(2)
C13'-C14'	1.403(4)	C17B-C18B	1.413(2)
C14'-C15'	1.431(4)	C17B-C22B	1.416(2)
C15'-C16'	1.525(4)	C18B-C19B	1.410(3)
C16'-C21'	1.417(4)	C19B-C20B	1.404(3)
C16'-C17'	1.427(4)	C19B-C23B	1.502(3)
C17'-C18'	1.408(4)	C20B-C21B	1.396(2)
C17'-C22'	1.529(4)	C21B-C22B	1.419(3)
C18'-C19'	1.398(4)	C21B-C24B	1.514(3)
C19'-C20'	1.405(4)	C23B-F15B	1.327(7)
C19'-C25'	1.531(4)	C23B-F14'	1.33(2)
C20'-C21'	1.405(4)	C23B-F14B	1.340(6)
C21'-C28'	1.536(4)	C23B-F13'	1.340(18)
C22'-C23'	1.547(4)	C23B-F13B	1.369(7)
C22'-C24'	1.556(4)	C23B-F15'	1.418(16)
C25'-C27'	1.541(4)	C24B-F18B	1.328(2)
C25'-C26'	1.551(4)	C24B-F16B	1.328(3)
C28'-C30'	1.552(4)	C24B-F17B	1.333(3)
C28'-C29'	1.554(4)	C25B-C26B	1.404(2)
C31'-C32'	1.536(5)	C25B-C30B	1.411(2)
C31'-C33'	1.542(4)	C26B-C27B	1.410(3)
C31'-C34'	1.569(5)	C27B-C28B	1.398(3)
C31'-P1'	1.906(4)	C27B-C31B	1.503(3)
C35'-C37'	1.540(5)	C28B-C29B	1.401(3)
C35'-C38'	1.560(4)	C29B-C30B	1.403(2)
C35'-C36'	1.559(4)	C29B-C32B	1.507(3)
C35'-P1'	1.890(4)	C31B-F20B	1.324(3)
B1B-C1B	1.645(3)	C31B-F19B	1.330(3)
B1B-C9B	1.653(3)	C31B-F21B	1.333(3)
B1B-C25B	1.656(3)	C32B-F23B	1.351(3)
B1B-C17B	1.664(3)	C32B-F22B	1.351(2)
C1B-C6B	1.415(3)	C32B-F24B	1.358(2)
C1B-C2B	1.417(2)		
C2B-C3B	1.395(3)	Angles:	
C3B-C4B	1.405(3)		
C3B-C7B	1.510(3)	C1A-Au1A-P1A	174.45(6)
C4B-C5B	1.393(3)	C1A-Au1A-C2A	34.53(7)
C5B-C6B	1.400(3)	P1A-Au1A-C2A	148.15(5)
C5B-C8B	1.512(3)	C2A-C1A-Au1A	78.96(12)
C7B-F1B	1.335(3)	C1A-C2A-C4A	120.71(19)
C7B-F3B	1.341(3)	C1A-C2A-C3A	121.04(19)
C7B-F2B	1.361(4)	C4A-C2A-C3A	117.64(17)
C8B-F6B	1.326(3)	C1A-C2A-Au1A	66.52(11)
C8B-F4B	1.327(3)	C4A-C2A-Au1A	102.34(12)
C8B-F5B	1.366(3)	C3A-C2A-Au1A	108.70(14)
C9B-C14B	1.409(2)	C9A-C4A-C5A	118.9(2)
C9B-C10B	1.433(3)	C9A-C4A-C2A	120.60(18)
C10B-C11B	1.398(3)	C5A-C4A-C2A	120.52(19)
C11B-C12B	1.404(3)	C6A-C5A-C4A	120.6(2)
C11B-C15B	1.526(3)	C7A-C6A-C5A	119.8(2)
C12B-C13B	1.410(3)	C6A-C7A-C8A	120.4(2)
C13B-C14B	1.410(3)	C9A-C8A-C7A	119.4(2)
C13B-C16B	1.509(3)	C8A-C9A-C4A	120.9(2)
C15B-F10"	1.171(7)	C15A-C10A-C11A	118.54(17)
C15B-F11'	1.232(8)	C15A-C10A-P1A	123.73(13)
C15B-F12B	1.315(4)	C11A-C10A-P1A	117.72(15)
C15B-F11B	1.362(5)	C12A-C11A-C10A	122.33(19)
C15B-F10'	1.365(14)	C13A-C12A-C11A	119.20(18)
C15B-F10B	1.367(5)	C12A-C13A-C14A	119.38(18)

C13A-C14A-C15A	122.67(18)	C15'-C10'-P1'	124.3(4)
C10A-C15A-C14A	117.85(16)	C11'-C10'-P1'	117.4(4)
C10A-C15A-C16A	126.90(15)	C12'-C11'-C10'	122.0(5)
C14A-C15A-C16A	115.25(15)	C13'-C12'-C11'	118.7(6)
C21A-C16A-C17A	119.16(15)	C12'-C13'-C14'	118.9(5)
C21A-C16A-C15A	119.88(15)	C13'-C14'-C15'	122.3(5)
C17A-C16A-C15A	119.90(15)	C10'-C15'-C14'	117.5(5)
C18A-C17A-C16A	119.65(15)	C10'-C15'-C16'	126.8(4)
C18A-C17A-C22A	118.46(16)	C14'-C15'-C16'	114.9(4)
C16A-C17A-C22A	121.77(15)	C21'-C16'-C17'	118.9(4)
C19A-C18A-C17A	121.85(16)	C21'-C16'-C15'	119.3(5)
C18A-C19A-C20A	117.64(16)	C17'-C16'-C15'	119.6(5)
C18A-C19A-C25A	122.11(16)	C18'-C17'-C16'	119.6(4)
C20A-C19A-C25A	120.16(16)	C18'-C17'-C22'	118.6(4)
C19A-C20A-C21A	122.67(16)	C16'-C17'-C22'	121.8(4)
C20A-C21A-C16A	118.98(16)	C19'-C18'-C17'	121.6(4)
C20A-C21A-C28A	119.21(15)	C18'-C19'-C20'	117.5(5)
C16A-C21A-C28A	121.71(15)	C18'-C19'-C25'	122.5(4)
C17A-C22A-C23A	110.51(17)	C20'-C19'-C25'	119.9(4)
C17A-C22A-C24A	111.43(16)	C21'-C20'-C19'	122.4(4)
C23A-C22A-C24A	110.50(18)	C20'-C21'-C16'	118.9(4)
C19A-C25A-C27A	114.21(17)	C20'-C21'-C28'	119.2(5)
C19A-C25A-C26A	109.22(17)	C16'-C21'-C28'	121.6(4)
C27A-C25A-C26A	111.09(19)	C17'-C22'-C23'	110.6(5)
C21A-C28A-C30A	112.13(16)	C17'-C22'-C24'	111.5(5)
C21A-C28A-C29A	110.54(17)	C23'-C22'-C24'	110.5(5)
C30A-C28A-C29A	111.04(18)	C19'-C25'-C27'	114.3(5)
C32A-C31A-C33A	109.0(2)	C19'-C25'-C26'	109.2(5)
C32A-C31A-C34A	108.9(2)	C27'-C25'-C26'	111.4(5)
C33A-C31A-C34A	108.3(2)	C21'-C28'-C30'	112.1(5)
C32A-C31A-P1A	108.07(15)	C21'-C28'-C29'	110.5(5)
C33A-C31A-P1A	114.16(19)	C30'-C28'-C29'	111.0(5)
C34A-C31A-P1A	108.22(18)	C32'-C31'-C33'	109.0(4)
C37A-C35A-C36A	106.6(2)	C32'-C31'-C34'	108.8(5)
C37A-C35A-C38A	108.1(2)	C33'-C31'-C34'	108.4(4)
C36A-C35A-C38A	111.4(2)	C32'-C31'-P1'	107.9(4)
C37A-C35A-P1A	106.62(15)	C33'-C31'-P1'	114.4(4)
C36A-C35A-P1A	115.58(18)	C34'-C31'-P1'	108.2(4)
C38A-C35A-P1A	108.20(18)	C37'-C35'-C38'	108.0(4)
C10A-P1A-C35A	107.93(10)	C37'-C35'-C36'	106.5(4)
C10A-P1A-C31A	107.73(11)	C38'-C35'-C36'	111.4(4)
C35A-P1A-C31A	111.80(11)	C37'-C35'-P1'	106.7(4)
C10A-P1A-Au1A	112.17(7)	C38'-C35'-P1'	108.3(4)
C35A-P1A-Au1A	108.96(8)	C36'-C35'-P1'	115.6(4)
C31A-P1A-Au1A	108.29(8)	C10'-P1'-C35'	108.0(3)
C1'-Au1'-P1'	163.3(5)	C10'-P1'-C31'	107.7(3)
C1'-Au1'-C2'	34.49(10)	C35'-P1'-C31'	112.2(3)
P1'-Au1'-C2'	147.8(4)	C10'-P1'-Au1'	112.4(3)
C2'-C1'-Au1'	78.6(2)	C35'-P1'-Au1'	109.0(3)
C1'-C2'-C4'	120.5(5)	C31'-P1'-Au1'	107.7(3)
C1'-C2'-C3'	121.2(5)	C1B-B1B-C9B	103.03(13)
C4'-C2'-C3'	117.7(4)	C1B-B1B-C25B	111.43(13)
C1'-C2'-Au1'	66.86(19)	C9B-B1B-C25B	112.61(14)
C4'-C2'-Au1'	101.9(3)	C1B-B1B-C17B	115.18(15)
C3'-C2'-Au1'	108.8(4)	C9B-B1B-C17B	112.54(13)
C9'-C4'-C5'	118.2(5)	C25B-B1B-C17B	102.41(13)
C9'-C4'-C2'	119.5(5)	C6B-C1B-C2B	116.17(15)
C5'-C4'-C2'	119.3(5)	C6B-C1B-B1B	120.47(15)
C6'-C5'-C4'	120.3(5)	C2B-C1B-B1B	122.98(15)
C7'-C6'-C5'	119.5(6)	C3B-C2B-C1B	121.61(17)
C6'-C7'-C8'	119.9(5)	C2B-C3B-C4B	121.13(18)
C9'-C8'-C7'	119.1(5)	C2B-C3B-C7B	121.71(18)
C8'-C9'-C4'	120.9(5)	C4B-C3B-C7B	117.03(18)
C15'-C10'-C11'	118.1(4)	C5B-C4B-C3B	118.22(17)

C4B-C5B-C6B	120.74(17)	F10"-C15B-C11B	115.1(4)
C4B-C5B-C8B	120.13(17)	F11'-C15B-C11B	118.0(4)
C6B-C5B-C8B	119.13(18)	F12B-C15B-C11B	115.7(2)
C5B-C6B-C1B	122.09(17)	F11B-C15B-C11B	113.3(3)
F1B-C7B-F3B	106.7(2)	F10'-C15B-C11B	115.1(7)
F1B-C7B-F2B	107.7(2)	F10B-C15B-C11B	112.8(3)
F3B-C7B-F2B	105.2(2)	F11"-C15B-C11B	108.9(5)
F1B-C7B-C3B	112.1(2)	F12"-C15B-C11B	106.7(3)
F3B-C7B-C3B	114.12(18)	F12'-C15B-C11B	109.1(3)
F2B-C7B-C3B	110.5(2)	F8B-C16B-F7B	107.89(16)
F6B-C8B-F4B	107.3(2)	F8B-C16B-F9B	106.62(16)
F6B-C8B-F5B	104.6(2)	F7B-C16B-F9B	104.56(16)
F4B-C8B-F5B	106.9(2)	F8B-C16B-C13B	112.59(17)
F6B-C8B-C5B	112.81(17)	F7B-C16B-C13B	112.46(16)
F4B-C8B-C5B	112.8(2)	F9B-C16B-C13B	112.22(15)
F5B-C8B-C5B	112.01(19)	C18B-C17B-C22B	115.08(16)
C14B-C9B-C10B	115.47(16)	C18B-C17B-B1B	118.49(15)
C14B-C9B-B1B	122.95(15)	C22B-C17B-B1B	126.00(14)
C10B-C9B-B1B	121.32(15)	C19B-C18B-C17B	122.25(16)
C11B-C10B-C9B	122.89(17)	C20B-C19B-C18B	121.55(16)
C10B-C11B-C12B	120.60(17)	C20B-C19B-C23B	119.63(17)
C10B-C11B-C15B	120.46(17)	C18B-C19B-C23B	118.75(17)
C12B-C11B-C15B	118.94(18)	C21B-C20B-C19B	117.57(16)
C11B-C12B-C13B	117.69(17)	C20B-C21B-C22B	120.60(16)
C12B-C13B-C14B	121.49(16)	C20B-C21B-C24B	118.88(16)
C12B-C13B-C16B	120.71(17)	C22B-C21B-C24B	120.52(15)
C14B-C13B-C16B	117.77(17)	C17B-C22B-C21B	122.92(15)
C9B-C14B-C13B	121.85(16)	F15B-C23B-F14'	88.8(7)
F10"-C15B-F11'	123.8(6)	F15B-C23B-F14B	108.0(4)
F10"-C15B-F12B	74.5(7)	F14'-C23B-F14B	117.4(8)
F11'-C15B-F12B	67.2(6)	F15B-C23B-F13'	118.4(8)
F10"-C15B-F11B	125.0(6)	F14'-C23B-F13'	103.3(10)
F11'-C15B-F11B	41.7(6)	F14B-C23B-F13'	16.5(7)
F12B-C15B-F11B	106.1(4)	F15B-C23B-F13B	106.0(3)
F10"-C15B-F10'	53.5(8)	F14'-C23B-F13B	18.1(8)
F11'-C15B-F10'	114.2(9)	F14B-C23B-F13B	105.6(3)
F12B-C15B-F10'	118.2(7)	F13'-C23B-F13B	89.8(6)
F11B-C15B-F10'	83.2(6)	F15B-C23B-F15'	14.6(8)
F10"-C15B-F10B	35.9(6)	F14'-C23B-F15'	103.1(9)
F11'-C15B-F10B	125.6(6)	F14B-C23B-F15'	98.6(7)
F12B-C15B-F10B	106.8(5)	F13'-C23B-F15'	111.5(9)
F11B-C15B-F10B	100.8(3)	F13B-C23B-F15'	119.9(7)
F10'-C15B-F10B	18.6(6)	F15B-C23B-C19B	113.9(3)
F10"-C15B-F11"	113.9(8)	F14'-C23B-C19B	114.6(8)
F11'-C15B-F11"	64.1(8)	F14B-C23B-C19B	111.9(3)
F12B-C15B-F11"	124.9(5)	F13'-C23B-C19B	114.5(7)
F11B-C15B-F11"	22.6(4)	F13B-C23B-C19B	111.0(3)
F10'-C15B-F11"	64.2(7)	F15'-C23B-C19B	109.2(5)
F10B-C15B-F11"	82.7(5)	F18B-C24B-F16B	105.8(2)
F10"-C15B-F12"	111.9(7)	F18B-C24B-F17B	105.25(19)
F11'-C15B-F12"	35.0(6)	F16B-C24B-F17B	106.0(2)
F12B-C15B-F12"	38.8(4)	F18B-C24B-C21B	111.94(16)
F11B-C15B-F12"	76.5(4)	F16B-C24B-C21B	114.44(16)
F10'-C15B-F12"	137.9(7)	F17B-C24B-C21B	112.72(17)
F10B-C15B-F12"	137.5(5)	C26B-C25B-C30B	116.10(16)
F11"-C15B-F12"	99.0(5)	C26B-C25B-B1B	124.50(15)
F10"-C15B-F12'	44.9(6)	C30B-C25B-B1B	118.96(15)
F11'-C15B-F12'	99.4(6)	C25B-C26B-C27B	121.87(17)
F12B-C15B-F12'	33.6(4)	C28B-C27B-C26B	121.05(17)
F11B-C15B-F12'	132.7(4)	C28B-C27B-C31B	120.17(17)
F10'-C15B-F12'	97.1(7)	C26B-C27B-C31B	118.78(18)
F10B-C15B-F12'	80.6(4)	C27B-C28B-C29B	117.96(17)
F11"-C15B-F12'	141.9(6)	C28B-C29B-C30B	120.57(17)
F12"-C15B-F12'	72.1(5)	C28B-C29B-C32B	120.47(16)

C30B-C29B-C32B	118.96(16)	F21B-C31B-C27B	113.73(18)
C29B-C30B-C25B	122.43(16)	F23B-C32B-F22B	107.45(17)
F20B-C31B-F19B	106.4(3)	F23B-C32B-F24B	105.77(16)
F20B-C31B-F21B	104.5(2)	F22B-C32B-F24B	105.91(16)
F19B-C31B-F21B	106.2(2)	F23B-C32B-C29B	111.61(16)
F20B-C31B-C27B	112.1(2)	F22B-C32B-C29B	112.60(16)
F19B-C31B-C27B	113.2(2)	F24B-C32B-C29B	113.02(15)

Table 9. Torsion angles [°] for complex 79.

P1A-Au1A-C1A-C2A	122.5(5)	C18A-C17A-C22A-C23A	68.8(2)
Au1A-C1A-C2A-C4A	90.74(17)	C16A-C17A-C22A-C23A	-107.1(2)
Au1A-C1A-C2A-C3A	-98.42(18)	C18A-C17A-C22A-C24A	-54.5(3)
P1A-Au1A-C2A-C1A	-171.10(10)	C16A-C17A-C22A-C24A	129.6(2)
C1A-Au1A-C2A-C4A	-118.36(19)	C18A-C19A-C25A-C27A	40.6(3)
P1A-Au1A-C2A-C4A	70.54(17)	C20A-C19A-C25A-C27A	-142.9(2)
C1A-Au1A-C2A-C3A	116.5(2)	C18A-C19A-C25A-C26A	-84.5(2)
P1A-Au1A-C2A-C3A	-54.58(19)	C20A-C19A-C25A-C26A	92.0(2)
C1A-C2A-C4A-C9A	26.7(3)	C20A-C21A-C28A-C30A	47.1(2)
C3A-C2A-C4A-C9A	-144.4(2)	C16A-C21A-C28A-C30A	-136.7(2)
Au1A-C2A-C4A-C9A	96.55(19)	C20A-C21A-C28A-C29A	-77.4(2)
C1A-C2A-C4A-C5A	-153.46(19)	C16A-C21A-C28A-C29A	98.8(2)
C3A-C2A-C4A-C5A	35.4(3)	C15A-C10A-P1A-C35A	-115.92(18)
Au1A-C2A-C4A-C5A	-83.61(19)	C11A-C10A-P1A-C35A	65.45(19)
C9A-C4A-C5A-C6A	-2.3(3)	C15A-C10A-P1A-C31A	123.20(18)
C2A-C4A-C5A-C6A	177.8(2)	C11A-C10A-P1A-C31A	-55.43(19)
C4A-C5A-C6A-C7A	1.5(4)	C15A-C10A-P1A-Au1A	4.12(19)
C5A-C6A-C7A-C8A	0.4(4)	C11A-C10A-P1A-Au1A	-174.51(15)
C6A-C7A-C8A-C9A	-1.4(4)	C37A-C35A-P1A-C10A	71.13(18)
C7A-C8A-C9A-C4A	0.6(4)	C36A-C35A-P1A-C10A	-47.1(2)
C5A-C4A-C9A-C8A	1.3(3)	C38A-C35A-P1A-C10A	-172.82(17)
C2A-C4A-C9A-C8A	-178.9(2)	C37A-C35A-P1A-C31A	-170.56(16)
C15A-C10A-C11A-C12A	1.0(3)	C36A-C35A-P1A-C31A	71.2(2)
P1A-C10A-C11A-C12A	179.7(2)	C38A-C35A-P1A-C31A	-54.5(2)
C10A-C11A-C12A-C13A	0.3(4)	C37A-C35A-P1A-Au1A	-50.91(17)
C11A-C12A-C13A-C14A	-1.5(4)	C36A-C35A-P1A-Au1A	-169.16(17)
C12A-C13A-C14A-C15A	1.5(4)	C38A-C35A-P1A-Au1A	65.14(19)
C11A-C10A-C15A-C14A	-1.0(3)	C32A-C31A-P1A-C10A	-36.82(19)
P1A-C10A-C15A-C14A	-179.67(16)	C33A-C31A-P1A-C10A	84.7(2)
C11A-C10A-C15A-C16A	178.39(19)	C34A-C31A-P1A-C10A	-154.65(18)
P1A-C10A-C15A-C16A	-0.2(3)	C32A-C31A-P1A-C35A	-155.24(17)
C13A-C14A-C15A-C10A	-0.1(3)	C33A-C31A-P1A-C35A	-33.8(2)
C13A-C14A-C15A-C16A	-179.6(2)	C34A-C31A-P1A-C35A	86.9(2)
C10A-C15A-C16A-C21A	97.9(2)	C32A-C31A-P1A-Au1A	84.71(18)
C14A-C15A-C16A-C21A	-82.6(2)	C33A-C31A-P1A-Au1A	-153.81(18)
C10A-C15A-C16A-C17A	-93.9(2)	C34A-C31A-P1A-Au1A	-33.1(2)
C14A-C15A-C16A-C17A	85.5(2)	C1A-Au1A-P1A-C10A	91.7(6)
C21A-C16A-C17A-C18A	-1.3(3)	C2A-Au1A-P1A-C10A	-153.31(12)
C15A-C16A-C17A-C18A	-169.53(18)	C1A-Au1A-P1A-C35A	-148.9(6)
C21A-C16A-C17A-C22A	174.54(18)	C2A-Au1A-P1A-C35A	-33.87(13)
C15A-C16A-C17A-C22A	6.3(3)	C1A-Au1A-P1A-C31A	-27.1(6)
C16A-C17A-C18A-C19A	0.0(3)	C2A-Au1A-P1A-C31A	87.94(14)
C22A-C17A-C18A-C19A	-176.05(19)	P1'-Au1'-C1'-C2'	110.6(15)
C17A-C18A-C19A-C20A	0.0(3)	Au1'-C1'-C2'-C4'	90.5(5)
C17A-C18A-C19A-C25A	176.61(19)	Au1'-C1'-C2'-C3'	-98.7(5)
C18A-C19A-C20A-C21A	1.4(3)	P1'-Au1'-C2'-C1'	-149.7(10)
C25A-C19A-C20A-C21A	-175.24(19)	C1'-Au1'-C2'-C4'	-118.3(5)
C19A-C20A-C21A-C16A	-2.8(3)	P1'-Au1'-C2'-C4'	92.1(10)
C19A-C20A-C21A-C28A	173.48(18)	C1'-Au1'-C2'-C3'	116.7(5)
C17A-C16A-C21A-C20A	2.7(3)	P1'-Au1'-C2'-C3'	-32.9(11)
C15A-C16A-C21A-C20A	170.88(17)	C1'-C2'-C4'-C9'	11(2)
C17A-C16A-C21A-C28A	-173.49(18)	C3'-C2'-C4'-C9'	-160(2)
C15A-C16A-C21A-C28A	-5.3(3)	Au1'-C2'-C4'-C9'	81(2)

C1'-C2'-C4'-C5' -149(2)
C3'-C2'-C4'-C5' 40(2)
Au1'-C2'-C4'-C5' -79(2)
C9'-C4'-C5'-C6' -2(4)
C2'-C4'-C5'-C6' 158(3)
C4'-C5'-C6'-C7' 13(5)
C5'-C6'-C7'-C8' -12(6)
C6'-C7'-C8'-C9' 0(7)
C7'-C8'-C9'-C4' 11(7)
C5'-C4'-C9'-C8' -10(5)
C2'-C4'-C9'-C8' -170(3)
C15'-C10'-C11'-C12' -4(5)
P1'-C10'-C11'-C12' 171(3)
C10'-C11'-C12'-C13' 15(5)
C11'-C12'-C13'-C14' -11(7)
C12'-C13'-C14'-C15' -3(8)
C11'-C10'-C15'-C14' -10(4)
P1'-C10'-C15'-C14' 175(3)
C11'-C10'-C15'-C16' -179(3)
P1'-C10'-C15'-C16' 6(3)
C13'-C14'-C15'-C10' 13(6)
C13'-C14'-C15'-C16' -176(4)
C10'-C15'-C16'-C21' 88(3)
C14'-C15'-C16'-C21' -82(4)
C10'-C15'-C16'-C17' -109(3)
C14'-C15'-C16'-C17' 81(4)
C21'-C16'-C17'-C18' -8(5)
C15'-C16'-C17'-C18' -171(4)
C21'-C16'-C17'-C22' 174(3)
C15'-C16'-C17'-C22' 11(4)
C16'-C17'-C18'-C19' 0(7)
C22'-C17'-C18'-C19' 178(4)
C17'-C18'-C19'-C20' 9(7)
C17'-C18'-C19'-C25' -175(4)
C18'-C19'-C20'-C21' -10(6)
C25'-C19'-C20'-C21' 174(4)
C19'-C20'-C21'-C16' 2(6)
C19'-C20'-C21'-C28' 176(4)
C17'-C16'-C21'-C20' 7(4)
C15'-C16'-C21'-C20' 170(3)
C17'-C16'-C21'-C28' -167(3)
C15'-C16'-C21'-C28' -4(3)
C18'-C17'-C22'-C23' 71(4)
C16'-C17'-C22'-C23' -110(4)
C18'-C17'-C22'-C24' -52(4)
C16'-C17'-C22'-C24' 126(4)
C18'-C19'-C25'-C27' 38(4)
C20'-C19'-C25'-C27' -147(4)
C18'-C19'-C25'-C26' -88(4)
C20'-C19'-C25'-C26' 88(4)
C20'-C21'-C28'-C30' 52(4)
C16'-C21'-C28'-C30' -134(3)
C20'-C21'-C28'-C29' -72(4)
C16'-C21'-C28'-C29' 102(3)
C15'-C10'-P1'-C35' -130.7(19)
C11'-C10'-P1'-C35' 54(3)
C15'-C10'-P1'-C31' 107.9(19)
C11'-C10'-P1'-C31' -67(3)
C15'-C10'-P1'-Au1' -10.5(19)
C11'-C10'-P1'-Au1' 174(3)
C37'-C35'-P1'-C10' 47.2(13)
C38'-C35'-P1'-C10' 163.2(13)
C36'-C35'-P1'-C10' -71.0(13)
C37'-C35'-P1'-C31' 165.7(13)
C38'-C35'-P1'-C31' -78.2(13)
C36'-C35'-P1'-C31' 47.6(13)
C37'-C35'-P1'-Au1' -75.1(12)
C38'-C35'-P1'-Au1' 41.0(12)
C36'-C35'-P1'-Au1' 166.7(13)
C32'-C31'-P1'-C10' -71.6(12)
C33'-C31'-P1'-C10' 49.9(12)
C34'-C31'-P1'-C10' 170.8(12)
C32'-C31'-P1'-C35' 169.8(12)
C33'-C31'-P1'-C35' -68.8(12)
C34'-C31'-P1'-C35' 52.1(12)
C32'-C31'-P1'-Au1' 49.8(12)
C33'-C31'-P1'-Au1' 171.3(12)
C34'-C31'-P1'-Au1' -67.8(12)
C1'-Au1'-P1'-C10' 93.9(19)
C2'-Au1'-P1'-C10' 179.0(10)
C1'-Au1'-P1'-C35' -146.5(19)
C2'-Au1'-P1'-C35' -61.4(10)
C1'-Au1'-P1'-C31' -24.5(19)
C2'-Au1'-P1'-C31' 60.5(10)
C9B-B1B-C1B-C6B 90.35(18)
C25B-B1B-C1B-C6B -30.6(2)
C17B-B1B-C1B-C6B -146.72(16)
C9B-B1B-C1B-C2B -82.32(19)
C25B-B1B-C1B-C2B 156.69(16)
C17B-B1B-C1B-C2B 40.6(2)
C6B-C1B-C2B-C3B 1.9(3)
B1B-C1B-C2B-C3B 174.89(17)
C1B-C2B-C3B-C4B -2.3(3)
C1B-C2B-C3B-C7B 173.4(2)
C2B-C3B-C4B-C5B 1.0(3)
C7B-C3B-C4B-C5B -174.9(2)
C3B-C4B-C5B-C6B 0.6(3)
C3B-C4B-C5B-C8B -178.60(19)
C4B-C5B-C6B-C1B -0.9(3)
C8B-C5B-C6B-C1B 178.28(18)
C2B-C1B-C6B-C5B -0.3(3)
B1B-C1B-C6B-C5B -173.49(17)
C2B-C3B-C7B-F1B 127.2(2)
C4B-C3B-C7B-F1B -56.9(3)
C2B-C3B-C7B-F3B 5.7(3)
C4B-C3B-C7B-F3B -178.4(2)
C2B-C3B-C7B-F2B -112.7(3)
C4B-C3B-C7B-F2B 63.2(3)
C4B-C5B-C8B-F6B -141.4(2)
C6B-C5B-C8B-F6B 39.4(3)
C4B-C5B-C8B-F4B -19.7(3)
C6B-C5B-C8B-F4B 161.1(2)
C4B-C5B-C8B-F5B 101.0(2)
C6B-C5B-C8B-F5B -78.3(2)
C1B-B1B-C9B-C14B 99.02(18)
C25B-B1B-C9B-C14B -140.80(16)
C17B-B1B-C9B-C14B -25.6(2)
C1B-B1B-C9B-C10B -74.85(19)
C25B-B1B-C9B-C10B 45.3(2)
C17B-B1B-C9B-C10B 160.48(15)
C14B-C9B-C10B-C11B 1.2(3)
B1B-C9B-C10B-C11B 175.50(16)
C9B-C10B-C11B-C12B -0.3(3)
C9B-C10B-C11B-C15B -179.88(18)
C10B-C11B-C12B-C13B -0.9(3)
C15B-C11B-C12B-C13B 178.64(18)
C11B-C12B-C13B-C14B 1.3(3)
C11B-C12B-C13B-C16B -176.67(16)

C10B-C9B-C14B-C13B -0.9(2)	C18B-C19B-C23B-F15B 177.7(3)
B1B-C9B-C14B-C13B -175.06(15)	C20B-C19B-C23B-F14' 94.9(8)
C12B-C13B-C14B-C9B -0.4(3)	C18B-C19B-C23B-F14' -82.1(8)
C16B-C13B-C14B-C9B 177.64(16)	C20B-C19B-C23B-F14B -128.3(3)
C10B-C11B-C15B-F10" 77.4(8)	C18B-C19B-C23B-F14B 54.8(3)
C12B-C11B-C15B-F10" -102.1(8)	C20B-C19B-C23B-F13' -146.0(7)
C10B-C11B-C15B-F11' -83.3(9)	C18B-C19B-C23B-F13' 37.0(7)
C12B-C11B-C15B-F11' 97.2(9)	C20B-C19B-C23B-F13B 114.1(3)
C10B-C11B-C15B-F12B -6.6(6)	C18B-C19B-C23B-F13B -62.8(3)
C12B-C11B-C15B-F12B 173.8(5)	C20B-C19B-C23B-F15' -20.2(7)
C10B-C11B-C15B-F11B -129.5(3)	C18B-C19B-C23B-F15' 162.8(7)
C12B-C11B-C15B-F11B 50.9(4)	C20B-C21B-C24B-F18B 137.2(2)
C10B-C11B-C15B-F10' 137.0(6)	C22B-C21B-C24B-F18B -43.4(3)
C12B-C11B-C15B-F10' -42.6(7)	C20B-C21B-C24B-F16B 16.9(3)
C10B-C11B-C15B-F10B 116.8(4)	C22B-C21B-C24B-F16B -163.8(2)
C12B-C11B-C15B-F10B -62.8(4)	C20B-C21B-C24B-F17B -104.3(2)
C10B-C11B-C15B-F11" -153.3(5)	C22B-C21B-C24B-F17B 75.0(2)
C12B-C11B-C15B-F11" 27.1(5)	C1B-B1B-C25B-C26B 139.19(17)
C10B-C11B-C15B-F12" -47.3(5)	C9B-B1B-C25B-C26B 24.0(2)
C12B-C11B-C15B-F12" 133.1(4)	C17B-B1B-C25B-C26B -97.15(19)
C10B-C11B-C15B-F12' 29.1(5)	C1B-B1B-C25B-C30B -48.8(2)
C12B-C11B-C15B-F12' -150.4(4)	C9B-B1B-C25B-C30B -163.97(14)
C12B-C13B-C16B-F8B -16.7(2)	C17B-B1B-C25B-C30B 74.90(18)
C14B-C13B-C16B-F8B 165.31(16)	C30B-C25B-C26B-C27B 1.3(3)
C12B-C13B-C16B-F7B -138.81(18)	B1B-C25B-C26B-C27B 173.58(17)
C14B-C13B-C16B-F7B 43.2(2)	C25B-C26B-C27B-C28B -1.0(3)
C12B-C13B-C16B-F9B 103.6(2)	C25B-C26B-C27B-C31B 179.62(19)
C14B-C13B-C16B-F9B -74.4(2)	C26B-C27B-C28B-C29B -0.1(3)
C1B-B1B-C17B-C18B -169.22(15)	C31B-C27B-C28B-C29B 179.30(19)
C9B-B1B-C17B-C18B -51.5(2)	C27B-C28B-C29B-C30B 0.7(3)
C25B-B1B-C17B-C18B 69.66(18)	C27B-C28B-C29B-C32B -178.92(17)
C1B-B1B-C17B-C22B 18.7(2)	C28B-C29B-C30B-C25B -0.3(3)
C9B-B1B-C17B-C22B 136.45(17)	C32B-C29B-C30B-C25B 179.32(16)
C25B-B1B-C17B-C22B -102.38(18)	C26B-C25B-C30B-C29B -0.7(2)
C22B-C17B-C18B-C19B 0.1(2)	B1B-C25B-C30B-C29B -173.39(15)
B1B-C17B-C18B-C19B -172.79(16)	C28B-C27B-C31B-F20B -113.1(3)
C17B-C18B-C19B-C20B -1.5(3)	C26B-C27B-C31B-F20B 66.3(3)
C17B-C18B-C19B-C23B 175.43(17)	C28B-C27B-C31B-F19B 126.5(3)
C18B-C19B-C20B-C21B 1.3(3)	C26B-C27B-C31B-F19B -54.1(3)
C23B-C19B-C20B-C21B -175.53(17)	C28B-C27B-C31B-F21B 5.2(3)
C19B-C20B-C21B-C22B 0.1(3)	C26B-C27B-C31B-F21B -175.4(2)
C19B-C20B-C21B-C24B 179.39(17)	C28B-C29B-C32B-F23B -95.3(2)
C18B-C17B-C22B-C21B 1.3(2)	C30B-C29B-C32B-F23B 85.0(2)
B1B-C17B-C22B-C21B 173.60(16)	C28B-C29B-C32B-F22B 143.70(18)
C20B-C21B-C22B-C17B -1.5(3)	C30B-C29B-C32B-F22B -36.0(2)
C24B-C21B-C22B-C17B 179.23(17)	C28B-C29B-C32B-F24B 23.7(3)
C20B-C19B-C23B-F15B -5.4(4)	C30B-C29B-C32B-F24B -155.94(16)

μ-Chloro bis-{[(2′,4′,6′-triisopropyl-1,1′-biphenyl-2-yl)di-tert-butylphosphine] gold(I)} tetrakis[3,5-bis(trifluoromethyl)phenyl] borate (85)

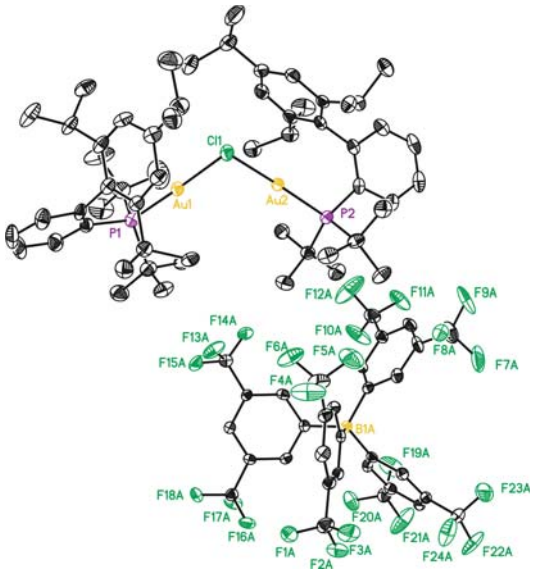

Table 10. Crystal data and structure refinement for 85.

Empirical formula	C91.30 H105 Au2 B Cl1.60 F24 P2
Formula weight	2181.76
Temperature	100(2) K
Wavelength	0.71073 Å
Crystal system	Triclinic
Space group	P-1
Unit cell dimensions	a = 12.6200(10) Å α= 75.106(3) °. b = 19.7026(15) Å β = 80.481(3) °. c = 19.7379(16) Å γ = 77.609(3) °.
Volume	4600.7(6) $Å^3$
Z	2
Density (calculated)	1.575 Mg/m^3
Absorption coefficient	3.359 mm^{-1}
F(000)	2178
Crystal size	0.20 x 0.10 x 0.06 mm^3
Theta range for data collection	1.66 to 30.41 °.
Index ranges	-17 <=h<=15 -28 <=k<=25 -27 <=l<=28
Reflections collected	59215
Independent reflections	24039 [R(int) = 0.0367]
Completeness to theta =30.41 °	86.4%
Absorption correction	Empirical
Max. and min. transmission	0.8239 and 0.5531
Refinement method	Full-matrix least-squares on F^2
Data / restraints / parameters	24039 / 343 / 1337
Goodness-of-fit on F^2	1.051

Final R indices [I>2sigma(I)]	R1 = 0.0334
	wR2 = 0.0640
R indices (all data)	R1 = 0.0557
	wR2 = 0.0707
Largest diff. peak and hole	1.043 and -0.929 e.Å^{-3}

Table 11. Bond lengths [Å] and angles [°] for 85.

Bond lengths:			
Au1-P1	2.2509(9)	C37-C42	1.523(4)
Au1-Cl1	2.3463(8)	C38-C39	1.384(5)
Au2-P2	2.2438(8)	C39-C40	1.406(5)
Au2-Cl1	2.3348(8)	C39-C45	1.517(5)
P1-C1	1.823(3)	C40-C41	1.390(5)
P1-C22	1.878(4)	C41-C48	1.527(5)
P1-C26	1.885(4)	C42-C43	1.532(4)
P2-C30	1.831(3)	C42-C44	1.539(4)
P2-C51	1.879(3)	C45-C46	1.523(6)
P2-C55	1.887(3)	C45-C47	1.527(6)
C1-C2	1.401(5)	C48-C50	1.529(5)
C1-C6	1.418(5)	C48-C49	1.537(5)
C2-C3	1.380(5)	C51-C52	1.527(5)
C3-C4	1.371(6)	C51-C53	1.530(5)
C4-C5	1.379(6)	C51-C54	1.537(5)
C5-C6	1.397(5)	C55-C58	1.536(5)
C6-C7	1.511(5)	C55-C56	1.539(5)
C7-C8	1.407(5)	C55-C57	1.542(5)
C7-C12	1.416(4)	B1A-C25A	1.632(4)
C8-C9	1.388(5)	B1A-C17A	1.640(5)
C8-C13	1.524(5)	B1A-C9A	1.641(5)
C9-C10	1.385(5)	B1A-C1A	1.651(5)
C10-C11	1.390(5)	C1A-C6A	1.393(4)
C10-C16	1.516(5)	C1A-C2A	1.402(4)
C11-C12	1.388(5)	C2A-C3A	1.389(4)
C12-C19	1.517(5)	C3A-C4A	1.387(4)
C13-C14	1.532(5)	C3A-C7A	1.505(5)
C13-C15	1.542(5)	C4A-C5A	1.381(5)
C16-C18	1.502(5)	C5A-C6A	1.399(4)
C16-C17	1.523(5)	C5A-C8A	1.493(5)
C16-C17'	1.538(6)	C7A-F3'	1.299(8)
C16-C18'	1.552(6)	C7A-F1A	1.306(4)
C19-C20	1.532(5)	C7A-F2'	1.312(9)
C19-C21	1.542(5)	C7A-F2A	1.326(5)
C22-C25'	1.479(14)	C7A-F3A	1.371(4)
C22-C23	1.509(6)	C7A-F1'	1.434(8)
C22-C24	1.518(6)	C8A-F4A	1.330(4)
C22-C25	1.573(6)	C8A-F5A	1.333(4)
C22-C24'	1.583(14)	C8A-F6A	1.342(4)
C22-C23'	1.666(13)	C9A-C14A	1.393(4)
C26-C27	1.519(5)	C9A-C10A	1.398(4)
C26-C29	1.526(5)	C10A-C11A	1.390(5)
C26-C28	1.539(6)	C11A-C12A	1.381(5)
C30-C31	1.405(4)	C11A-C15A	1.505(5)
C30-C35	1.414(5)	C12A-C13A	1.387(5)
C31-C32	1.380(5)	C13A-C14A	1.390(4)
C32-C33	1.378(5)	C13A-C16A	1.495(5)
C33-C34	1.377(5)	C15A-F7'	1.310(5)
C34-C35	1.396(5)	C15A-F9A	1.312(5)
C35-C36	1.512(5)	C15A-F8'	1.341(5)
C36-C37	1.401(4)	C15A-F8A	1.342(5)
C36-C41	1.408(4)	C15A-F7A	1.371(5)
C37-C38	1.393(5)	C15A-F9'	1.375(5)
		C16A-F10A	1.319(4)

C16A-F12A	1.323(4)	C3-C4-C5	120.0(4)
C16A-F11A	1.330(4)	C4-C5-C6	122.0(4)
C17A-C18A	1.393(4)	C5-C6-C1	118.1(3)
C17A-C22A	1.408(4)	C5-C6-C7	114.0(3)
C18A-C19A	1.397(4)	C1-C6-C7	127.7(3)
C19A-C20A	1.384(4)	C8-C7-C12	119.5(3)
C19A-C23A	1.486(4)	C8-C7-C6	117.8(3)
C20A-C21A	1.383(4)	C12-C7-C6	121.8(3)
C21A-C22A	1.387(4)	C9-C8-C7	118.9(3)
C21A-C24A	1.499(4)	C9-C8-C13	119.1(3)
C23A-F14A	1.329(4)	C7-C8-C13	122.0(3)
C23A-F15A	1.336(4)	C10-C9-C8	123.0(3)
C23A-F13A	1.349(4)	C9-C10-C11	117.1(3)
C24A-F16A	1.335(4)	C9-C10-C16	123.0(3)
C24A-F18A	1.341(4)	C11-C10-C16	119.9(3)
C24A-F17A	1.341(3)	C12-C11-C10	122.8(3)
C25A-C30A	1.393(4)	C11-C12-C7	118.7(3)
C25A-C26A	1.409(4)	C11-C12-C19	118.9(3)
C26A-C27A	1.392(4)	C7-C12-C19	122.4(3)
C27A-C28A	1.380(4)	C8-C13-C14	112.5(3)
C27A-C33A	1.490(4)	C8-C13-C15	110.7(3)
C28A-C29A	1.384(4)	C14-C13-C15	109.3(3)
C29A-C30A	1.396(4)	C18-C16-C10	112.1(4)
C29A-C32A	1.485(4)	C18-C16-C17	111.4(4)
C32A-F23A	1.298(4)	C10-C16-C17	108.8(3)
C32A-F23'	1.298(7)	C18-C16-C17'	69.2(5)
C32A-F24A	1.317(4)	C10-C16-C17'	116.3(5)
C32A-F22A	1.332(4)	C17-C16-C17'	43.6(5)
C32A-F24'	1.334(7)	C18-C16-C18'	44.5(4)
C32A-F22'	1.365(6)	C10-C16-C18'	115.2(5)
C33A-F21'	1.314(5)	C17-C16-C18'	135.4(5)
C33A-F21A	1.315(4)	C17'-C16-C18'	106.4(5)
C33A-F20'	1.327(5)	C12-C19-C20	111.3(3)
C33A-F20A	1.333(4)	C12-C19-C21	112.4(3)
C33A-F19A	1.340(4)	C20-C19-C21	109.5(3)
C33A-F19'	1.366(5)	C25'-C22-C23	74.2(7)
C1S-Cl1S	1.775(9)	C25'-C22-C24	125.5(8)
C1S-Cl2S	1.776(9)	C23-C22-C24	110.2(4)
C1R-C2R	1.516(5)	C25'-C22-C25	33.7(7)
C2R-C3R	1.521(5)	C23-C22-C25	107.7(4)
C3R-C4R	1.521(5)	C24-C22-C25	108.6(4)
C4R-C5R	1.516(5)	C25'-C22-C24'	109.7(8)
		C23-C22-C24'	124.7(8)
Angles:		C24-C22-C24'	22.4(6)
P1-Au1-Cl1	176.82(3)	C25-C22-C24'	87.1(7)
P2-Au2-Cl1	173.03(3)	C25'-C22-C23'	104.4(8)
Au2-Cl1-Au1	94.82(3)	C23-C22-C23'	33.7(5)
C1-P1-C22	107.52(17)	C24-C22-C23'	80.6(6)
C1-P1-C26	108.15(16)	C25-C22-C23'	134.7(6)
C22-P1-C26	112.01(16)	C24'-C22-C23'	100.2(8)
C1-P1-Au1	111.04(11)	C25'-C22-P1	113.1(7)
C22-P1-Au1	110.77(11)	C23-C22-P1	108.1(3)
C26-P1-Au1	107.35(12)	C24-C22-P1	116.0(3)
C30-P2-C51	107.71(14)	C25-C22-P1	105.9(3)
C30-P2-C55	107.00(15)	C24'-C22-P1	118.6(8)
C51-P2-C55	112.27(15)	C23'-C22-P1	109.2(5)
C30-P2-Au2	111.92(11)	C27-C26-C29	109.2(4)
C51-P2-Au2	110.60(11)	C27-C26-C28	108.7(3)
C55-P2-Au2	107.34(11)	C29-C26-C28	105.3(4)
C2-C1-C6	118.3(3)	C27-C26-P1	116.9(3)
C2-C1-P1	117.7(3)	C29-C26-P1	106.4(2)
C6-C1-P1	124.1(3)	C28-C26-P1	109.7(3)
C3-C2-C1	122.0(4)	C31-C30-C35	118.7(3)
C4-C3-C2	119.5(4)	C31-C30-P2	116.5(3)

C35-C30-P2	124.7(2)	F3'-C7A-F2A	121.9(6)
C32-C31-C30	122.0(3)	F1A-C7A-F2A	109.9(4)
C33-C32-C31	119.2(3)	F2'-C7A-F2A	21.1(5)
C34-C33-C32	119.7(3)	F3'-C7A-F3A	33.6(4)
C33-C34-C35	122.7(4)	F1A-C7A-F3A	105.5(4)
C34-C35-C30	117.6(3)	F2'-C7A-F3A	86.8(5)
C34-C35-C36	114.8(3)	F2A-C7A-F3A	105.7(4)
C30-C35-C36	127.6(3)	F3'-C7A-F1'	102.1(6)
C37-C36-C41	120.0(3)	F1A-C7A-F1'	33.7(3)
C37-C36-C35	119.3(3)	F2'-C7A-F1'	100.8(6)
C41-C36-C35	120.0(3)	F2A-C7A-F1'	81.2(5)
C38-C37-C36	118.9(3)	F3A-C7A-F1'	132.0(5)
C38-C37-C42	118.9(3)	F3'-C7A-C3A	118.8(5)
C36-C37-C42	122.0(3)	F1A-C7A-C3A	112.1(3)
C39-C38-C37	122.7(3)	F2'-C7A-C3A	112.9(6)
C38-C39-C40	117.3(3)	F2A-C7A-C3A	113.4(4)
C38-C39-C45	122.9(3)	F3A-C7A-C3A	109.7(3)
C40-C39-C45	119.8(3)	F1'-C7A-C3A	110.4(4)
C41-C40-C39	122.2(3)	F4A-C8A-F5A	107.4(3)
C40-C41-C36	118.9(3)	F4A-C8A-F6A	105.1(3)
C40-C41-C48	119.3(3)	F5A-C8A-F6A	104.6(3)
C36-C41-C48	121.7(3)	F4A-C8A-C5A	114.1(3)
C37-C42-C43	113.0(3)	F5A-C8A-C5A	112.5(3)
C37-C42-C44	109.5(3)	F6A-C8A-C5A	112.4(3)
C43-C42-C44	110.0(3)	C14A-C9A-C10A	115.6(3)
C39-C45-C46	113.8(3)	C14A-C9A-B1A	122.2(3)
C39-C45-C47	110.8(3)	C10A-C9A-B1A	121.8(3)
C46-C45-C47	109.6(4)	C11A-C10A-C9A	122.0(3)
C41-C48-C50	113.1(3)	C12A-C11A-C10A	121.1(3)
C41-C48-C49	110.6(3)	C12A-C11A-C15A	119.6(3)
C50-C48-C49	109.3(3)	C10A-C11A-C15A	119.2(3)
C52-C51-C53	107.6(3)	C11A-C12A-C13A	118.2(3)
C52-C51-C54	108.9(3)	C12A-C13A-C14A	120.2(3)
C53-C51-C54	108.9(3)	C12A-C13A-C16A	119.3(3)
C52-C51-P2	106.7(2)	C14A-C13A-C16A	120.5(3)
C53-C51-P2	116.2(2)	C13A-C14A-C9A	122.9(3)
C54-C51-P2	108.3(2)	F7'-C15A-F9A	79.8(4)
C58-C55-C56	108.4(3)	F7'-C15A-F8'	107.7(6)
C58-C55-C57	106.9(3)	F9A-C15A-F8'	116.2(8)
C56-C55-C57	108.5(3)	F7'-C15A-F8A	119.8(7)
C58-C55-P2	107.6(2)	F9A-C15A-F8A	108.3(6)
C56-C55-P2	115.7(2)	F8'-C15A-F8A	14.7(7)
C57-C55-P2	109.4(2)	F7'-C15A-F7A	26.8(4)
C25A-B1A-C17A	112.8(2)	F9A-C15A-F7A	105.4(5)
C25A-B1A-C9A	104.5(2)	F8'-C15A-F7A	89.2(6)
C17A-B1A-C9A	112.8(3)	F8A-C15A-F7A	103.4(5)
C25A-B1A-C1A	111.9(3)	F7'-C15A-F9'	106.0(4)
C17A-B1A-C1A	103.0(2)	F9A-C15A-F9'	26.2(4)
C9A-B1A-C1A	112.1(2)	F8'-C15A-F9'	105.6(5)
C6A-C1A-C2A	115.6(3)	F8A-C15A-F9'	93.4(6)
C6A-C1A-B1A	121.7(3)	F7A-C15A-F9'	131.0(5)
C2A-C1A-B1A	122.3(3)	F7'-C15A-C11A	115.7(4)
C3A-C2A-C1A	122.1(3)	F9A-C15A-C11A	118.5(5)
C4A-C3A-C2A	121.2(3)	F8'-C15A-C11A	113.8(6)
C4A-C3A-C7A	117.8(3)	F8A-C15A-C11A	111.3(6)
C2A-C3A-C7A	121.0(3)	F7A-C15A-C11A	108.6(4)
C5A-C4A-C3A	117.9(3)	F9'-C15A-C11A	107.2(4)
C4A-C5A-C6A	120.8(3)	F10A-C16A-F12A	106.3(4)
C4A-C5A-C8A	120.2(3)	F10A-C16A-F11A	105.7(3)
C6A-C5A-C8A	119.1(3)	F12A-C16A-F11A	105.2(3)
C1A-C6A-C5A	122.4(3)	F10A-C16A-C13A	113.6(3)
F3'-C7A-F1A	72.2(5)	F12A-C16A-C13A	112.4(3)
F3'-C7A-F2'	109.7(7)	F11A-C16A-C13A	113.0(3)
F1A-C7A-F2'	125.3(6)	C18A-C17A-C22A	115.5(3)

C18A-C17A-B1A	123.2(3)	F23A-C32A-F24'	44.3(4)
C22A-C17A-B1A	120.6(3)	F23'-C32A-F24'	104.8(5)
C17A-C18A-C19A	122.4(3)	F24A-C32A-F24'	131.9(4)
C20A-C19A-C18A	120.5(3)	F22A-C32A-F24'	64.8(4)
C20A-C19A-C23A	120.2(3)	F23A-C32A-F22'	60.6(4)
C18A-C19A-C23A	119.2(3)	F23'-C32A-F22'	104.3(5)
C21A-C20A-C19A	118.4(3)	F24A-C32A-F22'	50.8(4)
C20A-C21A-C22A	120.8(3)	F22A-C32A-F22'	130.7(4)
C20A-C21A-C24A	119.7(3)	F24'-C32A-F22'	99.2(5)
C22A-C21A-C24A	119.5(3)	F23A-C32A-C29A	111.8(3)
C21A-C22A-C17A	122.3(3)	F23'-C32A-C29A	115.5(4)
F14A-C23A-F15A	106.7(3)	F24A-C32A-C29A	112.0(3)
F14A-C23A-F13A	105.3(3)	F22A-C32A-C29A	113.1(3)
F15A-C23A-F13A	105.6(3)	F24'-C32A-C29A	115.3(4)
F14A-C23A-C19A	113.3(3)	F22'-C32A-C29A	115.7(3)
F15A-C23A-C19A	113.6(3)	F21'-C33A-F21A	122.6(6)
F13A-C23A-C19A	111.7(3)	F21'-C33A-F20'	108.3(6)
F16A-C24A-F18A	106.6(3)	F21A-C33A-F20'	68.4(5)
F16A-C24A-F17A	106.7(3)	F21'-C33A-F20A	31.0(4)
F18A-C24A-F17A	106.2(3)	F21A-C33A-F20A	106.4(4)
F16A-C24A-C21A	112.5(3)	F20'-C33A-F20A	130.5(5)
F18A-C24A-C21A	111.9(3)	F21'-C33A-F19A	73.3(5)
F17A-C24A-C21A	112.4(3)	F21A-C33A-F19A	106.5(4)
C30A-C25A-C26A	115.3(3)	F20'-C33A-F19A	42.0(4)
C30A-C25A-B1A	121.4(3)	F20A-C33A-F19A	103.2(3)
C26A-C25A-B1A	123.1(3)	F21'-C33A-F19'	105.7(6)
C27A-C26A-C25A	122.3(3)	F21A-C33A-F19'	34.0(4)
C28A-C27A-C26A	120.8(3)	F20'-C33A-F19'	101.6(5)
C28A-C27A-C33A	119.6(3)	F20A-C33A-F19'	79.4(5)
C26A-C27A-C33A	119.6(3)	F19A-C33A-F19'	133.9(5)
C27A-C28A-C29A	118.4(3)	F21'-C33A-C27A	117.3(5)
C28A-C29A-C30A	120.6(3)	F21A-C33A-C27A	115.3(3)
C28A-C29A-C32A	120.3(3)	F20'-C33A-C27A	113.7(5)
C30A-C29A-C32A	119.0(3)	F20A-C33A-C27A	112.5(3)
C25A-C30A-C29A	122.6(3)	F19A-C33A-C27A	112.0(3)
F23A-C32A-F23'	131.9(5)	F19'-C33A-C27A	108.9(5)
F23A-C32A-F24A	108.9(4)	Cl1S-C1S-Cl2S	110.1(8)
F23'-C32A-F24A	60.3(4)	C1R-C2R-C3R	110.9(7)
F23A-C32A-F22A	106.6(4)	C2R-C3R-C4R	110.4(7)
F23'-C32A-F22A	46.0(4)	C5R-C4R-C3R	110.4(8)
F24A-C32A-F22A	104.1(3)		

Table 12. Torsion angles [°] for 85.

P2-Au2-Cl1-Au1 -108.5(2)	C4-C5-C6-C1 -3.8(6)
P1-Au1-Cl1-Au2 -86.7(5)	C4-C5-C6-C7 170.7(4)
Cl1-Au1-P1-C1 -122.1(5)	C2-C1-C6-C5 3.3(5)
Cl1-Au1-P1-C22 118.5(5)	P1-C1-C6-C5 -177.9(3)
Cl1-Au1-P1-C26 -4.1(6)	C2-C1-C6-C7 -170.3(3)
Cl1-Au2-P2-C30 -127.8(3)	P1-C1-C6-C7 8.6(5)
Cl1-Au2-P2-C51 112.1(3)	C5-C6-C7-C8 -77.5(4)
Cl1-Au2-P2-C55 -10.7(3)	C1-C6-C7-C8 96.3(4)
C22-P1-C1-C2 -61.0(3)	C5-C6-C7-C12 91.8(4)
C26-P1-C1-C2 60.1(3)	C1-C6-C7-C12 -94.4(4)
Au1-P1-C1-C2 177.7(2)	C12-C7-C8-C9 2.0(5)
C22-P1-C1-C6 120.1(3)	C6-C7-C8-C9 171.6(3)
C26-P1-C1-C6 -118.7(3)	C12-C7-C8-C13 -176.7(3)
Au1-P1-C1-C6 -1.2(3)	C6-C7-C8-C13 -7.2(5)
C6-C1-C2-C3 -0.4(6)	C7-C8-C9-C10 -0.7(5)
P1-C1-C2-C3 -179.3(3)	C13-C8-C9-C10 178.1(3)
C1-C2-C3-C4 -2.2(6)	C8-C9-C10-C11 -0.9(5)
C2-C3-C4-C5 1.8(7)	C8-C9-C10-C16 178.5(3)
C3-C4-C5-C6 1.2(7)	C9-C10-C11-C12 1.2(5)

C16-C10-C11-C12 -178.2(3)	P2-C30-C35-C34 175.5(2)
C10-C11-C12-C7 0.0(5)	C31-C30-C35-C36 -178.3(3)
C10-C11-C12-C19 -178.6(3)	P2-C30-C35-C36 -2.3(5)
C8-C7-C12-C11 -1.7(5)	C34-C35-C36-C37 -83.1(4)
C6-C7-C12-C11 -170.8(3)	C30-C35-C36-C37 94.8(4)
C8-C7-C12-C19 176.9(3)	C34-C35-C36-C41 87.3(4)
C6-C7-C12-C19 7.8(5)	C30-C35-C36-C41 -94.9(4)
C9-C8-C13-C14 44.9(4)	C41-C36-C37-C38 3.5(5)
C7-C8-C13-C14 -136.4(3)	C35-C36-C37-C38 173.9(3)
C9-C8-C13-C15 -77.6(4)	C41-C36-C37-C42 -172.1(3)
C7-C8-C13-C15 101.1(4)	C35-C36-C37-C42 -1.7(5)
C9-C10-C16-C18 -3.1(6)	C36-C37-C38-C39 -0.8(5)
C11-C10-C16-C18 176.4(4)	C42-C37-C38-C39 174.9(3)
C9-C10-C16-C17 120.6(4)	C37-C38-C39-C40 -1.9(5)
C11-C10-C16-C17 -60.0(5)	C37-C38-C39-C45 179.7(4)
C9-C10-C16-C17' 73.8(7)	C38-C39-C40-C41 2.0(6)
C11-C10-C16-C17' -106.7(7)	C45-C39-C40-C41 -179.6(4)
C9-C10-C16-C18' -51.8(7)	C39-C40-C41-C36 0.6(5)
C11-C10-C16-C18' 127.7(6)	C39-C40-C41-C48 -174.9(3)
C11-C12-C19-C20 74.7(4)	C37-C36-C41-C40 -3.4(5)
C7-C12-C19-C20 -103.9(4)	C35-C36-C41-C40 -173.7(3)
C11-C12-C19-C21 -48.6(4)	C37-C36-C41-C48 171.9(3)
C7-C12-C19-C21 132.9(3)	C35-C36-C41-C48 1.6(5)
C1-P1-C22-C25' -152.2(8)	C38-C37-C42-C43 45.7(4)
C26-P1-C22-C25' 89.1(8)	C36-C37-C42-C43 -138.7(3)
Au1-P1-C22-C25' -30.7(8)	C38-C37-C42-C44 77.3(4)
C1-P1-C22-C23 -72.2(3)	C36-C37-C42-C44 98.2(4)
C26-P1-C22-C23 169.2(3)	C38-C39-C45-C46 8.6(6)
Au1-P1-C22-C23 49.3(3)	C40-C39-C45-C46 -169.8(4)
C1-P1-C22-C24 52.2(4)	C38-C39-C45-C47 -115.5(4)
C26-P1-C22-C24 -66.5(4)	C40-C39-C45-C47 66.1(5)
Au1-P1-C22-C24 173.7(3)	C40-C41-C48-C50 -45.9(5)
C1-P1-C22-C25 172.7(3)	C36-C41-C48-C50 138.7(3)
C26-P1-C22-C25 54.0(3)	C40-C41-C48-C49 77.0(4)
Au1-P1-C22-C25 -65.8(3)	C36-C41-C48-C49 -98.3(4)
C1-P1-C22-C24' 77.3(7)	C30-P2-C51-C52 -70.5(3)
C26-P1-C22-C24' -41.4(7)	C55-P2-C51-C52 172.0(2)
Au1-P1-C22-C24' -161.2(7)	Au2-P2-C51-C52 52.1(2)
C1-P1-C22-C23' -36.5(6)	C30-P2-C51-C53 49.4(3)
C26-P1-C22-C23' -155.2(6)	C55-P2-C51-C53 -68.1(3)
Au1-P1-C22-C23' 85.0(6)	Au2-P2-C51-C53 172.0(2)
C1-P1-C26-C27 -75.1(3)	C30-P2-C51-C54 172.4(2)
C22-P1-C26-C27 43.2(4)	C55-P2-C51-C54 54.8(3)
Au1-P1-C26-C27 165.0(3)	Au2-P2-C51-C54 -65.0(3)
C1-P1-C26-C29 47.2(3)	C30-P2-C55-C58 41.9(3)
C22-P1-C26-C29 165.5(3)	C51-P2-C55-C58 159.9(2)
Au1-P1-C26-C29 -72.7(3)	Au2-P2-C55-C58 -78.4(2)
C1-P1-C26-C28 160.6(3)	C30-P2-C55-C56 -79.5(3)
C22-P1-C26-C28 -81.1(3)	C51-P2-C55-C56 38.5(3)
Au1-P1-C26-C28 40.7(3)	Au2-P2-C55-C56 160.3(2)
C51-P2-C30-C31 -66.6(3)	C30-P2-C55-C57 157.7(2)
C55-P2-C30-C31 54.3(3)	C51-P2-C55-C57 -84.3(3)
Au2-P2-C30-C31 171.6(2)	Au2-P2-C55-C57 37.4(2)
C51-P2-C30-C35 117.3(3)	C25A-B1A-C1A-C6A 152.3(3)
C55-P2-C30-C35 -121.8(3)	C17A-B1A-C1A-C6A -86.3(3)
Au2-P2-C30-C35 -4.4(3)	C9A-B1A-C1A-C6A 35.3(4)
C35-C30-C31-C32 1.6(5)	C25A-B1A-C1A-C2A -35.3(4)
P2-C30-C31-C32 -174.8(2)	C17A-B1A-C1A-C2A 86.1(3)
C30-C31-C32-C33 -0.6(5)	C9A-B1A-C1A-C2A -152.3(3)
C31-C32-C33-C34 -1.4(5)	C6A-C1A-C2A-C3A -1.3(5)
C32-C33-C34-C35 2.5(5)	B1A-C1A-C2A-C3A -174.1(3)
C33-C34-C35-C30 -1.5(5)	C1A-C2A-C3A-C4A 0.4(5)
C33-C34-C35-C36 176.6(3)	C1A-C2A-C3A-C7A 178.9(3)
C31-C30-C35-C34 -0.5(4)	C2A-C3A-C4A-C5A 0.1(5)

C7A-C3A-C4A-C5A -178.4(3)
C3A-C4A-C5A-C6A 0.3(5)
C3A-C4A-C5A-C8A -179.2(3)
C2A-C1A-C6A-C5A 1.7(5)
B1A-C1A-C6A-C5A 174.6(3)
C4A-C5A-C6A-C1A -1.3(5)
C8A-C5A-C6A-C1A 178.2(3)
C4A-C3A-C7A-F3' -17.1(7)
C2A-C3A-C7A-F3' 164.4(5)
C4A-C3A-C7A-F1A 64.1(5)
C2A-C3A-C7A-F1A -114.4(4)
C4A-C3A-C7A-F2' -147.7(5)
C2A-C3A-C7A-F2' 33.8(6)
C4A-C3A-C7A-F2A -170.7(4)
C2A-C3A-C7A-F2A 10.8(5)
C4A-C3A-C7A-F3A -52.7(4)
C2A-C3A-C7A-F3A 128.7(4)
C4A-C3A-C7A-F1' 100.3(5)
C2A-C3A-C7A-F1' -78.2(5)
C4A-C5A-C8A-F4A -4.4(5)
C6A-C5A-C8A-F4A 176.1(3)
C4A-C5A-C8A-F5A 118.3(4)
C6A-C5A-C8A-F5A -61.2(5)
C4A-C5A-C8A-F6A -124.0(4)
C6A-C5A-C8A-F6A 56.6(4)
C25A-B1A-C9A-C14A 87.7(3)
C17A-B1A-C9A-C14A -35.1(4)
C1A-B1A-C9A-C14A -150.9(3)
C25A-B1A-C9A-C10A -85.1(3)
C17A-B1A-C9A-C10A 152.1(3)
C1A-B1A-C9A-C10A 36.3(4)
C14A-C9A-C10A-C11A 0.8(4)
B1A-C9A-C10A-C11A 174.0(3)
C9A-C10A-C11A-C12A 0.1(5)
C9A-C10A-C11A-C15A -179.3(3)
C10A-C11A-C12A-C13A -0.2(5)
C15A-C11A-C12A-C13A 179.2(3)
C11A-C12A-C13A-C14A -0.6(5)
C11A-C12A-C13A-C16A 177.0(3)
C12A-C13A-C14A-C9A 1.5(5)
C16A-C13A-C14A-C9A -176.1(3)
C10A-C9A-C14A-C13A -1.5(4)
B1A-C9A-C14A-C13A -174.7(3)
C12A-C11A-C15A-F7' -83.8(5)
C10A-C11A-C15A-F7' 95.6(5)
C12A-C11A-C15A-F9A 8.4(6)
C10A-C11A-C15A-F9A -172.1(5)
C12A-C11A-C15A-F8' 150.6(5)
C10A-C11A-C15A-F8' -29.9(6)
C12A-C11A-C15A-F8A 135.0(5)
C10A-C11A-C15A-F8A -45.6(6)
C12A-C11A-C15A-F7A -111.7(5)
C10A-C11A-C15A-F7A 67.7(5)
C12A-C11A-C15A-F9' 34.2(5)
C10A-C11A-C15A-F9' -146.4(4)
C12A-C13A-C16A-F10A 153.2(3)
C14A-C13A-C16A-F10A -29.2(5)
C12A-C13A-C16A-F12A -86.0(4)
C14A-C13A-C16A-F12A 91.6(4)
C12A-C13A-C16A-F11A 32.9(5)
C14A-C13A-C16A-F11A -149.5(3)
C25A-B1A-C17A-C18A -148.6(3)
C9A-B1A-C17A-C18A -30.6(4)
C1A-B1A-C17A-C18A 90.5(3)
C25A-B1A-C17A-C22A 41.1(4)
C9A-B1A-C17A-C22A 159.1(3)
C1A-B1A-C17A-C22A -79.8(3)
C22A-C17A-C18A-C19A -1.3(4)
B1A-C17A-C18A-C19A -172.0(3)
C17A-C18A-C19A-C20A 2.4(5)
C17A-C18A-C19A-C23A 178.3(3)
C18A-C19A-C20A-C21A -1.3(4)
C23A-C19A-C20A-C21A -177.1(3)
C19A-C20A-C21A-C22A -0.9(4)
C19A-C20A-C21A-C24A 178.4(3)
C20A-C21A-C22A-C17A 2.1(5)
C24A-C21A-C22A-C17A -177.2(3)
C18A-C17A-C22A-C21A -1.0(4)
B1A-C17A-C22A-C21A 170.0(3)
C20A-C19A-C23A-F14A -144.8(3)
C18A-C19A-C23A-F14A 39.3(4)
C20A-C19A-C23A-F15A -22.9(4)
C18A-C19A-C23A-F15A 161.2(3)
C20A-C19A-C23A-F13A 96.5(4)
C18A-C19A-C23A-F13A -79.4(4)
C20A-C21A-C24A-F16A -151.5(3)
C22A-C21A-C24A-F16A 27.8(4)
C20A-C21A-C24A-F18A -31.5(4)
C22A-C21A-C24A-F18A 147.8(3)
C20A-C21A-C24A-F17A 88.0(3)
C22A-C21A-C24A-F17A -92.7(3)
C17A-B1A-C25A-C30A -152.2(3)
C9A-B1A-C25A-C30A 85.0(3)
C1A-B1A-C25A-C30A -36.6(4)
C17A-B1A-C25A-C26A 33.8(4)
C9A-B1A-C25A-C26A -89.0(3)
C1A-B1A-C25A-C26A 149.5(3)
C30A-C25A-C26A-C27A 0.5(5)
B1A-C25A-C26A-C27A 174.8(3)
C25A-C26A-C27A-C28A 0.2(5)
C25A-C26A-C27A-C33A -178.5(3)
C26A-C27A-C28A-C29A -0.6(5)
C33A-C27A-C28A-C29A 178.1(3)
C27A-C28A-C29A-C30A 0.3(5)
C27A-C28A-C29A-C32A 178.7(3)
C26A-C25A-C30A-C29A -0.8(5)
B1A-C25A-C30A-C29A -175.2(3)
C28A-C29A-C30A-C25A 0.4(5)
C32A-C29A-C30A-C25A -178.0(3)
C28A-C29A-C32A-F23A 108.5(5)
C30A-C29A-C32A-F23A -73.1(5)
C28A-C29A-C32A-F23' -62.5(7)
C30A-C29A-C32A-F23' 115.9(6)
C28A-C29A-C32A-F24A -129.0(4)
C30A-C29A-C32A-F24A 49.5(5)
C28A-C29A-C32A-F22A -11.8(5)
C30A-C29A-C32A-F22A 166.7(4)
C28A-C29A-C32A-F24' 60.1(6)
C30A-C29A-C32A-F24' -121.4(6)
C28A-C29A-C32A-F22' 175.2(5)
C30A-C29A-C32A-F22' -6.3(6)
C28A-C27A-C33A-F21' 169.7(6)
C26A-C27A-C33A-F21' -11.6(7)
C28A-C27A-C33A-F21A 13.7(5)
C26A-C27A-C33A-F21A -167.6(4)
C28A-C27A-C33A-F20' -62.6(6)
C26A-C27A-C33A-F20' 116.1(6)
C28A-C27A-C33A-F20A 135.9(3)

C26A-C27A-C33A-F20A -45.4(4)	C26A-C27A-C33A-F19' -131.4(5)
C28A-C27A-C33A-F19A -108.4(4)	C1R-C2R-C3R-C4R 178(3)
C26A-C27A-C33A-F19A 70.3(4)	C2R-C3R-C4R-C5R 170(3)
C28A-C27A-C33A-F19' 49.9(5)	

DFT Calculations Data

(Ethynylbenzene) [(2′,4′,6′-triisopropyl-1,1′-biphenyl-2-yl) di-tert-butylphosphine] gold(I) hexafluoroantimonate (6)

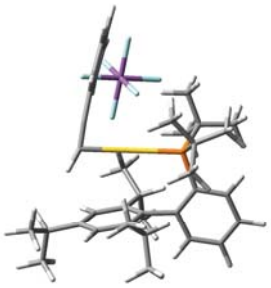

Row	Symbol	X	Y	Z
1	P	-1.4220890	-2.0874300	-0.4061630
2	C	0.1788090	-2.7175190	-1.2104470
3	C	-2.3153120	-3.4456610	0.5876250
4	Au	-0.9434760	-0.2923880	1.0399150
5	C	1.3957710	-1.2360410	4.0949600
6	C	2.4760610	-2.0838190	4.2892970
7	C	3.6327990	-1.9307820	3.5216410
8	C	3.7228000	-0.9230440	2.5640550
9	C	2.6539970	-0.0595050	2.3711790
10	C	1.4874140	-0.2185650	3.1318940
11	H	0.4784280	-1.3520800	4.6702980
12	H	2.4158710	-2.8737410	5.0348920
13	H	4.4688960	-2.6115660	3.6703340
14	H	4.6067580	-0.8157820	1.9387900
15	H	2.7139050	0.7190840	1.6144450
16	C	0.3725430	0.6196820	2.8438180
17	C	-0.5781180	1.3368720	2.5111430
18	H	-1.2502100	2.1795120	2.4827910
19	C	-2.5210790	-1.5086180	-1.7572370
20	C	-2.9429100	-2.4586420	-2.7017470
21	C	-2.9291850	-0.1600410	-1.9137830
22	C	-3.7108650	-2.1118780	-3.8040660
23	H	-2.6704540	-3.5046590	-2.5728890
24	C	-3.6863600	0.1657550	-3.0487360
25	C	-4.0690480	-0.7823320	-3.9879260
26	H	-4.0214930	-2.8762780	-4.5128460
27	H	-3.9956330	1.2034950	-3.1770130
28	H	-4.6597540	-0.4831810	-4.8514630
29	C	-2.2070640	-4.8571540	0.0121000
30	H	-2.8372620	-5.5196140	0.6233470
31	H	-2.5696570	-4.9347370	-1.0201900
32	H	-1.1863200	-5.2553190	0.0600040
33	C	-1.7319360	-3.4552040	2.0060440
34	H	-0.6485820	-3.6309680	2.0218870
35	H	-1.9292860	-2.5116270	2.5340660
36	H	-2.2098930	-4.2653660	2.5763260
37	C	-3.7905070	-3.0613580	0.6760800
38	H	-4.2965380	-3.7649150	1.3528810
39	H	-3.9249610	-2.0538660	1.0891040
40	H	-4.2945540	-3.1092090	-0.2980160
41	C	0.0123960	-3.8435040	-2.2312360
42	H	1.0136280	-4.1039740	-2.6036380
43	H	-0.4277290	-4.7560610	-1.8195040

44	H	-0.5776330	-3.5256090	-3.0995610
45	C	1.1219400	-3.1645390	-0.0914530
46	H	2.1084120	-3.3735230	-0.5296700
47	H	1.2631710	-2.3844280	0.6718980
48	H	0.7824320	-4.0845950	0.4023800
49	C	0.8005600	-1.5307280	-1.9417070
50	H	0.9963650	-0.6828040	-1.2768990
51	H	1.7726540	-1.8412600	-2.3505820
52	H	0.1758290	-1.2003210	-2.7829740
53	C	-2.7328260	0.9901980	-0.9613870
54	C	-3.7520550	1.2748630	-0.0227310
55	C	-1.6831980	1.9223200	-1.1421180
56	C	-3.6882610	2.4543690	0.7229560
57	C	-1.6678420	3.0846270	-0.3713560
58	C	-2.6572800	3.3761820	0.5654780
59	H	-4.4845950	2.6613170	1.4384670
60	H	-0.8551940	3.8017430	-0.5096930
61	C	-0.5904250	1.7220980	-2.1692570
62	H	-0.6556850	0.6875090	-2.5326010
63	C	-2.6135680	4.6887070	1.3181620
64	H	-1.5500900	4.9275280	1.4909570
65	C	-3.3158620	4.6513960	2.6694550
66	H	-2.9579290	3.8296240	3.3053370
67	H	-3.1473050	5.5922180	3.2083100
68	H	-4.4028960	4.5353670	2.5536960
69	C	-3.2059630	5.7982100	0.4472310
70	H	-3.1501280	6.7694350	0.9567270
71	H	-2.6792170	5.8828230	-0.5120460
72	H	-4.2639410	5.5862440	0.2328540
73	C	0.8047600	1.9309550	-1.5827950
74	H	0.9295710	1.4141500	-0.6177060
75	H	1.5833860	1.5529630	-2.2564340
76	H	1.0165720	2.9962830	-1.4133880
77	C	-0.8068610	2.6361860	-3.3758700
78	H	-0.7773280	3.6941600	-3.0781180
79	H	-0.0194190	2.4770860	-4.1247780
80	H	-1.7767950	2.4501640	-3.8565260
81	C	-4.9585830	0.3754150	0.1579310
82	H	-4.7401950	-0.5914250	-0.3188540
83	C	-5.2790720	0.1129760	1.6285090
84	H	-5.6902010	1.0054100	2.1199800
85	H	-6.0323700	-0.6813610	1.7192030
86	H	-4.3865300	-0.1920470	2.1951560
87	C	-6.1789520	0.9657840	-0.5505590
88	H	-7.0505060	0.3080020	-0.4317350
89	H	-6.4371810	1.9475370	-0.1283950
90	H	-5.9965090	1.0988180	-1.6250220
91	Sb	4.8787650	0.6956260	-0.8953340
92	F	4.6758450	1.5884500	0.7565870
93	F	3.9624760	2.0950200	-1.7563290
94	F	3.2422050	-0.1914300	-0.5760190
95	F	6.5137450	1.5721190	-1.1810540
96	F	5.7859810	-0.7017200	-0.0056140
97	F	5.0416060	-0.2238770	-2.5257130

(Ethynylbenzene) [(2′,4′,6′-triisopropyl-1,1′-biphenyl-2-yl) di-tert-butylphosphine] gold(I) tetrakis[3,5-bis(trifluoromethyl)phenyl] borate (83)

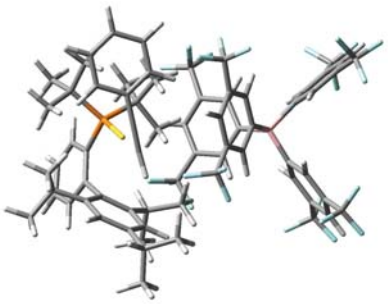

Row	Symbol	X	Y	Z
1	P	3.6413760	0.7558520	1.7393810
2	C	4.9163240	1.9952040	2.4240960
3	C	1.8480760	1.2686030	2.0874640
4	Au	3.9509760	0.6456680	-0.5912480
5	C	3.7843180	4.1131330	-2.4844230
6	C	4.0112810	5.4452710	-2.1722350
7	C	5.2795750	5.8578110	-1.7665560
8	C	6.3267120	4.9409080	-1.6759160
9	C	6.1092190	3.6043230	-1.9781390
10	C	4.8314270	3.1859860	-2.3799690
11	H	2.8013510	3.7753310	-2.8038790
12	H	3.1967930	6.1628550	-2.2457090
13	H	5.4556200	6.9033340	-1.5217710
14	H	7.3150970	5.2709620	-1.3640860
15	H	6.9143280	2.8750950	-1.9009860
16	C	4.5704810	1.8053940	-2.6271950
17	C	4.3296090	0.6071960	-2.8005940
18	H	4.2075550	-0.3537050	-3.2727890
19	C	3.9636340	-0.8626430	2.5566920
20	C	3.8756410	-0.9038910	3.9588450
21	C	4.3315890	-2.0459960	1.8668700
22	C	4.1721360	-2.0475510	4.6867180
23	H	3.5758130	-0.0159030	4.5083440
24	C	4.6590370	-3.1760660	2.6297290
25	C	4.5868860	-3.1900290	4.0153660
26	H	4.0865640	-2.0368650	5.7709800
27	H	4.9592240	-4.0795220	2.0984460
28	H	4.8428210	-4.0938810	4.5645750
29	C	1.5406900	1.6092760	3.5430810
30	H	0.4801080	1.8863540	3.6138790
31	H	1.6967680	0.7622530	4.2223650
32	H	2.1149880	2.4715290	3.9034430
33	C	1.4728200	2.4654860	1.2119210
34	H	1.9875630	3.3913210	1.4901730
35	H	1.6617350	2.2700740	0.1456190
36	H	0.3919910	2.6410050	1.3336670
37	C	0.9883680	0.0886420	1.6418580
38	H	-0.0727450	0.3663620	1.7339960
39	H	1.1672930	-0.1629030	0.5860820
40	H	1.1524400	-0.8073510	2.2539440
41	C	5.0170160	2.0694110	3.9486530
42	H	5.7002230	2.8933470	4.2009510
43	H	4.0623030	2.2781360	4.4444970
44	H	5.4437710	1.1549610	4.3759640
45	C	4.5914150	3.3878140	1.8769450
46	H	5.4597440	4.0401230	2.0514620
47	H	4.3929700	3.3885980	0.7943220
48	H	3.7372710	3.8443040	2.3915300
49	C	6.2841990	1.5693650	1.8930300

50	H	6.3325350	1.5994010	0.7964380
51	H	7.0415040	2.2661750	2.2810290
52	H	6.5619790	0.5612330	2.2290740
53	C	4.3401090	-2.2813520	0.3831140
54	C	3.2000220	-2.8692770	-0.2165750
55	C	5.5223840	-2.1311210	-0.3736230
56	C	3.2515330	-3.2229670	-1.5636280
57	C	5.5185010	-2.5041750	-1.7206420
58	C	4.3927330	-3.0365890	-2.3414100
59	H	2.3613910	-3.6574420	-2.0213490
60	H	6.4329360	-2.3874100	-2.3063390
61	C	6.8233330	-1.6718820	0.2523550
62	H	6.5903060	-1.2241510	1.2294550
63	C	4.4395180	-3.4584200	-3.7936250
64	H	5.3717270	-3.0507170	-4.2200840
65	C	3.2721160	-2.9164840	-4.6146850
66	H	3.1869390	-1.8224860	-4.5545660
67	H	3.3939960	-3.1851360	-5.6720460
68	H	2.3139770	-3.3353100	-4.2783970
69	C	4.5028540	-4.9816720	-3.9033530
70	H	4.5923580	-5.2949230	-4.9521620
71	H	5.3589810	-5.3870520	-3.3487190
72	H	3.5896300	-5.4376250	-3.4941040
73	C	7.5581630	-0.6233820	-0.5795890
74	H	6.8958220	0.2079240	-0.8651500
75	H	8.3999490	-0.2080370	-0.0087960
76	H	7.9708240	-1.0519070	-1.5035600
77	C	7.7349520	-2.8721790	0.5131500
78	H	7.9846120	-3.3830080	-0.4278000
79	H	8.6746740	-2.5500420	0.9819830
80	H	7.2576260	-3.6055450	1.1764690
81	C	1.9540250	-3.2154640	0.5778930
82	H	1.9696050	-2.6442360	1.5164420
83	C	0.6546210	-2.8764810	-0.1468450
84	H	0.4708860	-3.5471540	-0.9980950
85	H	-0.1919680	-2.9933700	0.5430310
86	H	0.6484280	-1.8484830	-0.5281680
87	C	1.9487750	-4.7002650	0.9487950
88	H	1.0500370	-4.9420790	1.5319900
89	H	1.9418110	-5.3242110	0.0431440
90	H	2.8268710	-4.9818840	1.5434040
91	B	-3.5704010	0.0204120	-0.0320330
92	C	-4.2433840	-1.3121570	-0.7019720
93	C	-4.3410340	-1.4775000	-2.0896730
94	C	-4.9039640	-2.2773450	0.0688360
95	C	-5.0286820	-2.5417440	-2.6693800
96	H	-3.8725760	-0.7476010	-2.7537000
97	C	-5.5901410	-3.3480940	-0.5011470
98	H	-4.8937470	-2.1962250	1.1580190
99	C	-5.6564700	-3.4976580	-1.8804790
100	H	-6.1876360	-4.3319360	-2.3295140
101	C	-4.8068900	1.0948730	-0.0034440
102	C	-5.7300680	1.1438880	1.0485430
103	C	-5.0955300	1.9148220	-1.1020330
104	C	-6.8545880	1.9673660	1.0165600
105	H	-5.5740220	0.5155500	1.9288420
106	C	-6.2177270	2.7385650	-1.1442140
107	H	-4.4267700	1.9140170	-1.9659060
108	C	-7.1107070	2.7800680	-0.0806040
109	H	-7.9842010	3.4252540	-0.1106260
110	C	-2.9415620	-0.2590750	1.4533570
111	C	-2.8299110	0.7588550	2.4050720
112	C	-2.3386740	-1.4824010	1.7911860
113	C	-2.1775390	0.5733270	3.6252620

114	H	-3.2610990	1.7404180	2.1963250
115	C	-1.6938050	-1.6782740	3.0084300
116	H	-2.3823470	-2.3080920	1.0796580
117	C	-1.6083900	-0.6498430	3.9445300
118	H	-1.1014130	-0.8035190	4.8952830
119	C	-2.2878630	0.5901560	-0.8775300
120	C	-1.4304200	-0.2391970	-1.6143980
121	C	-1.9171530	1.9385950	-0.7975620
122	C	-0.2967430	0.2562520	-2.2552390
123	H	-1.6591490	-1.3021330	-1.7035980
124	C	-0.7752480	2.4400050	-1.4189350
125	H	-2.5406250	2.6286720	-0.2269810
126	C	0.0464900	1.6024930	-2.1631360
127	H	0.9367070	1.9825960	-2.6657280
128	C	-5.0452650	-2.6402310	-4.1610140
129	C	-6.2155470	-4.3484900	0.4167540
130	C	-7.7688120	1.9562750	2.1994740
131	C	-6.4107940	3.6091770	-2.3439360
132	C	-1.0243090	-2.9722620	3.3469510
133	C	-2.1241870	1.7279030	4.5724090
134	C	-0.4888440	3.9068640	-1.3484540
135	C	0.5965720	-0.6337710	-3.0579490
136	F	-8.2359210	0.7240350	2.4518650
137	F	-7.1350730	2.3541670	3.3139070
138	F	-8.8297830	2.7558910	2.0421500
139	F	-7.6061390	4.2107020	-2.3602160
140	F	-5.4810580	4.5772330	-2.3994730
141	F	-6.2985670	2.9138680	-3.4852450
142	F	-5.4647210	-1.4989180	-4.7272800
143	F	-5.8379590	-3.6209860	-4.6078450
144	F	-3.8162900	-2.8728220	-4.6504860
145	F	-6.9462860	-5.2626640	-0.2310040
146	F	-5.2840130	-5.0135780	1.1196080
147	F	-7.0177660	-3.7616590	1.3174970
148	F	0.3183150	-2.8373450	3.3751120
149	F	-1.2930840	-3.9480740	2.4716970
150	F	-1.3776650	-3.4129720	4.5608350
151	F	-1.3270070	1.5006090	5.6223740
152	F	-1.6624020	2.8344880	3.9584830
153	F	-3.3353130	2.0404840	5.0495650
154	F	-1.1222020	4.5838320	-2.3153060
155	F	0.8221760	4.1741730	-1.4871480
156	F	-0.8738290	4.4424590	-0.1830480
157	F	0.0768510	-1.8435850	-3.2750600
158	F	0.8925430	-0.0983600	-4.2519070
159	F	1.7834940	-0.8262270	-2.4396530

(Ethynylbenzene) [(2´,4´,6´-triisopropyl-1,1´-biphenyl-2-yl) di-tert-butylphosphine] gold(I) tetrafluoroborate (84)

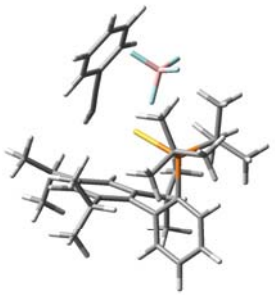

Row	Symbol	X	Y	Z
1	P	0.2976050	2.0708940	0.1254880
2	C	0.8539790	2.6707200	1.8350290
3	C	1.2660910	2.9359330	-1.2744850

4	Au	0.6120610	-0.2525830	-0.0481700
5	C	3.4936810	-1.4838780	-2.6134700
6	C	4.7287110	-1.0065410	-3.0294870
7	C	5.7206350	-0.7292730	-2.0895890
8	C	5.4850890	-0.9352050	-0.7306360
9	C	4.2561050	-1.4146390	-0.2991310
10	C	3.2558490	-1.6860200	-1.2460310
11	H	2.7031180	-1.6942020	-3.3328610
12	H	4.9192790	-0.8459730	-4.0885390
13	H	6.6861230	-0.3508590	-2.4204340
14	H	6.2652330	-0.7204150	-0.0032580
15	H	4.0350620	-1.5761780	0.7550030
16	C	1.9709350	-2.1167300	-0.7975320
17	C	0.8588390	-2.4564900	-0.3916490
18	H	0.0071460	-3.0319300	-0.0707780
19	C	-1.4775480	2.5141340	-0.0965780
20	C	-1.7995240	3.8812850	-0.1312960
21	C	-2.5130560	1.5701980	-0.2990330
22	C	-3.0897470	4.3349250	-0.3620880
23	H	-1.0186050	4.6208910	0.0234140
24	C	-3.8089270	2.0549370	-0.5362580
25	C	-4.1049650	3.4099040	-0.5703070
26	H	-3.2947640	5.4030870	-0.3820660
27	H	-4.6043510	1.3271210	-0.6991600
28	H	-5.1248500	3.7387910	-0.7597360
29	C	1.5856280	4.4125770	-1.0322970
30	H	2.1291640	4.7886170	-1.9114590
31	H	0.6899860	5.0362320	-0.9274870
32	H	2.2325770	4.5781940	-0.1632810
33	C	2.5828490	2.1770150	-1.4839060
34	H	3.2110550	2.1481730	-0.5859810
35	H	2.4091930	1.1405760	-1.8078530
36	H	3.1552200	2.6827520	-2.2757890
37	C	0.4499670	2.8193340	-2.5611950
38	H	1.0540740	3.2098370	-3.3931970
39	H	0.2058330	1.7756630	-2.7951800
40	H	-0.4829250	3.3964050	-2.5269630
41	C	0.4274220	4.0945280	2.1851380
42	H	0.8236210	4.3306650	3.1835180
43	H	0.8199030	4.8494090	1.4936000
44	H	-0.6638410	4.1953910	2.2363520
45	C	2.3752080	2.5428870	1.9325580
46	H	2.6632360	2.7058850	2.9817820
47	H	2.7242840	1.5401730	1.6568040
48	H	2.9039360	3.2939020	1.3330240
49	C	0.2186220	1.7147010	2.8444220
50	H	0.5633910	0.6811280	2.7126760
51	H	0.5016430	2.0365820	3.8579930
52	H	-0.8776620	1.7380060	2.7880400
53	C	-2.4129250	0.0710170	-0.2890200
54	C	-2.2726820	-0.6349100	-1.5041030
55	C	-2.6906260	-0.6418320	0.9009000
56	C	-2.3935950	-2.0265900	-1.5046630
57	C	-2.7706510	-2.0331250	0.8501610
58	C	-2.6351030	-2.7483240	-0.3398390
59	H	-2.2944450	-2.5591160	-2.4516640
60	H	-2.9820300	-2.5869650	1.7676160
61	C	-3.0155860	0.0637240	2.2031100
62	H	-2.6732690	1.1062330	2.1200130
63	C	-2.8356280	-4.2487290	-0.3341580
64	H	-2.4366030	-4.6248360	0.6233080
65	C	-2.1228690	-4.9807440	-1.4643340
66	H	-1.0521130	-4.7395510	-1.5130750
67	H	-2.2163810	-6.0655860	-1.3281870

68	H	-2.5653390	-4.7395370	-2.4413870
69	C	-4.3328460	-4.5627660	-0.3720490
70	H	-4.5085230	-5.6458380	-0.3245130
71	H	-4.8666110	-4.0911220	0.4632250
72	H	-4.7727350	-4.1872930	-1.3080120
73	C	-2.3386060	-0.5611050	3.4207520
74	H	-1.2658190	-0.7282480	3.2615100
75	H	-2.4639930	0.0949830	4.2932210
76	H	-2.7946780	-1.5269540	3.6802380
77	C	-4.5313990	0.1063810	2.4100910
78	H	-4.9413530	-0.9115530	2.4815030
79	H	-4.7779050	0.6339920	3.3416310
80	H	-5.0429670	0.6179560	1.5841150
81	C	-2.0500590	0.0693160	-2.8275970
82	H	-1.8611300	1.1332110	-2.6212540
83	C	-0.8385620	-0.4808960	-3.5794460
84	H	-0.9934430	-1.5231220	-3.8917180
85	H	-0.6490570	0.1086700	-4.4873680
86	H	0.0685730	-0.4542640	-2.9552670
87	C	-3.3017150	-0.0074660	-3.7016190
88	H	-3.1478740	0.5320250	-4.6459870
89	H	-3.5472760	-1.0502480	-3.9478020
90	H	-4.1725990	0.4307060	-3.1966190
91	B	2.0896860	-1.7503940	2.9331760
92	F	2.1892440	-1.9585020	4.2994290
93	F	0.7230240	-1.6812380	2.5678840
94	F	2.7050760	-0.5382500	2.5840780
95	F	2.7046820	-2.7896100	2.2323080

5. Towards the Total Synthesis of Rumphellaone A

All the reactants, ligands and the following reagents were purchased from comercial sources and used without further purification: (furan-2-yloxy)trimethylsilane, 2-(diethoxymethyl)furan, furan-2-carboxylic acid, maleic anhydride, 2-methylfuran, 6-methylhept-5-en-2-one, butane-1,4-diol, 2,2,7,7-tetramethyl-3,6-dioxa-2,7-disilaoctane, ethynylbenzene, 1-ethynyl-3-methylbenzene, 3-ethynylphenol, 1-ethynyl-3-methoxybenzene and BINOL. $Mn(dpm)_3$ and Crabtree's catalyst were synthesized as reported.[1,2] JohnPhosAuCl, ^{t}BuXPhosAuCl, IPrAuCl, Ph_3PAuCl, (THT)AuCl, (**44**)AuCl and complexes **E**, **V**, **W**, **X**, **Y**, **Z**, **LL** and **SS** were also prepared according to the literature.[3,4,5,6] Cyclobutene **19** was characterized in **Chapter 2** and complex **Q** in **Chapter 4**.[7,8]

Procedures for the Silyloxyalkynylfuran Approach

(Z)-4-Oxo-6-(trimethylsilyl)hex-2-en-5-ynoic acid (40)

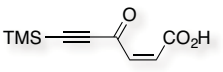

$AlCl_3$ (140 mg, 1.11 mmol) was added portion-wise to an ice-cooled solution of maleic anhydride (98 mg, 1.00 mmol) and 1,2-bis(trimethylsilyl)ethyne (170 mg, 1.00 mmol) in CH_2Cl_2 (8.5 ml). The mixture was stirred at 0 ºC for 2 h and then at 25 ºC for 20 h. The reaction was quenched with 1 M HCl and the phases were separeted. The organic layeres were washed with water and dried with $MgSO_4$. The crude was concentrated and purified with cyclohexane:ethyl acetate (2:1) with 1% formic acid. (Z)-4-oxo-6-(trimethylsilyl)hex-2-en-5-ynoic acid **40** was obtained in 25% isolated yield (46.2 mg, 0.24 mmol). ^{1}H NMR (500 MHz, $CDCl_3$, ppm) δ 7.10 (d, J = 15.67 Hz, 1H), 6.93 (d, J = 16.02 Hz, 1H), 0.29 (s, 9H); ^{13}C NMR (126 MHz, $CDCl_3$, ppm) δ 127.44 (s), 169.10 (s), 142.41 (s), 134.27 (s), 102.01 (s), 99.98 (s), – 0.68 (s). ESI$^-$ *m/z* calc for $C_9H_{11}O_3Si^+$ $[M-H]^-$ 195.0483, found 195.0483 (0.0 ppm).

---

[1] R. H. Crabtree and M. W. Davis, *J. Org. Chem.* **1986**, *51*, 2655–2661.
[2] K. Iwasaki, K. K. Wan, A. Oppedisano, S. W. M. Crossley and R. Shenvi, *J. Am. Chem. Soc.* **2014**, *136*, 1300–1303.
[3] Catalyst **V** was provided by Prof. Fernando P. Cossio's research group (Universidad del País Vasco). The complex was prepared by Dr. Iván Rivilla, who collaborated in the enantioselective synthesis of oxabicycles (**Chapter 2**).
[4] N. Delpont, I. Escofet, P. Pérez-Galán, D. Spiegl, M. Raducan, C. Bour, R. Sinisi and A. M. Echavarren, *Catal. Sci. Tech.* **2013**, *3*, 3007–3012.
[5] R. J. Felix, D. Weber, O. Gutierrez, D. J. Tantillo and M. R. Gagné, *Nat. Chem.* **2012**, *4*, 405–409.
[6] *(a)* M. J. Johansson, D. J. Gorin, S. T. Staben and F. D. Toste, J. Am. Chem. Soc. 2005, 127, 18002–18003; *(b)* E. Herrero-Gómez, C. Nieto-Oberhuber, S. López, B. Benet-Buchholz and A. M. Echavarren, *Angew. Chem. Int. Ed.* **2006**, *45*, 5455–5459; *(c)* D. V. Partyka, T. J. Robilotto, M. Zelles, A. D. Hunter and T. G. Gray, *Organometallics* **2008**, *27*, 28–32; *(d)* C. H. M. Amijs, V. López-Carrillo, M. Raducan, P. Pérez-Galán, C Ferrer and A. M. Echavarren, *J. Org. Chem.* **2008**, *73*, 7721–7730; *(e)* Y. Wang, K. Ji, S. Lan and L. Zhang, *Angew. Chem. Int. Ed.* **2012**, *51*, 1915–1918; *(f)* A. S. K. Hashmi, M. Hamzic, F. Rominger and J. W. Bats, *Chem. –Eur. J.* **2009**, *15*, 13318–13322; *(g)* I. Alonso, B. Trillo, F. Lopez, S. Montserrat, G. Ujaque, L. Castedo, A. Lledós and J. L. Mascareñas, *J. Am. Chem. Soc.* **2009**, *131*, 13020–13030; *(h)* A. S. K. Hashmi, T. Hengst, C. Lothschütz and F. Rominger, *Adv. Synth. Catal.* **2010**, *352*, 1315–1337; *(i)* M. Z. Wang, C. Y. Zhou, Z. Guo, E. L. M. Wong, M. K. Wong and C. M. Che, *Chem. Asian J.* **2011**, *6*, 812–824.
[7] C. Obradors and A. M. Echavarren, *Chem. –Eur. J.* **2013**, *19*, 3547–3551.
[8] C. Obradors, A. Homs, D. Leboeuf and A. M. Echavarren, *Adv. Synth. Catal.* **2014**, *356*, 221–228.

2-Iodo-5-methylfuran

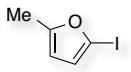

To a solution of 2-methylfuran (0.54 ml, 6.09 mmol) in THF (15.0 ml), 2 M ^{n}BuLi (3.35 ml, 6.70 mmol) was added at –10 ºC. The reaction mixture was stirred for 2 h and 1,2-diiodoethane (1.91 g, 6.70 mmol) was added. The solution was stirred for 18 h at 25 ºC. The product was extracted with diethyl ether and washed with brine. The organic layers were dried with Na_2SO_4 and concentrated carefully. 2-Iodo-5-methylfuran was obtained in 60% isolated yield (0.76 g, 3.67 mmol). ^{1}H NMR (500 MHz, $CDCl_3$, ppm) δ 6.40 (d, *J* = 3.02 Hz, 1H), 5.92 – 5.91 (m, 1H), 2.34 (d, *J* = 0.82 Hz, 3H); ^{13}C NMR (126 MHz, $CDCl_3$, ppm) δ 158.41 (s), 120.72 (s), 109.18 (s), 88.37 (s), 14.01 (s).

2-Tert-butyldimethylsilyloxyfuran

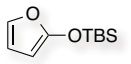

To a solution of furan-2(5H)-one (0.84 ml, 11.89 mmol) in CH_2Cl_2 (10.0 ml) was added Et_3N (3.32 ml, 23.79 mmol). The solution was cooled down in an ice bath for 30 min and *tert*-butyldimethylsilyl trifluoromethanesulfonate (3.28 ml, 14.27 mmol) was added. The reaction mixture was stirred at 25 ºC for 2 h and quenched with water. The phases were separated, the organic layers were dried with Na_2SO_4 and concentrated. Kugelrohr destillation at 100 ºC and 10 Torr afforded *tert*-butyl(furan-2-yloxy)dimethylsilane in 68% isolated yield (1.54 g, 7.80 mmol). ^{1}H NMR (500 MHz, CD_2Cl_2, ppm) δ 6.82 (dd, *J* = 2.32, 1.11 Hz, 1H), 6.21 (dd, *J* = 3.18, 2.23 Hz, 1H), 5.11 (dd, *J* = 3.17, 1.07 Hz, 1H), 0.96 (s, 9H), 0.23 (s, 6H); ^{13}C NMR (126 MHz, CD_2Cl_2, ppm) δ 157.52 (s), 132.77 (s), 111.54 (s), 84.01 (s), 25.98 (s), 25.76 (s), – 4.63 (s).

2-Triisopropylsilyloxyfuran

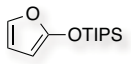

To a solution of furan-2(5H)-one (0.84 ml, 11.89 mmol) in CH_2Cl_2 (10.0 ml) was added Et_3N (3.32 ml, 23.79 mmol). The solution was cooled down in an ice bath for 30 min and triisopropylsilyl trifluoromethanesulfonate (3.95 ml, 14.27 mmol) was added. The reaction mixture was stirred at 25 ºC for 16 h and quenched with water. The phases were separated, the organic layers were dried with Na_2SO_4 and concentrated. Kugelrohr destillation at 100 ºC and 0.1 Torr afforded (furan-2-ylpxy)triisopropylsilane in 84% isolated yield (2.40 g, 9.97 mmol). ^{1}H NMR (400 MHz, $CDCl_3$, ppm) δ 6.80 (dd, *J* = 2.25, 1.07 Hz, 1H), 6.20 (dd, *J* = 2.98, 2.26 Hz, 1H), 5.12 (dd, *J* = 3.20, 1.12 Hz, 1H), 1.30 – 1.21 (m, 3H), 1.09 (d, *J* = 7.24 Hz, 18H); ^{13}C NMR (101 MHz, $CDCl_3$, ppm) δ 157.14 (s), 131.97 (s), 111.22 (s), 83.59 (s), 17.67 (s), 12.34 (s).

2-Trimethylsilylethynyl-5-methylfuran (41)

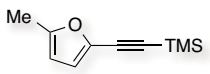

^{t}BuLi 1.5 M in diethyl ether (10.0 ml, 16.50 mmol) was added dropwise over 2-methylfuran (1.35 ml, 15.00 mmol) in diethyl ether (30.0 ml) under inert conditions at – 78 ºC. The solution was stirred for 1 h at this temperature and 1,2-diiodoethane (4.65 g, 16.50 mmol) in diethyl ether (45.0 ml) was added. The reaction mixture was stirred for an additional 30 min, warmed to 25 ºC and quenched it with a saturated solution of $Na_2S_2O_3$. Then, it was extracted with diethyl ether, washed with brine and dried with Na_2SO_4. THF (13.0 ml) was added to the crude and diethyl ether was evaporated under vacuum carefully. Ethynyltrimethylsilane (3.18 ml, 22.50 mmol) and Et_3N (6.28 ml, 45.00 mmol) were added and the solution was degassed with argon for 15 min. Bis(triphenylphosphine)palladium (II) dichloride (0.21 g, 0.30 mmol) was added and the reaction mixture stirred for 1 min at 25 ºC followed by CuI (0.11

g, 0.60 mmol). The solution was stirred for an additional 2 h. The crude was concentrated and purified by silica gel column chromatography eluting with pure cyclohexane to obtain trimethyl((5-methylfuran-2-yl)ethynyl)silane **41** in 35% isolated yield (0.93 g, 5.25 mmol). ^{1}H NMR (400 MHz, C_6D_6, ppm) δ 6.52 (dd, *J* = 3.27, 0.51 Hz, 1H), 5.66 (dq, *J* = 3.27, 1.00 Hz, 1H), 1.92 (dd, *J* = 1.14, 0.48 Hz, 3H), 0.27 (s, 9H); ^{13}C NMR (126 MHz, C_6D_6, ppm) δ 153.87 (s), 136.35 (s), 117.29 (s), 107.19 (s), 99.02 (s), 96.04 (s), 13.47 (s), – 0.19 (s).

2-Ethynyl-5-methylfuran

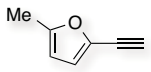

2-Trimethylsilylethynyl-5-methylfuran (516.0 mg, 2.89 mmol) was dissolved in methanol (15.0 ml) under inert conditions and K_2CO_3 (800.0 mg, 5.79 mmol) was added. The reaction mixture was stirred at 25 ºC for 15 min and was quenched with water. The solution was extracted with CH_2Cl_2, the organic layers dried with $MgSO_4$ and concentrated under vacuum without drying it. An exact solution was prepared in 5 ml of CH_2Cl_2 and the concentration was determined using diphenylmethane as internal standard. 2-Ethynyl-5-methylfuran was obtained in 60% yield (184.0 mg, 1.73 mmol). ^{1}H NMR (500 MHz, C_6D_6, ppm) δ 6.34 (d, *J* = 3.22 Hz, 1H), 5.62 (dq, *J* = 3.30, 0.95 Hz, 1H), 3.01 (s, 1H), 1.91 (s, 3H); ^{13}C NMR (126 MHz, C_6D_6, ppm) δ 154.08 (s), 135.16 (s), 117.56 (s), 107.09 (s), 81.73 (s), 74.76 (s), 13.50 (s).

2-Methyl-5-(3-methyl-3-phenylcyclobut-1-en-1-yl)furan (42)

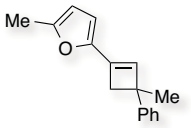

2-Ethynyl-5-methylfuran (21.00 mg, 0.20 mmol) was dissolvded in CH_2Cl_2 (0.40 ml) and α-methylstyrene (52.00 μl, 0.40 mmol) undert inert conditions, ^{t}BuXPhosAuCl (6.57 mg, 10.00 μmol) and $NaBAr^{F}_{4}$ (8.86 mg, 10.00 μmol) were added sequentially. The reaction mixture was stirred at 25 ºC for 24 h and quenched with a drop of Et_3N. The crude was concentrated and purified with silica gel preparative TLC eluting with pure pentane. 2-Methyl-5-(3-methyl-3-phenylcyclobut-1-en-1-yl)furan **42** was obtained in 64% isolated yield (28.8 mg, 0.13 mmol). ^{1}H NMR (400 MHz, $CDCl_3$, ppm) δ 7.40 – 7.37 (m, 2H), 7.35 – 7.30 (m, 2H), 7.22 – 7.18 (m, 1H), 6.43 (s, 1H), 6.17 (d, *J* = 3.16 Hz, 1H), 5.97 (dq, *J* = 3.26, 0.97 Hz, 1H), 2.91 (d, J = 12.44 Hz, 1H), 2.85 (d, J = 12.38 Hz, 1H), 2.33 (s, 3H), 1.63 (s, 3H); ^{13}C NMR (101 MHz, $CDCl_3$, ppm) δ 152.46 (s), 149.22 (s), 147.78 (s), 133.84 (s), 130.57 (s), 128.22 (s), 125.92 (s), 125.82 (s), 108.29 (s), 107.23 (s), 47.88 (s), 44.25 (s), 27.77 (s), 13.81 (s). APCI^{+} *m/z* calc for C16H17O^{+} [M+H]$^{+}$ 225.1274, found 225.1269 (2.4 ppm).

4-(4,4-Dimethyl-2-(5-methylfuran-2-yl)cyclobut-2-en-1-yl)butan-2-one (43)

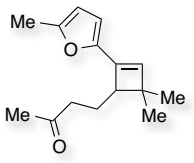

2-Ethynyl-5-methylfuran (106.0 mg, 1.00 mmol) was dissolved in DCE (5.0 ml) and 6-methylhep-5-en-2-one (295.0 μl, 2.00 mmol) under inert conditions, ^{t}BuXPhosAuCl (32.9 mg, 50.0 μmol) and $NaBAr^{F}_{4}$ (44.3 mg, 50.0 μmol) were added sequentially. The reaction mixture was stirred at 80 ºC for 2 h and quenched with a drop of Et_3N. The crude was concentrated and purified with silica gel column chromatography eluting with pentane:diethyl ether (20:1). 4-(4,4-Dimethyl-2-(5-methylfuran-2-yl)cyclobut-2-en-1-yl)butan-2-one **43** was obtained in 31% isolated yield (72.0 mg, 0.30 mmol). ^{1}H NMR (400 MHz, CD_2Cl_2, ppm) δ 6.15 (d, J = 3.20 Hz, 1H), 5.99 (s, 1H), 5.97 – 5.95 (m, 1H), 2.58 – 2.50 (m, 3H), 2.28 (s, 3H), 2.01 – 1.92 (m, 1H), 1.74 –

1.64 (m, 1H), 1.58 (s, 3H), 1.22 (s, 3H), 1.14 (s, 3H); ^{13}C NMR (126 MHz, CD_2Cl_2, ppm) δ 208.75 (s), 152.43 (s), 149.22 (s), 136.46 (s), 133.44 (s), 108.40 (s), 107.51 (s), 51.83 (s), 44.64 (s), 43.06 (s), 30.22 (s), 28.01 (s), 24.11 (s), 22.24 (s), 13.89 (s). APCI$^+$ *m/z* calc for C15H21O2$^+$ $[M+H]^+$ 233.1536, found 233.1531 (2.2 ppm).

Procedures for the Oxidation Approach

2-Methyl-2-(4-methylpent-3-en-1-yl)-1,3-dioxepane (55)

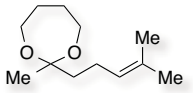

To a solution of 6-methylhept-5-en-2-one (4.43 ml, 30.00 mmol), triethoxymethane (5.49 ml, 33.00 mmol) and butane-1,4-diol (5.00 ml, 56.40 mol) in THF (60.0 ml) under inert conditions, $FeCl_3$ (487.0 mg, 3.00 mmol) was added. The reaction mixture was stirred at 25 ºC for 24 h and quenched with aqueous NaOH 10 %. The solution was extracted with CH_2Cl_2, the organic layers washed with water and dried with Na_2SO_4. The crude was purified by distillation at 120 ºC and 0.75 Torr and 2-methyl-2-(4-methylpent-3-en-1-yl)-1,3-dioxepane **55** was obtained in 83% isolated yield (4.91 g, 24.76 mmol). ^{1}H NMR (400 MHz, $CDCl_3$, ppm) δ 5.14 – 5.09 (m, 1H), 3.68 – 3.65 (m, 4H), 2.05 – 1.98 (m, 2H), 1.68 (d, *J* = 0.98 Hz, 3H), 1.65 –1.58 (m, 9H), 1.28 (s, 3H); ^{13}C NMR (101 MHz, $CDCl_3$, ppm) δ 131.70 (s), 124.32 (s), 102.63 (s), 62.11 (s), 37.81 (s), 29.93 (s), 25.82 (s), 23.29 (s), 22.54 (s), 17.76 (s).

2-(2-(4,4-Dimethyl-2-phenylcyclobut-2-en-1-yl)ethyl)-2-methyl-1,3-dioxepane (56)

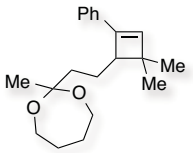

To a solution of 2-methyl-2-(4-methylpent-3-en-1-yl)-1,3-dioxepane **55** (44.0 μl, 0.20 mmol) and ethynylbenzene (220.0 μl, 2.00 mmol) under inert conditions, [^{t}BuXPhosAuNCMe]BAr$^F_4$ (15.0 mg, 10.00 μmol). The reaction mixture was stirred at 0 ºC for 48 h and quenched with a drop of Et_3N. The crude was concentrated and purified with silica gel prep-TLC eluting with cyclohexane:ethyl acetate (5:1). 2-(2-(4,4-Dimethyl-2-phenylcyclobut-2-en-1-yl)ethyl)-2-methyl-1,3-dioxepane **56** was obtained in 51% isolated yield (30.3 mg, 0.10 mmol).^{1}H NMR (400 MHz, $CDCl_3$, ppm) δ 7.34 – 7.28 (m, 4H), 7.23 – 7.19 (m, 1H), 6.29 (s, 1H), 3.69 – 3.64 (m, 4H), 2.71 (d, *J* = 10.94, 3.63 Hz, 1H), 1.87 – 1.78 (m, 1H), 1.75 – 1.65 (m, 1H), 1.61 – 1.57 (m, 4H), 1.53 – 1.40 (m, 2H), 1.27 (s, 3H), 1.25 (s, 3H), 1.19 (s, 3H).

4-(4,4-Dimethyl-2-phenylcyclobut-2-en-1-yl)butan-2-one (19)

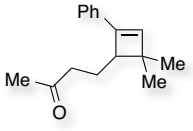

6-Methylhep-5-en-2-one (0,74 ml, 5.00 mmol) and ethynylbenzene (2.2 ml, 20.00 mmol) were dissolved in DCE (10.0 ml) under inert conditions and ^{t}BuXPhosAuCl (164.0 mg, 0.25 mmol) and NaBAr$^F_4$ (222.0 mg, 0.25 mmol) were added sequentially. The reaction mixture was stirred at 50 ºC for 19 h and quenched with 1 ml of Et_3N. The crude was concentrated and purified with silica gel column chromatography eluting with pentane:diethyl ether (20:1). 4-(4,4-Dimethyl-2-phenylcyclobut-2-en-1-yl)butan-2-one **19** was obtained in 78% isolated yield (0.89 g, 3.88 mmol). This compound was characterized in **Chapter 2**.

4-(2-(3-Hydroxyphenyl)-4,4-dimethylcyclobut-2-en-1-yl)butan-2-one (60)

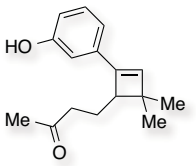

6-Methylhep-5-en-2-one (74.0 μl, 0.50 mmol) and 3-ethynylphenol (273.0 μl, 2.00 mmol) were dissolved in DCE (1.0 ml) under inert conditions and ^{t}BuXPhosAuCl (16.4 mg, 25.00 μmol) and $NaBAr^{F}_{4}$ (22.2 mg, 25.00 μmol) were added sequentially. The reaction mixture was stirred at 50 ºC for 19 h and quenched with 1 ml of Et_3N. The crude was concentrated and purified with silica gel column chromatography eluting with cyclohexane:ethyl acetate (5:1). 4-(2-(3-Hydroxyphenyl)-4,4-dimethylcyclobut-2-en-1-yl)butan-2-one **60** was obtained in 40% isolated yield (47.6 mg, 0.19 mmol). ^{1}H NMR (400 MHz, $CDCl_3$, ppm) δ 7.22 (t, *J* = 7.95 Hz, 1H), 6.92 (ddd, *J* = 7.58, 1.49, 1.21 Hz, 1H), 6.87 (dd, *J* = 2.67, 1.57 Hz, 1H), 6.77 (ddd, *J* = 8.17, 2.64, 0.84 Hz, 1H), 6.27 (s, 1H), 2.67 (dd, *J* = 10.73, 4.47 Hz, 1H), 2.53 – 2.47 (m, 2H), 2.14 (s, 3H), 2.12 – 2.05 (m, 1H), 1.71 – 1.61 (m, 1H), 1.23 (s, 3H), 1.15 (s, 3H); ^{13}C NMR (101 MHz, $CDCl_3$, ppm) δ 208.62 (s), 159.79 (s), 145.50 (s), 136.78 (s), 136.05 (s), 129.46 (s), 117.77 (s), 113.29 (s), 110.48 (s), 55.27 (s), 51.02 (s), 42.78 (s), 30.00 (s), 27.88 (s), 23.33 (s), 21.85 (s). ESI$^-$ *m/z* calc for $C_{16}H_{19}O_2^-$ $[M-H]^-$ 243.1391, found 243.1389 (0.2 ppm).

4-(2-(3-Methoxyphenyl)-4,4-dimethylcyclobut-2-en-1-yl)butan-2-one (61)

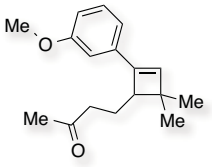

6-Methylhep-5-en-2-one (74.0 μl, 0.50 mmol) and 1-ethynyl-3-methoxybenzene (318.0 μl, 2.00 mmol) were dissolved in DCE (1.0 ml) under inert conditions and ^{t}BuXPhosAuCl (16.4 mg, 25.00 μmol) and $NaBAr^{F}_{4}$ (22.2 mg, 25.00 μmol) were added sequentially. The reaction mixture was stirred at 50 ºC for 19 h and quenched with 1 ml of Et_3N. The crude was concentrated and purified with silica gel column chromatography eluting with pentane:diethyl ether (20:1). 4-(2-(3-Methoxyphenyl)-4,4-dimethylcyclobut-2-en-1-yl)butan-2-one **61** was obtained in 65% isolated yield (83.6 mg, 0.32 mmol). ^{1}H NMR (400 MHz, $CDCl_3$, ppm) δ 7.25 (t, *J* = 7.91 Hz, 1H), 6.96 (ddd, *J* = 7.64, 1.60, 0.99 Hz, 1H), 6.91 (dd, *J* = 2.62, 1.51 Hz, 1H), 6.80 (ddd, *J* = 8.25, 2.59, 0.80 Hz, 1H), 6.30 (s, 1H), 3.83 (s, 3H), 2.71 (dd, *J* = 10.62, 4.31 Hz, 1H), 2.57 – 2.51 (m, 2H), 2.17 (s, 3H), 2.15 – 2.09 (m, 1H), 1.75 – 1.65 (m, 1H), 1.27 (s, 3H), 1.19 (s, 3H); ^{13}C NMR (101 MHz, $CDCl_3$, ppm) δ 208.55 (s), 159.73 (s), 145.43 (s), 136.72 (s), 135.98 (s), 129.42 (s), 117.71 (s), 113.22 (s), 110.42 (s), 55.19 (s), 50.95 (s), 42.76 (s), 42.70 (s), 29.95 (s), 27.84 (s), 23.26 (s), 21.80 (s). ESI$^+$ *m/z* calc for $C_{17}H_{22}NaO_2^+$ $[M+Na]^+$ 281.1512, found 281.1500 (1.2 ppm).

4-(4,4-Dimethyl-2-(m-tolyl)cyclobut-2-en-1-yl)butan-2-one (62)

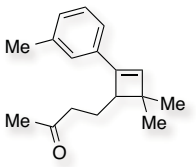

6-Methylhep-5-en-2-one (74.0 μl, 0.50 mmol) and 1-ethynyl-3-methylbenzene (200.0 μl, 1.75 mmol) were dissolved in dichloroethane (1.00 ml) under inert conditions and ^{t}BuXPhosAuCl (16.4 mg, 25.00 μmol) and $NaBAr^{F}_{4}$ (22.2 mg, 25.00 μmol) were added sequentially. The reaction mixture was stirred at 50 ºC for 19 h and quenched with 1 ml of Et_3N. The crude was concentrated and purified with silica gel column chromatography eluting with pentane:diethyl ether (20:1). 4-(4,4-Dimethyl-2-(m-tolyl)cyclobut-2-en-1-yl)butan-2-one **62** was obtained in 44% isolated yield (53.6 mg, 0.22 mmol). ^{1}H NMR (500 MHz, $CDCl_3$, ppm) δ 7.22 (t, *J* = 7.60 Hz, 1H), 7.17 – 7.14 (m, 2H), 7.05 (d, *J* = 7.54 Hz, 1H), 6.27 (s, 1H), 2.71 (dd, *J* = 10.86,

4.21 Hz, 1H), 2.58 – 2.45 (m, 2H), 2.35 (s, 3H), 2.16 (s, 3H), 2.15 – 2.08 (m, 1H), 1.73 – 1.35 (m, 1H), 1.25 (s, 3H), 1.18 (s, 3H); ^{13}C NMR (101 MHz, $CDCl_3$, ppm) δ 208.78 (s), 145.65 (s), 137.97 (s), 136.26 (s), 134.62 (s), 128.37 (s), 128.31 (s), 125.80 (s), 122.32 (s), 50.99 (s), 42.85 (s), 42.82 (s), 30.02 (s), 27.95 (s), 23.47 (s), 21.90 (s), 21.51 (s).

4-(2,2-Dimethyl-4-phenylcyclobutyl)butan-2-one (45)

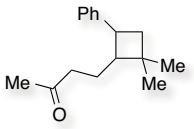

To a solution of 4-(4,4-dimethyl-2-phenylcyclobut-2-en-1-yl)butan-2-one **19** (59.8 mg, 0.26 mmol) in dry methanol (3.1 ml), Pd/C 10% (32.9 mg, 31.00 μmol) was added. The suspension was degassed with H_2 for 10 min and the reaction mixture was stirred at 25 ºC and under H_2 atmosphere (balloon) for 5 h. The crude was filtered through Teflon 0.22 and the solvent was removed under reduced pressure to obtain 4-(2,2-dimethyl-4-phenylcyclobutyl)butan-2-one **45** in 90% isolated yield as a mixture 1.6:1 of *cis*:*trans* diastereoisomers (53.9 mg, 0.23 mmol). ^{1}H NMR for the mixture of diastereoisomers (500 MHz, $CDCl_3$, ppm) δ 7.31 – 7.27 (m, 2H), 7.24 – 7.21 (m, 2H), 7.20 – 7.16 (m, 1H), 3.77 (q, *J* = 9.25 Hz, 0.7H), 2.96 (q, *J* = 8.77 Hz, 0.4H), 2.25 – 2.17 (m, 1H), 2.16 – 2.10 (m, 1H), 2.01 – 1.97 (m, 1H), 1.96 (s, 1.2H), 1.95 – 1.90 (m, 1H), 1.86 (s, 2H), 1.84 – 1.76 (m, 1H), 1.73 – 1.65 (m, 1H), 1.53 – 1.48 (m, 1H), 1.47 – 1.37 (m, 2H), 1.29 (s, 2H), 1.14 (s, 1.2H), 1.13 (s, 1.2H), 1.04 (s, 2H); ^{13}C NMR for the mixture of diastereoisomers (101 MHz, $CDCl_3$, ppm) δ 209.17 (s), 208.92 (s), 145.14 (s), 141.23 (s), 128.45 (s), 128.42 (s), 128.21 (s), 127.02 (s), 126.10 (s), 126.04 (s), 51.88 (s), 48.18 (s), 42.28 (s), 41.69 (s), 41.66 (s), 41.31 (s), 37.17 (s), 36.21 (s), 34.04 (s), 33.92 (s), 30.90 (s), 30.54 (s), 29.94 (s), 29.77 (s), 24.62 (s), 24.61 (s), 22.40 (s), 21.48 (s). ESI$^+$ *m/z* calc for $C_{16}H_{22}NaO^+$ $[M+Na]^+$ 253.1563, found 253.1558 (0.5 ppm).

2-Methyl-2-(4-methylpent-3-en-1-yl)-1,3-dioxane (63)[9]

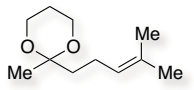

To a solution of 6-methylhept-5-en-2-one (1.48 ml, 10.00 mmol), triethoxymethane (1.83 ml, 11.00 mmol) and propane-1,3-diol (0.72 ml, 10.00 mmol) in THF (20 ml), $FeCl_3$ (0.16 g, 1.00 mmol) was added. The reaction mixture was stirred at 25 ºC for 12 h. Then, it was quenched with NaOH 10% and extracted with CH_2Cl_2. The combined organic layers were washed with water, dried over Na_2SO_4 and concentrated. The residue was purified with silica gel colum chromatography using a gradient of cyclohexane:ethyl acetate to obtain 2-methyl-2-(4-methylpent-3-en-1-yl)-1,3-dioxane **63** in 66% isolated yield (1.21 g, 6.57 mmol). ^{1}H NMR (440 MHz, $CDCl_3$, ppm) δ 5.15 –5.10 (m, 1H), 3.93 – 3.87 (m, 4H), 2.08 – 2.02 (m, 2H), 1.75 – 1.66 (m, 7H), 1.62 (s, 3H), 1.39 (s, 3H).

2-(2-(4,4-Dimethyl-2-phenylcyclobut-2-en-1-yl)ethyl)-2-methyl-1,3-dioxane (64)[9]

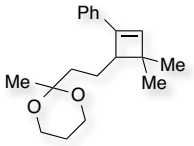

2-Methyl-2-(4-methylpent-3-en-1-yl)-1,3-dioxane **63** (0.1 g, 0.54 mmol) and ethynylbenzene (596.00 μl, 5.43 mmol) were dissolved in CH_2Cl_2 (1.00 ml) under inert conditions and [^{t}BuXPhosAuNCMe]$BAr^F{}_4$ (59.00 mg, 27.00 μmol) was added. The reaction mixture was stirred at 0 ºC for 24 h and quenched with 1 drop of Et_3N. The crude was concentrated and purified with silica gel column chromatography eluting with cyclohexane:ethyl acetate (99:1). 2-(2-(4,4-Dimethyl-2-phenylcyclobut-2-en-1-yl)ethyl)-2-methyl-1,3-dioxane **64** was obtained in 76% isolated

[9] Synthesized by Dr. Laura López.

yield (0.12 g, 0.41 mmol). ^{1}H NMR (500 MHz, $CDCl_3$, ppm) δ 7.35 – 7.29 (m, 4H), 7.23 – 7.20 (m, 1H), 6.29 (s, 1H), 3.95 – 3.82 (m, 4H), 2.72 (dd, *J* = 10.70, 4.28 Hz, 1H), 1.91 – 1.85 (m, 1H), 1.83 – 1.80 (m, 2H), 1.79 – 1.72 (m, 1H), 1.64 – 1.58 (m, 1H), 1.57 – 1.50 (m, 1H), 1.39 (s, 3H), 1.25 (s, 3H), 1.20 (s, 3H). ^{13}C NMR (75 MHz, $CDCl_3$, ppm) δ 145.94 (s), 136.49 (s), 134.99 (s), 128.43 (s), 127.36 (s), 125.28 (s), 99.40 (s), 59.80 (s), 59.79 (s), 52.08 (s), 43.06 (s), 37.39 (s), 27.97 (s), 25.70 (s), 23.37 (s), 22.02 (s), 20.92 (s). ESI$^+$ *m/z* calc for $C_{19}H_{26}NaO_2^+$ $[M+Na]^+$ 309.1825, found 309.1831 (0.6 ppm).

2-(2-(2,2-Dimethyl-4-phenylcyclobutyl)ethyl)-2-methyl-1,3-dioxane (65)[9]

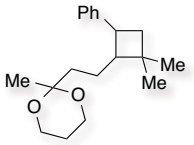

Ammonia (10 ml) was condensed in a trap cooled with acetone/dry ice and transferred to a flask at – 78 ºC. Then, metallic sodium (40 mg, 1.75 mmol) was added followed by a solution of 2-(2-(4,4-dimethyl-2-phenylcyclobut-2-en-1-yl)ethyl)-2-methyl-1,3-dioxane **64** (100 mg, 0.35 mmol) in THF (2 ml). The reaction mixture was stirred for 30 min and quenched with saturated NH_4Cl and the flask was left open while stirring for 2 h. The solution was extracted with cyclohexane and the organic layers were washed with brine, dried over Na_2SO4 and concentrated. The residue was purified by silica gel column chromatography using cyclohexane;ethyl acetate (98:2) to obtain *trans*-2-(2-(2,2-dimethyl-4-phenylcyclobutyl)ethyl)-2-methyl-1,3-dioxane **65** in 37% isolated yield (37 mg, 0.13 mmol). ^{1}H NMR (400 MHz, $CDCl_3$, ppm) δ 7.28 – 7.23 (m, 4H), 7.18 – 7.14 (m, 1H), 3.91 – 3.85 (m, 2H), 3.84 – 3.78 (m, 2H), 2.97 (q, *J* = 9.26 Hz, 1H), 2.03 – 1.94 (m, 2H), 1.79 – 1.65 (m, 3H), 1.60 – 1.52 (m, 4H), 1.35 (s, 3H), 1.15 (s, 6H). ^{13}C NMR (126 MHz, $CDCl_3$, ppm) δ 145.44 (s), 128.33 (s), 127.04 (s), 125.89 (s), 99.28 (s), 59.73 (s), 52.83 (s), 41.80 (s), 41.16 (s), 36.07 (s), 34.16 (s), 31.21 (s), 25.64 (s), 24.74 (s), 22.41 (s), 21.20 (s).

4-(4-(3-Hydroxyphenyl)-2,2-dimethylcyclobutyl)butan-2-one (67)

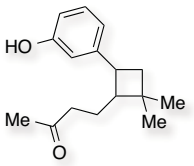

To a solution of 4-(2-(3-hydroxyphenyl)-4,4-dimethylcyclobut-2-en-1-yl)butan-2-one **60** (48.86 mg, 0.20 mmol) in dry methanol (2.40 ml), Pd/C 10% (21.00 mg, 19.73 μmol) was added. The suspension was degassed with H_2 gas for 10 min and the reaction mixture was stirred at 25 ºC and under H_2 atmosphere (balloon) for 5 h. The crude was filtered through Teflon 0.22 and the solvent was removed under reduced pressure to obtain 4-(4-(3-hydroxyphenyl)-2,2-dimethylcyclobutyl)butan-2-one **67** in 86% isolated yield as a mixture 1.7:1 of *cis*:*trans* diastereoisomers (43 mg, 0.17 mmol). ^{1}H NMR for the mixture of diastereoisomers (400 MHz, CD_3OD, ppm) δ 7.14 – 7.08 (m, 1H), 6.74 – 6.71 (m, 2H), 6.66 – 6.59 (m, 1H), 3.72 (q, *J* = 9.17 Hz, 0.7H), 2.90 (q, *J* = 9.05 Hz, 0.4H), 2.57 (q, *J* = 7.43 Hz, 0.4H), 2.34 – 2.28 (m, 0.7H), 2.19 – 1.86 (m, 7H), 1.76 – 1.61 (m, 1H), 1.51 – 1.44 (m, 1H), 1.31 (s, 2H), 1.15 (s, 1.2H), 1.15 (s, 1.2H), 1.05 (s, 2H); ^{13}C NMR for the mixture of diastereoisomers (101 MHz, CD_3OD, ppm) δ 212.07 (s), 211.82 (s), 158.39 (s), 158.28 (s), 147.96 (s), 143.97 (s), 130.27 (s), 130.04 (s), 120.85 (s), 120.09 (s), 119.29 (s), 116.23 (s), 114.70 (s), 113.91 (s), 52.80 (s), 49.15 (s), 42.90 (s), 42.81 (s), 42.22 (s), 42.06 (s), 38.12 (s), 36.94 (s), 34.70 (s), 34.63 (s), 31.04 (s), 30.81 (s), 29.80 (s), 29.63 (s), 25.41 (s), 24.81 (s), 22.60 (s), 22.43 (s). ESI$^-$ *m/z* calc for $C_{16}H_{21}O_2^-$ $[M-H]^-$ 245.1547, found 245.1545 (0.2 ppm).

4-(4-(3-Methoxyphenyl)-2,2-dimethylcyclobutyl)butan-2-one (68)

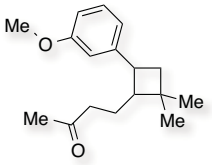

To a solution of 4-(2-(3-methoxyphenyl)-4,4-dimethylcyclobut-2-en-1-yl)butan-2-one **61** (85.14 mg, 0.33 mmol) in dry methanol (3.90 ml), Pd/C 10% (35.00 mg, 32.89 μmol) was added. The suspension was degassed with H_2 gas for 10 min and the reaction mixture was stirred at 25 ºC and under H_2 atmosphere (balloon) for 5 h. The crude was filtered through Teflon 0.22 and the solvent was removed under reduced pressure to obtain 4-(4-(3-methoxyphenyl)-2,2-dimethylcyclobutyl)butan-2-one **68** in 54% isolated yield as a mixture 1.7:1 of *cis*:*trans* diastereoisomers (46.3 mg, 0.18 mmol). ^{1}H NMR for the mixture of diastereoisomers (400 MHz, $CDCl_3$, ppm) δ 7.22 – 7.17 (m, 1H), 6.83 – 6.79 (m, 1H), 6.78 – 6.75 (m, 1H), 6.74 – 6.70 (m, 1H), 3.79 (s, 3H), 3.73 (q, *J* = 9.19 Hz, 0.7H), 2.93 (q, *J* = 9.02 Hz, 0.4H), 2.26 – 2.21 (m, 0.7H), 2.18 – 2.09 (m, 1.4H), 2.10 – 1.95 (m, 3H), 1.93 – 1.82 (m, 3H), 1.75 – 1.64 (m, 1H), 1.54 – 1.39 (m, 1H), 1.28 (s, 2H), 1.12 (s, 1.2H), 1.11 (s, 1.1H), 1.02 (s, 2H); ^{13}C NMR for the mixture of diastereoisomers (101 MHz, $CDCl_3$, ppm) δ 209.17 (s), 208.89 (s), 159.72 (s), 159.62 (s), 146.88 (s), 143.00 (s), 129.34 (s), 129.09 (s), 120.94 (s), 119.43 (s), 114.36 (s), 112.93 (s), 111.13 (s), 111.03 (s), 55.22 (s), 51.69 (s), 48.15 (s), 42.31 (s), 41.66 (s), 41.23 (s), 37.18 (s), 36.21 (s), 33.96 (s), 33.91 (s), 30.86 (s), 30.47 (s), 29.91 (s), 29.75 (s), 24.58 (s), 22.35 (s), 21.46 (s) and three carbon atoms missing due to overlapping. ESI$^+$ *m/z* calc for $C_{17}H_{24}NaO_2^+$ $[M+Na]^+$ 283.1669, found 283.1658 (0.9 ppm).

4-(2,2-Dimethyl-4-(m-tolyl)cyclobutyl)butan-2-one (69)

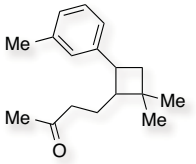

To a solution of 4-(2-(3-methoxyphenyl)-4,4-dimethylcyclobut-2-en-1-yl)butan-2-one **62** (53.34 mg, 0.22 mmol) in dry methanol (2.60 ml), Pd/C 10% (24.00 mg, 22.55 μmol) was added. The suspension was degassed with H_2 gas for 10 min and the reaction mixture was stirred at 25 ºC and under H_2 atmosphere (balloon) for 5 h. The crude was filtered through Teflon 0.22 and the solvent was removed under reduced pressure to obtain 4-(2,2-dimethyl-4-(m-tolyl)cyclobutyl)butan-2-one **69** in 84% isolated yield as a mixture 1.4:1 of *cis*:*trans* diastereoisomers (45.4 mg, 0.19 mmol). ^{1}H NMR for the mixture of diastereoisomers (400 MHz, $CDCl_3$, ppm) δ 7.19 – 7.15 (m, 1H), 7.03 – 6.98 (m, 3H), 3.72 (q, *J* = 8.94 Hz, 0.6H), 2.91 (q, *J* = 8.94 Hz, 0.4H), 2.33 (s, 3H), 2.26 – 2.08 (m, 1H), 2.20 – 2.10 (m, m, 1H), 2.05 – 1.94 (m, 3H), 1.93 – 1.80 (m, 3H), 1.75 – 1.64 (m, 1H), 1.53 – 1.40 (m, 1H), 1.28 (s, 2H), 1.13 (s, 1.2H), 1.12 (s, 1.2H), 1.03 (s, 2H); ^{13}C NMR for the mixture of diastereoisomers (101 MHz, $CDCl_3$, p pm) δ 209.26 (s), 208.98 (s), 145.04 (s), 141.11 (s), 137.85 (s), 137.60 (s), 129.15 (s), 128.28 (s), 128.06 (s), 127.74 (s), 126.78 (s), 126.76 (s), 125.49 (s), 124.01 (s), 51.75 (s), 48.13 (s), 42.30 (s), 41.69 (s), 41.57 (s), 41.25 (s), 37.05 (s), 36.17 (s), 33.97 (s), 33.87 (s), 30.87 (s), 30.48 (s), 29.88 (s), 29.69 (s), 24.62 (s), 24.59 (s), 22.35 (s), 21.55 (s), 21.52 (s), 21.49 (s). ESI$^+$ *m/z* calc for $C_{17}H_{24}NaO^+$ $[M+Na]^+$ 267.1719, found 267.1712 (0.7 ppm).

3,3-Dimethyl-2-(3-oxobutyl)cyclobutane-1-carboxylic acid (46)

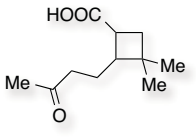

To a 1000 ml round-bottom flask, 4-(2,2-dimethyl-4-phenylcyclobutyl)butan-2-one **45** (287.5 mg, 1.25 mmol) was dissolved in 150 ml of a mixture of water:ethyl acetate (3:1) and cooled down to 4 ºC. Then, $NaIO_4$ (4.00 g, 18.75 mmol) followed by

ruthenium (IV) oxide monohydrate (20.00 mg, 0.13 mmol) were added sequentially. The reaction mixture was stirred vigorously for 30 h at 25 ºC. After extraction with ethyl acetate, the organic layers were washed with a mixture of brine:saturated Na_2SO_3 (10:1). The aqueous phase was acidified with concentrated HCl to pH 2 and extracted again. The combined organic layers were then washed with saturated Na_2CO_3 followed by extraction with CH_2Cl_2. The aqueous phase was acidified again and extracted with ethyl acetate. The solvent was evaporated under reduced pressure and 3,3-dimethyl-2-(3-oxobutyl)cyclobutane-1-carboxylic acid **46** was obtained in 80% isolated yield as a 1.4:1 mixture of diastereoisomers (210.7 mg, 1.06 mmol). ^{1}H NMR for the mixture of diastereoisomers (500 MHz, $CDCl_3$, ppm) δ 3.20 – 3.15 (m, 0.6H), 2.64 (q, *J* = 9.09 Hz, 0.4H), 2.47 – 2.24 (m, 3H), 2.14 – 2.07 (m, 4H), 1.92 – 1.66 (m, 3H), 1.09 (s, 2H), 1.04 (s, 1.1H), 1.02 (s, 2H), 1.01 (s, 1.1H); ^{13}C NMR for the mixture of diastereoisomers (126 MHz, $CDCl_3$, ppm) δ 209.26 (s), 209.24 (s), 181.83 (s), 180.99 (s), 47.76 (s), 46.43 (s), 42.05 (s), 41.28 (s), 39.26 (s), 36.51 (s), 35.94 (s), 35.86 (s), 34.57 (s), 33.93 (s), 31.01 (s), 30.17 (s), 29.96 (s), 29.92 (s), 23.97 (s), 23.26 (s), 22.32 (s), 21.49 (s).

Methyl 3,3-dimethyl-2-(3-oxobutyl)cyclobutane-1-carboxylate (66)

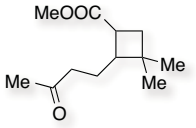

3,3-Dimethyl-2-(3-oxobutyl)cyclobutane-1-carboxylic acid **46** (76.50 mg, 0.39 mmol) were dissolved in 2 ml of a mixture of toluene:methanol (1:1) under inert conditions. The solution was cooled down to 0 ºC and 2 M trimethylsilyldiazomethane in diethyl ether (0.40 ml, 0.80 mmol) was added dropwise. The reaction mixture was stirred for 1.5 h and then directly concentrated under vacuum. Methyl 3,3-dimethyl-2-(3-oxobutyl)cyclobutane-1-carboxylate **66** was obtained in 91% isolated yield as a 1.1:1 mixture of diastereoisomers (75.1 mg, 0.35 mmol). ^{1}H NMR for the mixture of diastereoisomers (500 MHz, $CDCl_3$, ppm) δ 3.62 (s, 1.5H), 3.61 (s, 1.5H), 3.15 – 3.10 (m, 0.6H), 2.59 (q, *J* = 9.21 Hz, 0.5H), 2.36 – 2.19 (m, 3H), 2.09 – 2.05 (m, 4H), 1.82 – 1.73 (m, 1H), 1.64 – 1.56 (m, 2H), 1.07 (s, 1.5H), 1.02 (s, 1.5H), 1.00 (s, 1.5H), 0.99 (s, 1.5H); ^{13}C NMR for the mixture of diastereoisomers (126 MHz, $CDCl_3$, ppm) δ 208.52 (s), 208.40 (s), 175.82 (s), 174.99 (s), 51.59 (s), 51.38 (s), 47.68 (s), 46.34 (s), 41.98 (s), 41.32 (s), 39.24 (s), 36.33 (s), 36.11 (s), 35.69 (s), 34.53 (s), 34.09 (s), 31.04 (s), 30.16 (s), 29.93 (s), 29.89 (s), 24.01 (s), 23.29 (s), 22.30 (s), 21.58 (s).

Methyl 3,3-dimethyl-2-(2-(2-methyl-1,3-dioxolan-2-yl)ethyl)cyclobutane-1-carboxylate (71)

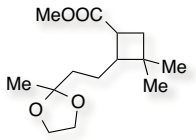

Trimethylsilyl trifluoromethanesulfonate (18.00 μl, 0.10 mmol) was dissolved in CH_2Cl_2 (200.00 μl). Then, 22.00 ml of this solution was added over methyl 3,3-dimethyl-2-(3-oxobutyl)cyclobutane-1-carboxylate **66** (21.00 mg, 0.10 mmol) at 0 ºC and under inert conditions followed by 2,2,7,7-tetramethyl-3,6-dioxa-2,7-disilaoctane (47.00 μl, 0.20 mmol). The reaction mixture was stirred for 1.5 h and quenched by a drop of pyridine. The solution was diluted with CH_2Cl_2 and washed with saturated $NaHCO_3$, aqueous $CuSO_4$ 1% and water, sequentially. The organic layers were dried with $NaSO_4$ and Na_2CO_3 and concentrated. Methyl 3,3-dimethyl-2-(2-(2-methyl-1,3-dioxolan-2-yl)ethyl)cyclobutane-1-carboxylate **71** was obtained quantitatively as a 1:1 mixture of diastereoisomers (27.4 mg, 0.10 mmol). *Note: Use 1.2 equiv. of 2,2,7,7-tetramethyl-3,6-dioxa-2,7-disilaoctane a in larger scale otherwise the purification is more complicated.* ^{1}H NMR for the mixture of diastereoisomers (500 MHz, $CDCl_3$, ppm) δ 3.95 – 3.89 (m, 4H), 3.66 (s, 1.5H), 3.65 (s, 1.5H), 3.20 – 3.15 (m, 0.5H), 2.64 – 2.59 (m, 0.5H), 2.28 – 2.23 (m, 0.5H), 2.16 – 2.10 (m, 1H), 1.90 – 1.86 (m, 0.5H), 1.80 – 1.76 (m, 1H),

1.55 – 1.45 (m, 4H), 1.30 (s, 1.5H), 1.29 (s, 1.5H), 1.12 (s, 1.5H), 1.08 (s, 1.5H), 1.05 (s, 1.5H), 1.03 (s, 1.5H); ^{13}C NMR for the mixture of diastereoisomers (126 MHz, $CDCl_3$, ppm) δ 176.10 (s), 175.33 (s), 110.09 (s), 110.04 (s), 64.78 (s), 64.75 (s), 51.69 (s), 51.40 (s), 48.47 (s), 47.17 (s), 39.44 (s), 37.70 (s), 36.85 (s), 36.53 (s), 36.10 (s), 35.73 (s), 34.70 (s), 34.12 (s), 31.31 (s), 30.52 (s), 24.91 (s), 23.86 (s), 23.82 (s), 23.44 (s), 22.33 (s), 22.11 (s).

Methyl trans-3,3-dimethyl-2-(2-(2-methyl-1,3-dioxolan-2-yl)ethyl)cyclobutane-1-carboxylate (trans-71)

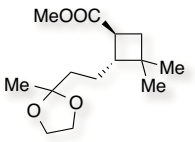

Methyl 3,3-dimethyl-2-(2-(2-methyl-1,3-dioxolan-2-yl)ethyl)cyclobutane-1-carboxylate **71** (30.00 mg, 0.12 mmol) was dissolved in 0.25 ml of THF under inert conditions and sodium methoxide (6.5 mg, 0.12 mmol) was added. Then, 0.25 ml of freshly distilled methanol were added and the reaction mixture was stirred at 70 ºC for 20 h, when the diastereoselectivity reached 97:3 by GC-MS. The solution was cooled down to 0 ºC and quenched with saturated NH_4Cl followed by extraction with ethyl acetate. The organic layers were washed with saturated $NaHCO_3$ and dried with Na_2SO_4. The solvent was removed under reduced pressure and methyl *trans*-3,3-dimethyl-2-(2-(2-methyl-1,3-dioxolan-2-yl)ethyl)cyclobutane-1-carboxylate ***trans*-71** was obtained in 77 % isolated yield (22.8 mg, 0.09 mmol). ^{1}H NMR (500 MHz, $CDCl_3$, ppm) δ 3.94 – 3.90 (m, 4H), 3.65 (s, 3H), 2.61 (q, *J* = 9.09 Hz, 1H), 2.16 – 2.11 (m, 1H), 1.87 (m, 1H), 1.78 (dd, *J* = 11.24, 8.71 Hz, 1H), 1.55 – 1.45 (m, 4H), 1.30 (s, 3H), 1.07 (s, 3H), 1.03 (s, 3H); ^{13}C NMR (126 MHz, $CDCl_3$, ppm) δ 176.09 (s), 110.04 (s), 64.76 (s), 51.69 (s), 48.47 (s), 39.43 (s), 36.84 (s), 36.09 (s), 34.69 (s), 30.51 (s), 24.90 (s), 23.85 (s), 22.32 (s). Stereochemistry confirmed with NOESY experiments (see **Chapter 5**).

1-(3,3-Dimethyl-2-(2-(2-methyl-1,3-dioxolan-2-yl)ethyl)cyclobutyl)ethan-1-one (trans-73)

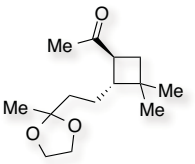

Methyl *trans*-3,3-dimethyl-2-(2-(2-methyl-1,3-dioxolan-2-yl)ethyl)cyclobutane-1-carboxylate ***trans*-71** (10.60 mg, 41.00 μmol) was dissolved in THF (0.10 ml) under inert conditions and *N*,*O*-dimethylhydroxylamine hydrochloride (4.50 mg, 45.10 μmol) was added. The solution was cooled down to 0 ºC and 2 M isopropylmagnesium chloride in diethyl ether (62.00 μl, 123.00 μmol) was added. The reaction mixture was stirred for 2 h and quenched with saturated NH_4Cl followed by extraction with CH_2Cl_2. The organic layers were washed with water and dried with $MgSO_4$. The Weinreb amide intermediate ***trans*-72** was obtained in 81 % yield and used directly. 1-(3,3-Dimethyl-2-(2-(2-methyl-1,3-dioxolan-2-yl)ethyl)cyclobutyl)-2-methoxypropan-1-one ***trans*-72** (16.30 mg, 57.00 μmol) was dissolved in THF (0.20 ml) under inert conditions and cooled down to 0 ºC. Then, 3 M methylmagnesium bromide in diethyl ether (35.00 μl, 102.60 μmol) was added and the solution was stirred for 1.5 h at 25 ºC. The reaction was cooled down to 0 ºC and quenched with saturated NH_4Cl followed by extraction with ethyl acetate. The organic layers were dried with Na_2SO_4 and concentrated. The crude was purified with neutral alumina column chromatography eluting with cyclohexane – cyclohexane:ethyl acetate (2:1) – ethyl acetate to obtain 1-(3,3-dimethyl-2-(2-(2-methyl-1,3-dioxolan-2-yl)ethyl)cyclobutyl)ethan-1-one ***trans*-73** in 65% isolated yield (9.5 mg, 0.04 mmol). ^{1}H NMR (400 MHz, $CDCl_3$, ppm) δ 3.94 – 3.89 (m, 4H), 2.73 (q, *J* = 9.52 Hz, 1H), 2.15 – 2.11 (m, 1H), 2.08 (s, 3H), 1.77 (t, *J*

= 9.32 Hz, 2H), 1.53 – 1.40 (m, 4H), 1.29 (s, 3H), 1.05 (s, 6H); ^{13}C NMR (101 MHz, $CDCl_3$, ppm) δ 210.29 (s), 110.00 (s), 64.78 (s), 47.59 (s), 47.03 (s), 37.18 (s), 36.25 (s), 33.95 (s), 30.61 (s), 28.47 (s), 25.05 (s), 23.87 (s), 22.59 (s). ESI$^+$ *m/z* calc for $C_{14}H_{24}NaO_3^+$ $[M+Na]^+$ 263.1618, found 263.1612 (0.6 ppm).

2,2,6-Trimethyl-6-(phenylethynyl)tetrahydro-2H-pyran (59)

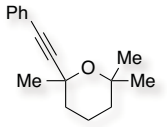

[(S,S,S)-(+)-(3,5-Dioxa-4-phosphacyclohepta[2,1-a:3,4-a']dinaphthalen-4-yl)bis(1-phenylethyl) amine] gold (I) chloride called **Z** (3.1 mg, 4.02 μmol) was dissolved in CH_2Cl_2 (0.05 ml) and added over silver bis(trifluoromethanesulfonyl)imide under inert conditions (1.5 mg, 3.87 μmol). The reaction mixture was stirred at 25 ºC for 15 min. The suspension was filtered through Teflon 0.22 and then concentrated. The crude was dissolved again in CH_2Cl_2 (0.15 ml) under inert conditions and ethynylbenzene (9 μl, 0.08 mmol) followed by 6-methylhep-5-en-2-one (49 μl, 0.33 mmol) were added. The reaction mixture was stirred at 25 ºC for 20 h and quenched with a drop of Et_3N. The crude was concentrated and purified by silica gel preparative TLC eluting with pentane:CH_2Cl_2 (2:1). 2,2,6-Trimethyl-6-(phenylethynyl)tetrahydro-2H-pyran **59** was obtained in 38% isolated yield (8 mg, 0.04 mmol). ^{1}H NMR (400 MHz, $CDCl_3$, ppm) δ 7.41 – 7.38 (m, 2H), 7.30 – 7.27 (m, 3H), 2.13 – 2.02 (m, 1H), 1.96 – 1.91 (m, 1H), 1.67 – 1.61 (m, 1H), 1.54 (s, 3H), 1.53 (s, 3H), 1.49 – 1.34 (m, 3H), 1.22 (s, 3H); ^{13}C NMR (101 MHz, $CDCl_3$, ppm) δ 131.46 (s), 128.35 (s), 128.00 (s), 123.71 (s), 94.69 (s), 83.46 (s), 73.64 (s), 67.96 (s), 38.68 (s), 36.76 (s), 33.30 (s), 32.69 (s), 25.55 (s), 17.96 (s). APCI$^+$ *m/z* calc for $C_{16}H_{21}O^+$ $[M+H]^+$ 229.1587, found 229.1586 (0.1 ppm).

DFT Calculations Data

2,6-Di(anthracen-9-yl)-4-methyl-4-(4-methylpent-3-en-1-yl)dinaphtho[2,1-d:1',2'-f][1,3]dioxepine (51)

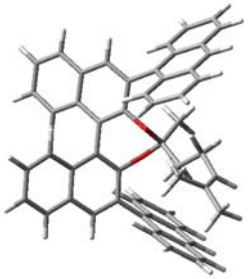

G = -2615.349893 Hartree/particle

Row	Symbol	X	Y	Z
1	C	-1.7409710	3.3448970	-0.1517820
2	C	-0.9756970	2.1485430	-0.3293030
3	C	-1.6138290	0.9290990	-0.1827300
4	C	-3.0208730	0.8057000	-0.0113420
5	C	-3.7627480	1.9630830	0.0483100
6	C	-3.1544700	3.2398680	0.0156460
7	H	-4.8464140	1.9012070	0.1608360
8	C	-3.9275880	4.4173270	0.1744630
9	C	-1.1559290	4.6354520	-0.0867800
10	C	-1.9291770	5.7564740	0.0889980
11	H	-1.4550760	6.7347730	0.1466600
12	C	-3.3323000	5.6524410	0.2065550
13	H	-3.9341360	6.5498000	0.3369580
14	H	-5.0072240	4.3153270	0.2863560
15	H	-0.0747190	4.7317240	-0.1625820
16	C	0.4731690	2.1402140	-0.6452370
17	C	1.0263070	2.8702160	-1.7469230

18	C	1.3109850	1.3279400	0.1030730
19	C	2.4390070	2.8527430	-1.9481070
20	C	2.7171410	1.2730200	-0.1157420
21	C	3.2532300	2.0627540	-1.1045000
22	H	4.3302580	2.0450340	-1.2801390
23	C	0.2317970	3.5775220	-2.6861430
24	H	-0.8510550	3.5601070	-2.5853690
25	C	3.0033630	3.5898810	-3.0187820
26	C	2.2078110	4.2902790	-3.8887900
27	C	0.8057210	4.2672780	-3.7259230
28	H	0.1718350	4.7957450	-4.4359250
29	H	4.0862340	3.5723480	-3.1434840
30	H	2.6506570	4.8472950	-4.7123440
31	O	-0.8715390	-0.2169400	-0.2769820
32	O	0.7915750	0.6001060	1.1392110
33	C	-0.0278130	-0.5288490	0.8225630
34	C	-0.8077000	-0.8119780	2.0854230
35	H	-1.5557430	-1.5936800	1.9085790
36	H	-0.1218460	-1.1403180	2.8754840
37	H	-1.3191560	0.0953860	2.4283440
38	C	0.8231390	-1.6905630	0.3489960
39	H	1.3375890	-1.3689300	-0.5687860
40	H	1.6057330	-1.8717030	1.1027040
41	C	0.0505840	-2.9769400	0.0520120
42	H	-0.8172450	-2.7379510	-0.5817170
43	H	-0.3558490	-3.3920420	0.9863710
44	C	0.9360240	-3.9927570	-0.6077110
45	H	1.4779880	-4.6699480	0.0594770
46	C	1.1659800	-4.0972960	-1.9230060
47	C	2.0994820	-5.1317320	-2.4730920
48	H	2.5391170	-5.7523850	-1.6822230
49	H	1.5835830	-5.7951800	-3.1843680
50	H	2.9230900	-4.6616030	-3.0342620
51	C	0.5403960	-3.2073770	-2.9545500
52	H	-0.0374800	-3.7952010	-3.6852500
53	H	-0.1294590	-2.4481270	-2.5326130
54	H	1.3201960	-2.6824920	-3.5292180
55	C	3.5582260	0.3364590	0.6735170
56	C	4.0460420	-0.8377940	0.0621480
57	C	3.8088700	0.5849940	2.0368610
58	C	4.7487620	-1.8089180	0.8583030
59	C	4.5267570	-0.3844150	2.8178670
60	C	4.9664350	-1.5611930	2.2125840
61	H	5.4957080	-2.3043960	2.8118810
62	C	-3.6400470	-0.5389420	0.1087480
63	C	-4.2618870	-0.9263580	1.3164590
64	C	-3.5591120	-1.4466600	-0.9688900
65	C	-4.7853780	-2.2612540	1.4463620
66	C	-4.0610340	-2.7838920	-0.8150610
67	C	-4.6593220	-3.1575780	0.3867400
68	H	-5.0408040	-4.1740240	0.5004190
69	C	-4.3639460	-0.0669420	2.4543090
70	C	-5.4084340	-2.6545390	2.6678200
71	C	-5.5027080	-1.7921350	3.7208200
72	C	-4.9628730	-0.4823160	3.6101490
73	H	-3.9477780	0.9365850	2.3949890
74	H	-5.0230500	0.1955500	4.4598990
75	H	-5.8043720	-3.6679850	2.7374590
76	H	-5.9792790	-2.1039920	4.6483850
77	C	-2.9957540	-1.0912870	-2.2319100
78	C	-3.9353160	-3.7070710	-1.8957850
79	C	-3.3660370	-3.3318710	-3.0776370
80	H	-3.2724360	-4.0447470	-3.8951400
81	C	-2.9017960	-1.9991410	-3.2485830

82	H	-2.4662310	-1.7015740	-4.2013610
83	H	-2.6410510	-0.0733750	-2.3820080
84	H	-4.3105820	-4.7203830	-1.7511220
85	C	3.3824990	1.7826150	2.6850520
86	C	4.7682340	-0.1237720	4.1988570
87	C	4.3366760	1.0327540	4.7817710
88	C	3.6379140	2.0006540	4.0094960
89	H	3.3068810	2.9246000	4.4806130
90	H	2.8552430	2.5352940	2.1010580
91	H	4.5291610	1.2223720	5.8363070
92	H	5.3107460	-0.8729300	4.7760050
93	C	3.8309200	-1.1437270	-1.3176530
94	C	5.1941480	-3.0203740	0.2504440
95	C	4.9676860	-3.2706610	-1.0715300
96	C	4.2759270	-2.3145070	-1.8636580
97	H	4.1005960	-2.5192320	-2.9194700
98	H	3.2915010	-0.4300040	-1.9381290
99	H	5.7222570	-3.7422390	0.8738700
100	H	5.3093760	-4.2002480	-1.5241640

(4-methyl-4-(4-methylpent-3-en-1-yl)dinaphtho[2,1-d:1',2'-f][1,3]dioxepine-2,6-diyl)bis(triphenylsilane) (52)

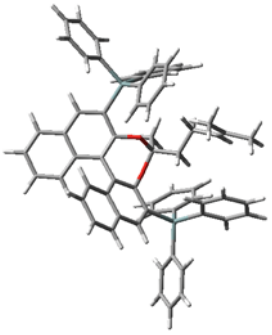

G = -3197.858361 Hartree/particle

Row	Symbol	X	Y	Z
1	C	-1.3915550	3.5081580	0.3934750
2	C	-0.7996040	2.2514820	0.0425700
3	C	-1.5588430	1.1051210	0.1977120
4	C	-2.9643840	1.1312060	0.4135380
5	C	-3.5422610	2.3586330	0.6570740
6	C	-2.7794970	3.5499020	0.7173190
7	H	-4.6203770	2.4359270	0.8126210
8	C	-3.3784780	4.7834440	1.0714170
9	C	-0.6505800	4.7142140	0.4734590
10	C	-1.2563600	5.8934840	0.8345670
11	H	-0.6638560	6.8045450	0.8997990
12	C	-2.6363170	5.9358260	1.1283670
13	H	-3.1032030	6.8786440	1.4072630
14	H	-4.4429830	4.7928190	1.3068840
15	H	0.4171300	4.6959930	0.2635070
16	C	0.5741040	2.1339830	-0.4962530
17	C	1.0040940	2.8739830	-1.6435470
18	C	1.4521080	1.2332260	0.0807380
19	C	2.3665840	2.7764250	-2.0523840
20	C	2.8215340	1.1336520	-0.2928630
21	C	3.2466320	1.9336890	-1.3338810
22	H	4.2934540	1.9135190	-1.6478780
23	C	0.1294020	3.6704310	-2.4265660
24	H	-0.9234090	3.7239230	-2.1569610
25	C	2.8144720	3.5087200	-3.1794820
26	C	1.9473410	4.2866490	-3.9033310
27	C	0.5884330	4.3542030	-3.5257640
28	H	-0.1044410	4.9505220	-4.1171300
29	H	3.8634890	3.4278020	-3.4653120

30	H	2.2970750	4.8404120	-4.7726000
31	O	-0.9733630	-0.1201320	0.0018430
32	O	1.0054190	0.4853430	1.1366330
33	C	0.0414370	-0.5418400	0.9167620
34	C	-0.5118950	-0.8271880	2.2933020
35	H	-1.2679020	-1.6181280	2.2567090
36	H	0.3092930	-1.1349680	2.9552290
37	H	-0.9720870	0.0792700	2.7064000
38	C	0.7013550	-1.7346230	0.2515740
39	H	1.1176690	-1.3925930	-0.7084850
40	H	1.5516530	-2.0288410	0.8850580
41	C	-0.1964070	-2.9440100	0.0010240
42	H	-1.0705990	-2.6352170	-0.5896820
43	H	-0.5899830	-3.3173690	0.9602260
44	C	0.5628770	-4.0428760	-0.6772390
45	H	1.2712350	-4.5842670	-0.0392250
46	C	0.5013700	-4.3934760	-1.9684140
47	C	1.3224010	-5.5263830	-2.5057610
48	H	1.9595730	-5.9776820	-1.7347090
49	H	0.6782050	-6.3147990	-2.9253290
50	H	1.9736270	-5.1909720	-3.3290240
51	C	-0.3573870	-3.7119750	-2.9887940
52	H	-1.0592960	-4.4197320	-3.4571650
53	H	-0.9437110	-2.8773420	-2.5873240
54	H	0.2675920	-3.3149620	-3.8050020
55	Si	4.0705270	-0.0434230	0.5060020
56	C	5.7722230	0.7738790	0.4406350
57	C	6.5660530	0.6438870	-0.7098260
58	C	6.2852570	1.5327610	1.5017500
59	C	7.8114510	1.2578140	-0.8056840
60	H	6.2067600	0.0420620	-1.5474750
61	C	7.5319210	2.1467600	1.4145870
62	H	5.7091460	1.6377240	2.4223130
63	C	8.2961780	2.0131700	0.2588700
64	H	8.4070530	1.1420090	-1.7100850
65	H	7.9094240	2.7285950	2.2543270
66	H	9.2720380	2.4915620	0.1897380
67	C	3.6226950	-0.4094140	2.2957950
68	C	3.5286690	-1.7103940	2.8048050
69	C	3.3530850	0.6537270	3.1717880
70	C	3.1865200	-1.9441500	4.1357780
71	H	3.7150500	-2.5639090	2.1508590
72	C	3.0182250	0.4295570	4.5023920
73	H	3.3775590	1.6813780	2.8009750
74	C	2.9350210	-0.8740440	4.9881620
75	H	3.1169860	-2.9658450	4.5065830
76	H	2.8104820	1.2720570	5.1603630
77	H	2.6705130	-1.0541400	6.0290670
78	C	4.1984380	-1.6066790	-0.5368160
79	C	5.0276580	-2.6619480	-0.1249100
80	C	3.5401630	-1.7390540	-1.7666580
81	C	5.1626390	-3.8168430	-0.8893760
82	H	5.5883270	-2.5793260	0.8089010
83	C	3.6782520	-2.8873760	-2.5417570
84	H	2.9023750	-0.9310540	-2.1307600
85	C	4.4837790	-3.9322350	-2.1000300
86	H	5.8056210	-4.6253950	-0.5445880
87	H	3.1514680	-2.9660270	-3.4929640
88	H	4.5866960	-4.8351690	-2.7007910
89	Si	-4.0331960	-0.4091810	0.1755030
90	C	-5.8324600	0.1632310	0.1595360
91	C	-6.7434180	-0.1297480	1.1814970
92	C	-6.2938170	0.9183060	-0.9313190
93	C	-8.0617840	0.3188880	1.1245100

94	H	-6.4223580	-0.7239780	2.0383620
95	C	-7.6066110	1.3718770	-0.9943120
96	H	-5.6098130	1.1588190	-1.7488830
97	C	-8.4939040	1.0720900	0.0376350
98	H	-8.7528650	0.0779340	1.9311060
99	H	-7.9401780	1.9580290	-1.8494920
100	H	-9.5235530	1.4238120	-0.0084650
101	C	-3.7131810	-1.1617810	-1.5218030
102	C	-4.4296060	-2.3021020	-1.9190190
103	C	-2.8801710	-0.5533490	-2.4712440
104	C	-4.3045080	-2.8263960	-3.2021980
105	H	-5.1127550	-2.7851230	-1.2161100
106	C	-2.7632280	-1.0625860	-3.7620690
107	H	-2.3133330	0.3401710	-2.2045210
108	C	-3.4720100	-2.2031930	-4.1285610
109	H	-4.8672610	-3.7154160	-3.4834350
110	H	-2.1127630	-0.5687990	-4.4827660
111	H	-3.3770140	-2.6063530	-5.1358950
112	C	-3.8070870	-1.6359890	1.5792590
113	C	-3.5021190	-2.9872820	1.3787900
114	C	-3.9423530	-1.1825850	2.9012440
115	C	-3.3360380	-3.8561880	2.4555110
116	H	-3.3754040	-3.3709230	0.3649900
117	C	-3.7821790	-2.0444650	3.9810750
118	H	-4.1622900	-0.1287780	3.0922110
119	C	-3.4759320	-3.3855710	3.7577940
120	H	-3.0939580	-4.9027600	2.2752540
121	H	-3.8888490	-1.6694860	4.9978400
122	H	-3.3446920	-4.0632210	4.5999140

4-Methyl-4-(4-methylpent-3-en-1-yl)-2,6-bis(2,4,6-triisopropylphenyl)dinaphtho[2,1-d:1',2'-f][1,3]dioxepine (53)

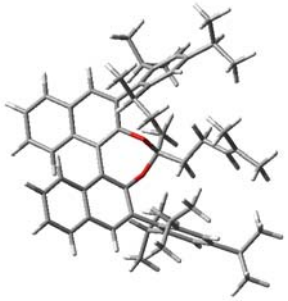

G = -2399.935166 Hartree/particle

Row	Symbol	X	Y	Z
1	C	-1.8848490	3.6288780	0.4167840
2	C	-1.0622860	2.5041030	0.0839600
3	C	-1.6416940	1.2480250	0.1084990
4	C	-3.0415330	1.0304820	0.2454200
5	C	-3.8389600	2.1337710	0.4290940
6	C	-3.2901590	3.4320840	0.5692400
7	H	-4.9208820	2.0147550	0.5038570
8	C	-4.1166070	4.5407240	0.8770310
9	C	-1.3609590	4.9256510	0.6476190
10	C	-2.1852930	5.9763400	0.9691530
11	H	-1.7579350	6.9608640	1.1517190
12	C	-3.5806330	5.7888550	1.0707180
13	H	-4.2243540	6.6312110	1.3173250
14	H	-5.1897970	4.3747540	0.9742550
15	H	-0.2855680	5.0799650	0.5813520
16	C	0.3612490	2.5978410	-0.3206680
17	C	0.8051890	3.4915110	-1.3521020
18	C	1.2763090	1.7090370	0.2240800
19	C	2.1971880	3.5489390	-1.6607440
20	C	2.6435000	1.6724760	-0.1735330

21	C	3.0856760	2.6371170	-1.0458710
22	H	4.1403850	2.6688690	-1.3239660
23	C	-0.0718430	4.3061380	-2.1144400
24	H	-1.1437260	4.2353070	-1.9482210
25	C	2.6635010	4.4664240	-2.6349080
26	C	1.7909070	5.2709770	-3.3216740
27	C	0.4063310	5.1706200	-3.0689030
28	H	-0.2917570	5.7781650	-3.6424040
29	H	3.7337520	4.5005880	-2.8406570
30	H	2.1586420	5.9673730	-4.0730990
31	O	-0.8467640	0.1457880	-0.0810970
32	O	0.8989470	0.8947790	1.2570580
33	C	0.0010600	-0.1888560	1.0024930
34	C	-0.7526610	-0.3942000	2.2973470
35	H	-1.5611890	-1.1196660	2.1529140
36	H	-0.0669810	-0.7693020	3.0675910
37	H	-1.1816130	0.5522770	2.6474430
38	C	0.7813370	-1.4095200	0.5609970
39	H	1.2545990	-1.1626440	-0.4004700
40	H	1.5964200	-1.5577270	1.2876310
41	C	-0.0324000	-2.6956980	0.4109910
42	H	-0.8833590	-2.5196960	-0.2642670
43	H	-0.4636460	-2.9747560	1.3869270
44	C	0.8634990	-3.7943290	-0.0698510
45	H	1.7194560	-3.9926770	0.5867590
46	C	0.8003260	-4.4876310	-1.2140700
47	C	1.8623360	-5.4836950	-1.5709300
48	H	2.6288610	-5.5719120	-0.7912410
49	H	1.4335390	-6.4822760	-1.7455940
50	H	2.3622200	-5.1947900	-2.5095350
51	C	-0.2565740	-4.3201090	-2.2617030
52	H	-0.6695680	-5.2966020	-2.5573910
53	H	-1.0899700	-3.6831140	-1.9442790
54	H	0.1761280	-3.8781120	-3.1746920
55	C	3.5311410	0.5650010	0.2803030
56	C	3.8575250	-0.4727120	-0.6242910
57	C	3.9938560	0.5115310	1.6052910
58	C	4.6342320	-1.5384390	-0.1710950
59	C	4.7780320	-0.5713710	2.0066170
60	C	5.1045030	-1.6093400	1.1402690
61	C	-3.5605520	-0.3627060	0.1531290
62	C	-4.0901460	-1.0150090	1.2852270
63	C	-3.4313650	-1.0637980	-1.0665090
64	C	-4.4140850	-2.3704790	1.1863240
65	C	-3.7867550	-2.4098780	-1.1162320
66	C	-4.2507230	-3.0921110	0.0088710
67	H	5.1477900	-0.6115070	3.0336560
68	H	4.8795030	-2.3442500	-0.8652520
69	C	3.4033630	-0.4599150	-2.0761070
70	H	2.5403050	0.2193450	-2.1571140
71	C	4.5138860	0.0816070	-2.9787880
72	H	5.3986780	-0.5698350	-2.9259910
73	H	4.1826490	0.1147580	-4.0259050
74	H	4.8283930	1.0918570	-2.6891920
75	C	2.9581370	-1.8257710	-2.5981470
76	H	2.2218580	-2.3079650	-1.9394580
77	H	2.5064000	-1.7128180	-3.5934390
78	H	3.8075010	-2.5157620	-2.7075990
79	C	5.9281090	-2.7834680	1.6170290
80	H	6.2212890	-2.5733110	2.6589750
81	C	5.1057530	-4.0704530	1.6151720
82	H	4.1901210	-3.9591920	2.2112640
83	H	4.8100320	-4.3439900	0.5919040
84	H	5.6852540	-4.9071700	2.0285130

85	C	7.2044860	-2.9576650	0.7975060
86	H	7.8106550	-2.0425690	0.7984020
87	H	7.8170160	-3.7752050	1.2011470
88	H	6.9725520	-3.2046630	-0.2483600
89	C	3.7014830	1.6186290	2.5961220
90	H	2.9642050	2.2967910	2.1439890
91	C	4.9623170	2.4380850	2.8673540
92	H	5.7451960	1.8205430	3.3310800
93	H	5.3711730	2.8526800	1.9352540
94	H	4.7470740	3.2733630	3.5479380
95	C	3.0936250	1.0896940	3.8914410
96	H	2.1947730	0.4937790	3.6821740
97	H	3.8013540	0.4590480	4.4478820
98	H	2.8086240	1.9214180	4.5499920
99	H	-4.8043320	-2.8901510	2.0632700
100	H	-3.6930760	-2.9460410	-2.0636200
101	C	-4.5804080	-4.5659770	-0.0438260
102	H	-4.8215120	-4.8812540	0.9847490
103	C	-5.8069360	-4.8319240	-0.9144620
104	H	-6.0649230	-5.8997400	-0.9108620
105	H	-6.6793660	-4.2669200	-0.5614020
106	H	-5.6171910	-4.5388460	-1.9571980
107	C	-3.3900720	-5.3938870	-0.5233820
108	H	-3.1677050	-5.1854030	-1.5800940
109	H	-2.4819170	-5.1751570	0.0563880
110	H	-3.6045580	-6.4677380	-0.4390380
111	C	-4.3634220	-0.2928470	2.5930710
112	H	-3.7721320	0.6346860	2.6041670
113	C	-3.9889630	-1.0963730	3.8369720
114	H	-4.1018680	-0.4711480	4.7324760
115	H	-4.6434470	-1.9688470	3.9696580
116	H	-2.9526370	-1.4568750	3.8054140
117	C	-5.8422540	0.0957890	2.6716690
118	H	-6.0498810	0.6585770	3.5921630
119	H	-6.1549770	0.7105830	1.8174370
120	H	-6.4743500	-0.8043530	2.6774720
121	C	-2.9935860	-0.3697030	-2.3443700
122	H	-2.5928660	0.6193620	-2.0845120
123	C	-4.2117250	-0.1350200	-3.2386910
124	H	-4.6593300	-1.0887240	-3.5543770
125	H	-4.9853680	0.4385210	-2.7092460
126	H	-3.9316420	0.4215120	-4.1435780
127	C	-1.8930420	-1.1065890	-3.1008420
128	H	-2.2278940	-2.0878840	-3.4672990
129	H	-1.5870430	-0.5222650	-3.9794480
130	H	-1.0057420	-1.2577850	-2.4699410

2,6-Bis(3,5-bis(trifluoromethyl)phenyl)-4-methyl-4-(4-methylpent-3-en-1-yl)dinaphtho[2,1-d:1',2'-f][1,3]dioxepine (54)

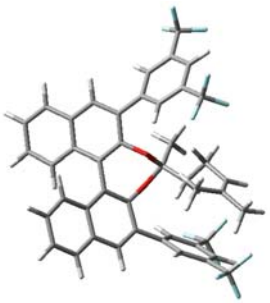

G = -3041.103987 Hartree/particle

Row	Symbol	X	Y	Z
1	C	-1.8499860	3.8365240	0.3378900
2	C	-1.0671100	2.7081580	-0.0595170
3	C	-1.6752490	1.4674670	-0.1230100

4	C	-3.0755240	1.2842340	0.0526290
5	C	-3.8369430	2.3913870	0.3522840
6	C	-3.2552760	3.6673940	0.5252800
7	H	-4.9167120	2.2905680	0.4718060
8	C	-4.0461290	4.7808540	0.9035730
9	C	-1.2874960	5.1104820	0.6031730
10	C	-2.0775670	6.1653440	0.9889480
11	H	-1.6223500	7.1326680	1.1938910
12	C	-3.4737990	6.0065870	1.1278890
13	H	-4.0883600	6.8540810	1.4251880
14	H	-5.1194630	4.6357850	1.0265000
15	H	-0.2114340	5.2440660	0.5107020
16	C	0.3753990	2.7750910	-0.3981010
17	C	0.8945050	3.6491690	-1.4072710
18	C	1.2276100	1.8643940	0.2019480
19	C	2.2922620	3.6140470	-1.6964770
20	C	2.6131490	1.7970870	-0.1095960
21	C	3.1197310	2.6811270	-1.0328700
22	H	4.1818780	2.6529160	-1.2810160
23	C	0.0801430	4.5162690	-2.1806920
24	H	-0.9949350	4.5225490	-2.0175460
25	C	2.8268970	4.4831040	-2.6798340
26	C	2.0148020	5.3329120	-3.3852390
27	C	0.6245980	5.3342960	-3.1397820
28	H	-0.0243280	5.9850430	-3.7232170
29	H	3.8992920	4.4485100	-2.8722130
30	H	2.4334710	5.9932900	-4.1421210
31	O	-0.9018370	0.3680150	-0.3949720
32	O	0.7259450	1.0033970	1.1438950
33	C	-0.0638890	-0.0896060	0.6619670
34	C	-0.8524440	-0.5680820	1.8588390
35	H	-1.5357980	-1.3768000	1.5740460
36	H	-0.1622170	-0.9407210	2.6249420
37	H	-1.4339500	0.2556850	2.2891700
38	C	0.8252720	-1.1510480	0.0439900
39	H	1.3831910	-0.6746850	-0.7762140
40	H	1.5632430	-1.4536840	0.8019610
41	C	0.1021670	-2.3790850	-0.5072630
42	H	-0.7036510	-2.0489510	-1.1755110
43	H	-0.3829980	-2.9350910	0.3092770
44	C	1.0627290	-3.2720890	-1.2347600
45	H	1.5646670	-4.0359080	-0.6337400
46	C	1.4075420	-3.1642760	-2.5247200
47	C	2.4278790	-4.0753200	-3.1372070
48	H	2.8043950	-4.8140710	-2.4194460
49	H	2.0091040	-4.6157070	-3.9998430
50	H	3.2879680	-3.5043480	-3.5199970
51	C	0.8381220	-2.1438730	-3.4644170
52	H	0.3516770	-2.6320040	-4.3225450
53	H	0.1042770	-1.4760840	-2.9968200
54	H	1.6421410	-1.5183910	-3.8816160
55	C	3.4650820	0.7410520	0.4780670
56	C	4.1400010	-0.1381060	-0.3723560
57	C	3.5668510	0.5564790	1.8585540
58	C	4.8776550	-1.1949550	0.1472210
59	C	4.3266630	-0.4887580	2.3705290
60	C	4.9764840	-1.3781560	1.5211920
61	C	-3.6726450	-0.0628950	-0.0469360
62	C	-4.6123720	-0.4849070	0.8961850
63	C	-3.2801010	-0.9607350	-1.0467330
64	C	-5.1273060	-1.7767000	0.8531560
65	C	-3.7765560	-2.2563950	-1.0659530
66	C	-4.7034660	-2.6764910	-0.1171440
67	H	-4.9148400	0.1912440	1.6936230

68	H	-5.0839100	-3.6970270	-0.1303020
69	H	-2.5665030	-0.6446570	-1.8021900
70	H	3.0468270	1.2314820	2.5337190
71	H	4.0471480	-0.0167060	-1.4505040
72	H	5.5570520	-2.2056650	1.9272430
73	C	4.4195130	-0.7253560	3.8467160
74	C	5.5367330	-2.1982620	-0.7480680
75	C	-3.2776980	-3.2596390	-2.0614250
76	C	-6.1564770	-2.2308890	1.8424790
77	F	-2.4916350	-2.7118330	-2.9940460
78	F	-2.5622670	-4.2175040	-1.4531240
79	F	-4.2853820	-3.8749310	-2.6906680
80	F	-5.8630350	-3.4423680	2.3317750
81	F	-7.3657580	-2.3302270	1.2725520
82	F	-6.2727090	-1.3952470	2.8776180
83	F	5.4747170	-1.8546040	-2.0372910
84	F	4.9618810	-3.4035630	-0.6260160
85	F	6.8288460	-2.3578880	-0.4329490
86	F	5.6816620	-0.9673090	4.2234920
87	F	3.9775180	0.3134830	4.5594950
88	F	3.6994640	-1.7964180	4.2105590

Trans-methyl 3,3-dimethyl-2-(3-oxobutyl)cyclobutane-1-carboxylate (Trans-66)

G = -694.265538 Hartree/particle

Row	Symbol	X	Y	Z
1	C	-0.7141700	-0.6673380	-0.3236750
2	C	-2.0442940	-1.4033600	-0.0057830
3	C	-2.6297370	-0.0273840	0.3894650
4	C	-1.1998930	0.5276290	0.5438120
5	H	-0.7465250	-0.3451810	-1.3793370
6	H	-3.2785650	0.0119120	1.2738270
7	H	-3.1346050	0.4586240	-0.4561670
8	H	-0.8169000	0.4601830	1.5705760
9	C	-1.9494570	-2.3329970	1.1942770
10	H	-2.9532540	-2.6769170	1.4821390
11	H	-1.3443070	-3.2221150	0.9653050
12	H	-1.5071150	-1.8412000	2.0719990
13	C	-2.6878600	-2.1137760	-1.1787980
14	H	-2.0827560	-2.9791650	-1.4898850
15	H	-3.6898050	-2.4859840	-0.9202520
16	H	-2.7882350	-1.4431630	-2.0438120
17	C	0.6224070	-1.3046120	-0.0214150
18	H	0.7386100	-2.2209180	-0.6211860
19	H	0.6653470	-1.6250880	1.0307580
20	C	1.7805510	-0.3633720	-0.2995020
21	H	1.7119890	0.5473920	0.3199660
22	H	1.7477000	0.0061310	-1.3397600
23	C	3.1425130	-0.9764740	-0.0771300
24	C	4.3130530	-0.0380840	-0.1933770
25	H	5.2530780	-0.5972490	-0.1807490
26	H	4.2479210	0.5672880	-1.1065450
27	H	4.3031560	0.6635860	0.6521480
28	C	-0.9279230	1.8811970	-0.0302950
29	C	0.2830820	3.8716120	0.2038710
30	H	0.9991560	4.2952630	0.9099910
31	H	0.7364420	3.7728330	-0.7880340
32	H	-0.6016450	4.5123400	0.1287330

33	O	3.2853030	-2.1547640	0.1909100
34	O	-1.3886440	2.2930650	-1.0740500
35	O	-0.0703240	2.5895970	0.7220890

Cis-methyl 3,3-dimethyl-2-(3-oxobutyl)cyclobutane-1-carboxylate (Cis-66)

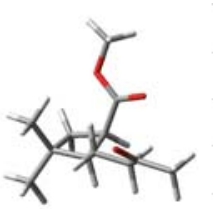

G = -694.261089 Hartree/particle

Row	Symbol	X	Y	Z
1	C	0.3802700	-1.0344310	0.5589870
2	C	1.6953560	-1.5505280	-0.0894150
3	C	2.4749890	-0.6051280	0.8582180
4	C	1.1770780	0.1568000	1.1876870
5	H	0.1183960	-1.7145390	1.3871000
6	H	3.2908720	-0.0240810	0.4131700
7	H	2.8563730	-1.1330080	1.7419410
8	H	0.9648170	0.3040470	2.2547210
9	C	1.9441050	-3.0355620	0.0901220
10	H	1.2059020	-3.6261100	-0.4739840
11	H	2.9426970	-3.3206780	-0.2717130
12	H	1.8716410	-3.3279520	1.1475400
13	C	1.8559640	-1.1633740	-1.5515700
14	H	2.8781890	-1.3911570	-1.8869030
15	H	1.1615140	-1.7267040	-2.1914150
16	H	1.6851490	-0.0930520	-1.7217450
17	C	-0.8542770	-0.8099280	-0.2871040
18	H	-1.0837820	-1.7420270	-0.8286500
19	H	-0.6727170	-0.0529820	-1.0652210
20	C	-2.0570200	-0.3960970	0.5419800
21	H	-1.8433860	0.5438620	1.0782790
22	H	-2.2636480	-1.1380140	1.3322800
23	C	-3.3219180	-0.2047590	-0.2568250
24	C	-4.5405270	0.1974760	0.5306230
25	H	-4.3704110	1.1661810	1.0195680
26	H	-5.4126610	0.2697000	-0.1256960
27	H	-4.7392620	-0.5282500	1.3302340
28	O	-3.3585100	-0.3607930	-1.4637590
29	C	0.9316370	1.4942210	0.5501980
30	O	1.9262690	1.9160390	-0.2410870
31	C	1.7209130	3.1868090	-0.8578180
32	H	1.5973630	3.9655120	-0.0981480
33	H	2.6127180	3.3781010	-1.4566080
34	H	0.8301640	3.1656730	-1.4942200
35	O	-0.0764280	2.1463140	0.7372190